THE DEVELOPMENT OF A TEST METHODOLOGY AND NEW FINDINGS IN SILICATE SCALE FORMATION AND INHIBITION

A thesis by

ROZANA AZRINA BINTI SAZALI

Thesis Submitted for the Degree of

Doctor of Philosophy in Petroleum Engineering

Institute of Petroleum Engineering
School of Energy, Geoscience, Infrastructure & Society
Heriot Watt University
Edinburgh UK

May 2018

ABSTRACT

Silicate scale is a well-known problem associated with certain EOR methods such as *Alkaline Surfactant Polymer* (ASP) Flooding and Thermal Oil Recovery. The kinetics of this silicate scale formation during ASP flooding is poorly understood due to the complexity of the (several) reactions that occur simultaneously and the strong dependency of these reactions on a range of factors in the reservoir.

An experimental methodology has been developed in this work to produce a well defined silicate scale in the laboratory. This has then been used in silicate inhibition efficiency experiments in order to study potential silicate inhibitors/dispersants. The produced silicate scale has been studies using elemental analysis for Mg and Si (by ICP) to quantify the severity of silicate scaling. In addition, the precipitated silicate deposits have also been examined using several spectroscopic methods such as ESEM/EDAX, FTIR, and XRD. A number of specific aspects of silicate scaling are studied in this thesis, as follows: (i) silicate scale formation and the related mechanisms of inhibition by chemical scale inhibitors (ii) the sensitivities of silicate scaling to various factors such as pH, temperature, initial Si:Mg molar ratio and brine ageing, (iii) the development of experimental methodology to study the effect of ferrous ion in reducing environments, and (iv) the effect of ferrous iron in the formation and inhibition of silicate scale.

These studies have enabled us to develop some new insights into the mechanisms of silicate scale formation and inhibition. The experimental methodology developed proved to be repeatable and reproducible. Results from the application of various spectroscopic methods enabled us to establish the morphology of the silicate scale formed and its stoichiometry in terms of the *Si:Mg molar ratio*. Factors governing the formation of silica and metal silicate in aqueous systems *w*ere studied and evaluated by establishing the types and morphology of the silicate precipitates produced using spectroscopic analysis and by measuring the *Si:Mg molar ratio*. It has been demonstrated that the amorphous silicate scale can be inhibited using the tested inhibitor A5 (and this has an MIC of ~ 50ppm); and how various functional groups affect IE % of silicates. An anaerobic experimental methodology was developed in this work and it is shown that the ferrous iron does enhance the silicate scale formation and the Fe itself is fully incorporated into the silicate scale which is formed that degrades the performance of the silicate inhibitors studied.

DEDICATION

To my lovely husband Mohd Khairul Azuan bin Jasni and beautiful children Putra Iszkandar and Aryan Rizqin

ACKNOWLEDGEMENT

Bismillahirrahmanirrahim. In the name of Allah, the Most Gracious and the Most Merciful.

Alhamdulillah, all praises to Allah for the strengths and his blessing in completing this thesis.

I would like to express my special appreciation and thanks to my supervisor Professor Ken Sorbie. You have been an incredible mentor for me! I would like to thank you for encouraging my research and for allowing me to grow as a research scientist. It would have been difficult for me to have reached this point in my academic journey, your invaluable help of constructive comments and suggestion throughout the experimental and thesis work have contributed to the success of this research. You have inspired and motivated me during difficult times when I needed words of encouragement. You deserve a big thank you from me. You are a legend!

Another appreciation goes to Professor Eric MacKay for his kindness, care, effort, and advice, with both academic and non-academic issues. I would especially like to thank Dr. Lorraine Boak for her guidance in the laboratory especially for lab training, experimental design procedures and the ICP, Dr. Jim Buckman for his help in obtaining ESEM/EDAX images, Mike Singleton for his valuable and constructive comment during the dry run presentation, Wendy McEwan and Katherine McIver for ICP analysis, I will also like to thank Alan Beteta, Tom Clark and Thomas McGravie for their expertise in manufacturing and installing the nitrogen glove box and other help in the laboratory. Not forgotten my appreciation to Heather O'Hara, thanks for the administrative help and care throughout my hard time. My colleagues in the flow assurance and scale team (FAST), thanks for the company and great times we spent together which made my stay at Heriot-Watt, an unforgettable moment. Every little help is very much appreciated!

I am also grateful and would like to acknowledge the Ministry of Education Malaysia and Universiti Teknologi MARA, Malaysia for their sponsorship and funding my Ph.D. at Heriot-Watt University, Edinburgh, UK. My sincere gratitude goes to FAST sponsors (Apache, Baker Hughes, BG Group, BP, Cairn, Chevron, Clariant, Clariant Oil Services, Conoco-Phillips, Equion, Foundation CMG, Galp Energia, Maersk, MI Swaco, Multi-chem, MWV, Nalco Champion, Nexen, Pemex, PETROBRAS, PETRONAS, Recherche

Exploitation Produits, Repsol Sinopec, Schlumberger, Saudi Aramco, Shell, Statoil, Talisman, Sinopec Energy UK, Total and Wintershall) for their feedback, insight and expertise during the steering meeting.

Special thanks go to my parents, Mr Sazali bin Sajari and Mrs Hamidah bin Mat, my parents in laws, Haji Mohd Ridza bin Abdul Hamid and Hajjah Azizah binti Taksir, sisters and family members who encouraged and supported me throughout my stay in the UK. Their prayers, eternal love and understanding helped me get through the ups and downs of my PhD journey.

Finally, above all, I am sincerely grateful to my beloved husband and my best friend Mohd Khairul Azuan. To the world, you may be one person, but to me, you are the world! You are the air that I breathe and my steps when I am weak. I couldn't be where I am right now without your endless love and support. I can't imagine how life would be without my children, Putra Iszkandar and Aryan Rizqin. They are the best thing that ever happened to me, without them I don't think that I could make it through each and every day. They are some of the most important people in my life and I don't think that I could survive without them. They sacrificed a lot and were always there when I needed them. I owe you my deepest gratitude for everything you guys have done. I love you guys to the moon and back!

Thank you all.

ACADEMIC REGISTRY
Research Thesis Submission

Name*:*	Rozana Azrina binti Sazali		
School:	EGIS		
Version: *(i.e. First, Resubmission, Final)*	Final	Degree Sought:	PhD Petroleum Engineering

Declaration

In accordance with the appropriate regulations I hereby submit my thesis and I declare that:

1) the thesis embodies the results of my own work and has been composed by myself
2) where appropriate, I have made acknowledgement of the work of others and have made reference to work carried out in collaboration with other persons
3) the thesis is the correct version of the thesis for submission and is the same version as any electronic versions submitted*.
4) my thesis for the award referred to, deposited in the Heriot-Watt University Library, should be made available for loan or photocopying and be available via the Institutional Repository, subject to such conditions as the Librarian may require
5) I understand that as a student of the University I am required to abide by the Regulations of the University and to conform to its discipline.
6) I confirm that the thesis has been verified against plagiarism via an approved plagiarism detection application e.g. Turnitin.

* *Please note that it is the responsibility of the candidate to ensure that the correct version of the thesis is submitted.*

Signature of Candidate*:*		Date:	25.5.2018

Submission

Submitted By *(name in capitals):*	
Signature of Individual Submitting:	
Date Submitted:	

For Completion in the Student Service Centre (SSC)

Received in the SSC by *(name in capitals):*			
Method of Submission *(Handed in to SSC; posted through internal/external mail):*			
*E-thesis Submitted (**mandatory for final theses**)*			
Signature:		Date:	

TABLE OF CONTENTS

LIST OF FIGURES

LIST OF TABLES

NOMENCLATURE

0.1% EDTA/NaOH	0.1 vol% of EDTA/NaOH quenching solution
1% EDTA/NaOH	1 vol% of EDTA/NaOH quenching solution
A5	Terpolymer of acrylic acid, 2-acrylamido-2-methylpropane sulfonic acid, non-ionic monomer
AC	After centrifuge
$Al(OH)_3$	Aluminium hydroxide
Al_2O_3	Aluminium oxide
Al^{3+}	Aluminium ion
ASP	Alkali-Surfactant-Polymer flooding
ATBS (AMPS)	2-acrylamido-2-methypropane sulphonic acid
BA	Non-polymeric inhibitor boric acid
$BaSO_4$	Barium sulfate
BC	Before centrifuge
Br^-	Bromide ion
Ca^{2+}	Calcium ion
$CaCO_3$	Calcium carbonate
$CaCl_2$	Calcium chloride
CaO	Calcium oxide
Ca/Mg	Molar ratio of calcium ion to magnesium ion
C_e	Solubility of amorphous silica in ppm
C_{es}	Molal solubility of amorphous silica in salt
C_e	Molal solubility of amorphous silica in salt-free water
$C_{e,mix}$	Molal solubility in a mixed electrolyte solution

CEOR	Chemical Enhanced Oil Recovery
CHP	Combined Heat and Power (CHP)
Cl^-	Chloride ion
CO_2	Carbon dioxide
C_O	Concentration of silicon (or other cations) originally in solution (i.e. t=0)
C_I	Concentration of silicon (or other cations) at sampling
C_B	Concentration of silicon (or other cations) in the blank solution (no inhibitor) at the same conditions and sampling time as C_I above
CP1	Proprietary blended copolymers
CP3	Proprietary blended copolymers
CP4	Proprietary blended copolymers
CP5	Proprietary blended copolymers
CP6	Proprietary blended copolymers
CP7	Proprietary blended copolymers
CMI	Carboxymethylinulin
D	Setchenow parameter solubility in multicomponent electrolyte solutions
D_i	D parameter of an individual electrolyte i
DETPMP (DTPMP)	Diethylene triamine penta methylene phosphonic acid
DTC	Differential thermochemical
DTG	Differential thermo-gravimetric
DW	Distilled water
EDAX (EDS)	Energy-dispersive X-ray spectroscopy analysis
EDTA	Ethylenediaminetetra acetic acid

EOR	Enhanced Oil Recovery
ESEM	Environmental Scanning Electron Microscope
ESPs	Electrical Submersible Pumps
Fe	Iron
Fe:Mg	Molar ratio of ferrous ion to magnesium ion
Fe:Si	Molar ratio of ferrous ion to silicon ion
$Fe(OH)_3$	Iron(III) hydroxide (hydrated iron oxide or yellow iron oxide)
$Fe(OH)_2$	Ferrous hydroxide
$Fe_2(OH)_3$	Ferric hydroxide
Fe_2O_3	Ferric oxide/ Iron(III) oxide
$Fe_2(SiO_3)_3$	Amorphous iron(III) silicate
$FeSiO_3$	Amorphous ferrous silicate
Fe_2SiO_4	Amorphous fayalite
$(Fe^{++}, Mg)_3Si_4O_{10}(OH)_2$	Minnesotaite
Fe^{2+}	Ferrous ion/ Iron(II) ion
Fe^{3+}	Ferric ion/ Iron(III) ion
FTIR-ATR	Fourier Transform Infrared - Attenuated Total Reflectance
H^+	Hydrogen ion
H3	Vinylamide / Vinylsulfonate co-polymer
H_2O	Water molecule
H_2S	Hydrogen sulphide
H_2SO_4	Sulfuric acid
$H_3SiO_4^-$	Monomeric silica ion
$H_4SiO_4^o$	Uncharged silicic acid
H_4SiO_4 ($Si(OH)_4$)	Silicic acid

$H_6Si_2O_7$	Dimers in silica polymerization reaction
HCl	Hydrochloric acid
HDPE	High-density polyethylene
HEDP	1-Hydroxyethylidine-1,1-diphosphonic acid
HF	Hydrogen fluoride
HPAM	Hydrolyzed polyacrylamide
HTHP	High Temperature High Pressure fields
ICP	Abbreviation of ICP-OES
IFT	Interfacial tension
ICP-OES	Inductively Coupled Plasma Atomic Emission Spectroscopy
IE	Inhibition efficiency
IE_{Mg} % (Mg_{IE} %)	Inhibition efficiency percentage calculated using magnesium (Mg) as the scaling ion
IE_{Si} % (Si_{IE} %)	Inhibition efficiency percentage calculated using silicon (Si) as the scaling ion
IR	Infra-red spectroscopy
I^-	Iodide ion
K_1	Dissociation constant
KCl	Potassium chloride
KCl/PVS	Potassium chloride/ Poly(vinyl Sulphonate) quenching solution
KNO_3	Potassium nitrate
K^+	Potassium ion
KCl	Potassium chloride
K_2O	Potassium oxide
LiCl	Lithium chloride

LiNO	Lithium salt of oxonitrate
$LiNO_3$	Lithium nitrate
M	Moles per litre
M	Molar solubilities of silica in qater
MB	Magnesium brine
MgO	Magnesium oxide
m	Molality of added salt
m_i	Molality of individual electrolyte i
MIC_{static} (MIC_{ST})	Minimum inhibitor concentration under static conditions in ppm
MIC_{TB}	Minimum inhibitor concentration under dynamic condition (in tube blocking test) in ppm
ml	Millilitres
μm	Micrometre
Li^+	Lithium ion
M^{2+}	Divalent cations
M^{3+}	Trivalent cations
$MgCl_2$	Magnesium chloride
$MgCl_2.6H_2O$	Magnesium chloride hexahydrate
$Mg(OH)_2$	Magnesium hydroxide
$MgO.SiO_2$	Magnesium silicate ($MgSiO_3$)
$MgSO_4$	Magnesium sulfate
$Mg_3Si_2O_5(OH)_4$	Chrysotile
Mg_2SiO_4	Amorphous forsterite
$MgSiO_3$	Amorphous enstatite

$(Mg,Fe)_2SiO_4$	Amorphous olivine - A name for a series between two end members, iron rich member (fayalite) and magnesium rich member (forsterite).
$Mg,FeSiO_4$	
$Mg_{0.8}Fe_{1.2}SiO_4$	
$MgFeSi_2O_6$	
Mg^{2+}	Magnesium ion
[Mg]	Magnesium ion concentration in ppm
$[Mg]_o$	Initial magnesium ion concentration in ppm
$[Mg]_f$	Final magnesium ion concentration in ppm
$[Mg]_{molar, rx}$	Magnesium ion reacted in molar
$[Mg]_{rx}$	Magnesium ion reacted in ppm
MB	Magnesium brine
M_B	Mass of silicon (or other cations) precipitated in supersaturated blank solution
M_I	Mass of silicon (or other cations) precipitated in test solution
Mg:Si	Molar ratio of magnesium ion to silicon ion
Mol	Moles
MS	Mass Spectroscopy
M. Wt.	Molecular weight
Na^+	Sodium ion
NaAc	Sodium acetate
NaBr	Sodium bromide
NaCl	Sodium chloride
$NaClO_4$	Sodium perchlorate
NaHCOO	Sodium formate
NaI	Sodium iodide

NaOH	Sodium hydroxide
$NaNO_3$	Sodium nitrate
Na_2CO_3	Sodium carbonate
Na_2O	Sodium oxide
Na_2SO_4	Sodium sulfate
$Na_2SiO_3.5H_2O$	Sodium metasilicate pentahydrate
n_i	Hydration number of cation i
NF	Non-filtered brine
NH_4HF_2	Ammonium bifluoride
$(NH_4)2Fe(SO_4)_2.6H_2O$	Ammonium iron (II) sulphate hexahydrate (Mohr's Salt)
NOCs	National Oil Companies
(nt)	Direct sampling
O_2	Oxygen
OH^-	Hydroxide ion
^oC	Degrees Celsius
P	Pressure
PAA	Poly(acrylic acid)
PALAM	Polyallylamine
PAMALAM	Poly(acrylamide-co-diallyl-dimethylammonium chloride)
PBTC	2-Phosphonobutane 1,2 4-tricarboxylic acid
PEI	Polyethyleneimine
PEOX	Poly(2-ethyl-2-oxazoline)
PGL	Propylene glycol
pH	Potential of hydrogen, the absolute value of base-ten logarithm of the hydrogen ion activity in solution

pH_{Nat}	Natural pH of solution
pH_o	Initial pH of mixed brine of Si/Mg
PL68	Ethylene oxide propylene oxide block co-polymer
PMA	Poly(maleic acid)
PPCA	Phosphino poly carboxylic acid
ppm	Parts per million (weight / volume unless otherwise stated)
PQ	Performance Quotient
PVS	Poly(vinyl sulphonate)
PVP	Poly(vinylpyrrolidone)
RO	Reverse osmosis
S_o (Mg)	Initial solubility of amorphous silica as a function of magnesium ion concentration
S_o (pH)	Initial solubility of amorphous silica as a function of pH
SB	Silicon brine
SDR	Silica Dissolution Ratio
SI	Scale inhibitor
[Si]	Silicon ion concentration in ppm
$[Si]_o$	Initial silicon ion concentration in ppm
$[Si]_{molar, rx}$	Silicon ion reacted in molar
$[Si]_{rx}$	Silicon ion reacted in ppm
SiO_2	Silica
Si:Mg	Molar ratio of silicon ion to magnesium ion
Si:Fe	Molar ratio of silicon ion to ferrous ion
$(Si:Mg)_o$	Initial molar ratio of silicon ion to magnesium ion
$Si(OH)_4$	Silicic acid

SiO_3^{2-}	Silicate anion
$Si(O_3)_3^{6-}$	Cyclic trimers
$Si(O_3)_6^{12-}$	Cyclic hexamers
$Si_2O(OH)_6$	Dimers in silica polymerization reaction
$Si_3O_2(OH)_8$	Trimers in silica polymerization reaction
$Si_4O_3(OH)_{10}$	Tetramers in silica polymerization reaction
SO_3	Sulfur trioxide
Sr^{2+}	Strontium ion
$SrCl_2$	Strontium chloride
SI	Scale inhibitor
[SI]	Scale inhibitor concentration (ppm active)
SEM	Scanning Electron Microscope
SP	Surfactant/ Polymer Flooding
SR	Saturation Ratio
SSI	Silica Saturation Index
SSI (pH)	Supersaturation index as a function of pH
SSI (Mg)	Supersaturation index as a function of magnesium ion present
T	Temperature / ^oC unless stated as ^{o}Kelvin in the text
t	Time / Hours
(t)	Sampling time
TDS	Total Dissolved Solid
TEM	Transmission electron microscopy
TG	Thermogravimetric
VS-Co	Vinylsulphonated acrylic acid co-polymer

XRD	X-Ray Diffraction Analysis
%	Percentage
[]	Concentration in ppm
γ	Activity coefficient

LIST OF PUBLICATIONS

1. Factors Affecting The Morphology And Constituents Of Silicate Scale - NACE Milano Italia Section Conference & Expo 2016 “A European event for the Corrosion Prevention of Oi l& Gas industry”, Genoa, Italy, 29-31 May 2016.

2. Quantifying the Severity of Silicate Scaling Using ICP-EOS - Chemistry in the Oil Industry XlV Chemistry: Challenges and Responsibilities, Manchester, United Kingdom, 2 - 4 November 2015.

3. The Effect of pH on Silicate Scaling - 11th SPE European Formation Damage, Budapest, Hungary, 3 – 5 June 2015.

CHAPTER 1. INTRODUCTION

1.1. SILICATE SCALE IN ASP FLOODING

The Alkali-Surfactant-Polymer (ASP) process combines alkali, surfactant and polymer (often in the same composite slug) to recover additional oil from the reservoir by reducing the oil/water interfacial tension and controlling the mobility ratio of the fluid displacement process. Alkali is added in ASP flooding to produce in-situ surfactants by reacting with the carboxylic acids in the oil to enhance the action of the (synthetic) injected surfactants. The high alkali conditions also reduce the loss of surfactant and polymer onto the rock surface by adsorption.

There have been over 30 field applications of ASP flooding, many of them in the Daqing field in China (Sheng, 2014). In these ASP applications, more than 70% of the producers have reported as experiencing scaling issues involving a mixture of carbonate and silicate scale. It has been reported that the initial scale would be mainly carbonate, followed later by silicate scale as the main component (Cheng et al., 2014). The main cause of both of these scales, especially the silicate scale is the presence of the strong alkali, i.e. the high pH conditions. Even when weaker alkalis were applied, such as sodium carbonate, these scaling problems persisted. The alkali conditions also led to the formation of oil/water emulsions in the separators which was an additional problem.

As well as silicate production in ASP floods, silicates can also form in steam floods due to quartz dissolution at high temperatures and also in conventional oil production. There is also experience of silicate scales in the geothermal industry and some experience with managing this problem also comes from this source.

1.2. CURRENT ADVANCES IN THE SILICATE SCALING AND KNOWLEDGE GAP

Generally, silicate scaling can be an *in situ* problem in the reservoir (i.e. it may lead to formation damage), it can be deposited in the production tubulars or downhole equipment (e.g. in ESPs) or silicate scales may form in the production system. In ASP Flooding, the origin of the silicate problem is that the ASP slug solubilises silica in the formation rock at higher pH conditions.

This solubilised silica is then transported to the producer well where it may mix with lower pH brines (pH ~ 7) which also contain divalent Mg^{2+} and Ca^{2+} ions. Both amorphous silica and also Mg-silicates may form but the aqueous chemistry of silicates is quite complex and no prediction models exist at present.

Many reports have appeared in the literature on the complexity of the reactions involved in the silicate scaling process, making this scaling problem very difficult to solve. The kinetics of silicate scaling reaction are not completely understood, including the formation of amorphous silica via silica polymerization, colloidal silica suspension, precipitation of metal silicates and co-precipitation of silica with mineral salts (e.g., calcium carbonate, calcium sulfate etc.).

It is currently common practice in the oil industry to study silicate scaling using quite qualitative approaches. For example, silicate scaling processes are often observed simply by using solution turbidity as a scaling measure. However, this approach only enables us to study the kinetics of silicate scaling in its early stages because of the colloidal solution it produces. In the previous work of Arensdorf et al. (2010), silicate scale severity was determined qualitatively by measuring the turbidity using a spectrophotometer while Sonne et al. (2012) carried out similar studies to test the severity of the silicate scales formed by enhancing the static testing method proposed by Arensdorf et al. Sonne et al. still measure the silicate scale formed qualitatively. In their work, they improve the experimental procedure by measuring the turbidity using an optical scanning device which is able to measure the light transmission at multiple locations.

Researchers have reported on the efficiency of a number of conventional scale inhibitors for inhibiting silicate scaling in industrial water systems, but to date none of them has fully solved the problem. Polymeric and non-polymeric (phosphonate) scale inhibitors that work by controlling the silicate formation either by crystal growth inhibition or crystal modification, failed to inhibit silicate scale, probably because the silicate scale is amorphous in nature. Amjad and Zuhl (2011) reported that carboxylic acid, sulfonic acid, and non-ionic groups present in the polymers exhibit poor interaction with silane groups present in silica with less than 20% efficiency. They claimed that potential candidates for silicate scale inhibitors must be able to disperse the silica-based deposit especially colloidal silica and magnesium silicate. In addition, they must also efficiently disperse any other scales that might act as nuclei for silicate precipitation, such as calcium carbonate and calcium sulfate.

The primary objectives of our silicate research are to develop an experimental bulk silicate scaling and inhibition method, and then to go on to use this to understand the mechanisms of silicate scale formation and its subsequent inhibition/dispersal. Silicate scale is very different from other types of scales (for example; barium sulfate scale which fully precipitates out from a scaling brine solution leaving a clear supernatant). Many researchers who study silicate scaling use more qualitative test methods in their attempts to evaluate the severity of the scale formed. Researchers such as Arensdorf et al. (2010) and Sonne et al. (2012) studied the extent of the silicate reaction using a measure of the turbidity. This solution turbidity was due to the amorphous nature of the silicate scale formed which produced different levels of cloudiness. However, in our study we have found that this method is not accurate; it is not reliable (or quantifiable) to measure the extent of the reaction based on the cloudiness of the brine at that particular time and, indeed, neither is it reproducible.

In spite of the considerable volume of research conducted to date, there is no comprehensive data available on silicate scale formation and its inhibition. There are no commercially available (or even research stage) silicate scale prediction models to help us in this task. Also, the effect of ferrous ion on the silicate scale formation and inhibition is not yet conclusive and carrying out experimental scaling studies with Fe^{2+} under anaerobic conditions is not well established.

1.3. AIMS AND OBJECTIVES OF THIS STUDY

The aim of this thesis is to improve our understanding of the conditions under which silicate scales form in oilfield systems, and what are the key parameters affecting the silicate scaling, such as solution pH, temperature (T), the presence of divalent ions (Mg^{2+}), the effect of Fe^{2+} etc. In order to carry out this study in a systematic manner, there was a need to establish an experimental methodology that enable us to ***quantify*** the severity of silicate scaling under various test conditions and to understand both the silicate formation and inhibition mechanisms for various types of potential silicate inhibitor. This thesis focuses on the mechanism of silicate scale formation under various test conditions and its inhibition. The following research objectives were established at the start of this study:

1) To develop more quantitative experimental methodologies to study both bulk silicate scaling and also silicate inhibition;
2) To understand the mechanisms of silicate scale formation and investigate several influencing factors affecting scaling conditions (in ASP flooding or in other systems);
3) To understand the mechanisms and the performance of various polymeric and other potential inhibitors in silicate scale inhibition;
4) To extend our experimental methodology to allow us to study the effect of ferrous ion on the silicate scaling system in a reducing environment (i.e. under anaerobic conditions);
5) To study the effect of ferrous ion on (i) the silicate scaling system; (ii) the performance of potential silicate inhibitor A5 in silicate inhibition.

1.4. RESEARCH OUTLINE

This study consists of the following areas of research:

Chapter 1 briefly reviews the basic problems with and the occurrence of silicate scale during ASP flooding and in other reservoir processes. It also considers the approaches to silicate scale control (mainly in industrial water system) which were current at the start of this work. The main objectives of the study as well as the thesis outline is also described here.

Chapter 2 review the occurrence and formation of silicate scaling in various areas in much more detail, particularly in ASP flooding, geothermal power plants and in industrial water systems. This includes a detailed discussion of the amorphous silica solubility, the kinetics and mechanisms of silicate scaling under various condition. The control of silicate scaling mainly in industrial water systems using scale inhibitors is also summarized here. The study approach of previous researchers towards silicate scale formation and inhibition is also described. Some discussion of the effect of ferrous ion on silicate scale formation and inhibition is also presented.

Chapter 3 explains the experimental methodology developed in this work which is subsequently used to study the silicate scaling formation. The novelty of this developed experimental method is also explained here. The reason behind the investigation of three "base cases" is also discussed in this chapter.

Chapter 4 presents the preliminary results of our study in our effort to develop a bulk (bottle) test for the first forming silicate scale in a reproducible manner. Many issues which arose due to the colloidal nature of the silicate scale produced are also discussed before a systematic approach was developed considering all these issues so that a satisfactory experimental methodology could be established. A sensitivity analysis was also conducted using this new methodology, so that effect of various parameters on silicate scaling could be evaluated, i.e. temperature (T), pH, brine ageing and the initial Si:Mg molar ratios were all evaluated. These results greatly improved our understanding of silicate scale formation and inhibition.

Chapter 5 addressed the matter of the high sensitivity of the silicate system to initial pH and how this issue was successfully resolved through the development of our very strict static inhibition efficiency test. This chapter also presents results on the performance of various potential silicate scale inhibitors for controlling the silicate deposits formed. The various silicate systems studied ranged from a "worst" base case to a "manageable" base case, using the potential polymeric silicate inhibitors VS-Co, H3 and A5.

Chapter 6 presents results which examine the effect of ferrous ion on silicate scale formation and inhibition under reducing conditions (i.e. in anaerobic conditions). This chapter explains the experimental methodology adopted in order to achieve the fully anaerobic conditions in a nitrogen glove box. Several results on the effect of Fe^{2+} on silicate formation and inhibition are presented.

Chapter 7 presents a summary and the overall conclusions from the above experimental Chapters 3, 4, 5 and 6. Recommendations for future research in the area of silicate scaling and its inhibition are also presented in this chapter.

All literature references are given at the end of this thesis along with a number of technical appendices.

CHAPTER 2. LITERATURE REVIEW

A detailed literature review surveying the work carried out by other researchers on silicate scaling relevant to this thesis is presented in this chapter. Topics reviewed include a discussion of silicate dissolution and deposition, the occurrence and kinetics of silica scaling, the experimental methodology for forming silicates and for testing silicate inhibitors/dispersants. The effects of ferrous ion on silicate scaling and on silicate inhibitor performance are also explored here.

2.1. OILFIELD SCALE

Oilfield scales has been recognized as a major problem in oil and gas production for many years. These mineral scales may block tubulars, damage downhole equipment and cause safety valves to block and fail. In addition, scaling may also occur in the reservoir formation where it may plug the pores and restrict the flow of reservoir fluid into the well.

Scale may typically form due to reduction in mineral solubility in produced formation waters as a result of changes during production i.e. changes in temperature T, pressure P, pH and CO_2/ H_2S partial pressures. At any point downstream from such changes, scale can form if supersaturation conditions occur. Common mineral scales that occur in oilfields include calcium carbonate, barium sulphate and iron sulphide. Work done by many researchers concluded that carbonate scale may form when there is changes in pressure and pH of the production fluid, whereas sulfate scale generally occur due to the mixing of incompatible brines i.e. formation water and injection water. However, a less well recognised group of scales are the silicate type deposits, e.g. amorphous silica, magnesium silicate etc.

2.2. ASP FLOODING

Enhanced Oil Recovery (EOR) techniques are being seriously considered for field application by virtually all the major multi-national and national oil companies (NOCs) due to the (relatively) high oil price and the reducing quantities of new oil reserves being discovered. A number of EOR projects are currently in progress worldwide including

CO_2 injection and Chemical EOR (CEOR). Due to the unavailability of CO_2 gas offshore in many regions, chemical EOR appears to be more widely applicable in many cases, considering its technically successful history in recovering additional oil from mature fields.

In particular, CEOR techniques such as polymer flooding, surfactant/polymer (SP) flooding and alkali/ surfactant/polymer (ASP) flooding are under active consideration and a number of companies are currently planning pilot and field wide floods using these methods. More than 30 ASP field pilots and large-scale applications worldwide have been carried out since 1994. These are mainly located in China, USA and Canada with more emerging in other parts of the world including India, Venezuela, and Malaysia. ASP flooding particularly aims to improve the water → oil microscopic displacement efficiency by reducing the interfacial tension (IFT) between the water and oil through the addition of synthetic surfactant to the water and through *in situ* generated surfactant from the alkali used. The polymer is added to match the oil and water mobility while the alkali is added to reduce adsorption of the high cost surfactant onto the rock and to control the local salinity to ensure the minimum IFT is obtained. The addition of alkali greatly improves the performance of surfactant and polymer causing earlier incremental oil production due to faster surfactant front propagation and quicker oil mobilization (Mayer et al., 1983; Hirasaki et al., 2011; Charest, 2013; Sheng, 2013; Sheng, 2014).

Singhal (2011) summarizes in his preliminary review of Innovative Energy Technologies Program (IETP) projects using polymers on the basic requirements of chemical flooding as being:

1) To propagate chemicals (polymers or surfactants) deep inside the reservoir
2) To overcome chemical adsorption or consumption, and
3) To improve sweep efficiency by reducing the interfacial tension between oil and water.

Sodium carbonate was used in 14 field cases, sodium hydroxide was used as the alkaline solution in seven cases, and NaOH and Na_2CO_3 were combined in one case (Sheng, 2014). Synergistic effects between alkali, surfactant and polymer have been observed in laboratory evaluations by Olsen et al. (1990). This has shown that post-waterflood oil recoveries up to 45.3% can be achieved when sodium bicarbonate or sodium carbonate is

used as compared to the conventional high pH chemicals that are typically used i.e. sodium hydroxide or sodium orthosilicate. Samanta et al. (2012) in their work proved the synergistic effect of ASP and they recommended a concentration range of 0.7 to 1.0 wt% alkali, 1,500 to 2,500 ppm polymer, and 0.2 wt% surfactant for successful ASP flooding, based on the experimental data and the relative cost of the various chemicals.

Work by Flaaten et al. (2008) showed that using a novel alkali such as metaborate can be used with hard brine at ~pH11 without the risk of carbonate scale precipitates forming i.e. which occurs since sodium carbonate is used in conventional ASP processes. This is due to metaborate being able to sequester divalent cations and achieve high performance and its ability to handle optimum salinity values of 120,000 ppm TDS with 6600ppm Mg^{2+} and Ca^{2+}.

Although all EOR processes are aimed at increasing the oil recovery through a range of mechanisms, all methods also have some downsides in terms of the problems which occur with them. Generally, these are either *in situ* problems in the reservoir (e.g. formation damage by polymers) or production problems which may occur at the producer well. Examples of production problems are as follows: (i) the CO_2 in gas injection may solubilise carbonate rocks leading to an increased scale deposition at the production well, (ii) demulsification problems can arise when surfactants are applied in SP flooding where the reservoir mechanism of oil mobilisation must be "undone" at the producer in order to release the recovered oil, (iii) where the high alkalinity in ASP flooding can lead to much more difficult carbonate scaling problems by increasing the saturation ratio (SR) of calcite, and (iv) when the alkali in ASP flooding may dissolve the silica in the rock to produce silicates at high pH (>10) which may deposits as pure amorphous silica and metal silicates at the producer well when the pH drops down to pH ~7 - 8 (Sheng (2013), Sheng (2014), Stoll et al. (2010)). It is this latter problem, the formation and prevention of silicate scaling, that is the primary focus of this thesis.

2.2.1 Alternative Alkalis in ASP Flooding

The addition of alkali in the ASP flooding produce negatively charged rock surfaces that generate repulsive forces with anionic surfactant hence surfactant retention is much reduced. Surfactant retention is also reduced because the anionic soap formed by alkali-oil reactions partly satisfies rock adsorption. Accordingly, minimizing surfactant

retention reduces the mass of surfactant required to recover the oil and thus the cost of recovery per barrel of incremental oil.

Alkalis such as sodium hydroxide, sodium carbonate and sodium orthosilicate are used instead of synthetic surfactant chemical packages due to their lower costs. The alkali can react with naphthenic acids in the oil to create *in situ* surfactants (or "soaps"), which then act in the same way as the surfactants which are injected directly. However, it is usually difficult to lower the interfacial tension to a sufficiently large degree with alkalis to significantly reduce the residual oil saturation. According to Khan et al. (2009) and Singhal (2011), there are numerous alkalis that are typically applied in ASP flooding including sodium hydroxide, sodium orthosilicate, ammonium hydroxide, potassium hydroxide, trisodium phosphaste, and sodium carbonate. The first two chemicals are commonly used when the overall cost and their effectiveness are taken into consideration.

Sodium metaborate was studied by many researchers as an alternative alkali due to its sequestering capability for divalent cations i.e. magnesium and calcium (Flaaten et al. 2008; Unomah, 2013). A serious limitation of the use of sodium silicate as an alkaline agent was observed in cores containing gypsum and anhydrite due to increased alkali consumption. In addition to that, the high alkalinity of sodium silicate caused precipitation of divalent ions in the brine and unloaded ions from ion exchange with the clay to form highly insoluble silicates.

However, the alkali also reacts with the minerals in the rock such as clay minerals and consumption of the alkali is one of the complicating features of the ASP process. Silicate scales and reduced injectivity have been the biggest factors contributing to the lower production in ASP flooding in Alberta. The associated silicate scale problems require very frequent well servicing. Silicate scaling problems have been widely reported in the Daqing field, China due to the application of ASP technology and in fields in Alberta, Canada, mainly due to the application of thermal methods.

2.3. THE OCCURRENCE OF SILICATE SCALING

Silicate scale is a well-known problem associated not only with ASP Flooding but also in the water industry and in the management of geothermal wells. When high pH ASP water co-mingles with the low pH formation water (and connate water) this may produce silicate

scale especially around the well where it can cause serious production problems. Silicate precipitates tends to be very complex chemically due to their dependence on the degree of silicate ion polymerization, which is a function of pH and the concentrations of the various silicate species. A laboratory study carried out by Gill (1998) examined a number of important aspects of silica scaling. Silicate scaling not only depends on the saturation level with respect to the mineral but also on a range of other processes, such as degree of silicate polymerization, colloidal silica suspension, precipitation of silicate minerals, biological activity such as diatoms, and co precipitation of silica. All of these factors have a profound effect on silica deposition and the concurrent participation of several of these processes makes the control of silicate deposition much more challenging.

The solubility of silicates varies considerably with pH and with the type and concentration of multivalent cations present. Most commonly, the precipitates and scales are salts of magnesium and calcium. Krumrine et al. (1985) reported that if carbonate scale exists, the silicates will also build to form a mixed scale. Later work by Gill (1998) also concluded that calcium carbonate can aggravate the silicate scale formation by providing nuclei for the development of silicate scale.

In this work, we will focus on the silicate problem which may arise in ASP flooding although silicates can also be observed in other oil recovery processes such as in thermal flooding and even in more conventional waterflooded reservoirs. For example, two production systems operated by Talisman in the North Sea were reported as having deposits of silicate scale incorporating both magnesium and iron.

2.3.1 Silicate Scaling in ASP Flooding

ASP flooding has been applied in the field with considerable technical success e.g. in the Daqing Field, China. ASP is also being actively evaluated for application in a number of oilfields worldwide. However, the high pH of the ASP solution, which is essential for efficient incremental oil recovery, can create significant production problems. The high pH fluid can dissolve silica from the rock formation i.e. rocks which may contain feldspar, illite, kaolinite and montmorillonite. This silica rich brine may later co-mingle with low pH formation water in the reservoir to produce silicate scale. This process tends to occur close to producers where it causes silicate deposition in the wells although the process can actually occur anywhere from the deep reservoir to the surface pipe network, as

described by Jing et al. (2013). According to Ahmed and Elraies (2014) silicate scaling issues are prevalent and have interrupted the smooth operations associated with the ASP flooding processes in many parts of the world, including in the western United States, Alberta, Hawaii, China, Puerto Rico, Mexico, the Middle East and Southeast Asia.

Krumrine et al. (1985) reported on scaling problems which were observed in the Long Beach Unit, Wilmington, California alkaline pilot plant. This pilot plant experienced scales made up variously of calcium carbonate, magnesium silicate and amorphous silica. The cause of these problems appeared to be the mixing of very hard waters from one subzone with moderately alkaline water from the other subzone, which eventually produced scale in the producers closest to the injectors. The silicate precipitates observed by Krumrine et al. were highly hydrated and amorphous in nature and they had a slimy texture. They did not readily adhere to or develop at metal surfaces, but instead adsorbed onto calcite (carbonate scale) and oxide surfaces.

Hou et al. (2005) reported that pump-sticking was observed in most wells in the pilot area of ASP flooding in the Daqing Oilfield due to the occurrence of alkali scales. This led to the use of electric submersible pumps (ESPs) or screw pumps and sucker rod pumps were used alternately, though their working lives were all very short before malfunction occurred.

Li et al. (2009) studied the characteristics of the formation of silicate scales and how this scaling impacts sucker rod pumps during ASP flooding. Li et al. found that the scales formed in the Daqing Oilfield did not have a single composition. They consisted of silica scale, carbonate scale and organic impurities. In their study, the silica exists in these deposits as silicate or SiO_2, Ca^{2+} and Mg^{2+} existed as carbonate while Fe occurred as its oxide or sulphide or carbonate. They also concluded that the presence of Ca^{2+}, Mg^{2+}, Al^{3+}, hydrolyzed polyacrylamide (HPAM) polymer, and surfactant increases the silicate scaling tendency and rate of silicate scale formation.

The occurrence of amorphous silica scale at production wells has been reported by Cenovus Energy (2009) in *Suffield Upper Mannville UU Commercial ASP Flood (1249B) project*. Increasing pH due to injection of alkali plays a role in the deposition of both calcium carbonate and also these amorphous silica based scales; in these wells, the sucker rods had to be pulled every six to nine months (if scale coupons show positive) and any existing scale had to be mechanically removed. It was reported that the silicate scale was

first observed when the pH increased to values in the range pH ~ 8.3 to 9 before the scale is aggravated by calcium and magnesium that acted as a 'glue' to bridge colloidal silica.

Husky Oil Operations Limited (2010) reported that silicate scale and the resulting reduced injectivity have been the biggest factors contributing to the lower production in *Taber S Mannville B Commercial ASP Flood (10418B)* project. Significant periods of downtime were reported for the wells, and that offsetting injection had to be shut-in to service most of them. They reported that scale became evident when the pH of the produced water was between 9 and 11. Outside this range, scales were not deposited in the well equipment.

The Fourth Plant of Daqing oilfield also experienced a serious foul water problem as a result of ASP Flooding. Jing et al. (2013) reported that the produced silicon weight from the formation accounted for 0.55 in 10000 of the total reservoir rock weight. In their work, the effect of aluminosilicate ion concentration, the influence of aluminosilicate ion ratio, the presence of calcium and magnesium ions, the temperature and the pressure on the silicate scale were investigated. This work concluded that the higher the concentration of aluminosilica ions in solution before reaction, the more severe the silicate scaling was. When the concentration of Si ion to Al ions were kept constant at 3:1 ratio, the produced water was most likely to scale followed by the formation water and the injection water. It was observed that the silicate scale started to form when the concentration of silicon ions was about 310mg/L.

2.3.2 Silicate Scaling in Geothermal Power Plants

Geothermal activity is a phenomenon that is closely associated with active volcanoes where heat transfer by convection instead of conduction will be possible when a sufficient amount of water is available to set up a hydrothermal convective system. High quality steam generated from this hot geothermal fluid due to pressure drop (accompanied with lowering in boiling point) can be utilised to generate electricity in a geothermal power plant and the still very hot pressurised separated water can be used to heat up cold water for district heating and domestic use; this total process is known as combined heat and power (CHP) plant.

A typical well or borehole in high temperature geothermal fields in Icelandic is generally between 2km to 3km deep, where the temperature of the geothermal fluid brought up

from such conventional boreholes can be up to 360°C. Nevertheless, the benefit of the exploitation of this geothermal fluid can be hindered by amorphous silica scale formation, as reported by many researchers (Ellis and Mahon, 1977; Stefánsson et al., 2011; Björke et al., 2012). Mineral precipitation is an inevitable problem in the exploitation of geothermal energy. According to Brown (2011), typical compounds that are found in geothermal operations are silica (SiO_2) and calcium carbonate ($CaCO_3$) except for a few isolated cases. According to Kristmanndóttir et al. (1989), the magnesium silicate formed in the Icelandic district heating systems is confirmed to be amorphous based on X-ray diffraction (XRD) analysis. Its structure is apparently similar to chrysotile ($Mg_3Si_2O_5(OH)_4$) with the Mg:Si ratio is close to 1 with small variations.

According to Gunnarsson and Arnórsson (2003, 2005) the silica deposits once caused operational problems and may even clog pipelines and injection drillholes in Nesjavellir geothermal power station, Iceland. Amorphous silica scale formation in wells, separators, pipes and heat exchangers at the Mutnovskoe Hydrothermal Field, Russia is a problem which makes the wide usage of geothermal resources difficult (Kashpura and Potapov, 2000). Chernev et al. (2015) identified the technogenic precipitation in the structures of Mutnovsky Geothermal Power Complex as being due to two types of precipitations; (i) first type of deposits consist of sulfide (troilite, marcasite, pyrite) border on the outer layer of SiO_2 into pipe wall and (ii) the second type of deposits with a large range minerals. Among diagnosed ore minerals which occurred were pyrite, troilite, chalcopyrite, sphalerite, oxides and hydroxides of iron and of nonmetallic - minerals, and silica compounds, carbonates, adularia. These included different forms of silica from amorphous (opal - chalcedony), crystalline (quartz) to spherical silica nanoparticles and possibly pure silicon.

Park et al. (2006) observed minerals that precipitated near the injection well at Coso Injection Well, California which included amorphous silica and small amounts of calcite. These mineral precipitates occurred in many parts of the operation including turbines, pipelines and injection wells, and cleaning was reported to be a costly operation (Henley, 1983). McLin et al. (2006) confirmed that the precipitate formed at Coso was due to deposits of amorphous silica associated with traces of calcite. These in the reservoir rocks adjacent to the original injection well 68-20 which had experienced a significant loss in injectivity over a period of 7 years. McLin et al. (2006) also confirmed that at Salton Sea, scale deposited in the reservoir rocks mainly consisted of alternating layers of barite and

fluorite with minor quantities of anhydrite, copper arsenic sulfides and amorphous silica was also present.

Gunnarsson, and Arnórsson (2005) suggested that a solution to the silicate scaling problem was to prevent the water from becoming oversaturated with respect to amorphous silica by carefully controlling the temperature and the pressure of the water. It is also reported that the amount of silica that precipitated out of geothermal waste water in Iceland amounts to over 40,000 tonnes annually. This precipitated silica was in itself a valuable product that is heavily used in a wide variety of industries.

2.3.3 Silicate Scaling in Industrial Water System

According to Iler (1979) silica dissolution and deposition occurs in a wide variety of environmental and industrial processes including ceramic and catalytic applications, water heater scaling, biomineralization, coating applications to improve adhesion and wetting properties, reverse osmosis, paper mills and so forth, making silica scaling (in industrial systems) a much-studied subject.

Silica and magnesium silicate present a difficult challenge for industrial water systems because they can cause catastrophic operational failures in process water systems due to deposit formation (Demadis et al., 2007). Silica-silicate scaling may form in various industrial water system including brackish water reverse osmosis processes (Darton, 1999), evaporative cooling water systems and water boiler and geothermal water systems (Amjad et al., 1997). Demadis and Neofotistou (2004) also claimed that silica scale is very difficult to manage. They claimed that developing a successful inhibition program is almost impossible using conventional scale inhibitors, e.g. phosphonate failed to prevent silicate scales from forming. In addition, the cleaning process is a difficult to carry out as it requires hazardous chemicals as well as operational shut-downs.

Scale is observed when the dissolved silica level in re-circulating water or a reverse osmosis system reject stream exceeds the amorphous silica solubility limit (~100 mg/L at ambient temperature) while silica-scale formation typically occurs when brine is cooled during brine handling and energy extraction in geothermal systems.

2.4. AMORPHOUS SILICA SOLUBILITY

The solubility of amorphous silica is a very important parameter to understand the precipitate that may formed under specific condition. Brown (2013) defined *silica saturation index (SSI)* as the ratio of the silica concentration in the brine divided by the equilibrium amorphous silica solubility at the conditions prevailing. Silica scaling is possible when SSI >1.0 whereas the silica scaling may not generally occur when SSI <1.0. It is impossible to review all silicate solubility data across a range of highly specialized fields since many studies have appeared (although insufficient data available for systems at elevated temperature, pH and in solutions containing multi-component salts).

The solubility of amorphous silica, in ppm (mg/kg) in salt-free neutral water solution at vapor pressure of the solution from 0° to 250°C, was determined by Fournier and Rowe (1977) and plotted in Figure 2-1;

$$\log C_e = - 731/T + 4.52, \text{ T in K} \quad \textbf{2.1}$$

At a constant high pressure of 1000atm, from 0 to 380°C, the amorphous silica solubility was found to be approximately a linear function of pressure in the range from 200 to 265°C (Figure 2-2). Generally, the pressure effect is less significant than the temperature effect.

$$\log C_e = - 810/T + 4.82, \text{ T in K} \quad \textbf{2.2}$$

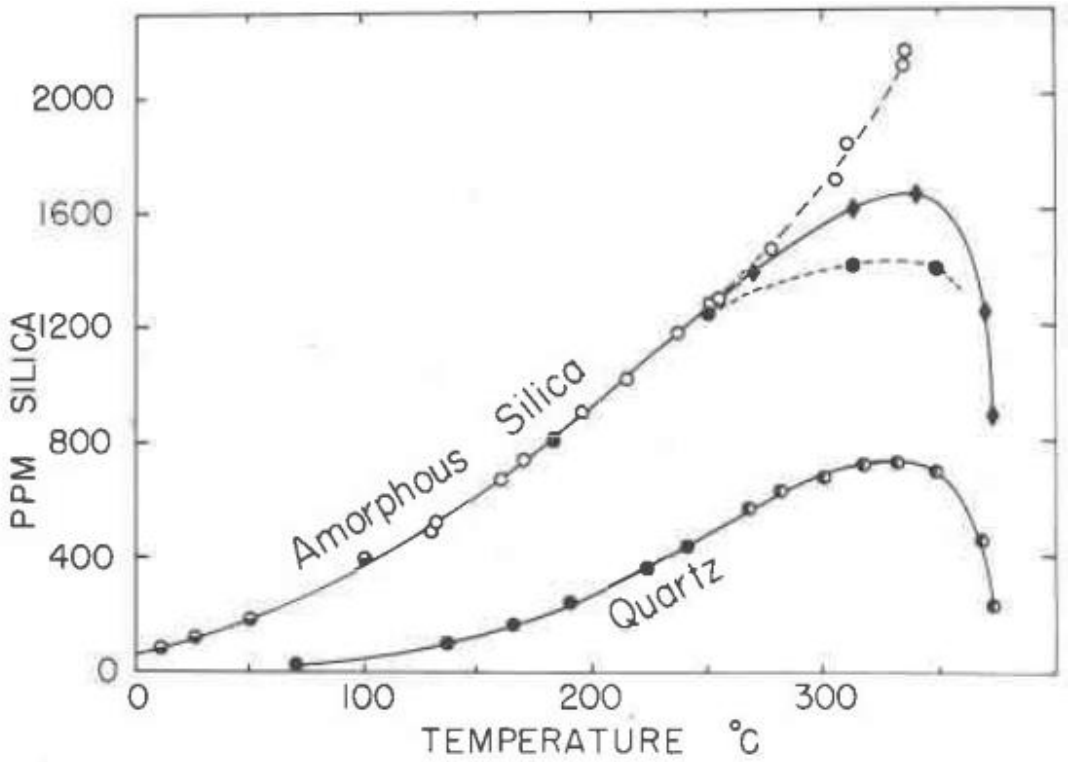

Figure 2-1 Solubility in water of amorphous silica relative to quartz at the vapour pressure of the solution (Fournier and Rowe, 1977).

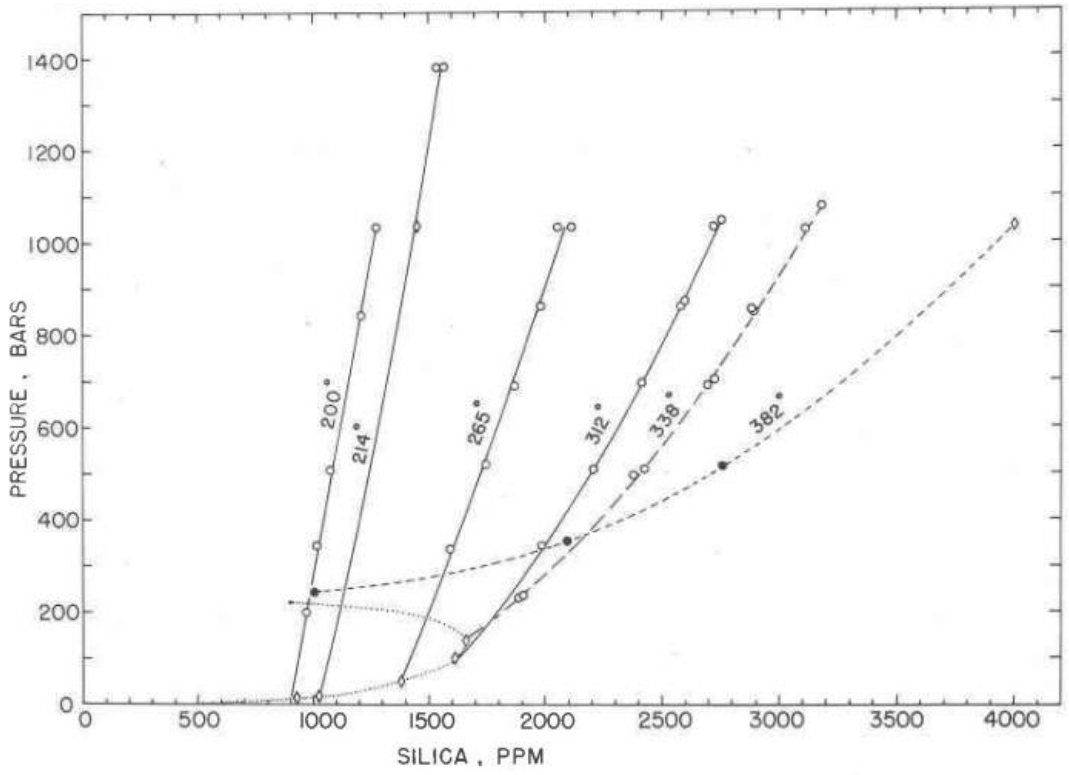

Figure 2-2 The solubility of amorphous silica (colorimetrically-reactive silica in solution) at various constant temperatures and variable pressure (Fournier and Rowe, 1977).

Marshall (1980) studied the solubility of amorphous silica as a function of temperature in neutral pure water at elevated temperatures (25^{o}C to 300^{o}C) and at the corresponding saturation pressures while Willey (1974) reported the effect of pressure on the solubility of amorphous silica in seawater at 0°C from 1 to 1200 atm. Other studies on the solubility of amorphous silica are listed in Table 2-1.

Table 2-1 Solubility of amorphous silica in aqueous solution (Chan, 1989)

SOLUBILITY OF AMORPHOUS SILICA IN AQUEOUS SOLUTION			
Researcher (Year)	Parameter study	Scope of study	Findings
Fournier and Rowe (1977)	***Temperature*** in neutral pure water at elevated temperatures and at the correspondin g saturation pressures	Amorphous silica solubilities along the liquid-vapor curve from 180 to 382°C and 200 to 1379bars (20Mpa to 157.9Mpa)	The solubility of amorphous silica, in ppm (mg/kg) in salt-free neutral water solution at vapor pressure of the solution from 0° to 250°C, was expressed by; **$\log C_e = -731/T + 4.52$**, T in K At a constant high pressure of 1000atm, from 0 to 380°C **$\log C_e = -810/T + 4.82$**, T in K C_e is amorphous silica solubility at equilibrium
Fournier and Rowe (1977)	high ***pressure***	From 200 to 1379 bars (20 Mpa to 157.9 Mpa) from 200 to 265°C	The amorphous silica solubility to be approximately a linear function of pressure in the range from 200 to 265°C (Figure 2-2). Generally, the pressure effect is less significant than the temperature effect.
Marshall (1980)	***Temperature*** in neutral pure water at elevated temperatures and at the correspondin g saturation pressures	298 and 573 K (25^{o}C to 300^{o}C)	**$\log M = -0.1185 - 1.1260 \times 10^3/T + 2.3305 \times 10^5/T^2 - 3.6784 \times 10^7/T^3$** where T is temperature in K ***M*** is molar solubilities of silica in water
Willey (1974)	***Pressure***	In seawater at 0°C from 1 to 1200atm	Solubility increased from 65 to 71ppm when pressure was increased from 1 to 150atm and then increased linearly to 94ppm at 1200atm.
Alexander et al. (1954)	***pH***	pH1 to 10.2 at 25^{o}C	Increasing solubility of amorphous silica with increasing pH. The solubility of silica in these systems was relatively constant;

			pH**2.1** to **2.7:** the solubilitv of monomeric silica from polymerized polysilicic acid is approximately **0.010%** SiO_2; pH***5*** to **8: 0.012-0.014%** **pH>9**: solubility of silica increases at high pH because of the formation of silicate (dissolved monomeric silica) ion in addition to $Si(OH)_4$, in solution
Jørgensen (1968)	***Salinity***		77 ppm at 25° C in 1.0M $NaClO_4$ solution, much smaller than 100-120 ppm in neutral water without salt.
Jephcott and Johnston (1950)	***Salinity***		Solubility was reduced significantly when aluminum was added or was present.
Marshall (1980)	***Salinity***	In aqueous sodium nitrate solutions 25° to 300°C	The solubility of amorphous silica in aqueous sodium nitrate solutions up to 6 molal
Marshall and Warakomski (1980)	***Salinity***	25°C in aqueous salt solutions (containing any of these salts): LiCl, NaCl, KCl, MgCl, CaCl, LiNO, $LiNO_3$, $NaNO_3$, $MgSO_4$, and Na_2SO_4.	*about the same result as Chan et al. (1987a, b)
Chan et. al. (1987a)	***Salinity*** Effect of ***cation***	Eleven salts: NaCl, NaBr, NaI, LiCl, KCl, $NaNO_3$, NaAc, Na_2SO_4, $MgCl_2$, $CaCl_2$ and $SrCI_2$ between 25 to 70°C	Amorphous silica solubility can be well correlated by hydration number of salts At a given dissolved salt concentration and 25°C, $\boldsymbol{C_{es}/C_e = 1 - 3.46\ n_i}$ Where; C_{es} = molal solubility in salt C_e = molal solubility salt-free water; n_i is the hydration number of cation i.

			the decreasing effect of cation on amorphous silica solubility: Mg^{2+} > Ca^{2+} > Sr^{2+} > Li^{+}> Na^{+} > K^{+}
Chan et. al. (l987b)	***Salinity*** effects Effect of ***anion***	The presence of sodium halide salts (NaCI, NaI, and NaBr)	I^{-} > Br^{-} > Cl^{-}
Chen and Marshall (1982)	***Salinity*** effects	In separate aqueous solutions of NaCl, Na_2SO_4, MgCl and $MgSO_4$ over the range of 100-300°C at various salt molalities.	Amorphous silica solubility data in NaCl, Na_2SO_4, $MgC1_2$, $MgSO_4$, $NaNO_3$, KCI, KNO_3, LiCl and $LiNO_3$ from 25 to 300 ° C could be fitted to the *Setchenow equation* (with a maximum average deviation of 17%), *Setchenow equation*: **$\log (C_e/C_{es}) = D\ m$;** m is the molality of added salt and D is the Setchenow parameter solubility in multicomponent electrolyte solutions be estimated from the solubilities in single salt solutions **$\log (C_e/C_{e,mix}) = \sim m_i D_i$;** where $C_{e,mix}$ is the molal solubility in a mixed electrolyte solution, and D_i and m_i are the D parameter and molality, respectively, of an individual electrolyte i.

2.4.1 pH Dependence of Silica Solubility

Brown (2013) discussed the effect of pH on amorphous silica solubility where the hydrogen atom can dissociate so silicic acid (also known as aqueous silica or dissolved silica) which is a weak acid according to:

H_4SiO_4 (or $Si(OH)_4$) $\leftrightarrow H^+ + H_3SiO_4^-$

Log K_1 (the first dissociation constant) for this reaction is given by:

$$\text{Log } K_1 = -2549/T - 15.36 \times 10^{-6} T^2 \quad (T = \text{abs K}) \qquad \textbf{2.3}$$

If the effects of the second order ionisation are neglected, and it is assumed that the solubility of silica is due entirely to the reaction:

$SiO_2 + 2H_2O \leftrightarrow H_4SiO_4$

Then the solubility of amorphous silica, S as a function of pH can be derived as:

$$S = C_e [1 + \{10pH * K_1 / \gamma(H_3SiO_4^-)\}] \qquad \textbf{2.4}$$

where C_e = Solubility in mg/kg from Equation 1

K_1 = Dissociation constant in equation 2.3

$\gamma(H_3SiO_4^-)$ = Activity coefficient of $H_3SiO_4^-$

The activity coefficient $\gamma(H_3SiO_4^-)$ is calculated from the extended Debye Huckel equation and the ionic strength of the solution which tabulated in following Table 2-2.

Table 2-2 Mean activity coefficient $\gamma(H_3SiO_4^-)$ (Fleming and Crerar, 1982)

Table 1. Mean activity coefficient $\gamma_\pm$ calculated from equations 3 and 9 for saturated solutions in equilibrium with quartz or amorphous silica.*

t(°C)	pH = 7		pH = 8		pH = 9		pH = 10		pH = 11		pH = 12	
	Quartz	Amorphous	Quartz	Amorphous	Quartz	Amorphous	Quartz	Amorphous	Quartz	Amorphous	Quartz	Amorphous
0	0·9993	0·9984	0·9989	0·9962	0·9978	0·9893	0·9942	0·9677	0·9831	0·9041	0·9491	0·7485
25	0·9990	0·9971	0·9978	0·9919	0·9940	0·9757	0·9821	0·9267	0·9459	0·7965	0·8449	0·6125
50	0·9982	0·9950	0·9952	0·9851	0·9857	0·9547	0·9565	0·8669	0·8723	0·6761	0·6888	0·5996
75	0·9969	0·9921	0·9907	0·9759	0·9715	0·9267	0·9138	0·7933	0·7646	0·5868	0·5754	0·4715
100	0·9949	0·9886	0·9841	0·9645	0·9506	0·8928	0·8541	0·7142	0·6480	0·5387	0·5376	
125	0·9920	0·9843	0·9750	0·9513	0·9232	0·8550	0·7820	0·6381	0·5532	0·5023	0·4463	
150	0·9886	0·9798	0·9643	0·9375	0·8916	0·8163	0·7056	0·5704	0·4868	0·4386		
175	0·9849	0·9755	0·9530	0·9242	0·8584	0·7795	0·6322	0·5113	0·4325			
200	0·9814	0·9717	0·9420	0·9126	0·8264	0·7471	0·5656	0·4580	0·3721			
225	0·9782	0·9687	0·9323	0·9035	0·7982	0·7205	0·5056	0·4071	0·2936			
250	0·9758	0·9668	0·9247	0·8972	0·7750	0·7006	0·4505	0·3563				
275	0·9741	0·9658	0·9193	0·8939	0·7576	0·6874	0·3985	0·3043				
300	0·9732	0·9658	0·9163	0·8934	0·7463	0·6812	0·3492	0·2516				

*Total ionic strength $I \leqslant 0{\cdot}01$ M except in the boxed-in area on the right; for $I \leqslant 0{\cdot}01$ M the Debye – Huckel theory matches the tabulated values to better than ± 0·4%.

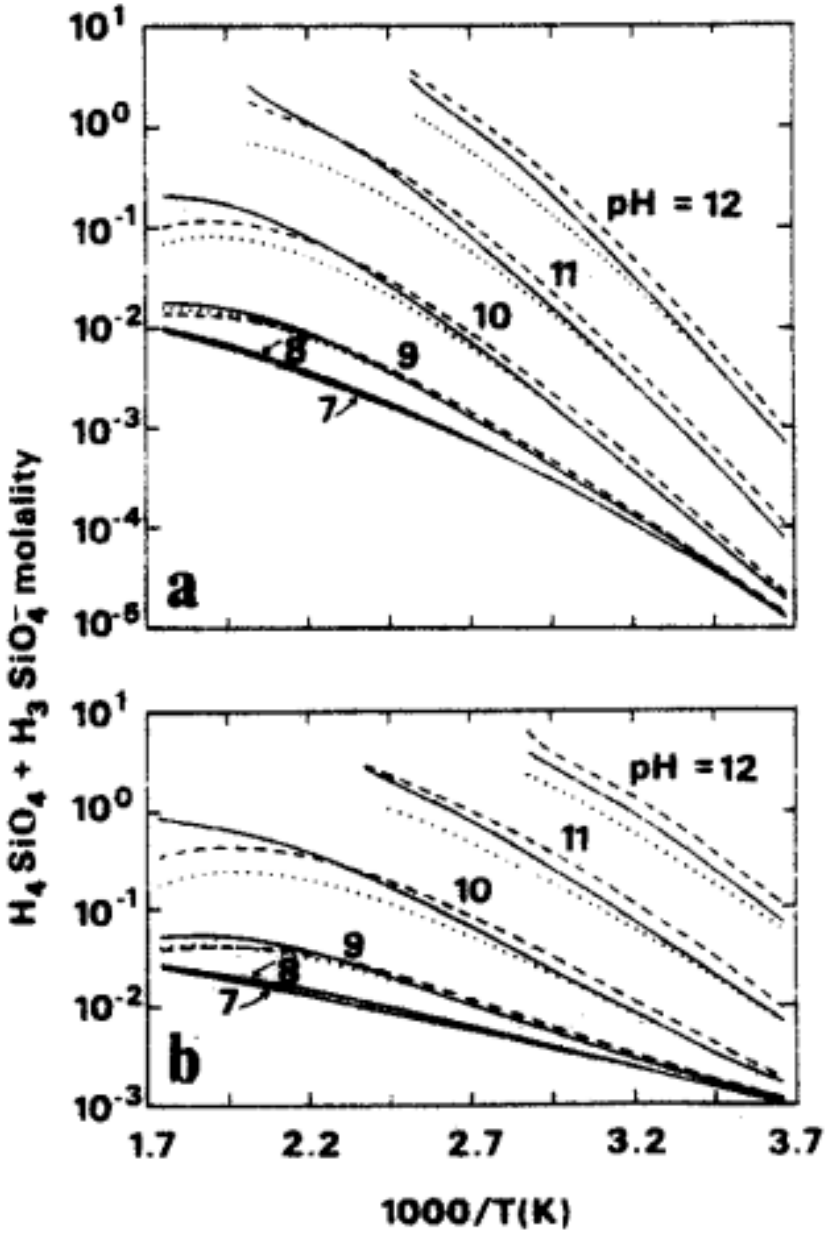

Figure 2-3 Solubility of (a) α-Quartz and (b) amorphous silica as a function of temperature at various pH (Fleming and Crerar, 1982).

2.4.2 Behaviour in Aqueous Sodium Chloride, Sodium Sulfate, Magnesium Chloride, and Magnesium Sulfate Solutions up to 350°C

Chen and Marshall (1982) investigated the solubility of amorphous silica in various aqueous solutions of sodium chloride, sodium sulfate, magnesium chloride and magnesium sulfate. Amorphous silica solubilities were most depressed by magnesium chloride, followed by magnesium sulfate and less by sodium chloride.

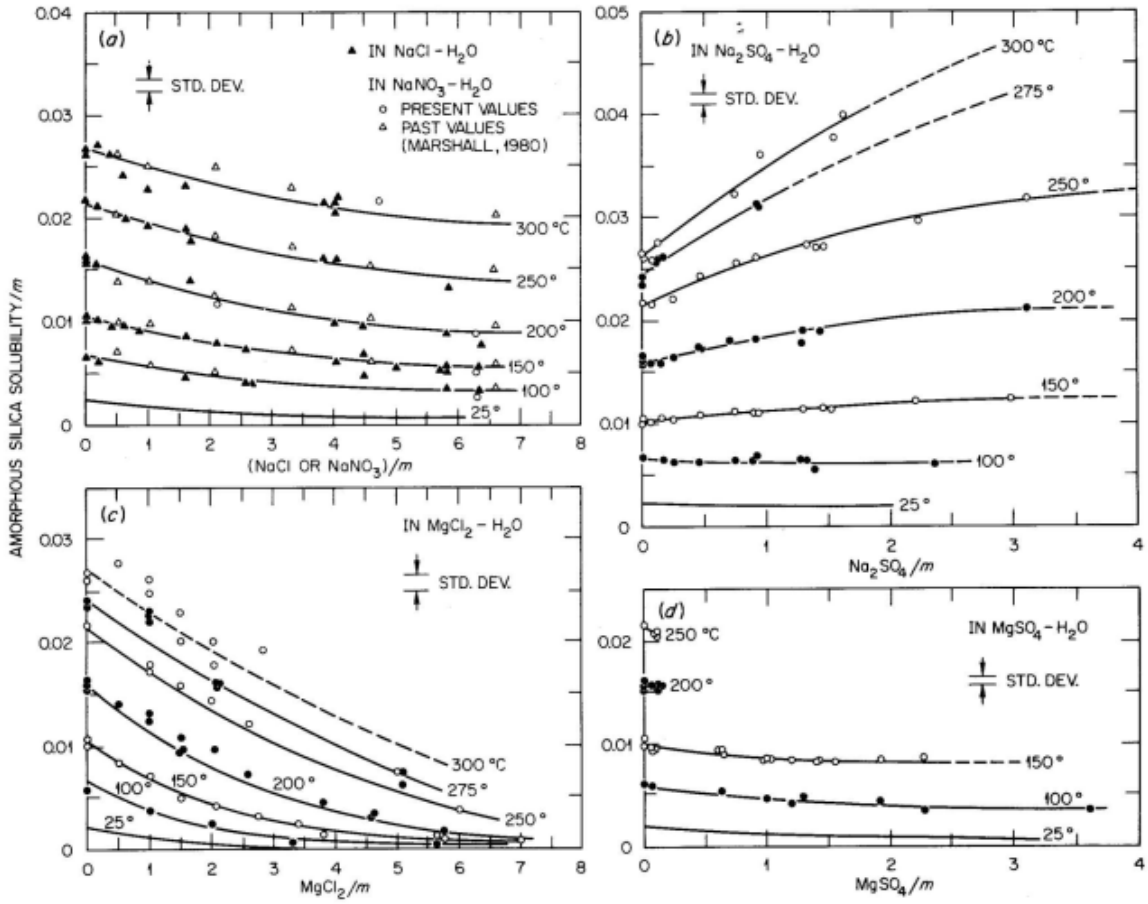

FIG. 3. The molal solubility of amorphous silica in aqueous NaCl, Na_2SO_4, $MgCl_2$, and $MgSO_4$ solutions, 25–300°C.

Figure 2-4 The molal solubility of amorphous silica in aqueous NaCl, Na_2SO_4, $MgCl_2$ and $MgSO_4$ solutions, 25-300°C (Chen and Marshall, 1982).

2.5. KINETICS OF SILICATE SCALING

Many reports have appeared in the literature on the complexity of the reactions involved in the silicate scaling process, making this scaling problem very difficult to solve (Meyers, 1999; Ning, 2002; Meyers, 2004; Icopini et al., 2005; Umar and Saaid 2013). The kinetics of silicate scaling reactions are not completely understood as compared to the thermodynamics (since the thermodynamics essentially represent the worst possible case). These kinetic reactions include the formation of amorphous silica via silica polymerization, colloidal silica suspension, precipitation of metal silicates, and co-precipitation of silica with mineral salts (e.g., calcium carbonate, calcium sulfate etc.).

Silica and silicate scale formation during ASP flooding is a complex process which proceeds in 4 stages as follows (i) silica dissolution, (ii) silica polymerization, (iii) silica-silicate scale formation and (iv) co-precipitation of silicate scale with other minerals (Meyers, 1999; Ning, 2002; Demadis, 2003; Icopini et al., 2005; Brown, 2011). These processes are described in turn below:

(i) ***Silica Dissolution***

Silica, SiO_2 (formation rock) dissolves slightly in water to produce silicic acid – $Si(OH)_4$. In this dissolution stage, the high pH (typically pH ~ 11) ASP water dissolves quartz in the rock formation forming silicic acid that later ionized to dissolved monomeric silica $H_3SiO_4^-$ or the silicate anion, SiO_3^{2-} (also known as monosilicate ion or silicate ion). The monomeric silica species will remain stable in solution at this high pH water.

Hydrolysis or dissolution of solid silica is expressed by Dowas et al. (1976):

$$x(SiO_2) + 2H_2O \leftrightarrow (x - l)(SiO_2) + Si(OH)_4$$

The **ionization** of silicic acid (Fleming and Crerar, 1982) is commonly expressed:

$$(A)\ H_4SiO_4 \leftrightarrow H_3SiO_4^- + H^+$$

However, Meyers (1999) reported that the ionization of silicic acid at neutral pH, depends on the concentration of hydrogen ions. K_1 for silicic acid is

known being very low, hence very little silicic acid can ionize when H^+ is present.

Lindsay (1972) reported that the uncharged silicic acid, $H_4SiO_4^o$ is the dominant species of Si below pH 8 while Said (1997) noted that monomeric silica, $H_3SiO_4^-$ represents only 0.19% of the total solubility of the pure silica, SiO_2 at pH 7.

The abundance of dissolved monomeric silica when high pH ASP solution present explained that the silicic acid starts to ionize in the highly alkaline condition and the hydroxyl ion catalysed the polymerization reaction; hence, below expression is more accurate to represent the ionization of silicic acid:

An alternative neutralization reaction is as follows:

(B) $H_4SiO_4 + OH^- = H_3SiO_4^- + H_2O$,

(ii) ***Silica Polymerization***

ASP water travel through the formation to the near (producer) well bore region. As it does so it co-mingles with the connate water that is at approximately neutral pH and the pH of the mixture will be lowered. It is known that solubility of monomeric silica decreases significantly at pH values below pH ~ 10.5. Under these lowered pH (supersaturated) conditions, the dissolved monomeric silica begins to polymerize and colloidal silica nanoparticles start to form.

Silica polymerization had been studied in detailed by many researchers (Alexander, 1954; Baumann, 1959; Kitahara, 1960; Bishop and Baer, 1972; Rothbaum and Wilson, 1977; Rothbaum and Rohde, 1979; Iler, 1979; Weres et al., 1979, 1980, 1981).

As pH increases, the solubility of the silicate ion also increases. Chan (1989) concluded that polymerization is at a maximum over the pH range $6 < pH < 9$, and will continue to polymerize until the silicate ion concentration falls to the solubility of amorphous silica (i.e. SiO_2).

According to Bishop and Baer (1972), the simplest condensation reaction to form a neutral dimer is likely to proceed as follows:

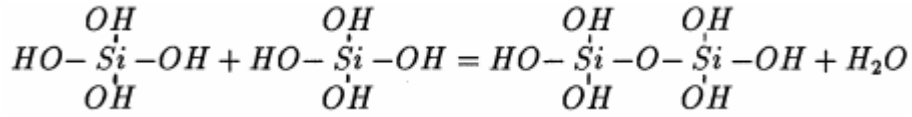

Silinol groups (-OH) between two monomers may form the Si-O-Si bonding into dimers ($H_6Si_2O_7$). This is the initial step towards the formation of higher molecular weight polymers. The silicate ion readily polymerizes by dehydration reaction (by loss of H_2O molecule) that may build up to *dimer - $Si_2O(OH)_6$, trimer - $Si_3O_2(OH)_8$, tetramer - $Si_4O_3(OH)_{10}$* silica and so on.

(iii) Silica-Silicate Scale Formation

Polymeric silicates can also form cyclic oligomer (instead of forming long chain open structure - pyroxene) by link the chain and eliminate the oxide where the most common cyclic polysilicates are the *cyclic trimers, $(SiO_3)_3^{6-}$* and the *cyclic hexamers $(SiO_3)_6^{12-}$* .

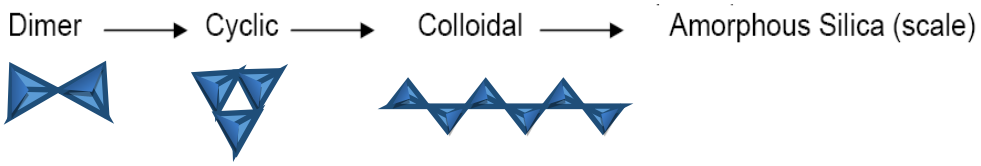

The polymerized silicate may continue to grow and form a “pure” amorphous silica scale if there are no divalent cations present.

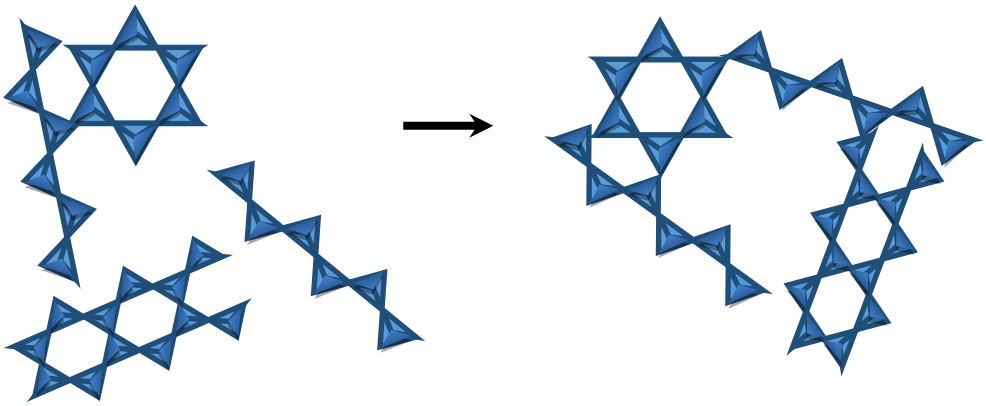

However, the presence of divalent cations (such as Mg^{2+}) in the solution can affect the precipitation reaction. Meyers (1999) reported that solubility decreases with pH when divalent cations were present.

The magnesium ion that presents in the connate/ formation water may bridges the colloidal silicate particles to form amorphous magnesium silicate scale. As the solution pH increases (especially at pH > 9), magnesium silicate scale is very likely to form because silica forms reactive silicate ions.

Below pH 7, magnesium silicate does not occur because silica is present essentially in an un-ionized form. Demadis (2010) reported that at pH less than 8, magnesium silicate is rarely observed in the deposit.

From colloidal form → silica scale formation as Mg^{2+} poly-silicates form and precipitate (also Fe, Al, Ca but Mg worst).

+ Mg^{2+} → Ppt. of Mg silicates

(iv) Co-Precipitation of Silicate Scale with Other Minerals

Possible Co-Precipitation with $CaCO_3$

The presence of calcium ions in the connate water will also promote the formation of calcium carbonate scale which may additionally provide the nuclei for the development of silicate scales

Depends on => pH, M^{2+}/M^{3+}, Ca/Mg ratio → various silicates form

Table 2-3 Summary of reported experimentally derived kinetic models for the decrease in monosilicic acid during the process of silica polymerisation (Tobbler, 2008)

Study	pH	T (°C)	SiO_2 (ppm)	max. reaction time (h)	[1]Reaction order, n
Alexander (1954)	1 - 6	1.9	6000	170	3 for pH<3.2 2 for pH>3.2
Goto (1956), Okamoto et al. (1957)	7-10	22.3	200 - 900	144	3
Baumann (1959)	0.5 - 9	30	400 - 4000	7	1 to 5
Kitahara (1960)	3 - 10	0 - 100	500 - 800	5	2 for pH<7.5 3 for pH>7.5
Bishop and Bear (1972)	8.5	25 - 45	300	200	2
Rothbaum and Wilson (1977)	7.8 - 8.7	50 - 120	500 - 1000	1000	5 to 8
Rothbaum and Rhode (1979)	7-8	5 - 180	300 - 1300	1200	4
Markrides et al. (1977, 1980)	4.5 - 6.5	75 - 105	700 - 1200	22	[3]0
[2]Peck and Axtmann (1979)	4.5 - 8.5	25 - 95	400 - 1000	-	1
[4,5]Weres et al. (1981)	2.5 - 8	50 - 100	500 - 1200	1.5	1 for $S>S_t$ 5 for $S<S_t$
Crerar et al. (1981)	7	25	1000	22	1
Icopini et al. (2005), Conrad et al. (2007)	3 - 11	25	250 - 1250	3000	4

[1]Reported rate laws were derived via the equation $-dC / dt \sim k(C-C_s)^n$ following the method described by Goto (1956).
[2]Peck and Axtmann (1979) analysed experiments reported by Makrides et al. (1980) and Rothbaum and Wilson (1977).
[3]Makrides (1977, 1980) postulated that particle growth preceeding the induction and nucleation phase was linear with time.
[4]Weres et al. (1981) used the same model as proposed by Makrides et al. (1977, 1980) and Peck and Axtmann (1979).
[5]Weres et al. (1981) proposed a 5th order rate law up to a certain silica concentration, S_t (unknown), and a 1st order rate > S_t

2.6. INHIBITION OF SILICATE SCALING

Work conducted by various researchers has suggested that silicate scale formation in many industries may be managed by reducing its formation rate. One of the possible solutions in geothermal systems is by aging the amorphous silica over-saturated waters. This will allow the monomeric silica that is in excess to polymerize to colloidal silica, and it is known that polymeric silica has less tendency to precipitate from solution than monomeric silica (Weres and Apps, 1982; Mroczek and McDowell, 1990; Gunnarsson and Arnórsson, 2003; Arnórsson, 2004).

Kashpura and Potapov (2000) concluded that an acidification technique was an acceptable and inexpensive alternative as a silicate scaling control method in geothermal systems particularly in wells and surface technical equipment. Guerra and Jacobo, (2012) reported that brine acidification using HCl and H_2SO_4 at pH5.5-6.0 was found to be effective for silicate scale control in the Berlin and Ahuachapan Geothermal field. However, alkalization is a more reliable method of water treatment before reinjection on a long-term basis as the former technique exposes the system to corrosion and does not eradicate the risk of silica deposition in the reservoir.

Apart from the two techniques described above, Weres and Apps (1982) and Arnórsson (2004) outlined several other possible control measures using (i) using chemical inhibitors, (ii) precipitation of the silica with lime or by bubbling CO_2 through the solution, (iii) mixing the brine with steam condensate; and (iv) by removal of colloidal silica by coagulation and settling.

The application of boric acid and/or its water-soluble salts to prevent silica polymerization in industrial waters has also been reported. It has been suggested that silica inhibition by borate is perhaps due to the formation of more soluble borate-silicate complexes. Dublin (1986) claimed the boric acid and/or its water-soluble salts may be used at concentrations of at least 10 ppm, as boric acid with the most preferred concentration is at least 50 ppm, as boric acid. Boric acid dissolves to form the orthoborate ion which apparently must be present to show activity in regard to inhibition of silica scales and precipitates. The water-soluble salts of boric acid include, but are not limited to, lithium, sodium, potassium, ammonium, and quaternary ammonium salts and may also include alkaline earth metal salts, aluminum salts, and transition metal salts if the presence of these types of cations can be tolerated in the industrial waters being treated.

Several approaches to prevent silica/silicate fouling in industrial water systems have been suggested by Perez et al. (1993) and Amjad and Zuhl (2008a, 2008b, 2009, 2010 and 2011). These can be grouped into two main categories. They can either be controlled by operating the systems at low concentrations that will involve a high volume of water or by incorporating chemical silica/silicate control agents in the water treatment programs as listed below:

1. Minimizing silica-based fouling by reducing the system silica concentrations by pre-treating the feed water with, for example $Al(OH)_3$, $Fe(OH)_3$, and $Mg(OH)_2$. These chemicals can effectively remove both soluble and colloidal silica (through chemical reaction and/or adsorption).

2. Through the use of additives that effectively inhibit silica polymerization in aqueous solutions. It was reported that homopolymers (e.g. Poly (maleic acid) PMA and poly(acrylic acid) PAA) and copolymers (proprietary blended namely CP1, CP3, CP4, and CP5) where carboxylic monomer groups dominate (>50%) of all these polymer compositions achieved less than 20% efficiency when tested up to 350ppm. Proprietary and patented CP6 and CP7 copolymer blends which contain <50% carboxylic acid monomer groups showed very good inhibition efficiency of up to 85% for silicate scale when tested up to 35ppm.

3. The use of boric acid and/or its water-soluble salts to control silica-based deposits. The formation of borate-silicate complexes which are more soluble than silica is a good alternative in silicate controls. However, this method has two main drawbacks; the high cost of the boron-based compounds and the limitations on the effluent discharge.

4. Polymeric dispersants that impart negative charge via adsorption onto suspended particles have also been used for minimizing silica-silicate fouling in industrial water systems. A blend of hydroxyl phosphono acetic acid and a copolymer of acrylic acid hydroxyl sulfonate; a blend of phosphonate and a copolymer of acrylic acid and 2-acrylamido-2-methyl propane sulfonic acid was reported an effective solution that extended the amorphous silica operating limit up to 300ppm.

Researchers have reported on the efficiency of a number of conventional scale inhibitors in inhibiting silicate scaling, but none of them successfully fully solved the silicate scaling problem. Polymeric and non-polymeric (phosphonate) scale inhibitors that work by controlling silicate formation either by crystal growth inhibition or crystal modification, failed to inhibit silicate scale probably because it is amorphous in nature. Several tested chemicals by other researchers are discussed in following section.

2.7. SCALE INHIBITOR TESTED FOR SILICATE SCALE

Silicate scales are covalently bonded and amorphous in nature and hence conventional polymeric and phosphonate scale inhibitors (SI) cannot inhibit them through either a nucleation or crystal growth inhibition/ crystal modification mechanism. “Pure” (no divalents) silicate scale is generally amorphous in nature. Since it is not a conventional crystal, then conventional scale inhibitors may be less effective since they are known to inhibit mineral scales through either nucleation inhibition or crystal growth inhibition mechanisms.

Chemicals are normally used for controlling/preventing silica scale either by inhibition or dispersion. The former approach prevents the dissolved monomeric silica from undergoing the oligomerization or polymerization reaction; which means this silica remains soluble and reactive. In contrast, the latter approach prevents the particle from further agglomerating to form larger sized particles as well as preventing surface adhesion or attachment of these particles to any surfaces in the system. Typical minimum inhibitor concentration (MIC) levels for conventional scales such as barium sulphate and calcium carbonate are [MIC] ~ 0.5 to 20ppm (Sorbie and Laing, 2004) whereas severe scale problems under high temperature high pressure (HTHP) fields may have MIC up to some 100s of ppm (Fan et al., 2011).

The use of non-polymeric inhibitors, such as phosphonates, to control scaling especially calcium carbonate is well known. However, these inhibitors suffer from the disadvantage that under high pH, high temperature or high hardness condition, they can react stoichiometrically with calcium ions leading to calcium phosphonate precipitation.

As such, phosphonates that are proven an effective crystalline scale threshold inhibitor cannot inhibit silica scale formation whereas even “small molecules” (cationic or anionic) in polymeric inhibitors are not active to inhibit silica scale in water treatment systems. Euvrard et al. (2007) tested the influence of a polymeric inhibitor, PPCA (phosphino poly carboxylic acid) and a phosphonate inhibitor, DETPMP (diethylene triamine penta methylene phosphonic acid) on silica fouling. Tests showed that the inhibition efficiency (IE) levels were calculated as IE ~30% and ~84% at concentrations of 100 and 1000ppm PPCA, while DETPMP recorded IE ~28% and ~80% at the same concentrations. Amjad and Zuhl (2009) also confirmed that phosphonates type inhibitors i.e. 1-Hydroxyethylidine-1,1-diphosphonic acid (HEDP), and 2-Phosphonobutane 1,2 4-

tricarboxylic acid (PBTC); and non-polymeric inhibitor boric acid (BA) are poor silica polymerization inhibitors.

Amjad et al. (1997) evaluated various products which included several polymeric-based and several non-polymeric inhibitors containing various functional groups (e.g., carboxylic acid, sulfonic acid, phosphonate, borate, etc.) to inhibit silica polymerization. Most of the polymers that demonstrated some efficacy in controlling foulants were homopolymers (i.e., polyacrylic acid, polymaleic acid), acrylic copolymers, or maleic copolymers. Product F (which is new proprietary product) had a marked inhibitory effect on silica polymerization and was superior to other commercial products including those meant for reverse osmosis (RO) pretreatment and silica control in particular. Amjad and Zuhl (2011) reported later that active ingredients such as carboxylic acid, sulfonic acid, and non-ionic groups present in the polymers exhibit poor interaction with silane groups present in silica with less than 20% efficiency. In addition, the candidates which were successful silicate scale inhibitors must be able to inhibit/ disperse the silica-based deposit especially colloidal silica and magnesium silicate and to disperse any other scale that can act as nuclei in silicate precipitation such as calcium carbonate and calcium sulfate.

Nonetheless, some inhibitor/dispersant chemistries are known, such as certain cationic polymers, that can inhibit silicate scales to some extent since the silicon concentration in the system was found to increase when the inhibitor dosage was increased (Amjad and Zuhl, 2008a, 2008b). Also, if the silicate can be dispersed, it will prolong the time before silicate scale could be formed. Amjad and Zuhl (2009) noted that a good dispersant would be a polymer species with M.Wt. < 10,000 Da with carboxylic acid and sulfonic acid groups.

Demadis et al. (2007) and Stathoulopoulou and Demadis (2008) tested several polymers as potential silica scale inhibitors, as follows, (i) neutral polymer PEOX (poly(2-ethyl–2–oxazoline)); (ii) Cationic additives included PEI (polyethyleneimine), PALAM (polyallylamine) and PAMALAM (poly(acrylamide-co-diallyl-dimethylammonium chloride)); and (iii) Blends of cationic/anionic polymers were PEI+CMI (CMI = carboxymethylinulin), PEI+PAA (PAA = polyacrylate). These workers found that cationic polymer worked to some extent as a function of time and inhibitor dosage.

Harrar et al. (1982) claimed that a mixture of cationic nitrogen-containing compounds, acid and (crystal) scale inhibitors (particularly polymeric imines, polymeric amines, and

quaternary ammonium compounds) could be effective for silicate inhibition in geothermal brines. These chemicals were found to stabilize colloidal silica and hinder agglomeration of the particles, hence the subsequent scale may be inhibited. Amjad and Yorke (1985) also proposed cationic-based copolymers to control silica scaling formation which found to be effective silica polymerization inhibitors but exhibited poor silica/silicate dispersing activity.

Neofotistou and Demadis (2004) identified and exploited some novel dendrimer chemistries; ethylenediamine polymer with dendrimer branches via amide chemical linkages as effective SiO_2 scale growth inhibitors in industrial waters known as polyaminoamide (PAMAM) STARBURST® dendrimers. They concluded that the performance of these dendrimers as silica polymerization inhibitors strongly depended on the branching present in the dendrimers though some of the dendrimers may have been entrapped within the SiO_2 matrix making them less efficient over time.

Amjad (2016) conducted experimental work to evaluate the performance of three non-ionic polymers, poly(2-ethyl-2-oxazoline) (PEOX); poly(vinylpyrrolidone) (PVP); ethylene oxide propylene oxide block co-polymer (PL68) and a non-polymeric additive i.e. propylene glycol (PGL). Results showed that the addition of 50ppm of each polymer tested in the presence of 650ppm silica as SiO_2 at pH 7.0, 40°C only achieved 40-70% efficiencies whereas PGL showed < 10% efficiency.

The using of ammonium bifluoride, NH_4HF_2 as a cleaning agent for silicate scale sparked some interest among researchers to find chemicals that can dissolve silica scales with less environmental effect. Demadis and colleagues (2007) found that the performance of a proprietary blend of additives namely Genesol 40, Carboxymethyl inulin, and polyacrylate as silica dissolver exhibited a rather random and inconsistent pattern which depended on the structure of the dissolver, testing time and the product dosage level.

A number of potential silicate scale inhibitors/dispersants have been tested as discussed above but none of these chemicals can fully inhibit silicate scaling even at very high concentration of chemicals (up to 1000ppm). Following evidence suggested by Amjad and Zuhl (2009), three polymeric SI have been tested in this work that contain various functional groups i.e. acrylamide, sulfonate, carboxylate, maleic acid, and another non-ionic monomers. These were tested in silicate *inhibition efficiency* (IE) tests carried; specifically, we evaluated Vinyl Sulfonated Acrylic Acid Co-polymer (*Inhibitor 1*),

Vinylamide / Vinylsulfonate Co-polymer (*Inhibitor 2*) and a Terpolymer of acrylic acid, 2-acrylamido-2-methylpropane sulfonic acid, non-ionic monomer (*Inhibitor 3*).

2.8. EXPERIMENTAL METHODOLOGY BY PREVIOUS RESEARCHERS IN SILICATE SCALING

Before the experimental methods reported in this thesis were developed and published, the study of silicate scaling was carried out mainly using qualitative experimental methods. The silicate scaling process was observed simply by using solution turbidity as a scaling measure or simply by visual inspection. This approach only enabled us to study the inhibition and kinetics of silicate scaling in its early stages because of the colloidal solution it produced when precipitation was taking place. In the previous work of Arensdorf et al. (2010) silicate scale severity was determined qualitatively by measuring the turbidity using a spectrophotometer, while Sonne et al. (2012a, 2012b) carried out studies using a similar approach to test the severity of the silicate scales formed by enhancing the static testing method proposed by Arensdorf et al. (2010). Sonne et al. (2012a, 2012b) still measured the silicate scale formed qualitatively. In their work, they improved the experimental procedure by measuring the turbidity using an optical scanning device which was able to measure the light transmission at multiple locations. This allowed for the settling of the silicate deposit and the dispersant effect of inhibitor could be observed, and more comprehensive data was generated by this type of multiple-point measurement.

Arensdorf et al. (2010) reported laboratory results of both static and dynamic testing that replicated the silicate scaling levels for a typical oil production well in a field under ASP flooding. The screening tests were used to evaluate the performance of chemical inhibitors in stopping the formation of magnesium silicate scaling by the mixing of Mg-containing brine (at natural pH) with Si-containing brine (at pH 10.7) at room temperature to give a final mixed brine ranging from 45-120ppm Mg and 470ppm Si. None of the chemicals tested acted as a “threshold” inhibitor but they resulted in significant delay in scaling when 50 to 100 ppm (as active) chemical were used.

In the work of Sonne et al. (2012a, 2012b), the mixed synthetic brine consisted of 20ppm Mg and 233.5ppm Si and was allowed to react at pH10 before adding inhibitor; i.e. the

effect of delayed chemical injection was studied. Various silicate brine scaling systems have been studied by other workers (Sui et al., 2014; Jing et al., 2013).

Sinclair (2012) conducted a series of experiments which were designed to test the effect of hydrodynamics on colloidal silica deposition in cylindrical pipe flow. The method of testing involved the use of a synthetic colloidal silica solution in a laboratory water tunnel. In the laboratory, better control could be achieved in terms of the ability to alter the chemical conditions, to have better control of the hydrodynamic conditions and to be able to monitor, control and adjust experimental conditions.

Umar and Saaid (2014) examined the effect of temperature on inhibitor performance by adopting some modified silicate scale polymerization procedure (Arensdorf et al., 2010; Amjad and Zuhl, 2008a, 2008b) in both static and dynamic test methods.

Kashpura and Potapov (2000) studied amorphous silica scales formation at The Mutnovskoe Hydrothermal Field (Russia) by examining the silicate scale produced by XRD and thermochemical analyses such as differential thermochemical (DTC), thermogravimetric (TG) and differential thermo-gravimetric (DTG) analyses. XRD suggested that the silicate scales produced were amorphous in nature, having maxima corresponding to quartz and pyrite FeS_2. DTG revealed that the endothermic minimum at a temperature of 125°C corresponded to opal. Possible measures to overcome these silicate scale problems were numerically modelled as described by Karpov et al. (1997).

Andhika and Regenspurg (2013) and Andhika et al. (2015) applied geochemical and mineralogical methods to characterize the solid silica precipitates and used measurements of ultrasonic velocity to study the polymerization of silica in solution where the aim was to understand the precipitation process in order to prevent such uncontrolled silica precipitation.

Basbar et al. (2013) studied the formation of silicate scale and its inhibition during alkaline flooding in static conditions. They studied selected scale inhibitors, namely Boric Acid (BA) and Poly Acrylic Acid (PAA). It was found that by introducing 250mg/L of PAA, the silica dissolution ratio (SDR) reduce to 0.21% in the case of low alkali concentration (0.4% alkali) and to 2.2% in the case of high alkali concentration (1.2% alkali). They concluded that the best inhibitor (PAA) does not prevent silicate scale, but rather somewhat reduced the SDR by 51% and 80% in the low alkali and high alkali concentrations, respectively.

2.9. EFFECT OF FERROUS ION IN SILICATE SYSTEM AND INHIBITOR PERFORMANCE

2.9.1 Occurrence of Fe-silicate Deposit

Most oil reservoirs exist as anaerobic and reducing environments created by bacterial activity consuming oxygen or redox reaction with the crude oil itself. Iron occurs in nature in its trivalent state (ferric/ Fe^{3+}) in an oxidising environment or its divalent state (ferrous/ Fe^{2+}) in a reducing environment. This Fe^{2+} can be oxidized to Fe^{3+} at the surface or upon contact with brine containing dissolved oxygen.

Evidence gathered from the Salton Sea geothermal field has shown that hypersaline brine containing ~500 ppm silica with more than 500 ppm iron (total) showed the formation of iron silicate scale. This ferrous scale was of a unique type, which was a hard, vitreous material which caused persistent trouble to the operation of the facilities in the field, as reported by Gallup (1989) and Gallup and Reiff (1991). The same scale, but amorphous in nature, was found in the wellhead piping at the Tiwi, Philippines geothermal field.

Gallup (1989) proposed the deposition of amorphous silica arises from the polymerization steps of mono-silicic acid through a condensation reaction as below:

$$2\ Si(OH)_4 \leftrightarrow (HO)_3Si\text{-}O\text{-}Si(OH)_3 + H_2O$$

The mono-silicic acid or the silicic acid oligomers further reacted with the hydrated ferric oxyhydroxide which consequently produced iron silicate scale. It is known that ferric iron has a strong affinity for silica, thus this reaction occurs quite rapidly as follows:

$$OFeOH.H_2O + Si(OH)_4 \leftrightarrow Fe(OH)_3.\ SiO_2 + 2H_2O$$

Later, Gallup and Reiff (1991) observed that ferric-rich silicates and corrosion products are dominantly detected in scales deposited from acidified brines at high temperature whereas ferrous-rich silicates are predominant in scales deposited at relatively low temperatures. As reservoir brine is known to exist in reducing conditions, ferric iron levels are anticipated to be very low which is consistent with produced brine analyses. Various spectroscopic analyses have been carried out including, Mőssbauer (Fe-57) spectroscopy, XRD and infra-red (IR) spectroscopy and analysis confirmed the scale resemble the structure of hisingerite, a hydrous Fe-Si oxide. Further IR spectra investigation and solubility observations suggest the presence of Fe-O-Si bonds. In

addition, iron deposited in the scales is believed to derive mainly from the brine, however some iron is also present as poorly-crystalline steel corrosion products. According to Marshall and Chen (1982), cations in the hypersaline brines decrease the solubility of silica resulting in the formation of iron silicate which may still form at temperatures as much as 50°C higher than pure amorphous silica.

Manceau et al. (1995) confirmed that scales precipitated in Salton Sea Geothermal Field at 250^{o}C are composed of hisingerite, whereas at temperature around 100^{o}C the scales are a mix of Al-containing opal and hydrous ferrous silicate, whose local structure similar to minnesotaite and greenalite.

Fe-oxide and Fe-silicate scale have been found by Fortin et al. (1998) in samples collected near hydrothermal vents on the Southern Explorer Ridge in the northeast Pacific Ocean. They propose that bacteria and their associated exo-polymers acted as nucleation sites for Fe-oxide and Fe-silicate formation and these scales structure had been verified by transmission electron microscopy (TEM) and energy dispersive X-ray spectroscopy (EDS) analysis.

Rodríguez (2006) reported on scales deposited in surface pipelines resulted from the mixing of the neutral pH and the low pH (acidic) fluids at the Miravalles geothermal field. These scales were found to be chemically homogeneous amorphous iron silicate with a stoichiometry that resemble of minnesotaite with the formula molecule, $(Fe^{++},Mg)_3Si_4O_{10}(OH)_2$.

2.9.2 Inhibition of Fe-silicate Deposit

Iron in aqueous solution is subject to hydrolysis that produces very low solubility ferric hydroxide. A report from the U.S. Geological Survey (1962) reported that the pH in most natural waters is not low enough to prevent these hydroxides from forming and under oxidizing environments, practically all the iron is readily precipitated as ferric hydroxide.

Gallup and Reiff (1991) believe the scale deposition can be controlled by adding reducing agents to convert ferric iron to ferrous iron, which forms a more soluble ferrous-silicates scale. The decreasing of the concentration of ferric iron also controls corrosion. Gallup (1989) reported that brine acidification is very effective scale control measure in geothermal field as this low pH condition not only shift equilibrium conditions away from

the Fe-silicate formation and/ or interfere the Fe-silicate formation; but it also stops the monomeric silica from further polymerizing.

2.9.3 Effect of Fe on Silicate Scaling

Work have been carried out by a number of researchers on the effect of Fe^{3+} in water treatment systems. The effects studied have included the antagonistic effect on the scale inhibitor and how ferric hydroxide $Fe_2(OH)_3$ seeded the silica polymerization on the membrane systems. Even when the ferric hydroxide was removed, silica scaling continued to grow. It was also reported that, in the presence of as low as 0.05ppm Fe^{3+}, the silica tended to precipitate even below its saturation level.

According to Zuhl and Amjad (2013), the Fe^{3+} ion present in the water as a result of raw water or carry over from the clarifier, is able to form soluble and insoluble complexes with hydroxide or/ and inhibitors. Therefore, less inhibitor is available to inhibit the silicate scale formation. It was reported that Fe^{3+} negatively affects the calcium phosphate inhibitor and iron oxide dispersant due to the formation of $Fe(OH)_3^-$. Fe^{3+} can complex or absorb onto the silica or it can catalyse the precipitation of silica scale. Malki (2014) concluded that the oxidation of Fe^{2+} to Fe^{3+} directly results in silica scale formation in reverse osmosis systems, despite the fact that the silica concentration was at a level that was not considered problematic.

Rodríguez (2006) detected not only ferric ion but also ferrous ion in the iron silicate scales in the surface pipelines of the Miravelle Geothermal Field, Costa Rica. He suggested that Fe^{2+} is more soluble so that reducing agent, sodium formate (NaHCOO), was used to effectively convert 99% of the ferric iron into ferrous ion which is more soluble at high temperature (250^{o}C). This also acted as a corrosion mitigation process since ferric iron is a well-known corrosive agent towards metallic materials.

Gallup (1989) studied iron silicate scale formation and inhibition at the Salton Sea Geothermal Field where they claimed that Fe^{2+} had been hydrolysed by water to Fe^{3+}; as the brine contained only 2-10ppm Fe^{3+} compared to 30ppm found in the scale. In summary, most of the research carried out to date has been on the effect of Fe^{3+} and not Fe^{2+}. Moreover, none of the techniques investigated have proved to be reliable in providing the necessary reducing environment.

2.9.4 Effect of Fe on Inhibitor Performance

Shupe (1981) reported solutions of polyacrylamide PAA polymers are adversely affected by metals, ferrous iron salts, certain biocides, or any free radical initiators when oxygen is present.

Stoppelenburg and Yuan (2000) found that Fe(II) did not have a significant effect on the DETPMP performance on barium sulfate inhibition efficiency. Indeed, it seemed to improve the DETPMP performance. However, they demonstrated that the presence of Fe(III) ions (as a result from the oxidation of Fe(II) under aerated condition) caused a detrimental effect on the DETPMP performance. Amjad (2014) also demonstrated that the addition of 10 mg to 100 mg of Fe_2O_3 i.e. Fe(III) ion to the calcium phosphate supersaturated solution exhibited a marked antagonistic effect on inhibitor performance.

In contrast, Gaffney et al. (1988) concluded that the presence of iron (II) in a system tend to have a remarkable effect on phosphonate barium sulphate scale inhibition performance; hence there was a need to consider the effect of iron (II) when designing a scale inhibitor efficiency test in the laboratory. The presence of ferrous ion showed antagonistic effects on various scale inhibitors including poly(vinylsulphonate) PVS under carbonate scaling conditions as reported by Graham et al. (2003). Alforjani (2005) also reported that the presence of ferrous ion in their inhibited test samples severely impaired the performance of phosphate esters and phosphonates in inhibiting calcium sulfate scale formation.

Kelland (2011) reported that, for both sulfate and carbonate scaling, ferrous iron severely affected the small amino phosphonate scale inhibitors i.e. diethylene triamine penta methylene phosphonates but has little significant effect on the performance of polysulfonate scale inhibitors, whereas polycarboxylate scale inhibitors were intermediately affected by iron (II) ions.

Zhang et al. (2015, 2016) reported that under barium sulfate scaling conditions, Fe(III) and Fe(II) both impair DTPMP, PPCA and PVS performance significantly, with Fe(III) affecting them all more.

CHAPTER 3. BASE CASE EXPERIMENTAL DEVELOPMENT

3.1. INTRODUCTION

The two primary objectives of the silicate research reported in this thesis are (i) to develop an experimental bulk silicate scaling and inhibition method, and (ii) to go on to use this to understand the mechanisms of silicate scale formation and its subsequent inhibition/dispersal. Silicate scale is very different from other types of scales (for example; barium sulfate scale which fully precipitates out from a scaling brine solution leaving a clear supernatant). Several previous researchers who have studied silicate scaling use more qualitative test methods in their attempts to evaluate the severity of the scale formed. Researchers such as Arensdorf et al. (2010) and Sonne et al. (2012) studied the extent of the silicate reaction using a measure of the turbidity. This solution turbidity was due to the amorphous nature of the silicate scale formed which produced different levels of cloudiness. However, in this study we have found that this method is not accurate, reliable or indeed quantifiable to measure the extent of the silicate reaction based on the cloudiness of the brine. In addition, this simple approach is not very reproducible.

In our experimental work, we have performed a structured study by reproducing various silicate scales in the laboratory, thus validating some results reported by Arensdorf et al. (2010). A static experimental methodology has been developed to produce a well defined silicate scale by modifying the approach reported by Arensdorf et al. (2010). The experimental approach has been extended by including elemental analysis for Mg and Si (by ICP) and examining the precipitated silicate deposits by several spectroscopic methods such as *Environmental Scanning Electron Microscopy/ Energy Dispersive X-ray Analysis* (ESEM/EDAX), *Fourier Transform Infrared Spectroscopy* (FTIR), *X-ray Powder Diffraction* (XRD) and *Mass Spectroscopy* (MS). Although we note that the data from MS is very difficult to analyse. Applying the methodology developed in this work, we are able to quantify give a much more quantitative assessment of the severity of the silicate scales formed.

There was a need to investigate the *minimum* magnesium ion concentration at which silicate scaling was initiated at 60^{o}C and pH8.5 to replicate the near well conditions and to gain an insight of the silicate scaling reaction which may occur in ASP flooding. Three

cases were studied and presented in this chapter; there are 60Mg:940Si representing the "*worst"* base case; 60Mg:470Si representing the "*intermediate"* base case and 30Mg:75Si representing a "*manageable"* base case at pH8.5, 60^{o}C.

After establishing acceptable "base case" scaling conditions for the silicate system (severe, intermediate and mild or *"manageable"*), a number of further investigation on the effect of various parameters were carried out. The parameters studied included pH, temperature, brine composition, and brine ageing (before scaling). The effects of all of these parameters were monitored using the range of analytical tools listed above and our more important results are presented in Chapter 4.

The ultimate aim of this work is to develop a methodology to tests chemicals that can inhibit the silicate scale which is produced during ASP flooding, steam flooding or during other more conventional reservoir processes. Several spectroscopic methods have been applied to the silicate deposits and these have confirmed that the silicate scales formed predominantly by covalently bonded amorphous silica. Since this is not crystalline, like a normal ionic salt, then this makes it difficult to inhibit using the conventional scale inhibitors which work through either nucleation or crystal growth inhibition mechanisms. Amjad and Zuhl (2009) suggested that polymers that exhibit good dispersion properties are typically low molecular weight (M.Wt. < 10,000 Da) and contain both carboxylic acid and sulfonate functional groups; hence several polymers that fall within that category were tested. Silicate systems were also found to be very sensitive to slight changes in pH; therefore, an *Inhibition Efficiency* (IE) Test was developed whereby the initial pH value of all mixed brines are adjusted to be very close to the nominal value through a very consistent procedure that is described under section 5.2.6 (pH adjustment techniques) in Chapter 5.

3.2. NOVELTY IN OUR SILICATE SCALING APPROACH

Our initial experiments followed and then significantly extended the previous work by Arensdorf et al. (2010) who demonstrated that magnesium silicate scaling can be formed reproducibly in the laboratory. We have extended this silicate methodology to include a quantitative ICP assay for [Mg] and [Si] and to study the silicate precipitated by various spectroscopic techniques such as ESEM/EDAX, XRD, FTIR and MS.

The methodology to perform silicate static bottle tests has been developed and a number of technical issues arising in the silicate system have been successfully addressed. Issues such as the appropriate reactor vessel materials (i.e. glass, plastic); ICP sampling procedure (i.e. sampling technique, appropriate quenching solution, ICP analysis *'waiting-time'*, etc.); the high sensitivity to pH and many more issues have been resolved and each is discussed in detailed in Chapter 4 and Chapter 5.

The approach used in this work has enabled us to establish an acceptable "base case" silicate scaling system. This 60Mg:940Si case was chosen as "*worst"* base case – which should be read as 60ppm of Mg ion and 940ppm of Si ion at 60^{o}C and pH 8.5. This case was used to study both the occurrence and inhibition of silicate scales (both amorphous silica and Mg-silicates). The mechanisms involved in forming silicates have been studied by reacting several brines at various conditions over relatively long periods (up to 8 days) and the *extent of reaction* under a range of conditions was evaluated. Several factors that influence the silicate system such as pH, temperature, initial ion concentrations, and brine age were studied and discussed in detailed in Chapter 4. The *extent of reaction* for each factor studied was evaluated (and compared) using the amount of Mg or Si which has ***reacted*** according to Equation 3.1;

$$\text{Mg } \textit{ion reacted} = [\text{Mg}]_o - [\text{Mg}]_f. \qquad \textbf{3.1}$$

where [Mg]o and [Mg]f are the initial and final values of magnesium concentration respectively; the notation for Si is the same.

What is actually measured in these experiments (by ICP) is the concentration of [Mg] and [Si] ***remaining*** in solution after any silicate precipitation has occurred. However, it is convenient here to plot the amount of Mg or Si which has ***reacted***, i.e. the amount missing from solution, which we refer to as the "*ion reacted*" (since it is in the precipitate). The *ion reacted* Si value is defined in the same way as for Mg.

The amount of ions reacted (Si and Mg) as calculated by Equation 3.1 were eventually converted into *Si:Mg molar ratio* in the solid silicate scale and these can be compared with the ESEM/EDAX Analysis. This has enabled us to establish the morphology of the silicate scale formed and its stoichiometry in terms of the *Si:Mg molar ratio*. This stoichiometry result was found to be very consistent by the two methods used, viz. (a) the solution ICP ion ***reacted*** results, and (b) the independent ESEM/EDAX results on the actual precipitate.

Later in our studies, it was found necessary to also study an "*intermediate"* base case and a "*manageable"* silicate scale base case to ensure the system studied can be fully inhibited. The reason why these cases were analysed are explained in the test.

3.3. EXPERIMENTAL DETAILS

An experiment method was initially set up (as shown schematically in Figure 3-1) to repeat some of the silicate scaling results reported by Arensdorf et al. (2010). However, this test was modified by taking a brine containing only magnesium ions to represent the connate brine (formation water). The other brine only contained silicon (as silicate) to represent the leachate by the ASP water (or any other silicate ion source in the reservoir).

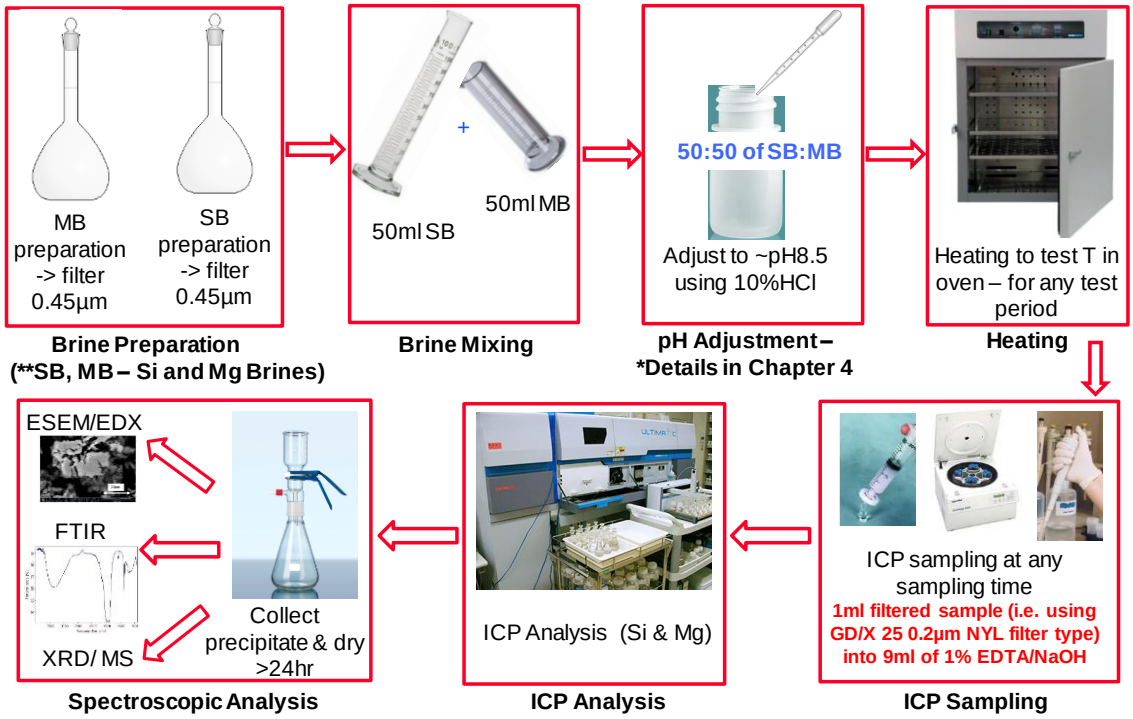

Figure 3-1 Silicate Static Bottle Test experimental methodology

The objective of these preliminary experiments was to establish that a reproducible silicate scale could be formed in the laboratory, in order that its formation and inhibition could then be studied in detail. In these initial experiments, the severity of the magnesium silicate scaling problem was yet to be quantified. Essentially, we formed the silicate scale by mixing the silicon brine (Si Brine) with the magnesium brine (Mg Brine) in a 50:50 ratio at 60^{o}C. The magnesium and silicon brines were prepared by dissolving appropriate

quantities of salts ($MgCl_2.6H_2O$ and $Na_2SiO_3.5H_2O$) in distilled water with the compositions given in Table 3-1. This brine was then filtered using a 0.45 µm filter size.

50ml samples of the Mg Brine and Si Brine were prepared in order to achieve a range of final mixed concentrations (i.e. from 30ppm to 1200ppm of Mg ion and 75ppm to 940ppm of Si ion respectively). These mixed brines were then pH-adjusted to the test pH i.e. pH=8.5, before being heated in the oven to the required test temperature i.e. 60°C.

Table 3-1 The brine composition and preparation for difference base cases studied

	Ion	**Mg^{2+} Concentration {ppm (mg / L)} x**	**Amount of $MgCl_2.6H_2O$ Required**				
			g / L	**g / 5L**	**g / 10L**	**g / 15L**	**g / 20L**
"Worst" base case Scenario	Mg^{2+}	120	1.003	5.017	10.035	15.052	20.069
	Mg^{2+}	180	1.505	7.526	15.052	22.578	30.104
	Mg^{2+}	240	2.007	10.035	20.069	30.104	40.138
60Mg:940Si	Mg^{2+}	600	5.017	25.087	50.173	75.260	100.347
	Ion	**Si^{4+} Concentration {ppm (mg / L)}**	**Amount of $Na_2SiO_3.5H_2O$ Required**				
			g / L	**g / 5L**	**g / 10L**	**g / 15L**	**g / 20L**
	Si^{4+}	1880	14.20	71.00	142.00	213.00	284.00
"Intermediate" base case Scenario	**Ion**	**Mg^{2+} Concentration {ppm (mg / L)}**	**Amount of $MgCl_2.6H_2O$ Required**				
			g / L	**g / 5L**	**g / 10L**	**g / 15L**	**g / 20L**
	Mg^{2+}	120	1.003	5.017	10.035	15.052	20.069
	Ion	**Si^{4+} Concentration {ppm (mg / L)}**	**Amount of $Na_2SiO_3.5H_2O$ Required**				
60Mg:470Si			**g / L**	**g / 5L**	**g / 10L**	**g / 15L**	**g / 20L**
	Si^{4+}	940	7.1	35.5	71	106.5	142
"Manageable" base case Scenario	**Ion**	**Mg^{2+} Concentration {ppm (mg / L)}**	**Amount of $MgCl_2.6H_2O$ Required**				
			g / L	**g / 5L**	**g / 10L**	**g / 15L**	**g / 20L**
	Mg^{2+}	60	0.5018	2.5088	5.0175	7.5263	10.035
	Ion	**Si^{4+} Concentration {ppm (mg / L)}**	**Amount of $Na_2SiO_3.5H_2O$ Required**				
30Mg:75Si			**g / L**	**g / 5L**	**g / 10L**	**g / 15L**	**g / 20L**
	Si^{4+}	150	1.1330	5.6649	11.3300	16.9947	22.6596

The mixed solutions of Mg brine and Si brine were visually inspected (often photographed) and samples for ICP analysis were taken at 2 hours and 22 hours (or any required sampling time). In order to stabilise the samples in conventional scaling studies

we usually use a "quenching solution". For the silicate mixed brine stabilisation, quenching solution were prepared for ICP analysis, viz. 1% EDTA/NaOH.

The silicate precipitated samples produced in these tests were filtered (using 0.2 μm paper filters and rinsed using distilled water) and the filtered cakes were left to dry at room temperature for at least 24 hours. A wide range of analytical techniques were applied to study the composition of the silicate scales formed, including: (i) *Environmental Scanning Electron Microscopy/ Energy Dispersive X-ray Analysis* (ESEM/EDAX), (ii) *Fourier Transfer Infrared Spectroscopy* (FTIR), and (iii) *Powder X-Ray Diffraction* (Powder XRD). The results from these techniques have given us some very useful interpretative clues as to the nature (and composition) of the silicate precipitates, as explained in detail in this section.

ESEM/EDAX analysis measures the proportions (in terms of both molar % and weight %) of the constituent elements and this was used in determining the stoichiometry of silicon to magnesium in the silicate precipitate; i.e. the *Si:Mg molar ratio*. The precipitates were also analysed using FTIR to compare the spectra produced, which reflects the chemical moieties and functional groups present. From XRD spectra one can infer the crystalline structure (from peak patterns), compositions (by peak location) and the degree of crystallinity (from peak width) of the silicate deposits.

3.3.1 Experimental Uncertainties and Minimizing Systematic Errors

Each analytical procedure should be tested thoroughly for its robustness to ensure that excellent repeatability can constantly be achieved. It is known that even under constant experimental conditions (i.e. same operator, same tools, and same laboratory, short time intervals between the measurements), repeated measurements of series of identical samples always lead to results which differ among themselves and from the true value (or accepted true value) of the sample. These differences or deviation resulted in what we called error that make quantitative measurements cannot be reproduced with absolute reliability. These types of error (differences/ deviation) can be distinguished and grouped into random error (that determine the precision) and systematic error (that determine accuracy) depending on their character and magnitude.

Precision which is also known as standard deviation, is defined as the degree of agreement between replicate measurements of the same quantity. In other words, precision is the ability to get the same result for the same sample when measured multiple times. It is the

repeatability of the result that is usually measured as % Relative Standard Deviation (RSD) or sometimes, SD % RSD = (SD / Mean Result) * 100. The estimated standard deviation i.e. the error range for a data set, is often reported with measurements because random errors are difficult to eliminate. Random errors are caused by uncontrollable fluctuations in variables such as measuring techniques (e.g. noise), sample properties (e.g. inhomogeneities), and chemical effects (e.g. equilibrium) that affect experimental results. Even under carefully controlled conditions random errors cannot, in principle, be avoided, they can only be minimized and evaluated with statistical methods. This positive and negative scattering of data i.e. vary in an unpredictable manner is characteristic of random errors in which low values indicate good precision. (ISO 3534-2, 2006).

However, good precision does not mean good accuracy, for instance, if there were a systematic error in the analysis. This error would not affect the precision, but it does affect the accuracy. Accuracy that determined from systematic error is the degree of agreement between the measured value and the true value or the accepted true value (an absolute true value is seldom known). In contrast to random errors, systematic errors can and must be avoided or eliminated if their origins become known, because they yield false results. The performance parameter of accuracy is the measurement uncertainty though these systematic errors cannot be statistically evaluated. Systematic (or determinate) errors are instrumental, methodological, or personal mistakes causing "lopsided" data, which is consistently deviated in one direction (i.e. to higher or lower values which lead to false results) from the true value. Examples of systematic errors: an *instrumental error* results when a spectrometer drifts away from calibrated settings; a *methodological error* is created by using the wrong indicator for an acid-base titration; and, a *personal error* occurs when an experimenter records only even numbers for the last digit of burette volumes. Systematic errors can be identified and eliminated after careful inspection of the experimental methods, cross-calibration of instruments, and examination of techniques (JCGM, 2008).

In short, random errors are due to the accuracy of the equipment and systematic errors are due to how well the equipment was used or how well the experiment was controlled. Following that, precision refers to the reproducibility (repeatability) of a measurement while accuracy is a measure of the closeness to true value (reliability).

In the context of this research, experiments and analysis done were carefully designed and conducted in a constant experimental condition. The laboratory balances are used both for

weighing out large amounts of salts for brine preparation, and smaller, more precise amounts of salts for brine reparation; chemicals for standard preparation; and for the preparation of scale inhibitor solutions. For these purposes, the top pan Sartorius LP2200S 2 decimal place balance (Readability 0.01g and / Repeatability – standard deviation ≤±0.01g and maximum reading of 2200g) is used for weighing larger amounts of chemicals, where precision up to four figures is not necessary *e.g.* during the preparation of large volume of brines. The four-figure Sartorius Secura 124-1S balance (Readability 0.0001g and / Repeatability – standard deviation ≤±0.0001g) is used for weighing small, *precise*, amounts of chemicals and has a maximum loading of 120g (including weighing vessel). It is worth mentioning here that the balance must ensure to be levelled and an internal calibration is performed if the balance has not been used recently to ensure accurate and precise measurement of samples.

All brines were prepared so that target concentration(s) were achieved (i.e. measured by ICP-EOS) by ensuring solve salts whilst preparing brines and to ensure efficient mixing of the freshly prepared brine as explained in detailed in Appendix. Any glassware used should be washed thoroughly using Decon labware wash and rinsed with distilled water for three time to ensure it is free from any contaminants. Oven were heated to test temperature and ensured was actually at the target temperature by switched it on for at least an hour before experiments started. All samples were ensured stabilized to the test temperature in the oven in an hour before the time was counted (i.e. 0 hour).

All measurements for samples preparation were done in measuring cylinder with appropriate volume accordingly (i.e. either in 10ml, 25ml or 100ml) by avoiding the parallax error. All solution for ICP sampled analysis of less than 10ml were measured using digital Eppendorf Reference variable pipette of appropriate volume (100-1000µL, 500-2500µL, 500-5000µL, or 1000-10000µL). The required volume was obtained by set the variable pipette, by pressing the black or blue button on the side and turn the top button (as indicated on the display) i.e. 0500µl = 0.5ml (Note: make sure the right volume is set in microliter unit). For the 5ml pipette, the volume was adjusted by just turn the top coloured section. The end button was pressed down to the first point of resistance before placing it in the liquid. The tip was placed in the liquid and the button was released slowly to draw up the liquid into the tip, i.e. making sure there are no air bubbles. The end button was depressed to the second point of resistance to dispense the liquid, i.e. to fully expel the liquid from the tip. The tip can then be released by fully depressing the end button to

the third point of resistance. The accurate volume was ensured by handling the variable pipette correctly as explained.

Systematic error associated to pH measurement was minimized by calibrate the pH meters at least once a day (on the day before the experiments conducted). pH10, pH 7 and pH 4 buffer solutions used in calibration is ensured aged no more than a month, otherwise new buffer solutions are used. All pH values of solutions were measured using Denver Instrument Model 215 pH/mV meter with accuracy of ±0.002pH, ±0.1mV, ±0.3^{o}C in aerobic tests and pH Mettler Toledo pH M300 with accuracy of ±0.03pH, ±2mV, in anaerobic tests. All pH was measured at room temperature i.e. the hot samples were ensured cooled down to room temperature before measurement were taken).

In order to confirm accuracy for ICP-EOS results, the results for a prepared standard were checked in which only certified reference materials were measured. Other quality control checks were also used to check analysis. Calibration standards should properly prepared and it is equally important to match to samples, prepare accurately and use them "fresh". For static test (quenched test), control samples of individual SB, MB, and mixed brine SB/MB were added to the ICP analysis of test samples were at regular intervals to allow for instrumental errors to be accounted for. For inhibition efficiency test, it is worth noting here C_O (as explained in detailed in Equation 5-1) is determined by adding the test SB and MB to the EDTA/NaOH quenching solution in the appropriate ratio, as used for the quenched test solutions. C_O samples are added to the ICP analysis of test samples at regular intervals to allow for instrumental errors to be accounted for. The limit of analytical error is defined by the difference between the estimated value of a quantity (i.e. ICP assayed concentration) and its true value. In this thesis, it is expressed as the percentage of the true values. In these tests each individual test condition is conducted in duplicate to allow anomalous results to be immediately recognised. Tests would be repeated if the difference in the recorded efficiencies was > 5 – 10%. Any divalent ion levels above stock solution concentration are not expected or must be within its analytical error of less than 5%. For ICP-OES, expect 1-2% RSD while the random error on the reading is 7.5 parts per billionth.

It must be noted that the EDAX signals are localized and variable and inaccurate values are expected depending on which point has been analysed. However, each sample for ESEM/EDAX was analysed for at least 3 different locations ensuring that they will better

represent the samples. Also, through the results obtained from ESEM/EDAX, all data obtained (at least for 3 locations of the same sample) were very close.

The samples for powder XRD need to be supplied as a finely ground powder with similar particle sizes, ideally sieved for better quality data. The amount should be a large spatula size to fill the sample holder of 25mm across and about 3mm deep. The sample is compacted into a sample holder, so it is flat and level with the top of the sample holder to minimise errors in peak positions. Detailed procedure is outlined in Appendix.

FTIR analysis require big chunks of "solid" samples to be crushed and make sure it is in small and tiny powder form using a mortar and pestel as described in Appendix. The crystal surface on the FTIR machine must all be covered with the sample by using a spatula and properly clamped so that it is stay and not fly away. The crystal and the tip were ensured free from any analysed samples by cleaning them using ethanol solution. It can be done by spraying a small amount of ethanol on a clean tissue before cleaning the crystal and the tip.

3.4. EXPERIMENTAL RESULTS AND DISCUSSION

3.4.1 Threshold Mg Concentration to Initiate Silicate Scaling (Conditions: pH8.5 and 60ºC)

There was a need to investigate the *minimum* magnesium ion concentration at which silicate scaling was initiated at 60^{o}C and pH8.5. Nominally, this is intended to replicate the near well conditions which might occur in ASP flooding.

All four brine concentrations i.e. 60Mg:940Si, 90Mg:940Si, 120Mg:940Si and 300Mg:940Si produced precipitate (through physical observation and from the ions reacted results based on the ICP data). Figure 3-2 shows that the higher the amount of magnesium ion present in the mixed brine, the higher the amount of magnesium ions reacted.

The ESEM/EDAX analysis indicated that all precipitates produced were amorphous in nature as shown in Figure 3-3.

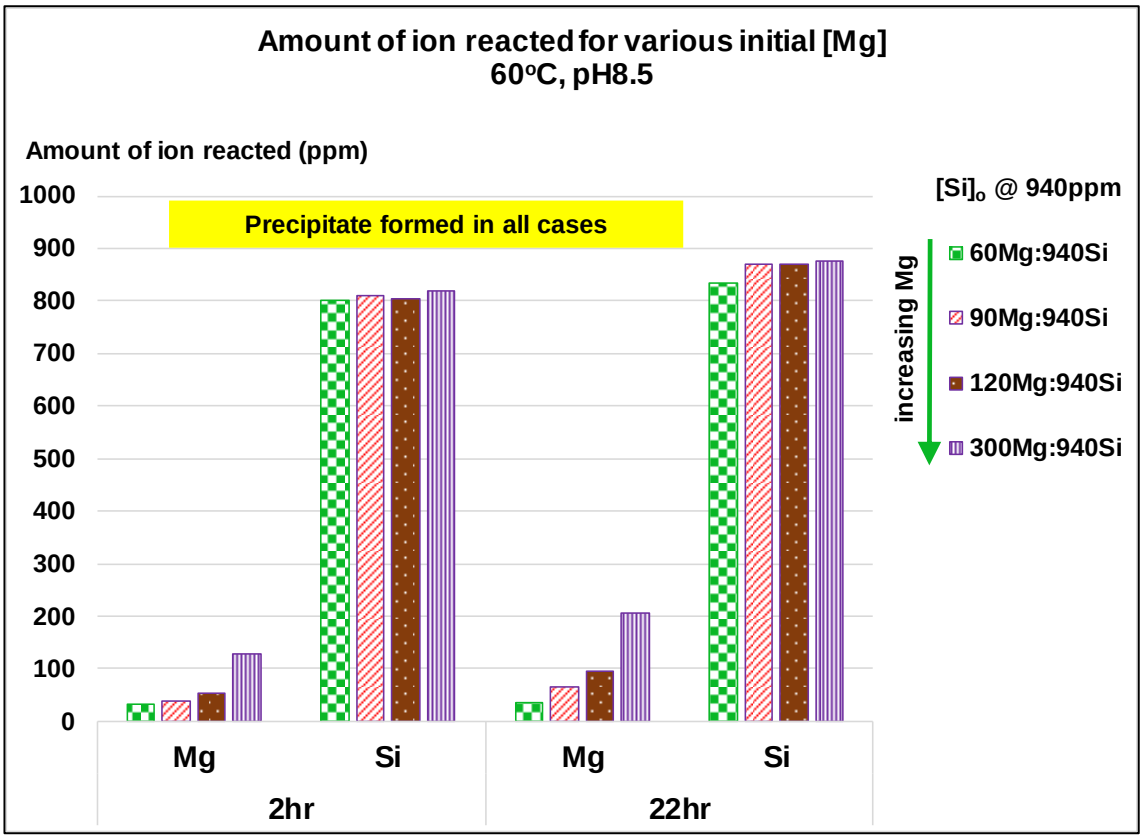

Figure 3-2 Amount of ion reacted for various magnesium levels (Si concentration is fixed at 940ppm) at 60°C, pH8.5

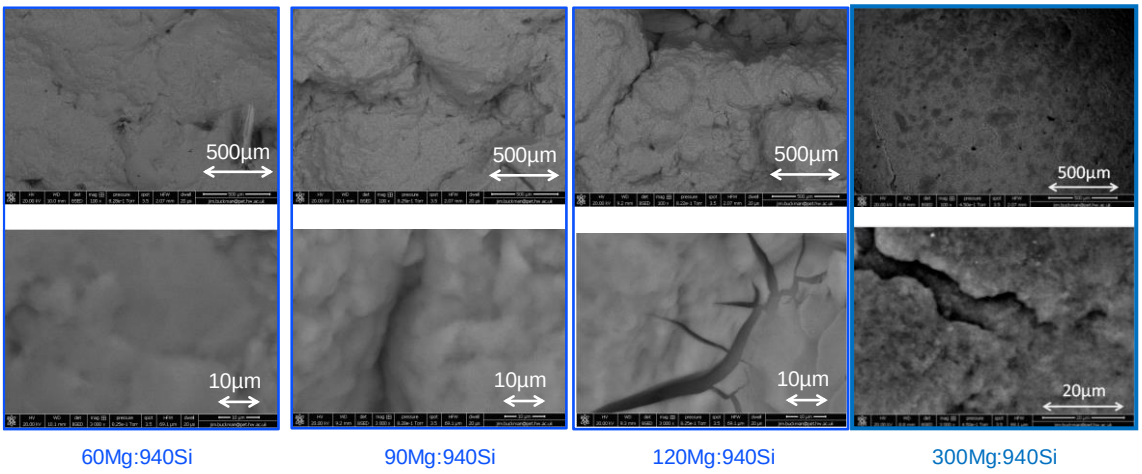

Figure 3-3 ESEM images for silicate deposits for various magnesium levels (Si concentration is fixed at 940ppm) at 60°C, pH8.5

The average values of Si:Mg molar ratio in the silicate deposits for each case were determined and these are plotted in Figure 3-4 for all test magnesium concentration at pH8.5 and 60°C test conditions. The Si:Mg molar ratio depends on the amount of magnesium present in the mixed solution and the Si:Mg ratio decreases as the amount of magnesium ion is increased. This was first indication (amplified in many later results) that the stoichiometry of Mg-silicate scale could have quite variable stoichiometry.

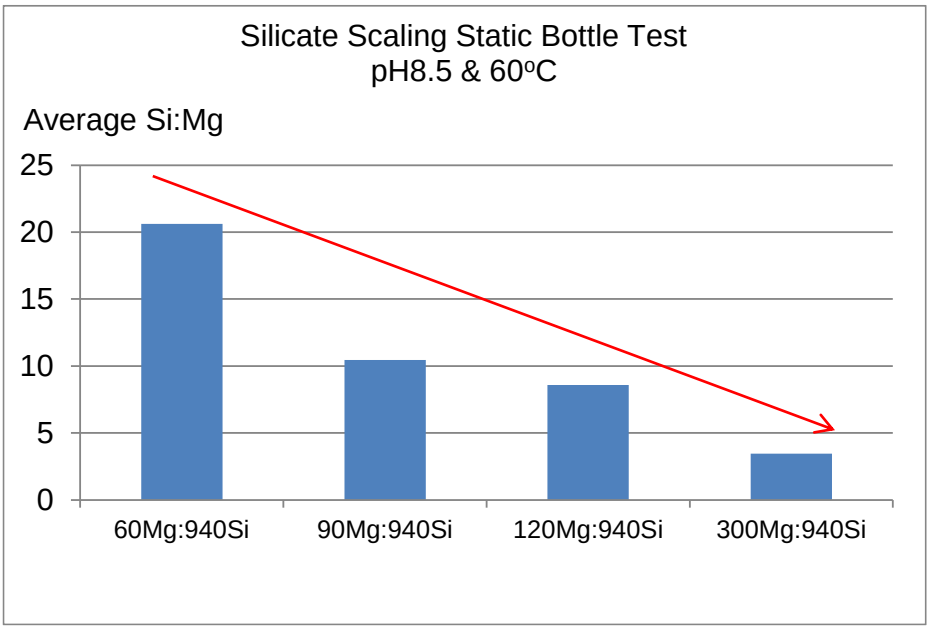

Figure 3-4 Average Si:Mg molar ratio for various magnesium levels (Si concentration is fixed at 940ppm) at 60°C, pH8.5

We now turn to the analysis of the magnesium silicate deposits which formed in this series of experiments by FTIR spectroscopy. The specific IR absorption peaks reflect the presence of particular chemical groups in the deposits. The FTIR spectrum shown in Figure 3-5 shows that the scale produced for all magnesium ion concentration consist of only magnesium silicate and amorphous silica. Peaks at ~1055 and ~790 cm^{-1} have been attributed to the presence of the amorphous silica, while peaks ~668, ~577 and ~565cm^{-1} has been demonstrated to be the identity of magnesium silicate scale. Much more detailed analyses of FTIR peaks for the silicate deposits can be seen in Figure 3-16 in this section, and in many more results in Chapter 4 and 5.

It is worth noted here that for the band due to Si-O-Si ~1100cm-1; the presence of higher amount of magnesium resulted in more magnesium bridging the amorphous silica scale to form amorphous Mg-silicate scale. Hence, band due to Si-O-Si may have already moved from 1055cm-1 to ~1000cm-1. This observation agreed with Hernández-Ortiz et al. (2012) that showed that absorption bands near 1100, 790, and 480cm-1 are common to all silicates with tetrahedrally coordinated silicon Si-O-Si and band due to SiO_2 can be seen at 1200cm-1.

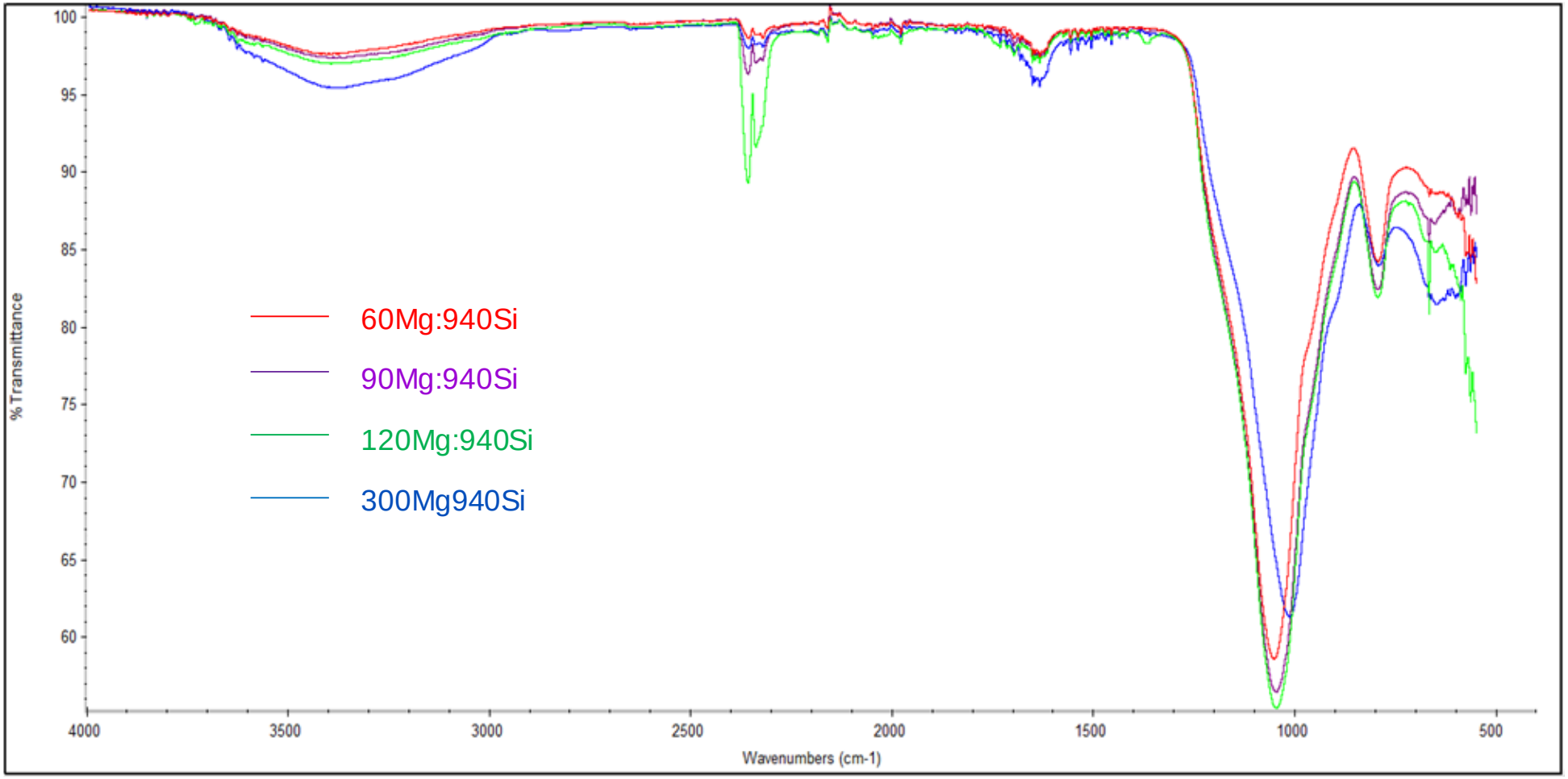

Figure 3-5 FTIR spectra for various magnesium levels (Si concentration is fixed at 940ppm) at 60°C, pH8.5

3.4.2 "Worst" Base Case Study (60Mg:940Si at 60ºC, pH8.5)

Based on results in previous section 3.4.1, the silicate system of 60Mg:940Si was chosen as a "*worst"* base case; set of concentrations and repeats proved the repeatability and reproducibility of the methodology adopted (as shown in Figure 3-6 and Figure 3-7 . For this case, it was found that 48.6% - 58.5% and 59.8% - 67.8% of magnesium ion was reacted after 2 and 22 hours respectively. 81.9% - 86.2% of silicon ion was reacted after 2 hours and this increased to 87.7% – 89.3% after 22 hours. Note that the range of percentage amount of ions reacted were calculated based on several experiments (blank samples) during the course of the work. The results for these "*worst"* case silicate scaling tests are clearly very repeatable.

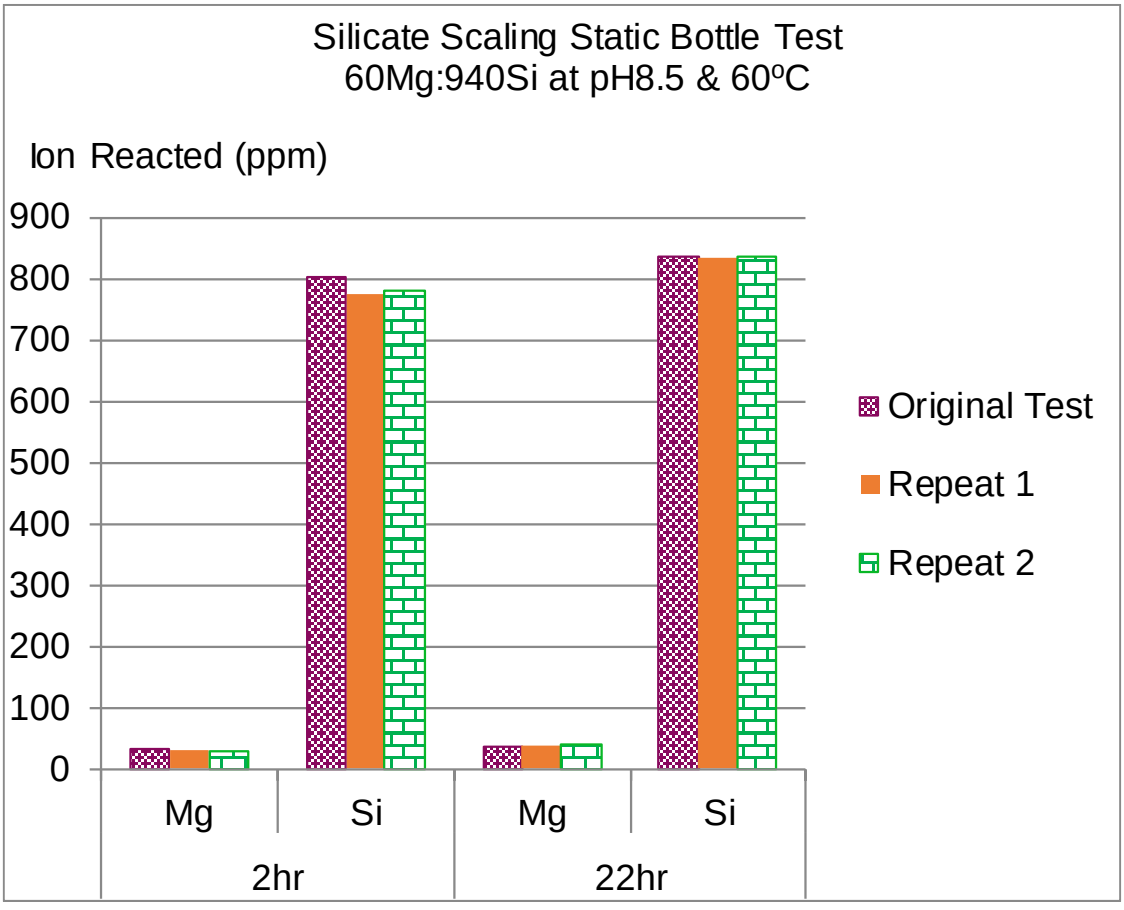

Figure 3-6 The amount of ion reacted (ppm) for *"worst"* base case (Blank) of 60Mg:940Si at 60ºC, pH8.5

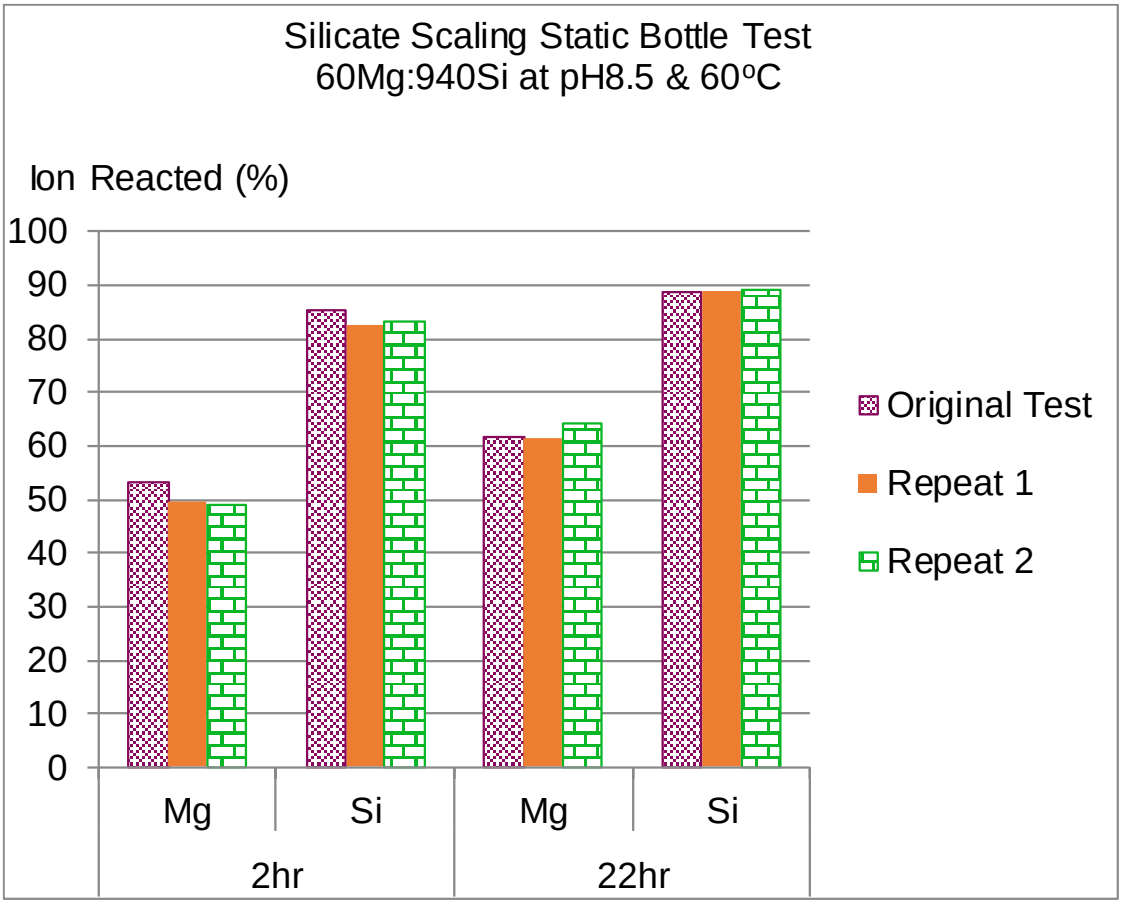

Figure 3-7 The amount of ion reacted (%) for *"worst"* base case (Blank) of 60Mg:940Si at 60ºC, pH8.5

The Si:Mg molar ratio in the silicate deposits for the 60Mg:940Si case was also determined for all tests and this is plotted in Figure 3-8. It is clearly shown that the Si:Mg molar ratio for all repeated tests agreed quite closely with each other and the average value for Si:Mg ration was found to be ~20 (Figure 3-8). As can be seen in Figure 3-9, the pH values recorded for the two repeat tests also matched very well at all reaction time; ~pH8.8 and ~pH8 after 2 hours and 22 hours reacted respectively. While the pH values were slightly change for *Original Test*; ~pH8.6 and ~pH8.4 after 2 hours and 22 hours reacted respectively.

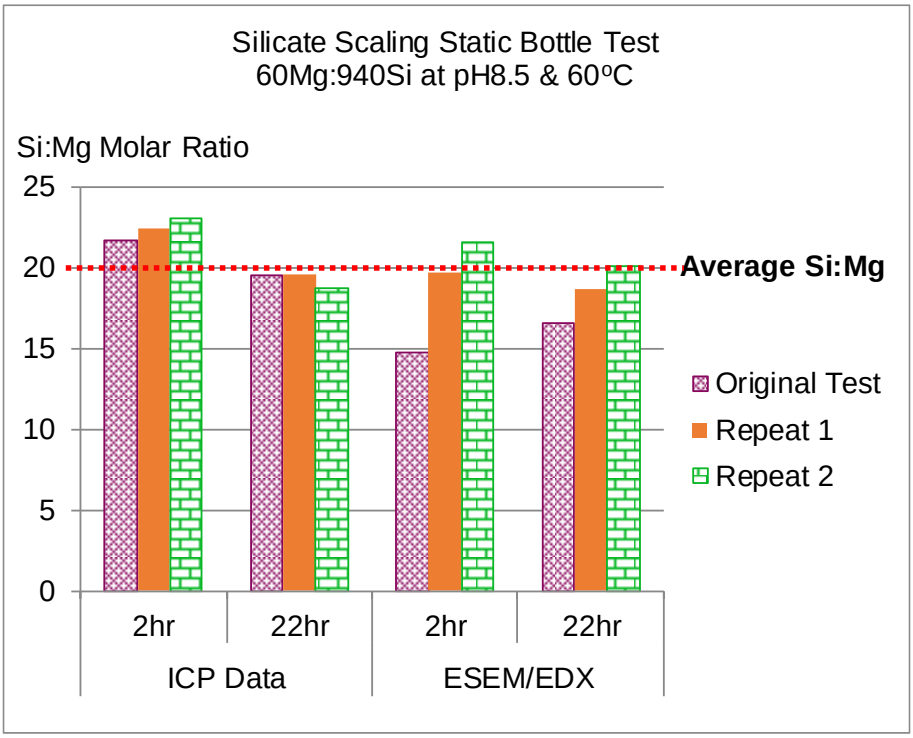

Figure 3-8 Si:Mg molar ratio in *"worst"* base case (Blank) of 60Mg:940Si at 60°C, pH8.5

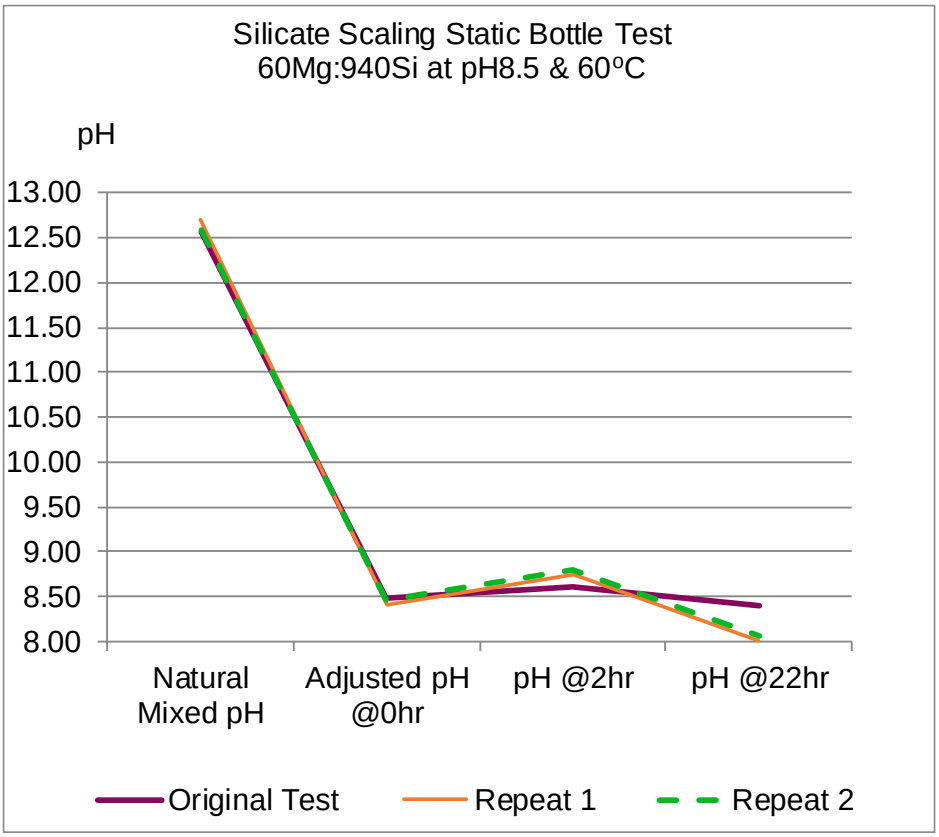

Figure 3-9 pH profile during scaling reaction of *"worst"* base case (Blank) of 60Mg:940Si at 60°C, pH8.5

Silica and silicate scale formation during ASP flooding is a complex process which proceeds in 4 stages as follows (i) silica dissolution, (ii) silica polymerization, (iii) silica scale formation (either as amorphous silica or as a Mg-silicate) and (iv) co-precipitation of silicate scale with other minerals (Arensdorf et al., 2011). The extent of silicate scale formation was further investigated by studying the rate of scaling reaction at early time. The experiment was designed to observe the scaling reaction of the "*worst"* base case at 15 minutes intervals – to get an estimate of how the scaling reaction rate proceeds, i.e. slowly and continuously or suddenly. The same experiment was then in some cases repeated to measure the severity of the scale produced (i.e. it was ICP sampled).

The silicate scale static bottle test was conducted in glass bottles to observe the formation of precipitate which allowed a visual observation and for the samples to be photographed*. The pH levels of all samples were closely adjusted to the nominal value using the consistent approach as described in section 5.2.6. (*Note: Although glass bottles were used here for the entire experiment, the short timescales, lower temperature and lower pH values ensured that the effects of Si leaching from the bottle were minimal. A fuller report on this issue of Si leaching from glass bottles is given in section 4.3.3, Chapter 4).

The extent of silicate scale formation was monitored throughout the reaction time through the physical observation, pH changes and amount of ions reacted viz. ICP sampling. The amount of ion reacted was verified by using several ICP sampling techniques.

Figure 3-10 shows that brine solution became cloudy 50 minutes after it was placed in the oven in the stabilizing period. As can be seen in Figure 3-11, gel precipitation was observed after one hour of reaction (reaction time started as 0hr after the brine solution left stabilizing to 60^{o}C for 1 hour). A thin clear layer appeared after 75 minutes and this layer then expanded after 90 minutes, as can be seen in Figure 3-11 and the appearance of the samples over 8 days can be seen in Figure 3-12.

The amounts of magnesium and silicon ion reacted throughout the reaction time were plotted in Figure 3-13 (in ppm) and Figure 3-14 (in %). We can see from these figures that amount of silicon ion reacted achieved equilibrium essentially after 2 hours while magnesium ion continues to react and only stabilized after 72 hours.

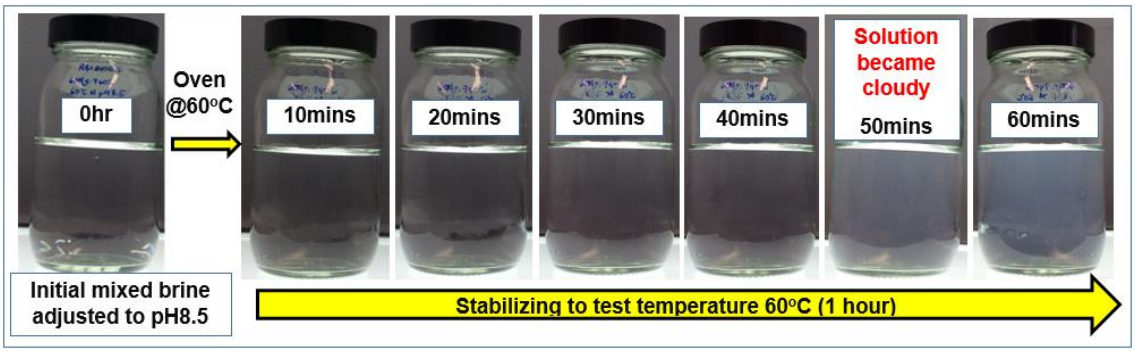

Figure 3-10 Physical observation of "*worst*" base case (Blank) of 60Mg:940Si at 60°C, pH8.5 (Stabilizing to test temperature for 1 hour)

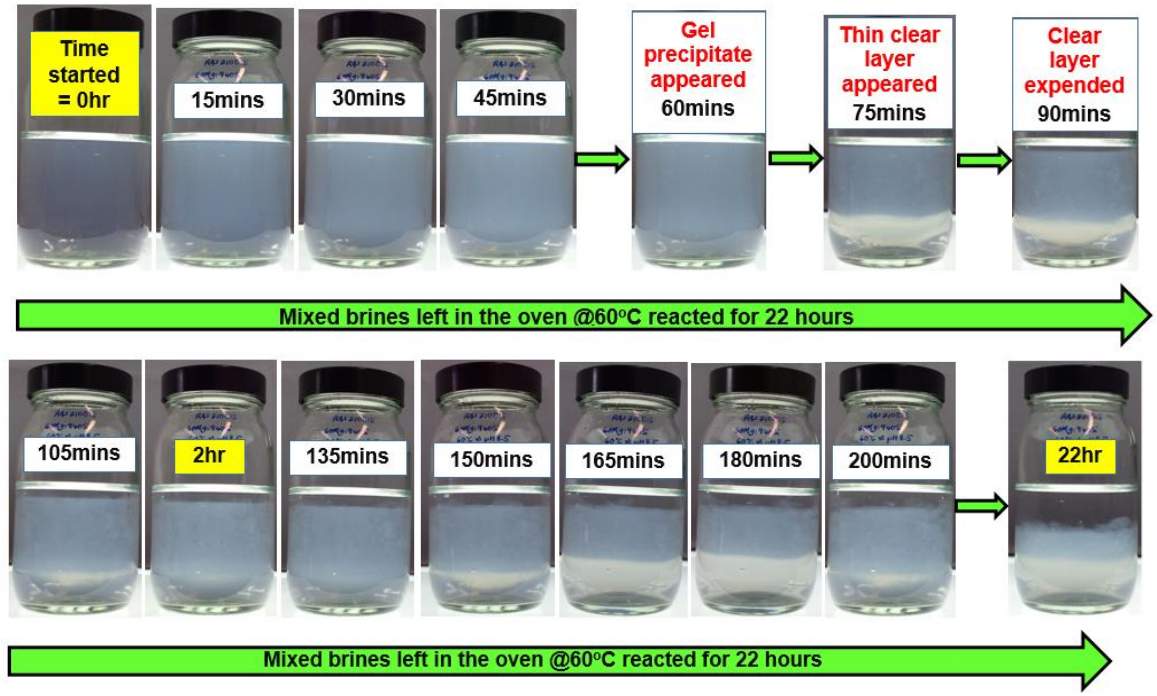

Figure 3-11 Physical observation of "*worst*" base case (Blank) of 60Mg:940Si at 60°C, pH8.5 (t=0 to 22 hour)

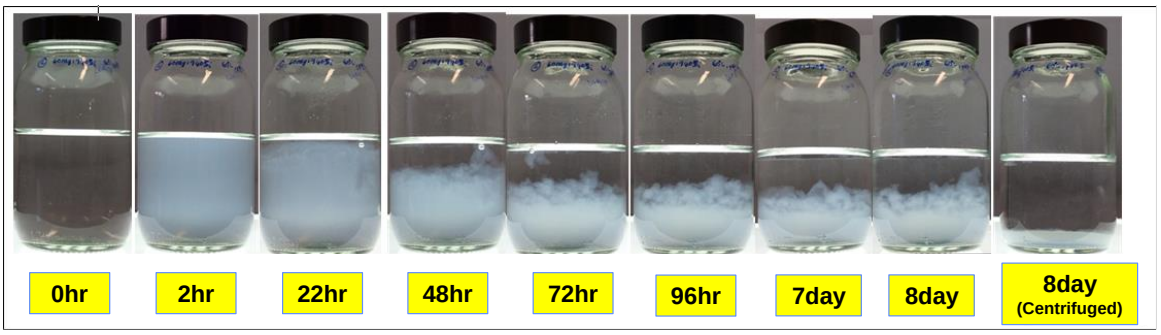

Figure 3-12 Physical observation of "*worst*" base case (Blank) of 60Mg:940Si at 60°C, pH8.5 (t=0 to 8 days)

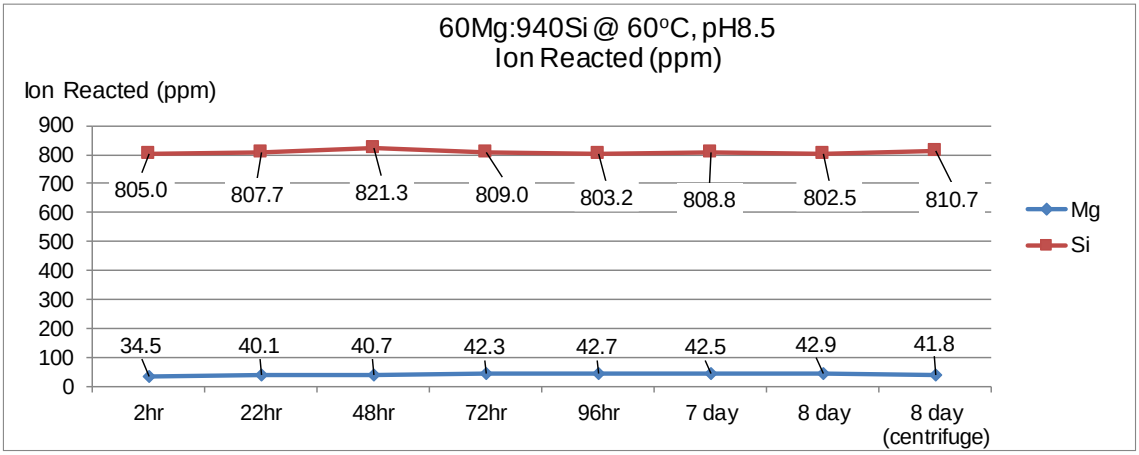

Figure 3-13 Amount of ion reacted for the "*worst*" base case (Blank) of 60Mg:940Si at 60°C, pH8.5 (t=0 to 8 days)

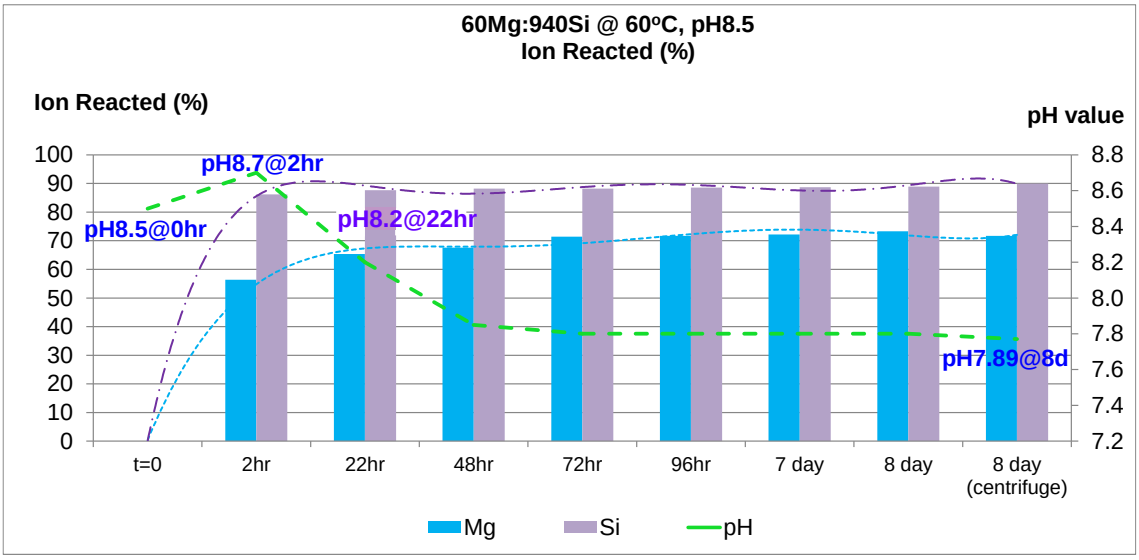

Figure 3-14 Percentage amount of ion reacted and pH profiles for the "*worst*" base case (Blank) of 60Mg:940Si at 60°C, pH8.5 (t=0 to 8 days)

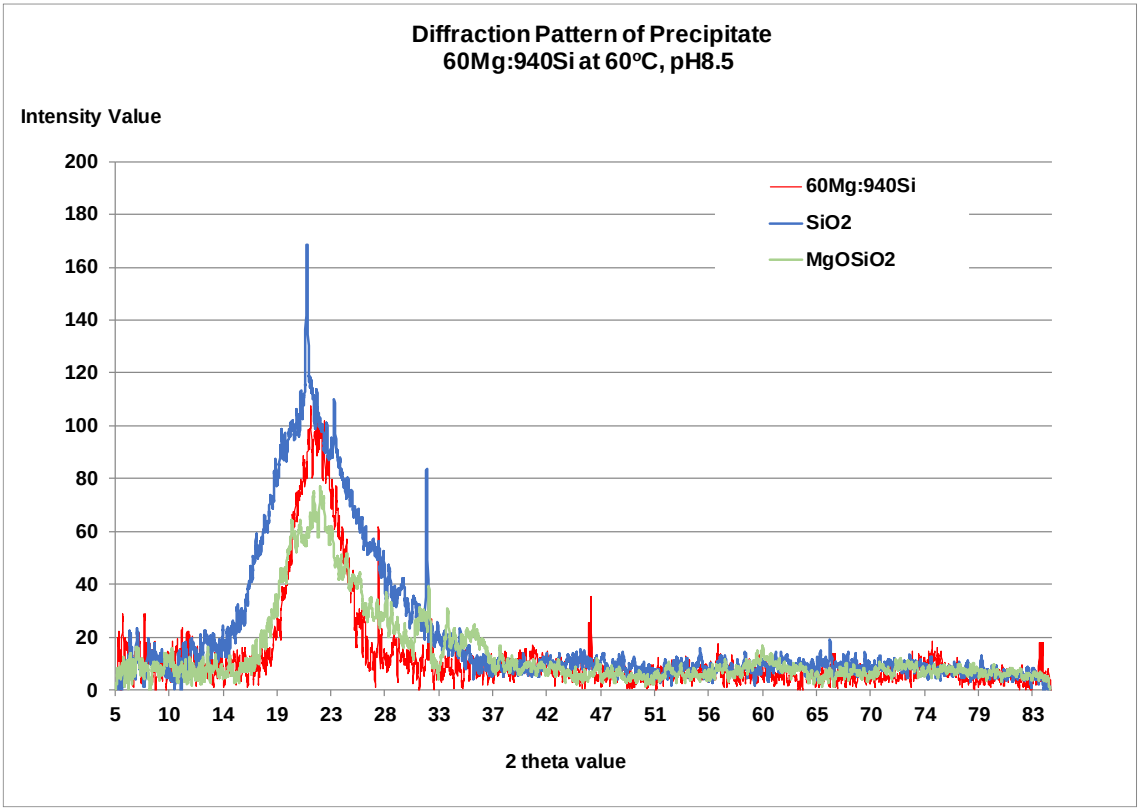

Figure 3-15 Diffraction pattern of "*worst*" base case (Blank) of 60Mg:940Si at 60ºC, pH8.5

The diffraction patterns shown in Figure 3-15 confirm the presence of amorphous silica and the amorphous form of magnesium silicate in the precipitate for this "*worst"* base case system. It is the wide peak width that reveals the clear crystal structure; if it were crystalline, then the peak will be very sharp. FTIR spectra shown in Figure 3-16 also confirmed the XRD results where peaks at ~1055 and ~790 cm^{-1} have been attributed to the presence of the amorphous silica, while peaks ~668, ~577 and ~565cm^{-1} has been demonstrated to be the identity of magnesium silicate scale. Based on empirical correlations between spectra and structure compiled by various researchers as tabulated in Table 3-2 and Table 3-3; and other works reported by various researchers as shown in Figure 3-16; confirmed the presence of Si-O-H, Si-O-Si in amorphous silica, Si-O-Si, Si-O-Mg and $MgSiO_3$ functional group and also the absence of $Mg(OH)_2$.

Table 3-2 Empirical correlations between spectra and structure

Group	Frequency in cm-1	Comments
Si—OH	3690 (free OH),	Isolated Si—OH groups on silica show a sharp band at 3750 cm-1 (McDonald, 1958)
Fluid water	3800-2750	with a shoulder around 3260 cm–1: this band feature is the same with that of simple fluid water which exists everywhere around us (Eisenberg & Kauzman, 1969)
-OH	3400-3200	3400 to 3200cm−1, are due to the symmetric and asymmetric stretching modes of the hydroxyl group (Dhaouadi et al., 2011)
Bending mode of fluid water	1600cm-1	The bending mode of fluid water, which should be seen at around 1600 cm–1, is hindered by many sharp Si-O stretching bands (Fukuda, 2012)
Bending mode of fluid water	1680	The bending modes of the adsorbed water molecules appear as a weak band around 1680cm−1 (Dhaouadi et al., 2011)
Si-OH	3585	–OH in chalcedonic quartz is mainly trapped as Si-OH by breaking the network of SiO_2 bonds; stretching band is sharp at 3585cm-1 (Kronenberg & Wolf, 1990)
O-H	3500, 1450, 2000-1800 1630	Broad band assigned to O-H stretching at 3500, 1450, 2000-1800 cm-1 and band due at 1630 cm-1 to scissor bending vibration of molecule water H_2O (Hernández-Ortiz et al., 2012)
Si-O-Si	1100 790 480	Absorption bands near 1100, 790, and 480 cm-1 are common to all silicates with tetrahedrally coordinated silicates (Hernández-Ortiz et al., 2012)
Si-O-Si	799-795	795–799 cm−1 can be assigned to the characteristics of the connection of many tetrahedron of Si–O–Si bond (Ying, 2007)
Si-O	2050-1400	Si-O stretching band (Fukuda, 2012)
Si-O-Si & Si-O-M (M=Al, Mg, Fe)	1200-950	Stretching vibrations of the Si-O-Si and Si O-M (M = A1, Mg, Fe) bridges occur (Karakassides, 1997 & 1999)
Si-O-Fe	974 967	The bond around 974 cm−1 and 967 cm−1 can be assigned to the stretching vibration of Si–O–Fe (Ying, 2007)

Table 3-3 Typical FTIR absorption peaks absorbed on magnesium hydroxide, amorphous silica, and magnesium silicate

Wavenumber cm-1	Mode	Comment
3699	-OH	Remarkable sharp and intense peak at 3699 cm^{-1} is assigned to the OH antisymmetric stretching vibration.
3440 & 1635	Stretching & bending vibration of water	The other absorption peaks at 3440 $cm^{-1}$and 1635 cm^{-1} could be due to the stretching vibration and the bending vibration of water, respectively.
1456	Bending vibration of -OH bond	The small peak at 1456 cm^{-1} is the bending vibration of OH bond.
436	Mg-O	The wide and strong absorption at 436 cm^{-1} is the stretching vibration of Mg-O.
	For $Mg(OH)_2$	(Jiang et al., 2009)
3437	stretching vibration of H_2O	3437 cm-1 is due to the stretching vibration of H_2O molecules
1632	Bending mode of fluid water	The IR band at 1632 cm-1 is due to the bending vibration of H_2O molecules
3246	Stretching vibrations of Si-OH	The shoulder at 3246 cm-1 could be assigned to the stretching vibrations of Si-OH groups in the structure of amorphous SiO_2. The presence of the Si-OH group is proved as bonded water.
1111	Si-O-Si	The very strong and broad IR band at 1111 cm-1 with a shoulder at 1188 cm-1 is usually assigned to the transverse optical mode (TO) and longitudinal optical mode(LO) of the Si-O-Si asymmetric stretching vibrations.
956	Silanol group/ Si-O-stretching vibration	The IR band at 956 cm-1 can be assigned to silanol groups. In the case of alkali silicate glasses, this band is assigned to Si-O- stretching vibrations.
800 474	Si-O-Si symmetric stretching vibration	The IR band at 800 cm-1 can be assigned to Si-O-Si symmetric stretching vibrations, whereas the IR band at 474 cm-1 is due to O-Si-O bending vibrations.
	For SiO_2	(Musić et al., 2011)
1000	Si-O stretching vibration	Amorphous magnesium silicates typically show two broad bands at about 10μm (1000cm-1) and 20μm (500cm-1) corresponding to Si-O stretching and bending vibrations. The large width of both bands results from a distribution of bond lengths and angles within the amorphous structure.
500	Si-O bending vibration	

500	Coupling of Si-O bending to the Mg-O stretching vibration Si-O-Si	The 20µm (500cm-1) band is additionally broadened due to the coupling of the Si-O bending to the Mg-O stretching vibration in this spectral region leading to a combined band of a huge width. The incorporation of Mg into the silicate network can occur in two different ways, as network former (4-fold coordination) and/or as network modifier (6-fold coordination).
800	Si-O stretching vibration (SiO_2)	The appearance of a third band at 12.5µm (800cm-1) visible in the SiO_2 spectrum, is typical for SiO_2 and disappears at a MgO content of 0.5. The band can be assigned to the symmetric stretching vibration of Si-O-Si bonds or to ring structures
1111.11 1030.93 975.61	Si-O stretching vibration **<u>For Mg-silicates</u>**	The position of the Si-O stretching vibration is shifted from 9µm (1111.11cm-1) for the pure SiO_2 to 9.7µm (1030.93cm-1) for $MgSiO_3$ and 10.25 µm (975.61cm-1) for the $Mg_{2.4}SiO_{4.4}$. (Jäger et al., 2003)

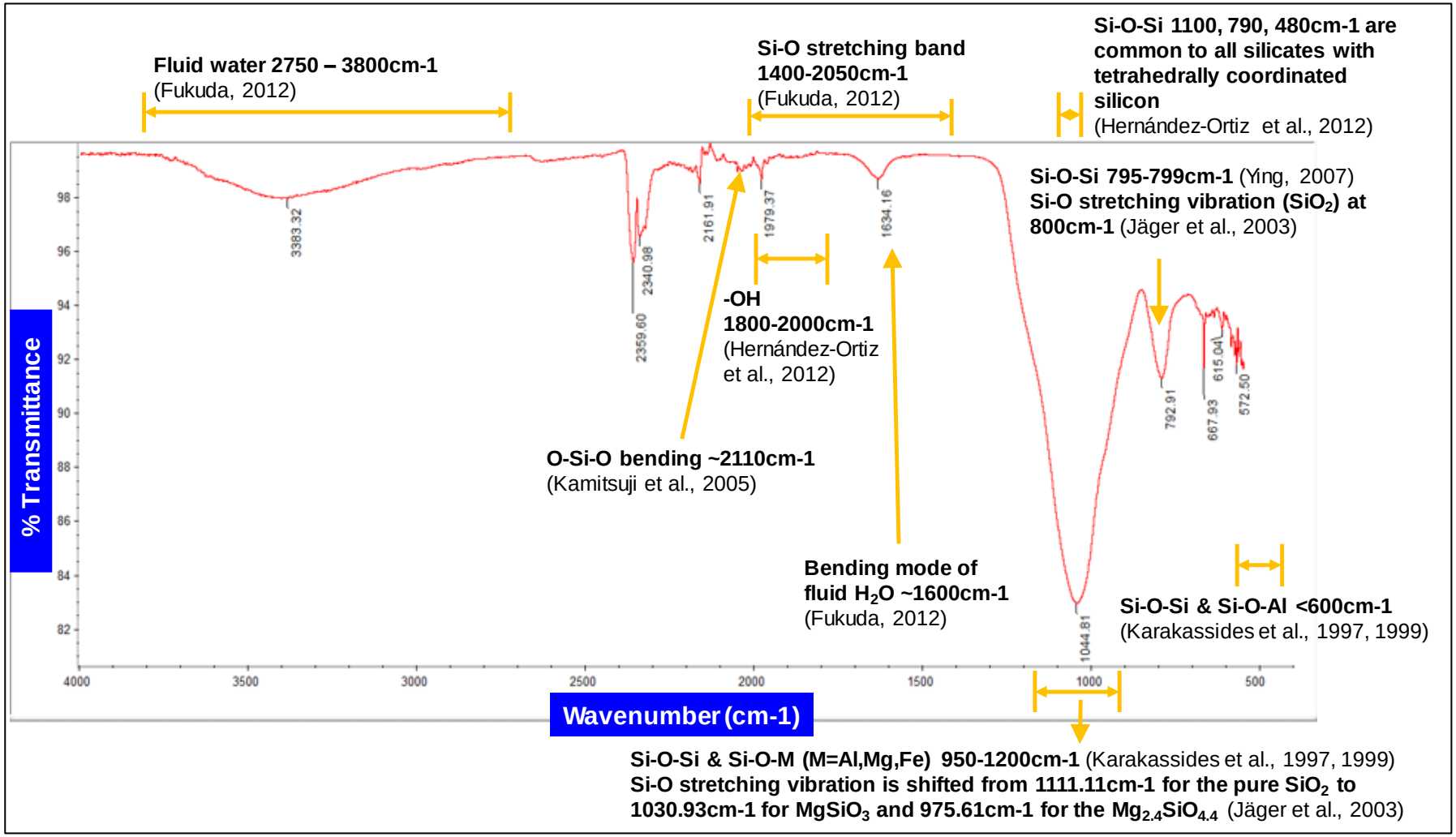

Figure 3-16 FTIR spectra of "*worst*" base case (Blank) of 60Mg:940Si at 60°C, pH8.5

3.4.3 "Intermediate" Base Case Study (60Mg:470Si at 60°C, pH8.5)

As will be shown later in Chapter 5, that the "*worst"* base case is very difficult to inhibit. Therefore, we have studied a more realistic case to allow us to find a chemical (or chemicals) that can inhibit the silicate scale. Two other base cases were developed i.e. 60Mg:470Si and 30Mg:75Si where we found the latter to be a "*manageable"* base case that can be successfully inhibited and this will be discussed in detailed in Chapter 5.

For the 60Mg:470Si case, the brine solution became slightly cloudy 1 hour after heating in the oven (the brine is left for one hour in the oven to stabilize the temperature to 60°C and this is t=0hr). The gel precipitate can be observed at 2 hour and a clear layer was observed at 22 hour. This clear layer expanded when all of the precipitate fell to the bottom of the bottle leaving a clear supernatant on top of the solution at 96 hour (see Figure 3-17).

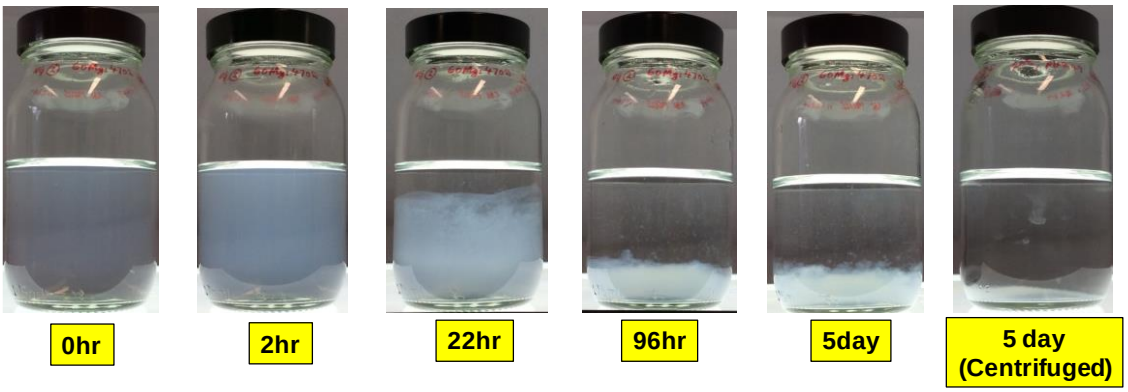

Figure 3-17 Physical observation of "*intermediate"* base case (Blank) of 60Mg:470Si at 60°C, pH8.5 (t=0 to 5 days)

The amounts of magnesium and silicon ion reacted over the reaction time in the "*intermediate"* base case are plotted in Figure 3-18(in ppm) and Figure 3-19(in %). We can see from these figures that the amount of silicon ion and magnesium ion reacted achieved equilibrium essentially after 4 days. Figure 3-19 shows the pH values recorded for the "*intermediate"* base case*;* these are reducing with reaction time; to ~pH7.9 after 5 days.

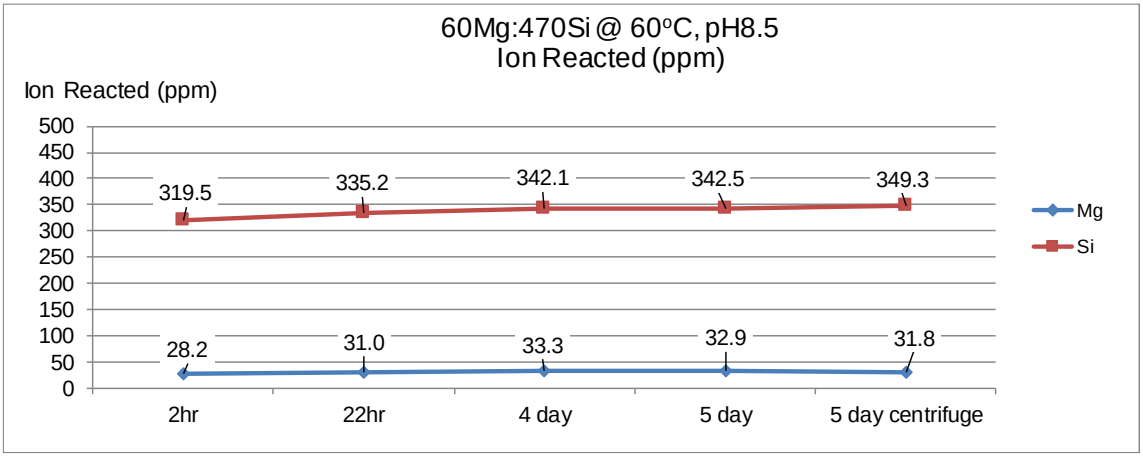

Figure 3-18 Amount of ion reacted for the "*intermediate*" base case (Blank) of 60Mg:470Si at 60°C, pH8.5 (t=0 to 5 days)

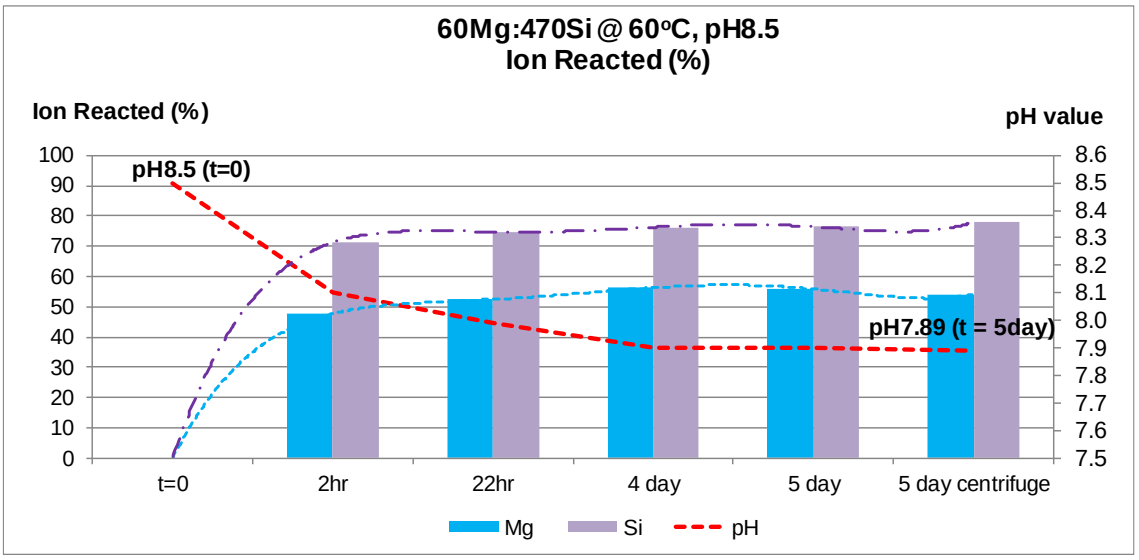

Figure 3-19 pH changes and ion reacted of "*intermediate*" base case (Blank) of 60Mg:470Si at 60°C, pH8.5 (t=0 to 5 days)

The diffraction pattern in the XRD Analysis shown in Figure 3-20 and FTIR spectra in Figure 3-21 confirmed that the silicate scale produced are the same as those found in the "*worst*" base case; i.e. the deposit is amorphous silica and amorphous magnesium silicate scale.

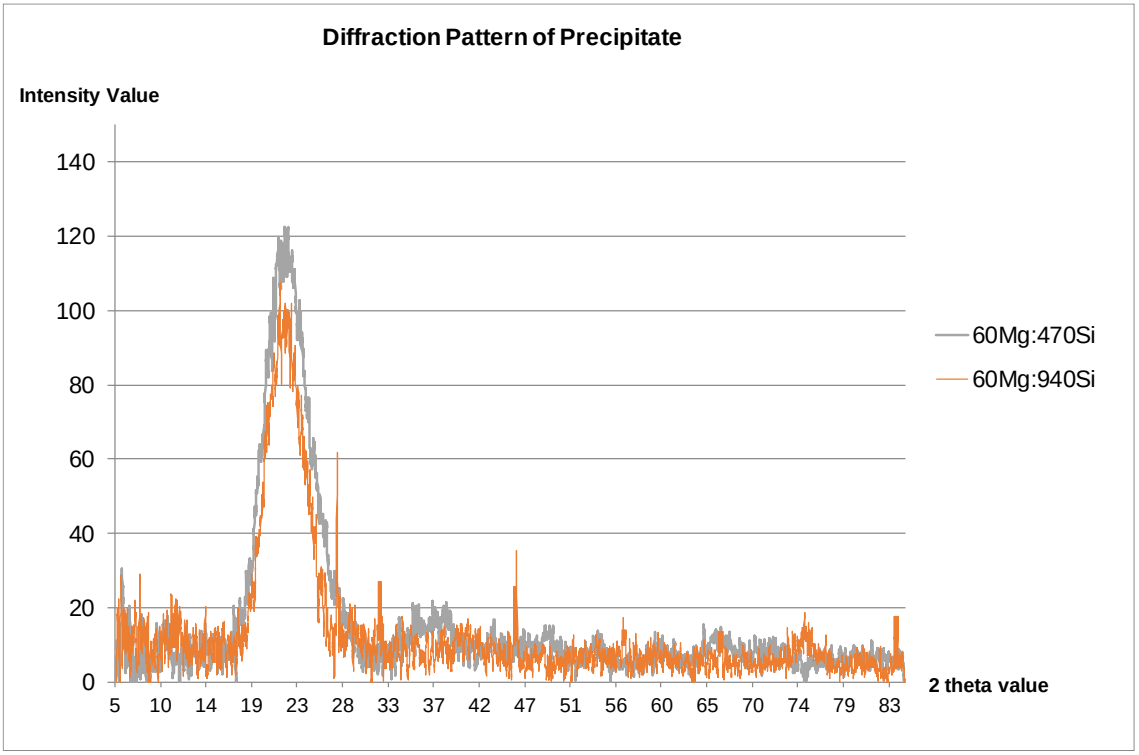

Figure 3-20 Diffraction pattern of "*intermediate*" base case of 60Mg:470Si at 60°C, pH8.5 – compare with "*worst*" base case (60Mg:940Si)

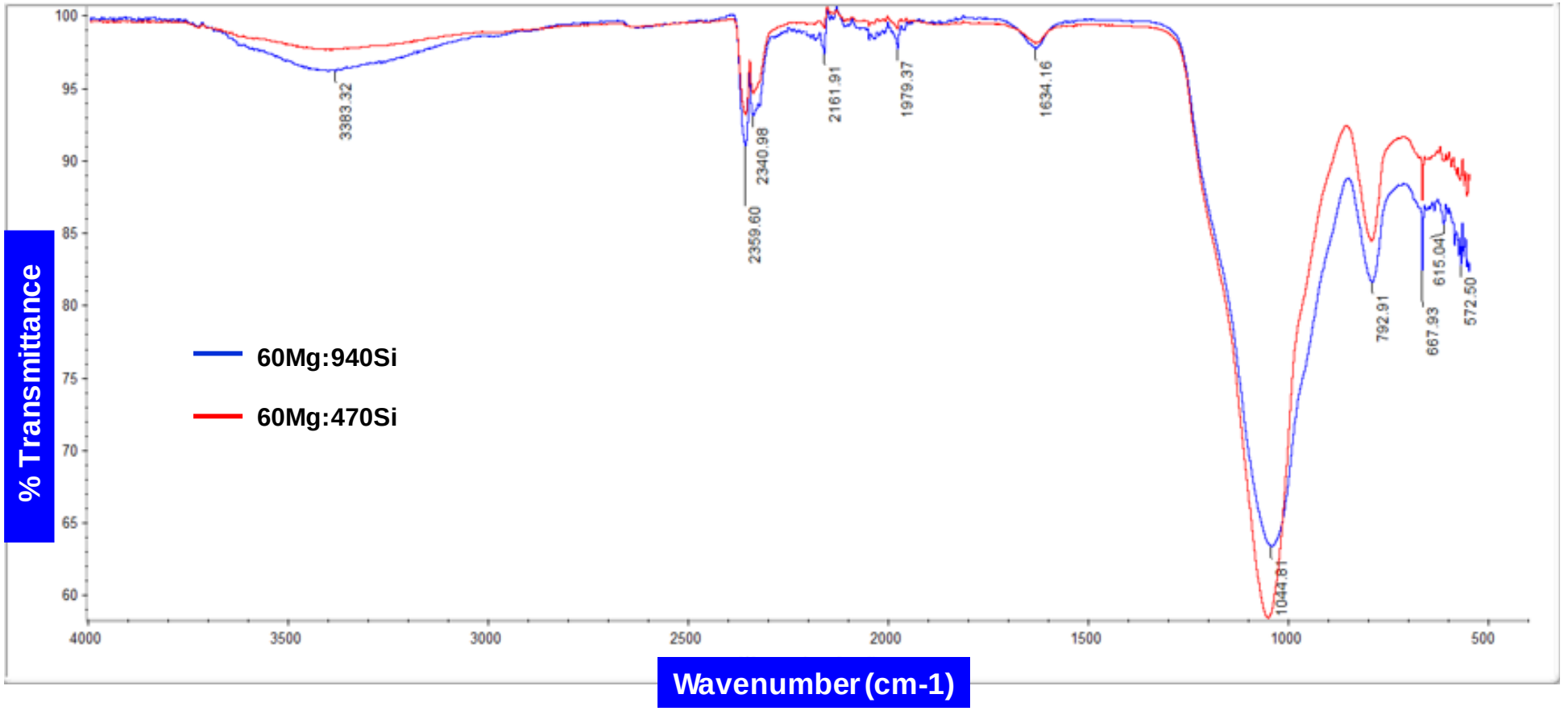

Figure 3-21 FTIR spectra for "*intermediate*" base case of 60Mg:470Si at 60ºC, pH8.5 – compare with "*worst*" base case (60Mg:940Si)

3.4.4 "Manageable" Base Case Study (30Mg:75Si at 60ºC, pH8.5)

As mentioned in 3.4.3, even the "*intermediate"* base case was found to be very difficult to inhibit as will be discussed in detail in Chapter 5. Therefore, a milder scaling "*manageable" Mg*:Si case that can be inhibited is studied. However, we note that this new case is more severe than that for some reported for some ASP oilfield conditions. Jing et al. (2013) reported that a case from the Daqing Oilfield contained 55ppm Si and 7.9, 16.5, 7.4 ppm Mg in the formation water, injection water and produced water respectively. Thus, our *"manageable"* case is much more severe than this field case. However, we show later in Chapter 5 that this case indeed be inhibited.

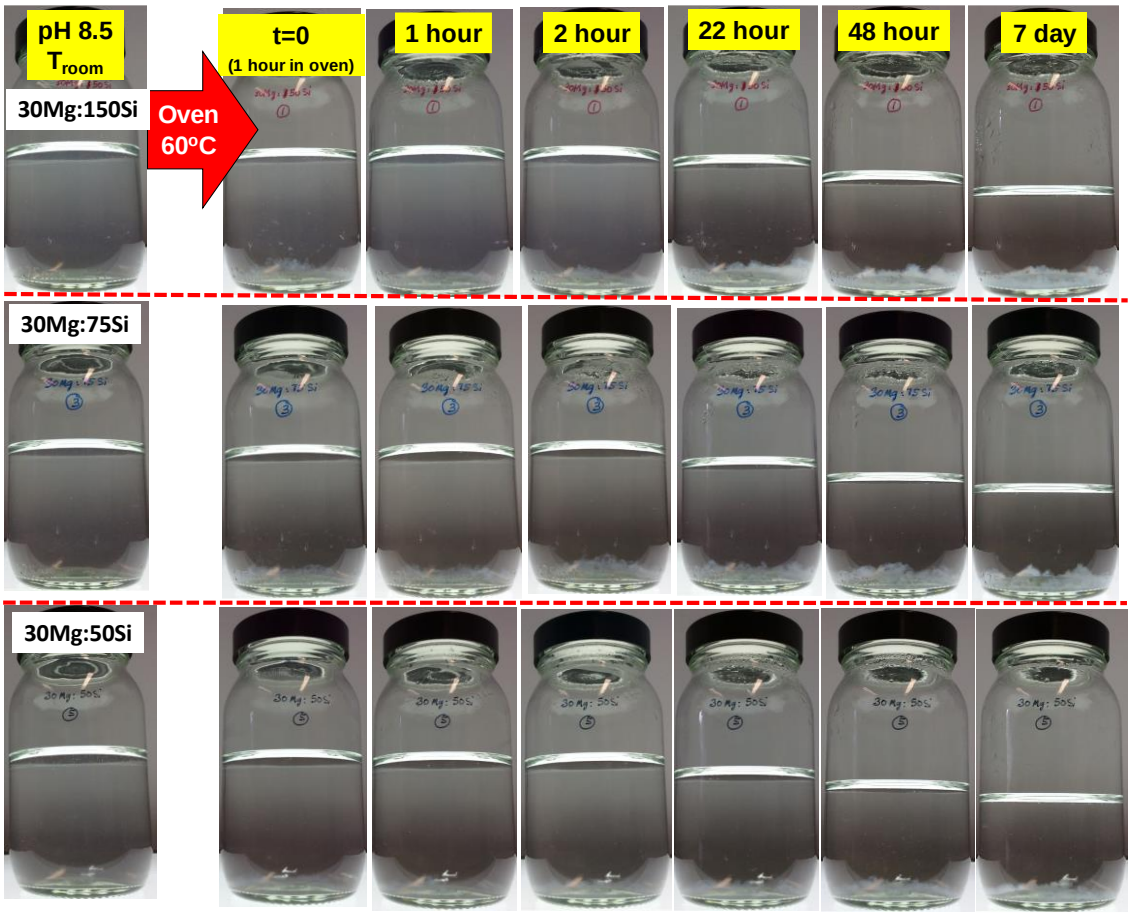

Figure 3-22 Physical observation of various silicon levels (Mg concentration is fixed at 30ppm) at 60ºC, pH8.5 in "*manageable*" base case (Blank) investigation study (t=0 to 7 days)

Therefore, three different silicate scaling brine mixes were studied; i.e. 30Mg:150Si, 30Mg:75Si and 30Mg:50Si respectively. 30Mg:50Si and 30Mg:75Si stay clear after being mixed and pH adjustment at room conditions, but the 30Mg:150Si became slightly cloudy (Figure 3-22). All of these brines produced scale as early as 1 hour after being heated at 60ºC in the oven (t=0hr).

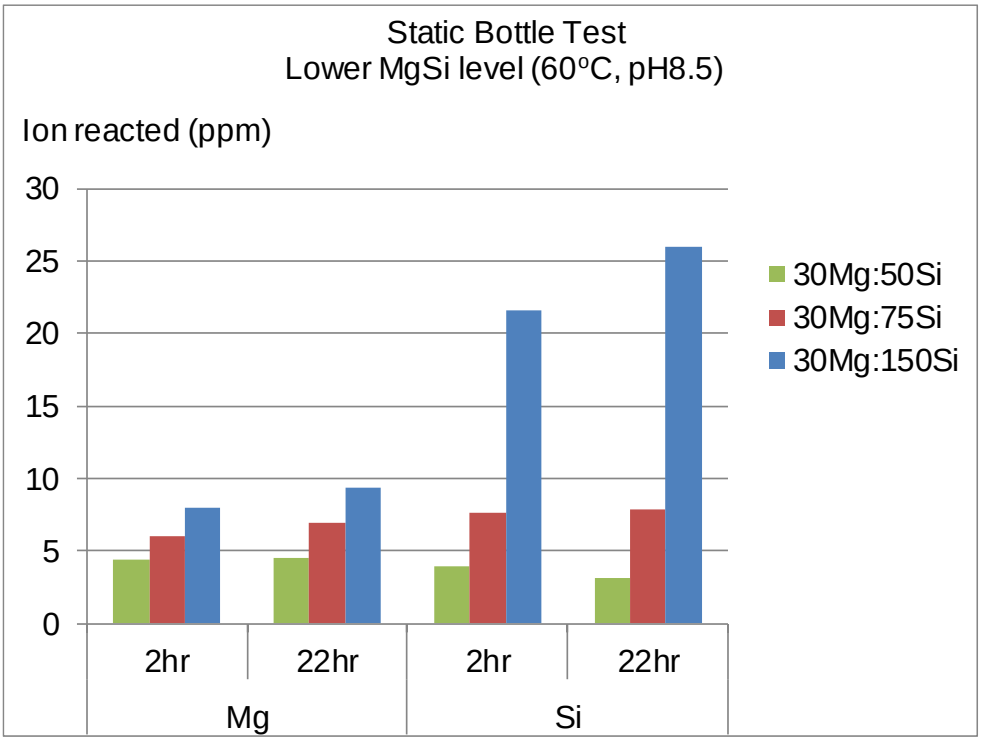

Figure 3-23 Amount of ion reacted for various silicon levels (Mg concentration is fixed at 30ppm) at 60°C, pH8.5 in "*manageable*" base case (Blank) investigation study (up to 22 hour)

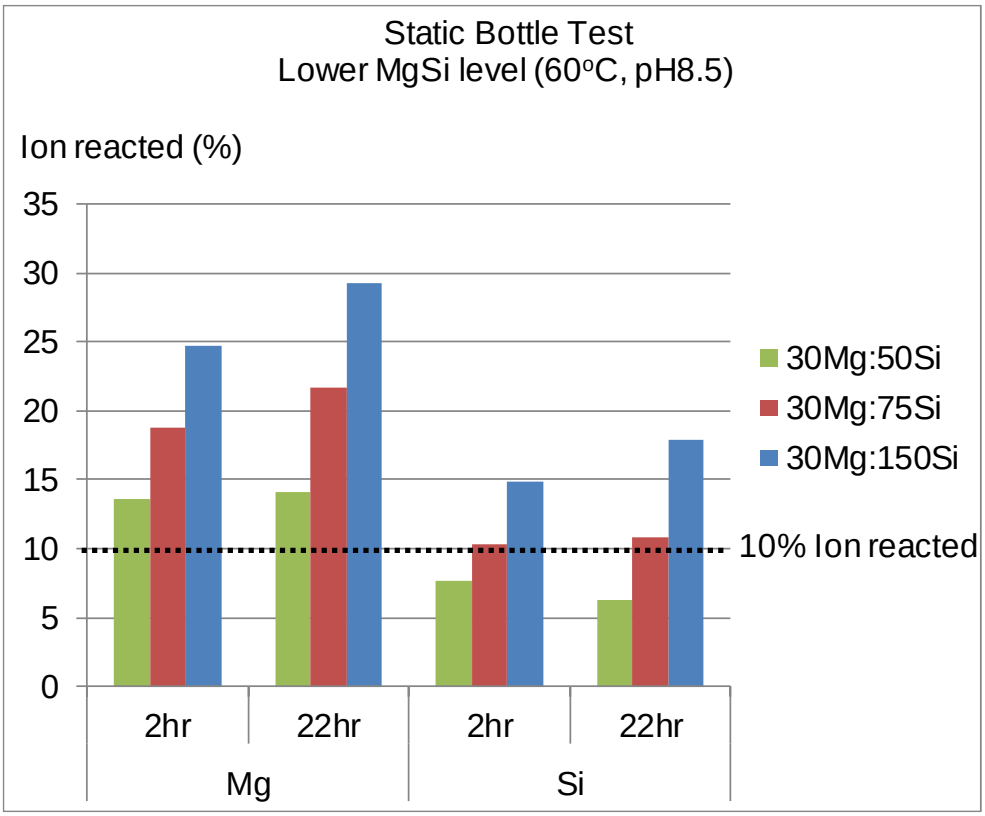

Figure 3-24 Amount of ion reacted (%) for various silicon levels (Mg concentration is fixed at 30ppm) at 60°C, pH8.5 in "*manageable*" base case (Blank) investigation study (up to 22 hour)

Figure 3-23 and Figure 3-24 show the amount of ion reacted in the three brine studied in ppm and percentage units respectively. From these figures, it can be seen that the 30Mg:75Si case resulted in about 10% and 18% of silicon and magnesium ion reacted at 2 hours respectively. This is sufficient to produce a visible and reproducible silicate scale. Hence, this brine condition (30Mg:75Si) was chosen as the "*manageable"* base case.

The Si:Mg molar ratio and pH profiles for these three brine conditions are plotted in **Figure 3-25** and Figure 3-26 respectively.

FTIR spectra shown in Figure 3-27 suggested that the scale produced in all brine solutions are almost the same as those produced in "*worst"* base case and "*intermediate"* base case; i.e. amorphous silica and amorphous magnesium silicate scale.

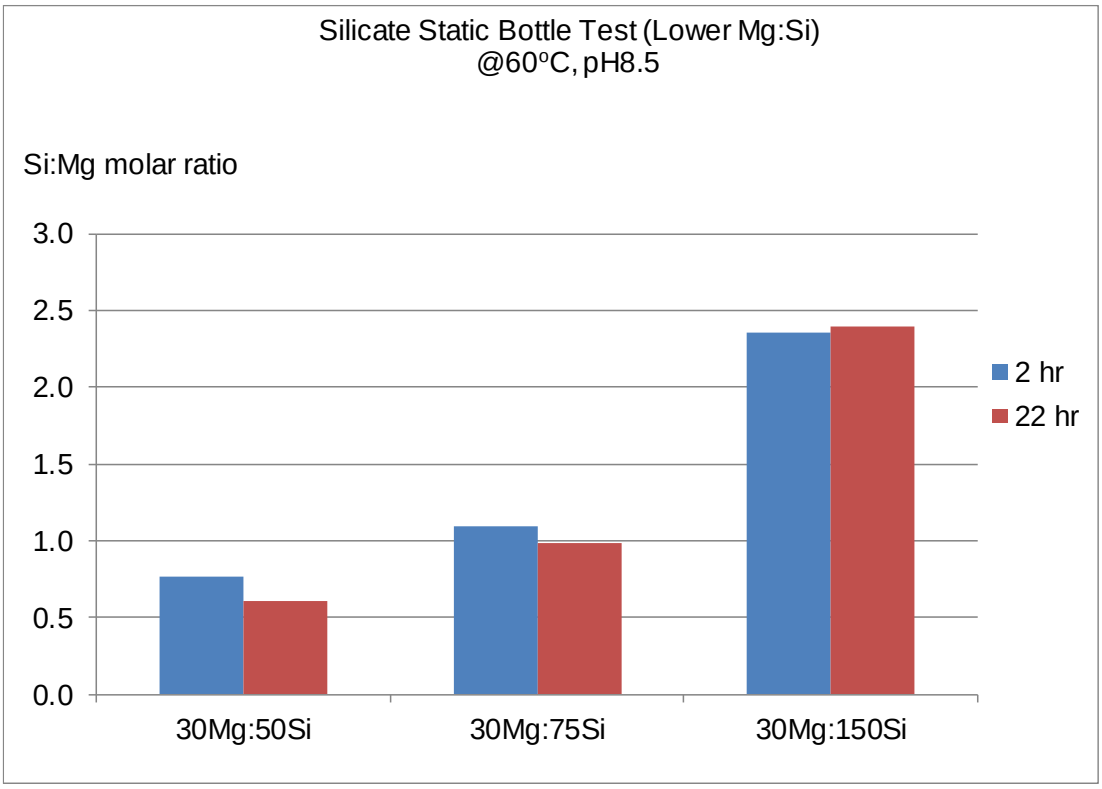

Figure 3-25 Si:Mg molar ratio for various silicon levels (Mg concentration is fixed at 30ppm) at 60°C, pH8.5 in "*manageable*" base case (Blank) investigation study (up to 22 hour)

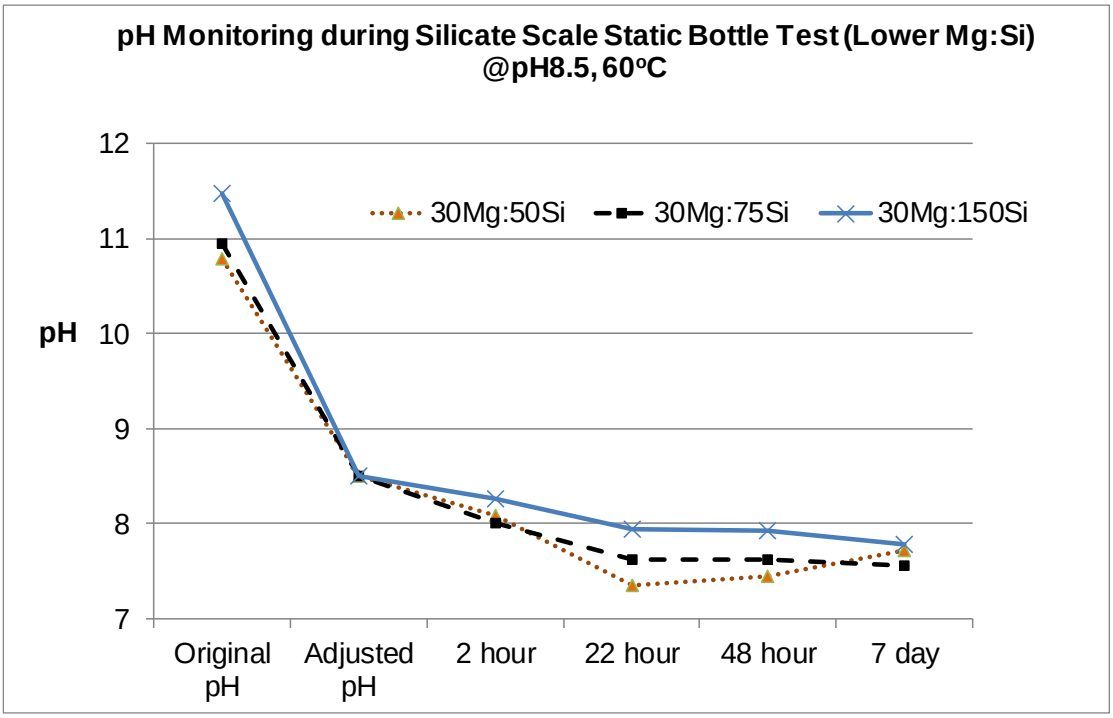

Figure 3-26 pH profile for various silicon levels (Mg concentration is fixed at 30ppm) at 60°C, pH8.5 in "*manageable*" base case (Blank) investigation study (up to 7 day)

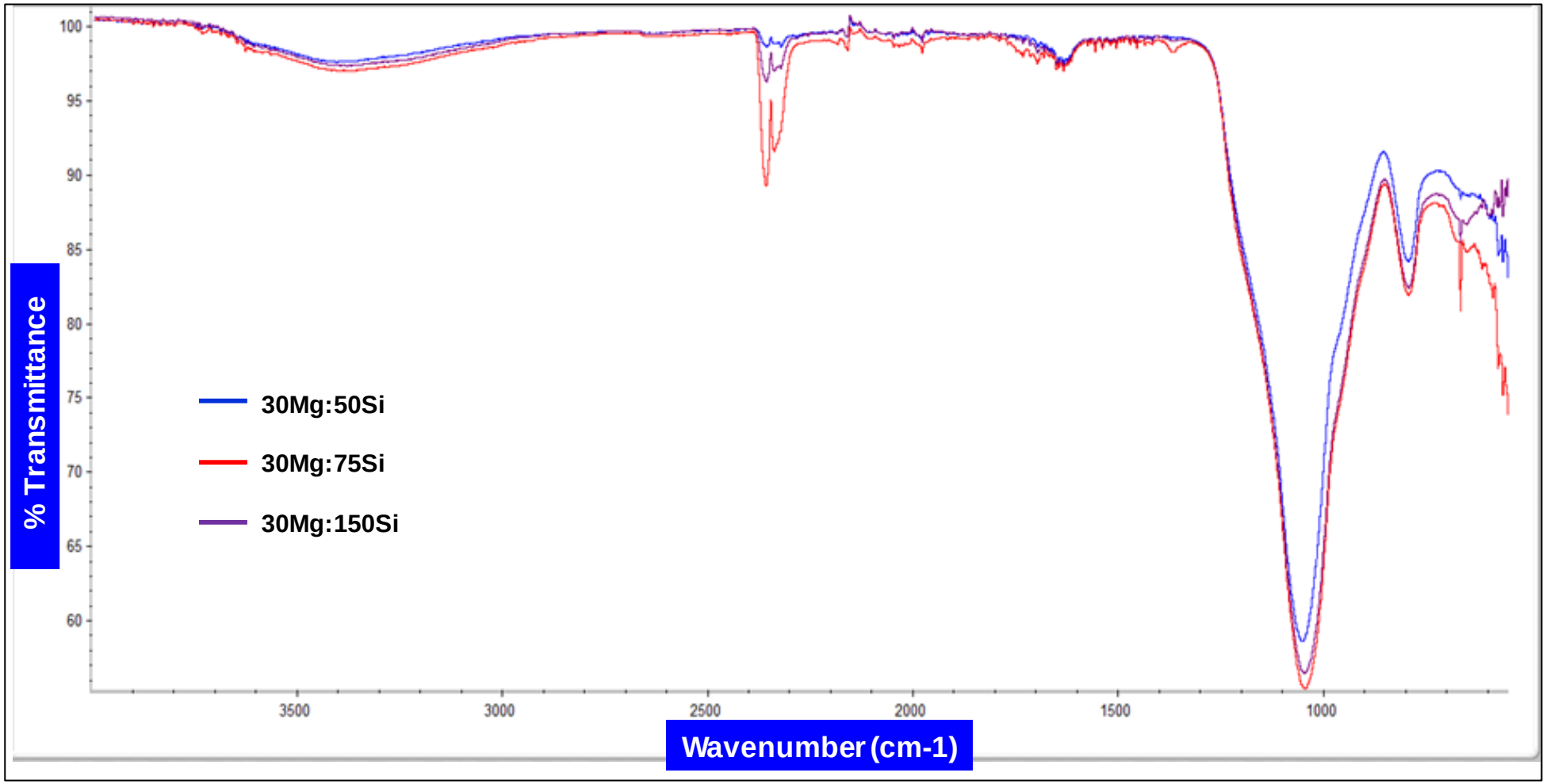

Figure 3-27 FTIR spectra for various silicon levels (Mg concentration is fixed at 30ppm) at 60ºC, pH8.5 in "*manageable*" base case (Blank) investigation study

3.5. SUMMARY AND CONCLUSIONS

The first objective of this thesis was to establish a quantitative, accurate and reproducible methodology for forming silicate scale in the laboratory. Our intention was to replace earlier more qualitative tests that did not characterize the silicate system very well. A much more quantitative silicate scaling test methodology has been developed in this work. ICP analysis of Mg and Si level in the test brine mixes are monitored from the initial conditions, over time until some final test time, usually 22 hours, but in some cases up to 8 days. This method is supplemented by using over other spectroscopic characterization methods on the silicate scale deposits themselves, such as ESEM/EDAX, FTIR and XRD.

This experimental method has been used to identify three "base cases" which are designate as a *"worst"* case, an *"intermediate"* case and a *"manageable"* silicate scaling case. These cases are defined by their initial Mg and Si compositions in the brine mix as follows:

- *"worst"* silicate scaling case, 60Mg:940Si (60ppm of Mg and 940ppm of Si in the initial brine mix);
- *"intermediate"* silicate scaling case, 60Mg:470Si;
- *"manageable"* silicate scaling case, 30Mg:75Si.

The reason for developing these 3 cases was that the *"worst"* and *"intermediate"* case were found to be too difficult for current silicate inhibitors/ dispersants to completely inhibit. However, these case yielded more silicate deposits in the experiments and they are very useful to establish the effect of various parameters (T, pH, etc.) on the stoichiometry and form of the silicate scale which were formed. The *"manageable"* silicate scaling case, as the name suggests, was found to one which could be completely inhibited by some (certainly not all) potential silicate inhibitors/ dispersants. This *"manageable"* case was still more severe than some field reported cases in terms of the silicate scaling tendency or severity (Jing et al., 2013).

Having established that well characterized and reproducible results can be obtained to produce a silicate scale, then this allows us to develop a scale inhibitor test method and this will be described in Chapter 5.

CHAPTER 4. INITIAL SILICATE STUDIES AND SENSITIVITIES

INTRODUCTION

In this chapter, a preliminary study of silicate scaling during chemical EOR, or other reservoir processes, is presented. Some preliminary laboratory results are presented on the development of silicate scaling where our first objective is to develop a bulk (bottle) test for first forming silicate scales in a reproducible manner and then for testing silicate scale "inhibitors" or dispersants. In this laboratory work, the aim was to produce silicate scale as the test scale or "the blank" scale for all tests.

This chapter gives a detailed description of all the initial experimental work carried out where various concentrations of magnesium brine were introduced to the silicon brine. The brines were mixed in a 50:50 mixing ratios in static bottle tests to give final mixed concentrations of magnesium ion ranging from [Mg] = 450ppm to 1200ppm for ***High Mg Test***; 45ppm to 120ppm for ***Low Mg Test*** and a fixed silicon (as element) concentration of [Si] ~1000ppm. The test was conducted at room temperature and left to react for 22 hours. The ion concentrations (Si and Mg) remaining in solution were quantified by sampling them using ICP analysis at 2 hours and 22 hours, in a manner well established in barium sulphate inhibition efficiency (IE) tests.

In *High Mg Tests*, it was observed that the mixture gave a cloudy solution immediately after mixing and that eventually three distinct layers could be observed in the test bottles after 22 hours. Therefore, the 22 hour sampling was performed taking samples from ***three*** levels in the bottles and the ICP values showed that these Mg/Si concentration can be different at each level. ESEM analysis was also carried out on the deposits in order to examine their crystal morphology and also their elemental composition using EDAX. The ESEM analysis shows that the silicate scales formed in our experiments were all amorphous in nature (not crystalline). The amorphous silicate is dispersed in the solution and settles to the bottom of the bottle by gravity. This resulted in the final concentrations of both Mg and Si ions being higher in the lower section of the bottles compared to the upper position after 22 hours mixing. Hence, a careful and well defined sampling technique for ICP must be used, probably by taking the supernatant at appropriate positions. For an initial Si:Mg less than 1 (Mg in excess), the atomic ratio of Si:Mg in the amorphous Mg silicate is ~1. However, when the initial Mg ion is in excess

(Si:Mg≥1), the atomic ratio of Si:Mg in the precipitate is ~1.3. This result was found consistently for the solution ICP *ion reacted* results and in the independent ESEM/EDAX results on the actual precipitate.

Later, we will also show that results obtained from ***Low Mg Test*** revealed the high pH solution stability such as silicon brine and quenching solution related to the usage of glass container. A detailed discussion of the issues which arose in developing the experimental methodology is presented in this chapter. Finally, further study of the silicate system sensitivities is presented i.e. the effects of pH, temperature, initial Si:Mg molar ratio and the ageing brine are reported here in order to develop a better understanding on the occurrence and prevention of silicate scales.

4.1. FIRST RESULTS FOR HIGH MAGNESIUM CONCENTRATION

4.1.1 Experimental Setup for Initial Silicate Study

As a starting point to initiate our programme of work on silicate formation and inhibition, an experiment was set up to repeat some of the results reported by Arensdorf et al. (2010) who studied the static and dynamic testing of silicate scale inhibitors. However, this test was modified by taking a brine containing only magnesium ions to represent the connate brine (formation water). The other brine only contained silicon (as silicate) to represent the leachate by the ASP water (or other reservoir process forming silicate in the reservoir). The objective of these preliminary experiments is to establish that we can reproduce a silicate scale in the laboratory so that we can study its formation and inhibition. The actual scale we are trying to form in these experiments is magnesium silicate. In these experiments, we also want to quantify the severity of the magnesium silicate scale formed; there are no commercially available (or even research stage) silicate scale prediction models to help us in this task. Essentially, we formed the magnesium silicate scale by mixing the silicon brine (Si Brine) with the magnesium brine (Mg Brine) in a 50:50 ratios at room temperature as shown in Table 4-1. The magnesium and silicon brines were prepared by dissolving appropriate quantities of salts (Magnesium chloride hexahydrate, $MgCl_2.6H_2O$ and sodium metasilicate pentahydrate, $Na_2SiO_3.5H_2O$) in distilled water with the compositions given in Table 4-2.

50ml samples of the Mg Brine were prepared in order to achieve a range of final mixed concentrations from 450ppm to 1200ppm while the 50ml Si Brine was fixed at ~1000ppm (initial Si concentration were actually measured and ranged between 1015 to 1080ppm by ICP analysis). 50ml of magnesium brine was added to 50ml of silicon brine in a glass bottle before being left to react on the lab bench for 22 hours. The original and final pH values of all brines were measured and their values are reported in Table 4-3.

The mixed solutions of Mg brine and Si brine were visually inspected and samples for ICP analysis were taken at 2 hours and 22 hours. In order to stabilise the samples in conventional scaling studies we must have a "quenching solution". For the silicate mixed brine stabilisation, two different quenching solutions were prepared for ICP analysis, viz. KCl/PVS and EDTA/NaOH. All 16 samples bottles (as shown in Table 4-4) were observed for any changes and photos were taken where appropriate. As noted above, we intend to establish the severity of the silicate scale formed as well as to establish its stoichiometry in a quantitative manner. In the previous work of Arensdorf et al., the silicate scale severity was determined qualitatively by measuring the turbidity using a spectrophotometer. Sonne et al. (2012) carried out a similar study to test the severity of the silicate scales formed by enhancing the static testing method proposed by Arensdorf et al. Sonne et al. still measure the silicate scale formed qualitatively. In their work, they improved the experimental procedure by measuring the turbidity using an optical scanning device which is able to measure the light transmission at multiple locations. By doing this, more comprehensive data can be generated.

Table 4-1 Initial condition of various silicate system tested at T_{room}, natural pH

Test condition **High Mg**	**Initial** condition of 50:50 mixed brine of SB:MB						
	Ion (ppm)		Ion (molar) $x10^{-3}$		Initial molar ratio $(Si:Mg)_o$	Initial mixed brine pH, pH_o	**Initial supersaturation relative to amorphous silica**
	Mg	Si	Mg	Si			
1	**447**	1015	18.625	36.140	**1.94**	12.25	16.062-17.347
2	**640**	1024	26.670	36.460	**1.37**	11.10	16.204-17.501
3	**948**	1080	39.500	38.450	**0.97**	9.92	17.091-18.458
4	**1188**	1050	49.500	37.386	**0.76**	9.70	16.616-17.946

Table 4-2 The brine composition and preparation

Ion	Concentration {ppm (mg / L)}	Formula Composition	g / L	g / 5L	g / 10L	g / 15L	g / 20L
Mg^{2+}	900	$MgCl_2.6H_2O$	7.53	37.63	75.26	112.89	150.52
Mg^{2+}	1200	$MgCl_2.6H_2O$	10.03	50.17	100.35	150.52	200.69
Mg^{2+}	1800	$MgCl_2.6H_2O$	15.05	75.26	150.52	225.78	301.04
Mg^{2+}	2400	$MgCl_2.6H_2O$	20.07	100.35	200.69	301.04	401.38
Si	1880	$Na_2SiO_3.5H_2O$	14.20	71.00	142.00	213.00	284.00

Table 4-3 Natural pH of brines, mixed brine and quenching solutions

Solution	Natural pH
Mg Brine 900ppm	6.12
Mg Brine 1200ppm	6.36
Mg Brine 1800ppm	6.39
Mg Brine 2400ppm	6.56
Si Brine 2049ppm	12.87
Quenching Solution 1% EDTA/NaOH	13.30
Quenching Solution KCl/PVS	8.06*
50:50 Mixed solution	11.82

*Adjusted using 10%HCl and concentrated NaOH Solution

Table 4-4 The 16 solutions test condition of [Mg^{2+}] and fixed [Si] of ~1000ppm in the mixed solution

Bottle No.	Quenching solution	Final Mix Mg concentration / ppm
1	KCl/PVS	450
2	KCl/PVS	450
3	KCl/PVS	600
4	KCl/PVS	600
5	KCl/PVS	900
6	KCl/PVS	900
7	KCl/PVS	1200
8	KCl/PVS	1200
9	1% EDTA/NaOH	450
10	1% EDTA/NaOH	450
11	1% EDTA/NaOH	600
12	1% EDTA/NaOH	600
13	1% EDTA/NaOH	900
14	1% EDTA/NaOH	900
15	1% EDTA/NaOH	1200
16	1% EDTA/NaOH	1200

4.1.2 Results and Discussion

(a) Physical Observations

In this chapter, a range of measurements were analysed to calculate the severity of the silicate scaling in the blank case (no inhibitor). Silicate scales were formed for a range of magnesium concentrations as listed in Table 4-4.

When analysed by ICP, the actual initial concentrations of the magnesium and silicon concentration varied somewhat from the initial target concentrations by less than 9% and 16% respectively. Note that initial target for magnesium ion concentration in the mixed solution are [Mg] ~ 450, 600, 900, and 1200ppm while the silicon target concentration is [Si] ~1000ppm.

It was observed that all bottles became cloudy immediately after mixing the two brines as can be seen in Figure 4-1. After 2 hours of mixing, three distinct layers can be seen in the test bottles, as follows – a clear solution at the top, a cloudy solution in the middle and a sediment layer at the bottom. This sediment layer is particularly noticeable for the higher magnesium concentrations at 900ppm and 1200ppm (see Figure 4-2). The initial ICP sampling at 2 hours was taken as per standard procedure for the $BaSO_4$ inhibition efficiency test, slightly below the surface, i.e. in the cloudy solution.

In these static bottle tests, the pH of the initial magnesium brine was found to be in the range pH 6.12 to 6.56 while the pH of the silicon brine was found to be 12.87 to give the mixed solution pH of 11.82 (see Table 4-3).

After 22 hours of mixing, it was seen that the clear layer had expanded and the cloudy and sediment layers were smaller, especially for the higher magnesium concentrations (900ppm and 1200ppm) as shown in Figure 4-3. It is worth mentioning that the 22 hour ICP sampling was taken at three different positions at the top, middle and bottom of the bottle (see Figure 4-4). This step was required to determine whether there were differences in [Mg] and [Si] (from ICP) measured at different positions before a final sampling technique could be established.

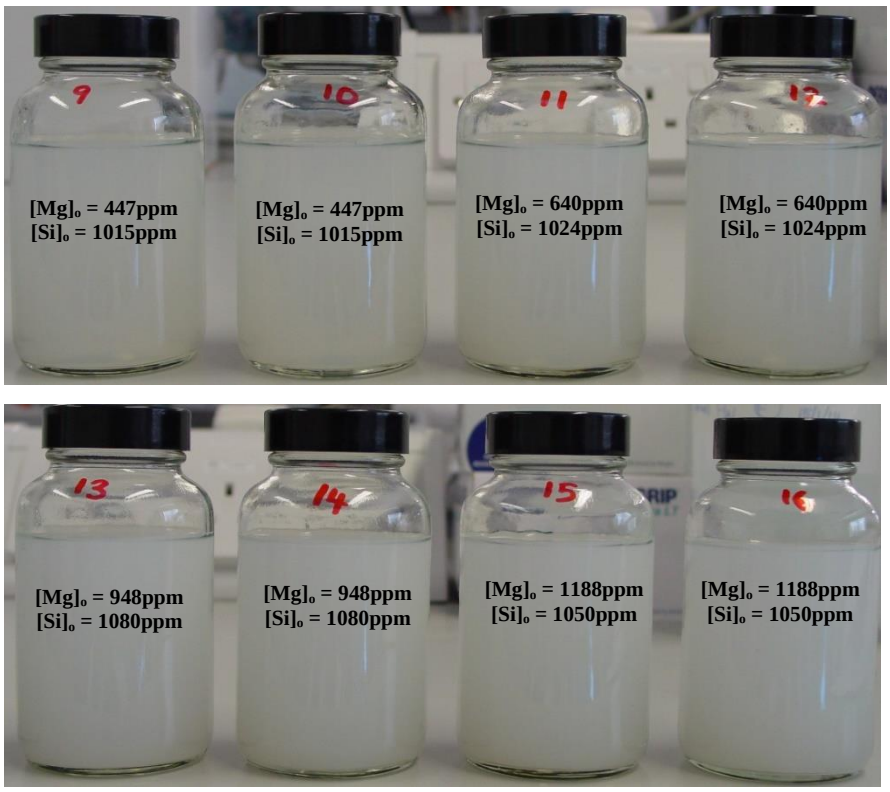

Figure 4-1 Mixed Mg brine and Si brine solution immediately after mixing (time = 0 hour). Note that the concentration values are the initial actual concentration in mixed solution

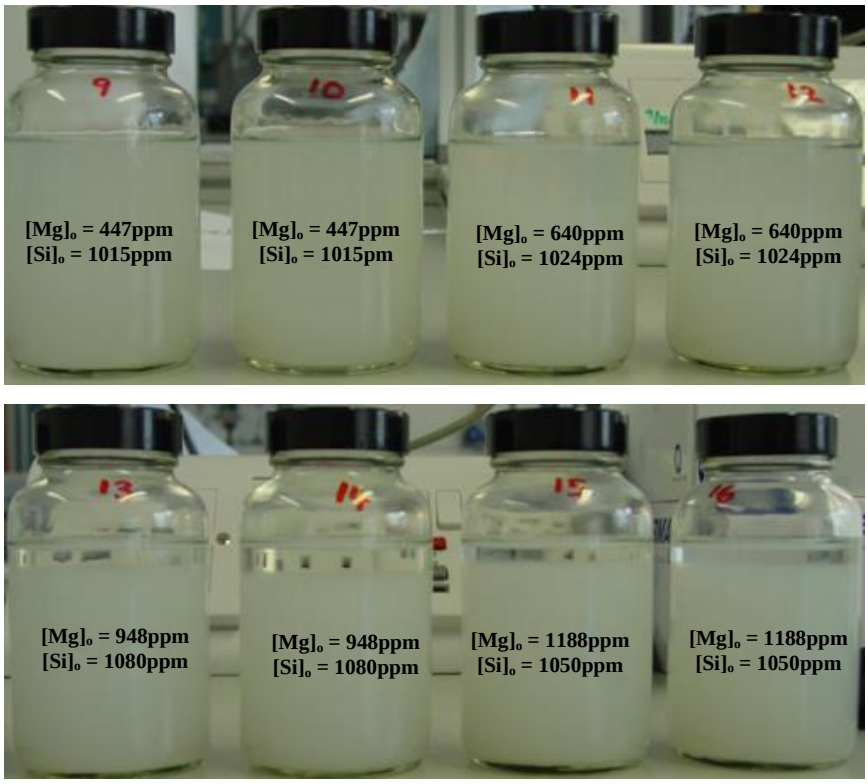

Figure 4-2 Mixed Mg brine and Si brine solution after 2 hours mixing (time = 2 hour)

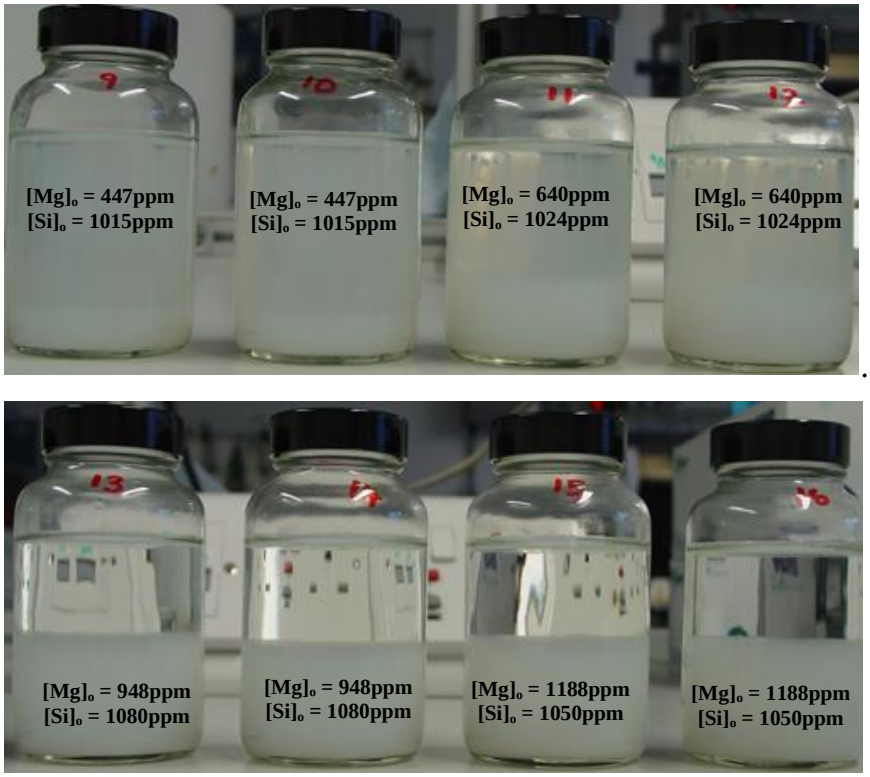

Figure 4-3 Mixed Mg brine and Si brine solution after 22 hours mixing (time = 22 hour)

Several problems were encountered while measuring the concentrations using the ICP due to the colloidal nature of these silicate solutions. The ICP machine experienced blocks in the nebulizer which caused delays in the analysis schedule. After 7 days, the samples quenched in KCl/ PVS solution had changed in turbidity indicating that some reaction had occurred either within the samples itself or between the sample and the quenching solution. Possibly the KCl/PVS (at pH ~8) was not suitable for the system as the mixed solution experienced a further reduction in pH value that may have promoted the polymerization of monomeric silica (pH of the mixed solution is 11.82). Hence, it was decided to discontinue with the KCl/PVS quenching solution and only use the 1% EDTA/NaOH quenching solution.

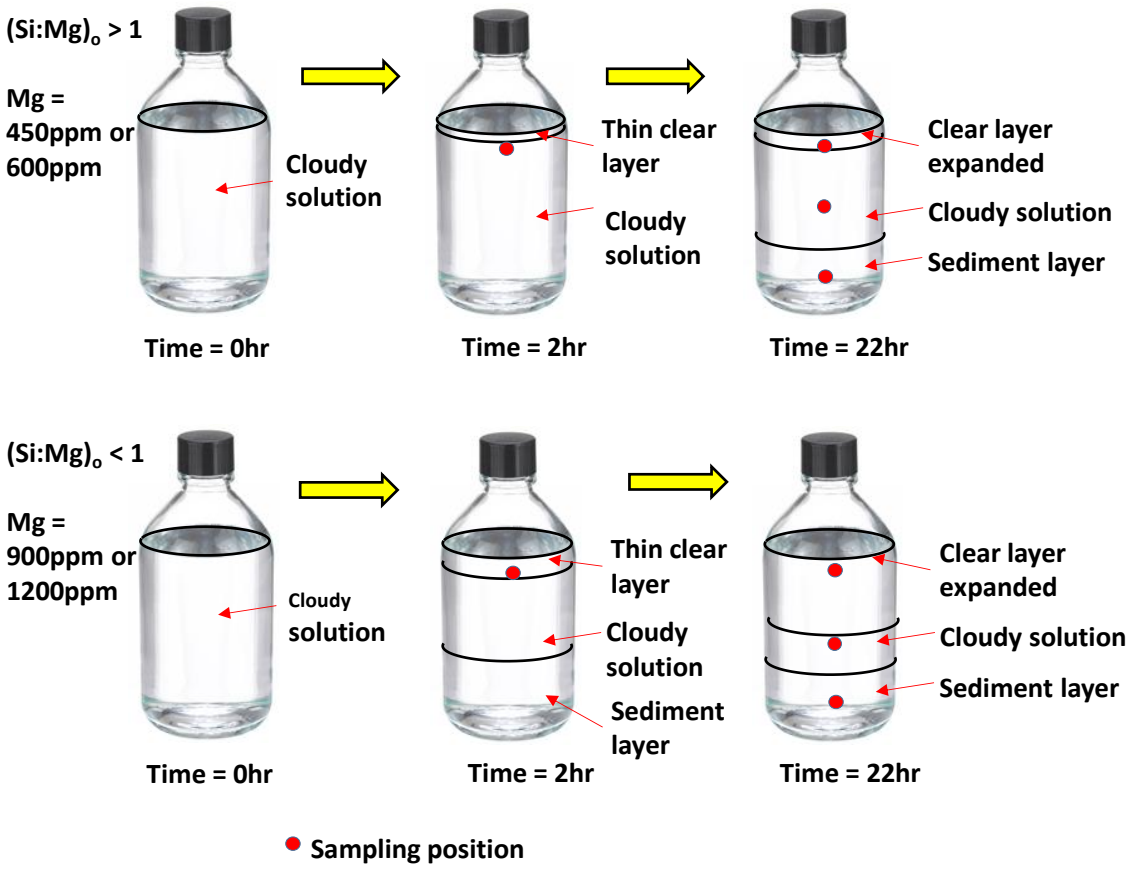

Figure 4-4 ICP sampling position – direct sampling technique (High Mg concentration of 450-1200ppm)

(b) ICP Analysis

The [Mg] and [Si] remaining in the system after 2 hours and 22 hours mixing were measured by sampling and analysing them by ICP. The two hour ICP samples were taken from the middle position of the bottle while the 22 hours samples were taken at three positions as shown in Figure 4-4.

For the 22 hours samples, the middle and bottom positions give cloudy solutions in the quenching solution matrix. This became a problem for the ICP machine as it blocked the nebulizer and the machine stopped analysing these samples. Hence, the samples were re-prepared by taking only the supernatant to be analysed by ICP.

The "*ion reacted"* value for the Mg and Si ions is defined in the same way as described earlier as per equation 3.1. Figure 4-5 and Figure 4-6 show the *ion reacted* values for Mg and Si, respectively, as a function of the (average) measured initial [Mg] values in the samples; initial [Mg] = 446.5ppm, 640.4ppm, 948ppm and 1187.7ppm. Also shown on

these figures is the actual (ICP measured) initial [Si] for each Mg level which should all be equal in this experiment (although they show a little variability); initial [SI] = 1014.9ppm, 1023.8ppm, 1080.0ppm and 1050.1ppm corresponding to the [Mg] order above. For the "*ion reacted*" value of [Mg] (Figure 4-5) and [Si] (Figure 4-6), there is *one* result at 2 hours since a single sample was taken (from the middle cloudy region) and *three* results at 22hours referring to the various levels within the bottle at which samples were taken, i.e. top, middle and bottom (Figure 4-4).

Results in both Figure 4-5 and Figure 4-6 show that the 22 hours upper sampling position give the highest values of magnesium and silicon *ion reacted* for all test conditions. Note that this is the clear region of the solution where there is no cloudiness (colloidal silicate or precipitate) and this is as we might expect. The maximum amount of ion reacted is expected in this clear (top) region since the lower samples at 22 hours (middle and bottom) are actually collecting both the solution plus some of the already formed colloidal silicate or precipitate. Thus, these lower apparent amounts of ion reacted are observed because of this "contamination" by already formed magnesium silicate. This indicated that it was important to carry out the sampling at the different levels in the bottle or this result would be masked.

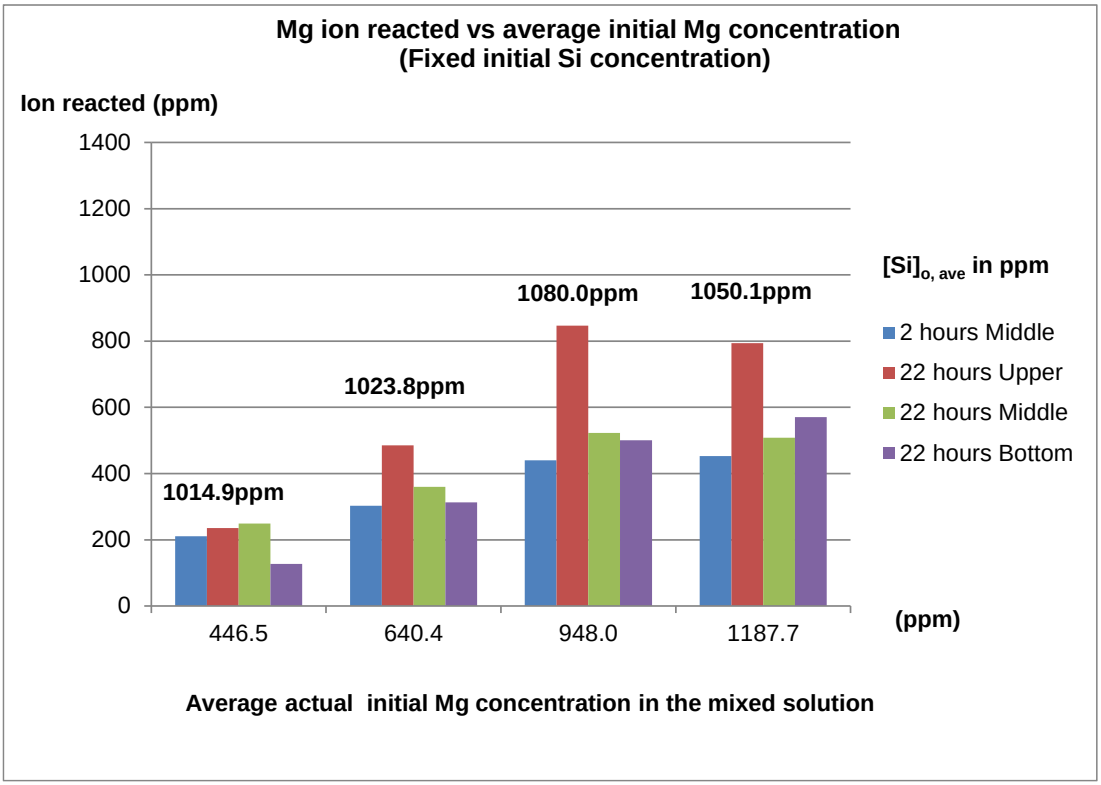

Figure 4-5 Magnesium *ion reacted* after 2 hours and 22 hours sampling

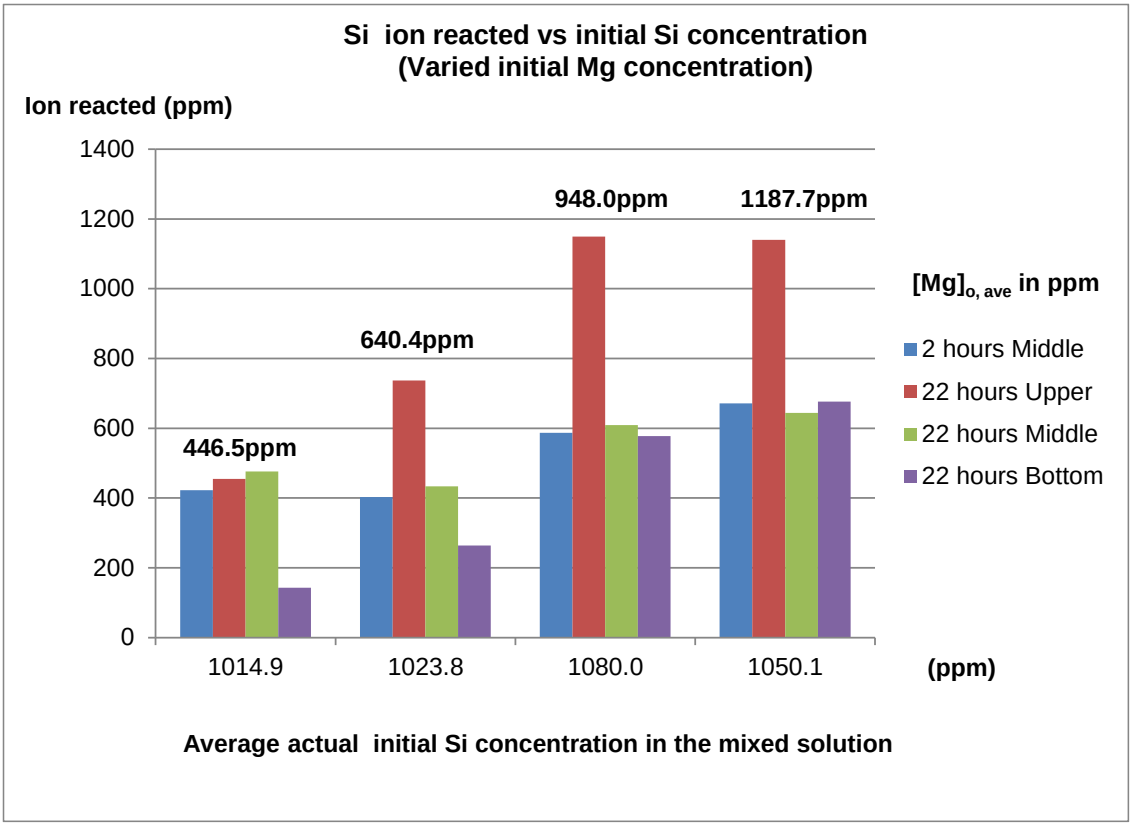

Figure 4-6 Silicon *ion reacted* after 2 hours and 22 hours sampling

Exactly the same data as shown in Figure 4-5 and Figure 4-6 are plotted in terms of the Molar concentrations in Figure 4-7 and Figure 4-8.

From the molar results in Figure 4-7 and Figure 4-8, we can calculate the effective stoichiometry – i.e. the Si:Mg molar atomic ratio in the silicate precipitate – for each set of experimental conditions. The stoichiometry of the silicate precipitate from the ICP measurements is shown in Figure 4-9 in terms of the Si/Mg molar atomic ratio; corresponding measurement by ESEM/EDAX also shown in this figure, as discussed below.

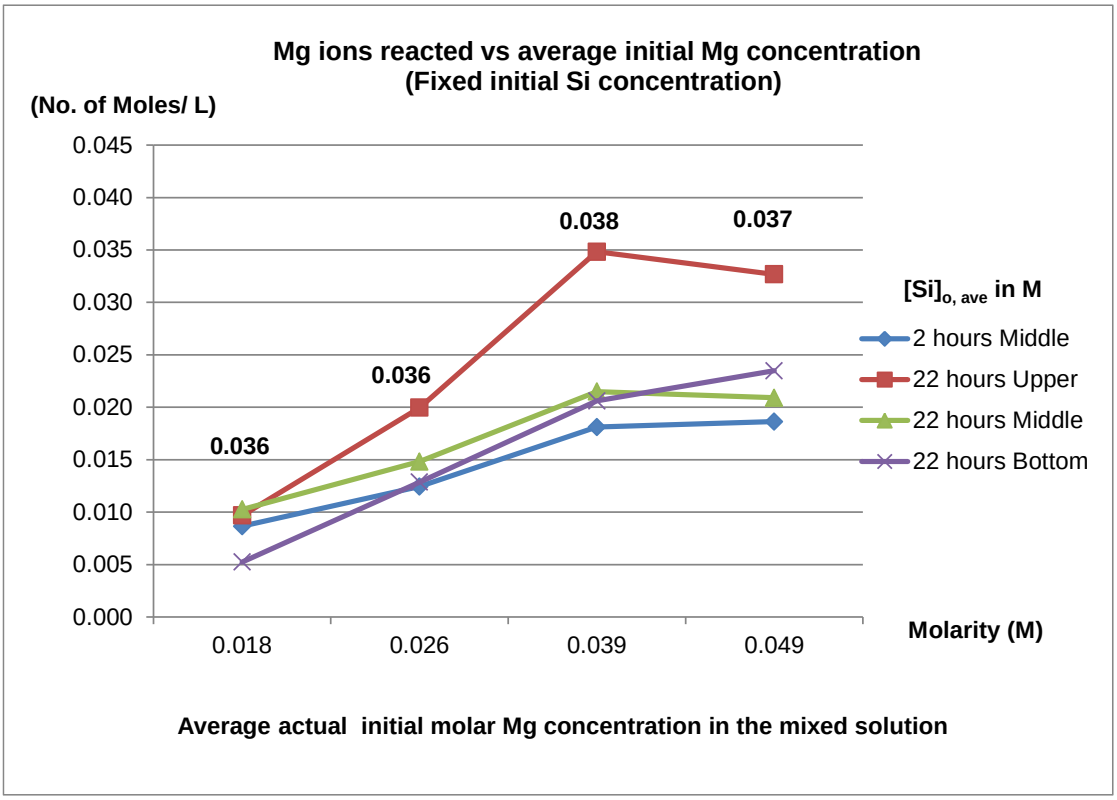

Figure 4-7 Trend of magnesium ion reacted in moles vs. Initial average (molar) concentration of Mg

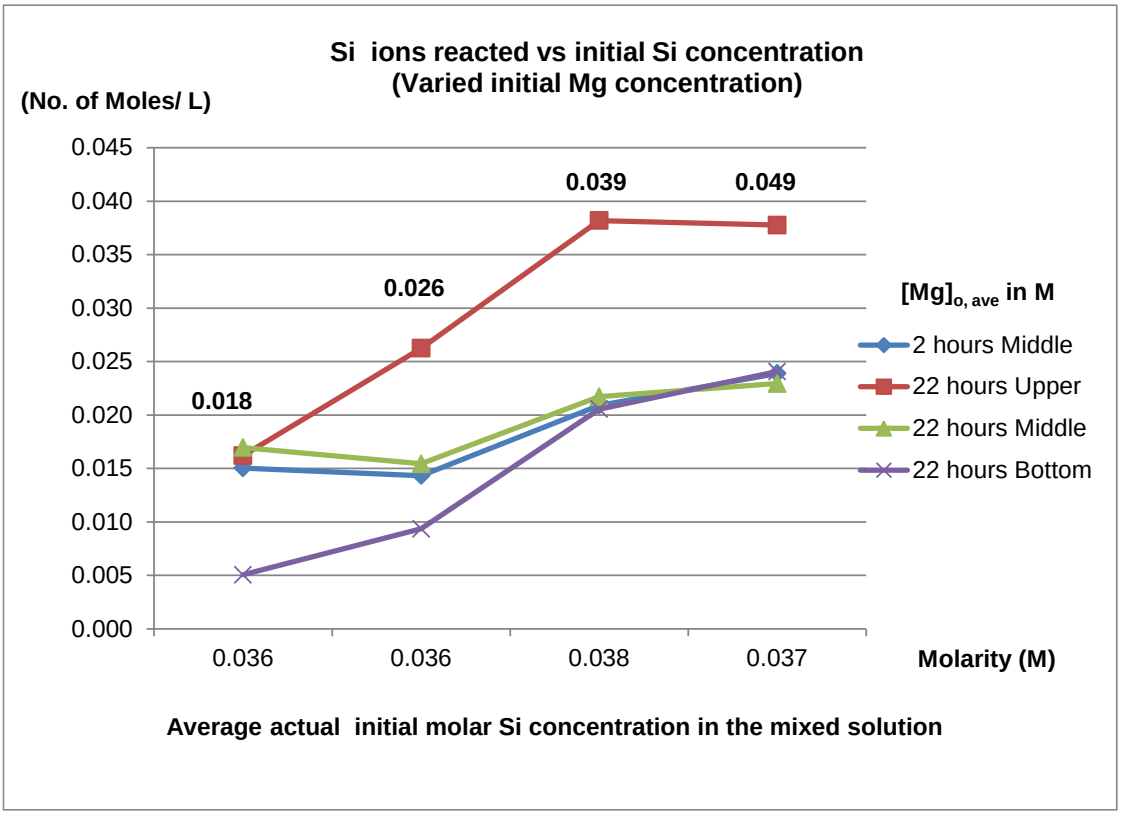

Figure 4-8 Trend of Si ion reacted in moles vs. Initial average (molar) concentration of Si

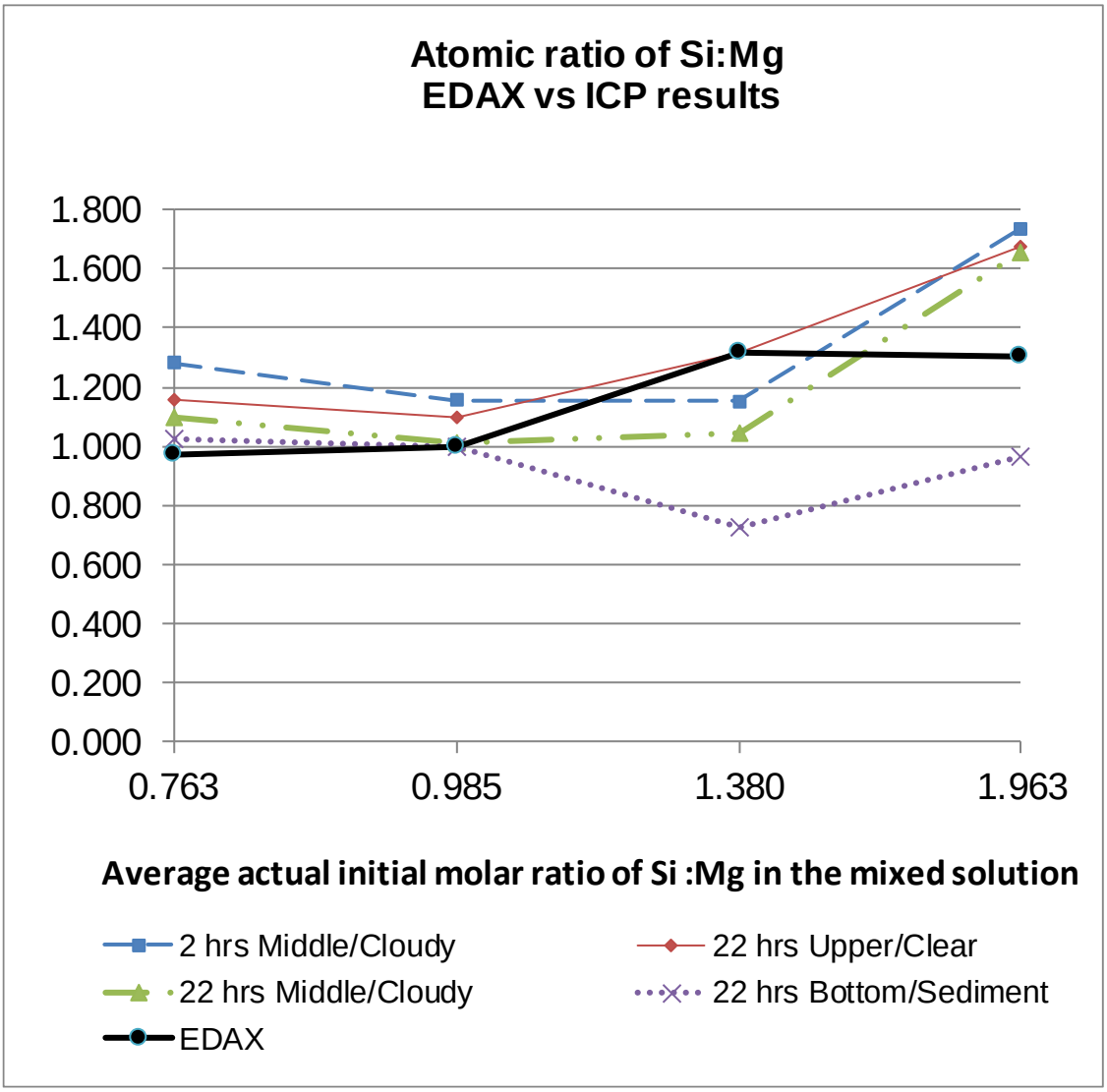

Figure 4-9 Stoichiometry in terms of the Si:Mg molar atomic ratio calculated from ICP analysis with the corresponding measurement by ESEM/EDAX also shown

In Figure 4-9, all the ICP data agree very well except for the samples from the bottom sediment (which are expected to be most in error for the reasons explained above). We will therefore, neglect the stoichiometry data from the bottom sediment region. As can be seen from stoichiometry data (except bottom sample) in Figure 4-9, both the ICP and the ESEM/EDAX data shows that when initial molar ratio for Si:Mg is more than 1 (i.e. the silicon ion is supplied in excess); the atomic ratio of Si:Mg in the precipitated amorphous magnesium silicate is approximately 1.3. However, when the initial magnesium ion in the mixed solution is supplied in excess (Si:Mg $\leq$ 1) , the atomic ratio of Si:Mg in the silicate precipitate is approximately 1. Only a slight change is recorded by EDAX when initial molar ratio of Si:Mg is increased from 0.76 to 0.98 to give the atomic ratio of Mg:Si from 1.002 to 1.027, respectively. Recall that, according to

Arensdorf et al. (2010) magnesium silicate scale typically has non-stoichiometric ratios of magnesium to silicate. Also, the results of Kristmanndóttir et al. (1989) reviewed above showed a Si:Mg ratio of ~ 1:1 which was the same whether the mother liquor contained a 1:2 or 2:1 mole ratio of silica to magnesium and whether the precipitation took place at room temperature or 75°C.

(c) ESEM/EDAX Analysis

The silicate precipitated samples produced in these tests were filtered and examined by ESEM analysis with EDAX to study the composition and the nature of the scale. All of the mixed solution were filtered using 0.2 μm paper filters and rinsed using distilled water.

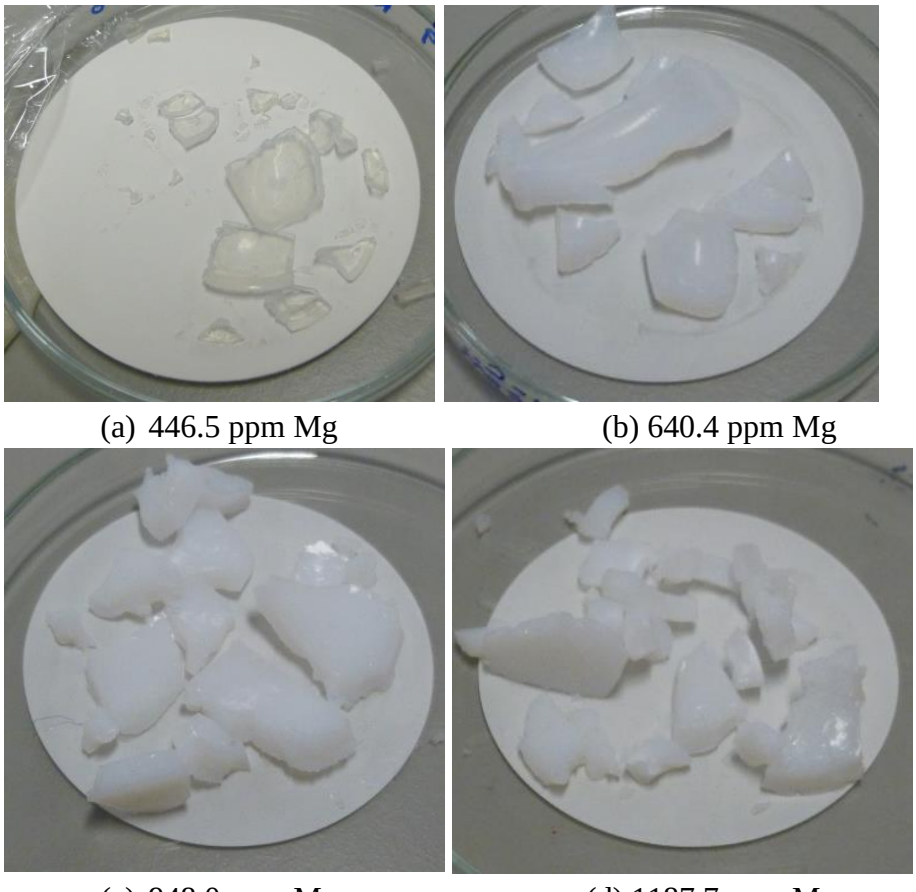

(a) 446.5 ppm Mg (b) 640.4 ppm Mg

(c) 948.0 ppm Mg (d) 1187.7 ppm Mg

Figure 4-10 Filtered cake of produced scale sent for ESEM analysis (labelled as average value of actual initial magnesium concentrations from the mixed 50:50 ratio brine)

The filtered cakes, as shown in Figure 4-10 were left to dry at room temperature for at least 24 hours. It was observed that the higher the initial magnesium concentration present in the mixed solution, the thicker the precipitated filter cake that was collected; that is, more mass of magnesium silicate was formed as the Mg:Si molar ratio increased to above 1, exactly as would be expected.

From the ESEM analysis, it was found that the scale produced is not crystalline but appeared to be a sort of gel-like structure. The main constituents were identified to be of oxygen (the highest percentage; 58 to 69% in weight percentage), magnesium (9.15 to 13.13% in weight percentage) and silicon (12.68 to 22.63% in weight percentage). Other elements were present as traces included sodium, carbon, and chloride. The intensity and atomic percentage ratio of silicon to magnesium were calculated and are presented in Figure 4-11.

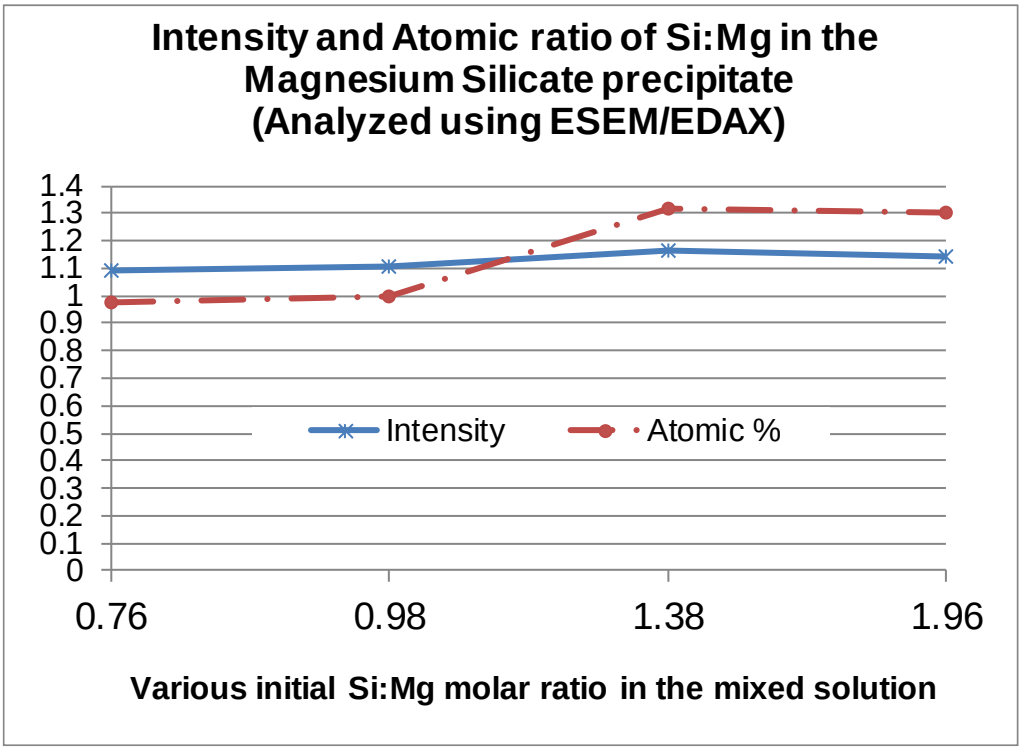

Figure 4-11 Intensity and atomic percentage ratio of silicon to magnesium in the precipitated scale

The ESEM images of the precipitated scale are shown in Figure 4-12, Figure 4-13, Figure 4-14, and Figure 4-15.

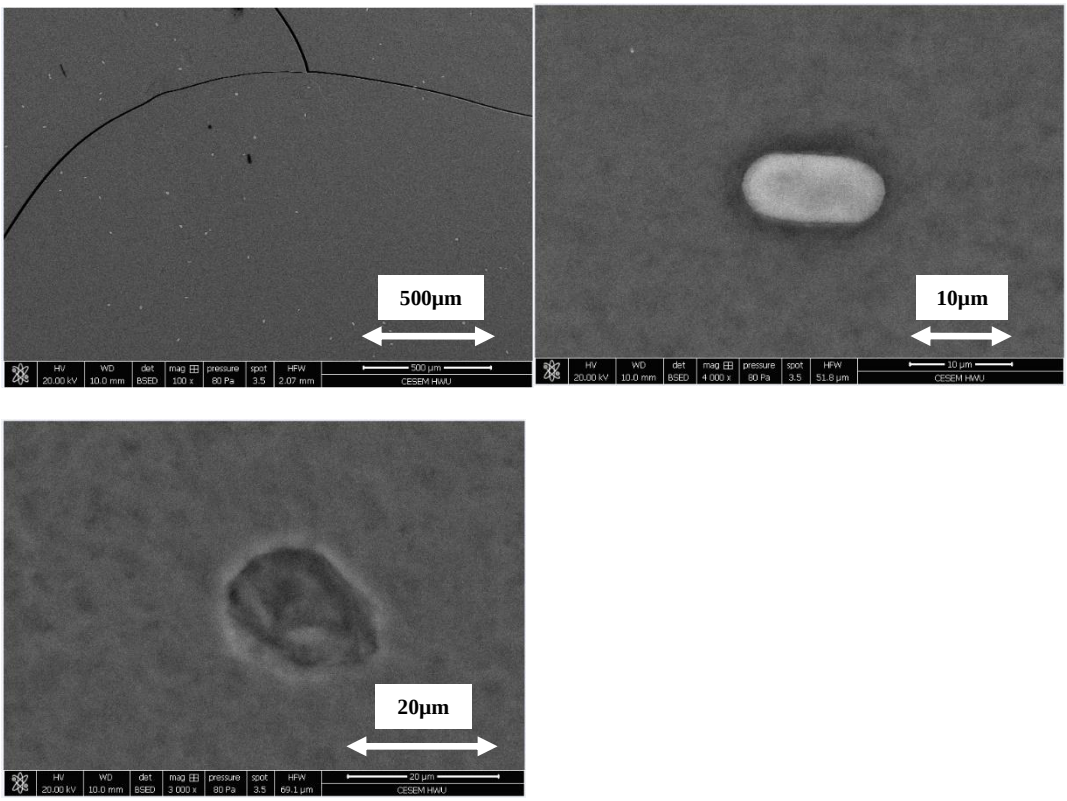

Figure 4-12 ESEM images of silica particles (Mg concentration of 446.5ppm in the mixed 50:50 ratio)

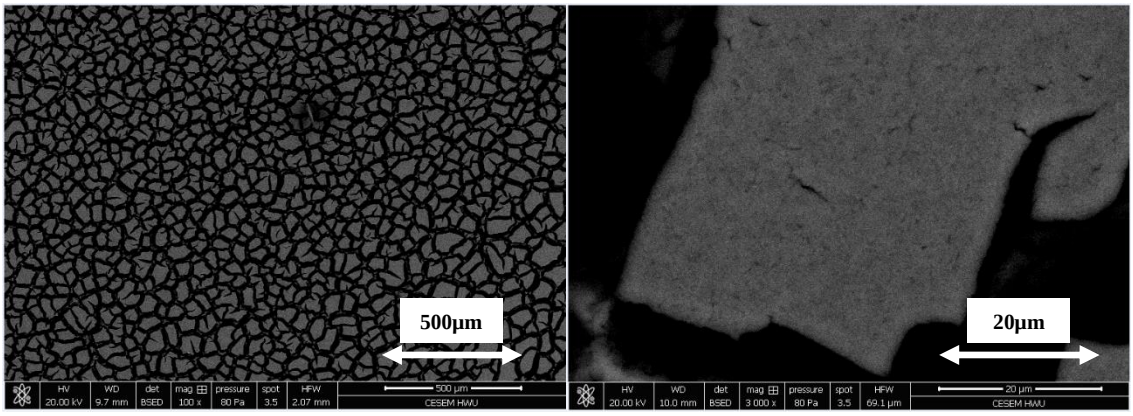

Figure 4-13 ESEM images of silica particles (Mg concentration of 640.4ppm in the mixed 50:50 ratio)

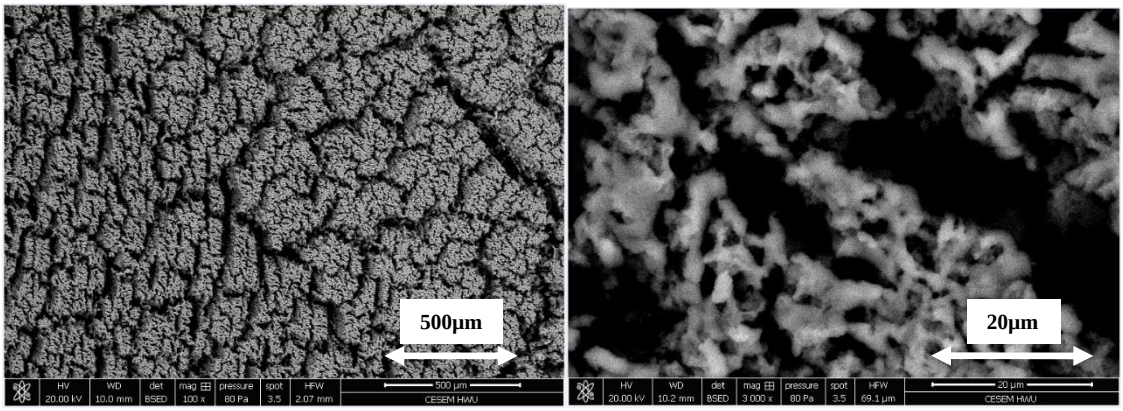

Figure 4-14 ESEM images of silica particles (Mg concentration of 948.0ppm in the mixed 50:50 ratio)

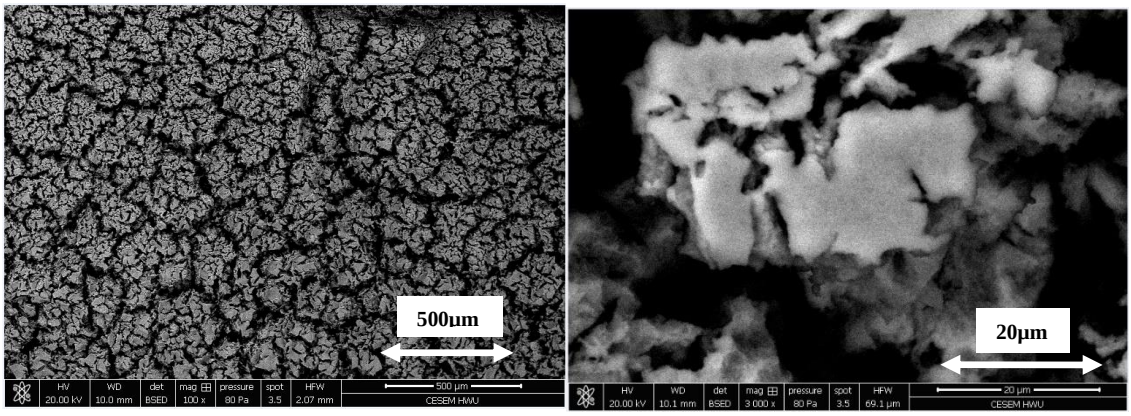

Figure 4-15 ESEM images of silica particles (Mg concentration of 1187.7ppm in the mixed 50:50 ratio)

4.1.3 Summary and Conclusions

This work initiated the study of silicate scaling for this PhD study and the experiments reported here are the first to be carried out by the FAST group on this research topic. The primary objectives of the FAST silicate research (and of this thesis) are to develop an experimental bulk silicate scaling and inhibition method, and then to go on to use this to understand the mechanisms of silicate scale formation and its subsequent inhibition/dispersal. Our initial experiments have followed the previous work by Arensdorf et al. (2010) and we have shown that magnesium silicate scaling can be reproduced in the laboratory. However, we have already extended the methodology to include a quantitative assay for [Mg] and [Si] and also to study of the magnesium silicate precipitated by ESEM/EDAX. Further investigation on the effect of various parameters such as pH, temperature, initial brine composition and brine ageing can now be carried

out in order to develop a better understanding of silicate scaling during ASP flooding (and in other more conventional processes).

The preliminary detailed conclusions of this *High Mg Test* are as follows:

(i) A static experimental methodology has been developed to produce a reasonably well defined magnesium silicate scale by modifying the approach reported by Arensdorf et al. (2010). Our experimental approach is extended by including elemental analysis for Mg and Si (by ICP), sampling at various levels within the reactor bottle and examining the precipitated Mg silicate deposits by ESEM/EDAX. The sampling position in the test bottle is important since the precipitate can interfere with the Mg and Si analysis; this observation provides the ground to investigate the most appropriate ICP sampling technique that reported in section 4.3.

(ii) The approach used in this work has enabled us to establish the morphology of the Mg silicate which is formed and its stoichiometry in terms of the Mg: Si molar ratio. The Mg silicate formed was found to be amorphous and the stoichiometry varied somewhat with the [Mg] in solution. For an initial Si:Mg more than 1 (i.e. Si ion in excess), the atomic ratio of Mg:Si in the amorphous Mg silicate is approximately 1.3. However, when the initial Mg ion in the mixed solution is in excess (Si:Mg $\leq$ 1), the atomic ratio of Si:Mg in the precipitate is approximately 1. This result was found consistently by the two methods used here, viz. (a) the solution ICP *ion reacted* results, and (b) the independent ESEM/EDAX results on the actual precipitate.

4.2. FIRST RESULTS FOR LOW MAGNESIUM CONCENTRATION

4.2.1 Experimental Details

This experiment was designed to determine the minimum concentration of magnesium ion required (threshold concentration) to initiate silicate scaling when mixed with silicon ion in a 50:50 ratio (where [Si] = 1025ppm in the final mix to make it comparable with *High Mg Test*).

Previous results *High Mg Test* (i.e. initial mixed magnesium ion concentration in 50:50 ratio are 450ppm, 600ppm, 900ppm & 1200ppm) showed that the silicate scale had already formed in the lowest Mg concentration case, i.e. [Mg^{2+}] = 450ppm, in which based on the ICP analysis, it was found that ~50% of the magnesium and silicon were reacted to form silicate scale.

Essentially, this *Low Magnesium Test* was performed as per methodology described in section 4.1.1 by mixing the silicon brine (Si Brine) with the magnesium brine (Mg Brine) in a 50:50 ratios at room temperature as shown in Table 4-5.

The original pH values of all brines were measured and their values are reported in Table 4-6.

Table 4-5 Initial condition of various silicate system tested at T_{room}, natural pH

Test condition **Low Mg**	Initial condition of 50:50 mixed brine of SB:MB						
	Ion (ppm)		Ion (molar)x10^{-3}		Initial molar ratio $(Si:Mg)_o$	Initial mixed brine pH pH_o	Initial supersaturation relative to amorphous silica
	Mg	Si	Mg	Si			
1	45.8	*619.1	1.876	22.115	11.788	~12.40	9.829-10.615
2	61.0	*627.1	2.514	22.392	8.907	~12.40	9.952-10.749
3	91.2	*619.2	3.752	22.018	5.868	~12.33	9.786-10.569
4	120.6	*623.3	4.945	22.079	4.465	~12.55	9.813-10.569

***Please note target Si concentration in 50:50 mixed brine is 1025ppm as comparable with the high Mg test; however, ICP measure the silicon concentration in the *control* solution as only ~620ppm. This will be discussed in detail in the following section 4.3.3.**

Table 4-6 Natural pH of brines, mixed brine and quenching solutions

Solution	Natural pH
Mg Brine 90ppm	6.12
Mg Brine 120ppm	6.36
Mg Brine 180ppm	6.39
Mg Brine 240ppm	6.56
Si Brine ***2050ppm (Target Si)**	12.87
Quenching Solution EDTA/NaOH	13.30
Tested Temperature	T_{room}

*** Please note that the silicon brine was prepared to contain ~2050ppm silicone; however, ICP measure the silicon concentration in the *control* solution as only 1025ppm. This will be discussed in detail in the following section 4.3.3.**

4.2.2 Results and Discussion

(a) Physical Observations

The visual inspection of the mixed brine allows us to monitor any physical changes that occur to the silicate system studied. The mixed brine were carefully inspected and photograph were taken as shown in Figure 4-16. We can see in this figure that for silicate system of 45Mg:620Si and 60Mg:620Si; the mixed brine stays clear up to 48 hours as shown in Figure 4-16.

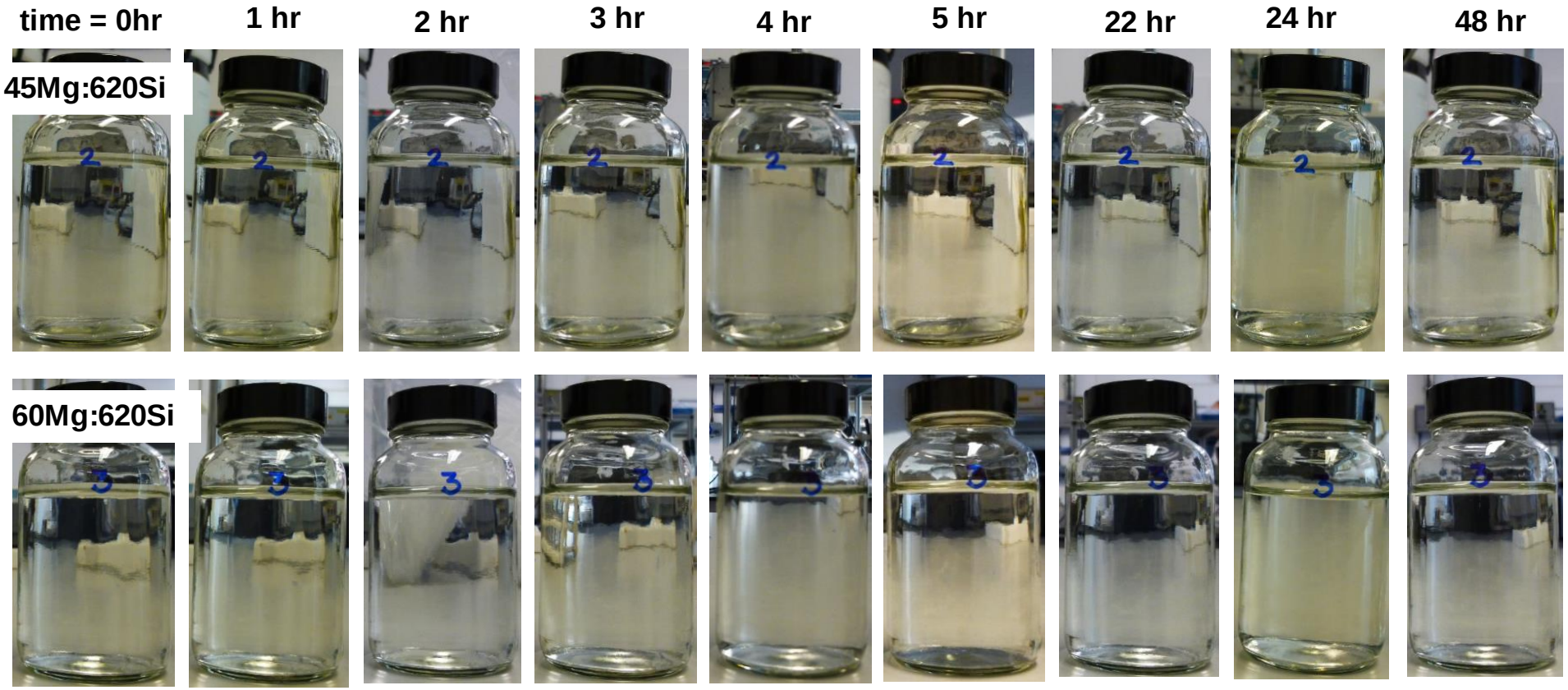

Figure 4-16 Silicate system of 45Mg:620Si and 60Mg:620Si at natural pH, T_{room}

For a silicate system of 90Mg:620Si and 120Mg:620Si, the mixed brine became slightly cloudy immediately after being mixing (i.e. at 0hr) as can be seen in Figure 4-17. However, no visible precipitate can be observed for any of the silicate system tested in this *Low Mg Test.*

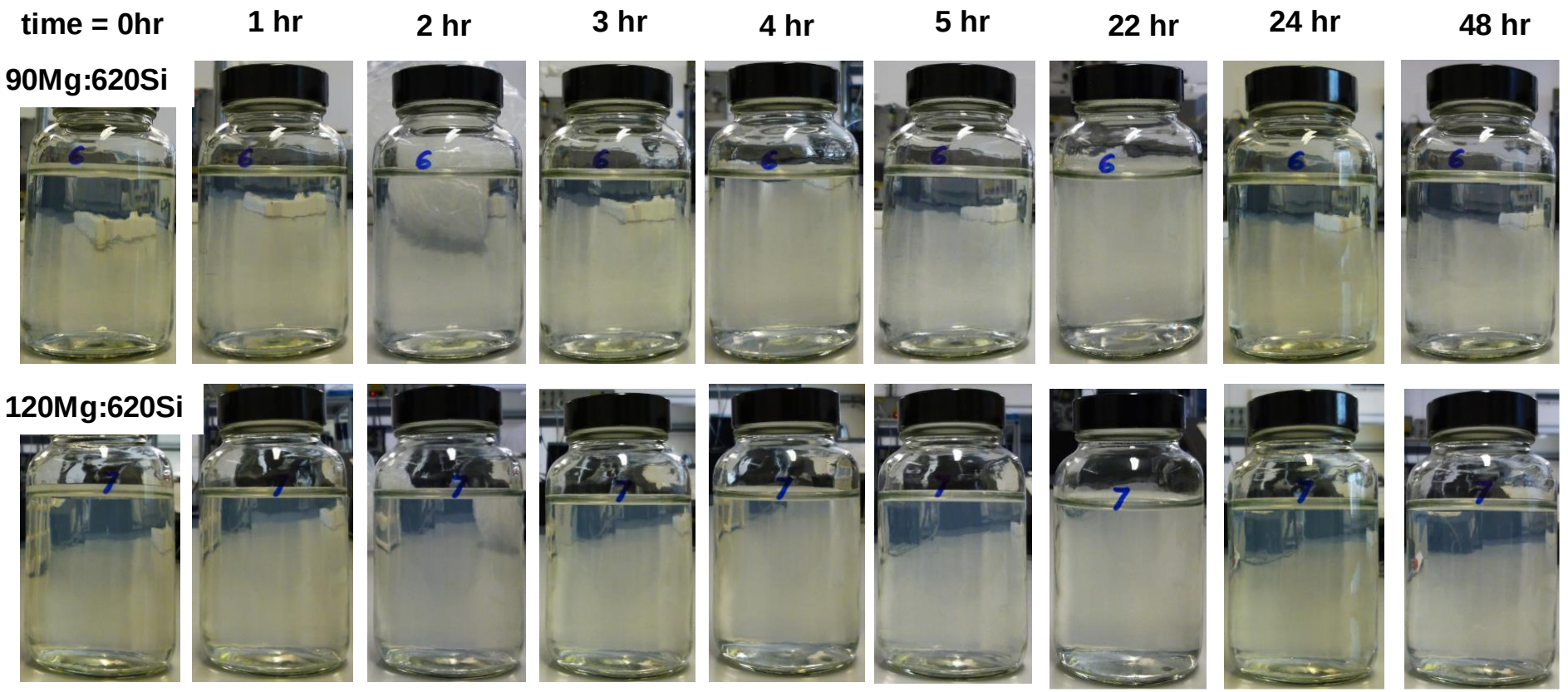

Figure 4-17 Silicate system of 90Mg:600Si and 120Mg:600Si at natural pH, T_{room}

(b) ICP Analysis

We continue with a detailed analysis of ICP measurement to confirm the observations made above. As mentioned earlier, the target silicon concentration in 50:50 mixed brine is ~1025ppm however only ~620ppm obtained by ICP analysis (i.e. ~39.5% reduction Si target). Also, the *control* solution of 2050ppm Si stock solution also revealed that the ICP value is only ~1250ppm. We further investigate the cause of reduction and detailed discussion about this issue is reported in section 4.3.3.

Despite this observation on reduction from [Si] target, we further determine the extent of reaction in *Low Magnesium Test* using equation 3.1. The amount of magnesium and silicon ion reacted are then plotted in Figure 4-18 and Figure 4-19 respectively.

The amount of magnesium and silicon ion reacted are <2.5ppm and <18ppm respectively that confirm the observation made earlier.

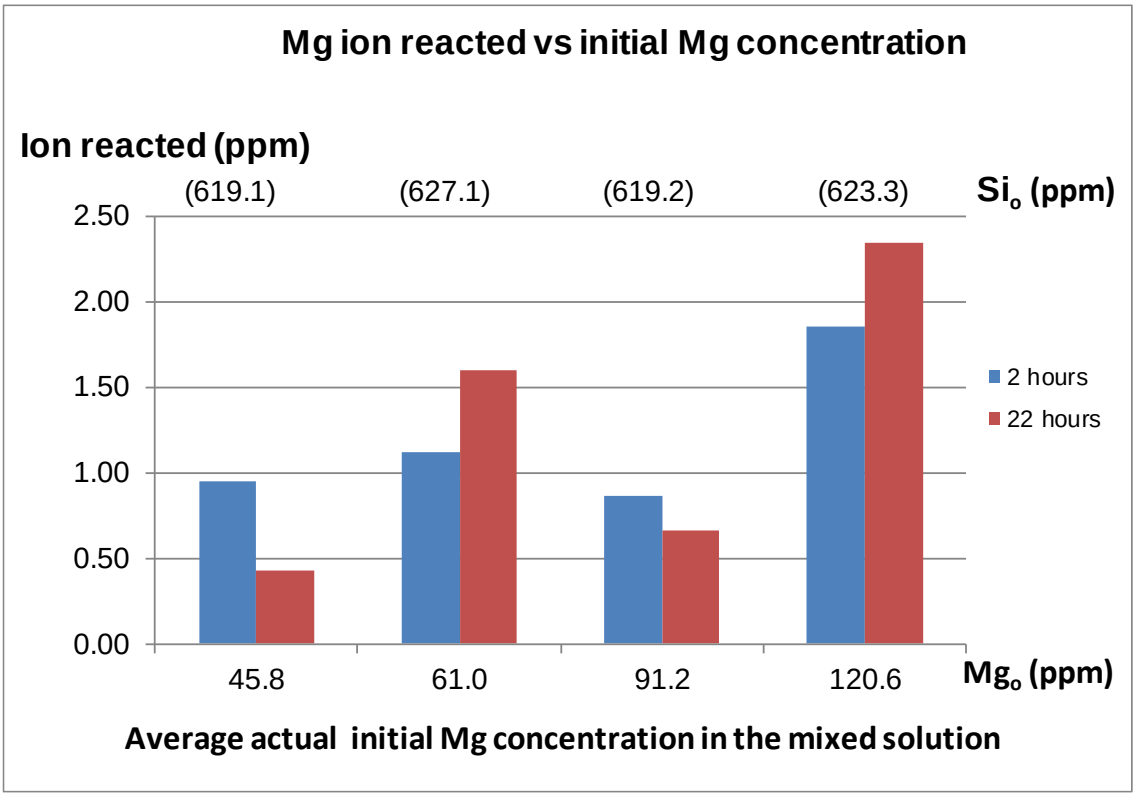

Figure 4-18 Amount of magnesium ion reacted in *"Low Magnesium Test"* at natural pH, T_{room}

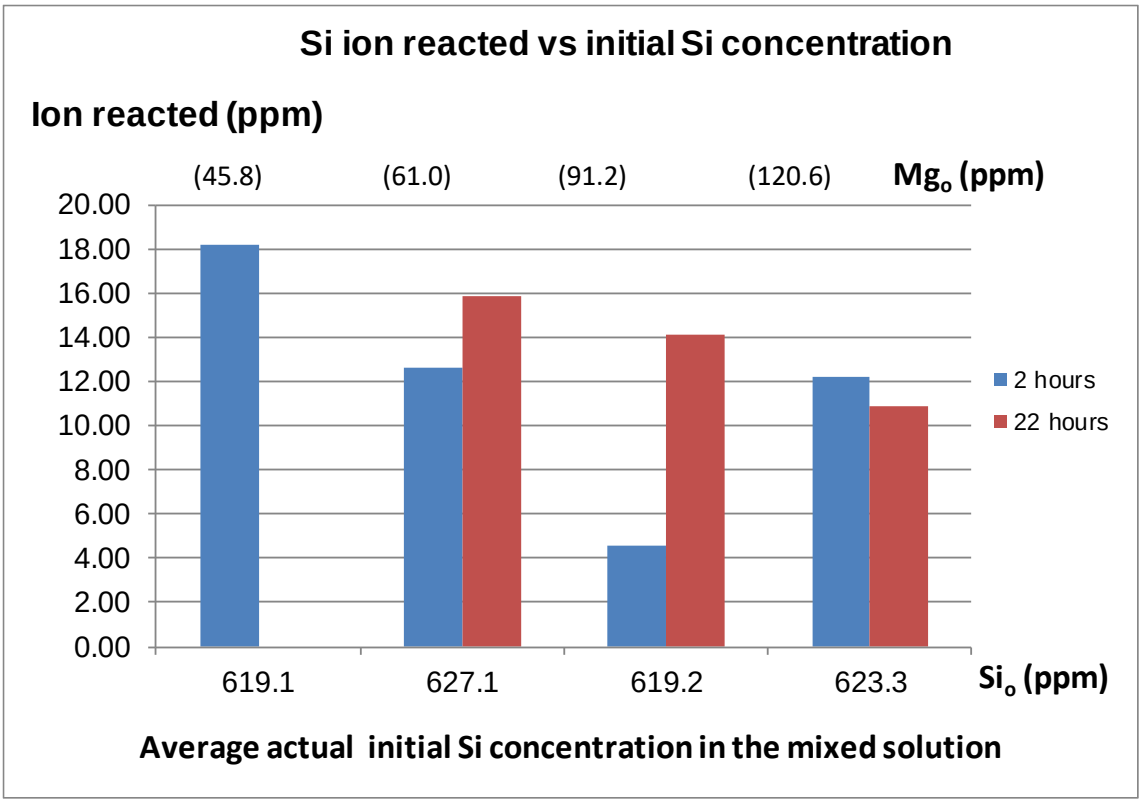

Figure 4-19 Amount of silicon ion reacted in *"Low Magnesium Test"* at natural pH, T_{room}

4.2.3 Summary and Conclusions

Silicate Scale Formation Static Bottle Tests for low concentrations of magnesium (i.e. initial mixed magnesium ion concentration in 50:50 ratios are 45ppm, 60ppm, 90ppm & 120ppm) revealed that no Mg-silicate scale was formed (at least it was not visible and the ion compositions of Mg and Si had not changed to within experimental accuracy); <3% Mg ion reacted (<3ppm Mg) & <3% Si ion reacted (<18ppm Si).

The brine instability issues observed in this particular test provides the motivation behind the systematic investigation of various parameters in our effort to establish the experimental methodology for silicate scaling static bottle tests. All of these parameters were examined in detailed and results are reported in the following sections.

4.3. DEVELOPING THE STATIC BOTTLE TEST OF SILICATE SYSTEM

In section 4.1 and 4.2, static tests were developed to study the reproducibility of silicate scaling in the laboratory by extending the work of Arensdorf et al. (2010) and by further quantifying the silicate scaling using ICP analysis. Initial static tests successfully measured the amount of silicate scale produced when mixing solutions with relatively high magnesium concentrations ($[Mg^{2+}]$ = 450ppm to 1200ppm in mixed brine) or low magnesium concentrations ($[Mg^{2+}]$ = 45ppm to 120ppm in mixed brine) with silicon brine (with [Si] = ~1000ppm in the mixed brine). However, several issues were identified while using this earlier approach on the high magnesium concentrations (as discussed in section 4.1.2(b)) based on the ICP analysis due to the colloidal nature of the Mg-silicate scale produced as well as on the low magnesium concentrations (as discussed in section 4.2.2(b)) due to the brine stability/ contamination issues.

Following the above issues observed, we undertook a systematic investigation whereby several experiments were set up in order to study the following:

(i) Establishing the correct quenching solution to be used in the ICP sampling

(ii) The issue of using glass bottles as opposed to HDPE bottles in the static bottle tests, and

(iii) Establishing if there is a need to centrifuge or stir the forming Mg-silicate solution while sampling.

4.3.1 Quenching Solution for ICP Sampling

(a) Quenching Solution for ICP Sampling – Test Set up

In this experiment, 1% EDTA/NaOH solution was prepared by mixing 50g of EDTA (Ethylene diamine tetra acetic acid disodium salt dihydrate) with 50g sodium hydroxide and then making the solution up to 5 litres using distilled water. The pH of the quenching solution is pH ~13 to ~13.5. Silicon brines (SB) with concentrations of 1880ppm was prepared by dissolving an appropriate amount of sodium metasilicate pentahydrate ($Na_2SiO_3.5H_2O$) in distilled water in the quantities indicated in Table 4-2. For the purpose

of checking the Si concentration only, the brines were not filtered. In the current test, a 100ppm silicon ICP standard solution was also prepared to check its stability.

In this experiment, ***test samples*** and ***control samples*** of the following solutions were prepared as below (refer Table 4-7) and ICP-samples at sampling time of up to 15 days in two different quenching solution i.e. 1% EDTA/NaOH and Distilled Water respectively (refer Table 4-8); giving final solution of:

(i) 1880ppm silicon brine was diluted into three different dilution factors of (x100), (x200) and (x400)

(ii) 100ppm silicon ICP standard solution was diluted by (x100)

Table 4-7 Static test samples

Tube No	Description	*Amount of 1880ppm SB (ml)	Amount of Quenching Solution (ml)	Final Mix [Silicon] ppm
1	(x10) of 1880ppm SB in 1% EDTA/ NaOH	10	90	188
2		10	90	188
3	(x10) of 1880ppm SB in DW	10	90	188
4		10	90	188
5	(x20) of 1880ppm SB in 1% EDTA/ NaOH	5	95	94
6		5	95	94
7	(x20) of 1880ppm SB in DW	5	95	94
8		5	95	94
9	(x40) of 1880ppm SB in 1% EDTA/ NaOH	2.5	97.5	47
10		2.5	97.5	47
11	(x40) of 1880ppm SB in DW	2.5	97.5	47
12		2.5	97.5	47
13	(x10) of 1000ppm Spectrol Si Standard in 1% EDTA/ NaOH	*10	90	100
14		*10	90	100
15	(x10) of 1000ppm Spectrol Si Standard in DW	*10	90	100
16		*10	90	100

*13-16: 1000ppm Spectrol Si Standard

Table 4-8 Test-tube list

Tube No	Descriptions	Quenching solution	Final Mix [Si] after quenching (ppm)
1	(x100) of 1880ppm SB in 1% EDTA/ NaOH	1% EDTA/NaOH	18.8
2		1% EDTA/NaOH	18.8
3	(x100) of 1880ppm SB in DW	DW	18.8
4		DW	18.8
5	(x200) of 1880ppm SB in 1% EDTA/ NaOH	1% EDTA/NaOH	9.4
6		1% EDTA/NaOH	9.4
7	(x200) of 1880ppm SB in DW	DW	9.4
8		DW	9.4
9	(x400) of 1880ppm SB in 1% EDTA/ NaOH	1% EDTA/NaOH	4.7
10		1% EDTA/NaOH	4.7
11	(x400) of 1880ppm SB in DW	DW	4.7
12		DW	4.7
13	(x100) of 1000ppm Spectrol Si Standard in 1% EDTA/ NaOH	1% EDTA/NaOH	10
14		1% EDTA/NaOH	10
15	(x100) of 1000ppm Spectrol Si Standard in DW	DW	10
16		DW	10

(b) Quenching Solution for ICP Sampling - Test Results and Discussion

Distilled water as quenching solution

[Si] in ***test samples*** for (x100), (x200) & (x400) dilution of *1880ppm Silicon Brine* and (x100) *Si ICP Standard Solution* sampled in ***distilled water*** **agreed** with each other at all sampling time i.e. from 22 hours to 15 days (see Figure 4-20). In other word, % deviation of [Si] in ***test samples*** for (x100), (x200) & (x400) dilution of 1880ppm Silicon Brine and (x100) of *Si ICP Standard Solution* solution against targeted value is **<8%.**

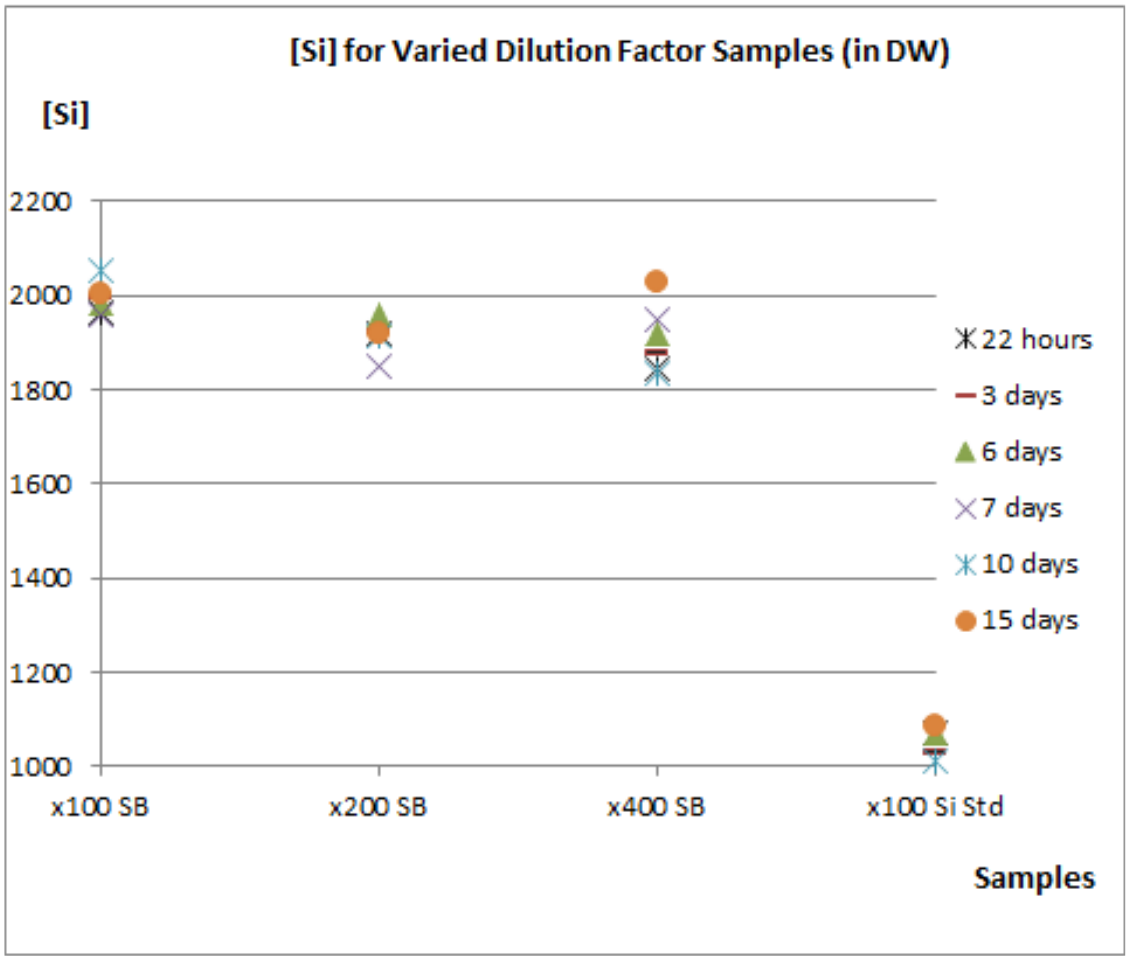

Figure 4-20 Distilled water as quenching solution in *test samples*

Further analysis of [Si] in ***control samples*** for (x100), (x200) & (x400) dilution of *1880ppm Silicon Brine* and (x100) of *Si ICP Standard Solution* sampled in ***distilled water*** also revealed that all values **agreed** with each other at all sampling time i.e. from 22 hours to 15 days. % deviation of [Si] in ***control samples*** for (x100), (x200) & (x400) dilution of *1880ppm Silicon Brine* and (x100) of *Si ICP Standard Solution* against targeted value is **<8%** (Refer Figure 4-21)**.**

Results suggest that distilled water may be a suitable quenching solution for our system as the samples and controls do not experience any interaction between ions of interest or with distilled water. However, this basic test only used silicon ion. Later we have to quench our mixed brine that consist of both silicon and magnesium ions which may require higher dilutions (40x) for control sample preparation.

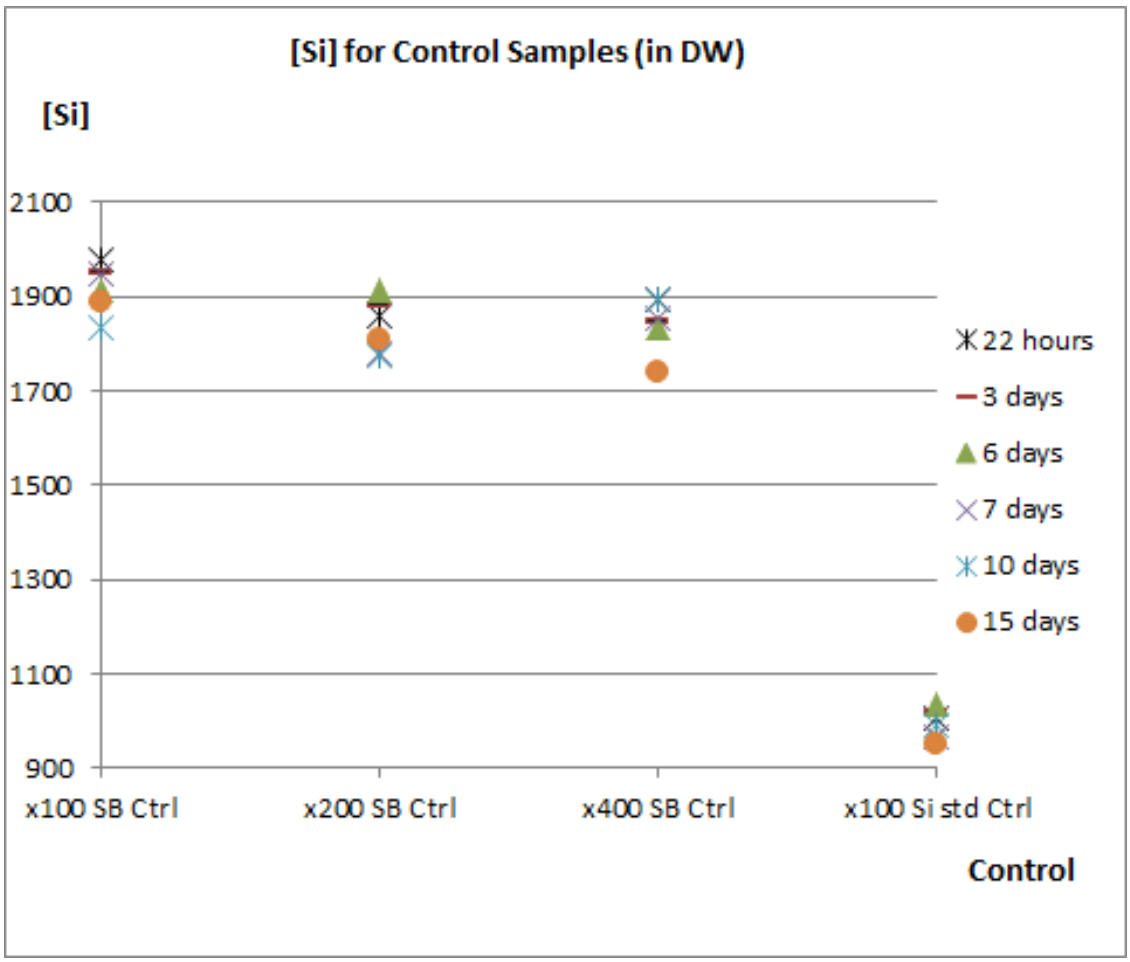

Figure 4-21 Distilled water as quenching solution in *control samples*

1% EDTA/NaOH as quenching solution

[Si] in ***test samples*** for (x100), (x200) & (x400) dilution of *1880ppm Silicon Brine* and (x100) *Si ICP Standard Solution* sampled in 1% EDTA/NaOH as quenching solution are **much higher** than the targeted values. % deviation of [Si] in samples for (x100), (x200) & (x400) dilution of *1880ppm Silicon Brine* and (x100) *Si ICP Standard Solution* against targeted value is up to **50%** (Refer Figure 4-22)**.**

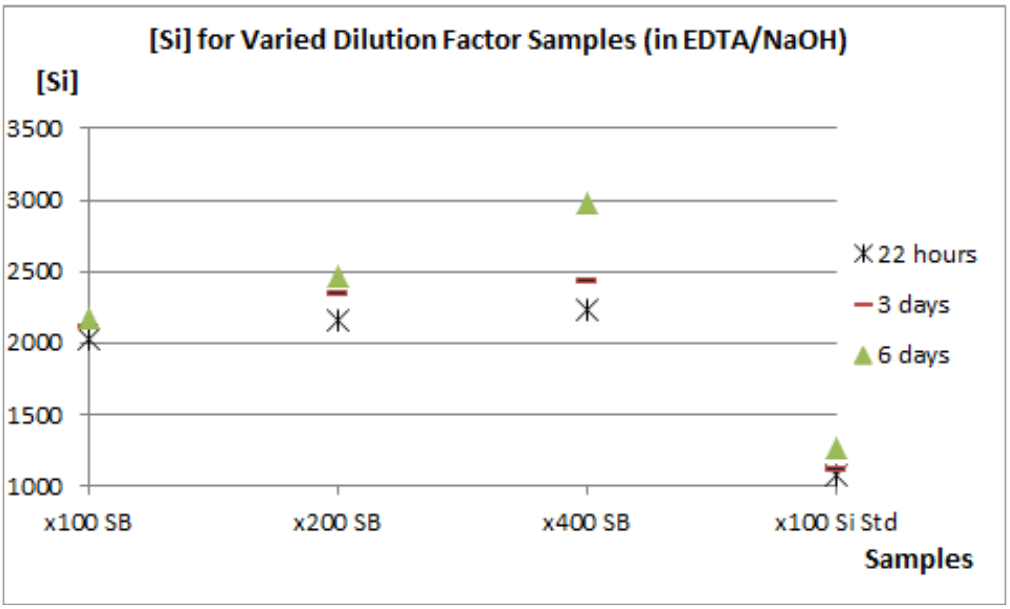

Figure 4-22 1% EDTA/NaOH as quenching solution in *test samples*

[Si] in the ***control samples*** for (x100), (x200) & (x400) dilution of *1880ppm Silicon Brine* and (x100) *Si ICP Standard Solution* sampled in 1% EDTA/NaOH as quenching solution **agreed** with each other at all sampling time. % deviation of [Si] in ***control samples*** for (x100), (x200) & (x400) dilution of *1880ppm Silicon Brine* and (x100) *Si ICP Standard Solution* sampled against targeted value is <5% (See Figure 4-23).

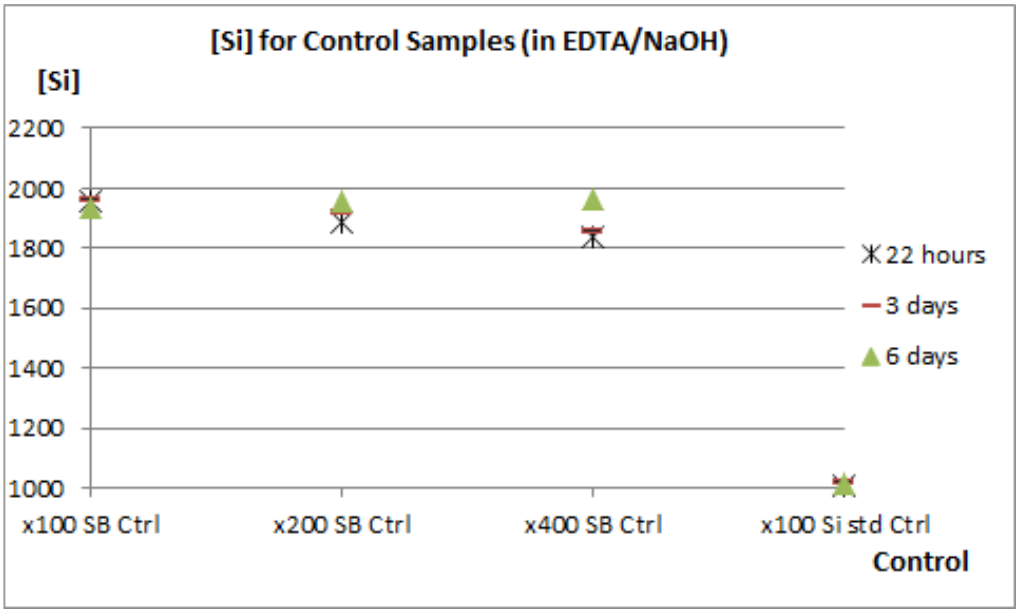

Figure 4-23 1% EDTA/NaOH as quenching solution in *control samples*

4.3.2 1% EDTA/NaOH Stability as Quenching Solution for ICP Sampling

(a) 1% EDTA/NaOH Stability Test Set up

This experiment was designed to study the stability of ICP-sampled brine in the test tubes before ICP analysis was carried out. In this experiment, 1% EDTA/NaOH solution was prepared by mixing 50g of EDTA (Ethylene diamine tetra acetic acid disodium salt dihydrate) with 50g sodium hydroxide and then making the solution up to 5 litres using distilled water. The pH of the quenching solution is pH ~13 to ~13.5. Several magnesium brines (MB) with concentrations of [Mg^{2+}] = 90ppm, 120ppm, 180ppm and 240ppm were made up along with a [Si] = 1880ppm silicon brine (SB) by dissolving an appropriate amount of magnesium chloride hexahydrate ($MgCl_2.6H_2O$) and sodium metasilicate pentahydrate ($Na_2SiO_3.5H_2O$) separately in distilled water in the quantities indicated in Table 4-9.

The fresh brines were diluted immediately to control concentrations i.e. x20 => 5ml various MB or SB brine/100ml 1% EDTA/NaOH solution and ICP analysed to measure their concentrations. For the purpose of checking the Si and Mg concentration only, the brines were not filtered. The same test tubes were ICP re-analysed after 5 days to check the stability of the quenching solution. These brines were then being used in magnesium silicate scaling tests (i.e. filtered brine) which follow a similar procedure to our normal silicate scaling static tests. This is the reason for still including the procedure for static tests. The results obtained were analysed and compared to determine the stability of 1%EDTA/NaOH as the quenching solution and to see if there is any reaction between the quenching solution and brine samples.

Table 4-9 Brine composition and preparation for "Quenching Solution for ICP Sampling" test

Ion	Concentration {ppm (mg / L)}	Formula Composition	g / L	g / 5L	g / 10L	g / 15L	g / 20L
Mg^{2+}	90	$MgCl_2.6H_2O$	0.753	3.76	7.53	11.29	15.05
Mg^{2+}	120	$MgCl_2.6H_2O$	1.003	5.02	10.03	15.05	20.07
Mg^{2+}	180	$MgCl_2.6H_2O$	1.505	7.53	15.05	22.58	30.10
Mg^{2+}	240	$MgCl_2.6H_2O$	2.007	10.03	20.07	30.10	40.14
Si^{4+}	1880	$Na_2SiO_3.5H_2O$	14.20	71.00	142.00	213.00	284.00

(b) 1% EDTA/NaOH Stability Test Results and Discussion

This experiment was designed to check the [Mg] and [Si] in the experimental controls (i.e. 1% EDTA/NaOH quenching solution) when prepared in a similar manner to a controls used in a set of silicate scaling static tests. Previously, there were errors and fluctuation in concentration recorded in our previous Silicate Scaling Static Bottle Tests for Low Magnesium. These errors were *not* found in our Silicate Scaling Static Bottle Tests for *High Magnesium Concentration Test*, reported in section 4.1 in which all brines and quenching solutions were freshly made and immediately ICP analysis was carried out as soon as sampling was done (this was not the case for the low magnesium tests). Therefore, this experiment was conducted to investigate whether or not reaction(s) occurred between 1% EDTA/NaOH solution and brine.

Previously, problems were encountered when conducting silicate scaling static tests for *Low Magnesium Concentration Test* discussed in section 4.2 in which the [Si] was reported to be much lower than targeted values.

Figure 4-24 clearly shows that ion concentration values recorded by ICP for magnesium and silicon brine precisely met the target concentration with <2 to 3% deviation from the target brine concentrations for the first run and then the re-run, respectively.

Brine concentrations for [Si] and [Mg] agreed with each other after ICP re-analysed (after 5 days from the first run) with a % deviation between the two values of only up to 3%, as shown in Figure 4-25. These results demonstrated that there is no adverse reaction between samples and 1% EDTA/NaOH quenching solution when the samples were left in ICP test tubes for up to 5 days. Therefore, the 1% EDTA/NaOH solution could be used as the quenching solution for Silicate Scaling Static Bottle Tests in which the waiting time for ICP analysis after each experiment was up to 5 days. This also meant that there was no necessity to immediately analyse the samples after each experiment which gives us some flexibility when scheduling the ICP runs for different experiments.

The stability of the brine with 1% EDTA/NaOH failed to explain the observation made in *Low Magnesium Test*. This leads us to the assumption that the brine may have already undergone some adverse reaction during the static test. This in tune led us to further investigate the usage of glass bottles as the reactor. Later, it will be shown that the high-pH solutions may have experience the adverse reaction even before the static test is conducted when stored in glass container (from which some additional Si can be etched).

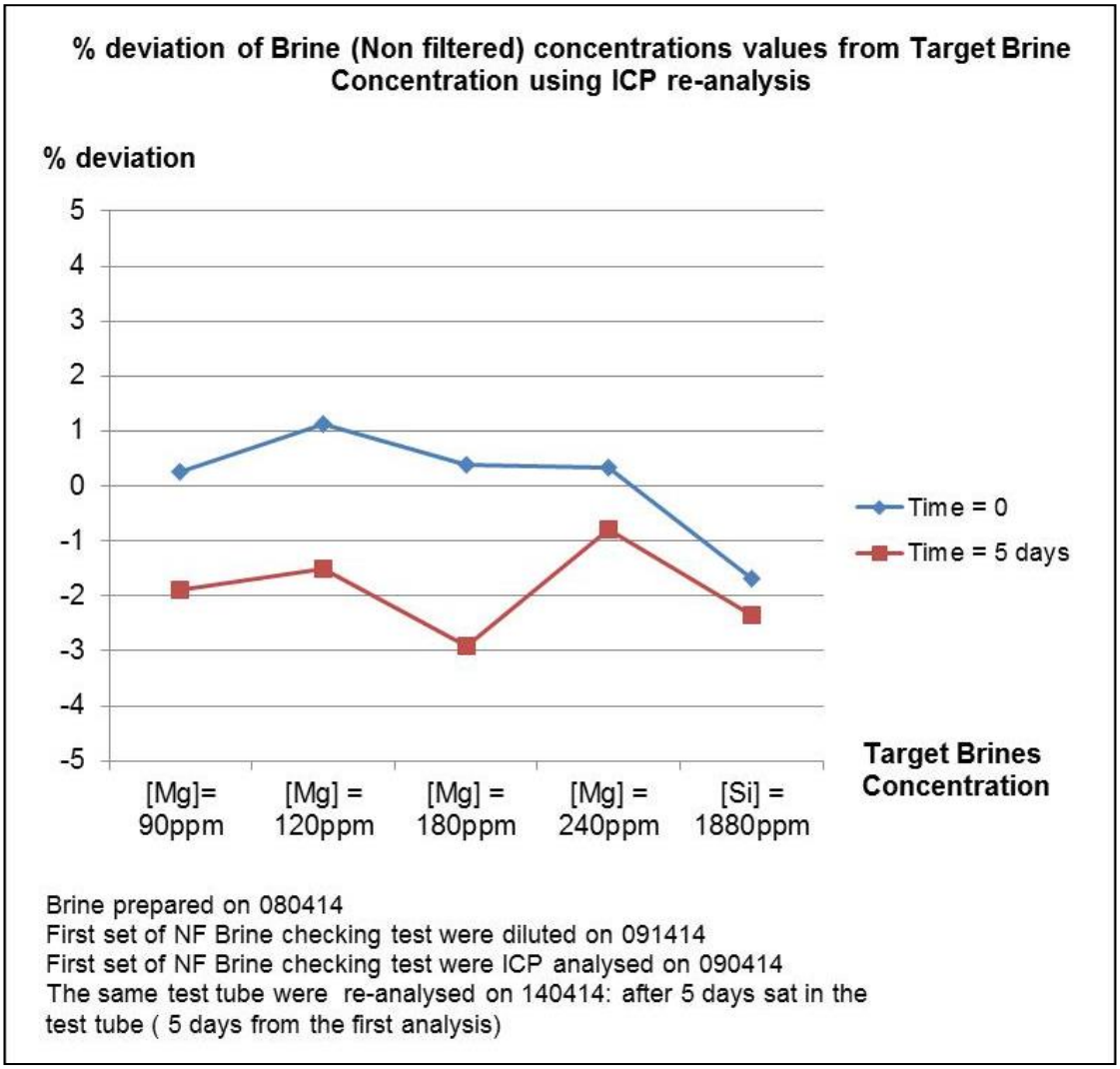

Figure 4-24 Percentage deviation of brines from the target brine concentration

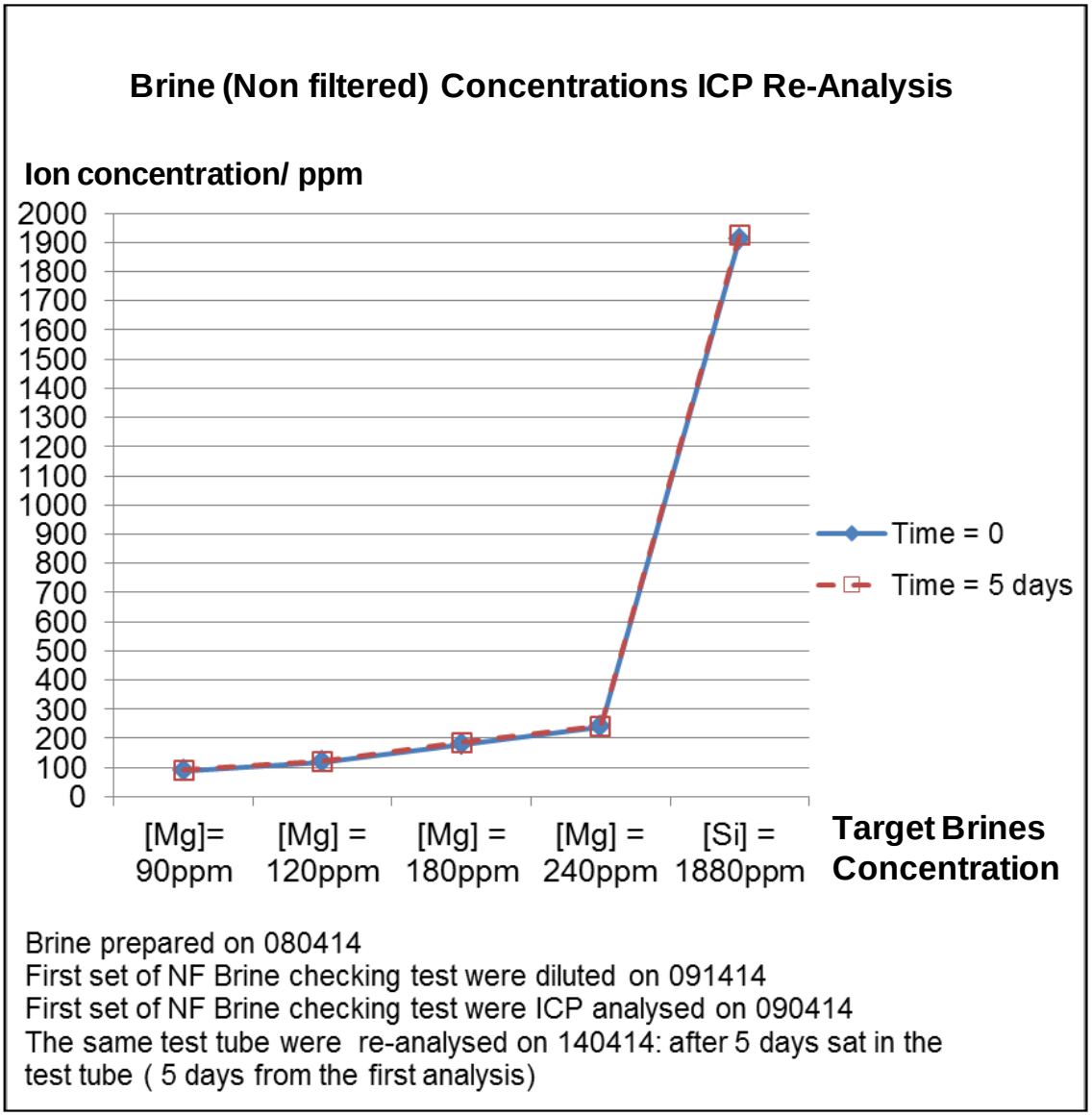

Figure 4-25 ICP analysis of "Waiting Time Effect Investigation" on 1%EDTA/NaOH quenching solution (x20 dilution of NF brines)

4.3.3 Glass Bottle Etch Test

(a) Glass Bottle Etch Test Set up

This experiment was set up to check whether any silicon (Si) is etched from the moulded glass used into the test solution in the Silicate Scale Static Bottle Tests. Results for Silicate Scaling Static Bottle Tests reported in section 4.1 and 4.2 had used glass bottles for the entire 22 hours at room temperature and natural pH condition of the mixed solution (i.e. 45ppm – 1200ppm Mg : ~1000ppm Si in 50:50 mixed ratios with natural pH value of approximately 9.7 to 12.5).

Moulded glass (Borosilicate glass) is known to experience some degree of bottle etch (Si dissolution) if contacted with high pH i.e. pH > 8; high ionic strength, i.e. >0.1M of alkaline salts and complexing agents, e.g. EDTA. Hence, a series of distilled water solution at various pH values and temperatures were ICP sampled to determine the silicon concentration (and Ca, Mg, Al, Fe) after several ageing times (22hours, 3 days, 7 days, 10 days and 15 days). Glass bottle compositions used in this test (and previous test) is given in Table 4-10.

Two sets of pH conditions in distilled water were prepared and placed in the test glass bottles; one set of 100ml distilled water at its natural pH and another set adjusted to pH12 by adding 2M NaOH solution. All glass bottles were left on the lab bench at room temperature for 15 days. The composition of this water was sampled at several ageing times as mentioned above by directly transferring 10ml samples (no dilution) from each glass bottles into test tubes which were then ICP analysed for silicon (Si), magnesium (Mg), calcium (Ca), aluminum (Al), and iron (Fe). pH values were also measured at each sampling time to monitor any pH changes if any (this was an initial indicator, as the solution will experience pH reduction if silicon is etched into the solution).

After 15 days, all glass bottles were heated up to 95^{o}C in the oven and were again ICP sampled at 22 hours and 44 hours (two sets of sampling: direct sampling without dilution; and x10 dilution - in case the amount of ion etched is too high without dilution). Precautionary steps were taken by replacing the glass lid by a new one after 22hour sampling to avoid them from expanding and breaking which would affect the experiment. All ICP results were analysed and plotted to see if any ion etched into the solution.

Table 4-10 Typical glass compositions of soda-lime-silica glasses

	AMBER	WHITE FLINT
Constituent	%	%
SiO_2	73.0	73.0
Al_2O_3	1.6	1.6
Fe_2O_3	0.3	0.04
CaO	11.5	11.5
MgO	0.1	0.1
Na_2O	12.9	13.1
K_2O	0.9	0.6
SO_3	0.1	0.3

Note that all glass testing performed by Glass Technology Services, Sheffield

(b) Glass Bottle Etch Test Results and Discussion

This experiment was designed to check if any silicon (and possibly other ions i.e. calcium, magnesium, aluminium and iron) was etched from the moulded glass used in the Silicate Scaling Static Bottle Tests. Moulded glass (Borosilicate glass) is known to experience bottle etch if contacted with high pH fluids, i.e. pH>8; high ionic strength, i.e. >0.1M of alkaline salts and complexing agents, e.g. EDTA.

Previous tests (Silicate Scaling Static Bottle Tests for high magnesium and low magnesium concentration) reported in section 4.1 and 4.2 were conducted with the natural fluid pH range from pH ~9.7 to 12.5 at room temperature. The same tests were repeated in this work to study the effects of pH and temperature and hence to establish the suitability of the glass bottle could be evaluated for this type of silicate testing.

Initially, the water temperature was increased to 95^{o}C by heating the glass bottle in the water bath. However, the glass bottle lid expanded and essentially disintegrated thus losing the sample into the water bath (Refer Figure 4-26). Therefore, the glass bottles were again tested at 95^{o}C by putting them into the oven but taking the precaution of replacing the lid by a new one after the 22 hour sampling event.

Figure 4-26 Broken lid when heated up in water bath

Based on the results plotted in Figure 4-27, no significant trend can be observed for the natural pH DW tests which were conducted at room temperature. The highest levels of silicon and magnesium ions etched into the distilled water after 15 days were ~ 0.9ppm and ~0.4ppm respectively. Hence, we can conclude that this glass bottle is suitable to be used for the silicate scale static bottle test at room temperature and ~pH6. Results from

similar Si etching experiments are presented in Figure 4-28 for the room temperature pH ~ 12 experiments. From these results, we can observe an increasing trend of Si and Ca ion concentrations etched with time for the pH 12 DW case. However, the amount of silicon dissolved into the distilled water is less than 9ppm and the amount of calcium is less than 2ppm while the rest are all dissolved to a level <1ppm after 15 days. Note that the pH value of the 50:50 mixes SB:MB solution in previous silicate scale static test (high Mg concentration) was approximately 9.7 to 12.5 and it was conducted at room temperature. Hence, the test results that were samples at 22 hours were only slightly influenced by the silicon etch (< 2ppm after 22 hours – Refer Figure 4-28).

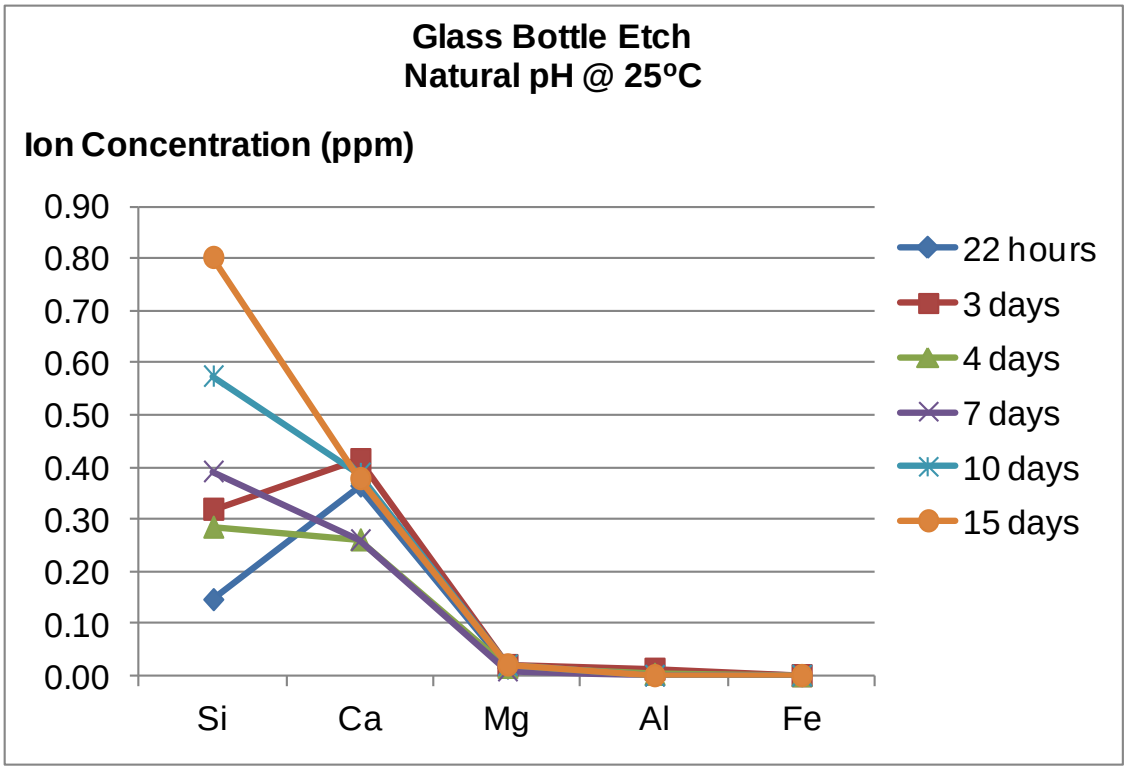

Figure 4-27 Ions etched into distilled water at natural pH and room temperature

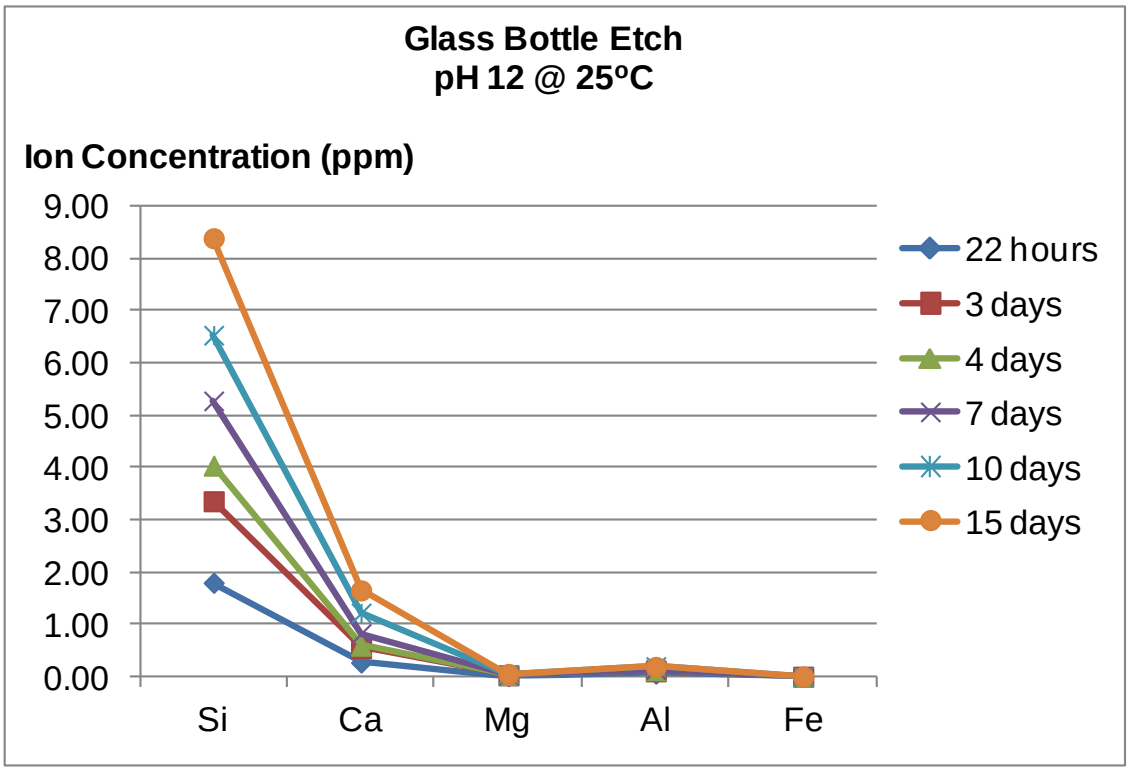

Figure 4-28 Ions etched into distilled water at pH12 and room temperature

Results from the 95ºC bottle etch tests are presented in Figure 4-29 and Figure 4-30 for the natural pH and high pH (~12) cases, respectively. As can be seen in Figure 4-29; silicon dissolution is up to 10 to 20ppm while Ca is etched up to ~3 to 4ppm into the natural pH water, after being heated up to 95ºC for 22hrs and 44hrs respectively.

Results in Figure 4-30 indicate that the amount of silicon and calcium ion etched in the pH12 water after being heated up to 95ºC for 22 hours were 85ppm and 1.5ppm respectively. This amount was further increased to 105ppm and 2.5ppm silicon and calcium ion respectively after 44hrs. Note that (nt) means direct sampling without quenching solution while (x10) means dilution in DW; the results agree very well whether they are diluted or not.

The high temperature (95ºC), high pH 12 results as expected give the highest level of Si etching (~ 100ppm Si) from the test bottles. This level of Si is sufficiently high for us to avoid using such glass bottles in all tests in future. In any case, we have shown that the glass bottle lids are unstable at this temperature (see Figure 4-26) and this also weighs against their use.

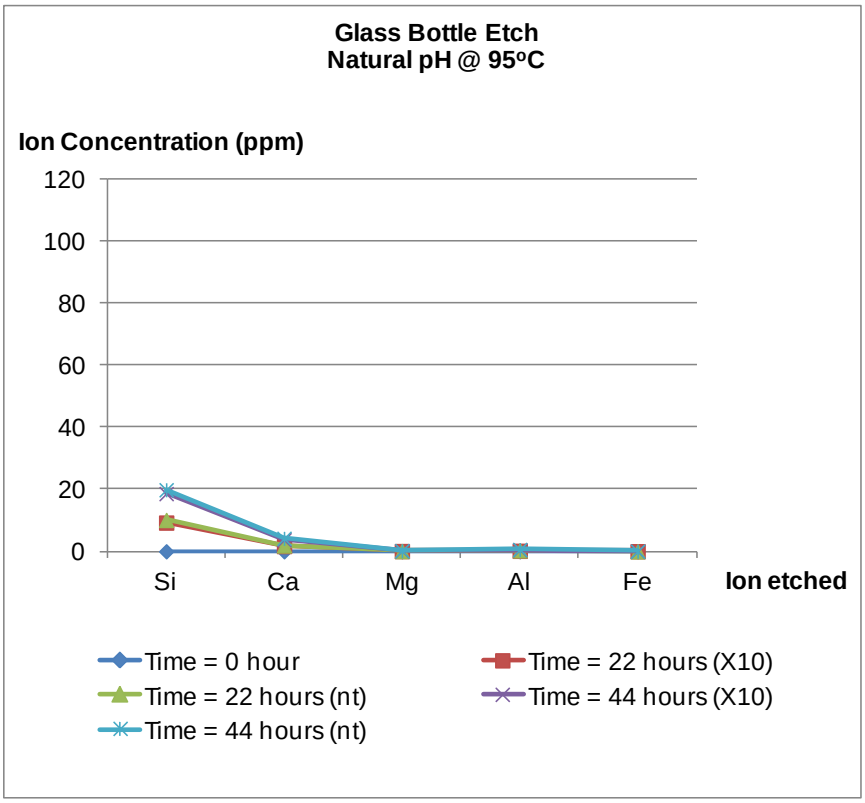

Figure 4-29 Ions etched into distilled water at natural pH and high temperature (95ºC)

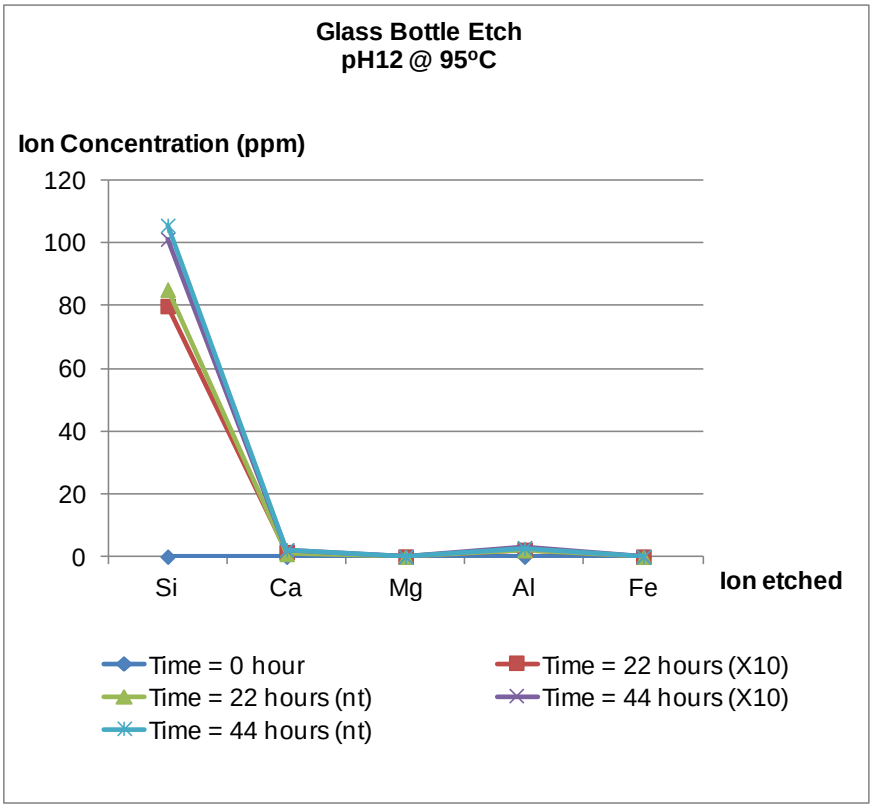

Figure 4-30 Ions etched into distilled water at pH 12 and high temperature (95ºC)

The pH test results in Figure 4-31 show that for the Natural pH DW, the pH values were increased from their initial values at the end of both test conditions (i.e. room T and 95ºC) while for pH12 DW, the pH values are slightly reduced from its initial values at the end of both test condition (i.e. room T and 95ºC).

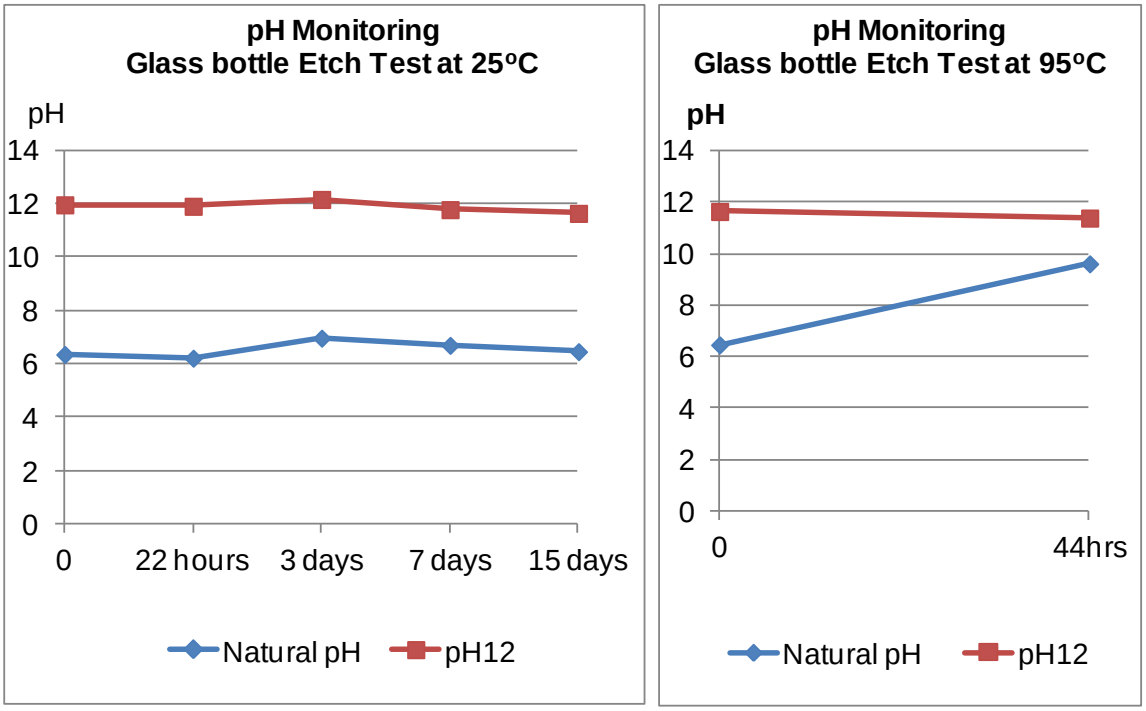

(a) **(b)**

Figure 4-31 pH monitoring for distilled water in Glass Bottle Etch Test at (a) 25ºC and (b) 95ºC

In other tests, a set of fresh non-filtered of magnesium and silicon brines were diluted and measured by ICP analysis. The non-filtered brines were then left in their individual glass volumetric flasks for 16 days before half of the water volumes were filtered using 0.45µm filter paper. The aged non-filtered and aged filtered brines were then diluted and ICP analysed and the results are plotted in Figure 4-32. Figure 4-32 shows that the fresh brines successfully met their target concentrations for both magnesium and silicon ion. The analysis of the aged filtered and non-filtered magnesium brines completely agreed with each other, with deviation of less than 6%. However, analysis of the aged filtered and non-filtered silicon brines showed reductions of 35% and 37% from the value measured for fresh non-filtered silicon brine. The pH value for magnesium brine is around pH6 while for silicon brine is around pH13. This demonstrated that the high pH of silicon brine resulted in silicon ion being etched into the brine. This actual level of Si could not explain the change but it may have shifted the supersaturation further which consequently promoted the polymerization of colloidal silica (and hence led to a lower amount of

silicon ion measured by ICP). This explain the reduced silicon concentration from the target value recorded in Figure 4-32.

In *Low Magnesium Test* discussed in section 4.2; 2050ppm stock Si brine (pH solution were measured as pH 12.87) were prepared and stored in volumetric glass (i.e. the silicon brine is under saturated at this condition of room temperature and highly alkaline). Initially the Si ion were kept stabilize at this high pH. However, this high pH caused the silicon ion etching from the glass -> glass bottle etch test revealed that ~10ppm Si (~21.4ppm SiO_2) were etched from the volumetric glass at room temperature (pH of DW is pH12) and this had caused the pH of the DW to drop about 0.5.

At high pH values, the mechanism of glass degradation changes from the leaching of alkali elements to the dissolution of silicate network as shown in below equations;

$$SiO_2 + 2H_2O \leftrightarrow H_4SiO_4 \quad \textbf{4.1}$$

$$H_4SiO_4 + OH^- \leftrightarrow H_3SiO_4^- + H_2O \quad \textbf{4.2}$$

Reaction (*Equation* 4.2) increases the solubility of the silicic acid in solution, driving the reaction forward. At some point the limit of solubility (increase in amorphous silica concentration) is exceeded, and non visible particles are formed. If the solution is not buffered, a decrease in the solution pH will take place (Hunt, 2012).

The reduction in the pH of the silicon brine that were kept in the volumetric glass (we assumed the pH reduction will be more than 0.5) disturbed the stability of the amorphous silica and reduce its solubility. The non visible particles which were formed act as nuclei that further speed up the polymerization rate to form colloidal silica. This is why we found a decrease in the 2050ppm Si stock solution that were kept in the volumetric flask for more than 6 days by ~40%. This did not happen in the magnesium brines since there was no ion etched into brine at pH6.

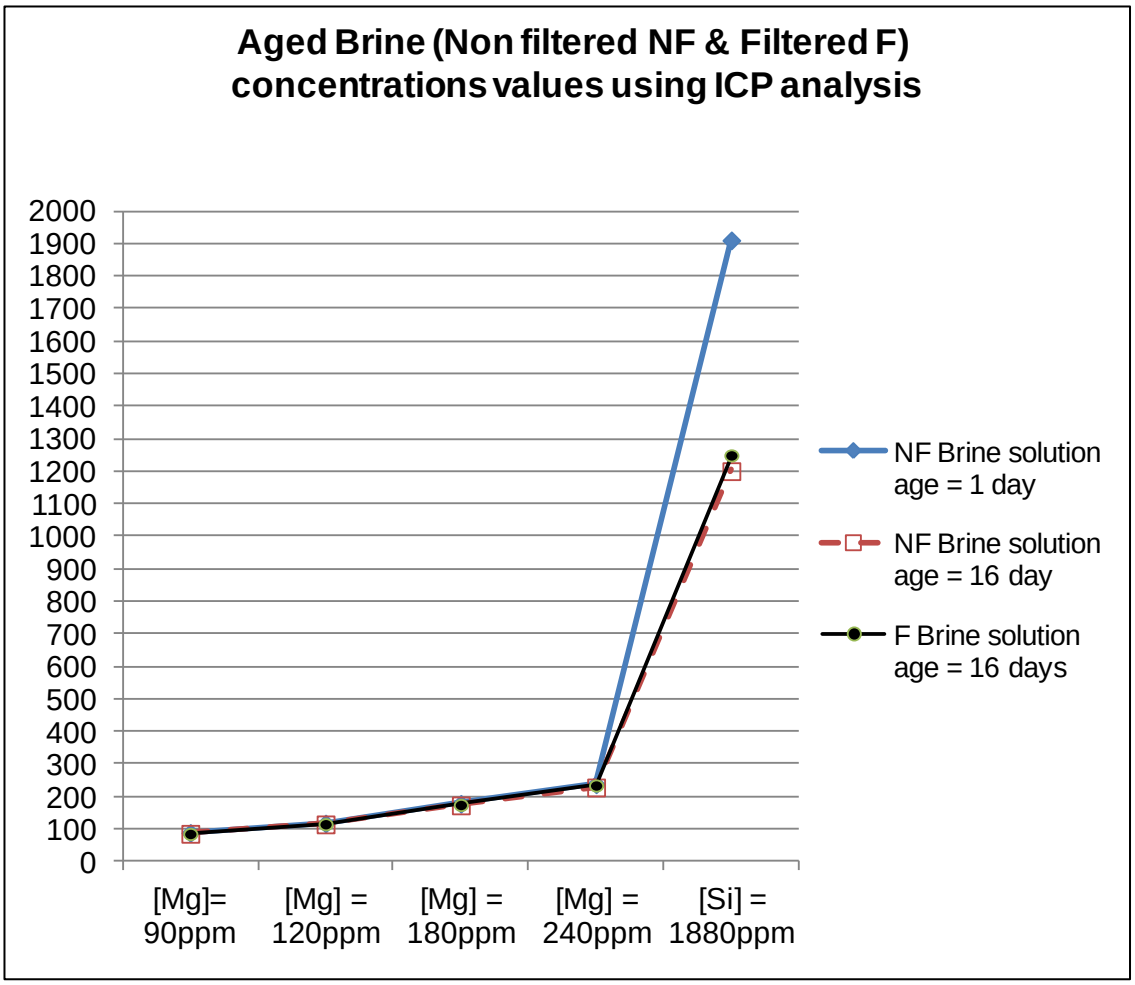

Figure 4-32 Fresh vs. Aged brines concentration (Filtered & Non-Filtered) ICP measured

The analytical silicon profile for 1% EDTA/NaOH is shown in Figure 4-33. These quenching solutions were prepared at different times and stored in volumetric flasks or HDPE bottle and were then ICP analysed. Results in Figure 4-33 clearly show that the aged 1% EDTA/NaOH quenching solution that was stored in the glass volumetric flask was contaminated with silicon. The longer the solution resided in the glass volumetric flask, the higher the amount of silicon which was etched into the solution (i.e. Silicon etched in 1% EDTA 23/4 is higher than silicon etched in 1% EDTA 24/6). Note that 1% EDTA 23/4 is the quenching solution that was prepared on 23/4/2014 and stored in the glass volumetric flask until the sampling time i.e. 75 days and 1% EDTA 24/6 was prepared on 24/6/14 and stored in the glass volumetric flask for 13 days.

1% EDTA 7/7 glass was prepared on the sampling day 7/7/14 and stored in glass volumetric flask and half of this solution was transferred into HDPE bottle and labelled as 1% EDTA 7/7 plastic. Both of these solutions showed no silicon contamination. These profiles revealed that 1% EDTA/NaOH quenching solution that is around pH 13 to 13.5 will etch silicon ion from the glass container and the longer the solution was left in the glass container, the higher amount of silicon ion that will be etched into the solution.

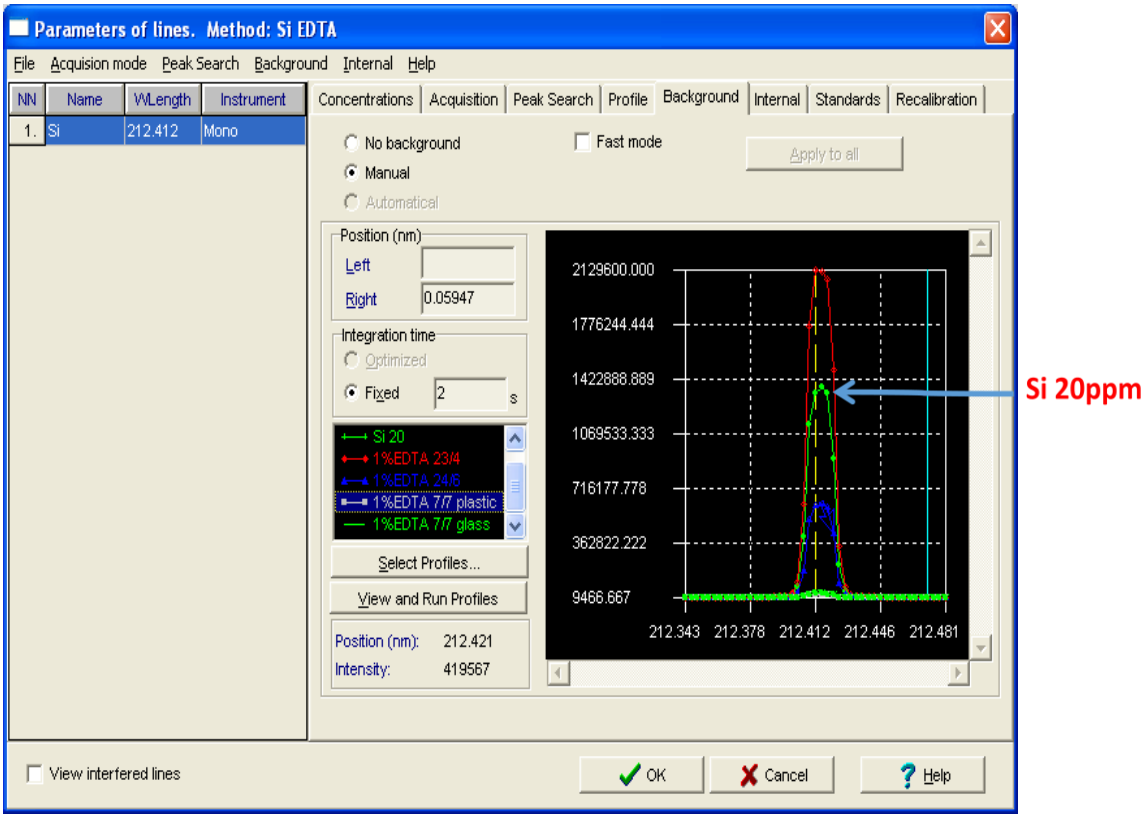

Figure 4-33 Silicon profile for 1% EDTA/NaOH quenching solution

4.3.4 Centrifuging Effect while ICP Sampling

(a) Centrifuging Effect Test Set up

Previous results from the Silicate Scaling Static Bottle Tests for *High Magnesium Concentration Test* were discussed in section 4.1.2(b) and in these it was shown that the sampling position in the test bottle was important since the precipitate can interfere with the Mg and Si analysis. It was observed that the upper fluid layer was clear; the middle layer was cloudy and distinct white sediment had settled at the bottom of the bottle. This

experiment was conducted to check the most appropriate method for ICP sampling of a colloidal silicate solution. Previous results for first results showed that the sampling position (upper – clear; middle – cloudy & bottom – sediment as shown in Figure 4-34) in the test bottle was important since the precipitate can interfere with the Mg and Si analysis as can be observed in Figure 4-5 and Figure 4-6. These results were obtained because of the colloidal nature of the mixed solution where the scale that formed continuously settled to the bottom of the bottle over time, leaving a distinct clear layer in the upper zone, a cloudy layer in the middle zone and thick white sediment in the bottom zone.

Two sets of brines - namely Mg-Brine (MB, i.e. 180ppm Mg and 1800ppm Mg), and Si-brine (SB, i.e. 1880ppm Si) were prepared and vacuum filtered separately through 0.45μm membrane filter paper, as shown in Table 4-11. The initial pH of all filtered brines were check separately before re-measuring the pH of the mixed solution of "*50ml 180ppm MB with 50ml 1880ppm SB"* and "*50ml 1800ppm MB with 50ml 1880ppm SB*" mixed in 50:50 proportions.

100ml of the 50:50% mixes were prepared by mixing 50ml MB and 50 ml SB (gave final concentrations of 90ppm Mg: 940ppm Si and 900ppm Mg: 940ppm Si) before immediately shaking the MB/SM solution mixture vigorously. The clear glass bottles containing the MB/SB were placed on the lab bench with their lids on and experiments were conducted at room temperature and at their natural pH conditions. The cloudiness/turbidity of the solution was observed and pictures were taken where appropriate.

In this test, the samples were analysed by ICP for the particular ions of interest, e.g. silicon and magnesium after 22 hours mixing as per $BaSO_4$ Inhibition Efficiency Test. This was compared with the data taken from the previous *High Magnesium Concentration Test* (i.e. ICP results taken at upper clear position).

Then, the mixed samples at 22 hours were centrifuged to separate the clear solution from the precipitate. From this, the clear solution was analysed again by ICP for [Si] and [Mg] to observe any differences between the two ICP sampling techniques (Non-centrifuged vs. centrifuged).

Photographs were taken, pH values were measured and ICP sampling was repeated once the top clear solution was apparent visually.

Table 4-11 Brine composition and preparation for "Centrifuging Effect during ICP Sampling" test

Ion	Concentration {ppm (mg / L)}	Formula Composition	g / L	g / 5L	g / 10L	g / 15L	g / 20L
Mg^{2+}	180	$MgCl_2.6H_2O$	1.505	7.53	15.05	22.58	30.10
Mg^{2+}	1800	$MgCl_2.6H_2O$	15.05	75.3	150.5	225.8	301.0
Si^{4+}	1880	$Na_2SiO_3.5H_2O$	14.20	71.00	142.00	213.00	284.00

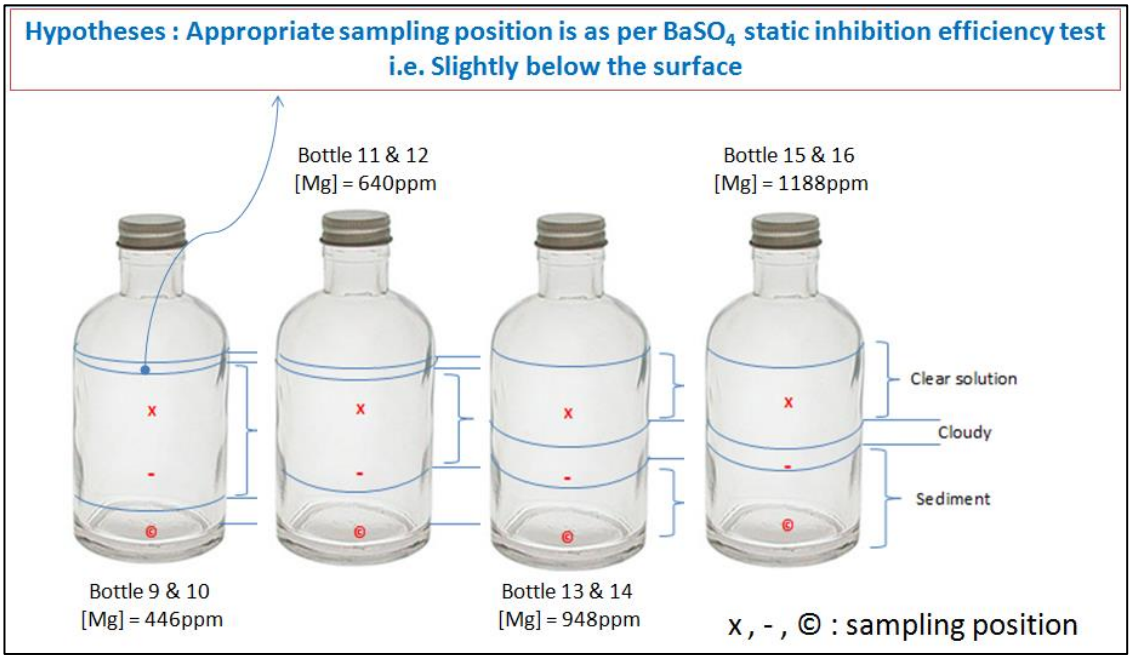

Figure 4-34 ICP sampling position for previous Silicate Scaling Static Bottle Test (section 4.1) and sampling hypotheses

(b) Centrifuging Effect Test Results and Discussion (90Mg:940Si and 900Mg:940Si)

The high concentration magnesium solution, i.e. 900ppm Mg: 940ppm Si, gave a cloudy solution immediately after mixing. After two hours, a clear cloudy layer could be observed and this layer expanded after 22 hour as shown in Figure 4-35, Figure 4-36, and Figure 4-37. However, there was no change in cloudiness in the low magnesium concentration i.e. 90Mg:940Si for the entire 22 hours.

(a)
90ppm Mg : 940ppm Si

(b)
900ppm Mg : 940ppm Si

Figure 4-35 Observation of the mixed brine at time = 0hour

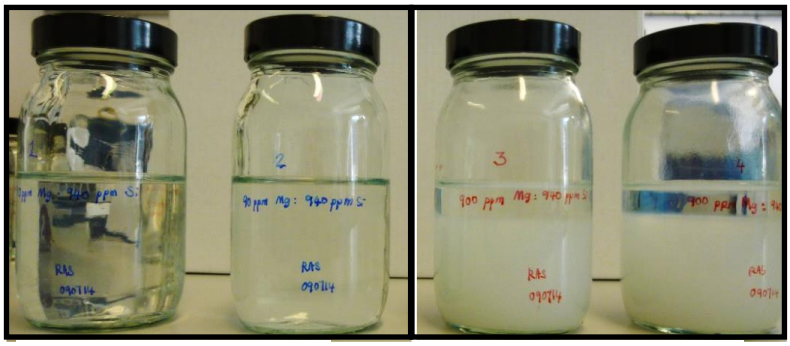

(a)
90ppm Mg : 940ppm Si

(b)
900ppm Mg : 940ppm Si

Figure 4-36 Observation of the mixed brine at time = 2hour

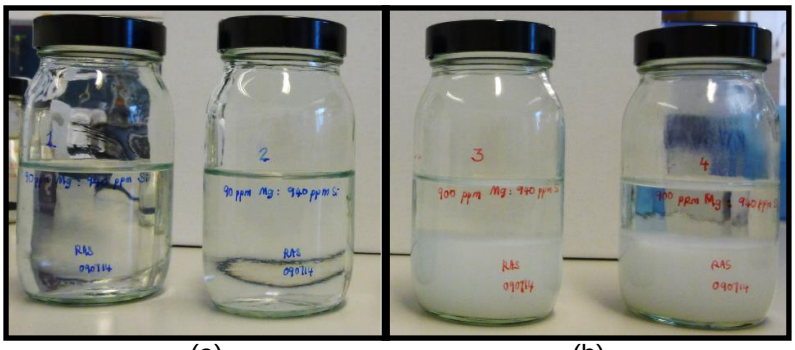

(a)
90ppm Mg : 940ppm Si

(b)
900ppm Mg : 940ppm Si

Figure 4-37 Observation of the mixed brine at time = 22 hour

The clear solution in the 900Mg:940Si was further expanded when centrifuged at approximately 3600rpm for 30 minutes as show in Figure 4-38; no differences were observed after these samples were further centrifuged for another 1 hour.

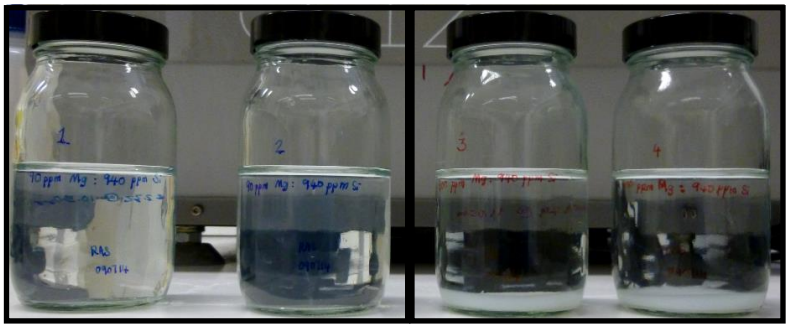

(a) 90ppm Mg : 940ppm Si

(b) 900ppm Mg : 940ppm Si

Figure 4-38 Observation of the mixed brine after centrifuged

Figure 4-39 shows that 794.1ppm and 792.5 ppm magnesium ion was reacted when calculated using equation 3.1 for before and after centrifuging, i.e. < 2ppm difference. For the silicon ion, then 929.6ppm and 940.6ppm silicon ion was reacted before and after centrifuge (~11ppm difference). These figures are essentially identical for these two cases.

The repeatability and reproducibility of the ICP sampling technique was proven when comparing above results with previous silicate scaling static bottle test for the same magnesium concentration as reported in sections 4.1.2(b) and 4.2.2(b). As shown in Figure 4-40, there is less than a 1% differences in silicon and magnesium ions reacted between the two tests. It is worth noting that the "percentage ion reacted" was plotted in Figure 4-40 instead of "amount of ion reacted" since the control values for high Mg cases were different in both tests.

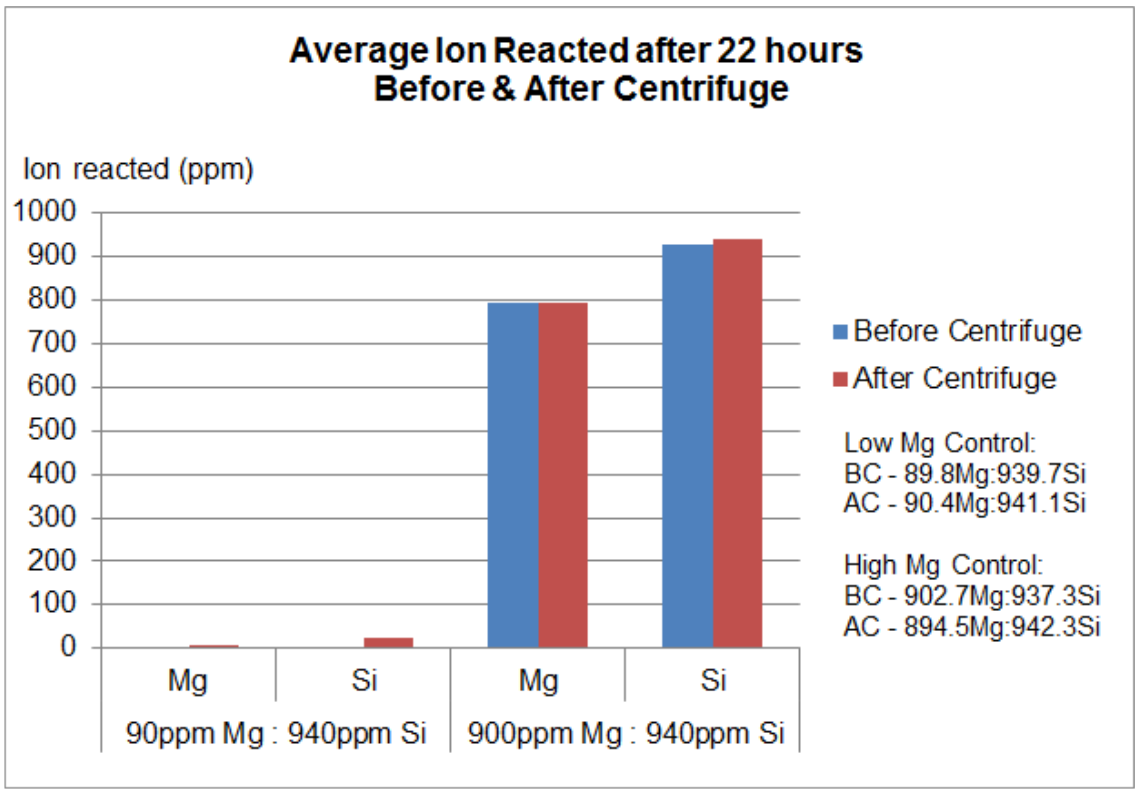

Note: BC – Before Centrifuge & AC – After Centrifuge

Figure 4-39 Average calculated ion reacted after 22 hours before and after centrifuge in "Centrifuge Test"

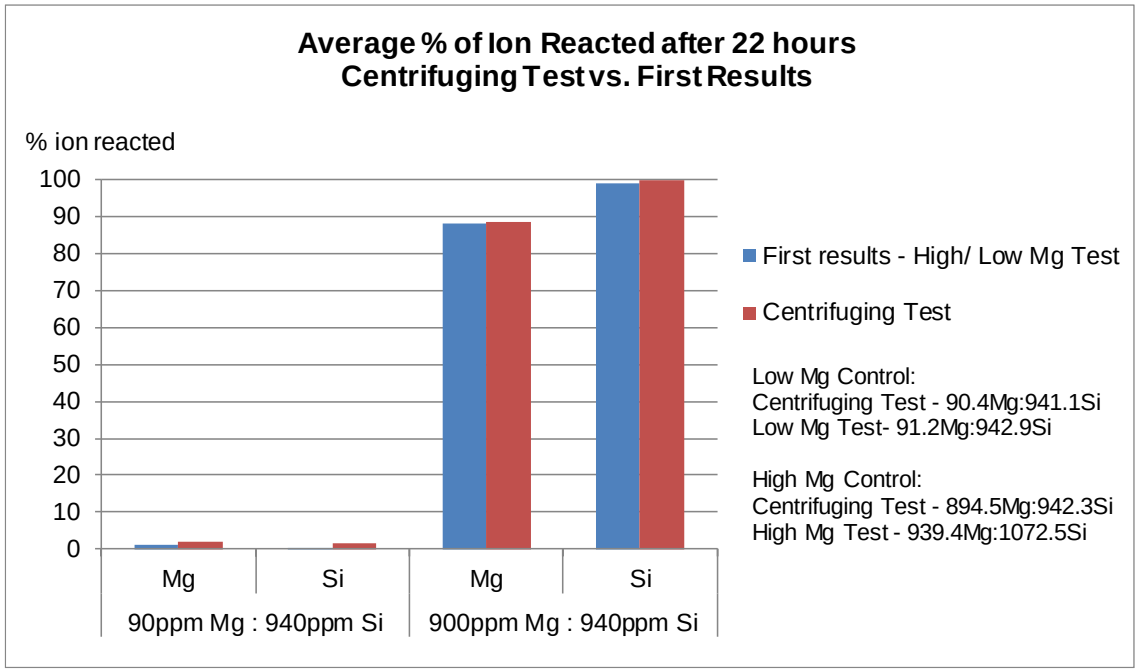

Figure 4-40 Average percentage of ions reacted after 22 hours (Centrifuging Test vs. previous Silicate Scaling Static Bottle Test – reported in section 4.1.2(b) and 4.3.4(b))

(c) Centrifuging Effect Test Results and Discussion (300Mg:940Si)

Figure 4-41 was plotted when 50:50 mixed ratio of magnesium brine was added to silicon brine giving the final mixed concentration of 300ppm Mg : 940ppm Si. The test was conducted at room temperature, natural pH and using HDPE bottles. The mixed solutions were allowed to react for 22 hours and samples for ICP analysis were taken at 2 hours and 22 hours before centrifuging; ICP sampling was repeated to check any differences in ICP ion values. However, only 22 hours ICP data before and after centrifuging were analysed and presented here as part of our investigation into whether there is a need for centrifuging for these ion concentrations.

Figure 4-41 clearly shows that greater than 50% differences for [Mg] reacted and larger than 20% differences for [Si] reacted in ICP values were calculated using equation 3.1. The physical observations at 2 hours and 22 hour reaction time show that the mixed solution produced scales with a cloudy layer being produced in all zones across the bottle (Refer Figure 4-42). Figure 4-43 shows that there were significant differences in the degree of cloudiness observed in the solutions before and after centrifuging. When the mixed solutions were centrifuged at 3600rpm for 30 minutes, a clear solution was produced leaving a white sediment layer at the bottom of the glass.

The above observation suggested that the need for Mg/silicate sample centrifuging will depend on the condition of the mixed solution at the given sampling time, as shown in Figure 4-44. If there is no scale formed in the mixed solution (i.e. cases such as in 90ppm Mg : 940pm Si) or there is scale formed but a clear upper zone is produced (i.e. cases such as 900ppm Mg : 940 ppm Si) at the sampling time, there will be no differences in ICP values measured between before and after centrifuging. However, if there is scale formed but a cloudy layer is produced in the upper zone at the sampling time, then there will be significant differences in ICP values measured for samples before and after centrifuging. Figure 4-44 shows the comparison between all brine concentrations tested in this centrifuging test after 22 hours of reaction.

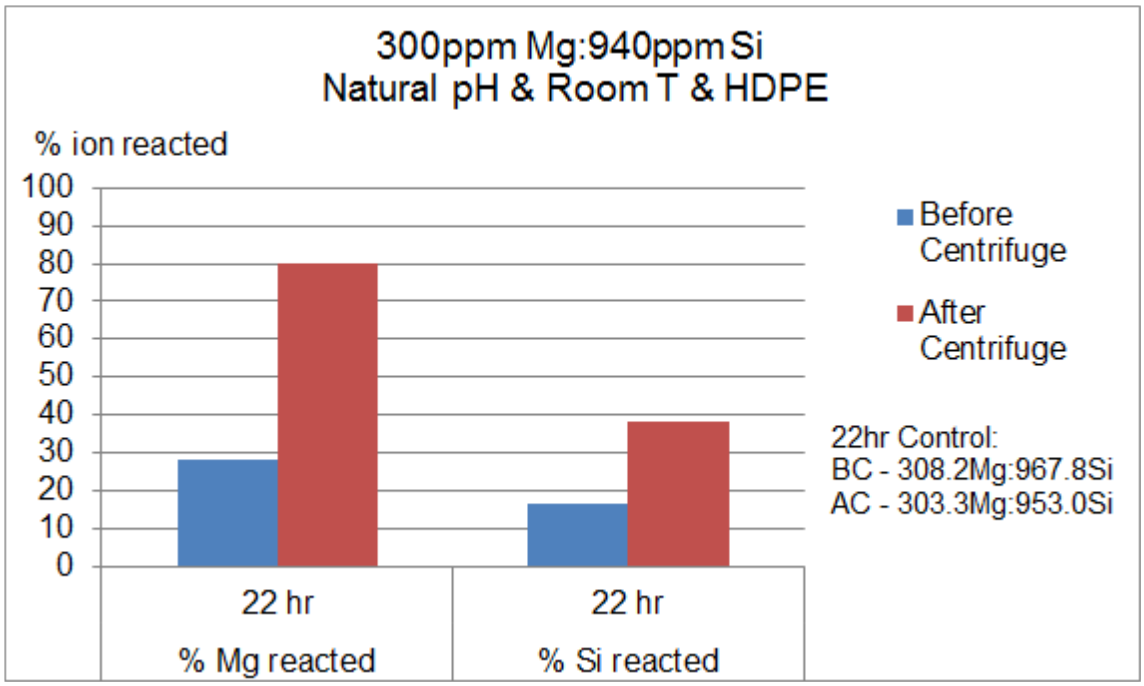

Figure 4-41 Percentage of magnesium and silicon ion reacted at 22 hour before and after centrifuge

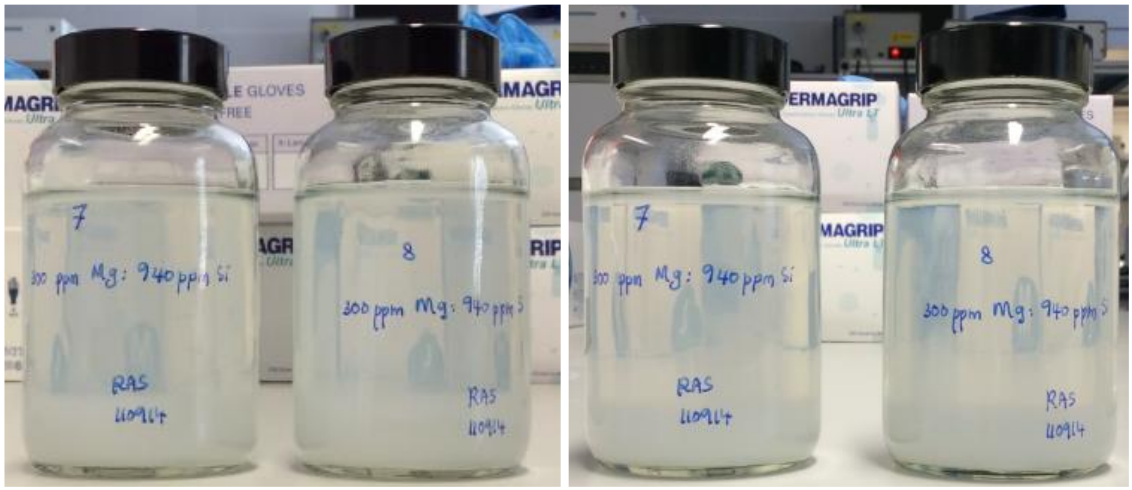

(a) 2 hour (b) 22 hour

Figure 4-42 Observation of 300ppm Mg : 940ppm Si at 2 and 22 hours of reaction time

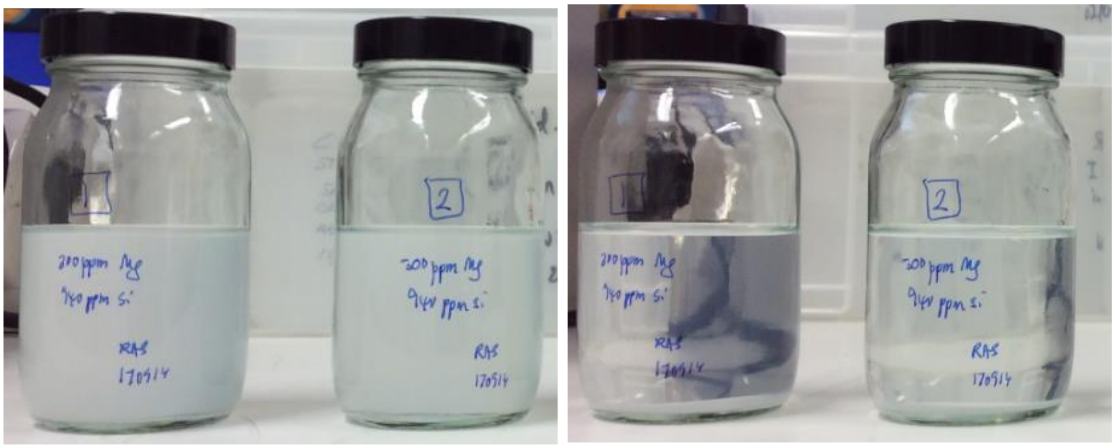

(a) Before Centrifuge (22 hour) (b) After Centrifuge

Figure 4-43 Observation of 300ppm Mg : 940ppm Si at 22 hours (Before and after centrifuge)

(a)
90ppm Mg : 940ppm Si
No scale

(b)
900ppm Mg : 940ppm Si
Scaled & Upper Clear

(c)
300ppm Mg : 940ppm Si
Scaled & Upper Cloudy

Figure 4-44 Observation at sampling time, 22 hour

4.3.5 Stirring Effect while ICP Sampling

(a) Stirring Effect Test Set up

Previous tests (4.1.2(a)) have shown that the mixed solution of magnesium brine and silicon brine produced a colloidal solution in which the precipitate settled to the bottom of the bottle after a period of time. Therefore, sampling in different zones within the bottle (i.e. upper, middle and sediment zones) strongly affected the ion concentrations measured.

Due to the colloidal nature of the mixed solution while the Mg-silicate scaling reaction was taking place, it was necessity to investigate whether stirring the scaling mixture

would affect the ICP values measured. In this experiment, two sets of brines namely MB (i.e. 600ppm Mg), and SB (i.e. 1880ppm Si) were prepared and vacuum filtered separately through 0.45μm membrane filter paper as shown in Table 4-12. The same procedure as that used for the silicate scaling static bottle tests was conducted for final mixed concentrations in 50:50 ratios of 300ppm Mg and 940ppm Si. Two sets of mixed solutions were tested with one set being magnetically stirred for the entire test duration while the other set was left unstirred on the lab bench at room condition. ICP sampling was carried out at 2 and 22 hours for silicon and magnesium ions. Both sets were then centrifuged and ICP sampled to see if any differences in the ICP results were obtained.

Table 4-12 Brine composition and preparation for "Stirring Effect while ICP sampling" test

Ion	Concentration {ppm (mg / L)}	Formula Composition	g / L	g / 5L	g / 10L	g / 15L	g / 20L
Mg^{2+}	600	$MgCl_2.6H_2O$	5.02	25.09	50.17	75.26	100.35
Si^{4+}	1880	$Na_2SiO_3.5H_2O$	14.20	71.00	142.00	213.00	284.00

(b) Stirring Effect Test Results and Discussion

Figure 4-45 and Figure 4-46 shows the amount and percentage of ion reacted at 2 hour and 22 hours with and without stirring. The amount of magnesium and silicon ion reacted without stirring is always higher than in the case with stirring. This may be explained due the fact that stirring probably helped to disperse the colloidal and particulate Mg-silicate thus leading to a higher measured ICP concentration. The amount of magnesium reacted without stirring was calculated to be 6% higher than the same mixed solution with stirring at 2 and 22 hours. The amount of silicon ion reacted in the mixed solution without stirring was calculated to be 3 % higher at 2 hours and 9% higher at 22 hours compared with the stirred mixed solution. However, the differences were less than 1% when both mixed solution was centrifuged for 30 minutes at 3600rpm. These results suggested that stirring has no effect in total ion reacted but rather simply helped to disperse the Mg-silicate that was formed.

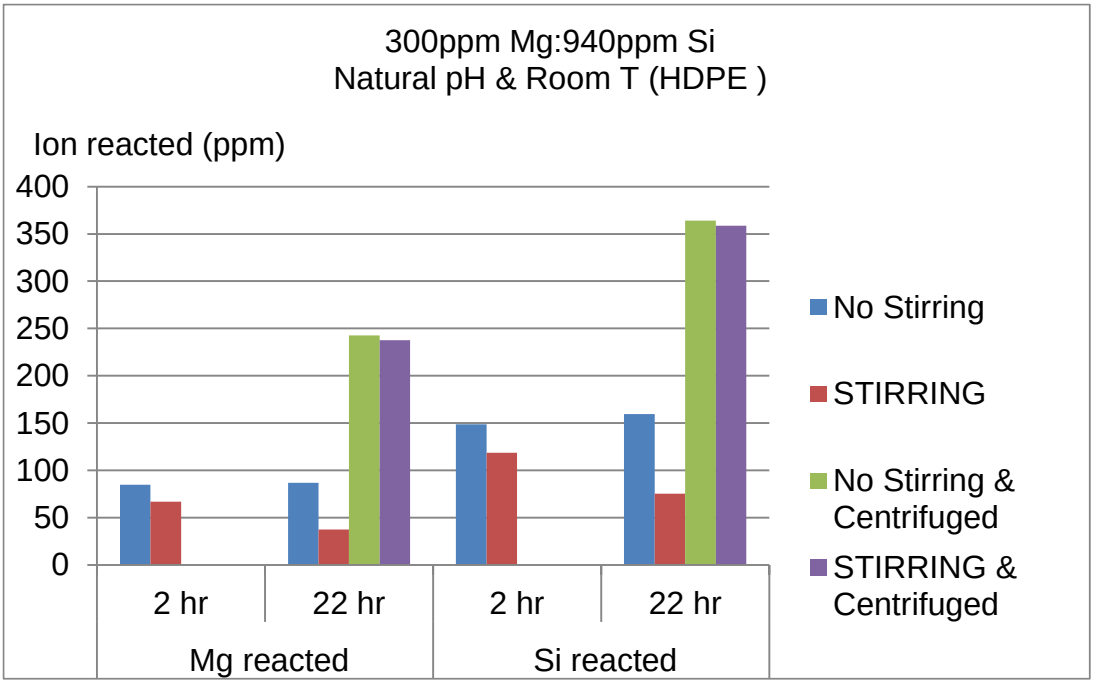

Figure 4-45 Amount of ion reacted at 2 and 22 hours for "Stirring Effect Test"

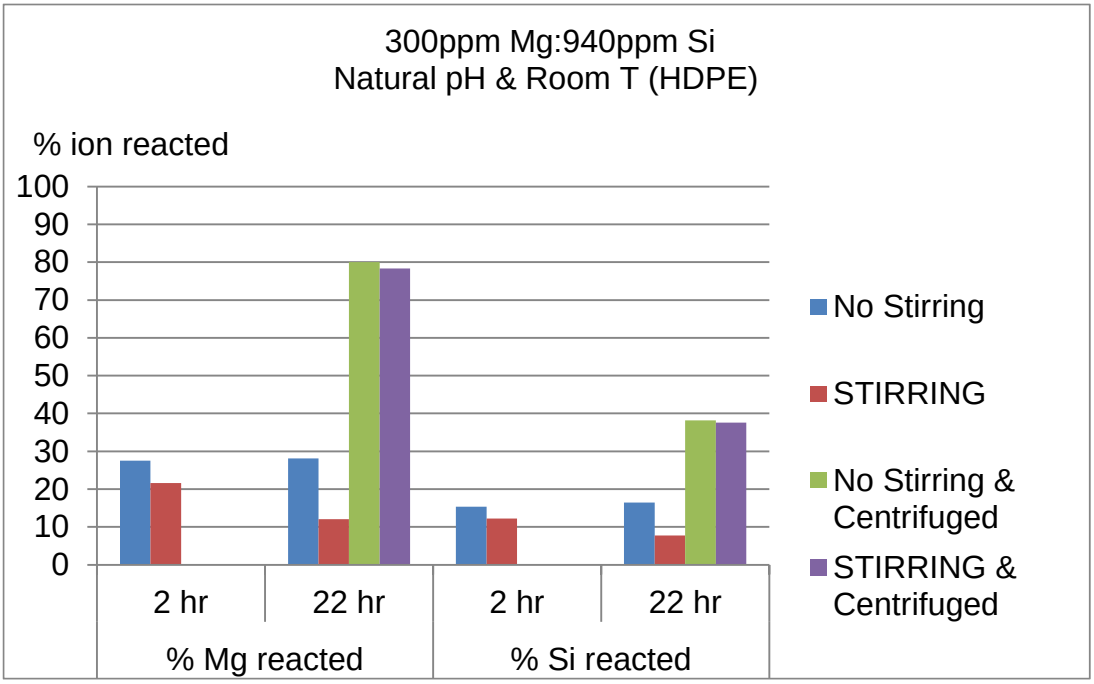

Figure 4-46 Percentage of ions reacted at 2 and 22 hours for "Stirring Effect Test"

4.3.6 Filtering Option & Filter Type Evaluation Test

(a) Filtering Option & Filter Type Test Set up

In the experiment described here, the filtering option was further evaluated as oppose to centrifuging while sampling. It was conducted with the following aims (i) to examine if filtering can replace the centrifuging steps while ICP sampling, and (ii) to evaluate the appropriate filter type for the silicate system.

Filtering Option

Test results in section 4.3.4 (refer to Figure 4-44) show that the mixed solution condition in the test bottle at sampling time (No scale – clear solution or Scaled with upper clear layer or Scale with cloudy solution) is important since the precipitate can interfere with the Mg and Si analysis. As can be observed for 300ppm Mg: 940ppm Si, the mixed 50:50 magnesium brine and silicon brine was found to produce a cloudy solution after reaction at room temperature at its natural pH (~pH12.4) for 22 hours. Therefore, this concentration was chosen as a base case to check the repeatability and reproducibility of the filtering technique in ICP sampling as compared to the centrifuging technique.

The rationale behind this part of the study is to simplify the ICP sampling procedure without the need for sample centrifuging. The centrifuge is limited to four samples only at one time; while the centrifuging process itself is time consuming and involves complex scheduling when large numbers of samples are involved in an experiment. The test was conducted to evaluate the performance of both techniques at two different test conditions (i.e. 300Mg:940Si at room temperature and pH8.5; and 300Mg:940Si at 60^{o}C and pH8.5) using the same procedure of silicate scaling static bottle test. The latter silicate system was heated to 60^{o}C using an oven.

Duplicate samples were tested to check the ICP ion values at 22 hour for both techniques (filtering and centrifugation) at both test conditions. After 22 hours, duplicate samples were centrifuged at speed ~3600rpm for 30 minutes before being ICP sampled and analysed as in standard $BaSO_4$ Static Inhibition Efficiency Tests i.e. slightly below the top surface of the scaling solution (by taking 1 ml of this centrifuged solution and diluted into 9ml of 1% EDTA/NaOH quenching solution).

Other corresponding duplicate samples were filtered using a syringe filter to get at least 10ml of the test samples as per the $BaSO_4$ Static Inhibition Efficiency Tests before 1ml

of the filtered samples was then quenched in the 1% EDTA/NaOH quenching solution for ICP analysis. Note that the filter type used in this analysis is Anatop 25 plus.

Filter Type Evaluation Test

The filter type was further evaluated for the silicate system of 60Mg:940Si at test condition of 60^{o}C, pH8.5. Several filter types were evaluated as following:

i. GD/X 25 0.2µm NYL

ii. GD/X 25 0.2µm PES

iii. Anotop Plus 25 0.2µm

(b) Test Results and Discussion – Filtering vs. Centrifuging Techniques

To further simplify the ICP sampling procedure, the filtering technique appears to be a promising alternative for avoiding the tedious and time consuming procedures involved in centrifuging the sample before the ICP sampling can be performed. In this experiment, a 10 ml test sample was filtered using a syringe filter as per the $BaSO_4$ Static Inhibition Efficiency sampling procedure, i.e. slightly below the top surface of the scaling reaction. From this filtered sample, a further 1ml sample was then quenched in 9ml of 1% EDTA/NaOH quenching solution.

Figure 4-47 show the percentage amount of ion reacted in the silicate scaling static bottle tests that were conducted at room temperature, pH 8.5 and 60^{o}C, pH8.5 respectively. As can be seen in the figure, for 300Mg:940Si reacted at room temperature (and pH 8.5), the differences in values calculated for both techniques are <2% and <9% for percentage amount of magnesium and silicon ions reacted, respectively. The amount of ion reacted calculated from ICP values were found to be higher when using filtering than when centrifuging the samples. However, the results are reversed for the scaling reaction of 300Mg:940Si at 60^{o}C (and pH 8.5). For this case, it was found that the differences between these techniques are <5% and <1% for percentage amount of magnesium and silicon ions reacted, respectively, as can be seen in the figure.

The filtering procedure is a promising technique that could replace centrifuging in due course within an acceptable margin of experimental error. Centrifuging techniques may

have the possibility of not all the precipitate falling to the bottom which can interfere with the ICP value even although the test samples were centrifuged for long enough (in this test all test samples were centrifuged for 30 minutes). While the precipitate is completely filtered in the filtering technique.

However, care should be taken in choosing the correct syringe filter that will suit the purpose; i.e. filter material does not contain elements that could interfere the ICP analysis and the filter can adequately withstand the test temperature. The syringe filter i.e. Anatop 25 Plus used in the experiment could only withstand temperature up to 40^{o}C that probably contributed to some of the differences in results, and this had been remedied in the results discussed in next section.

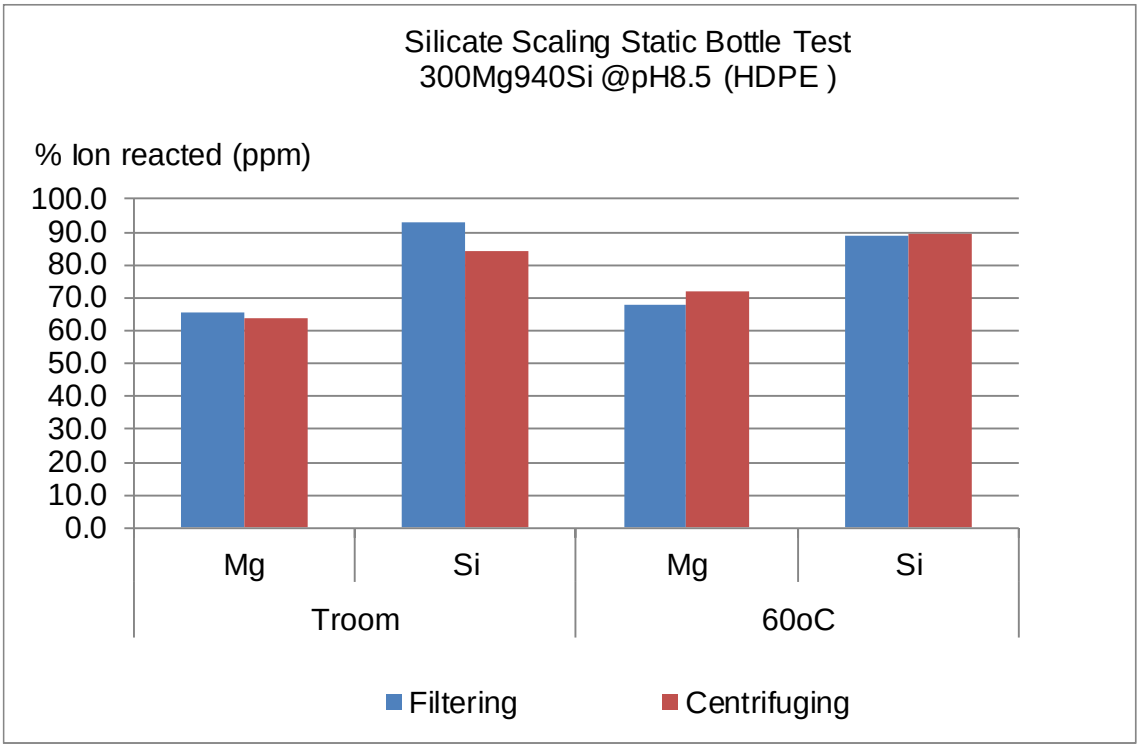

Figure 4-47 Filtering (using Anatop 25 Plus) vs. Centrifuging techniques while ICP sampling

(c) Test Results and Discussion – Filter Type Evaluation Test

The amount of ion reacted determined from the ICP analysis for all filter types are shown in Figure 4-48 and the differences in the values with the ones obtained by the centrifuging technique are shown in Figure 4-49. Direct sampling gave the closest value of the amount magnesium ion reacted as determined by centrifuging technique (but the largest in the

amount of silicon ion reacted) while the Anotop 25 plus gave the opposite results from direct sampling. It can be concluded that the GD/X 25 0.2µm Nylon filter gave the most reasonable values closest to those determined from the centrifuging technique and also the lowest error between duplicates (Refer Figure 4-50).

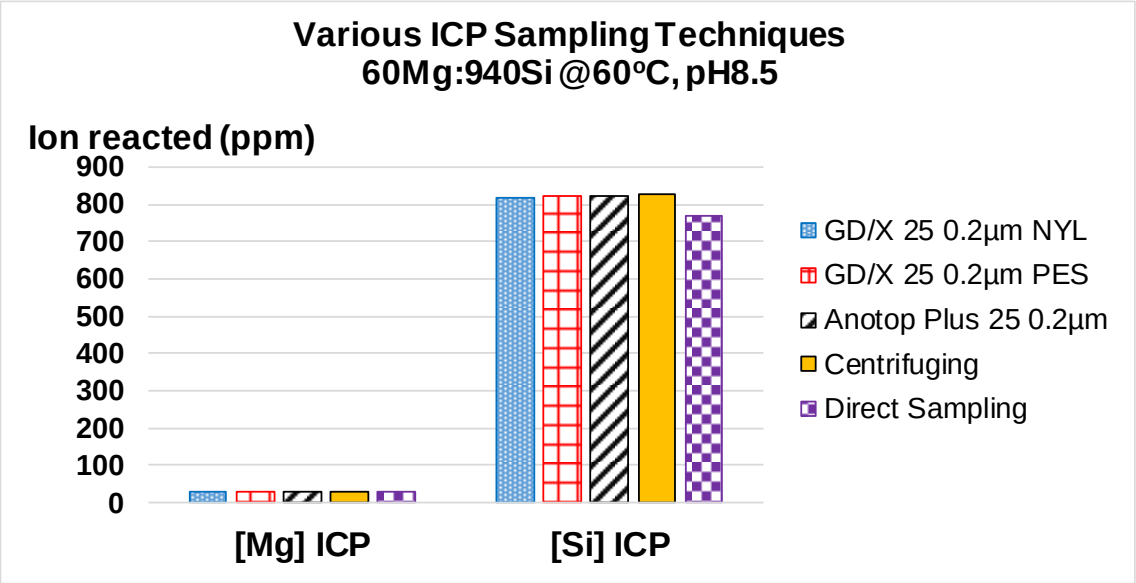

Figure 4-48 Comparison in amount of ion reacted determined from ICP analysis using various filters, direct sampling and centrifuging technique.

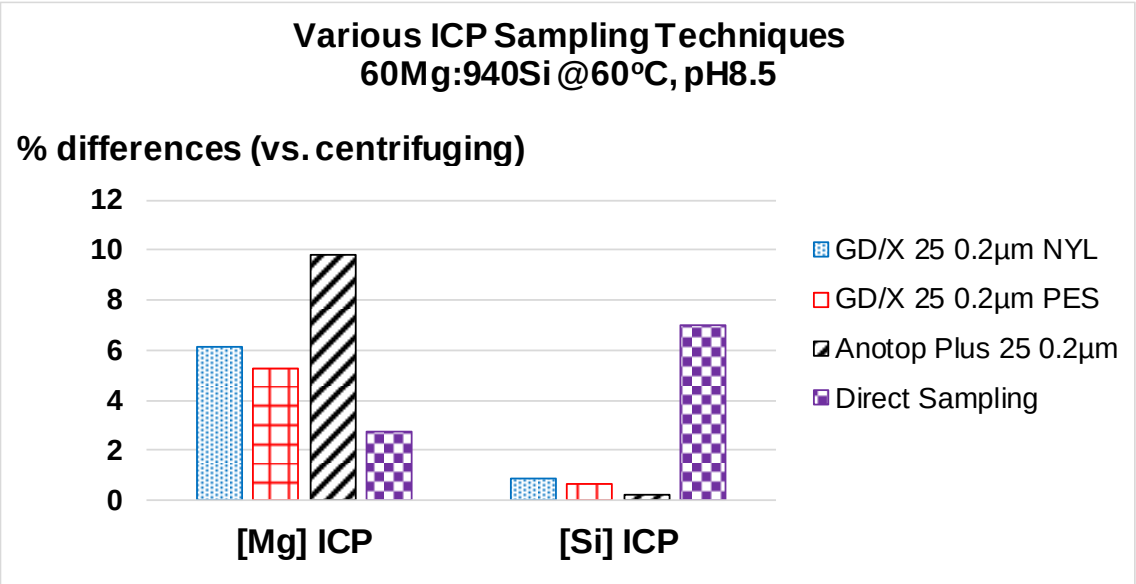

Figure 4-49 Percentage differences of amount of ion reacted when using various filter type and direct sampling as compared to centrifuging technique.

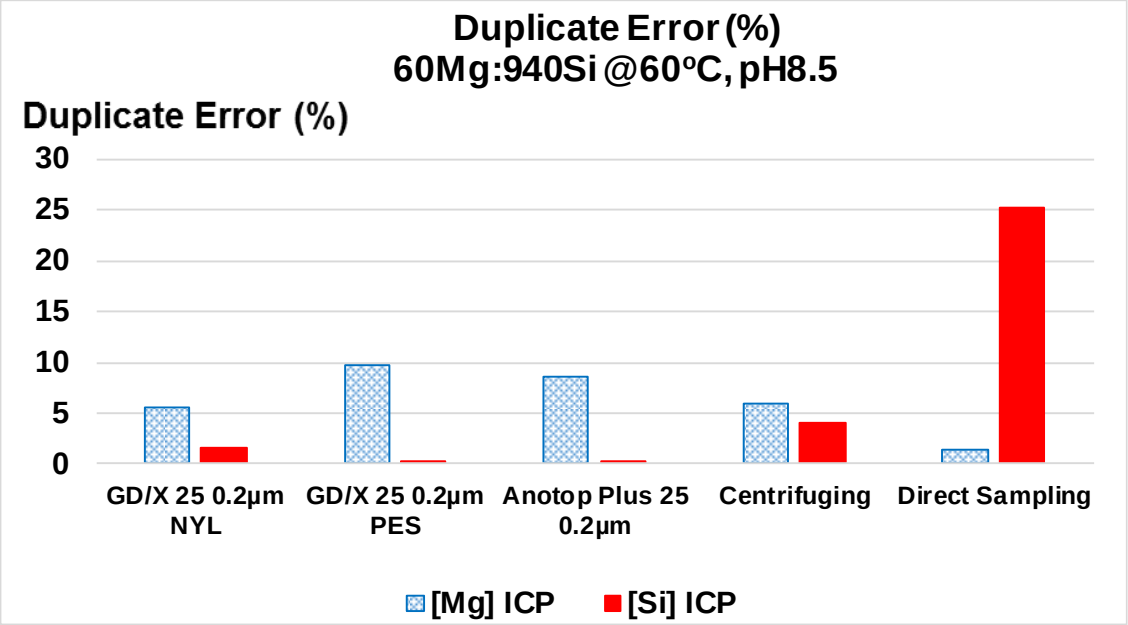

Figure 4-50 Difference error in duplicates in various filter types, direct sampling and centrifuging technique

4.3.7 Summary and Conclusions of Silicate Scale Static Test Development

A methodology for quantifying silicate scale formation using ICP analysis has been developed. This methodology has solved several issues which have arisen while dealing with the colloidal nature of the mixed solution produced in the silicate scaling reaction. Among the issues that have been solved in this work include establishing the correct quenching solution, the location of ICP sampling, the effect of sample centrifuging and stirring and filtering while sampling, and the use of glass or HDPE bottles for the tests. The methodology which has now been fully established is summarized in Figure 4-51.

The preliminary detailed conclusions on the developed methodology for quantifying silicate scaling using ICP analysis are as follows:

1. ICP results were found to be repeatable and reproducible and are hence suitable for quantifying silicate scale formation;

2. A 1% EDTA/NaOH solution is the correct quenching solution for use in ICP sampling since it has been shown that there is no further reaction between the solutions and the sample. The waiting time for the sample quenched in 1% EDTA/NaOH is up to five days which provides flexibility in scheduling the ICP analysis.

3. HDPE bottles were found to be suitable for Silicate Scaling Static Bottle Test since there was no additional magnesium or silicon ion etched into the solution

4. Glass Bottles may suitable to be used for Silicate Scaling Static Bottle Test at room temperature and pH up to 12 for experimental times up to 22 hours, but it is probably best to avoid them. However, glass bottles are not suitable for use at 95^{o}C due to high silicon etch which may be observed, i.e. up to 80ppm at pH 12 solution as early as 22 hours. The higher the pH value of the solution, the higher the amount of ion will etch into the solution. Therefore, any solutions that is high in pH such as 1880ppm silicon brine (~pH13) and 1% EDTA/NaOH quenching solution (~pH13.5) must be immediately transferred into HDPE container once prepared. It is worth noting here that the use of glass bottles in our silicate system at 60^{o}C, pH8.5 is acceptable.

5. ICP sampling techniques;

    (i) ICP sampling should be taken as per $BaSO_4$ Static Inhibition Efficiency Tests i.e. slightly below the top surface of the scaling solution.

    (ii) The need to centrifuge the sample will depend on the upper zone condition at the sampling time. If there is no scale produced, then there will no need to centrifuge the mixed solution. Centrifuging is also not required if scale is formed but there is a clear upper layer zone. However, if scale is produced but the the upper layer zone remain cloudy, then there will be significant differences in values of ICP measured (Si and Mg) concentrations before and after centrifuging.

    (iii) Stirring at sampling time make no differences in total values reacted but rather helps to disperse the solution. It is closely related to the need for centrifuging and the same argument in the above point also applies here.

    (iv) Based on the results and arguments discussed in this section, we conclude that filtering using GD/X 25 0.2µm NYL is the most appropriate ICP sampling technique. The filtering assured there was no precipitate sampled which would interfere with the ICP sampling and measurement. In addition, the filtering techniques eliminated the complexity in the experimental schedule i.e. the tedious handling between ICP sampling and

the centrifuging process. The number of samples required was also halved, i.e. separate test bottles for 2 and 22hour samplings were not required, which meant that the difficulty in the pH adjustment of samples was greatly reduced.

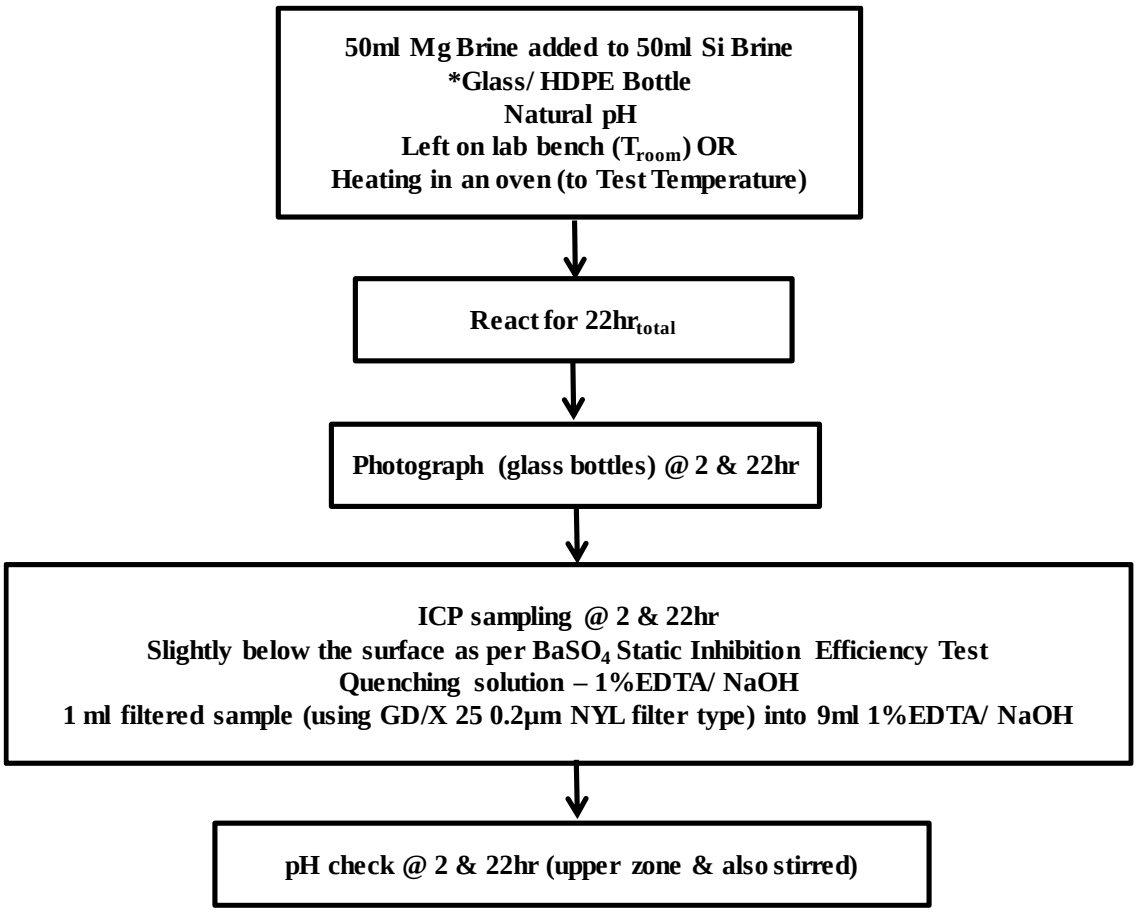

Figure 4-51 General experimental methodology developed for Silicate Scale Static Bottle Test

4.4. SENSITIVITY ANALYSIS

Silicate scaling in oil wells involves some very complex aqueous solution chemistry and is not yet fully understood. This is due to the fact that a number of chemical reactions are occurring simultaneously, the high dependency of silica solubility on pH and the insolubility of certain metal-silicate scales. Therefore, there is a need to study how these various factors (i.e. pH, temperature, divalent ions etc.) will affect the type, extent and morphology of silicate scales which form and the kinetics of the silicate scaling reactions.

The methodology which has now been established has then been applied to study (a) the effect of pH on the severity and composition of silicate scaling which is observed and, (b) the minimum magnesium concentration (threshold value) required to initiate the silicate scaling reaction, (c) the effect of temperature, and (d) the effect of ageing the original silicon brine before forming the magnesium silicate scales. A number of interesting, novel and important findings have been uncovered in this study and these are reported here.

The effect of any factors studied was evaluated through qualitative analysis (i.e. types and morphology of silicate scales formed using various spectroscopic techniques) and quantitative analysis (i.e. establishing the *Si:Mg molar ratio* determined from the ICP analysis and EDAX analysis). A wide range of analytical techniques have been investigated to study the composition of the silicate scales formed, as follows:

(i) *Environmental Scanning Electron Microscopy/ Energy Dispersive X-ray Analysis* (ESEM/EDAX);

(ii) *Fourier Transform Infrared Spectroscopy* (FTIR); and

(iii) *X-ray Powder Diffraction* (XRD).

The results from these techniques have given us some excellent interpretive clues as to the nature of the silicate precipitates, as explained in some detail in this section.

4.4.1 Effect of pH

(a) Experimental Set up

Previous ESEM/EDAX analysis in section 4.1.2(b) and 4.1.2(c) revealed that the Mg-silicate scale formed was found to be amorphous in nature and that the stoichiometry varied somewhat with the initial [Mg^{2+}] in solution. For an initial Si:Mg molar ratio less than 1 (i.e. Si ion in excess), the atomic ratio of Si:Mg in the amorphous Mg silicate was found to be approximately 1.3. However, when the initial Mg ion in the mixed solution is in excess (Si:Mg ≤ 1), the atomic ratio of Si:Mg in the precipitate is approximately 1. Though, ESEM/EDAX are only able to identify what those particular elements are and their relative proportions (Atomic % for example) but not the actual compounds which were formed. For example, the ESEM/EDAX can provide relative proportion of Mg, Si, and O but cannot identify whether the Mg containing compound is magnesium silicate or magnesium hydroxide.

Hence, in this test, two sets of brines were prepared as shown in Table 4-13 before duplicate sets of bottle tests (with 900ppm Mg and 940ppm Si in a 50:50 mix ratio) were carried out with lowered pH values to pH 8.5 to ensure that no magnesium hydroxide was formed. Typically, magnesium hydroxide is formed at pH ≥ 9.5 while colloidal silica will be formed at pH < 8.5 and magnesium silicate is formed at pH≥8.5. One set of the same magnesium and silicon concentrations were allowed to react at its natural pH (pH >10) while another set were allowed to react at its natural pH for 22 hours, before the mixed pH solution was pH re-adjusted to pH ~8.5. ICP sampling was carried out at 22 hours. The various precipitates were collected and analysed by ESEM/EDX (and also with FTIR, Powder XRD and by mass spectrometry MS in some cases). Reference chemicals for FTIR, Powder XRD (and mass spectroscopy) are magnesium hydroxide, magnesium silicate and amorphous silica. This test protocol is shown schematically in Figure 4-52.

Table 4-13 Brine composition and preparation for "pH Effect on Silicate Scaling" test

Ion	Concentration {ppm (mg / L)}	Formula Composition	g / L	g / 5L	g / 10L	g / 15L	g / 20L
Mg^{2+}	1800	$MgCl_2.6H_2O$	15.05	75.3	150.5	225.8	301.0
Si^{4+}	1880	$Na_2SiO_3.5H_2O$	14.20	71.00	142.00	213.00	284.00

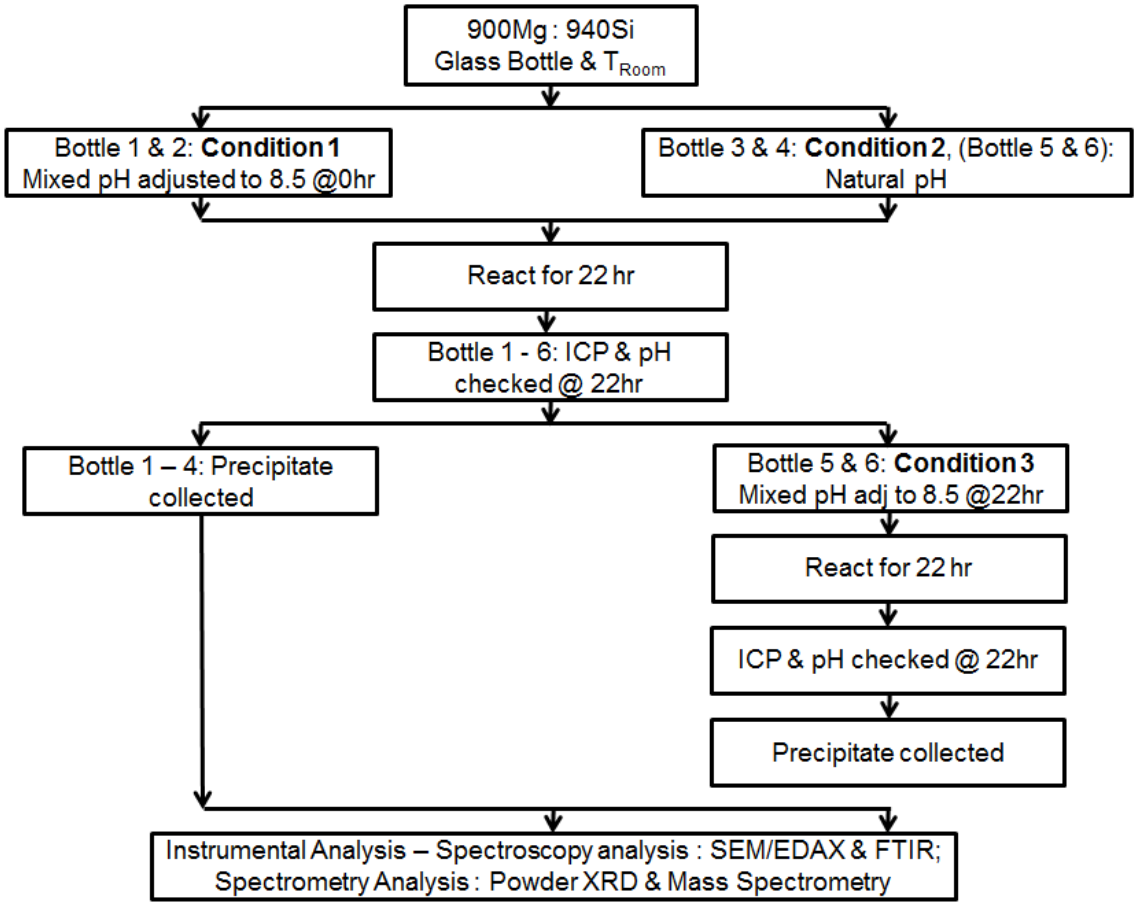

Figure 4-52 Experimental procedure for "pH Effect on Silicate Scaling" test

(b) Experimental Results and Discussion

The effect of pH on silicate scale formation is studied in this work by reacting a 50:50 mixed solutions of 1880ppm silicon brine with an 1800ppm magnesium brine (giving a final solution of 900Mg:940Si) for 22 hours at 3 pH conditions, which were (i) Condition 1 - fixed pH8.5 at 0 hour; (ii) Condition 2 - its natural pH condition ~pH10.1; and (iii) Condition 3 - its natural pH condition ~pH10.1 for 22 hours followed by pH being re-adjusted to pH8.5 and then allowing the reaction to continue for another 22 hours.

Physical Observation

It was observed that for all conditions a mixed a cloudy solution appeared immediately after the solutions were mixed. However, the colloidal solution started to settle to the bottom of the bottle at different rates (time = 2 hour & 22 hour) as can be seen in Figure 4-53 and Figure 4-54.

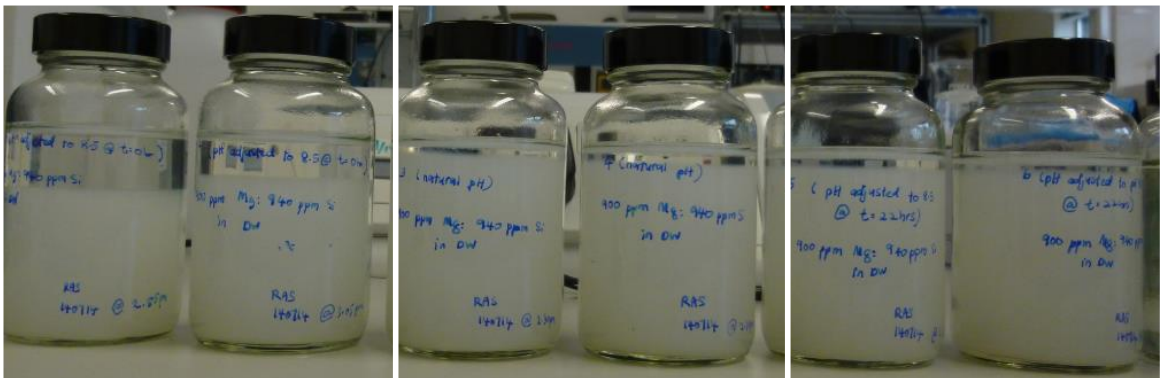

(a) Test condition 1: pH8.5 adjusted @ 0hr

(b) Test Condition 2: Natural pH

(c) Test Condition 3: Natural pH, then pH8.5 adjusted@22hr

Figure 4-53 Physical observation after 2 hour of mixing of 900ppm Mg : 940ppm Si

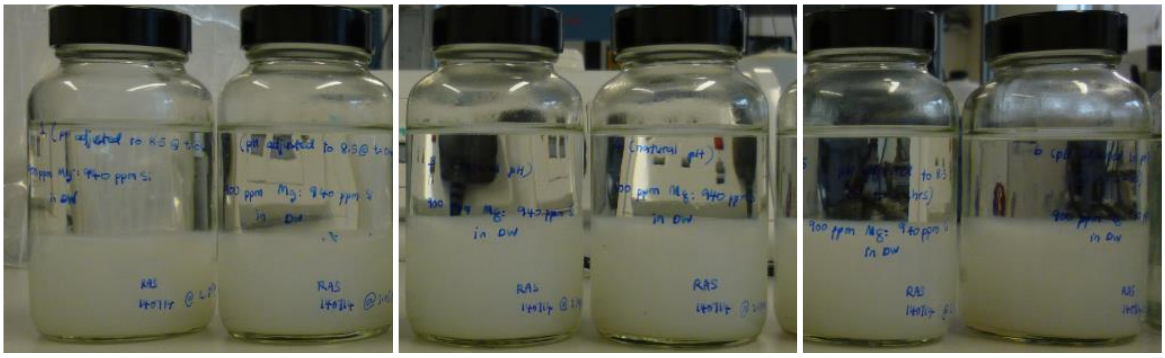

(a) Test condition 1: pH8.5 adjusted @ 0hr

(b) Test Condition 2: Natural pH

(c) Test Condition 3: Natural pH, then pH8.5 adjusted@22hr

Figure 4-54 Physical observation after 22 hour (Condition 1 & 2) and 44 hour (Condition 3) of mixing of 900ppm Mg : 940ppm Si

ICP Results and Analysis

The results plotted in Figure 4-55 show that there are differences in the amounts of ions which have reacted (calculated from the ICP data) under each of the three different conditions. This may be an indicator of slightly different compounds being formed in the scale which is precipitated under each of the different pH conditions; e.g. we note that much lower magnesium ion reacted is observed in Condition 1 (pH8.5 for 22 hours) than in Condition 2 (Natural pH ~ 10.15 for 22 hours). This was due to the fact that more magnesium hydroxide $Mg(OH)_2$ was formed under pH Condition 2. However, this $Mg(OH)_2$ was re-dissolved when the pH was re-adjusted down to pH8.5 in condition 3, before being allowed to react for another 22 hours.

ICP analysis plotted in Figure 4-56 found that the percentage of magnesium ions reacted after 22 hours of mixing are 41.7%, 88.8% and 75.1% while the percentage of silicon ion reacted are 94.0%, 99.6% and 98.7% for Condition 1, Condition 2 and Condition 3,

respectively. The amount of magnesium and silicon ion reacted in Condition 2 (i.e. Natural pH) agreed with previous Silicate Scaling Static Bottle Tests reported in section 4.1.2(b) that shows the repeatability and reproducibility of the ICP sampling method with less than 1% differences.

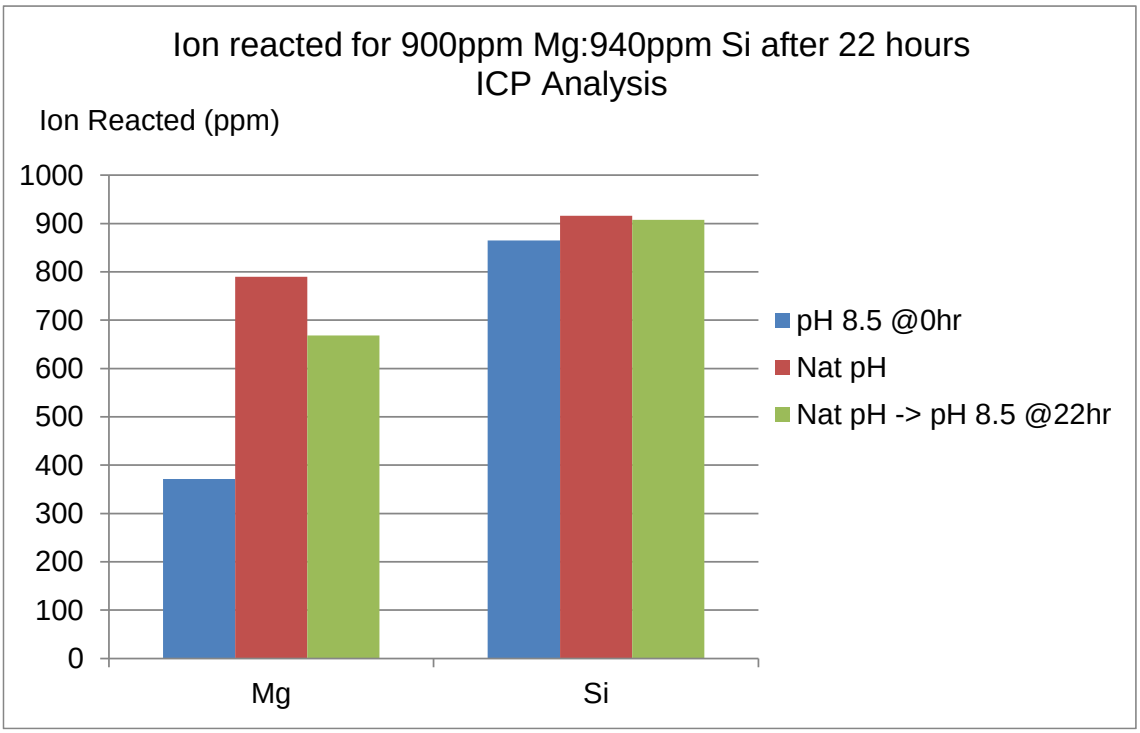

Figure 4-55 Amount of ions reacted for different pH condition for 900ppm Mg : 940ppm Si

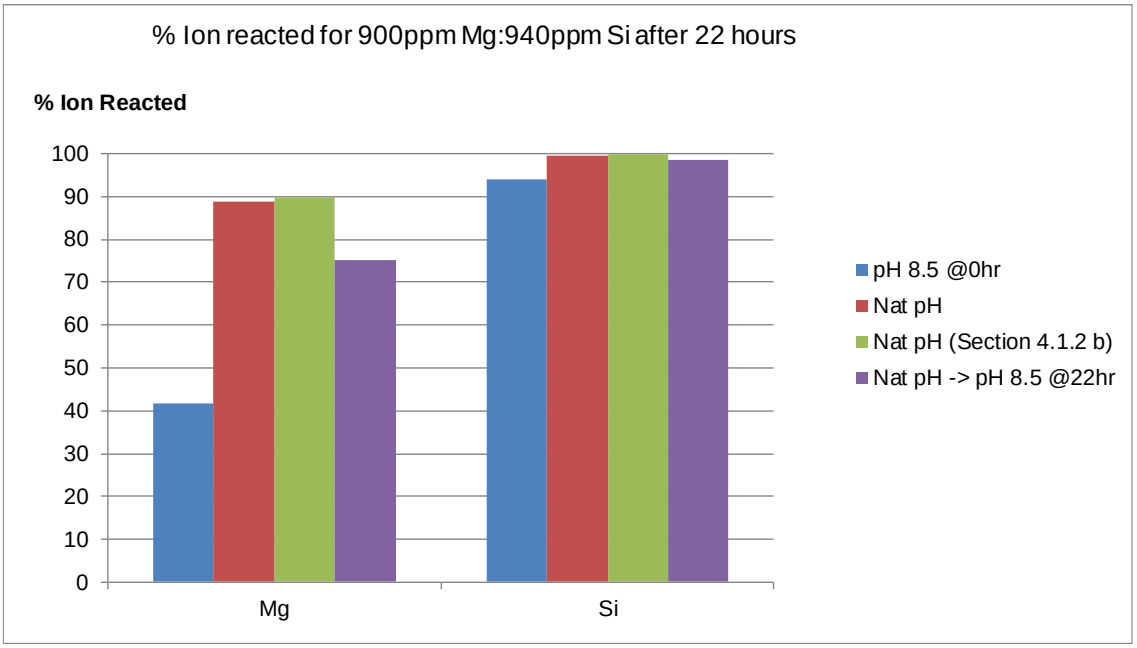

Figure 4-56 Percentage of ions reacted for different pH condition for 900ppm Mg : 940ppm Si

Figure 4-57 shows the (Molar) ion reacted for magnesium $[Mg]_{molar, rx}$ and silicon $[Si]_{molar, rx}$ at each of the 3 conditions. It is evident that for condition 1 (pH8.5@0hr); the $[Si]_{molar, rx}$ was higher than $[Mg]_{molar, rx}$ which *may* be due to the fact that the silicon polymerization is favoured at pH less than 8.5. At natural pH (Condition 2); molar ratio of magnesium to silicon Mg:Si ~ 1 indicated that magnesium silicate and magnesium hydroxide both co-precipitate at this pH condititon. $[Mg]_{molar, rx}$ in Condition 3 (Natural pH then pH8.5@22hr) it was found that the Mg reacted less than in Condition 2 which indicated that some of the magnesium hydroxide which had initially formed was re-dissolved as the pH dropped from its natural pH (>10) to pH8.5 at 22 hour. pH values were slightly reduced from its initial values in all 3 test conditions, as can be seen in Figure 4-58.

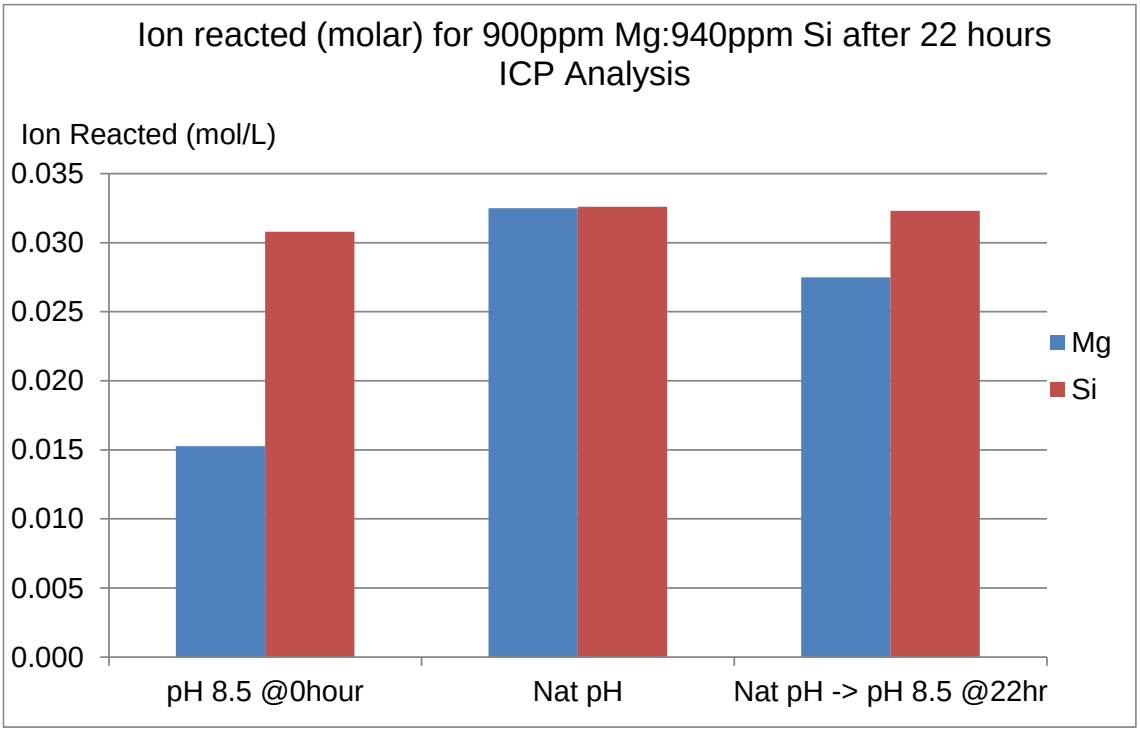

Figure 4-57 Molar ion reacted (calculated from ICP data) for 900ppm Mg : 940ppm Si after 22 hours

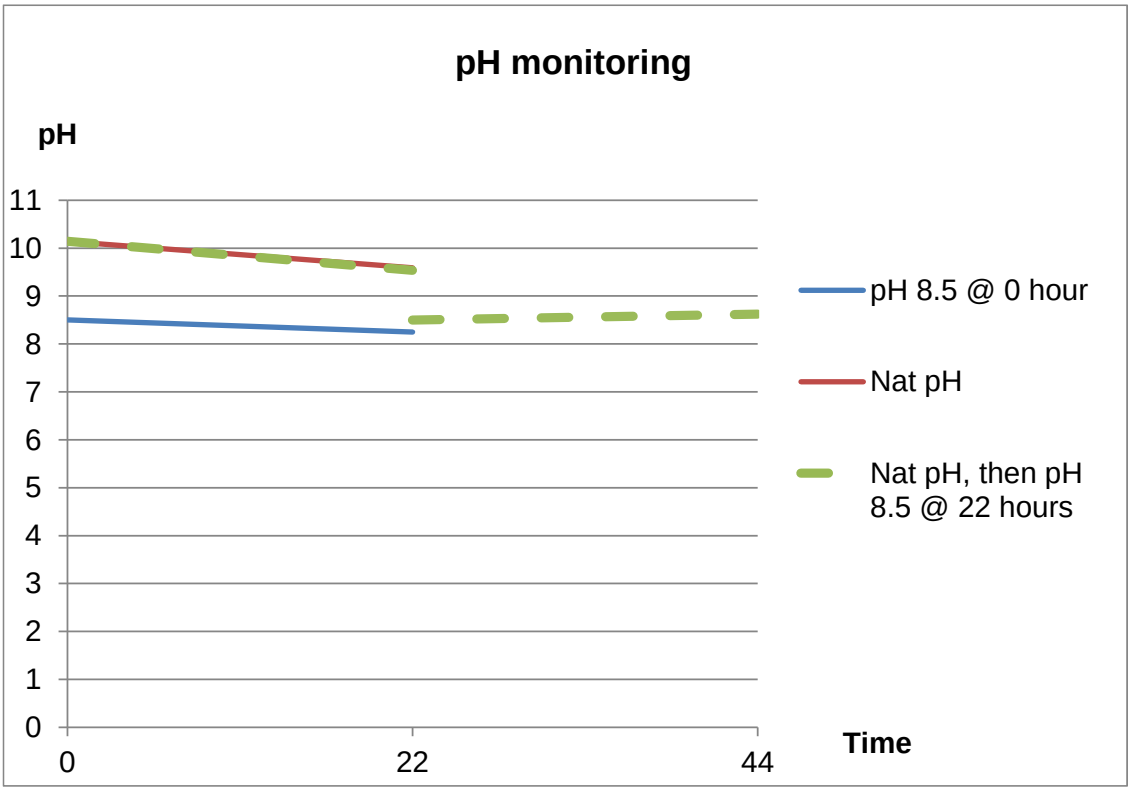

Figure 4-58 pH Monitoring in "pH Effect on Silicate Scaling" test

Note that pH8.5@0hr is **Condition 1**; Nat pH is **Condition 2** while Nat pH -> pH8.5@22hr is **Condition 3**. Also note that the plotted amount of ion reacted in Figure 4-55 to Figure 4-57 for Condition 3 is after 44 hour.

ESEM/EDAX Results and Analysis

All precipitates were collected by filtration using a 0.2μm filter paper, dried in a desiccator for at least 24 hours before then being analysed by different types of spectroscopic analysis, namely ESEM/EDAX, FTIR, Powder XRD and Mass Spectrometry (MS). See Figure 4-59 and Figure 4-60.

(a) Test condition 1: pH8.5 adjusted @ 0hr

(b) Test Condition 2: Natural pH

(c) Test Condition 3: Natural pH, then pH8.5 adjusted@22hr

Figure 4-59 Precipitate collected after 22 hours (Condition 1 & 2) and 44 hours (Condition 3)

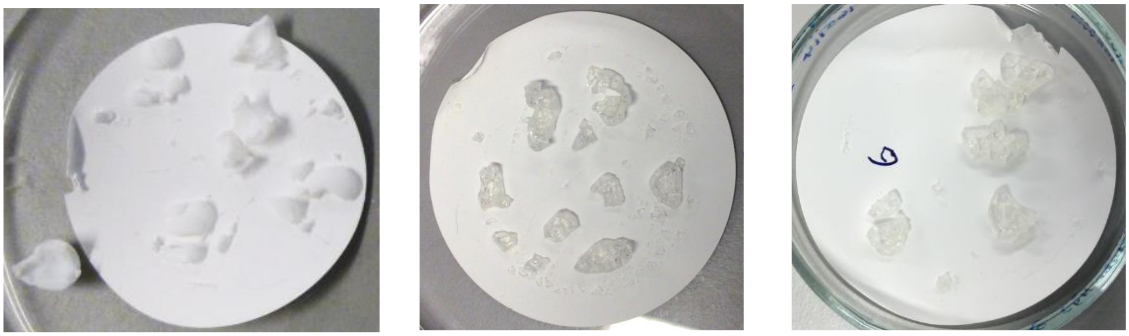

(a) Test condition 1: pH8.5 adjusted @ 0hr

(b) Test Condition 2: Natural pH

(c) Test Condition 3: Natural pH, then pH8.5 adjusted@22hr

Figure 4-60 Precipitate collected after desiccated for >24 hour

Based on the ESEM images in Figure 4-61, Figure 4-62 and Figure 4-63, it is conclusive that all of the solid silicate scale formed in these tests is amorphous in nature (i.e. they are not crystalline). The main constituents in the precipitates were found to be Oxygen (58.21 to 64.80 wt.%), Magnesium (8.95 to 15.62 wt.%), Silicon (14.52 to 25.87 wt.%) with traces of sodium, carbon, and chloride.

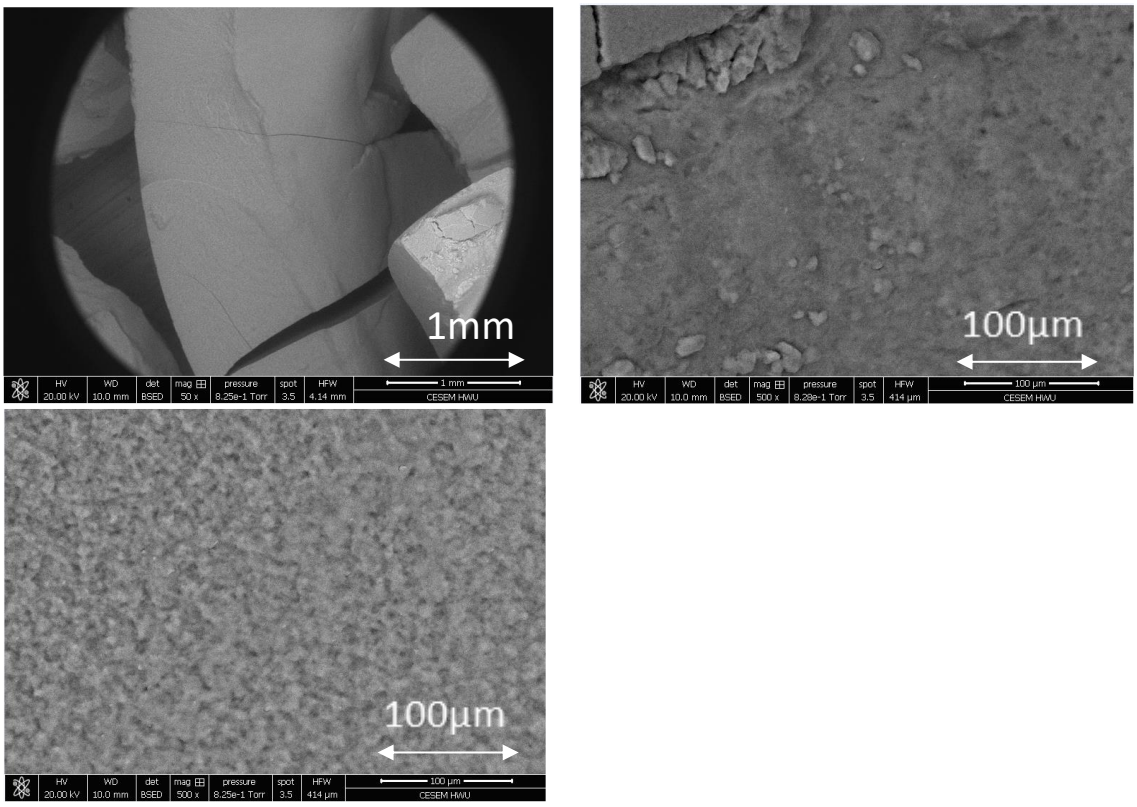

Figure 4-61 ESEM images for precipitate formed in Test Condition 1 (pH8.5 adjusted @0hr)

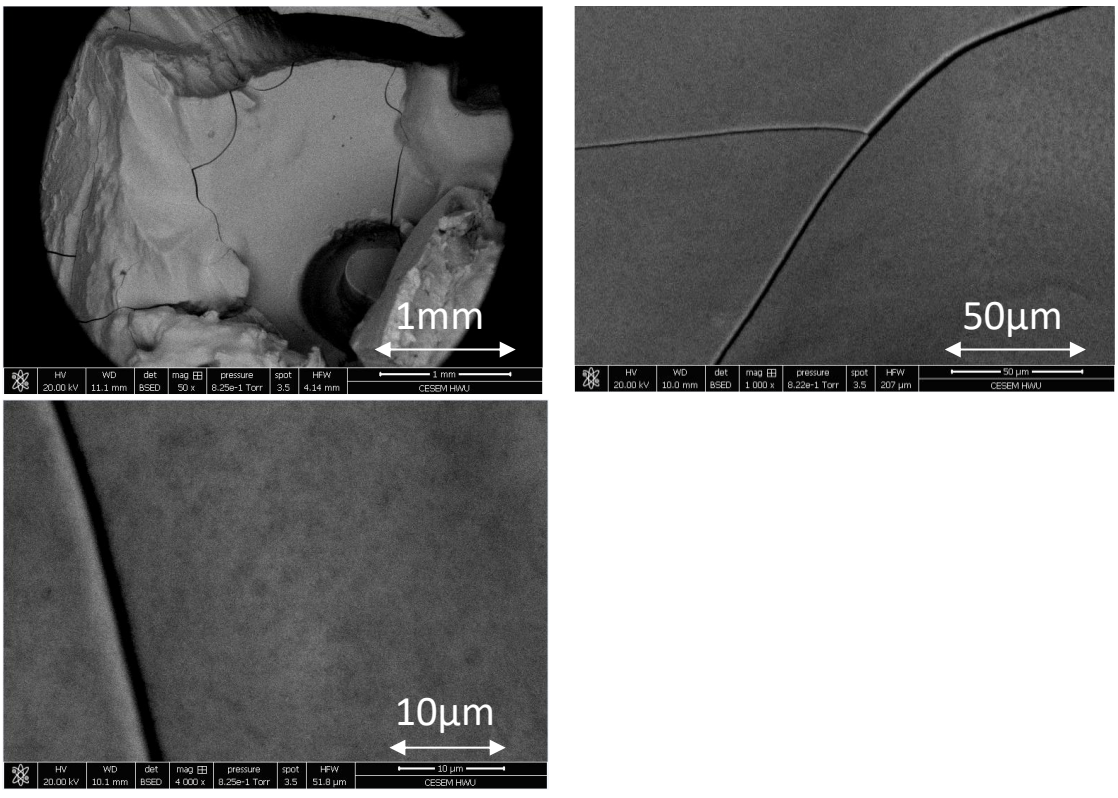

Figure 4-62 ESEM images for precipitate formed in Test Condition 2 (Natural pH)

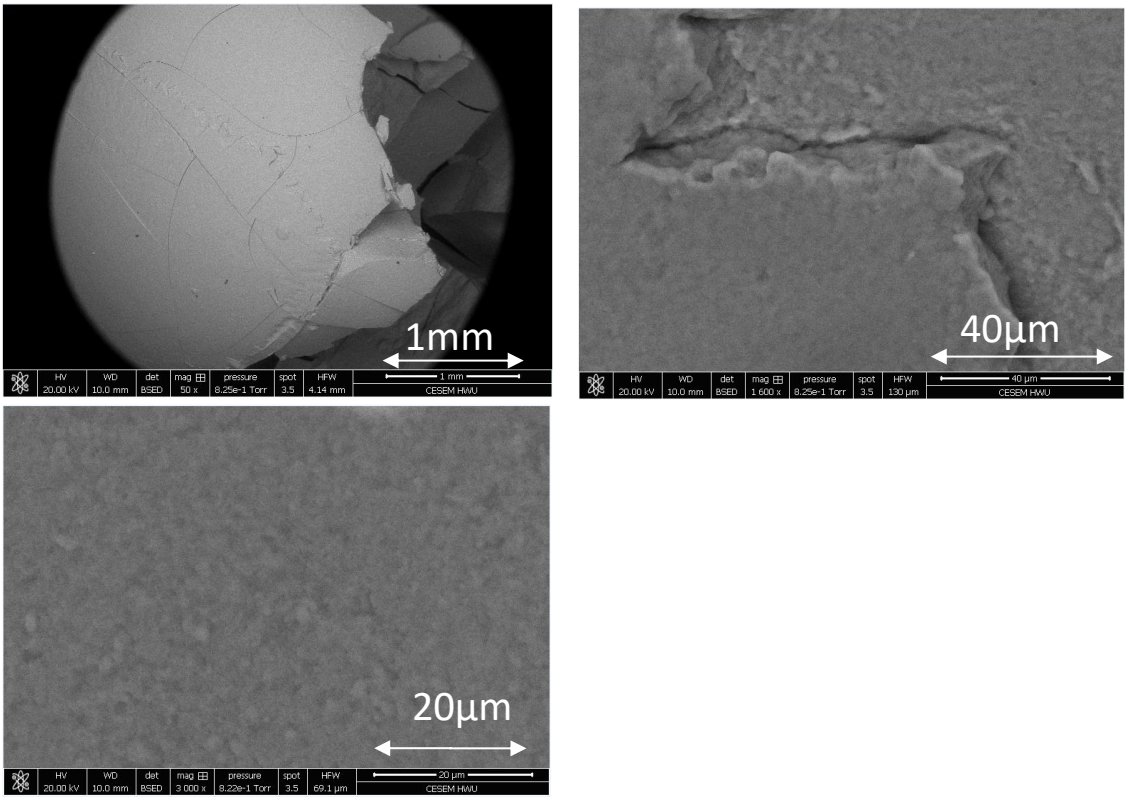

Figure 4-63 ESEM images for precipitate formed in Test Condition 3 (Natural pH, then pH8.5 @22hr)

ESEM/EDAX results showed that the atomic ratio of Si:Mg is 2.08, 1.01 and 1.30 for Condition 1, Condition 2 and Condition 3, respectively. ICP analysis and ESEM/EDAX analysis for Condition 2 closely agreed with the previous results found under the same conditions in Silicate Scaling Static Bottle Test (reported in section 4.1.2(b)). This finding confirms the repeatability and reproducibility of the Mg-silicate methodology which is developed here.

The Si:Mg ratio under various solution conditions is shown in Figure 4-64. These values of Si:Mg ratio were calculated based on the assumption that all reacted magnesium ions were reacted only with silicon ions to form magnesium silicate ($MgO.SiO_2$) scale. This may not be true in some conditions since part of the reacted magnesium ions $[Mg]_{rx}$ may have formed magnesium hydroxide $Mg(OH)_2$. In addition, some of the reacted silicon ions $[Si]_{rx}$ may have polymerized to form colloidal amorphous silica.

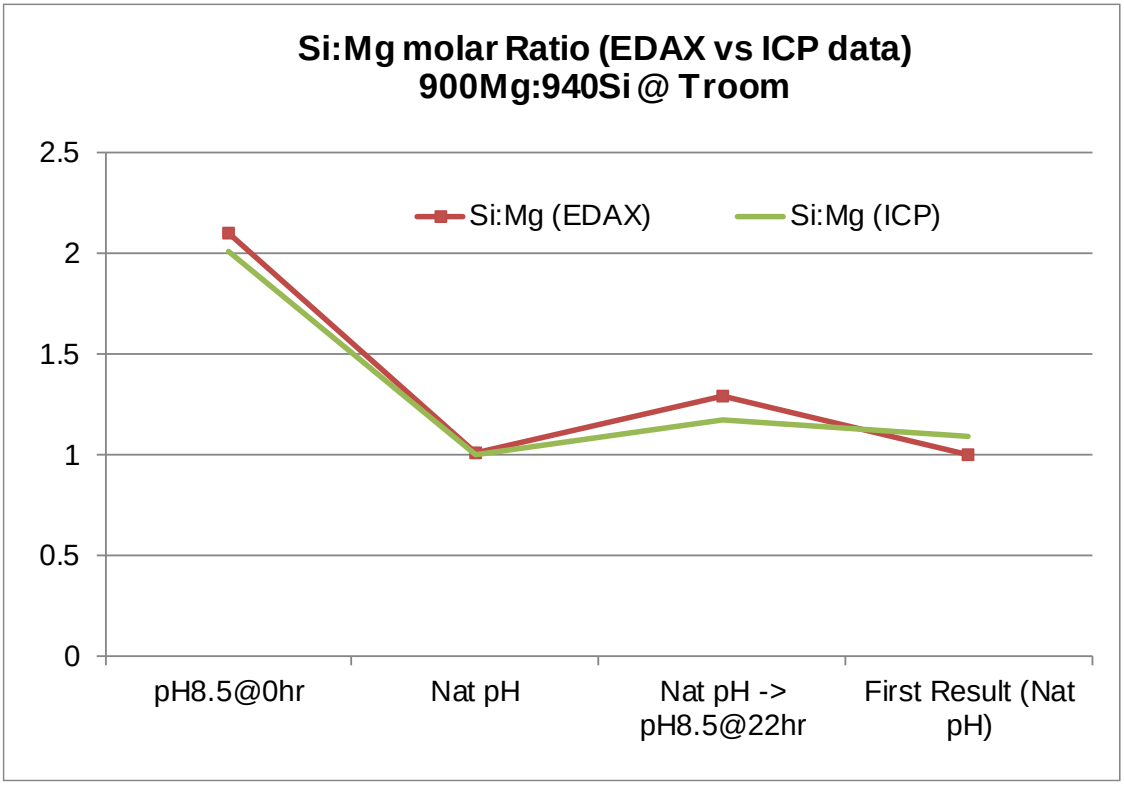

Figure 4-64 Si:Mg molar ratio in precipitate (ESEM/EDAX vs. ICP results)

Note that results for *First Result (Nat pH)* is Si:Mg molar ratio from section 4.1.2(b).

Figure 4-65 shows the elemental data from ESEM/EDAX analysis. It is shown that the magnesium and silicon atomic percentage trends agree with the [ion] reacted values calculated from the ICP results (Figure 4-55) as below;

Mg Atomic %: "pH8.5@0hr" < "Natural pH then pH8.5@22hr" < "Natural pH"

Si Atomic %: "Natural pH" < "Natural pH then pH8.5@22hr" < pH8.5@0hr

O Atomic %: "Natural pH then pH8.5@22hr" < "pH8.5@0hr" < "Natural pH"

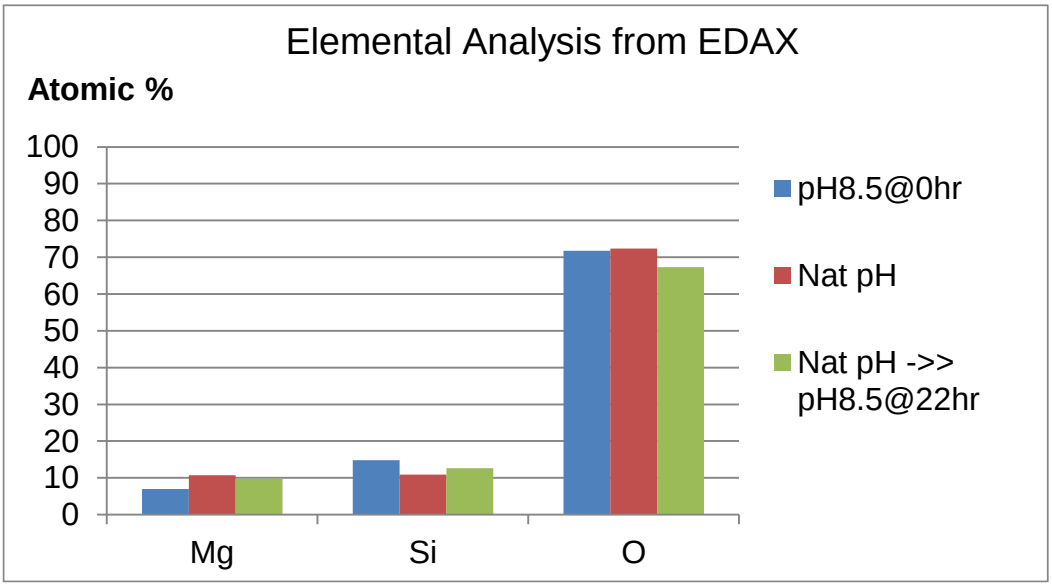

Figure 4-65 Elemental analysis from ESEM/EDAX

FTIR Results and Analysis

The FTIR spectrum obtained for the precipitate is shown in Figure 4-67. These FTIR results show the presence of amorphous silica, magnesium hydroxide and Si-O-Metal bonding while the powder XRD recorded broad peaks (discussed below) which confirmed that the precipitate formed has a non- crystalline structure, but rather is amorphous in nature. From Figure 4-67, the FTIR spectrum suggested the presence of Si-O-Si in amorphous silica (~800cm^{-1}) while there is no magnesium hydroxide present in precipitate for Condition 1 (pH8.5). The spectra also suggested the presence of magnesium hydroxide (~1417cm-1) and Si-O-Metal (1000-900cm^{-1}) but no amorphous silica in precipitate for Condition 2 (Natural pH~10.1) and Condition 3 (Natural pH~10.1 followed by pH8.5 adjusted at 22hour). Rashid et al. (2009) show that metal silicates have common FTIR features with respect to the vibrational band at 1039 cm-1, which is due to the Si–O–Si symmetrical stretching vibration. In addition, the Si–O bending vibration of the metal silicate occurs at 432 cm-1. The other bands in the spectra around ~600 and ~3300 cm-1 are probably associated with various metal–O modes and water molecules, respectively.

Differences in the amount of magnesium ion reacted $[Mg]_{rx}$ and silicon ion reacted $[Si]_{rx}$ calculated from ICP data indicated that different compound were produced in the precipitates for each of the 3 different conditions. This revealed that the pH values during the scaling reaction will affect the compound presented in the precipitate. The formation of amorphous silica, SiO_2, is favored when the pH is less than 8.5 while the formation of magnesium silicate $MgO.SiO_2$ will increased when the pH is greater than 8.5. If the pH value of the mixed solution is higher than pH9.5, magnesium hydroxide will started to precipitate out (Refer Figure 4-66 – At pH ~10.1, Total Soluble Magnesium is ~150ppm; hence concentration 900ppm is higher than solubility->> Supersaturated). As expected, band due to $Mg(OH)_2$ can only be seen in Condition 2 and 3 shown in Figure 4-68.

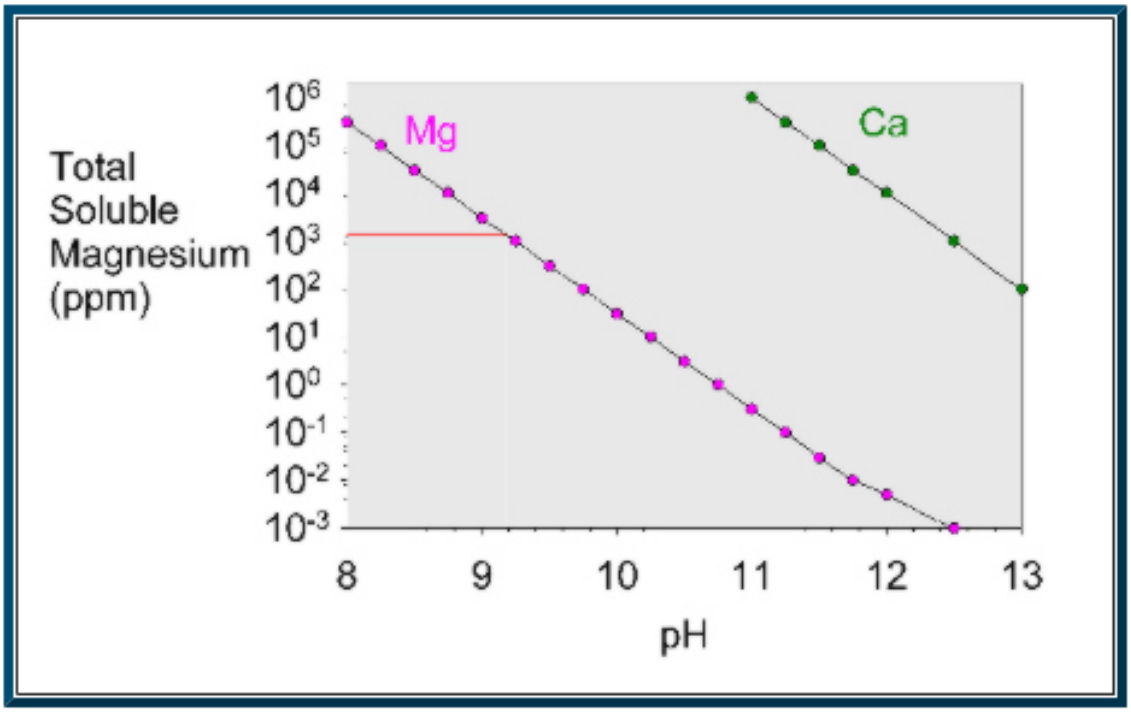

Figure 4-66 The solubility of magnesium as a function of pH

"What is that Precipitate in My Reef Aquarium?", by Holmes-Farley, S.R. 2005, retrieved from http://reefkeeping.com/issues/2005-07/rhf/index.htm#20 Copyright 2005 by ReefKeeping Magazine™ Reef Central, LLC.

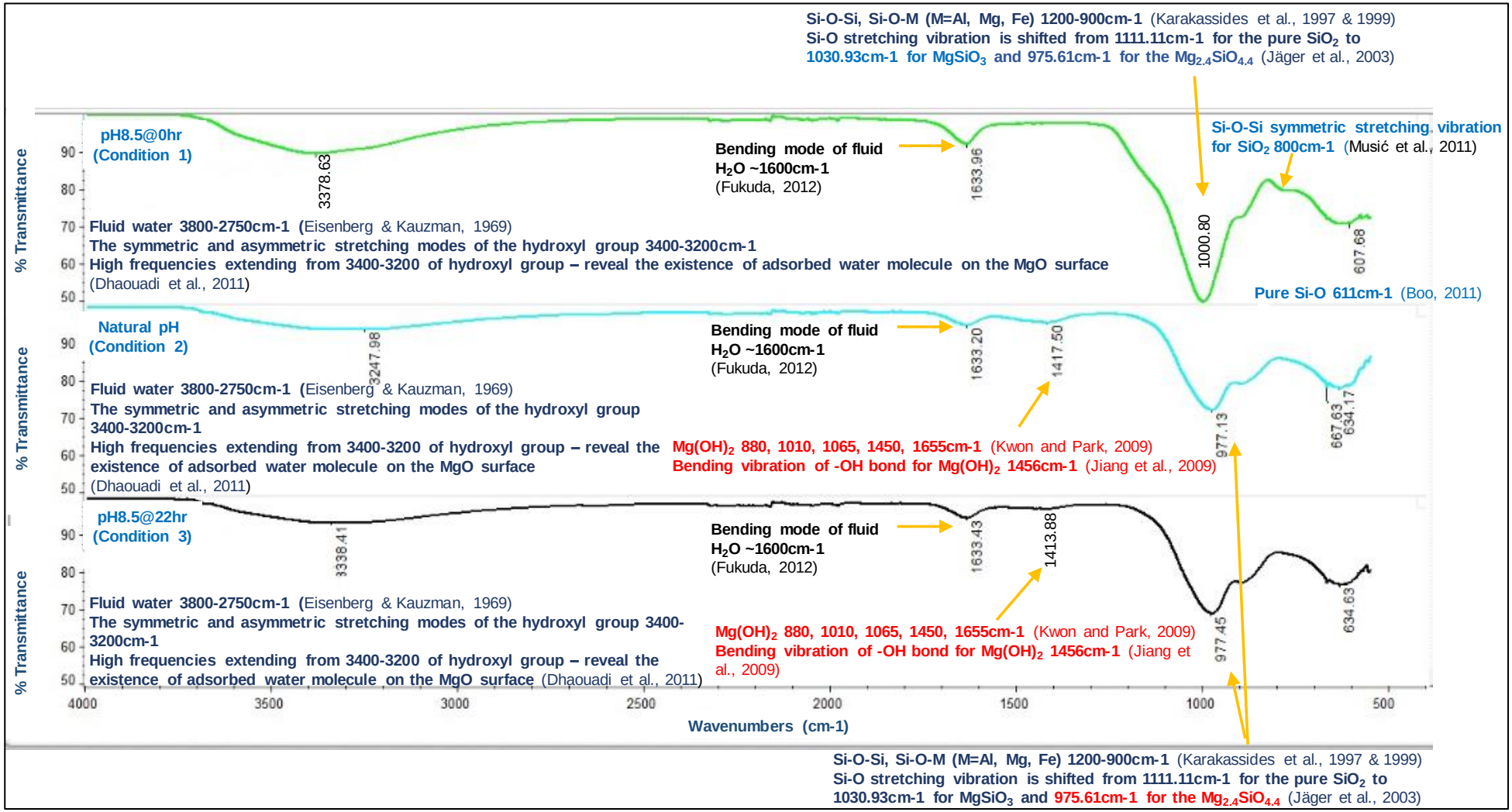

Figure 4-67 FTIR spectrum for precipitate formed of 900ppm Mg : 940ppm Si at various pH conditions

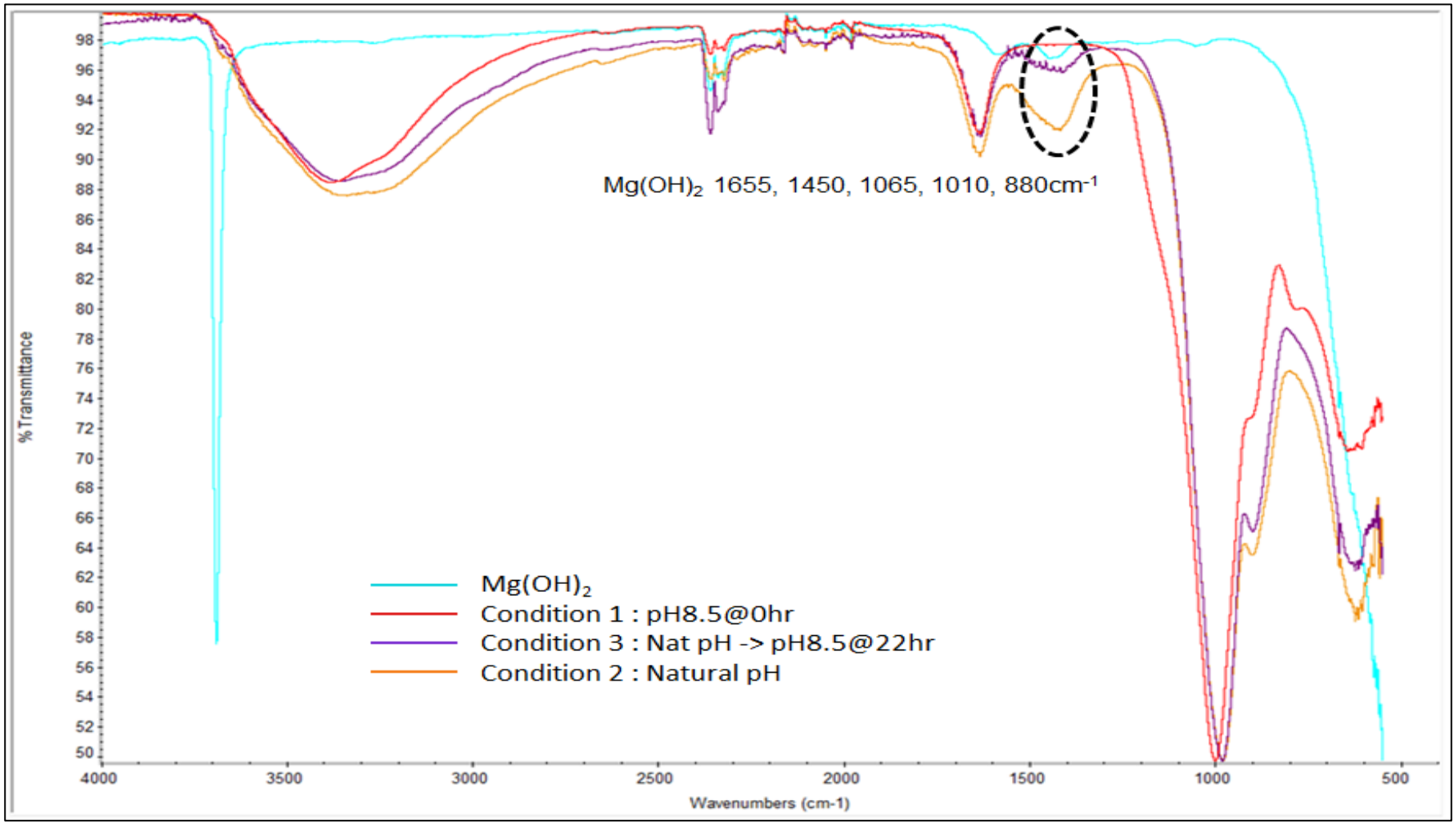

Figure 4-68 FTIR spectrum for precipitate formed (of 900ppm Mg : 940ppm Si) vs. Spectrum for reference sample $Mg(OH)_2$

- Intensity for $MgO.SiO_2$ spectrum (A):

The FTIR spectrum in Figure 4-69 shows that the intensity of the magnesium silicate peak is increased when the pH increased and that the higher the pH value of the mixed solution, the higher the amount of magnesium silicate produced. Above pH 9, magnesium silicate $MgO.SiO_2$ is very likely to form along with $Mg(OH)_2$ and silicate ions (Amjad and Zuhl, 2008b). Therefore, the precipitate produced in Condition 2 which was reacted at its natural pH (i.e. pH10.14) for 22 hours will have the highest amount of magnesium silicate compared to the precipitate that was produced in Condition 1 in which the mixed pH solution was adjusted to pH 8.5. The amount of magnesium silicate in the precipitate produced in Condition 3 was in between the amount produced in the other two conditions because it started in its natural pH condition 10.1 but was subsequently re-adjusted to pH8.5 after 22 hours of mixing.

Therefore, the amounts of magnesium silicate in all precipitate are in order of:

"pH8.5@0hr" < "Natural pH then pH8.5@22hr" < "Natural pH"

- Intensity for SiO_2 spectrum (B):

Based on spectrum presented in Figure 4-69, a weak broad spectrum of amorphous silica can only be observed in the precipitate produced from Test Condition 1 (i.e. "pH8.5@0hr"). This peak was not present in precipitate formed in Conditions 2 and 3 the reaction took place at their natural pH values i.e. pH10.14. This is consistent with the work by Demadis (2010) which reported that at pH less than 8.5, polymerization of silica is favoured which eventually forms amorphous silica scale, while Amjad and Zuhl (2009) reported that at pH larger than 8.5, the mixed solution may experience magnesium silicate $MgO.SiO_2$ formation.

- Intensity for $Mg(OH)_2$ spectrum (C):

The FTIR spectrum in Figure 4-69 clearly shows the presence of magnesium hydroxide $Mg(OH)_2$ peaks in the precipitate produced in Condition 2 and Condition 3 while no such peak was seen in the FTIR spectrum of the precipitate produced in Condition 1.

Magnesium hydroxide would probably have precipitated out when the pH was higher than pH 9, but this would not have occurred in the solution with pH8.5 in Condition 1. This caused the intensity of the peak in the precipitate of Condition 2 to be higher than for Condition 3. The magnesium hydroxide formed in the solution in Condition 3 was re-dissolved when the pH was subsequently re-adjusted to pH8.5 after 22 hours mixing at its natural pH (pH10.14).

Therefore, the amounts of magnesium hydroxide in all precipitate are in order of:

"Nat pH then pH8.5@22hr" < "Nat pH (pH ~ 10)"

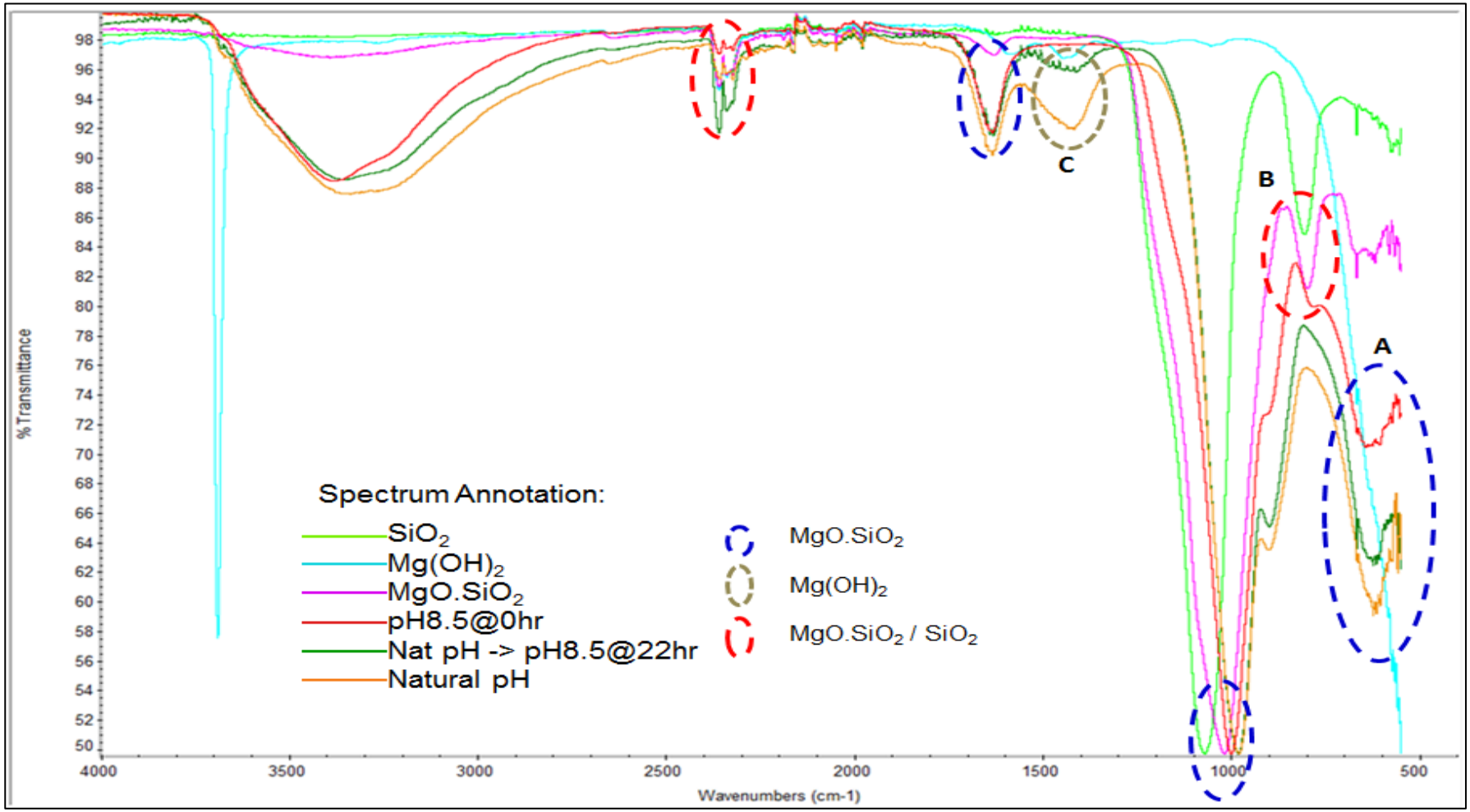

Figure 4-69 FTIR spectrum for precipitate formed (of 900ppm Mg : 940ppm Si) vs. Spectrum for reference sample $Mg(OH)_2$, $MgO.SiO_2$, and amorphous SiO_2

Powder XRD Results and Analysis

Figure 4-70 shows the X-Ray Diffraction (XRD) pattern for all the precipitates produced in Conditions 1, 2 and 3. The Powder XRD patterns supported the same conclusions drawn from the FTIR spectra. As can be seen in Figure 4-70, there was no magnesium hydroxide formed in the precipitate produced in Condition 1 (i.e. pH8.5@0hr). This is because at pH less than 8.5, where the reaction favoured amorphous silica SiO_2 formation and at pH more than 8.5 magnesium silicate $MgO.SiO_2$ may form but not magnesium hydroxide $Mg(OH)_2$ that only precipitated out when the pH exceeds pH 9. The pattern of reference samples are shown in Figure 4-71.

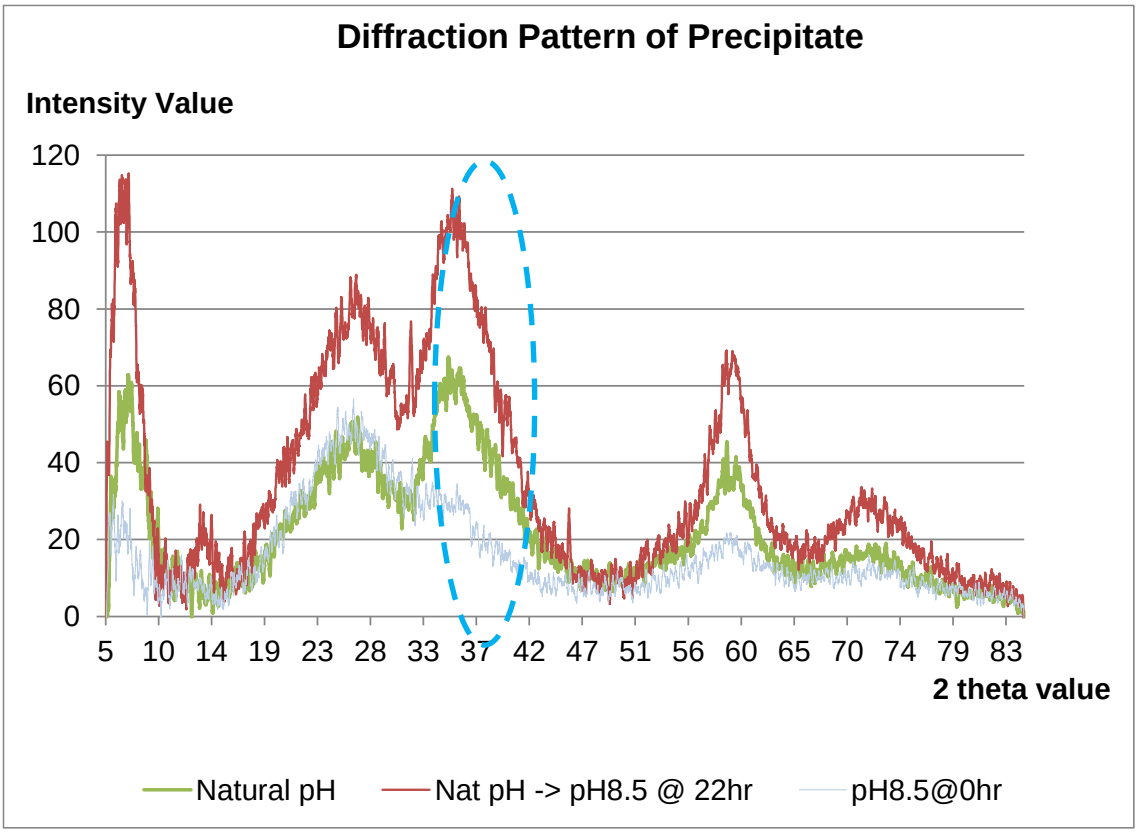

Figure 4-70 Diffraction pattern of precipitate formed of 900ppm Mg : 940ppm Si

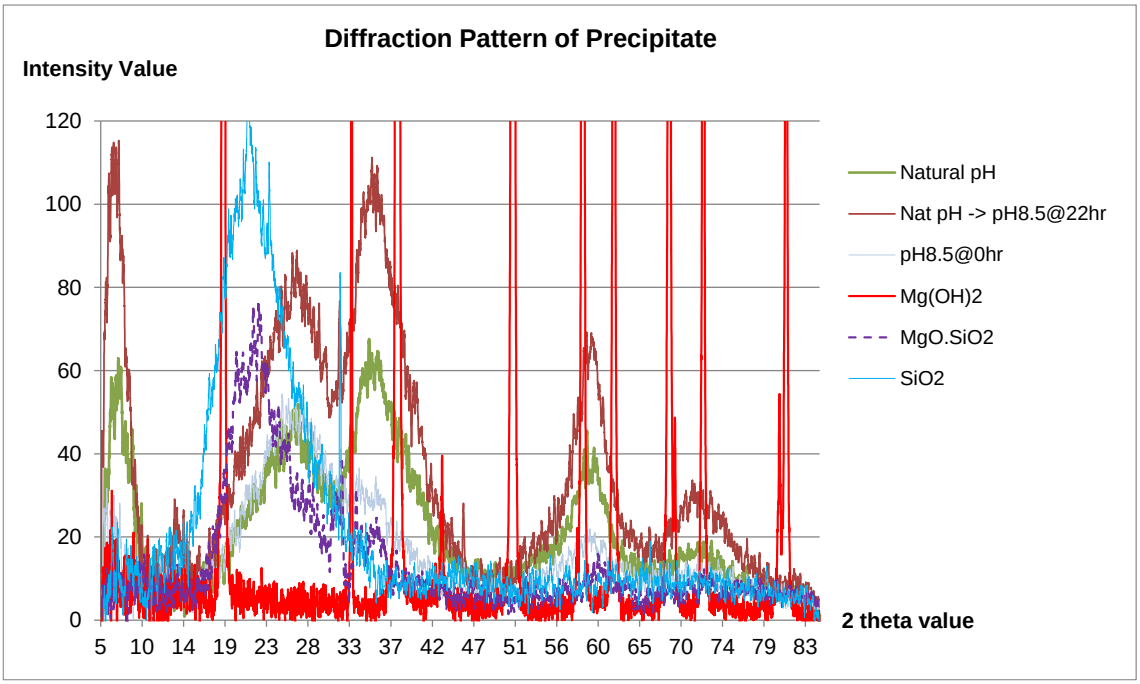

Figure 4-71 Diffraction pattern of precipitate formed (of 900ppm Mg : 940ppm Si) vs. Reference samples

(c) Summary and Conclusions

The conclusions on the efffect of pH on silicate scaling can be summarized as follows:

1. Different amounts of magnesium ion reacted $[Mg]_{rx}$ and silicon ion reacted $[Si]_{rx}$ calculated from ICP analysis indicated that different compounds were produced in the precipitates which formed under different pH conditions.

2. Based on ESEM, FTIR and powder XRD, the silicate precipitates formed were not crystalline but rather amorphous in nature.

3. Precipitate formed in Test Condition 1 (i.e. pH8.5@0hr) mostly contained amorphous silica SiO_2 and formed some amount of magnesium silicate $MgO.SiO_2$ but no magnesium hydroxide $Mg(OH)_2$.

4. Precipitate formed in Test Condition 2 (i.e. Natural pH) mostly contain magnesium silicate $MgO.SiO_2$ and magnesium hydroxide $Mg(OH)_2$ but not amorphous silica SiO_2.

5. Precipitate formed in Test Condition 3 (i.e. Natural pH then pH8.5@22hr) contain the same compound as Test Condition 2 but some of magnesium hydroxide $Mg(OH)_2$ re-dissolved when the pH was reduced from pH10.15 to pH8.5.

6. Magnesium silicate scaling tendency increased as the pH increased as shown in the intensity (i.e. amount) of $MgO.SiO_2$ spectrum (A) in order of

   "pH8.5@0hr" < "Nat pH then pH8.5@22hr" < "Nat pH"

7. Magnesium hydroxide $Mg(OH)_2$ was re-dissolved when the initially high pH of the solution was lowered to pH 8.5 as was evident in the reduced intensity of the $Mg(OH)_2$ spectrum (C):

   "Nat pH then pH8.5@22hr" < "Nat pH"

(d) Additional Results – Effect of pH on Silicate Scaling System of 300Mg:940Si, T_{room}, Natural pH

This experiment was designed to check the repeatability of the above results on the much milder scaling silicate system of 300Mg:940Si. Figure 4-72 shows that for the 300Mg:940Si case, the amount of magnesium and silicon ion reacted were higher by ~30% and ~67% when they were reacted at pH 8.5 compared to when they were reacted at the natural pH (~pH12.41).

As discussed above, at pH > 9.5, we might expect that some of the magnesium ion was reacted to also produce magnesium hydroxide. That is why the Si:Mg molar ratio was found lower for reaction at its natural pH since the magnesium ion reacted to co-produce magnesium hydroxide and magnesium silicate as plotted in Figure 4-73.

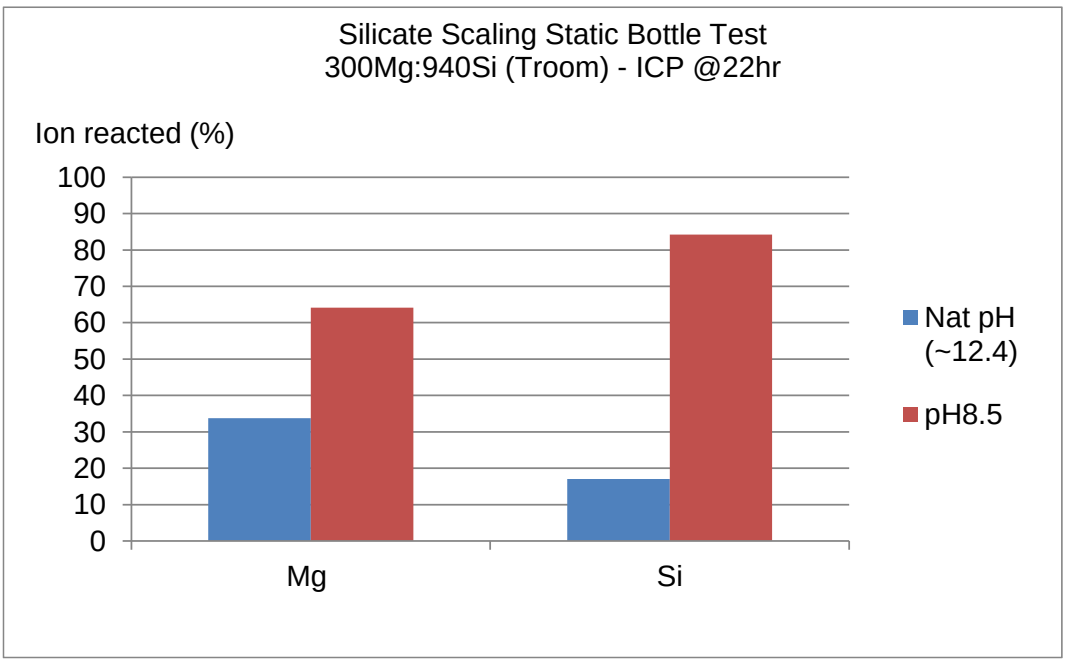

Figure 4-72 Percentage amount of ion reacted of 300Mg:940Si at T_{room} (Natural pH vs. pH8.5)

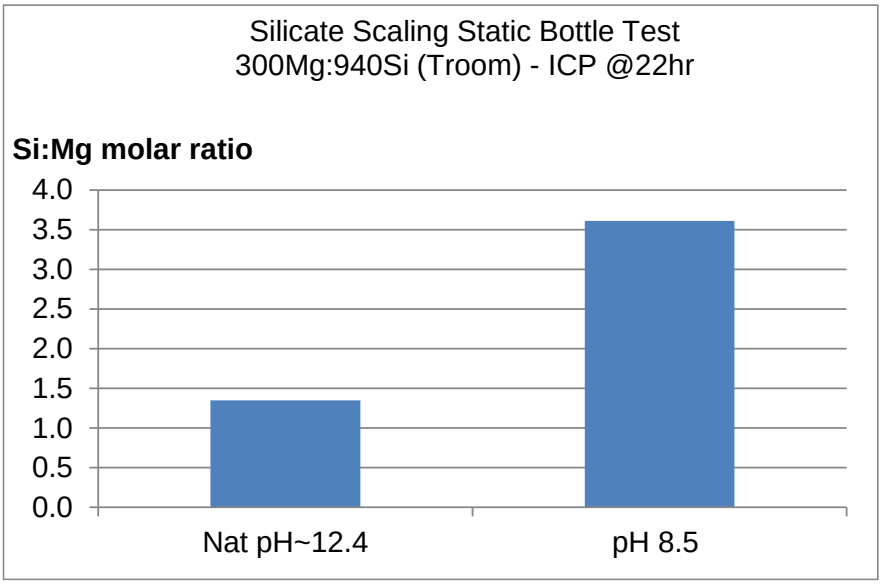

Figure 4-73 Si:Mg molar ratio of 300Mg:940 Si at T_{room} (Natural pH vs. pH8.5)

The FTIR spectrum of the precipitate for both pH conditions in Figure 4-74 clearly shows that scale produced from the reaction at ~pH12.4 contains magnesium hydroxide and magnesium silicate, but not amorphous silica. The precipitate formed in the reaction at ~pH8.5 only contains magnesium silicate and amorphous silica.

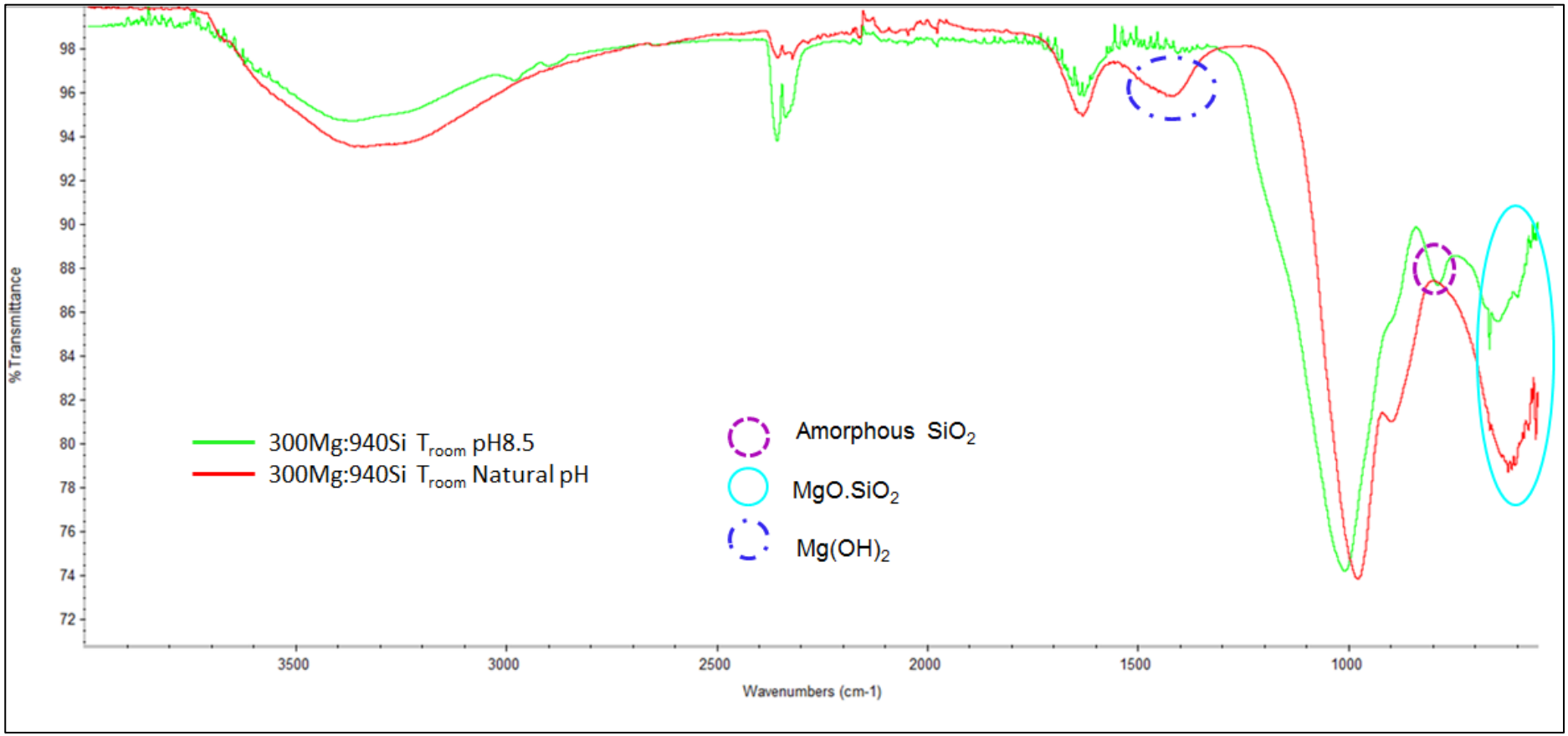

Figure 4-74 FTIR spectrum of 300Mg:940Si at T_{room} (Natural pH vs. pH8.5)

4.4.2 Effect of Temperature

(a) Experimental Details

600ppm magnesium and 1880ppm silicon brine were prepared and filtered using 0.45µm. These brines were mixed in a 50:50 molar ratio before being pH adjusted to pH8.5. One duplicate was left reacting at room temperature whereas another duplicate was heated in the oven at 60°C for 22 hours. Both duplicates were ICP sampled at 22 hour before the precipitates formed were filtered and analysed by ESEM/EDAX.

(b) Experimental Results and Discussion

Figure 4-75 shows that the amount (%) of magnesium and silicon ions reacted were higher by ~8% and ~5%, respectively, when tested at 60°C as compared to room temperature. At elevated temperature, the solubility of Mg-silicate will reduce, concentration>solubility; hence more Mg reacted to form Mg-silicate. Solubility of amorphous silica increases at 60°C but the polymerization rate is also increased; hence more Si ions polymerize to form amorphous silica.

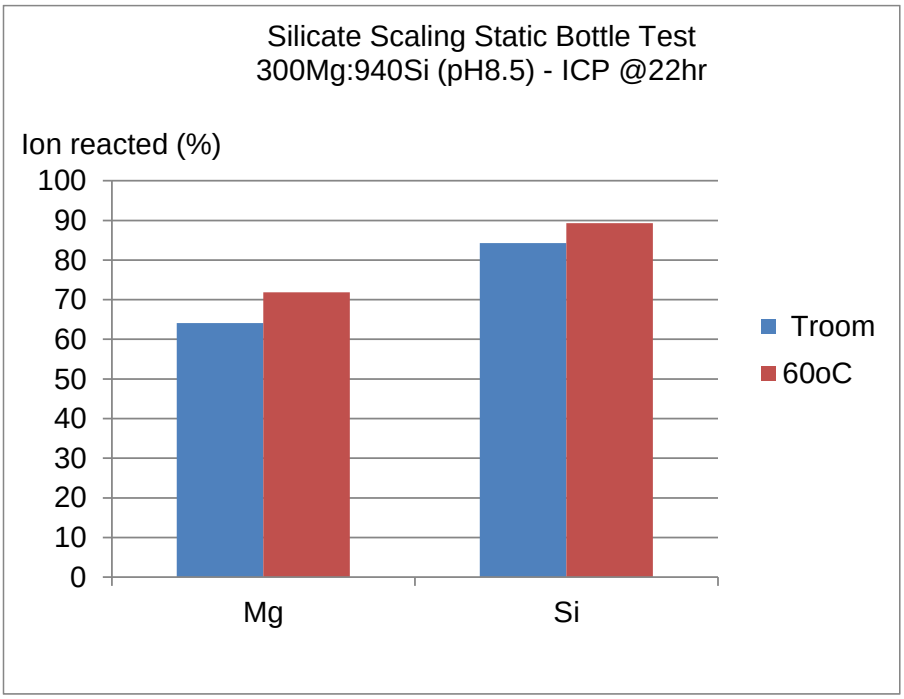

Figure 4-75 Percentage amount of ion reacted of 300Mg:940Si at pH8.5

Figure 4-76 shows the Si:Mg molar ratio for the 300Mg:940Si case at pH8.5 (calculated from the ICP values) in which there is no significant differences observed between the results at each test temperature. The Si:Mg molar ratios agreed closely with the values obtained from the ESEM/EDAX as shown in Figure 4-77.

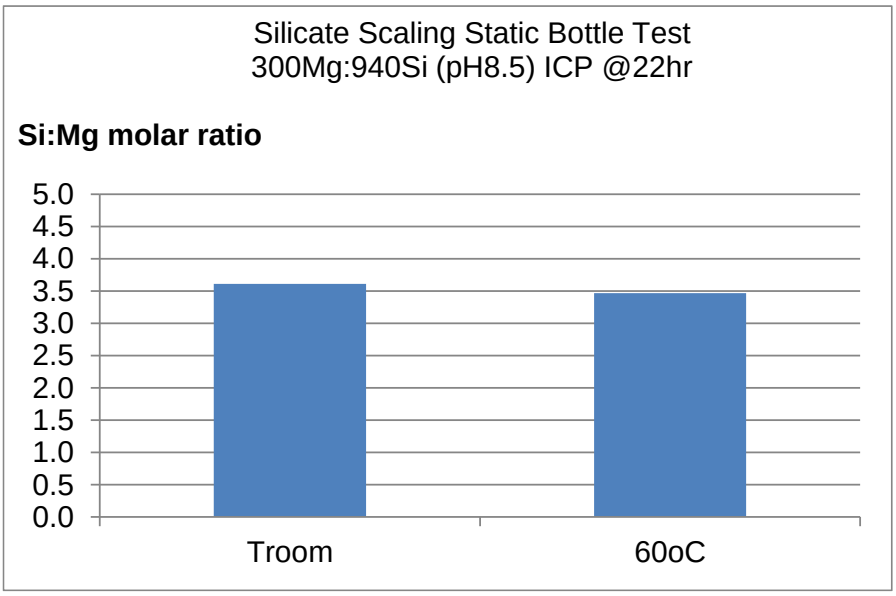

Figure 4-76 Si:Mg molar ratio of 300Mg:940Si at pH8.5

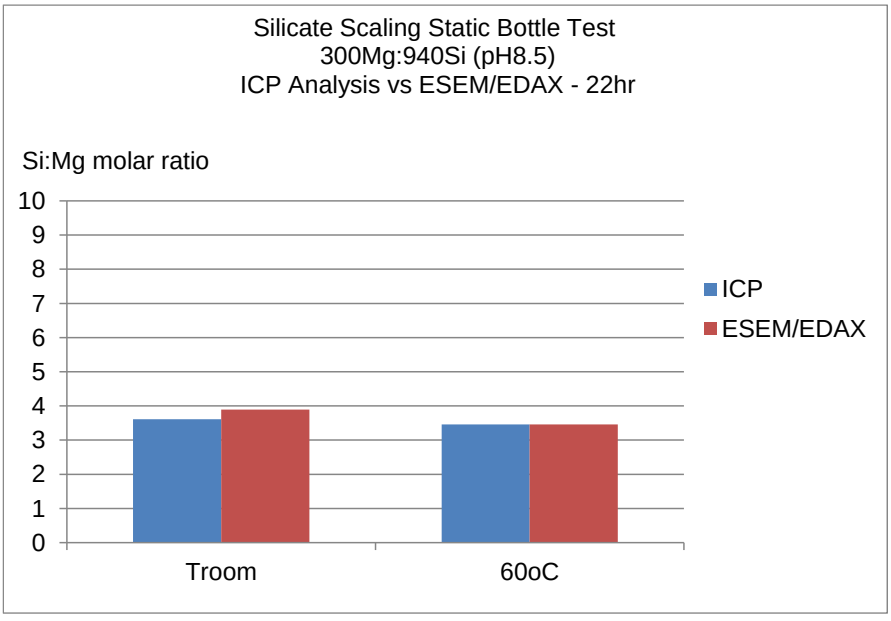

Figure 4-77 Si:Mg molar ratio of 300Mg:940Si (ICP analysis vs. ESEM/EDAX analysis)

ESEM images of the precipitate produced from the reaction for the 300Mg:940Si case at pH 8.5 (room temperature vs. 60^{o}C) presented in Figure 4-78 and Figure 4-79 shows that the scale is amorphous in nature.

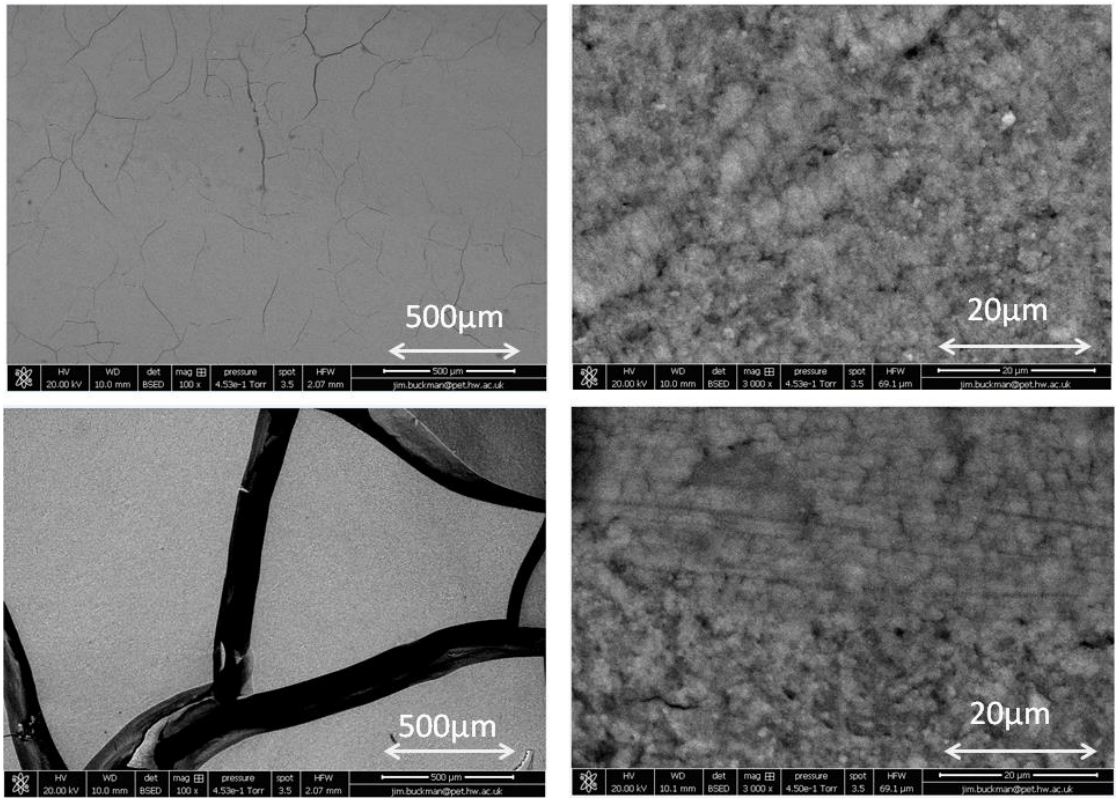

Figure 4-78 ESEM images of 300Mg:940Si (pH8.5 and T_{room})

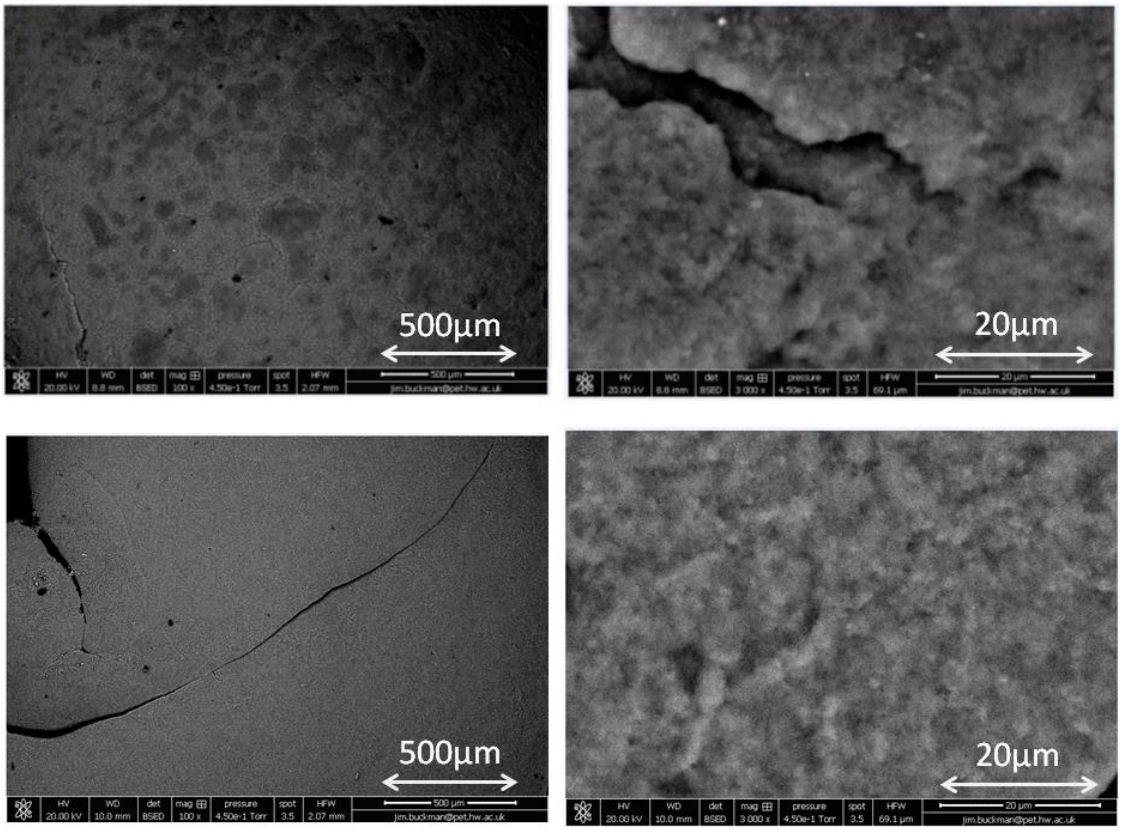

Figure 4-79 ESEM images of 300Mg:940Si (pH8.5 and 60ºC)

FTIR spectra shown in Figure 4-80 for both test temperatures shows the presence of amorphous silica and magnesium silicate with the spectra at room temperature being more intense than at 60ºC.

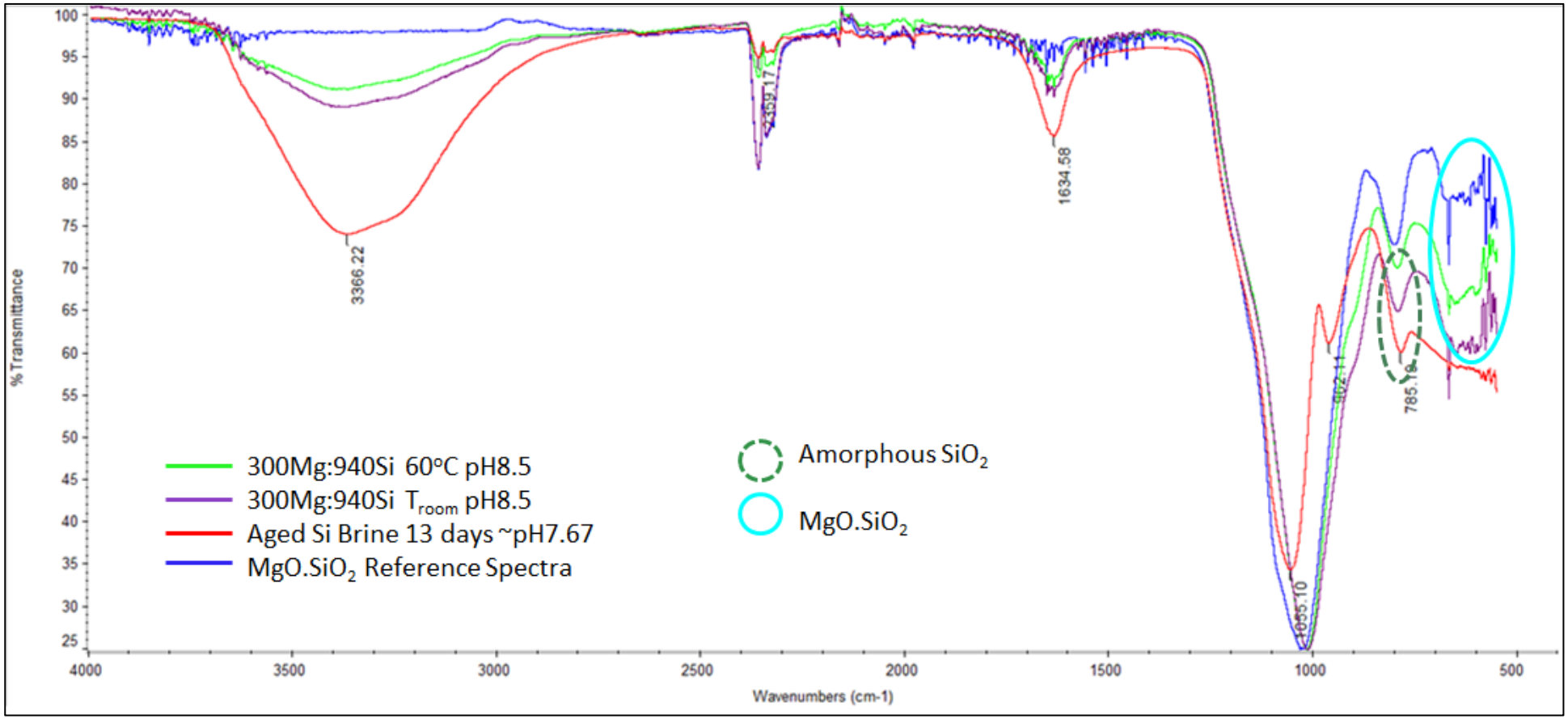

Figure 4-80 FTIR spectrum of 300Mg:940Si at pH8.5 (60ºC vs. T_{room})

(c) Summary and Conclusions

The effect of temperature and pH on the amount and morphology of the silicate scale produced is again examined in detailed here. In studying the effect of temperature, a 300ppm Mg: 940ppm Si mixed brine was reacted after pH was adjusted to pH 8.5 for 22 hours at 2 test temperatures (room temperature vs. 60^{o}C). Similar results are reported at "natural" pH levels for ASP, i.e. pH~12.4 to compare with the pH8.5 results. From the ICP results shown in Figure 4-81, it emerges that pH is the dominant factor that strongly influences the silicate scaling reaction compared to the effect of temperature. The Si:Mg molar ratio results for both temperature and pH conditions on the silicate scaling reaction in Figure 4-82 obviously shows that pH effect is dominant compared with the temperature effect.

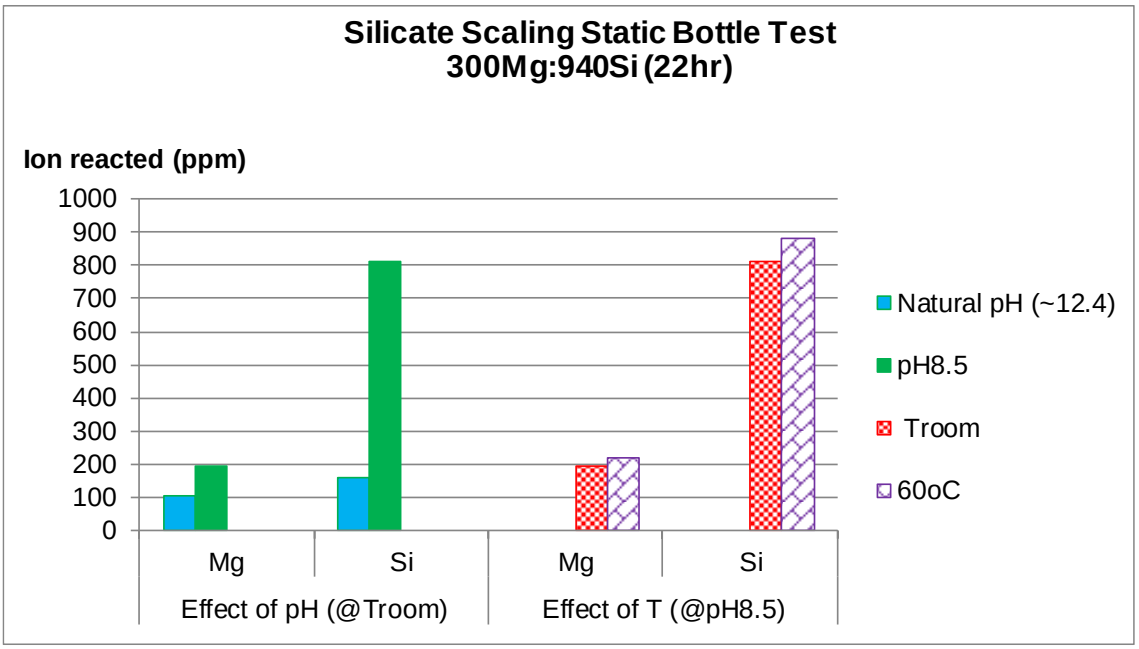

Figure 4-81 Temperature and pH effect on amount of ion reacted of 300Mg:940Si

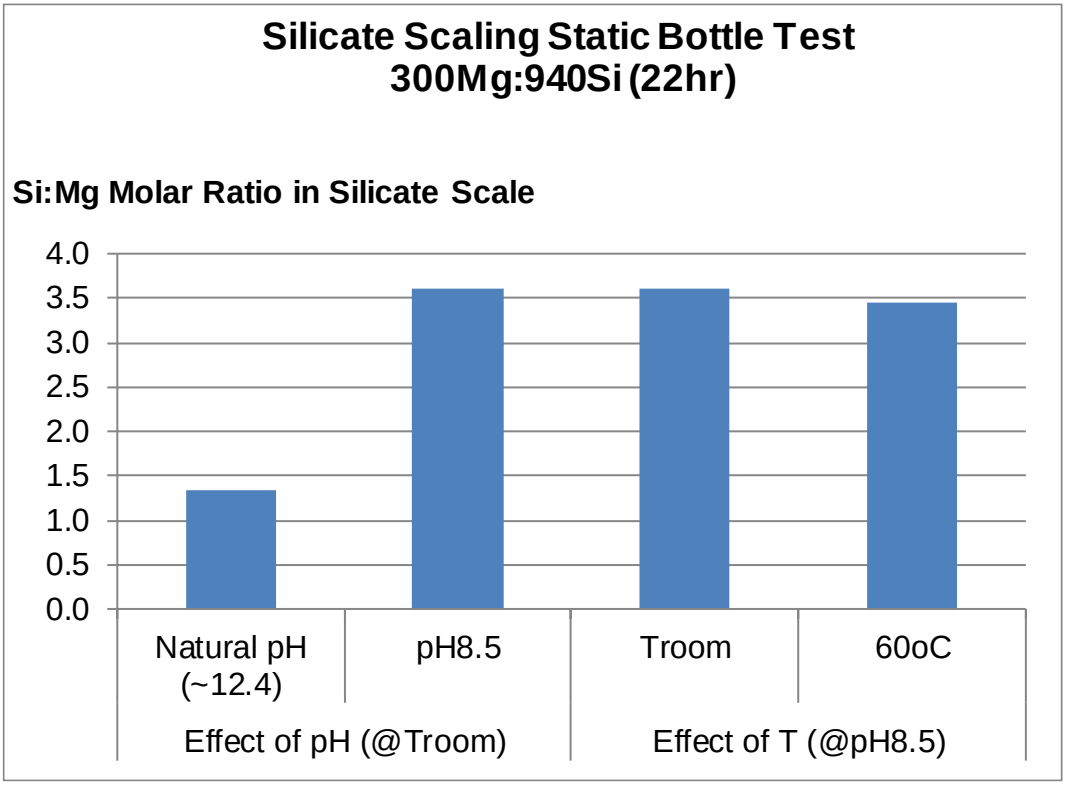

Figure 4-82 Temperature and pH effect on Si:Mg molar ratio of 300Mg:940Si

4.4.3 Effect of Initial Si:Mg Molar Ratio

Effect of Concentration of Magnesium Ion

The problem of silica scaling is exacerbated in the presence of low levels of polyvalent metal ions (i.e., aluminum, iron, calcium, magnesium, etc.). Therefore, the initial concentration of the magnesium ion present in the mixed brine was studied.

(a) Experimental Details

This experiment was designed to determine the minimum concentration of magnesium ion required to initiate silicate scaling when mixed with silicon ion in a 50:50 ratios. This result is used as a reference on setting the appropriate concentration of magnesium and silicon concentration in the base case condition as presented in *Chapter 3* before this base case condition being tested in Silicate Scale Static Inhibition Efficiency Tests.

Several experiments were conducted to determine the minimum amount of magnesium concentration (Refer Table 4-14 various initial Si:Mg molar ratio) that initiated silicate scaling in static bottle tests at room temperature and at their natural pH values.

Table 4-14 Test condition of various initial silicon to magnesium molar ratios $(Si:Mg)_o$ @T_{room}, natural pH

Test	$(Si:Mg)_o$	Mg_o (ppm)	Si_o (ppm)	T (^oC)	pH_{Nat}	S_o (pH)	S_o (Mg)	SSI (pH)	SSI (Mg)
1	0.76	1188	1050	25	9.70	191.76	121.17-135.19	11.7	16.62-17.95
2	0.90	900	940	25	10.1	310.98	121.17-135.19	6.45	14.88-16.07
3	0.97	948	1080	25	9.92	242.72	121.17-135.19	9.5	17.09-18.46
4	1.37	640	1024	25	11.10	2398.28	121.17-135.19	0.91	16.20-17.50
5	1.94	447	1015	25	12.25	41058.74	121.17-135.19	0.053	16.06-17.35
6	2.10	449	945	25	12.25	41058.74	121.17-135.19	0.049	14.95-16.15
7	3.11	304	945	25	12.42	60674.43	121.17-135.19	0.033	14.95-16.15
8	4.47	120	620	25	12.55	81806.84	121.17-135.19	0.016	9.81-10.60
9	5.87	91	618	25	12.33	49339.87	121.17-135.19	0.027	9.79-10.57
10	7.56	125	945	25	12.55	81806.84	121.17-135.19	0.025	14.95-16.15
11	8.91	61	629	25	12.40	57948.88	121.17-135.19	0.023	9.95-10.75
12	11.79	46	621	25	12.40	57948.88	121.17-135.19	0.023	9.82-10.62

S_o (pH) & SSI (pH) – solubility & supersaturation index as a function of pH by Brown (2013)
S_o (Mg) & SSI (Mg) – solubility & supersaturation index as a function of Mg present by Chen and Marshall (1982)

Also, there is a need to investigate the minimum magnesium ion concentration at which silicate scaling would be initiated at 60^{o}C and pH8.5 to replicate the near well conditions. Therefore, several experiments with various initial Si:Mg molar ratio were also conducted at a higher temperature (60^{o}C) and at pH8.5 as shown in Table 4-15.

In this experiment, various concentrations of magnesium and silicon ions were tested in 50:50 ratios at test temperature and pH values**.** The samples were then analysed by ICP for silicon and magnesium after 2 and 22 hours mixing.

Table 4-15 Test condition of various initial Si:Mg molar ratio (60ºC, pH8.5)

Test	$(Si:Mg)_o$	Mg_o (ppm)	Si_o (ppm)	T (ºC)	pH_{Nat}	S_o (pH)	S_o (Mg)	SSI (pH)	SSI (Mg)
Mg_o fix @30ppm									
1	1.41	30	50	60	10.80	241.77	220	0.44	0.49
2	2.16	30	75	60	10.95	241.77	220	0.66	0.73
3	4.33	30	150	60	11.50	241.77	220	1.33	1.46
Mg_o fix @60ppm									
4	4.33	60	300	60	11.82	241.77	220	2.65	2.92
5	8.13	60	564	60	12.10	241.77	220	4.99	5.48
6	10.85	60	752	60	12.25	241.77	220	6.65	7.31
7	13.56	60	940	60	12.40	241.77	220	8.32	9.14
Si_o fix @940ppm									
8	3.13	300	940	60	12.55	241.77	220	8.32	9.14
9	6.78	120	940	60	12.33	241.77	220	8.32	9.14
10	9.04	90	940	60	12.40	241.77	220	8.32	9.14
11	13.56	60	940	60	12.40	241.77	220	8.32	9.14

(b) Experimental Results and Discussion

The Effect of Initial Si:Mg Molar Ratio at Room Temperature, Natural pH

Various concentration of initial Si:Mg molar ratio were reacted at room temperature, natural pH (as shown in Table 4-14) and the extent of reaction values were determined, in order to understand the effect of this factor on the silicate system. Figure 4-83 shows that there is almost no magnesium and silicon ion reacted when the initial magnesium added into the mixed brine is up to 125ppm magnesium ion were mixed with either ~600ppm or ~940ppm silicon ion. This figure was re-plotted into Figure 4-84, Figure 4-85 and Figure 4-86 that show clearly the cut off concentration that initiate the silicate scaling at room temperature, natural pH. At this test condition, with less than ~120ppm magnesium added to ~600ppm Si or ~940ppm Si producing no precipitate. When ~300ppm magnesium ion was added to ~940ppm silicon, approximately 33.8% of magnesium and 17% of silicon ion was reacted.

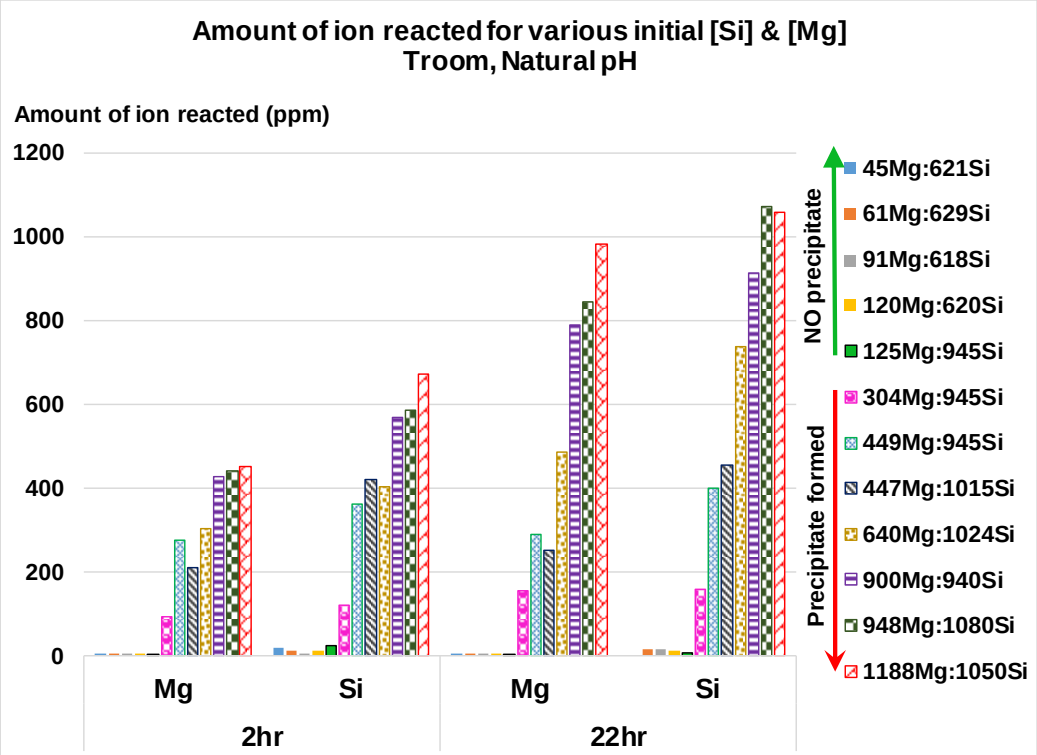

Figure 4-83 Extent of reaction for various initial Si:Mg molar ratios at T_{room}, natural pH

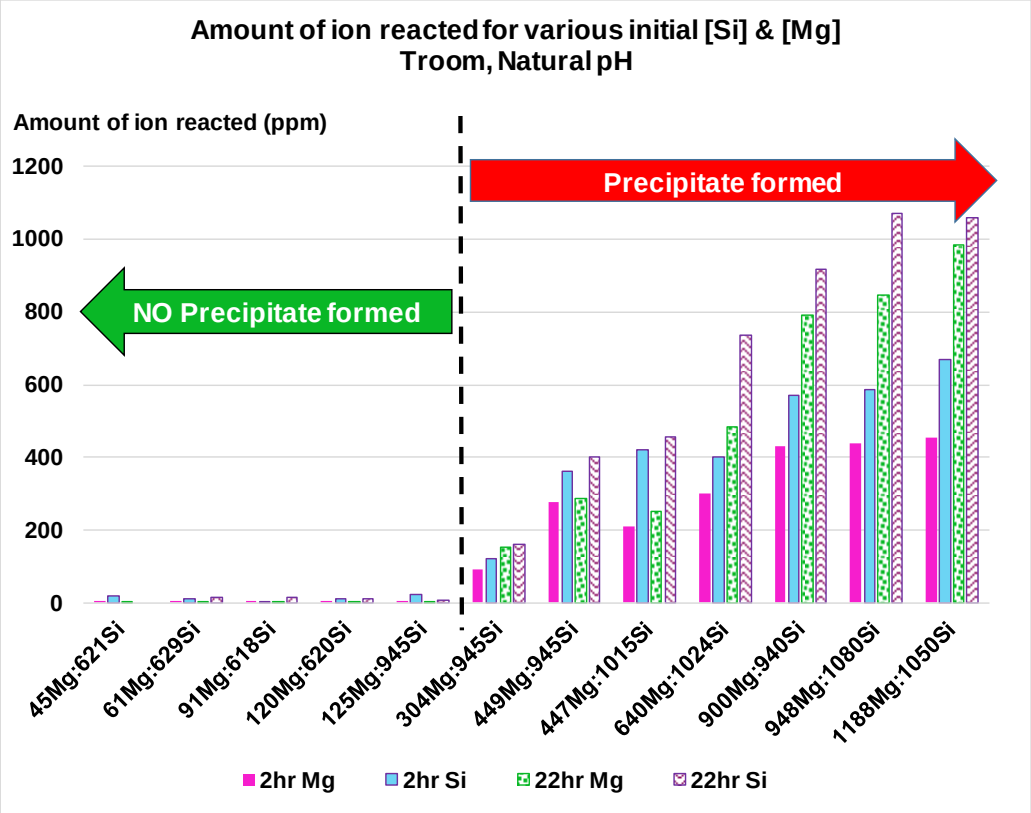

Figure 4-84 Extent of reaction for various initial Si:Mg molar ratios at T_{room}, natural pH

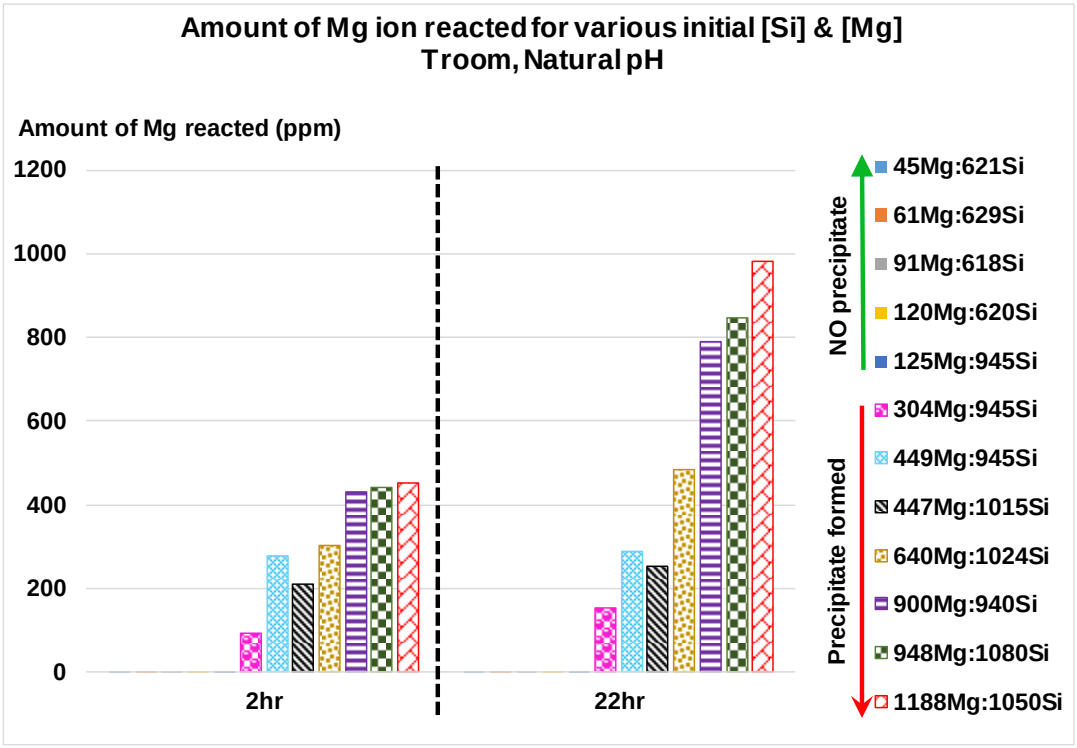

Figure 4-85 Amount of Mg ion reacted for various initial Si:Mg molar ratios at T_{room}, natural pH

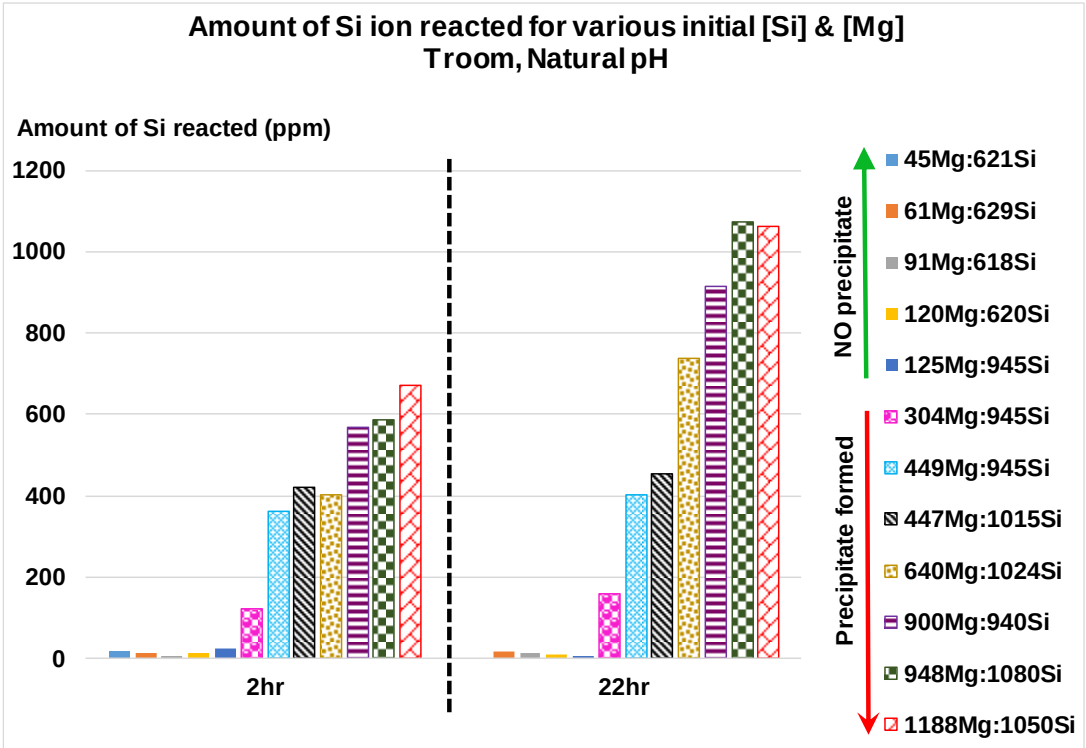

Figure 4-86 Amount of Si ion reacted for various initial Si:Mg molar ratios at T_{room}, natural pH

EDAX analysis of these precipitates were then used to determine the Si:Mg molar ratio in the silicate scale that is plotted in Figure 4-87. Further examination of the Si:Mg in the precipitate was shown to be grouped into 3 categories;

a) High Magnesium: Si:Mg in the precipitate ~ 1 when $(Si:Mg)_o<1$.

b) Medium Magnesium: Si:Mg in the precipitate ~ 1.3 when $1.37<(Si:Mg)_o<3.11$

c) Low Magnesium: No precipitate formed when $(Si:Mg)_o>4.47$

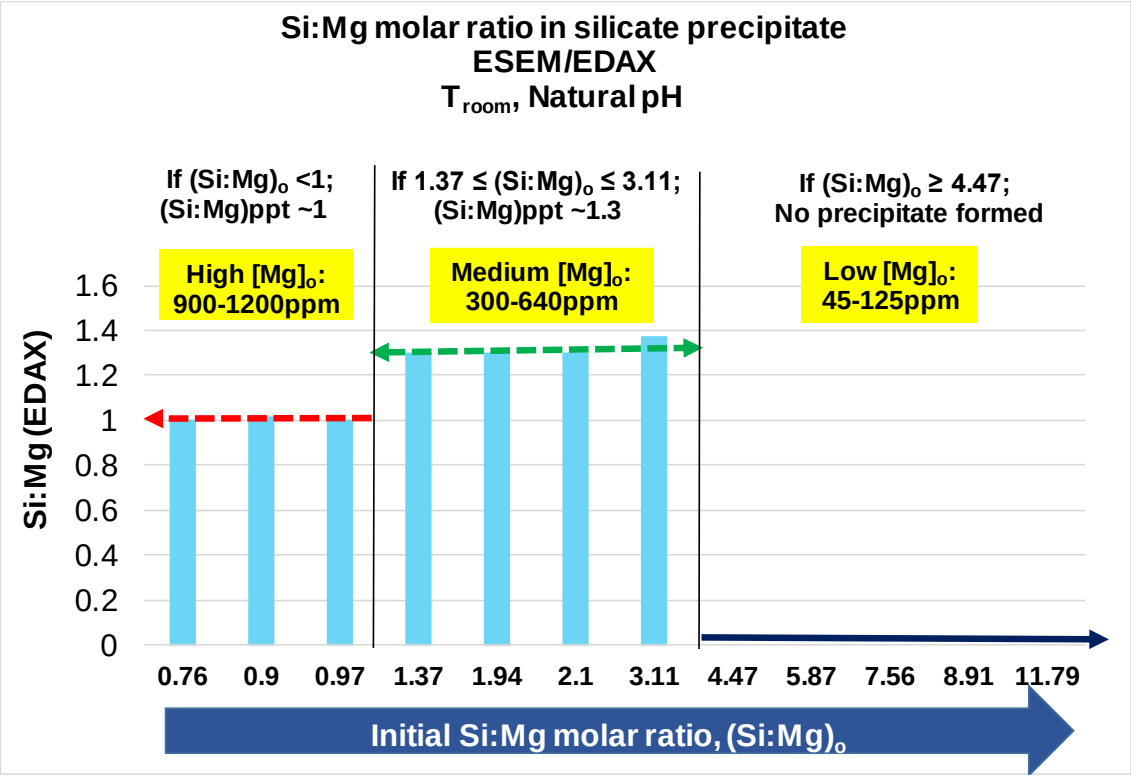

Figure 4-87 Si:Mg molar ratio in the silicate precipitate (Test condition: T_{room}, natural pH); $[Si]_{fixed}$ ~ 620/ 940/ 1050ppm

The Effect of Initial Si:Mg Molar Ratio at 60°C, pH8.5 - Fixed $[Mg]_o$

We also conducted the same test to understand the effect of this initial Si:Mg molar ratio on the silicate system, but at higher temperature (60°C) and lower pH (pH8.5). Various initial Si:Mg molar ratios as shown in Table 4-15 were studied and the extent of reaction is plotted in Figure 4-88. In this current experiment, $[Mg]_o$ was fixed at 2 values which are 30ppm and 60ppm. It is shown in this figure for $[Mg]_o$ = 60ppm that the amount of magnesium and silicon ion reacted were increasing as initial silicon added increased.

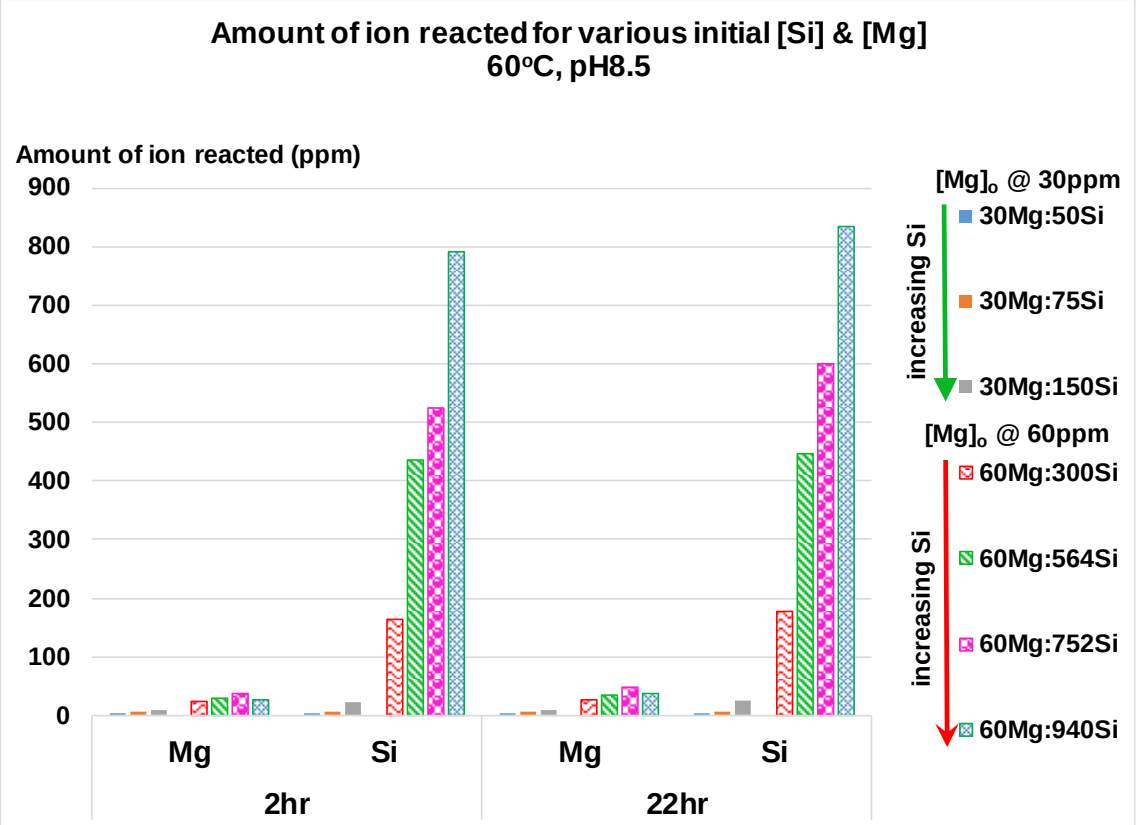

Figure 4-88 Extent of reaction for various initial Si:Mg molar ratios at 60°C, pH8.5; $[Mg]_{fixed,\ 1}$ = 30ppm & $[Mg]_{fixed,\ 2}$ = 60ppm

Generally, the amount of magnesium and silicon ion reacted was increasing with the reaction time, as shown in Figure 4-89, and visual inspection confirmed this ICP analysis which suggested that precipitate formed in all cases tested.

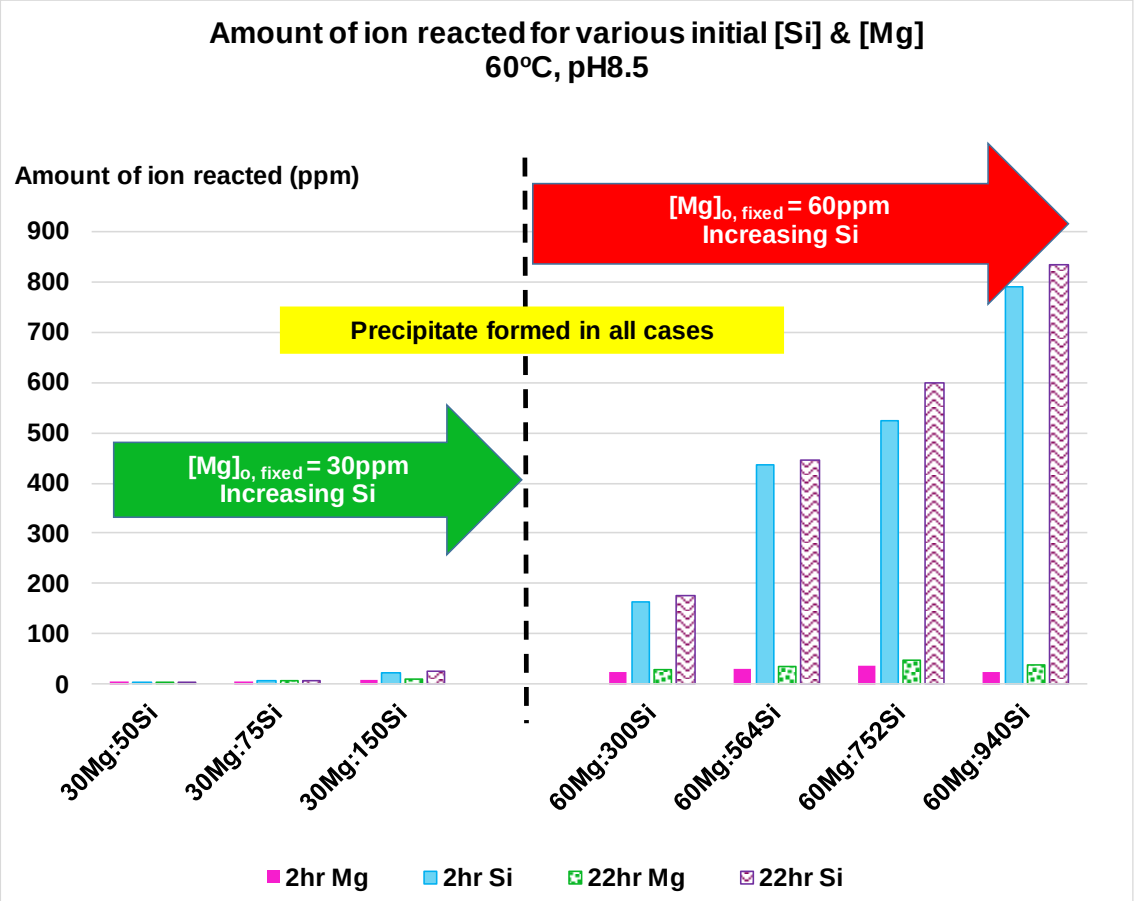

Figure 4-89 Extent of reaction for various initial Si:Mg molar ratios at 60°C, pH8.5; $[Mg]_{fixed,\ 1}$ = 30ppm & $[Mg]_{fixed,\ 2}$ = 60ppm

Likewise, close examination of the ICP analysis also showed that, for $[Mg]_o$ = 30ppm, the amount of magnesium and silicon ion reacted were increasing as initial silicon concentration increased, as shown in Figure 4-90 and Figure 4-91.

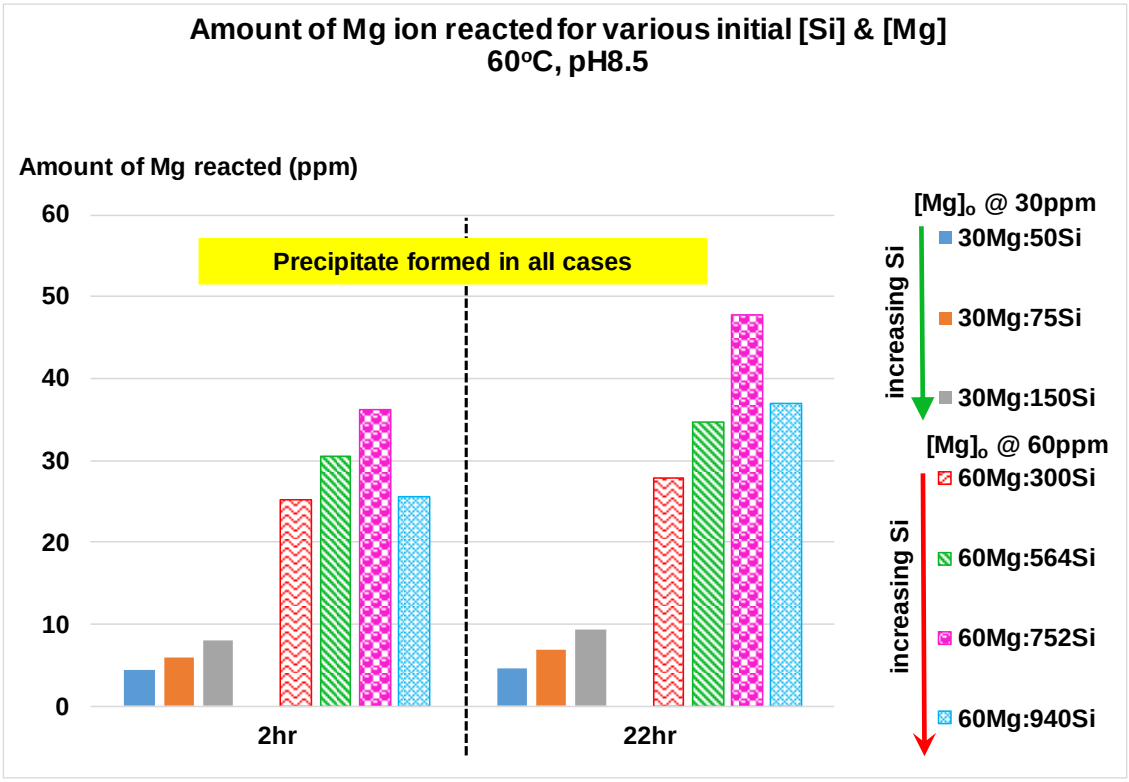

Figure 4-90 Amount of Mg ion reacted for various initial Si:Mg molar ratios at 60°C, pH8.5; $[Mg]_{fixed,1}$ = 30ppm & $[Mg]_{fixed,\ 2}$ = 60ppm

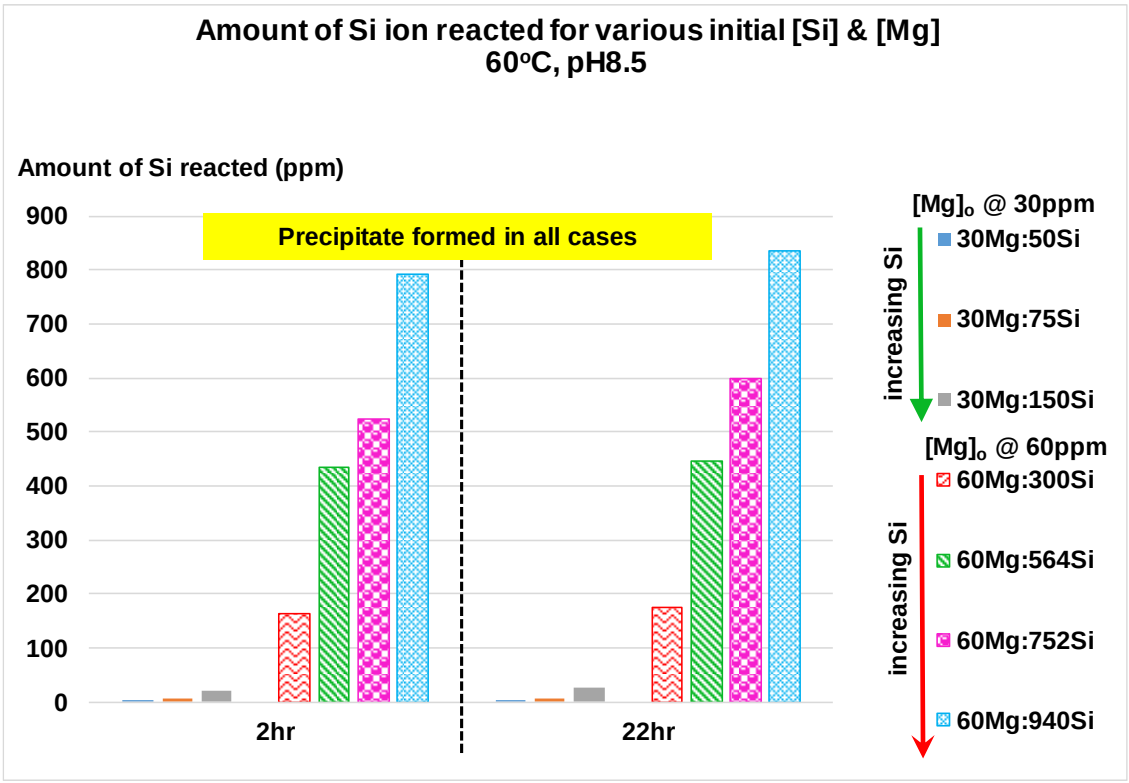

Figure 4-91 Amount of Si ion reacted for various initial Si:Mg molar ratios at 60°C, pH8.5; $[Mg]_{fixed,1}$ = 30ppm & $[Mg]_{fixed,\ 2}$ = 60ppm

Si:Mg molar ratios in the precipitate determined from EDAX analysis suggest that the values varied from 0.6 to 21, where this value increased with increasing initial silicon concentration (Refer Figure 4-92).

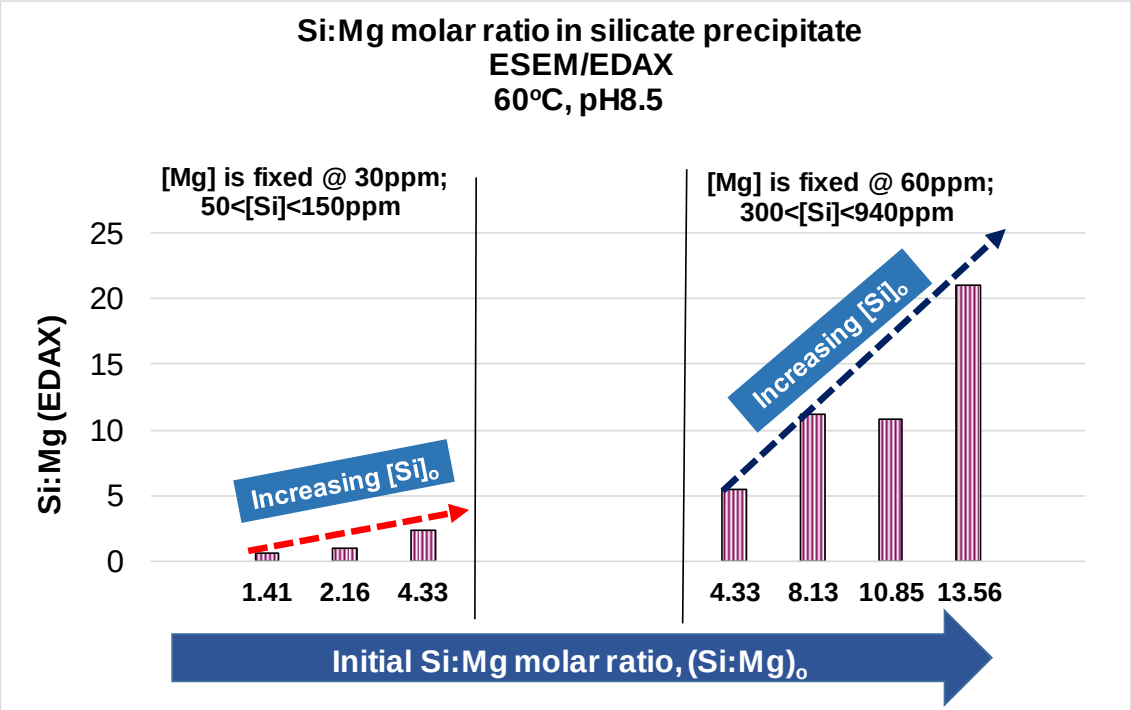

Figure 4-92 Si:Mg molar ratio in the silicate precipitate at test condition of 60°C, pH8.5; $[Mg]_{fixed,\,1}$ = 30ppm & $[Mg]_{fixed,\,2}$ = 60ppm

The Effect of Initial Si:Mg Molar Ratio at 60°C, pH8.5 - Fixed $[Si]_o$

Figure 4-93 shows that the *Si:Mg molar ratio* in the silicate deposit depends on the amount of magnesium present in the mixed solution. In addition, the *Si:Mg molar ratio* decreases as the amount of magnesium ion is increased. This finding suggests that the higher the concentration of magnesium present in the system, the higher tendency of magnesium silicate precipitation as more of these magnesium ions bridge to the the polymerized silica, resulting in a lower *Si:Mg molar ratio* (refer Figure 4-94). This is as expected, but it has not been firmly established in an oilfield appropriate system to date.

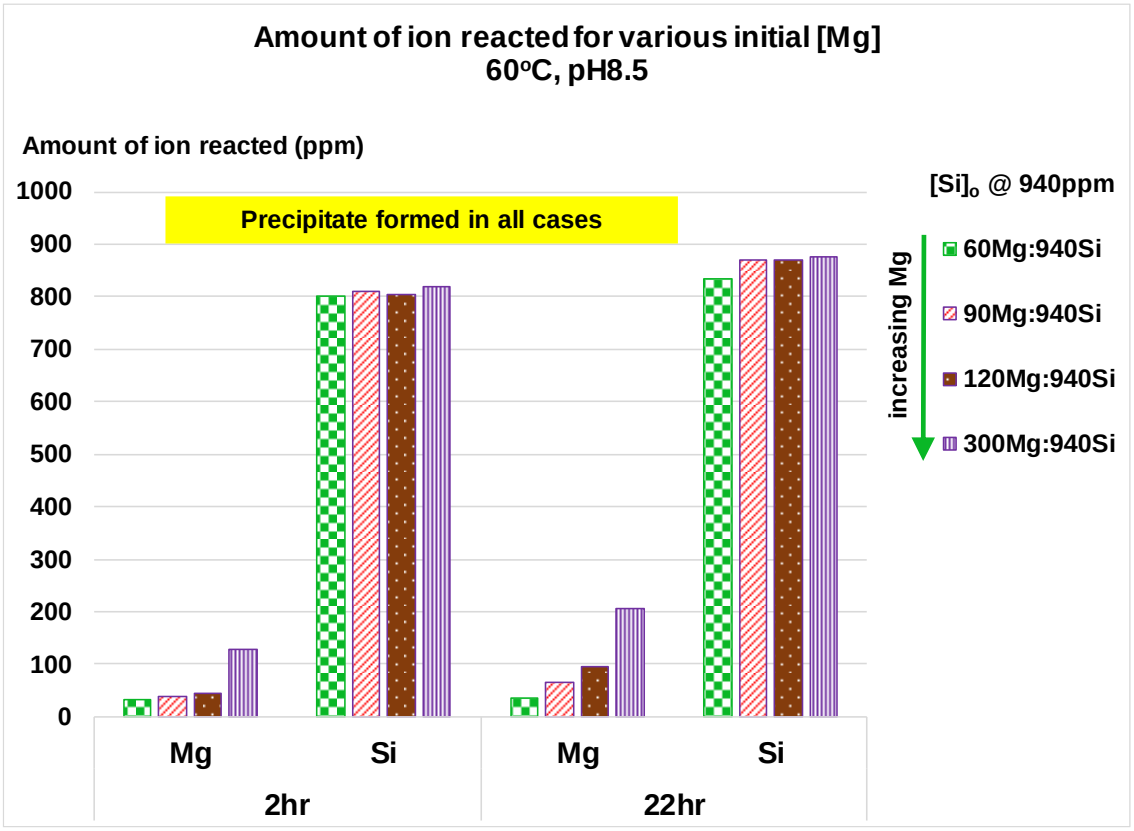

Figure 4-93 Amount of ion reacted for various initial Si:Mg molar ratios at 60°C, pH8.5; $[Si]_o$ = 940ppm

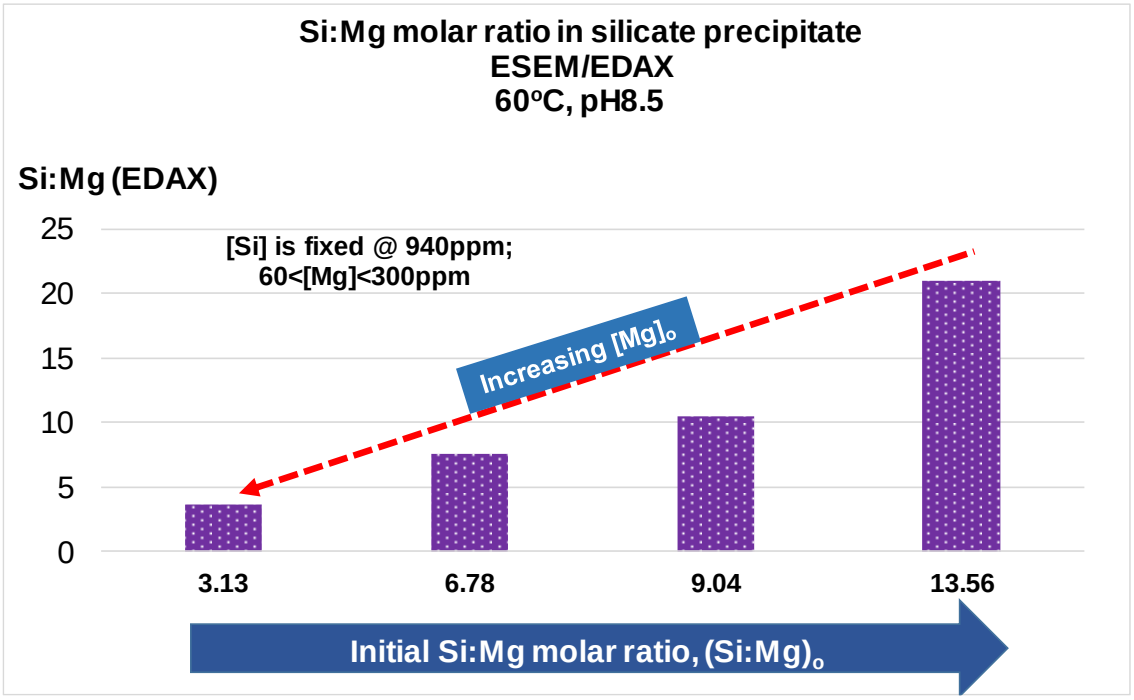

Figure 4-94 Si:Mg molar ratio in the silicate precipitate (Test condition: 60°C, pH8.5); $[Si]_{fixed}$ = 940ppm

(c) Summary and Conclusion

Following the previously obtained results, we found that the initial solution Si:Mg molar ratio definitely affected the final Si:Mg molar ratio in the precipitate. Two main conclusions are drawn as follows:

a) For silicate system reacted at room temperature at natural pH levels; the Si:Mg in the precipitate is between ~1 to ~1.3. Also, at high pH (>pH9.5) the reaction will results in co-produced Mg-silicate & $Mg(OH)_2$ as discussed in section 4.4.1.

a) For silicate system reacted at 60^{o}C and pH8.5; the Si:Mg ration in the precipitate will vary between ~0.6 to ~21, where only amorphous silica and amorphous Mg-silicate scale are produced.

4.4.4 Effect of Ageing Silicon Brine

(a) Experimental Details

Another experiment was also conducted to study the effect of ageing silicon brine at various pH values (pH8.5 and pH7.6) on the silica precipitation process. This was carried out to examine if any effects, such as silicate polymerization occurred before the Mg-silicate formed which would lead to changes in the stoichiometry of the final Mg-silicate scale which was formed. Interestingly, the precipitation reaction between fresh magnesium brine and aged silicon brine was found to produce magnesium silicate scales with very different stoichiometries, as compared with the freshly mixed magnesium and silicate brines. This has important implications in terms of which silicate brines may be forming in the reservoir and on the precise details of the laboratory procedures which we should be using to assess silicate scale inhibition. These issues are addressed below in this work on silicate scale management.

It was observed that during the pH adjustment of silicon brine from its natural pH ~12.9 to pH ~7.6, the solution became cloudy after 20 hours. Furthermore, a gel-liked precipitate appeared in the silicon brine after the solution was left at room temperature for another 7 days. The pH was recorded as pH ~8.57 after 7 days and it was believed that this gel precipitate was probably due to the polymerization of monomeric silicate ions.

Therefore, the same precipitation experiment was repeated with the two sets of aged silicon brines adjusted to pH 7.6 and pH 8.5, respectively. Magnesium brine was later added to the aged silicon brine to give an initial mixed concentration of 60Mg:940Si before being heated to the test temperature of 60^{o}C in the oven and then allowed to react for 22 hours.

The aim of this experiment was to determine if there were any differences in the Si:Mg ratio incorporated into the magnesium silicate scale in a fresh brine mix (i.e. fresh silicon brine is mixed with fresh magnesium brine) as compared with an aged brine mix (i.e. fresh magnesium brine is added to aged silicon brine that aged at certain pH value for 7 days). This would be an indirect way to test the hypothesis that the aged silicate solution had polymerised to some degree. There were two sets of aged silicon brine tested in this experiment which were at pH ~ 8.5 and pH ~ 7.6. If the silicate had actually polymerised, then we would expect the Si:Mg ratios to be rather higher than in the fresh silicate/Mg brine mix (where the silicate brine was not aged).

The experimental methodology involved 5 main steps as described below:

(i) 1880ppm silicon brine was pH adjusted to *test condition 2;* pH8.5 and *test condition 3;* pH7.6 respectively (Figure 4-95).

(ii) The silicon brines in (i) above were *aged* for 7 days (Figure 4-95). The pH of the aged silicon brine was monitored throughout the ageing process before being mixed with fresh magnesium brine.

(iii) Fresh 120ppm magnesium brine samples were added to (Figure 4-96);

   a. Fresh 1880ppm silicon brine gave final solution of *test condition 1;* gave final solution of 60Mg:940Si (blank sample).

   b. *Aged* Si brine at pH8.5; gave final solution of 60Mg:940Si

   c. *Aged* Si brine at pH7.6; gave final solution of 60Mg:940Si

(iv) All three conditions of above 60Mg:940Si were initially pH-adjusted to pH8.5 (Figure 4-96) just after mixing.

(v) All three brines were then heated to 60^{o}C and left reacted for 22 hours (Figure 4-97).

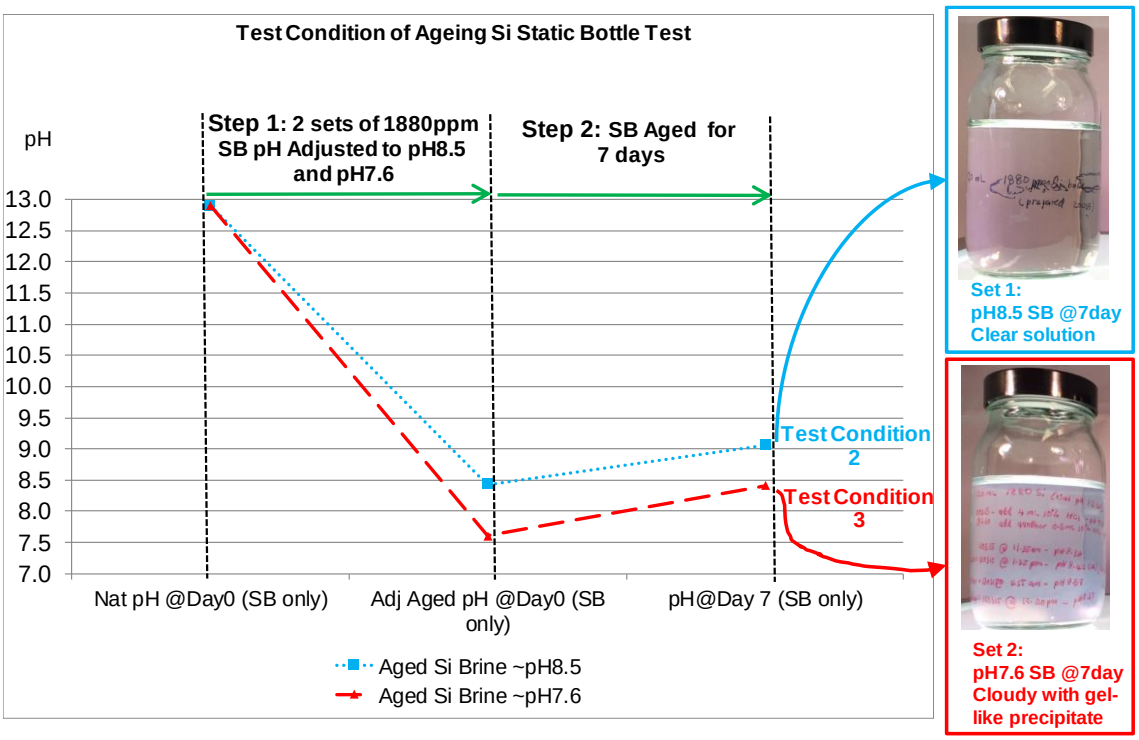

Figure 4-95 Silicon brine ageing (Step 1 & 2) in Test Condition 2 & 3

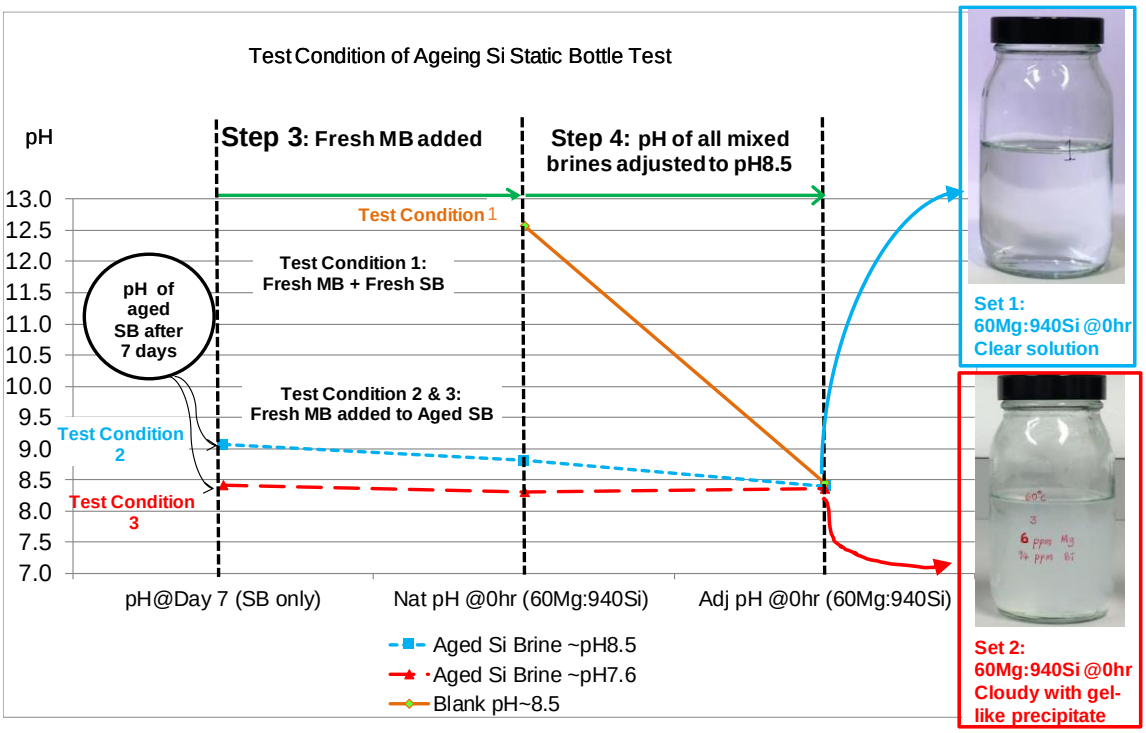

Figure 4-96 The addition of fresh magnesium brine (Step 3 & 4) in three different test conditions

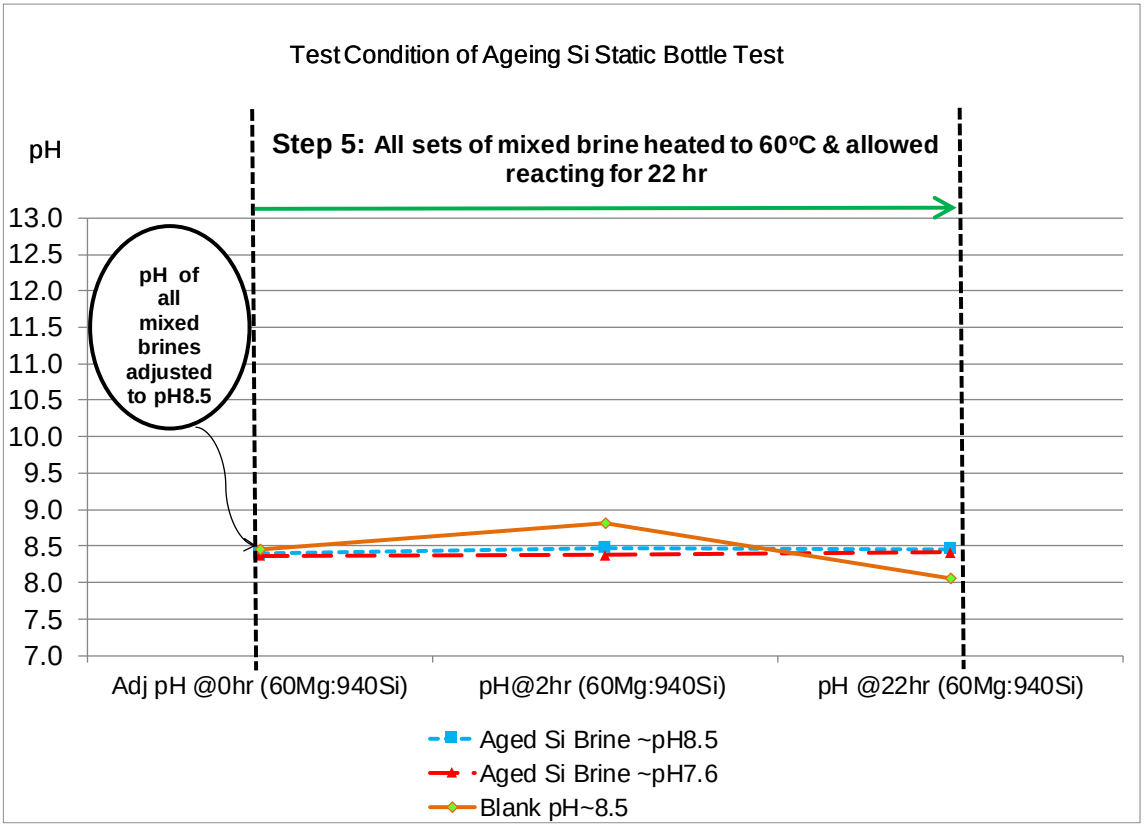

Figure 4-97 Heating to 60°C allowing reaction for 22 hours (Step 5)

(b) Experimental Results and Discussion

Figure 4-98 shows that the aged silicon brine in test condition 2 stays clear even after 7 days. In contrast, the aged silicon brine at pH7.6 in test condition 3 produced a gel-like precipitate after 7 days. The observations at all test conditions after 2 and 22 hour are shown in Figure 4-99. The results in this figure clearly demonstrate that the mixed brine of aged brine at pH8.5 (i.e. test condition 2) only became slightly cloudy after 2 hours. However, the gel-like precipitate can be seen after 22 hours; similar to observation for brine in test condition 1 and 3.

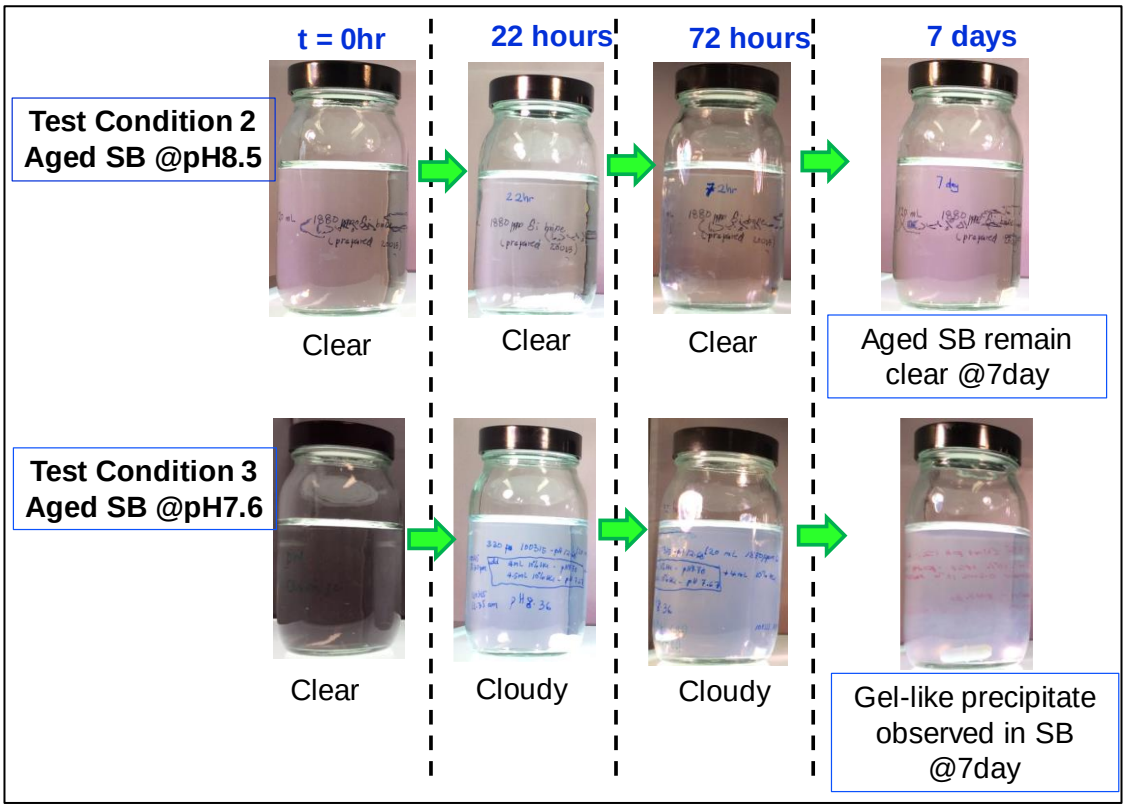

Figure 4-98 Observation for ageing silicon brine in Test Condition 2 & 3

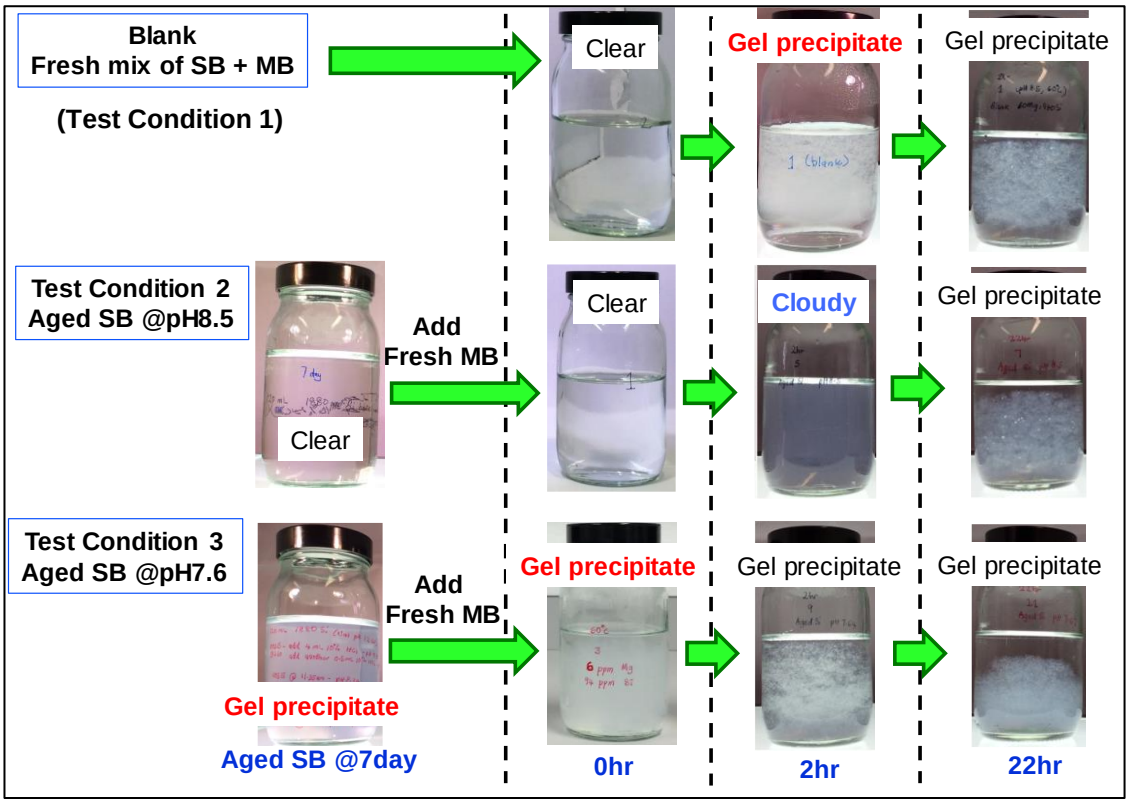

Figure 4-99 Observation in all test conditions up to 22 hours

As shown in Figure 4-100, a gel-like precipitate was observed in the *blank* solution and the solution with silicon brine aged at pH 7.6; while the solution with silicon brine aged at pH8.5 remained cloudy after 2 hours of being reacted. These solutions were centrifuged (as shown in Figure 4-101) before they could be ICP sampled, and the precipitates were collected for analysis of their morphologies and compositions using FTIR and ESEM/EDAX.

Figure 4-102 and Figure 4-103 show the conditions of the mixed solutions after reaction for 22 hours, before and after centrifuging. Gel-like precipitate was also observed in the solution with aged silicon brine aged at pH8.5, after it was reacted for 22 hours.

According to Gunnarsson and Arnórsson (2003), polymeric silica has less tendency to precipitate from solution than monomeric silica and colloids that formed during the polymerization reaction may remain suspended in the solution for long periods of time. They claimed that ageing reduces amorphous silica supersaturation in the waste water by a factor of ten or more, and therefore greatly decreases the potential for amorphous silica deposition.

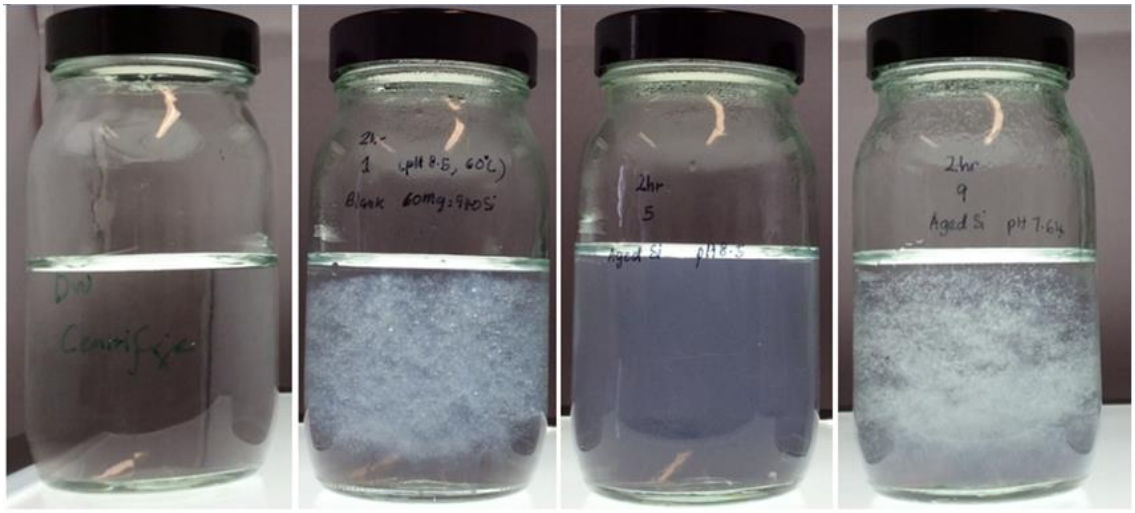

Figure 4-100 2hr observation blank samples vs. Aged silicon mixed brine (Before centrifuge)

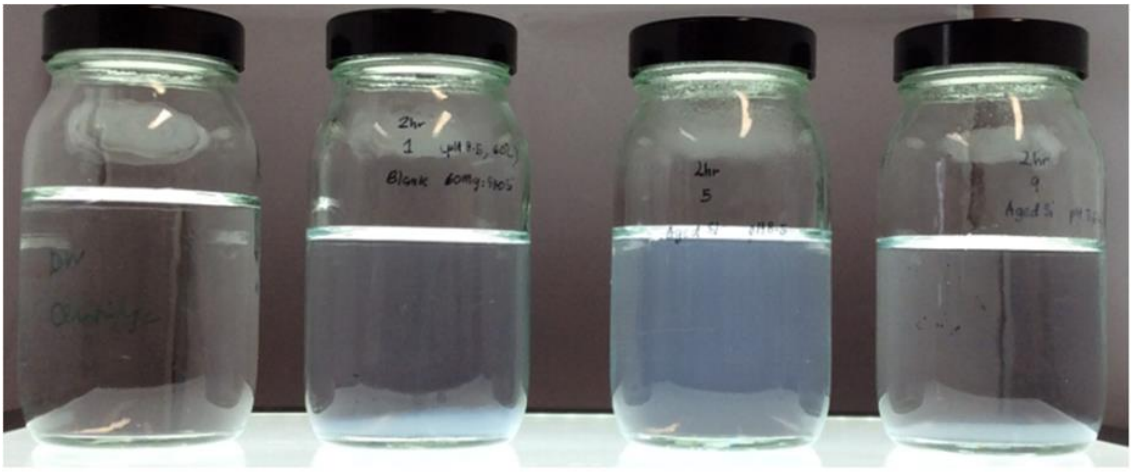

Figure 4-101 2hr observation blank samples vs. Aged silicon mixed brine (After centrifuge)

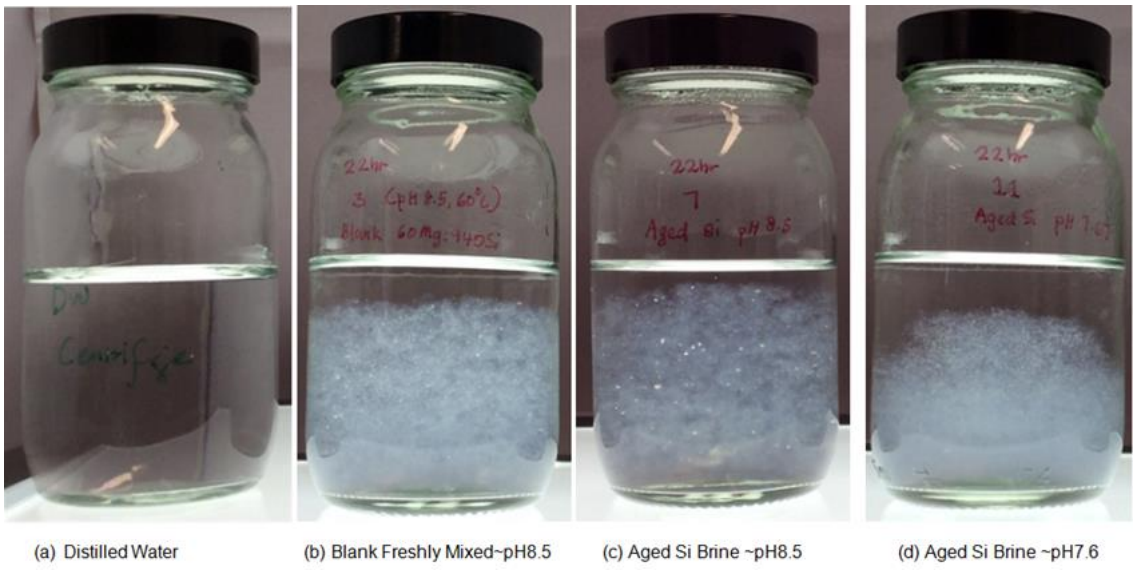

Figure 4-102 22hr observation blank samples vs. Aged silicon mixed brine (Before centrifuge)

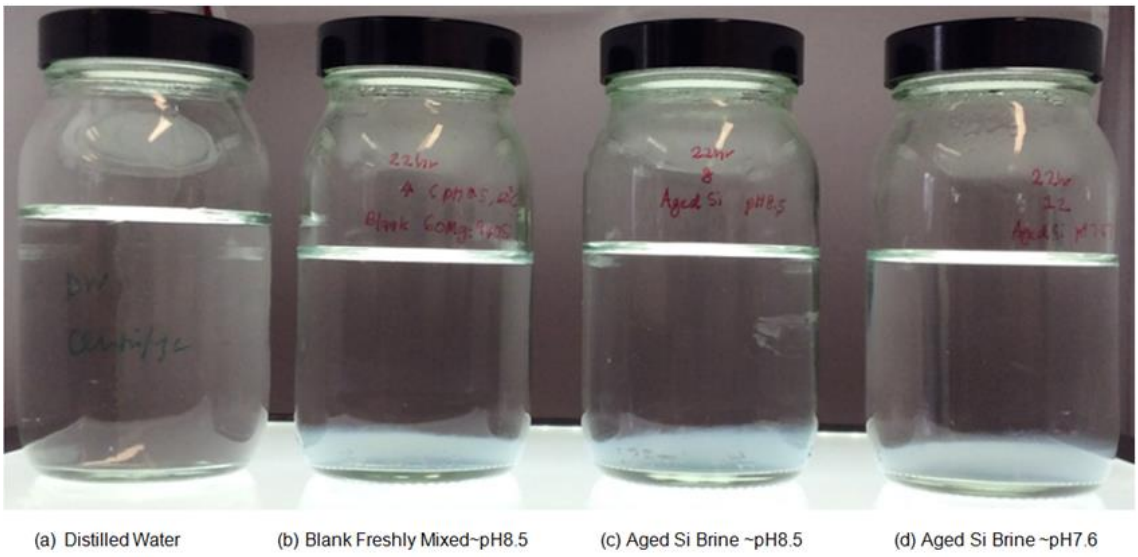

Figure 4-103 22hr observation blank samples vs. Aged silicon mixed brine (After centrifuge)

The amounts of magnesium and silicon ion reacted are plotted in Figure 4-104 and Figure 4-105 in actual concentration (ppm) and percentage values, respectively.

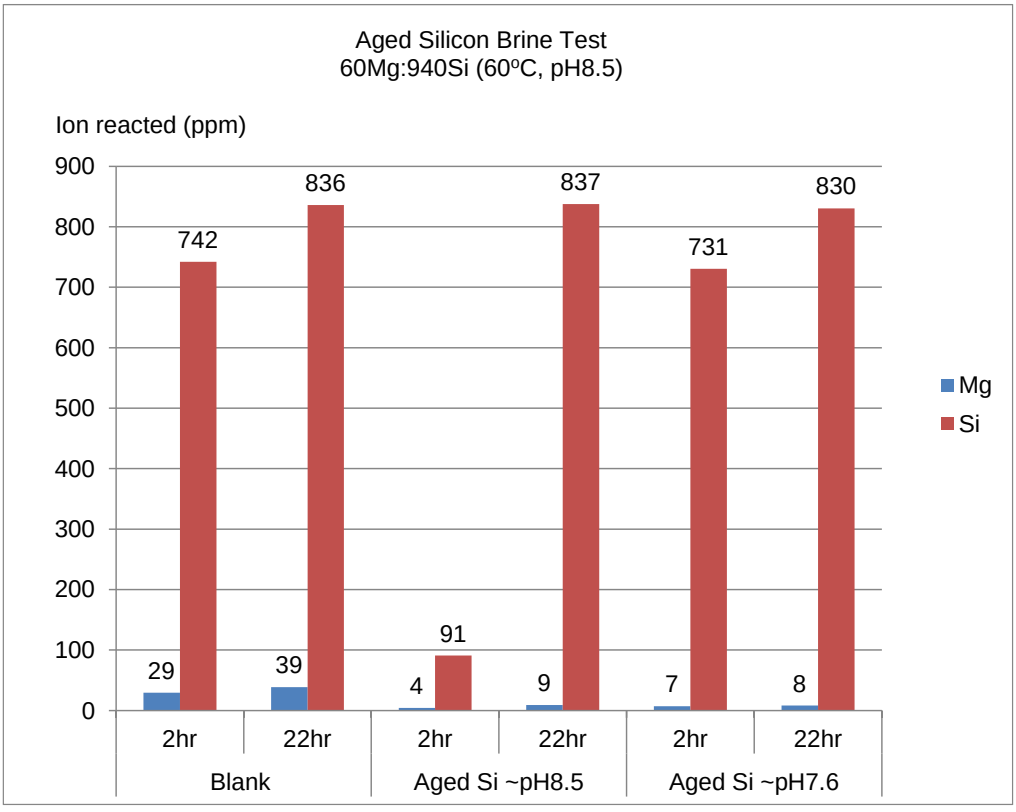

Figure 4-104 Amount of ion reacted of 60Mg:940Si (60°C and pH8.5) in "Aged Silicon Brine" test

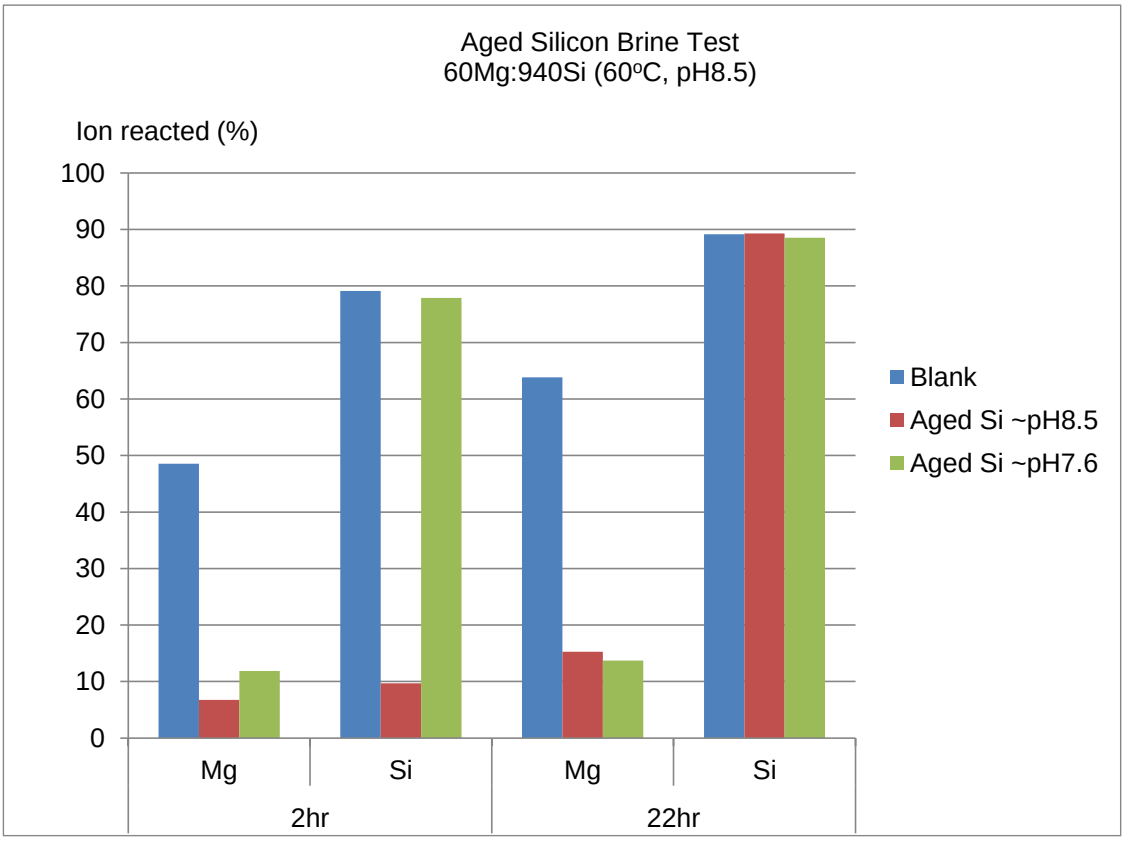

Figure 4-105 Percentage amount of ion reacted of 60Mg:940Si (60ºC and pH8.5) in "Aged Silicon Brine" test

The amounts of magnesium ion reacted in the aged silicon brine mixed solution were found to be much lesser compared to the blank solution. The ageing process appears to have reduced the amount of magnesium ion reacted by 86% and 76% for aged brine@pH8.5 and aged brine@pH7.6 respectively when compared to the blank solution at 2 hour. It was also observed that the percentage of magnesium ion reacted reduced by 76% and 78% for aged brine@pH8.5 and aged brine@pH7.6, respectively, in comparison to the blank solution after 22 hours of reaction. The high percentage reduction in the amount of magnesium ion reacted as shown in Figure 4-106 is thought to be a result of the reduced tendency for producing the amorphous magnesium silicate scale as this polymerized silica is believed to remain suspended (i.e. not deposited) in the solution.

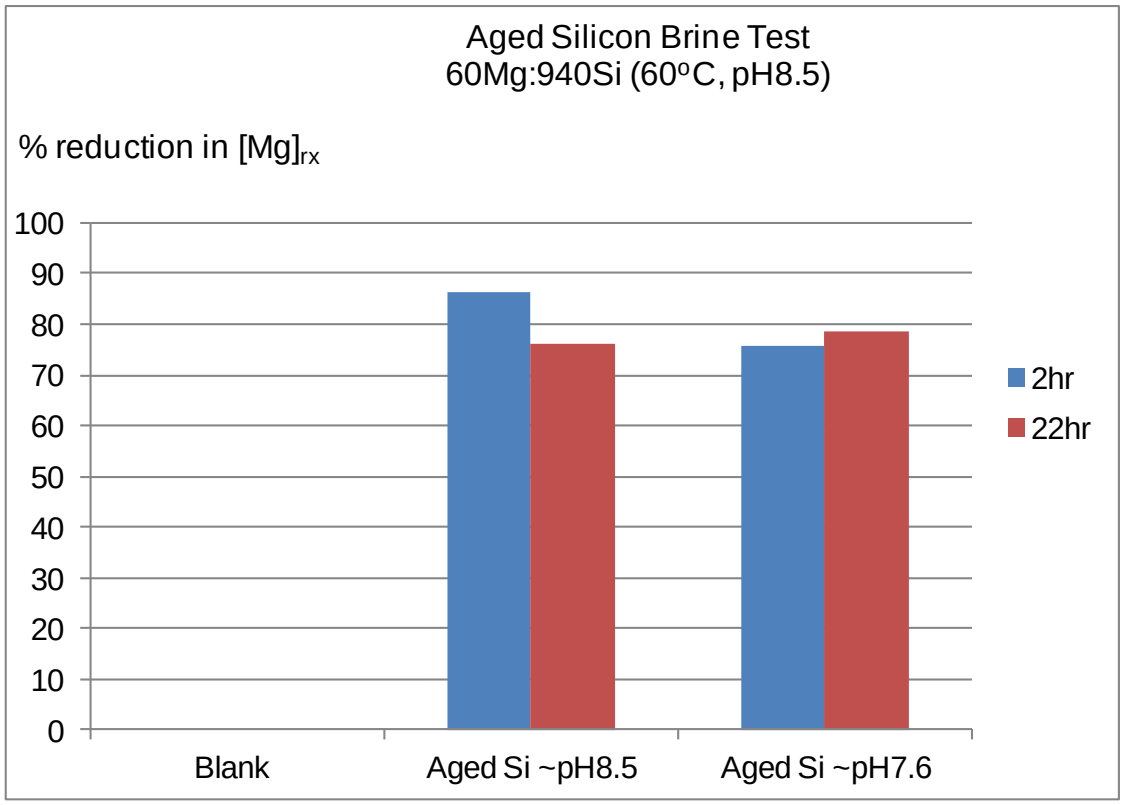

Figure 4-106 Percentage reduction in the amount of magnesium ion reacted as compared to blank solution

As shown in Figure 4-107, the aged SB gave silicate deposits with much higher *Si:Mg molar ratio* than the fresh mixed brine. Thus, our postulate appears to be correct that, in the aged SB, silica polymerization readily occurs. In turn, polymerization lowers the aqueous concentration of monomeric silica giving less tendency for Mg-silicate scale deposit and precipitation. These new findings in this work on the effect of aged silicate brine before Mg-silicate formation are important in the oilfield since the released Si may be formed some time before it encounters any Mg^{2+} ions in solution (i.e. before the Mg-silicate scale forms). This has clear implications for the test methodology when examining inhibitors/dispersants for use against silicate scales. The Si:Mg molar ratio of precipitate in test condition 2 is ~80 while in test condition 3 is ~90. These findings suggest that long chain silicate was form as compared in the blank solution where the value ~20 only. In the precipitate that produced from the *blank* solution, we might expect that the structure was much shorter with more magnesium ion bridge into this short amorphous silica structure.

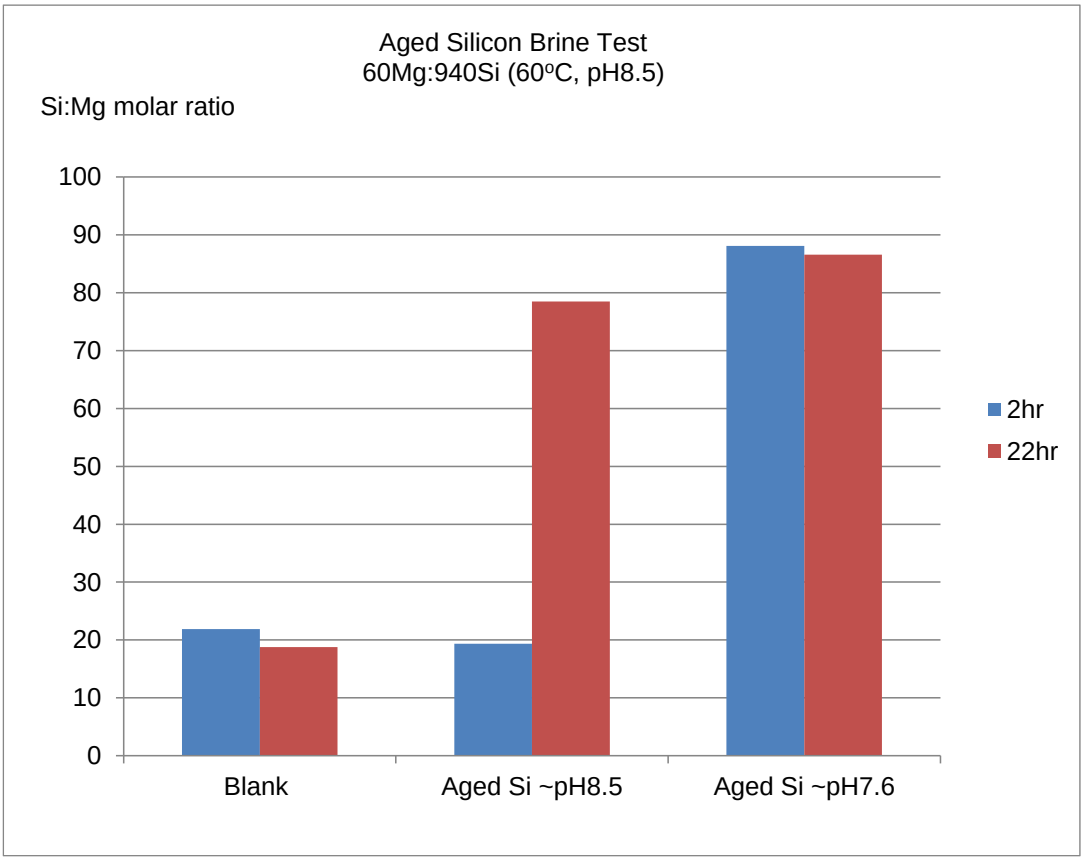

Figure 4-107 Si:Mg molar ratio determined from ICP data of 60Mg:940Si (60ºC and pH8.5) in "Aged Silicon Brine" test

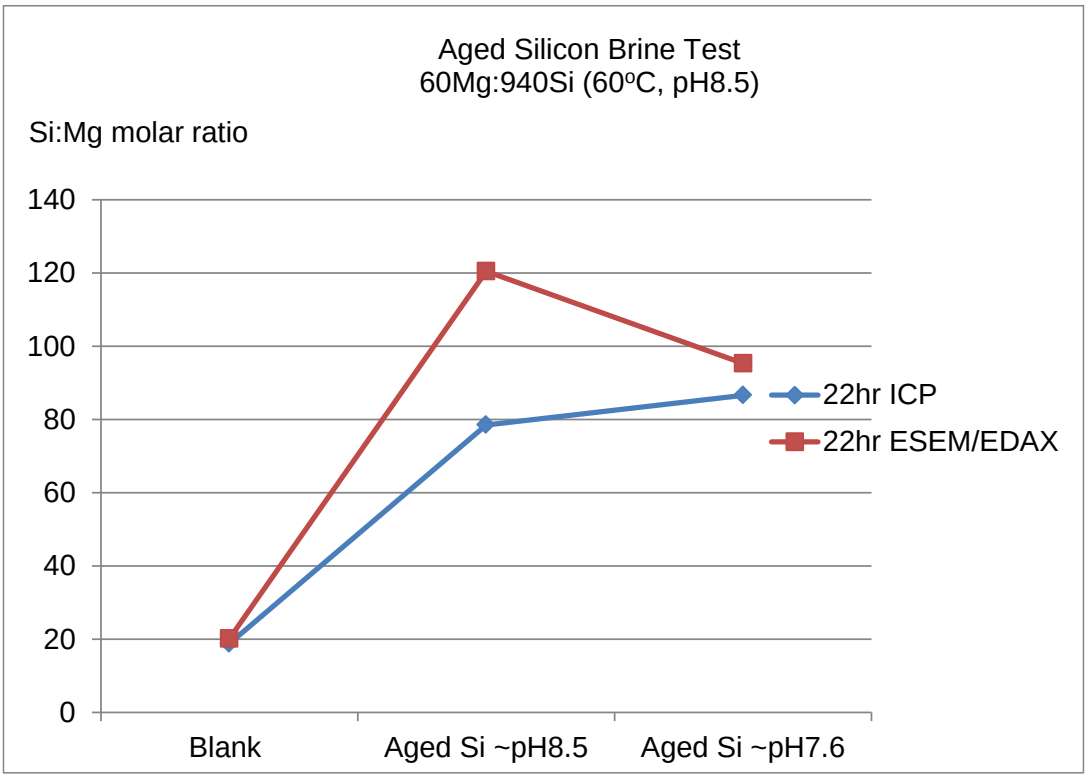

Figure 4-108 Si:Mg molar ratio of 60Mg:940Si (60ºC and pH8.5) in "Aged Silicon Brine" Test – ICP data vs. ESEM/EDAX data

Si:Mg molar ratios calculated from ICP data for all conditions in the aged silicon brine experiment are plotted in Figure 4-107, and these are then compared with the values obtained from the ESEM/EDAX studies which are plotted in Figure 4-108. The pH values throughout the reaction were monitored and plotted in Figure 4-109. It is observed that pH values after 2 hours of reaction were higher than the initial pH values then they subsequently reduced to lower than the initial pH value after 22 hours.

All FTIR spectra for the precipitates collected after 2 hours and 22 hours in this experiment are shown in Figure 4-110. This figure shows the same spectra acquired as per earlier tests at 60°C, pH8.5.

ESEM images for precipitates collected from the ageing silicon brine and precipitate collected from the ageing silicon brine reaction are also presented in Figure 4-111, Figure 4-112, Figure 4-113 and Figure 4-114.

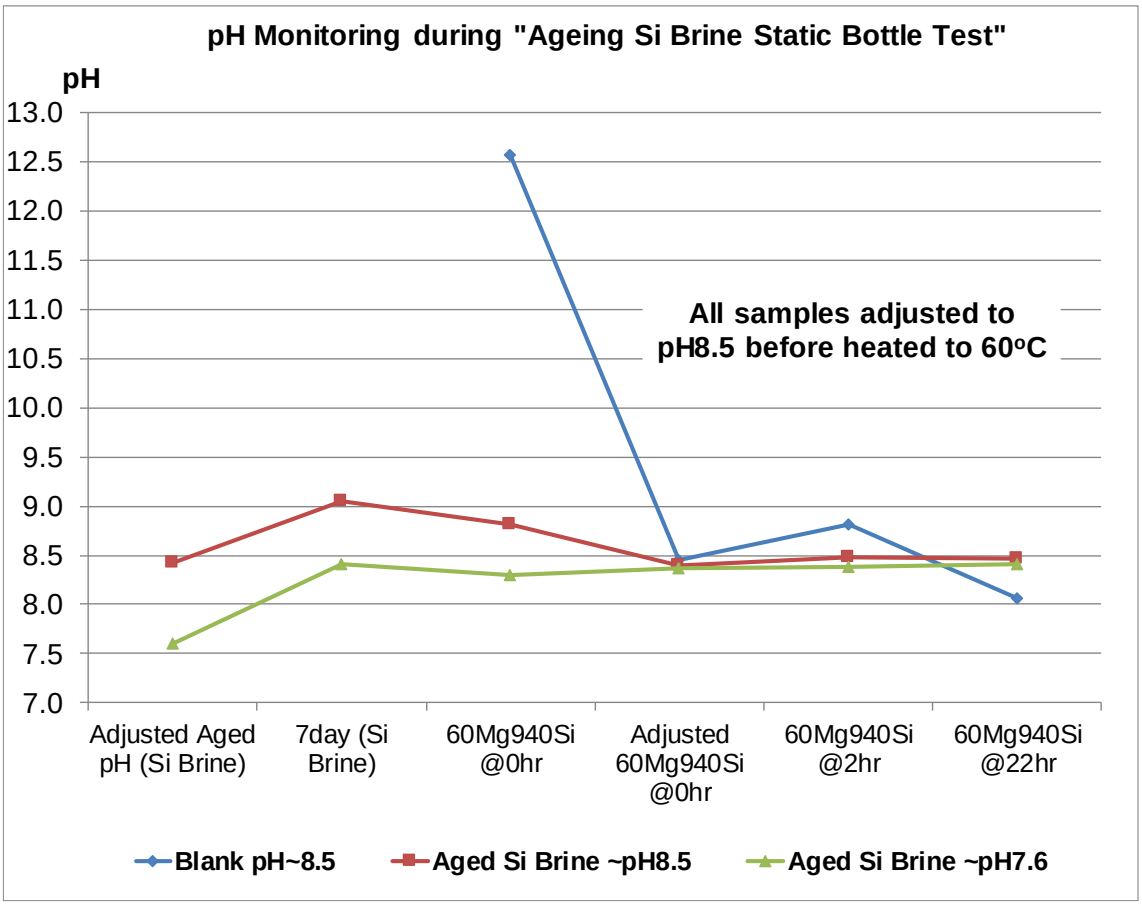

Figure 4-109 pH monitoring in "Aged Silicon Brine Test"

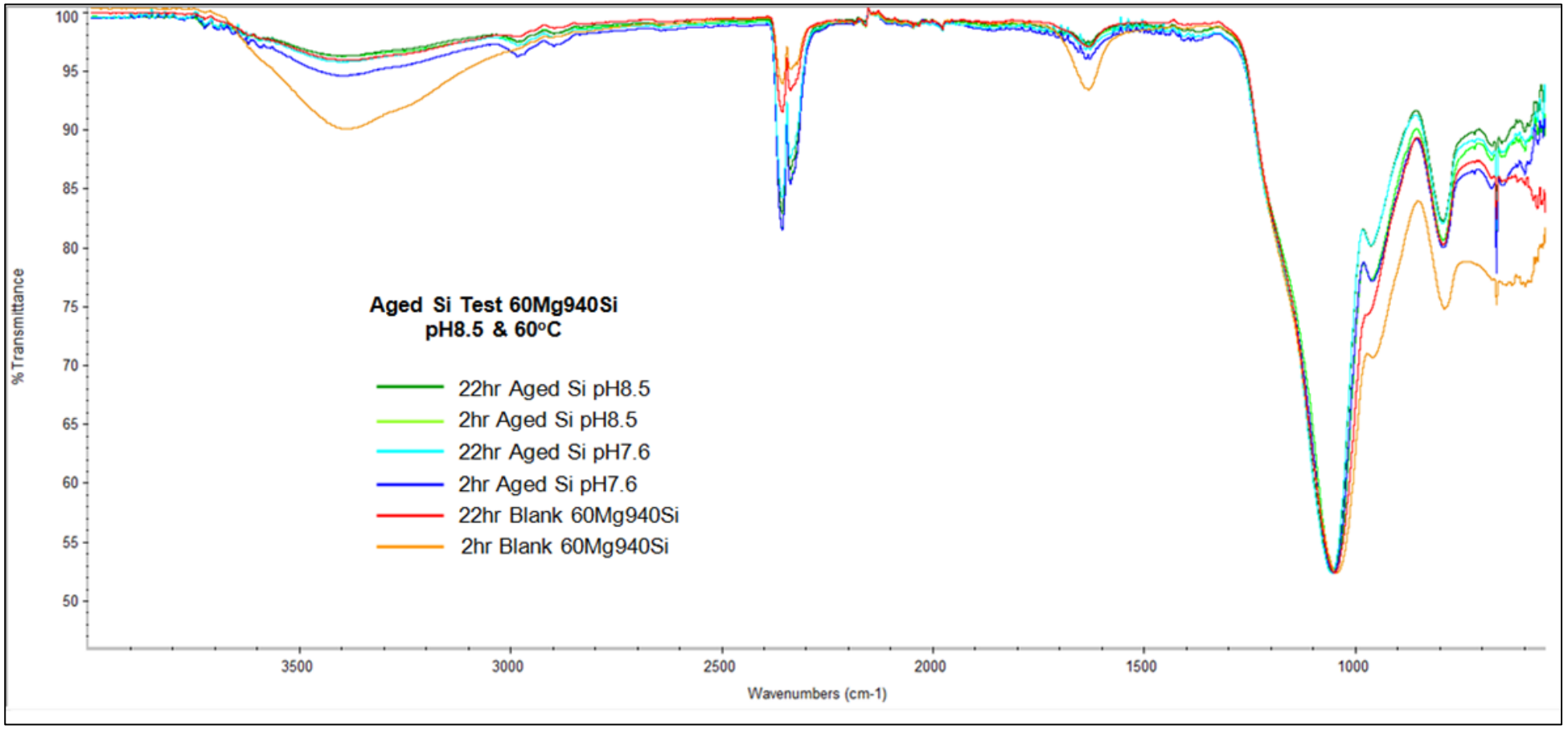

Figure 4-110 FTIR spectrum of precipitate produced after 2and 22hr reaction of 60Mg:940Si (60°C and pH8.5) in "Aged Silicon Brine Test"

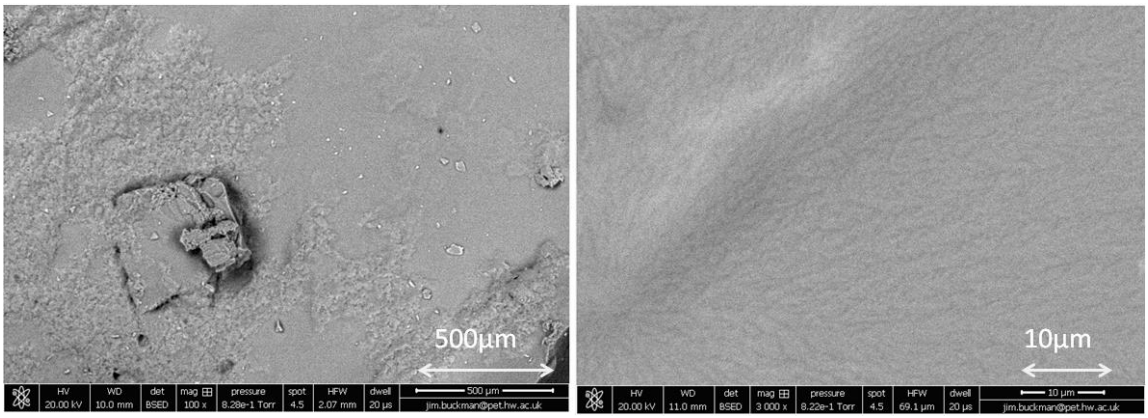

Figure 4-111 ESEM images of ageing silicon brine 13 days old at pH7.6

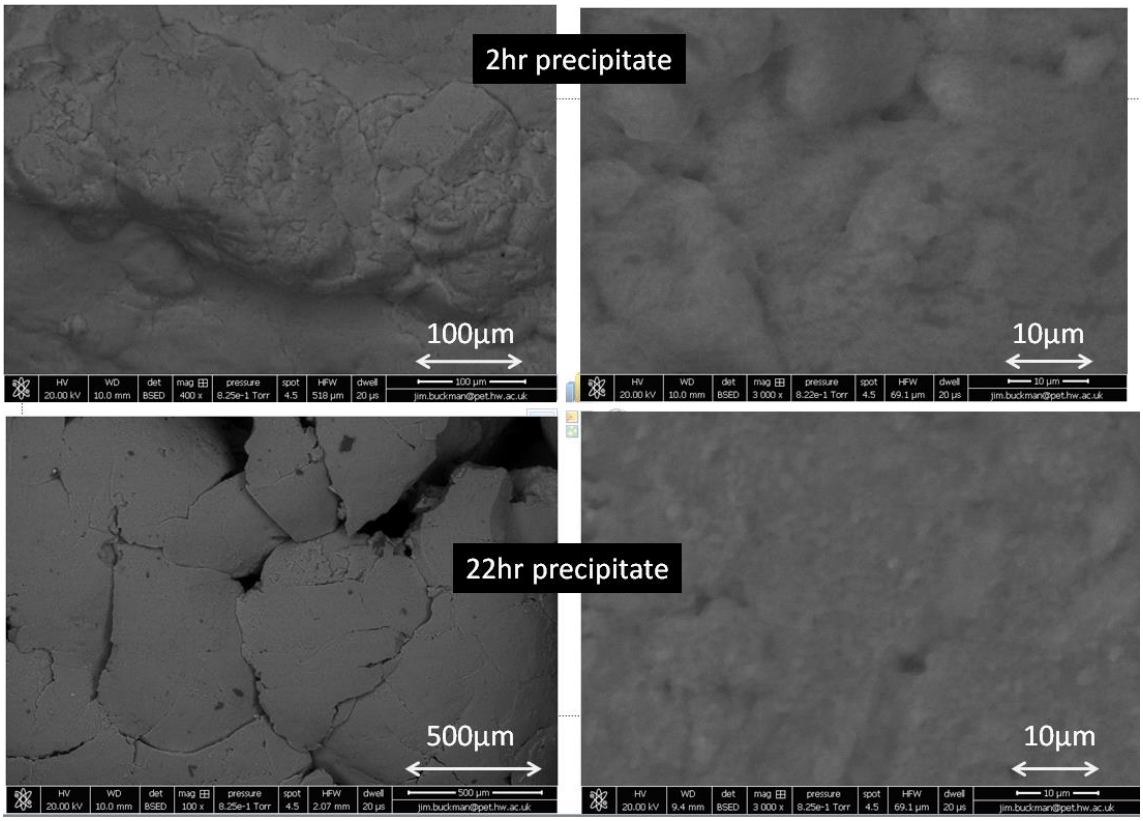

Figure 4-112 ESEM images of precipitate produced in blank solution (Reaction between fresh magnesium brine with fresh silicon brine)

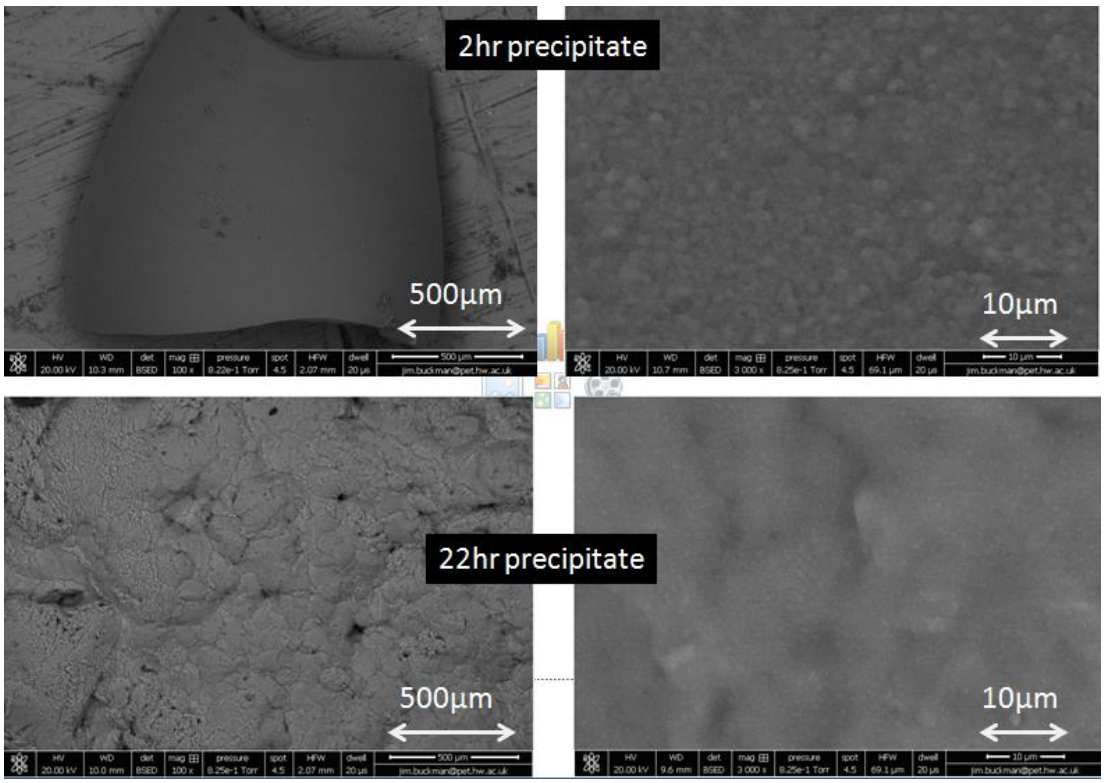

Figure 4-113 ESEM images of precipitate produced in reaction between fresh magnesium brine with 7 days old ageing silicon brine at pH8.5

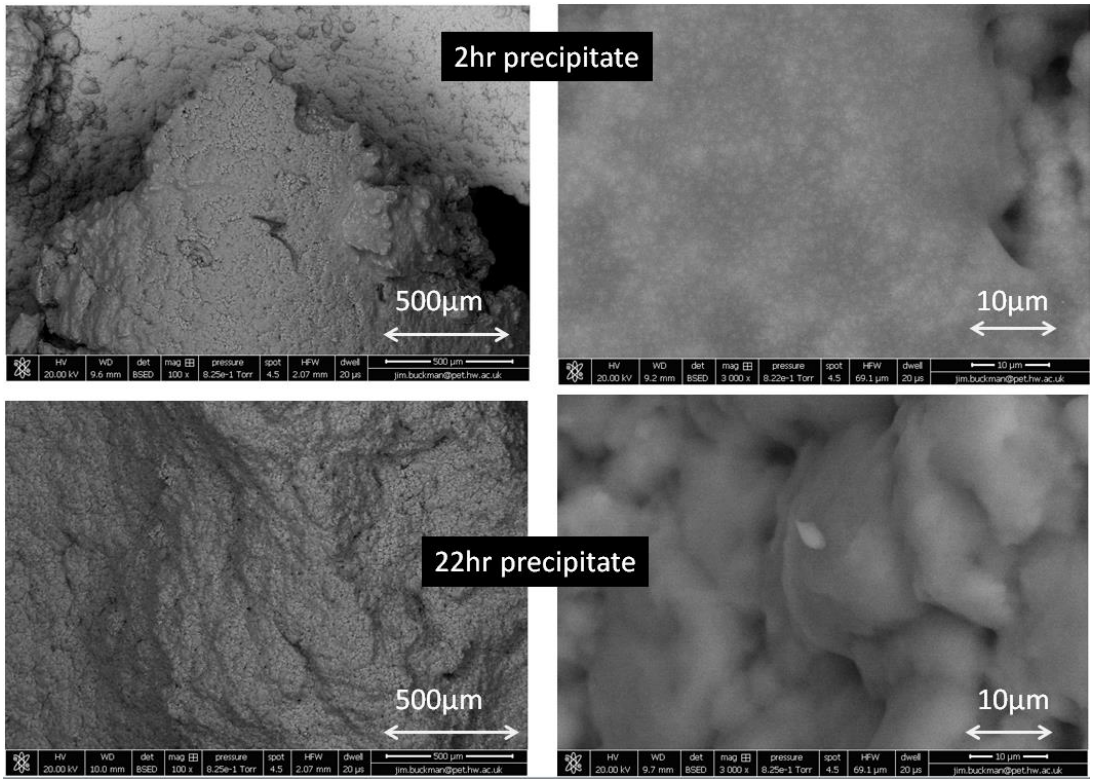

Figure 4-114 ESEM images of precipitate produced in reaction between fresh magnesium brine with 7 days old ageing silicon brine at pH7.6

(c) Summary and Conclusion - Silicate Brine Ageing Experiments

Two basic pathways for the precipitation of amorphous silica have been described by Weres et al. (1980) as (i) molecular deposition of monosicilic acid producing vitreous silica, a hard scale on the surface that was almost indestructible once formed except by the using of hot HF or caustic; and (ii) homogenous nucleation when monosilic acid bridged colloidal silica producing hard scale of the cemented colloidal aggregate type. Hence, the effect of ageing the silicon brine was to convert the dissolved silica to a much less adhesive "polymeric form" with a less than critical nucleus size. Ageing the silicon brine resulted in lower amounts of magnesium ion reacting which means lower risk of the deposition of amorphous magnesium silicate scale. Aged Silicon Brine (SB) showed extensive reaction of Si for both pH values studied (pH 8.5 and 7.6) at 22 hours but this was polymerized into amorphous silica and remain suspended in the solution i.e. the formation of hard scale vitreous silica on surface via molecular deposition of monomeric silica deposition will be avoided.

Aged SB gave silicate deposits with much higher Si:Mg molar ratio than measured for fresh (unaged silicate brine) mixed brine samples. This may due to the fact that silica polymerization occurs in the aged silicon brine which lowers the aqueous concentration of monomeric silica. Hence, there was less tendency for silicate scale deposition/ precipitation. The suspended polymerized scale formed in both aged solution is more of a "flocculate like" material. Hence, the supersaturation condition due to monomeric silica is now being diverted to a relatively nonadhesive polymeric form rather than conversion into amorphous magnesium silicate scale or hard vitreous silica. According to Weres et al. (1980) the formation of this nonadhesive polymeric form scale had reduce the dissolved silica concentration by allowing time for its conversion to colloidal silica.

Si:Mg molar ratio in the precipitate determine from ICP analysis and EDAX analysis agree very well with each other. FTIR spectra confirmed the presence of amorphous SiO_2 and amorphous Mg-Silicate scale under all test conditions.

4.5. SUMMARY AND CONCLUSIONS

We now summarize the novel contributions of the results in this chapter to the study of silicate scaling, as follows:

1. The experimental methodology for the silicate scaling static test is now established with all issues which arose due to (a) the colloidal nature of the silicate scale produced and (b) the repeatability and reproducibility of the test results,now being fully resolved.

2. A wide ranging sensitivity analysis of silicate scaling has been successfully conducted that shows clear results for all of the parameters tested. Our results show that the silicate system is most affected by the solution pH rather than the temperature. The initial Si:Mg molar ratio of the reacting brine will result in varied the Si:Mg molar ratios in the precipitate formed. Finally, the aged silicate brine led to ~80% less of magnesium ion reacted in the blank solution, which implying a lower amount of amorphous magnesium silicate scale reacted.

CHAPTER 5. SILICATE SCALE INHIBITION

INTRODUCTION

The kinetics of silicate scaling reactions are not completely understood since the process is very complex. It includes the formation of amorphous silica via silica polymerization, colloidal silica suspension, precipitation of metal silicates and co-precipitation of silica with mineral salts (e.g., calcium carbonate, calcium sulfate etc.). Researchers have reported on the efficiency of a number of conventional scale inhibitors in inhibiting silicate scaling but none of them fully solved the silicate scaling problem. Polymeric and non-polymeric (phosphonate) scale inhibitors that work by controlling the silicate formation either by crystal growth inhibition or crystal modification, have failed to inhibit silicate scale probably because it is amorphous in nature. A successful silicate scale inhibitor or dispersant must be able to prevent/disperse the silica-based deposit, especially if it is in the form of colloidal silica and magnesium silicate. In addition, it should also inhibit/disperse any other scale that can act as nuclei in silicate precipitation such as calcium carbonate and calcium sulfate.

Silicate scale is covalently bonded and amorphous in nature; hence conventional scale inhibitors (SI) cannot inhibit them through either a nucleation or crystal growth inhibition mechanism. However, if the silicate can be dispersed, it will prolong the time before silicate scale can be formed. Amjad and Zuhl (2009) noted that a good dispersant would be a polymer species with M.Wt. < 10,000 Da with carboxylic acid and sulfonic acid groups. A number of potential silicate scale inhibitors/dispersants have been tested in this work. Following evidence suggested by Amjad and Zuhl (2009), three different polymeric SI have been tested which are Vinyl Sulfonated Acrylic Acid Co-polymer (*Inhibitor 1- VS-Co*), Vinylamide / Vinylsulfonate Co-polymer (*Inhibitor 2 – H3*) and Terpolymer of acrylic acid, 2-acrylamido-2-methylpropane sulfonic acid, non-ionic monomer (*Inhibitor 3 – A5*).

In this chapter, we start by presenting the results and discussion on the initial studies of *Inhibition Efficiency* (IE) where experiments were performed using VS-Co and H3. A detailed analysis of inconsistency in the obtained IE results revealed a very basic problem in the silicate system. It is shown that the silicate system is extremely sensitive to the initial pH values of the mixed brine. This means a very stringent control in pH adjustment

is needed to get repeatable and reproducible results. Hence, a consistent procedure for brine mixing and the pH adjustment process must be maintained throughout any IE test. The inconsistencies in the results mentioned earlier has led us to perform silicate scale static tests with varying initial pH values of the mixed brine. Experimental results establish that a difference of 0.5 in pH can make a significant difference in the final IE results.

The generated data from this initial work will be used as a basis to further develop a simple and reproducible method for performing the silicate IE tests to allow a rapid screening of the potential scale inhibitor. In the corresponding static IE tests, experiments were performed to evaluate the SI performance in silicate systems at various (Si and Mg) concentration levels, since it will be shown later in this chapter that the silicate scale is very difficult to inhibit. As such, this chapter is written in a way that potential inhibitors are tested in a silicate system from "*worst"* case to "*manageable"* base cases. We show later that VS-Co and the H3 polymer failed to inhibit silicate scale even in the so-called *"manageable"* base case.

5.1. SCALE INHIBITOR TESTED

Several *polymeric* type inhibitors have been tested in this IE test which are Inhibitor 1 (VS-Co), Inhibitor 2 (H3) and Inhibitor 3 (A5).

Inhibition efficiency is calculated using a modification of the static method used for barium sulphate. However, since we are producing Mg-silicate scales, we carry out the measurements and calculations for both the Mg and the Si, as explained below. The *inhibition efficiency* of any scale inhibitors (SI) to inhibit the silicate scaling was calculated using Equation 5-1 (Shaw, 2012);

$$\%Efficiency(t) = \frac{(M_B - M_I)x100}{M_B} = \frac{(C_O - C_B) - (C_O - C_I)x100}{(C_O - C_B)} = \frac{(C_I - C_B)x100}{(C_O - C_B)}$$

Equation 5-1

Where;

M_B = Mass of silicon (or other cations) precipitated in supersaturated blank

M_I = Mass of silicon (or other cations) precipitated in test solution.

C_O = Concentration of silicon (or other cations) originally in solution (i.e. t=0).

C_I = Concentration of silicon (or other cations) at sampling.

C_B = Concentration of silicon (or other cations) in the blank solution (no inhibitor) at the same conditions and sampling time as C_I above.

(t) = Sampling time.

The IE_{Mg} % is the inhibition efficiency percentage calculated using magnesium (Mg) as the scaling ion; i.e. the percentage of magnesium ion that can be prevented from precipitating in the inhibitor-containing brine as compared to the amount of magnesium ion precipitated in the blank solution (uninhibited). The IE_{Mg} % value here is interpreted as the inhibition efficiency percentage of the tested inhibitor towards amorphous magnesium silicate scale formation.

The IE_{Si} % is the inhibition efficiency percentage calculated using silicon (Si) as the scaling ion; i.e. the percentage of silicon ion that can be prevented from precipitating in the inhibitor-containing brine as compared to the amount of silicon ion precipitated in the blank solution. The IE_{Si} % value here is interpreted as the inhibition efficiency percentage of the tested inhibitor towards amorphous silica scale formation.

Several inhibitors were tested in various silicate scaling systems i.e. different Mg and Si levels to study their inhibition efficiencies towards silicate scales using the established methodology.

5.1.1 Vinyl Sulfonated Acrylic Acid Co-polymer (VS-Co)

Following work reported by Amjad and Zuhl (2009) which conclude polymers that exhibit good dispersion properties are typically low molecular weight (M.Wt. < 10,000 Da) species and contain both carboxylic acid and sulfonic acid groups. Thus, following this suggestion, Vinyl sulfonated acrylic acid co-polymer, also known as VS-Co scale inhibitor was used which contains both carboxylate and sulfonate functional groups was chosen in the first silicate inhibition efficiency tests carried out in this work. This experiment was conducted to study the efficiency of a type II polymer; VS-Co to inhibit silicate scale formation at 60^{o}C and pH8.5.

VS-Co is a commercial liquid product from Company A with low molecular weight of <4000g/mol and 30% activity. The main functional groups are carboxylate and sulfonate as shown in Figure 5-1.

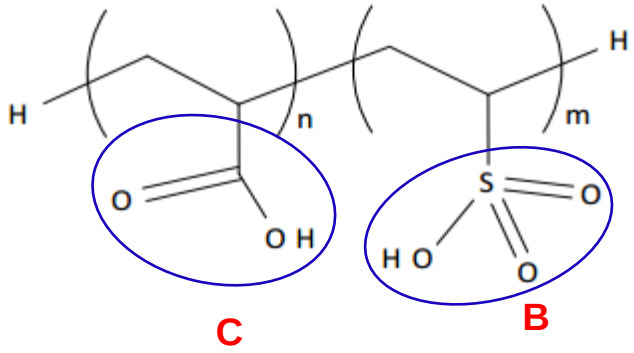

Note: B – Sulfonate C – Carboxylate

Figure 5-1 Functional groups available in VS-Co polymer

5.1.2 Vinylamide / Vinylsulfonate Co-polymer (H3)

H3 is a higher molecular weight terpolymer based on ATBS and vinylamide. H3 is a commercialized scale inhibitor supplied by Company B that contains the main functional groups of both amide and sulfonate – heteropolymeric. It came in powder form with activity of 100%. The main funtional groups can be seen in Figure 5-2.

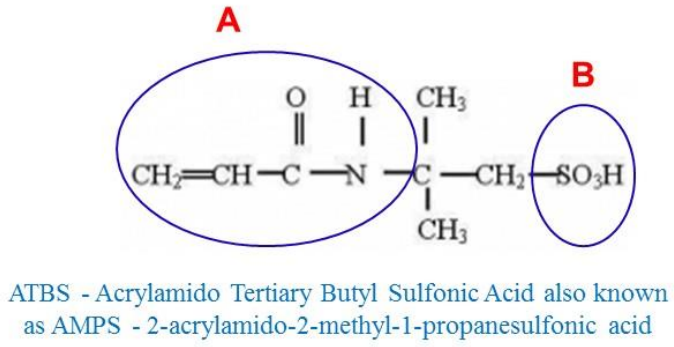

Note: A – Acrylamide B – Sulfonate

Figure 5-2 Functional groups available in H3 polymer

5.1.3 Terpolymer of acrylic acid, 2-acrylamido-2-methylpropane sulfonic acid, non-ionic monomer (A5)

A5 is a low molecular weight and water-soluble polymer that contains 2-acrylamido-2-methylpropane sulfonic acid (AMPS/ ATBS), acrylic, maleic and another non-ionic monomer but not the allyl oxybenzene sulfonate monomer. This polymer is a commercial product from Company C which was supplied as a clear to hazy mild odour liquid with activity of 42%. Some of the functional groups available in A5 are shown in Figure 5-3.

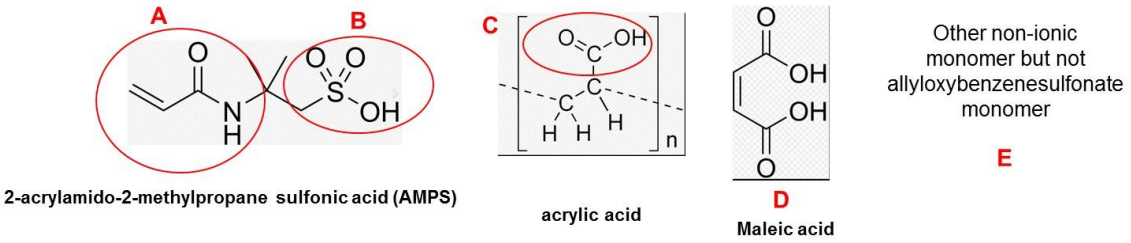

Note: A – Acrylamide B – Sulfonate C – Carboxylate D – Maleic Acid E – another non-ionic monomer

Figure 5-3 Functional groups available in A5 polymer

5.2. METHODOLOGY DEVELOPMENT OF SILICATE SCALE INHIBITION EFFICIENCIES STUDIES

5.2.1 Initial Study of Silicate Scale Inhibition Efficiency (60Mg:940Si, pH8.5 and 60ºC) – Experimental Details

The mixture of brine concentration (60Mg: 940Si) at test conditions of 60ºC and pH8.5 was chosen as the base case to study the efficiency of various scale inhibitors, in this initial experiment starting with the VS-Co and H3 as shown in Table 5-1.

Table 5-1 Scale inhibitor details

Scale Inhibitor name	Supplier	Activity %
VS-Co	Company A	30 (Thick liquid)
H3	Company B	100 (Fine solid powder)

10,000ppm active SI stock (of the VS-Co) was prepared before being further diluted in 250ml silicon brine to obtain various active SI concentrations (i.e. 20ppm, 50ppm and 100ppm) in the final mix brine of 50:50 ratios of 1880ppm silicon brine and 120ppm

magnesium brine. The diluted SI samples were prepared in 250ml of silicon brine to enables the same solution to be used in 4 bottles (4 x 50ml) i.e. a test and duplicate bottle at each sampling times i.e. 2 hr and 22 hr, for each test SI concentration.

It must be noted here that for a set of inhibitor concentration in these initial studies were conducted in eight different glass bottles to allow a duplicate of ICP measurement of *blank* and *samples* at 2 and 22 hours respectively (this is due to the fact that the samples were ICP sampling as per $BaSO_4$ inhibition efficiency test after samples were centrifuged). This mean, the pH of all four test samples were pH-adjusted differently that not only caused a lengthy and tedious procedure but also may lead to inconsistencies of the way final pH values were achieved in every samples.

The test samples were then ICP analysed at 2 and 22hr and precipitates were collected to analyse the morphology and chemical compositions of any precipitates which formed using EDAX analysis. EDAX analysis shows the proportion and molar (or weight) ratios of the constituent elements and was used in determining the stoichiometry of silicon to magnesium in the silicate precipitate. The precipitates were also analysed using FTIR to compare the spectra produced which reflect the chemical moieties present.

Another experiment was designed to study the efficiency of Vinylamide / vinylsulfonate polymer; H3 to inhibit silicate scale formation at 60^{o}C and pH8.5. The same methodology as per VS-Co was applied in this test using 5,000ppm active SI stock (of the H3).

It is worth mentioning here that all results reported in this chapter are the average of duplicate values where the percent difference between duplicates are shown for relevant experimental results in section 5.2.2 to 5.2.6.

5.2.2 First Results of Initial Inhibition Efficiencies Studies of 60Mg:940Si, pH8.5 and 60^{o}C

(a) VS-Co IE Tests

In this section, a detail discussion on the first results of VS-Co performance is presented from the results obtained in four repeated test i.e. *original* test, *repeat 1* test, *repeat 2* test and *repeat 3* test. In the *original* test, VS-Co showed some promising results in inhibiting silicate scale at least over a 2-hour period. Hence, the VS-Co IE Test was repeated to

verify the results obtained previously. However, there were inconsistencies between the results obtained for the repeated VS-Co IE Tests as shown in Figure 5-4 (IE $_{Si}$ %) and Figure 5-5 (IE $_{Mg}$ %).

It is worth noting that a set of inhibitor concentrations in these initial studies were conducted in eight different glass bottles to allow a duplicate of each ICP measurement of the *blank* (i.e. uninhibited brine) and *samples* (i.e. SI-containing brine) at 2 and 22 hours, respectively. This is due to the fact that the samples were ICP sampled as per $BaSO_4$ inhibition efficiency tests after samples were *centrifuged*. Hence, a duplicate *blank* at 2 hours will be different from a duplicate *blank* at 22 hours causing the IE results to be non repeatable and therefore inconsistent. Indeed, all four repeats using VS-Co produced quite different results.

VS-Co performance in stopping amorphous silica scale (IE $_{Si}$ %)

Figure 5-4 shows the inhibition efficiency at 2 and 22 hour calculated using the **silicon** ion as C_o in our IE % calculation where the IE $_{Si}$ % value here denotes the inhibition efficiency percentage of the tested inhibitor towards amorphous silica scale formation. In the *original* test shown in Figure 5-4a, VS-Co was found to be effective at 2 hour with more than 90% IE (i.e. IE $_{Si}$ % at 2hour > 90%) being achieved at the lowest scale inhibitor concentration tested, i.e. 20ppm. However, VS-Co demonstrates a poor IE % at 22 hours with only 1% even at the highest concentration tested, i.e. 100ppm (i.e. IE $_{Si}$ % at 22hour ~1%).

Repeat 1 test (Figure 5-4b) shows that the addition of 20ppm and 50ppm VS-Co resulted in no observed amorphous silica scale inhibition either at 2 hour or 22 hour i.e. IE $_{Si}$ % at 2 & 22hour ~0%. However, the same figure also shows that the addition of 100ppm VS-Co resulted in ~50% efficiency in stopping amorphous silica scale at 2 hour but showed little inhibition at 22 hour. Detailed examination of the ICP analysis by plotting the amount of ion reacted in the *blank* and test samples at 2 hour revealed that the IE $_{Si}$ % at 2 hour was found to be *zero* for 20ppm and 50ppm VS-Co as the amount of silicon ions reacted in the *blank* were much lower than the amount calculated for both VS-Co concentrations (see Figure 5-6b).

Results from the *Repeat 2* test shown in Figure 5-4c is the worst when the addition of up to 100ppm VS-Co totally fails to stop the formation of amorphous silica for either 2 or 22 hour tests; IE $_{Si}$ % at 2 & 22hour ~0%. As observed in Figure 5-6c, we found that VS-Co did not work to stop the silicate scale (i.e. both amorphous silica scale or amorphous magnesium silicate scale) formation at 2 hour because the VS-Co-containing brine produces more scale than in the *blank* samples.

In the *Repeat 3* test, VS-Co seems to work at least for the first 2 hours (refer to Figure 5-4d). There is no definite pattern observed in *Repeat 3* test in which the addition of 100ppm VS-Co can only inhibit ~50% of amorphous silica scale formation. By referring to the same figure, we found that the addition of 20ppm VS-Co can stop ~40% of amorphous silica scales. However, the addition of 50ppm VS-Co can only inhibit <20% of the scales.

It is quite clear from these results that the IE $_{Si}$ % test results are not reproducible whereby the VS-Co seems work in the *original* and *Repeat 3* test when the VS-Co-containing brine produce less scale than in the *blank* as presented in Figure 5-6a and Figure 5-6d. IE $_{Si}$ % is summarized in Table 5-2.

Table 5-2 IE $_{si}$ % (VS-Co performance in stopping amorphous silica scale)

Residence Time	IE $_{Si}$ % (VS-Co performance in stopping amorphous silica scale)			
	Original Test	*Repeat 1 Test*	*Repeat 2 Test*	*Repeat 3 Test*
2 hour	~90	0-45	0	17-47
22 hour	~1	0-4	0	0-1

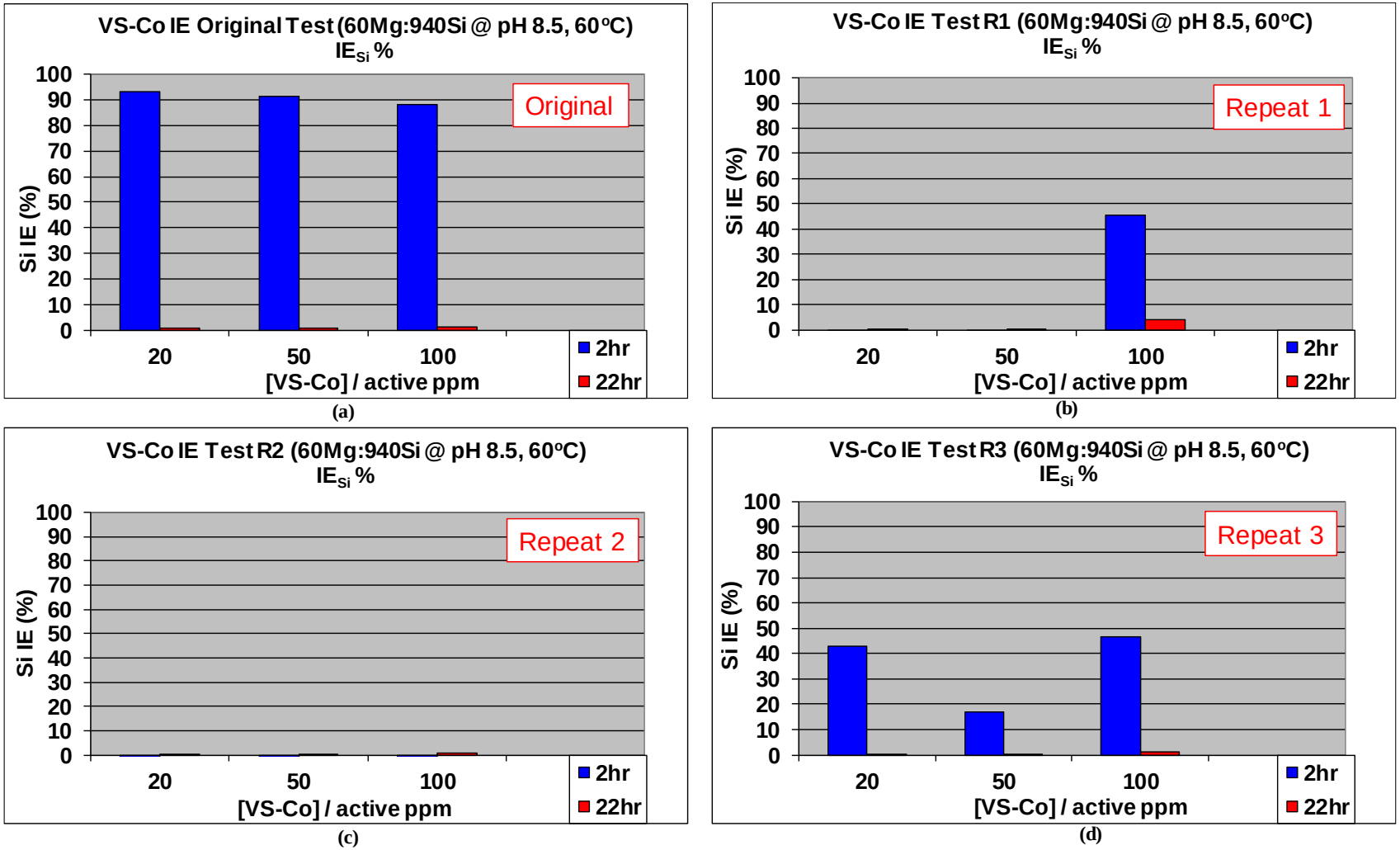

Figure 5-4 Inhibition efficiency (%) of VS-Co IE calculated using Si ion as C_o

VS-Co performance in stopping amorphous magnesium silicate scale (IE $_{Mg}$ %)

The corresponding IE results now using magnesium (Mg) as the primary scaling ion in our IE % calculation are shown in Figure 5-5 where the IE $_{Mg}$ % value here denotes the inhibition efficiency percentage of the tested inhibitor towards amorphous magnesium silicate scale formation.

The IE % determined using the magnesium ion as C_o shows a slightly different pattern in the *original* test (Figure 5-5a) with the IE at 2 hour being slightly lower than IE $_{Si}$ % (i.e. IE $_{Mg}$ % ~85% at 2 hr) for all concentration tested. The ability of VS-Co to stop amorphous magnesium silicate scale formation shows some variation in IE results at 22 hours with some improved level of IE up to 40% (as compared to IE $_{Si}$ % at 22 hour ~ 1%) but not in any definite pattern.

Figure 5-5b shows that the addition of 20ppm and 50ppm VS-Co in *Repeat 1* test resulted in no observed amorphous magnesium silicate scale inhibition at 2 hour i.e. IE $_{Mg}$ % at 2 hour ~0%). This is due to less ions reacting in the blank (see Figure 5-6b) as will be discussed in detail later in this section. However, by examining the figure closely we found that the IE $_{Mg}$ % showed little inhibition of 2 to 14% at 22 hours in the 20 and 50ppm VS-Co-containing brines. The same figure also shows that the addition of 100ppm VS-Co resulted in ~50% efficiency in stopping amorphous magnesium silicate scale at 2 hour but little inhibition of <10% at 22 hours (i.e. IE $_{Mg}$ % at 2 hour ~ 50% and IE $_{Mg}$ % at 22hour <10%).

The ability of VS-Co to stop or reduce amorphous magnesium silicate scale in *Repeat 2* test is not consistent as the inhibition percentage is *zero* at 2 hours (Figure 5-5c). However, an increase in the % inhibition is observed at 22 hour with increasing [VS-Co]. As observed in Figure 5-6c, we found that VS-Co did not work to stop the silicate scale formation at 2 hour because the VS-Co-containing brine produces <u>more</u> scale than in the *blank* samples.

IE $_{Mg}$ % results in Figure 5-5d again shows no definite pattern in the ability of VS-Co to stop amorphous magnesium silicate scale formation in *Repeat 3* test, where the addition of 20ppm VS-Co was able to achieve and IE ~ 40% at 22 hour. The addition of 50ppm VS-Co only gives an IE ~20% of the same scale but the addition of 100ppm VS-Co can only achieve IE ~ 40% at 2 hour. The addition of 20ppm and 50ppm VS-Co resulted in

~6% efficiency at 22 hour but no inhibition was observed in the 100ppm VS-Co-containing brine. IE $_{Mg}$ % results are summarized in Table 5-3.

Table 5-3 IE $_{Mg}$ % (VS-Co performance in stopping amorphous magnesium silicate scale)

Residence Time	IE $_{Mg}$ % (VS-Co performance in stopping amorphous magnesium silicate scale)			
	Original Test	*Repeat 1 Test*	*Repeat 2 Test*	*Repeat 3 Test*
2 hour	~85	0-50	0	20-42
22 hour	2-42	1-14	6-20	0-8

Results revealed that the amount of ions reacted in the blank were not in agreement with the results reported in section 3.4.2. It was reported in that section that 48.6% - 58.5% of magnesium ion and 81.9% - 86.2% of silicon ion was reacted after 2 hours. It is observed that the amount of magnesium ion reacted in the *blank* sample of this first IE tests varied between 29% - 47% whereas the amount of silicon ion reacted varied between 44% - 87% (Refer Figure 5-6). Duplicate samples also produced large discrepancies (i.e. percent difference that will be explained later) that meant a detailed analysis of all IE test results for VS-Co and H3 was necessary, and this was carried out and is reported in the following section.

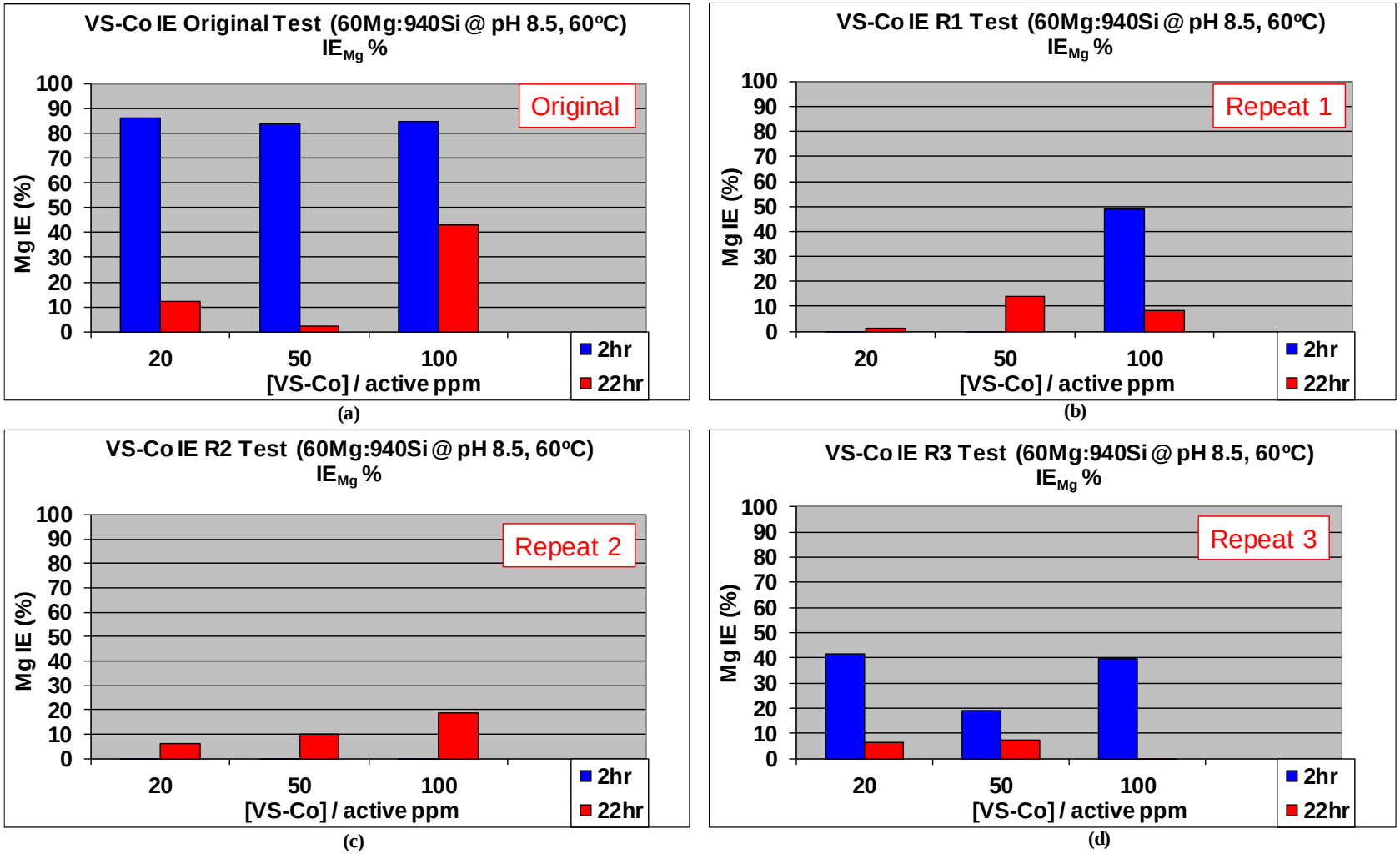

Figure 5-5 Inhibition efficiency (%) of VS-Co IE calculated using Mg ion as C_o

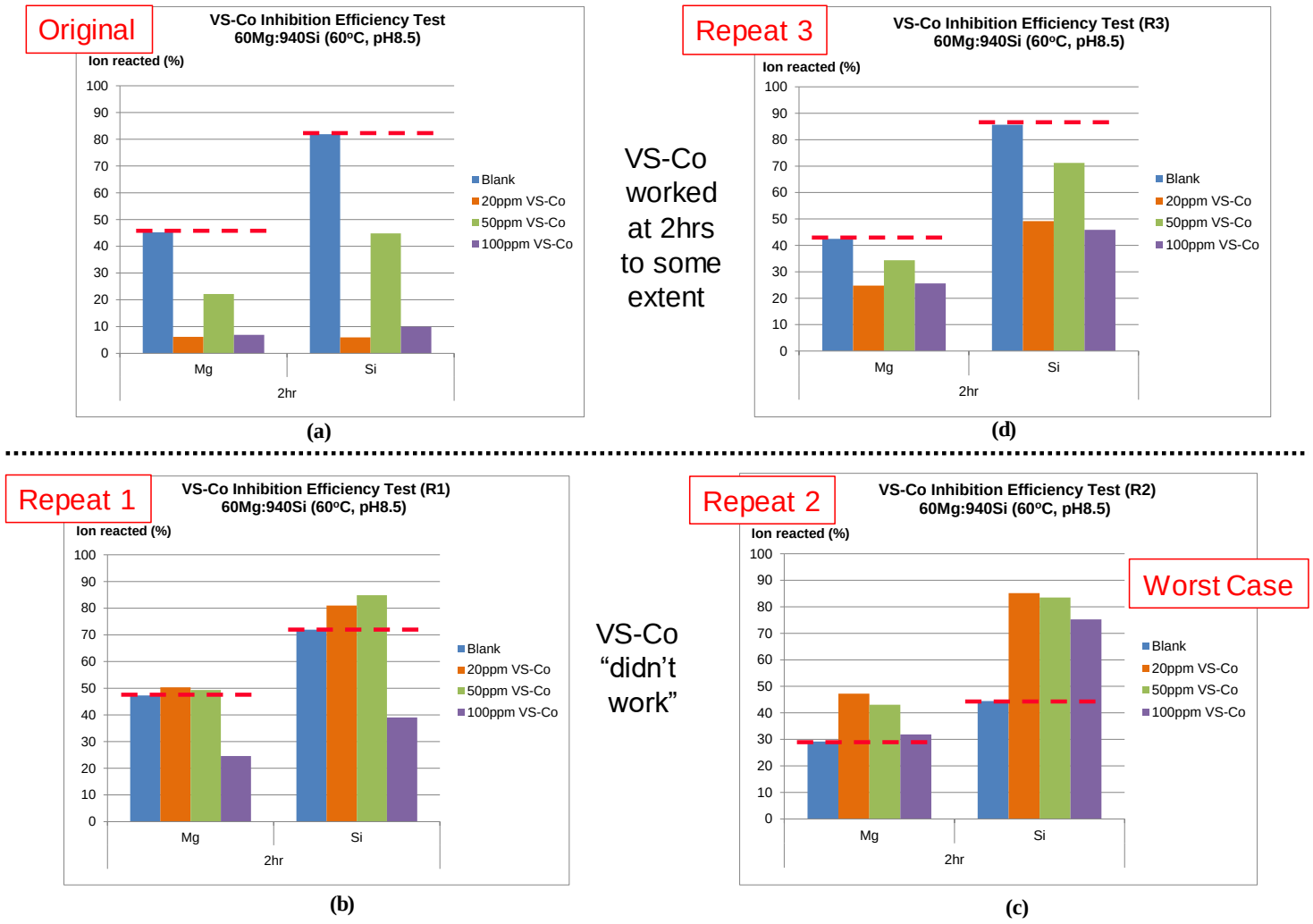

Figure 5-6 Percentage amount of ion reacted in blank & samples of all VS-Co IE Tests

Detailed analysis on blank and samples of initial VS-Co IE Tests

Generally, results obtained from the four IE repeat experiments were inconsistent and no obvious trend could be observed with respect to the silicon or magnesium ion results. As mentioned earlier, a set of inhibitor concentrations in this initial study were conducted in eight different bottles to allow a duplicate of ICP measurement of *blank* and *samples* at 2 and 22 hours respectively (this is due to the fact that the samples were ICP sampled as per $BaSO_4$ inhibition efficiency test after samples were centrifuged). For example, for tested concentration of 20ppm VS-Co containing brine; there was a duplicate (2 bottles) of blank and a duplicate of 20ppm VS-Co-containing brine for 2 hour ICP sampling; a duplicate (2 bottles) of blank and a duplicate of 20ppm VS-Co containing brine for 22 hour ICP sampling; making the total of 8 bottles for the concentration tested.

Results of the experiments must be described in terms of the accuracy and precision of the experimental measurements. Percent error (sometimes referred to as fractional difference) measures the accuracy of a measurement by the difference between a measured or experimental value *E* and a true or accepted value *A* as shown in Equation 5-2. However, the true values for these experiments are not known:

$$\text{Percent Error} = \frac{|E-A|}{A}$$

Equation 5-2

Hence, the percent difference (discrepancy) as shown in Equation 5-3 is calculated in this thesis. Percent difference measures precision of two measurements (duplicate) by the difference between the measured or experimental values minimum value, E_1 and maximum value, E_2 expressed as a fraction the average of the two values. The equation to use to calculate the percent difference is:

$$\text{Percent Difference} = \frac{|E_1-E_2|}{\left(\frac{E_1+E_2}{2}\right)}$$

Equation 5-3

Overall, the discrepancies calculated between duplicates over 2-hour sampling are up to 166.4% and 146.2% for the amounts of silicon and magnesium ion reacted in the scaling reactions, respectively. 22 hour ICP data were moderately affected, as the discrepancies calculated between duplicates were up to ~3.4% and 49.34% for silicon and magnesium ion reacted, respectively.

Original Test

The highest discrepancy calculated between duplicate in the *original* test found to be up to 166.4% and 133.8% in the 50ppm VS-Co containing brine for both Si and Mg ion reacted in the 2 hour scaling reaction.

The discrepancies calculated for duplicates in 22 hour scaling reaction found to be less than 7% for both amount of Si and Mg ion reacted except for duplicate of 100ppm VS-Co containing brine where the discrepancy in the amount of magnesium reacted was found to be ~49.3% (Refer Figure 5-11a).

Repeat 1 Test

The discrepancy between duplicates in the *blank* samples at 2 hour in *Repeat 1 Test*, as shown in Figure 5-11b was found to be 39.2% and 28.7% for magnesium and silicon ion, respectively, even although the pH values were adjusted close to the nominal pH initial value; these pH levels were pH 8.50 and pH 8.35 (nominal pH value is 8.50). Significant differences in the extent of reaction between both duplicates of blank samples can be seen clearly in the photograph shown in Figure 5-7. 22 hour ICP data in the blank solution were not affected as much as the discrepancies calculated were only ~1.3% and ~0.3% for magnesium and silicon ion reacted, respectively.

Other duplicates VS-Co containing brine produced discrepancy within the experimental error (~0.02% to ~7.5% for 2 hour and 22 hour reaction) except for 50ppm VS-Co with magnesium discrepancy is ~12.6% in 2 hour reaction; and for 100ppm VS-Co in which the discrepancies were ~79.3% and ~89.8% for magnesium and silicon ion reacted in 2 hour, respectively.

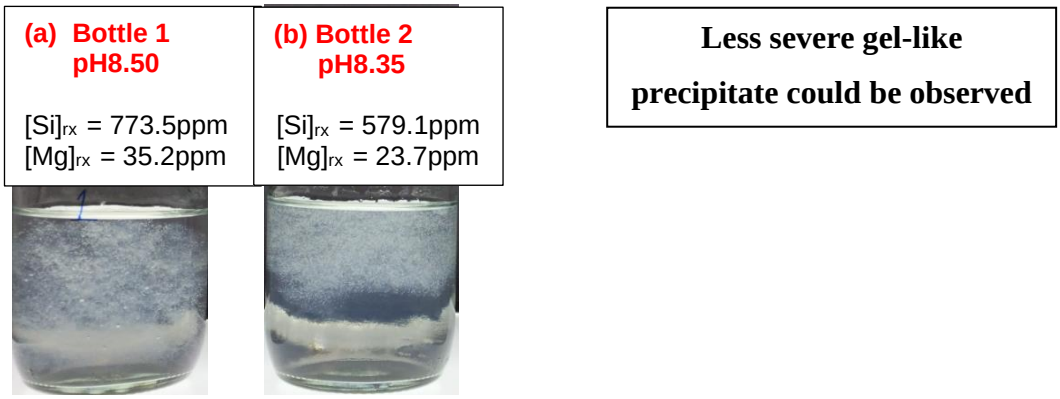

Figure 5-7 A duplicate of blank 60Mg:940Si at 2 hour in VS-Co IE Test *Repeat 1*

Repeat 2 Test

The discrepancies between duplicates in the *blank* at 2 hours in *Repeat 2 Test*, as shown in Figure 5-11c, were found to be 108.5% and 139.4% for magnesium and silicon ion, respectively, even although the pH values were adjusted close to the test pH. These pH values were pH 8.53 and pH 8.35. This was expected as the visual observation of both *blank* duplicates look completely different, as can be seen in Figure 5-8. Other duplicates were consistent enough within the experimental error (<10% error except for 100ppm VS-Co containing brine which produces discrepancies as much as 18.1% in silicon ion reacted in 2 hour and 21.2% in magnesium ion reacted in 22 hour) and it is worth noting that the initial pH of other samples was adjusted within the range pH 8.40 to pH 8.50.

It can be also clearly seen that ions reacted in the *blank* samples for this test were completely different from results obtained in VS-Co IE Test *(Repeat 1)* – refer to Figure 5-7. It is obvious that there is inconsistency in the *blank* samples even although the pH values were adjusted to values close to the initial test pH value. In fact, the same initial pH value (Duplicate in VS-Co IE Test *Repeat 1* and *Repeat 2* have same initial pH value i.e. 8.35) also resulted in significantly different extents of reaction.

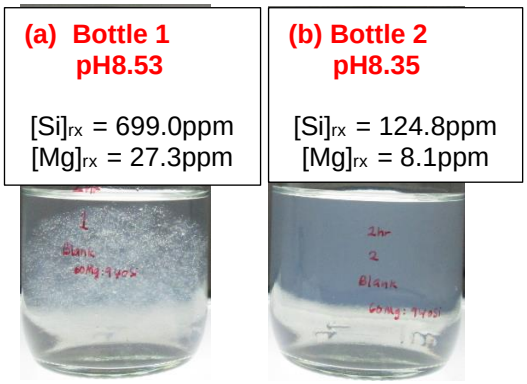

Figure 5-8 A duplicate of blank 60Mg:940Si at 2 hour in VS-Co IE Test *Repeat 2*

Repeat 3 Test

Further analysis of the ICP data revealed that the discrepancies between duplicates at 2 hours in *Repeat 3 Test* are too high for all VS-Co concentrations; ~16.3% to ~146.5% and ~28.4% to 153.4% for Mg and Si ions, respectively. These results are plotted in Figure 5-11d. For 20ppm VS-Co test for example, the discrepancy is up to 130.2% and 152.5% for Mg and Si ion respectively. This result was not expected since both duplicates were closely adjusted to the test pH values, which were pH 8.37 and pH 8.41, respectively. Physical observations of these samples are shown in Figure 5-9. The discrepancy for 100ppm VS-Co test is up to 146.5% and 153.4% for Mg and Si ion respectively where photographs of 100ppm VS-Co samples are also shown in Figure 5-10.

However, the discrepancies for *blank* at 2 and 22 hour and other VS-Co containing brines at 22 hours were not affected much that is within experimental error; i.e. ~0.005% to ~7.4% except for 20ppm VS-Co at 22 hour with percent difference in magnesium ion reacted of up to ~12.4%.

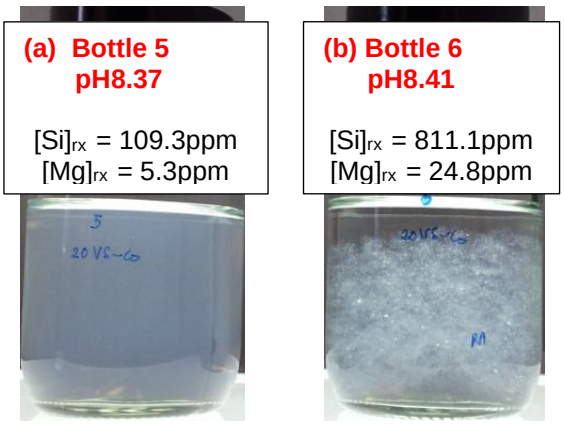

Bottle 5 became slightly cloudy after 2 hours of reaction while gel-like precipitate formed in Bottle 6

Figure 5-9 A duplicate of 20ppm VS-Co + 60Mg:940Si at 2 hour in VS-Co IE Test *Repeat 3*

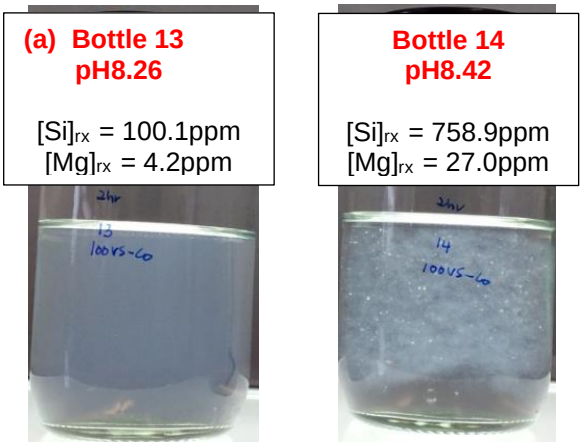

Bottle 13 became slightly cloudy after 2 hours of reaction while gel-like precipitate formed in Bottle 14

Figure 5-10 A duplicate of 100ppm VS-Co + 60Mg:940Si at 2 hour in VS-Co IE Test *Repeat 3*

This is evidence that the silicate system is very sensitive to a slight change in initial pH value. In addition, the process involved in brine mixing (the way the Mg brine is added into the SB brine) and the pH adjustment (including time needed to adjust the pH) are all believed to affect the extent of reaction of the silicate scaling system.

Because of the above inconsistencies, we cannot conclude that the VS-Co is successfully inhibiting the silicate scale. However, all of the above observation and findings are very important in our effort to develop the static IE test so that reliable silicate inhibition measurements can be carried out.

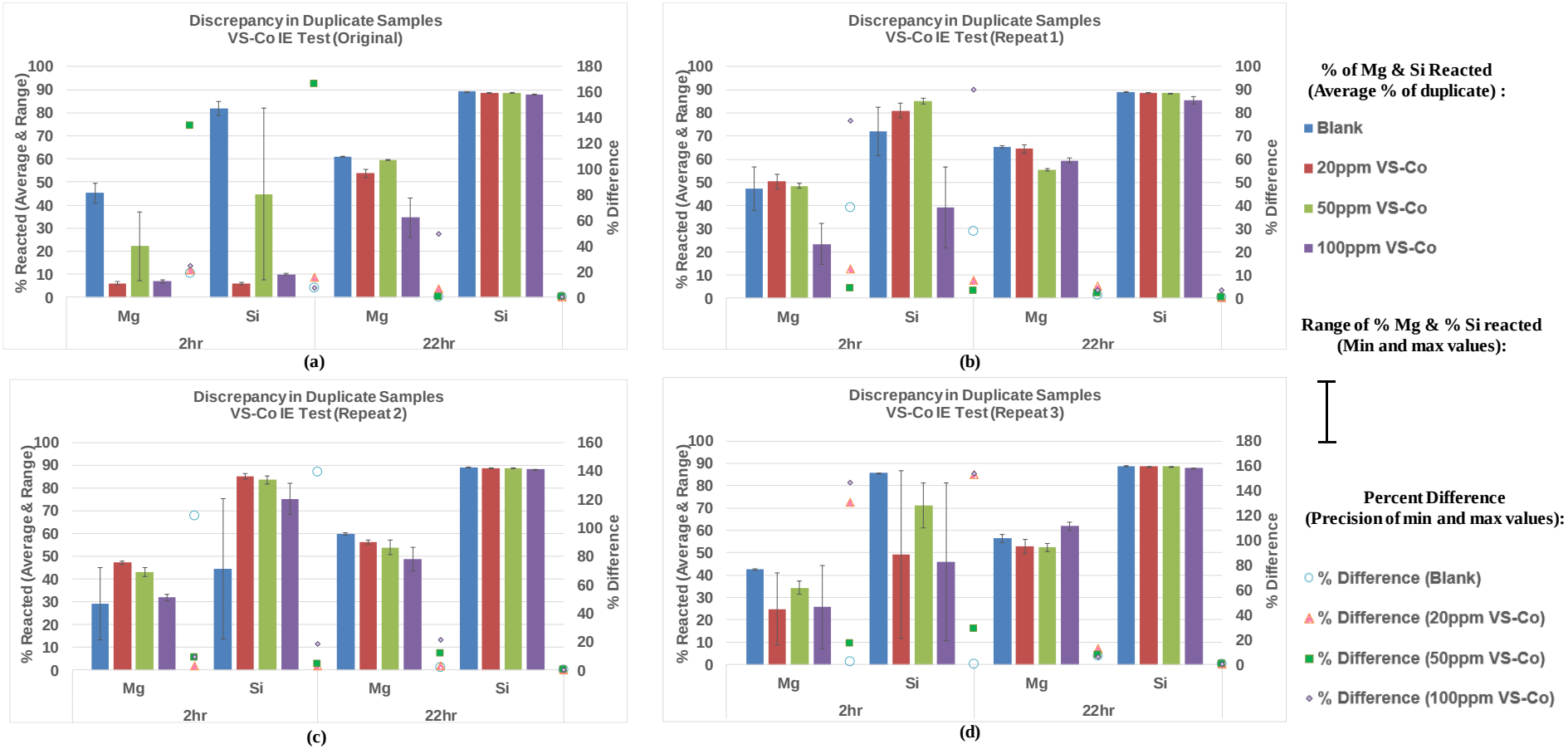

Figure 5-11 Discrepancy in duplicate samples of blank and inhibited test samples

(b) H3 IE Tests

H3 performance

Following a failure to obtain a reproducible result in the VS-Co IE Tests, no conclusions could be made on VS-Co efficiency towards silicate scale inhibition. The same inhibition efficiency tests were continued to study the potential of polymeric scale inhibitor H3 to inhibit silicate scale. The inhibition efficiency of the H3 IE Test at 2 and 22 hour calculated for the **silicon** ion (IE_{Si} %) as shown in Figure 5-12. From the analysed ICP data, IE % at 2 hours were found to be *zero* for all tested H3 concentrations as the amount of silicon ions reacted in the blank are much less than the amount calculated for H3-contained mixed brine. The IE % at 22 hour only has slight inhibition of <1% for all H3 concentrations tested.

The corresponding IE results using magnesium as the primary scaling ion in our IE % calculation (IE_{Mg} %) are shown in Figure 5-13. These results revealed that the IE % at 2 hours were *zero* when only 20ppm H3 was present in the blank; while the IE % were increased to ~12% and ~35% when 50ppm H3 and 100ppm H3 were added respectively. IE_{Mg} % at 22 hour also found increased with the increasing amount of H3 added from 7-47%.

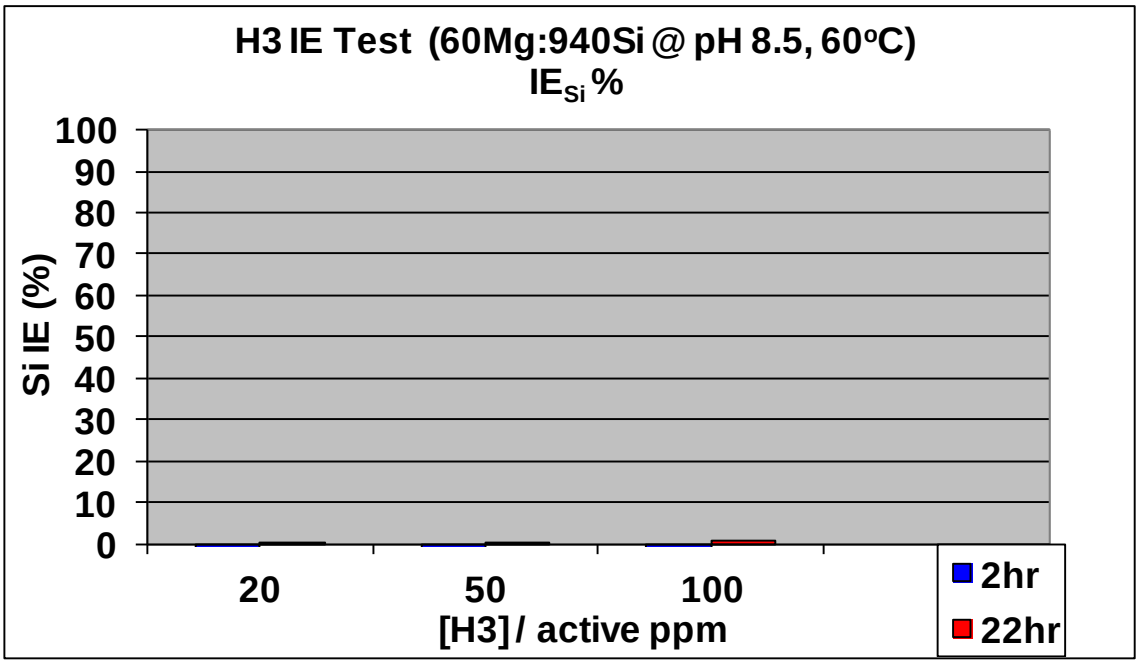

Figure 5-12 Inhibition efficiency (%) of H3 IE Test calculated using Si ion as C_o

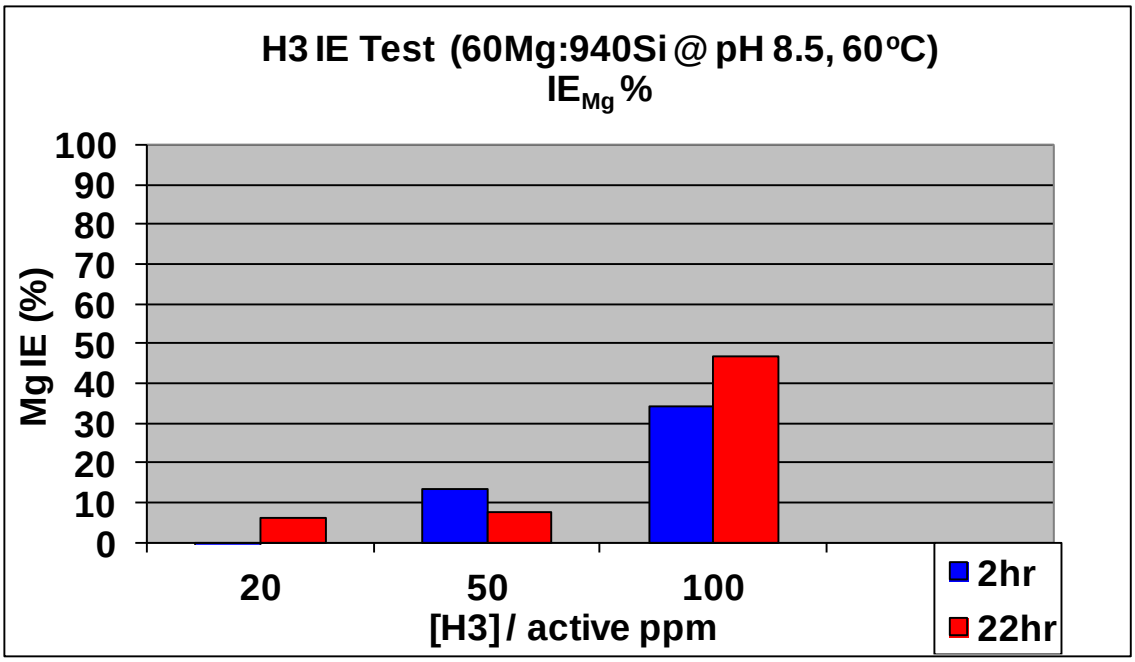

Figure 5-13 Inhibition efficiency (%) of H3 IE Test calculated using Mg ion as C_o

Detailed analysis on blank and samples of initial H3 IE Test

Further analysis showed that the discrepancy between duplicates in the *blank* samples at 2 hours was also found to be as high as 40% and 59.7% for magnesium and silicon ions, respectively (as shown in Figure 5-14). This is so even although the pH value of the blank duplicates were adjusted to be exactly the same value of pH (i.e. pH 8.42) while other duplicates of H3-contained mixed brine were consistent enough within the experimental error.

As can be seen in Figure 5-15, it is clear that blank sample in bottle 2 experienced more severe scaling reaction compared to that observed in bottle 1. Both duplicates were adjusted to pH 8.42; however, these initial conditions resulted in different amounts of magnesium and silicon ion reacted. The only difference between both duplicates was the time taken to adjust the pH where bottle 1 took ~10 minutes while bottle 2 took only ~6 minutes to stabilize to target pH. These findings suggest that all variants of the experimental method must be taken into account. Hence, a consistent procedure for brine mixing and pH adjustment must be developed as this appears to be important in the silicate system.

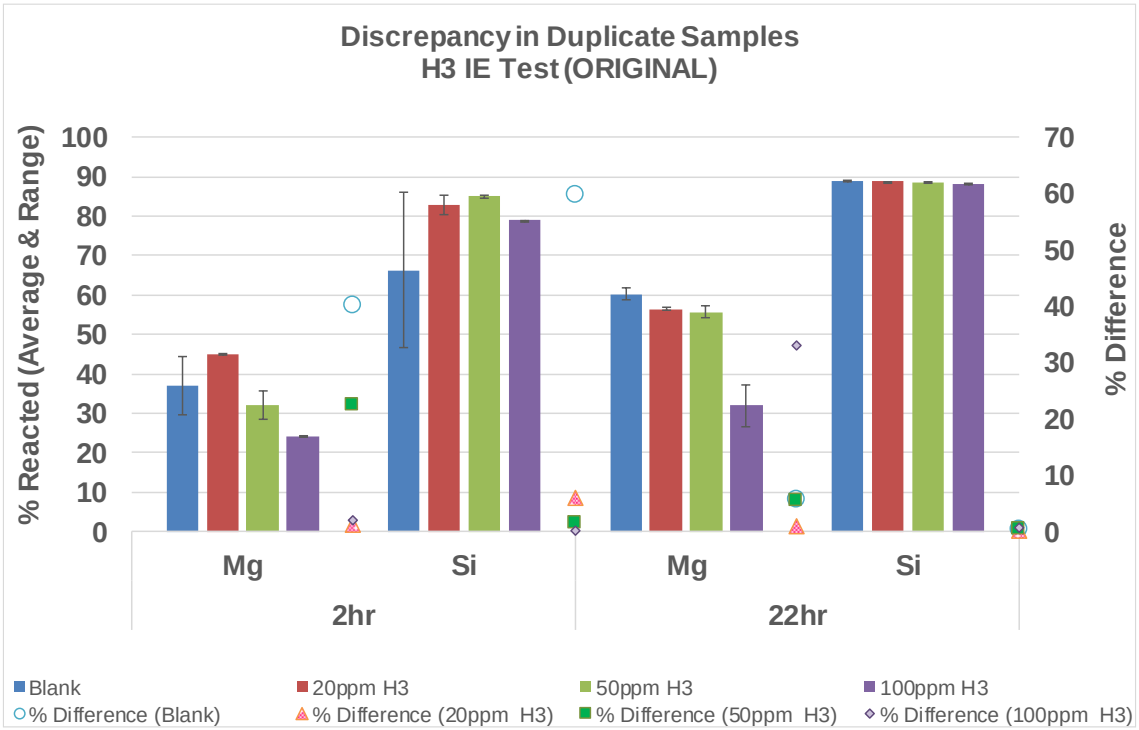

Figure 5-14 Discrepancy in duplicate samples of H3 IE Test

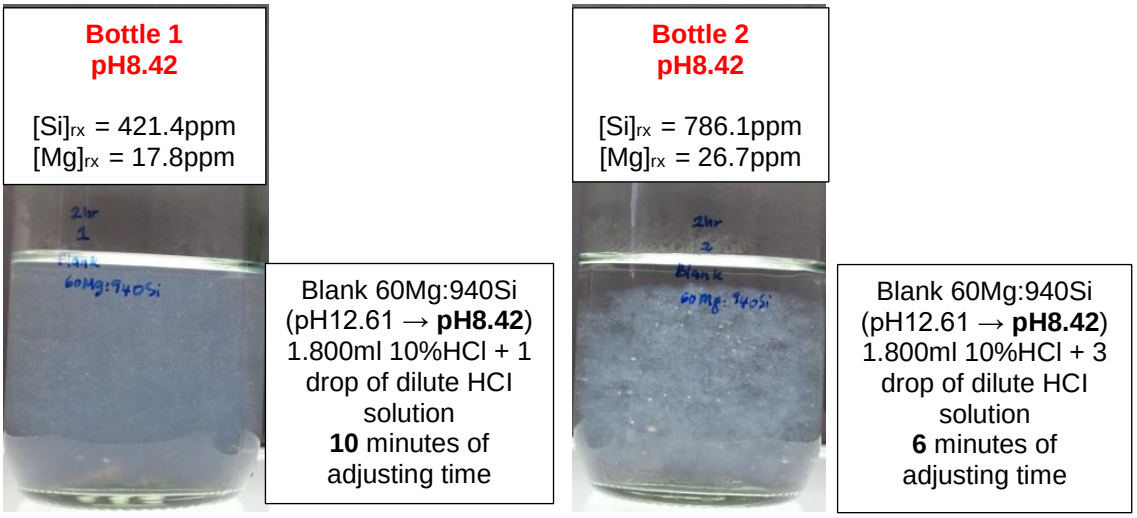

Figure 5-15 Blank 60Mg:940Si at 2 hour (H3 IE Test)

Other duplicates were not affected as much as the percent difference <6% except for 50ppm H3 with 22.3% in Mg ion reacted at 2 hour; and for 100ppm H3 with 33.1% Mg ion reacted at 22 hour. The results discussed above led us to further examine the initial pH of the *blank* in all VS-Co IE Tests and H3 IE Tests to support our earlier conjectures on the possible sources of discrepancies or experimental sensitivities in the following section.

5.2.3 Further Analysis of Initial pH of the Mixed Brine (Blank) in Initial Inhibition Efficiencies Studies i.e. Initial VS-Co & H3 IE Tests

Detailed analysis of ICP data was carried out in all IE tests. The evidence appears to show that the silicate system is extremely sensitive towards slight changes in initial pH value. Figure 5-16 and Figure 5-17 tabulates various initial blank pH values for the 60Mg:940Si case in various tests and its associated amount of ions reacted. Physical changes can also be observed in the photographs which were taken.

Test	VS-Co IE Test Original		VS-Co Repeat 1		VS-Co Repeat 2	VS-Co Repeat 3	H3 IE Test	
pH	8.48	8.40	8.50	**8.35**	8.53	8.41	**8.42**	**8.42**
$[Mg]_{rx}$ ppm	29.9	24.7	35.2	23.7	27.3	26.0	17.8	26.7
$[Si]_{rx}$ ppm	802.8	746.2	773.5	**579.1**	699.0	802.7	**421.4**	**786.1**
	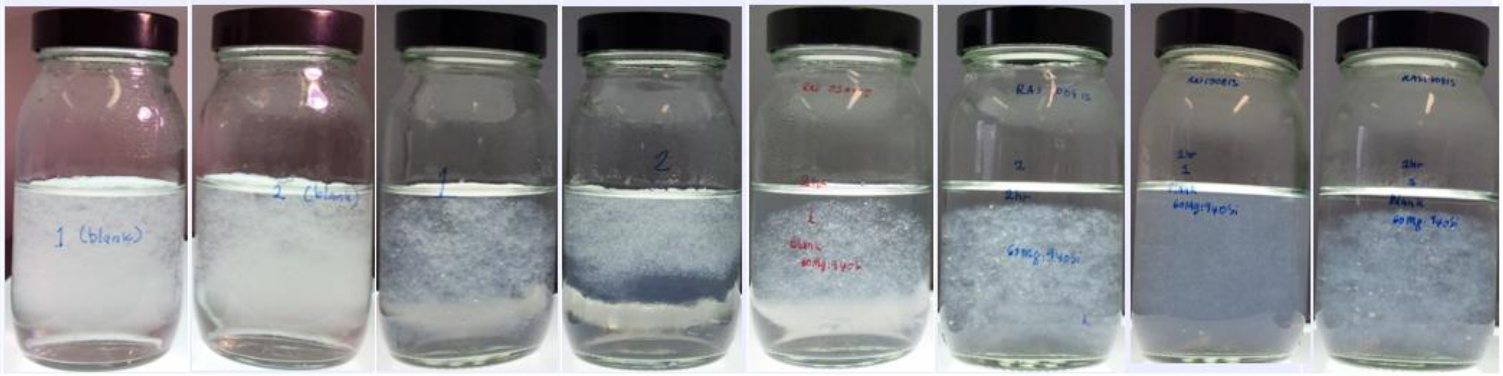							

Figure 5-16 Observation of blank 60Mg:940Si @pH8.5, 60ºC at 2 hour – Gel-liked precipitate observed

Test	VS-Co IE Repeat 2	VS-Co IE Repeat 3	Repeat Blank	
pH	8.35	8.37	**8.45**	8.40
$[Mg]_{rx}$ ppm	8.1	1.4	**5.4**	6.4
$[Si]_{rx}$	124.8	13.8	**65.1**	79.8
	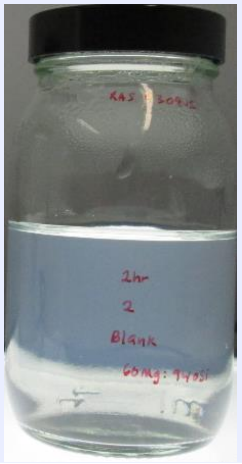	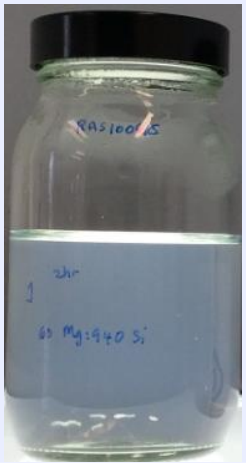	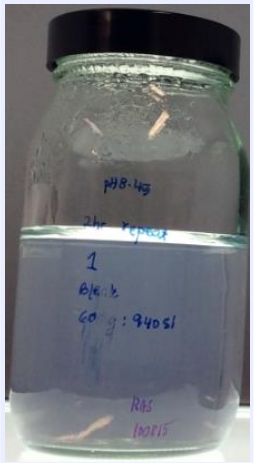	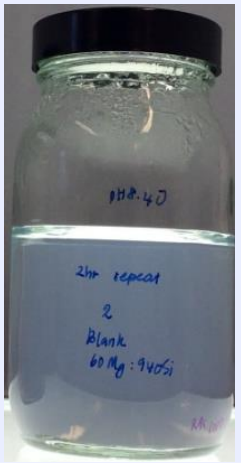

Figure 5-17 Observation of blank 60Mg:940Si @pH8.5, 60ºC at 2 hour – Solution became slightly cloudy (No gel-liked precipitate observed)

As can be seen in Figure 5-16, the *blank* samples in the H3 IE Test resulted in totally different amounts of ions reacted, even although both duplicates were adjusted to the same initial pH value, pH~8.42. Another *blank* in VS-Co IE Test Repeat 1 was adjusted to pH 8.35 (considered close enough to the nominal pH value) but resulted in completely different amounts of ions reacted as compared to its duplicate with pH 8.50. One of the *blanks* as shown in Figure 5-17 was adjusted to be very close to the test pH ~8.45. However, this *blank* only became slightly cloudy after 2 hours of reaction.

The amount of ion reacted in the *blank* samples was found to vary even although the initial pH values of the blank samples were adjusted to be very close to the nominal value (Refer Figure 5-18). The amount of magnesium ion reacted varied from ~1ppm to ~35ppm while the amount of silicon ion reacted was between ~14ppm to ~803ppm (Nominal values reported in Figure 3-6 in *Chapter 3* is ~29ppm to ~34ppm of magnesium ion reacted and ~770ppm to ~810ppm of silicon ion reacted). Hence, from all of the evidence, it appears to be vital to adjust the pH value of the mixed brine very close to the test pH and a very consistent approach seems to be required. All the *blanks* and samples in all of the tests above were adjusted to their initial pH values in a rather arbitrary way – no consistent brine mixing and pH adjustment procedures were applied i.e. it appeared they were not as close to the test pH as they should have been.

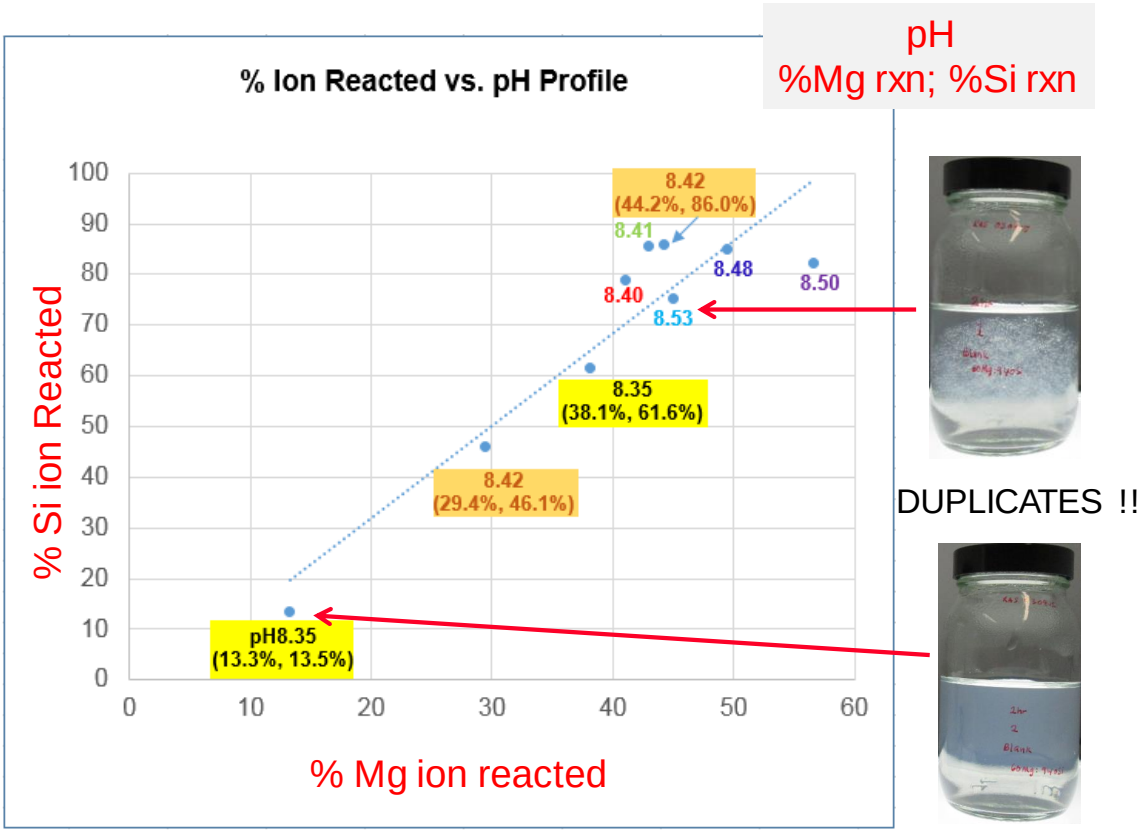

Figure 5-18 % Amount of ion reacted vs. Initial pH values (in the blank)

Further analysis of the IE tests revealed that there is a correlation between IE $_{Si}$ % and the initial pH of the mixed brine (Refer Figure 5-19, Figure 5-20 and Figure 5-21). Generally, for all VS-Co concentrations, it was found that the lower the initial pH of the mixed brine, the better the IE % (except for few samples that need further investigation to validate this hypotheses).

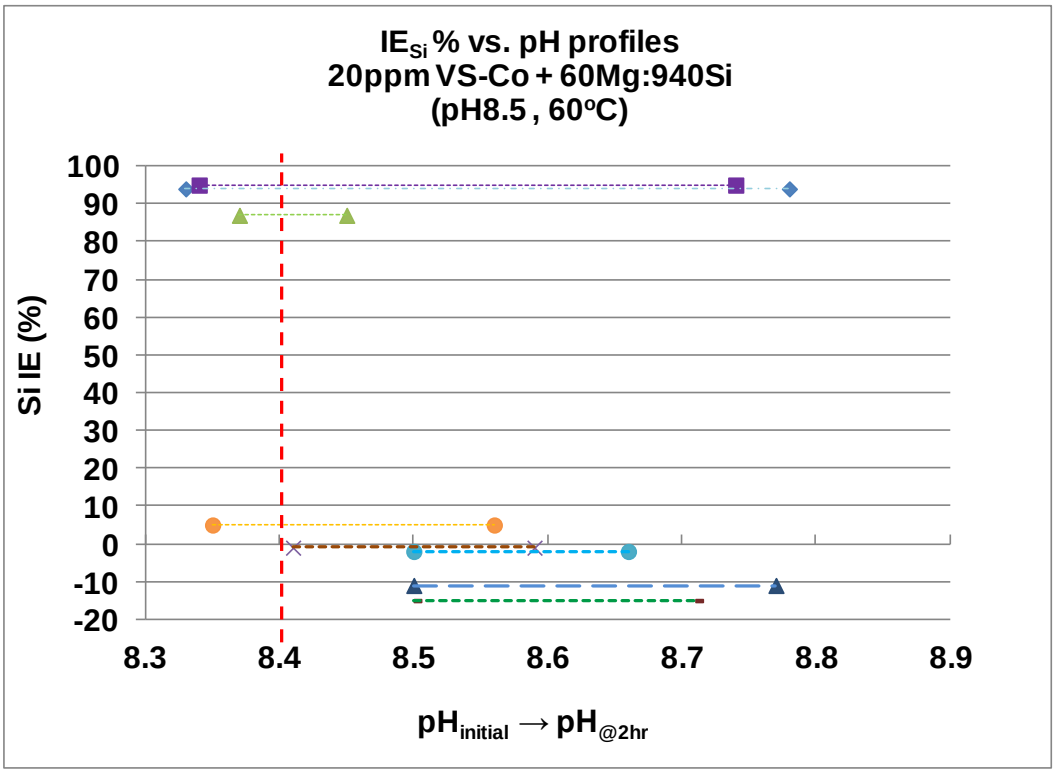

Figure 5-19 IE $_{Si}$ % vs. pH profile for 20ppm VS-Co + 60Mg:940Si

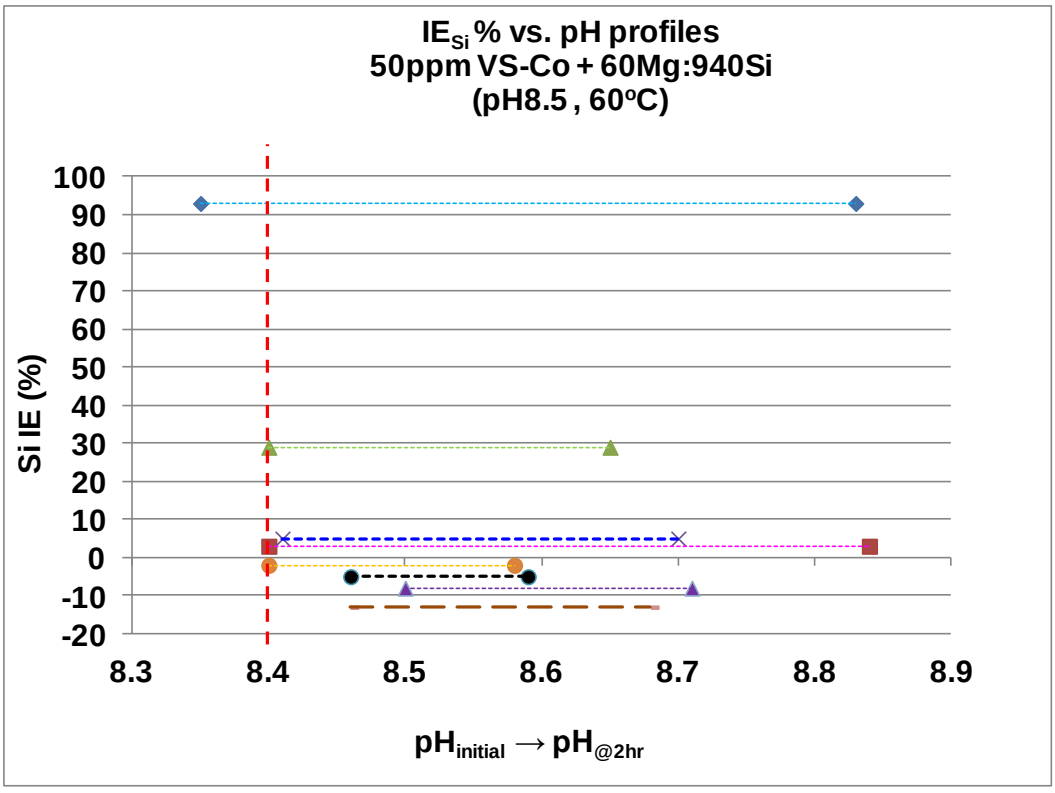

Figure 5-20 IE $_{Si}$ % vs. pH profile for 50ppm VS-Co + 60Mg:940Si

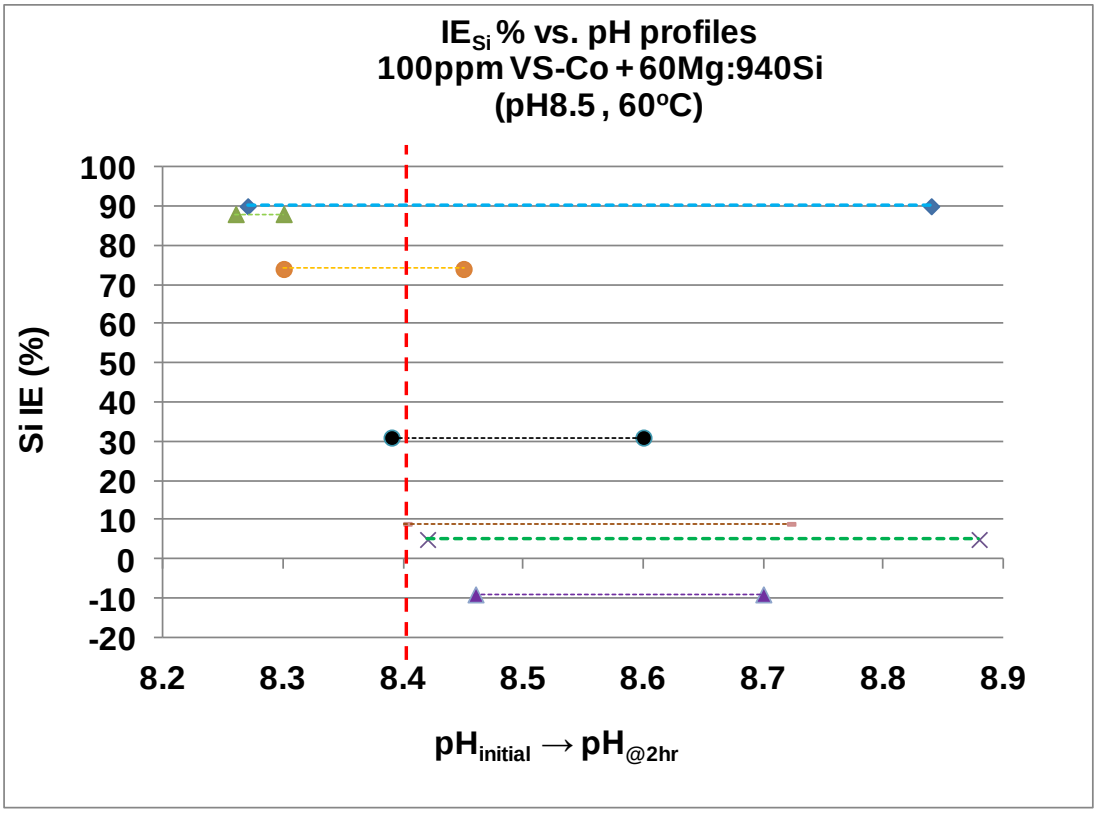

Figure 5-21 IE $_{Si}$ % vs. pH profile for 100ppm VS-Co + 60Mg:940Si

5.2.4 Silicate Scale Static Bottle Test (Blank 60Mg:940Si) at Varied Initial pH values

(a) Experimental Details

Further analysis of the IE test results in section 5.2.2 showed that the silicate system is not stable and it is very difficult to reproduce, probably because of its high sensitivity to initial pH values. For all IE tests that were conducted, the initial pH values of all samples were controlled between 8.35 - 8.50 where this was done arbitrarily hence the only concern was the initial pH values with little consistency in the brine mixing and pH adjusting procedures. This controlled pH values (i.e. pH8.35 – 8.50) was originally considered to be close enough to the nominal value. The amount of magnesium and silicon ion reacted in the *blank* in all tests was found to vary, as tabulated in Table 5-4 and plotted in Figure 5-22 (amount of ion reacted in ppm) and Figure 5-23 (amount of ion reacted in %).

Table 5-4 Amount of 2hr - Ion Reacted in *blank* 60Mg:940Si (at pH8.5, 60°C) in *First* IE Experiments & other sensitivities tests

Experiment	pH	$[Mg]_{rx}$ / ppm	$[Si]_{rx}$ / ppm	$[Mg]_{rx}$ / %	$[Si]_{rx}$ / %
VS-Co IE *Original Test*	8.48	29.9	802.8	49.8	86.4
	8.40	24.7	746.8	41.2	80.3
VS-Co IE *Repeat1*	8.50	35.2	773.5	58.7	82.2
	8.35	23.7	579.1	39.5	61.5
VS-Co IE *Repeat2*	8.53	27.3	699.0	45.5	75.3
	8.35	8.1	124.8	13.5	13.4
VS-Co IE *Repeat3*	8.47	26.0	802.7	43.3	85.9
	8.37	1.4	13.8	2.3	1.5
H3 IE Test	8.41 (10mins)	17.8	421.4	29.7	45.7
	8.41 (6mins)	26.7	786.1	44.5	85.3
Aged Si Test	8.47	29	742.0	48.3	79.1
	8.46	39	836	65.0	89.1
Blank repeat for observation	8.45	5.4	65.1	9.0	6.9
	8.40	6.4	79.8	10.7	8.5

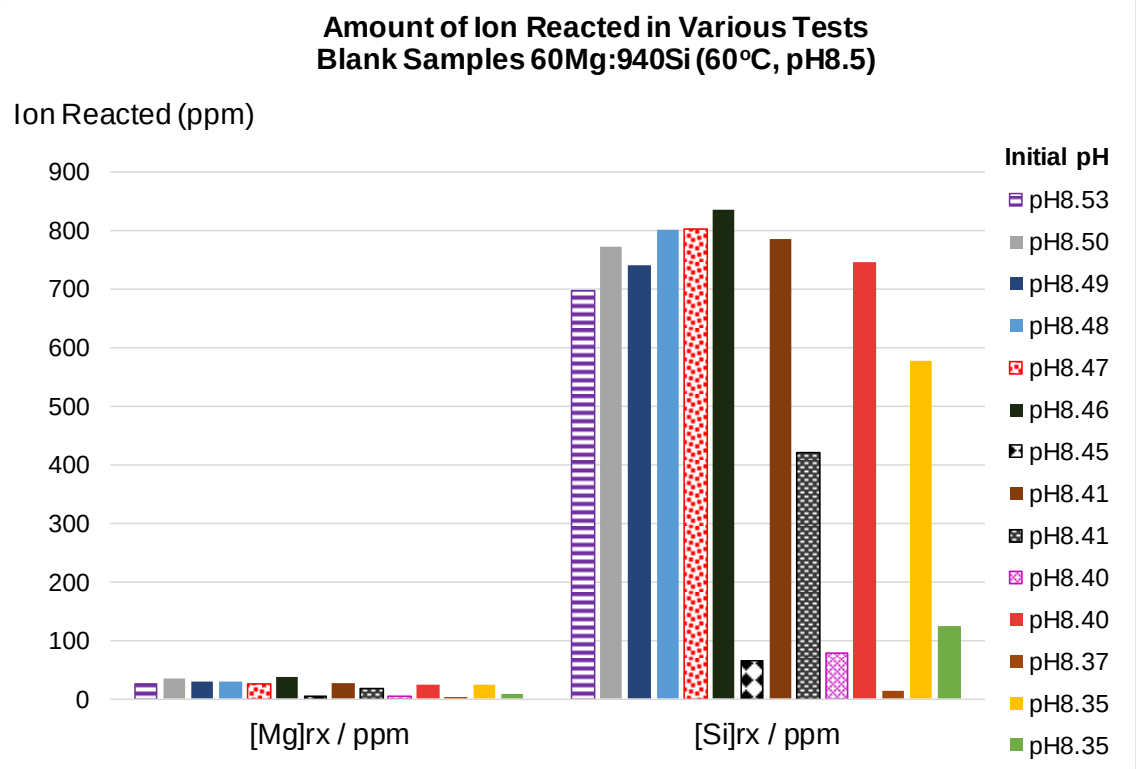

Figure 5-22 Amount of ion reacted (ppm) of *blank* samples in *First* IE Tests at 2 hours

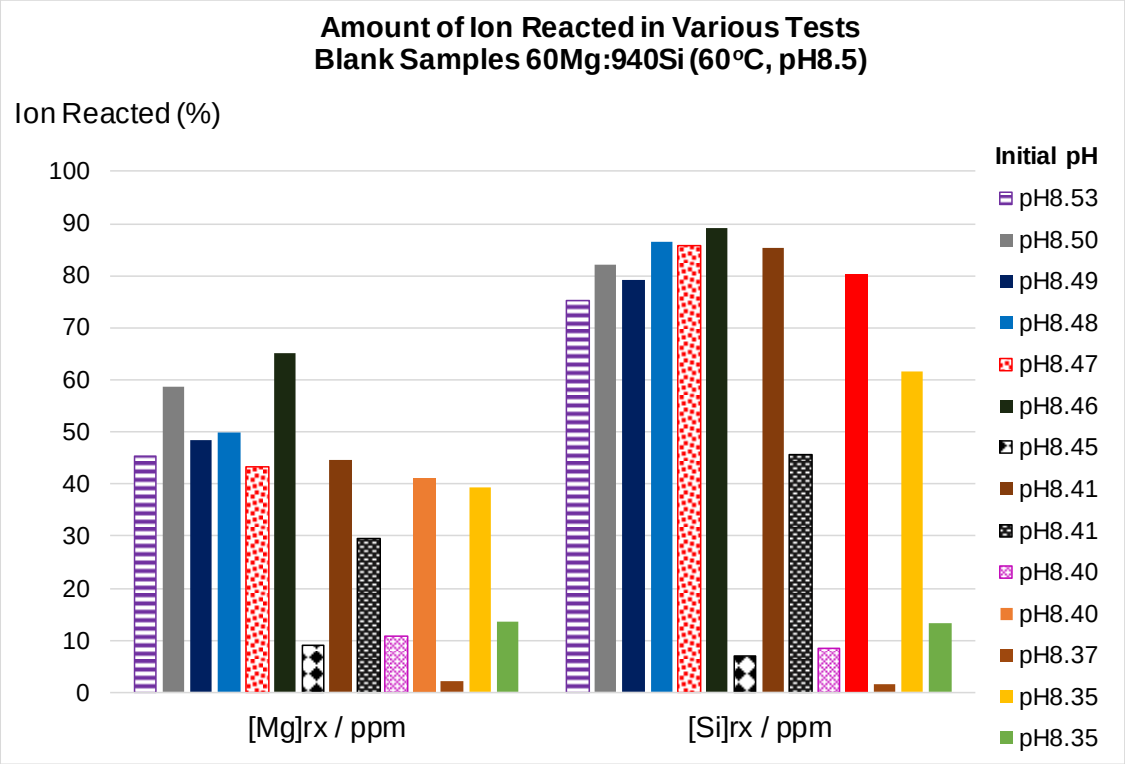

Figure 5-23 Amount of ion reacted (%) of *blank* samples in *First* IE Tests at 2 hours

Therefore, a series of "nominal pH 8.5" static bottle tests were performed at T = 60°C to study the extent of reaction when initial pH value of the mixed brines were adjusted to the pH values, pH 7.5, pH 8.0, pH 8.5 and were also tested at the systems natural pH (~pH 12.7).

In this experiment, the pH values were adjusted closely to the specific pH value and were adjusted within a specific time (i.e. 6 – 8 minutes only) with the stirring speed kept constant at speed 2. The brine mixing process was performed in a very consistent way for each sample where the Si brine and Mg brine were shaken vigorously (exactly 33 times) in their individual HDPE bottle. Then, Mg brine was added to the Si brine and again shaken vigorously (33 times). The natural pH of the mixed brine was then measured while stirring using a magnetic stirrer at speed 2. The pH probe was left in the solution until a stable value was reached ~12.70 (it took 2-3 minutes for the pH to reach a stable value). Then an appropriate amount of 10%HCl solution was added to the solution. The pH was adjusted to be very close to the nominal value (i.e. 8.48 – 8.52 for a test pH of 8.50) and the total time needed to adjust the pH was kept within 6-8 minutes (time was counted from when the brine was mixed).

(b) Experimental Results

This experiment was designed to study the effect of initial pH on the mixed brine (Magnesium brine and silicon brine in 50:50 mixed ratios – 60Mg:940Si) silicate scaling reaction. ICP sampling of the *first* inhibition efficiency tests (VS-Co and H3) revealed that different amounts of silicon and magnesium ion were reacted even for slightly different initial mixed pH values from the nominal pH value (i.e. pH 8.5).

Results in Figure 5-24 show that slight changes by 0.5 in the pH value of the mixed brine result in significantly different extents of reaction (i.e. pH 8 and pH8.5). For example, these results show that 22.1% and 41.6% of magnesium reacted while 69.6% and 86.2% of silicon ion reacted for this mixed brine at initial pH values of 8.0 and 8.5 respectively. The silicate ion is stable at high pH (i.e. pH12.7), hence no polymerization occurs. The solubility of silicate and magnesium silicate is quite high at this pH and hence almost no silicate scale formed at this pH. Since the amount of magnesium is very low, then magnesium hydroxide is not produced here (this can also be seen from physical observation of the samples in Figure 5-26).

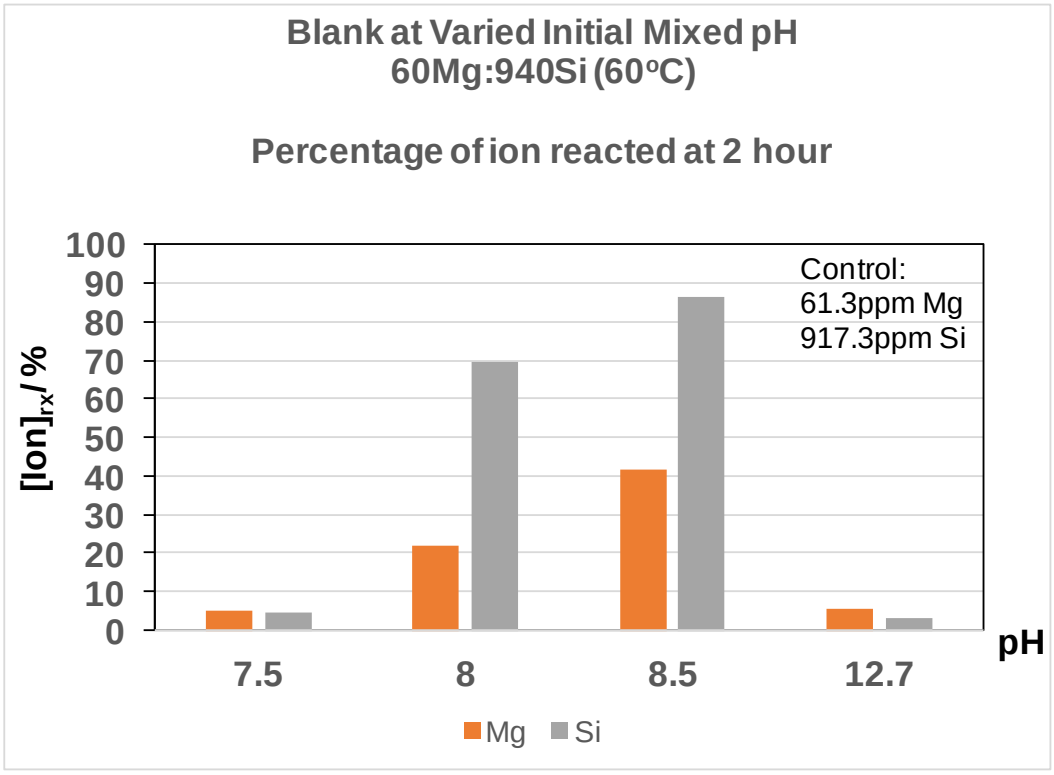

Figure 5-24 Percentage of ion reacted at 2 hour – Blank 60Mg:940Si at various initial mixed pH

According to Demadis (2010), at pH less than 8.0, magnesium silicate is unlikely to form since the silicate is in unionized form. Below pH 7, magnesium silicate does not occur because silica is present essentially in an unionized form (Meyers, 1999). That is why the brine at pH 7.5 only became slightly cloudy after 2 hours (Figure 5-26). According to Chan (1989), polymerization rate is maximum at 6 < pH <9 and its solubility is a minimum at pH ~7.6. Hence, it is believed that the cloudiness produced might be a sign of the brine starting to show silica polymerization.

The presence of divalent cations (such as Mg^{2+}) in the solution might affect the precipitation reaction. Meyers (1999) reported that solubility decreases with pH and divalent cations present. Amjad and Zuhl (2009) reported that magnesium silicate is favoured when pH is more than 8.5. Results obtained from the ICP data are consistent with the literature as the amount of magnesium and silicon ion reacted at pH8.5 is higher than at pH8.0. Physical observation on the samples also supports this view - see Figure 5-27.

The ICP data obtained are reliable since the pH values of all samples were strictly controlled close to the nominal value (i.e. pH = 7.5, 8.0, 8.5) in a very consistent manner, as described in Section 5.2.4. These were validated since we find a negligible discrepancy (i.e. <5.7% and <3.6% for magnesium and silicon ion respectively) between duplicates as shown in Figure 5-25.

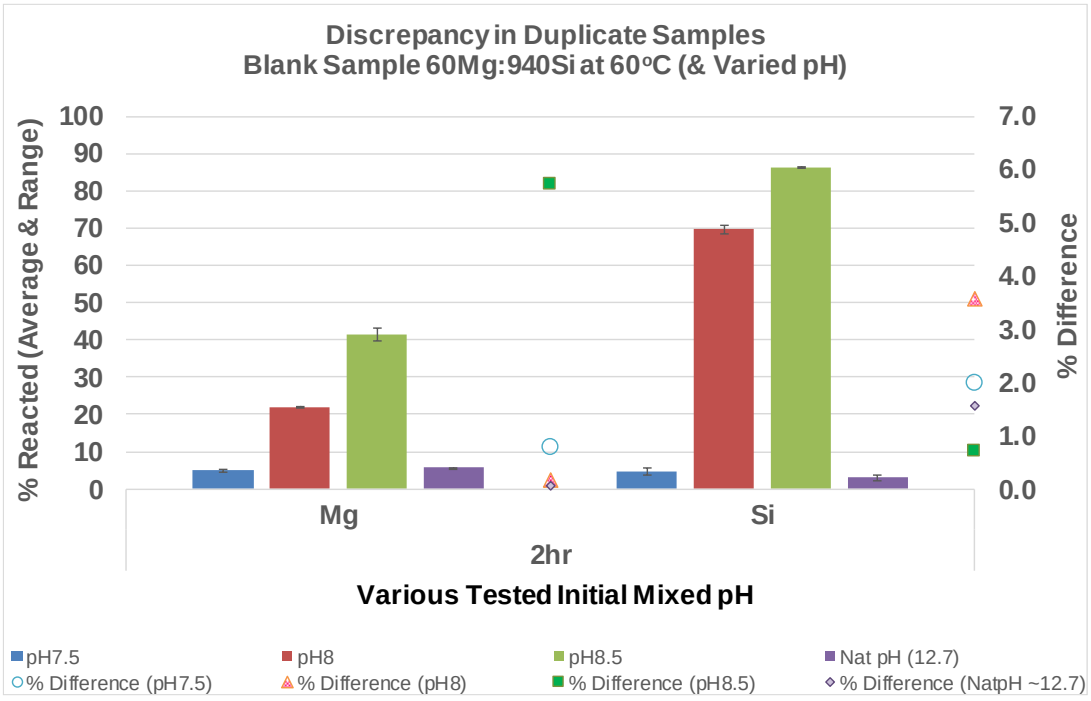

Figure 5-25 Discrepancy in duplicate samples of blank 60Mg:940Si at varied initial pH

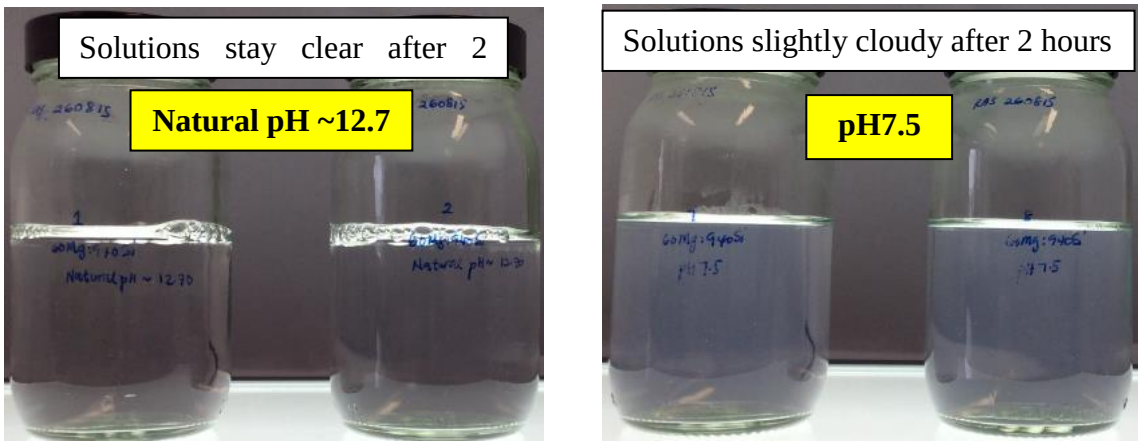

Figure 5-26 Blank 60Mg:940Si of natural pH~12.70 (left) and pH7.5 (right) after 2 hour

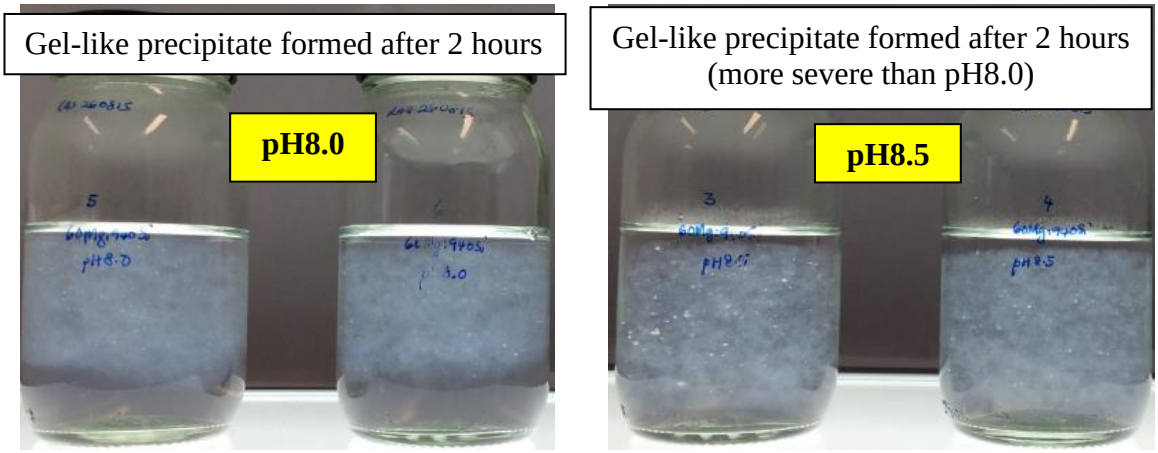

Figure 5-27 Blank 60Mg:940Si of natural pH~8.0 (left) and pH8.5 (right) after 2 hour

Generally, the pH values of the mixed brines increased after 2 hours of reaction except for the brine with natural pH~12.70, in which the pH was almost unchanged (Refer to Figure 5-28).

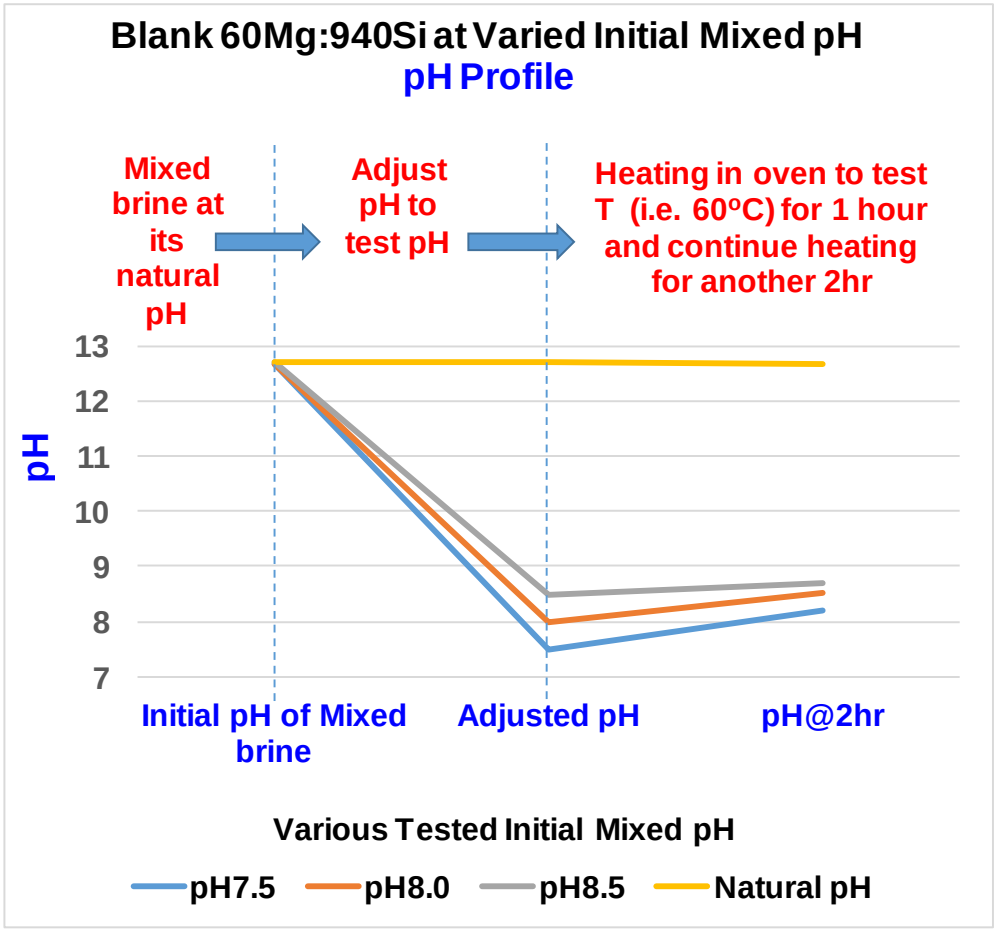

Figure 5-28 pH profile of blank 60Mg:940Si at Varied Initial Mixed pH

5.2.5 Buffering the Silicate System

Experimental results discussed in section 5.2.4 confirmed our initial conjecture that the silicate system is very sensitive to the initial pH of the mixed brine. Hence, the option of buffering the silicate system was considered in order to stabilize the system to obtain reproducible results. Borate buffer at pH 8.5 was tested to check the stability and reproducibility of the silicate system in a series of experimental tests. However, the addition of borate buffer directly into the mixed brine 60Mg:940Si (Natural pH of the mixed brine is ~12.70) did not change the pH to the test pH of 8.5. In fact, the pH of this mixed brine was relatively unchanged.

Therefore, the mixed brine was pH adjusted through the normal procedure i.e. The pH levels of the mixed brine were closely adjusted to the nominal value using the consistent approach as described in 5.2.4(a) before the borate buffer was added into the pH-adjusted mixed brine.

However, the borate buffer caused a slight increase in the pH value of the mixed brine; the pH increased as the amount of borate buffer increased. The pH was increased to 8.72 and 8.76 when 1ml and 2ml of borate buffer was added, respectively. As can be seen in Figure 5-29 and Table 5-5, the higher the initial pH values of the mixed brine, the higher the amount of magnesium reacted in the following order;

BLANK (pH8.5) < 1 ml Borate (pH8.72) < 2ml Borate (pH8.76)

Almost all of the magnesium ions were reacted after 22 hours; 94.9% and 89.3% in the brine with 2ml and 1ml of borate buffer respectively, as compared to only 66.7% in the blank. There are no significant differences in the total amount of silicon ion reacted for the three cases. We concluded that, although the addition of the borate buffer into the silicate system was quite efficient at keeping the pH of the mixed brine at the test pH (Refer Table 5-5), the borate buffer itself resulted in another additional step in the normal static test procedure and did not offer any particular advantage.

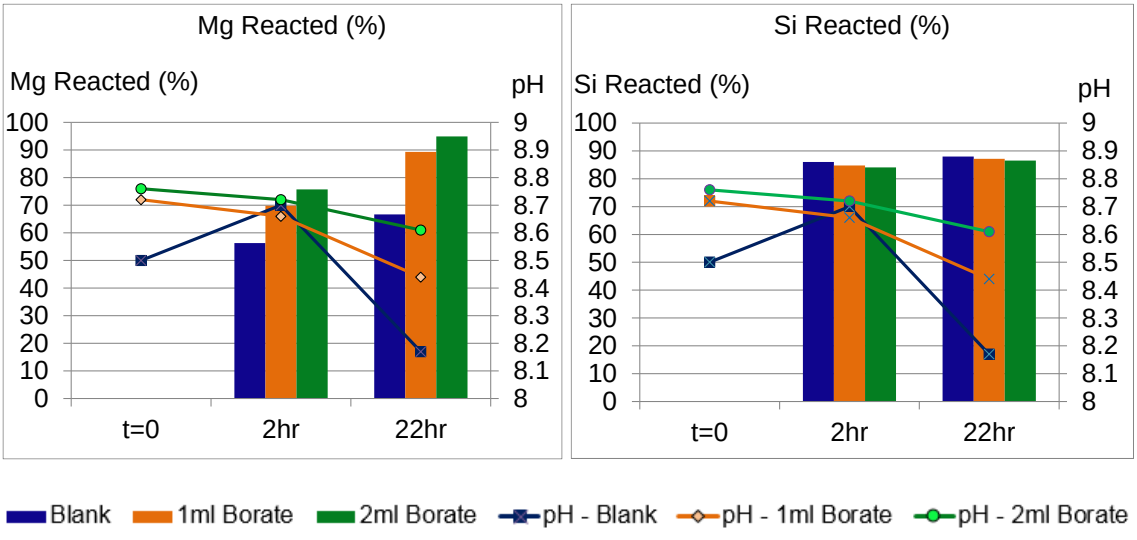

Figure 5-29 % Amount of ion reacted of base case (Blank) 60Mg:940Si at 60°C (With borate buffer)

Table 5-5 Borate buffer system of base case (Blank) 60Mg:940Si at 60°C

Test Condition (60Mg:940Si), 60°C		BLANK (No Borate)	Add 1 ml Borate	Add 2 ml Borate
Mg Reacted (%)	2 hour	56.3	69.8	75.7
	22 hour	66.7	89.3	94.9
pH Monitoring	Initial Adjusted pH (Add 10% HCl)	8.50		
	Initial pH @0hr (When Borate Buffer Added)	8.50	8.72	8.76
	pH @2hr	8.70	8.66	8.72
	pH @22hr	8.17	8.44	8.61
pH changes		8.17-8.70	8.44-8.72	8.61-8.76
Amount of pH changes		~0.53	~0.28	~0.15

In this experiment, the discrepancies between duplicate samples are very small as the percent difference calculated for all test conditions are less than 6% (Refer Figure 5-30). Hence, the pH adjustment procedure (as explained in 5.2.4(a)) adopted in this experiment was successful in obtaining reproducible results.

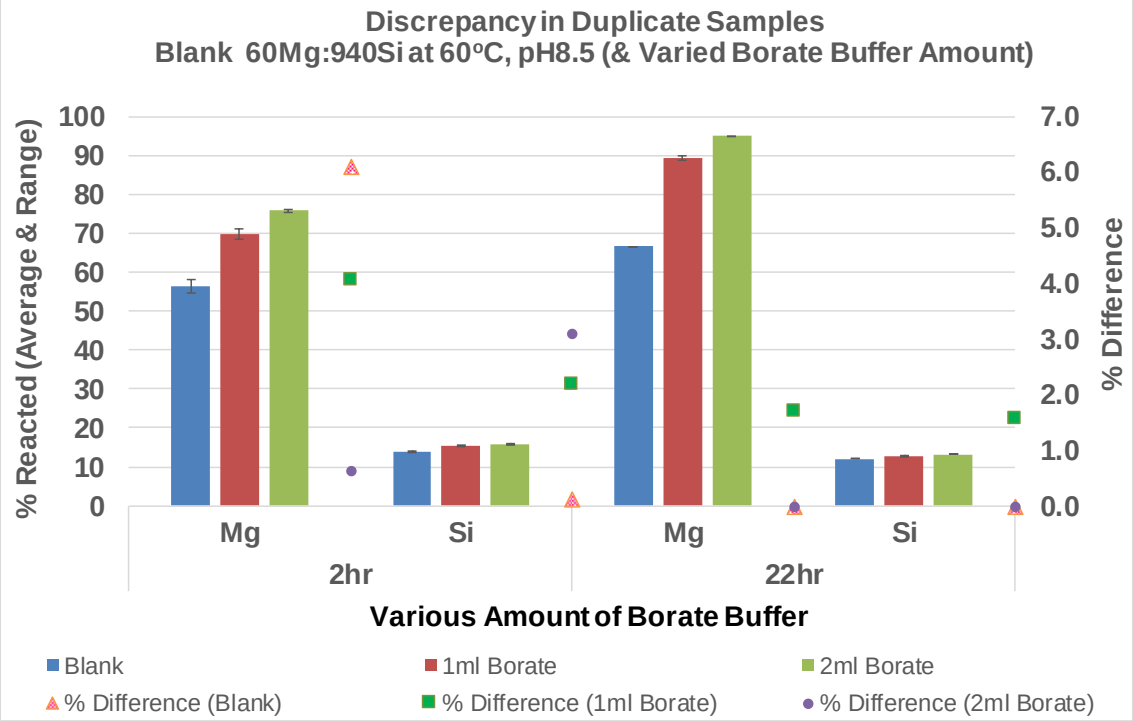

Figure 5-30 Discrepancy in duplicate samples of blank 60Mg:940Si (No borate) and various amount of borate buffer

5.2.6 Summary of Developed Inhibition Efficiency Test Methodology

Figure 5-31 shows a schematic of the procedure for carrying out *inhibition efficiency* tests for silicate scale using chemical scale inhibitors/dispersants. The scale inhibitor (SI) stock solution (at high active concentrations up to 10,000ppm) was prepared either in silicone brine (SB) – for A5 polymer; or distilled water (DW) for VS-Co or H3 polymer as summarized in Table 5-6. This stock solution was then further diluted to 250ml samples of silicone brine to obtain various active SI concentrations (i.e. 20ppm, 50ppm, 100ppm etc.) in the final 50:50 ratio mixed silicon and magnesium brine as summarized in Table 5-7.

The magnesium brine was then added to the silicon brine/ SI solution before these mixed Mg/Si/SI brines were then pH-adjusted (to the test pH) before being heated in the oven (to test temperature). The test samples were then ICP analysed at 2 and 22hr (or any other chosen sampling times) and precipitates were collected to analyse the morphology and chemical compositions of any precipitates which formed using ESEM/EDAX and FTIR analyses. It is worth mentioning here that the precipitates were not able to be analysed using XRD due to very small amount of precipitates formed (i.e. there was not enough material to carry out an accurate analysis by XRD).

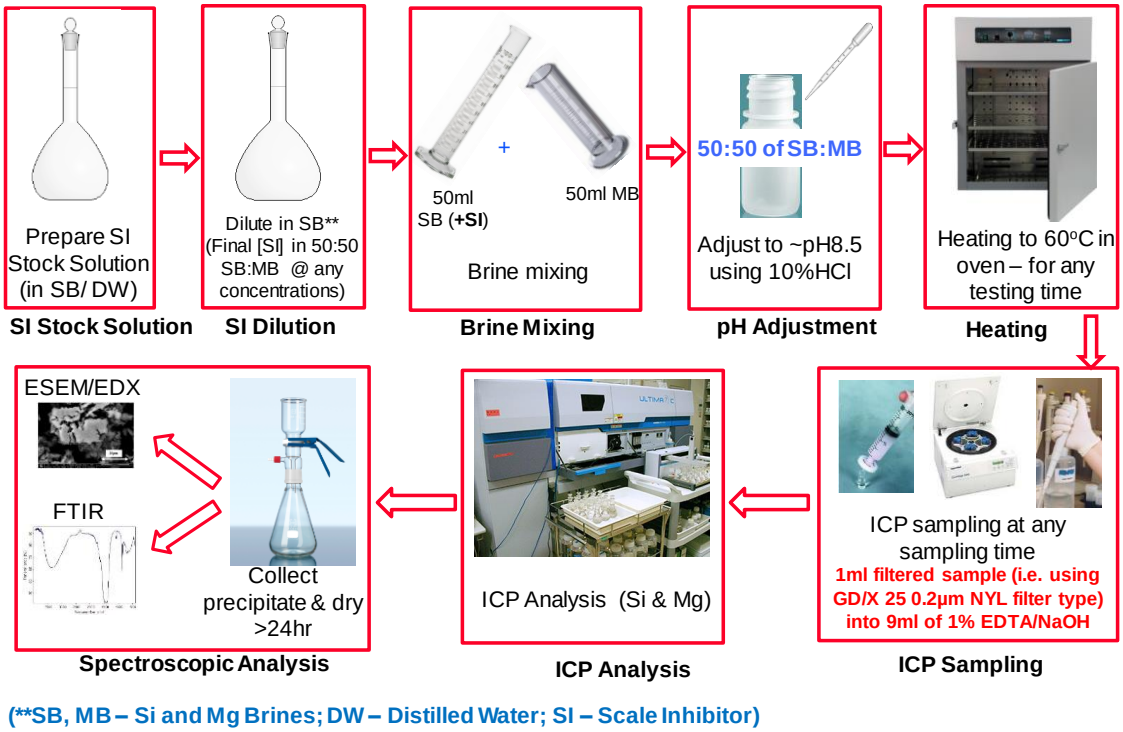

Figure 5-31 Silicate Scale *Inhibition Efficiency* Test experimental methodology

Table 5-6 Active stock solution preparation of scale inhibitor/ dispersant tested

Scale Inhibitor name	Supplier	Form	Activity (%)	Actual weight for 250ml	Concentration of active stock solution (ppm)
A5	C	Liquid	42	0.5952g in 250ml Si brine	1000
VS-Co	A	Liquid	30	8.33g in 250ml DW	10000
H3	B	Powder	100	1.25g in 248.75g DW	5000

Table 5-7 Scale inhibitor dilution in silicon brine (SB/SI solution)

Scale Inhibitor name	SI Activity (%)	Concentrations required v/v before mix / ppm active	Concentrations v/v after mix / ppm active	Volume of active SI stock solution diluted (in 250ml Silicone brine)
A5	42	40	20	40/1,000*250 = **10ml** of stock SI soln
		60	30	60/1,000*250 = **15ml** of stock SI soln
		80	40	80/1,000*250 = **20ml** of stock SI soln
		100	50	100/1,000*250 = **25ml** of stock SI soln
		150	75	150/1,000*250 = **37.5ml** of stock SI soln
		200	100	200/1,000*250 = **50ml** of stock SI soln
		400	200	400/1,000*250 = **100ml** of stock SI soln
		600	300	600/1,000*250 = **150ml** of stock SI soln
		800	400	800/1,000*250 = **200ml** of stock SI soln
		1000	500	1000/1,000*250 = **250ml** of stock SI soln
VS-Co	30	40	20	40/10,000*250 = **1.0ml** of stock SI soln
		100	50	100/10,000*250 = **2.5ml** of stock SI soln
		200	100	200/10,000*250 = **5.0ml** of stock SI soln
		1000	500	200/10,000*250 = **25ml** of stock SI soln

Scale Inhibitor name	SI Activity (%)	Concentrations required v/v before mix / ppm active	Concentrations v/v after mix / ppm active	Volume of active SI stock solution diluted (in 250ml Silicone brine)
H3	100	40	20	40/5,000*250 = **2.0ml** of stock SI soln
		100	50	100/5,000*250 = **5.0ml** of stock SI soln
		200	100	200/5,000*250 = **10ml** of stock SI soln

pH adjustment techniques

Further analysis of the IE test results showed that the silicate system was not very stable in that it could be difficult to reproduce because of its high sensitivity to initial pH values. Duplicate samples often produced large discrepancies as discussed in 5.2.3. Therefore, appropriate procedures had to be established for pH adjustment of the reacting system before any potential scale inhibitor can be reliably tested.

The silicate system is very sensitive to changes smaller than 0.5 pH units resulting in significant differences in the extent of reaction as shown in section 5.2.4. This was confirmed by the results obtained in Figure 5-24 where the initial pH of the base case was varied slightly but very different outcomes were observed.

The brine mixing process was carried out in a very consistent way for each sample where the Si brine and Mg brine were shaken vigorously (exactly 33 times) in their individual HDPE bottle. Then, Mg brine was added to the Si brine and again shaken vigorously (33 times). The natural pH of the mixed brine was then measured while stirring using a magnetic stirrer at speed 2. The pH probe was left in the solution until a stable value was reached ~12.70 (it took about 2-3 minutes for the pH to reach a stable value). Then an appropriate amount of 10% HCl solution was added to the solution (we know the exact amount of 10% HCl to be added through the pre-test of pH adjustment). The pH was adjusted (using dilute HCl solution) to be very close to the nominal value (i.e. 8.48 – 8.52 for a test pH of 8.50) and the total time needed to adjust the pH was kept within 6-8 minutes (time was counted as brine was mixed).

This procedure is illustrated in Figure 5-32.

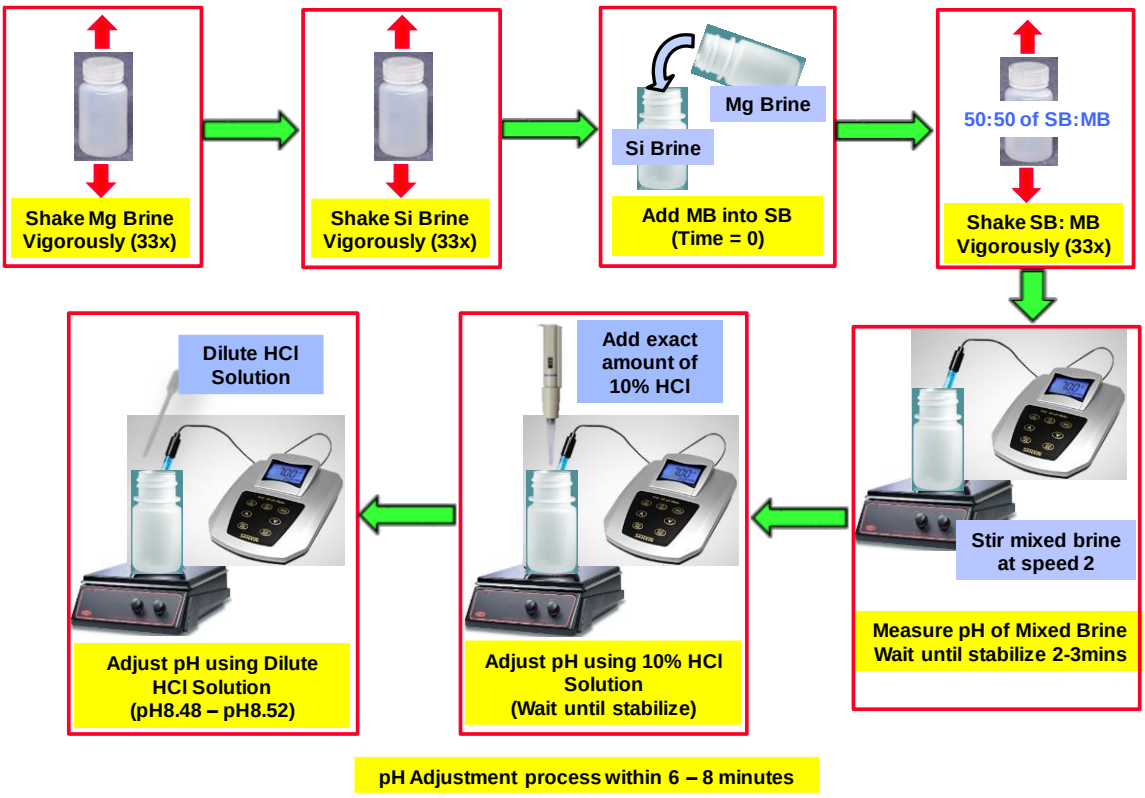

Figure 5-32 pH adjustment procedure

Following the establishment of the Inhibition Efficiency Test Methodology as described in section 5.2.6 where the samples will be ICP-sampled using GD/X 25 0.25µm Nylon filter type (refer section 4.3.6); hence H3 IE Test were repeated for two times to check its repeatability and reproducibility while adopting the pH adjustment procedures as described above. The filtering procedure assured there was no precipitate sampled which would interfere with the ICP sampling and measurement. In addition, the filtering techniques eliminated the complexity in the experimental schedule i.e. the tedious handling between ICP sampling and the centrifuging process. The number of samples required was also halved, i.e. separate test bottles for 2 and 22hour samplings were not required, which meant that the difficulty in the pH adjustment of samples was greatly reduced. Therefore, this H3 IE Test was simplified to exclude the need of centrifuging process and the difficulty in pH adjustment process.

Percent difference for both simplified test found to be less than 7% as shown in Figure 5-33 and Figure 5-34 that proof the repeatability and reproducibility of the developed IE test methodology. Following this, a series of various silicate static bottle tests (Section 5.3) and IE test (Section 5.4 to 5.8). It is worth noting here that all values reported are the average values of duplicate and the discrepancies i.e. percent difference are very small (not shown in the graph as the discrepancies are consistently appeared lower than 3%).

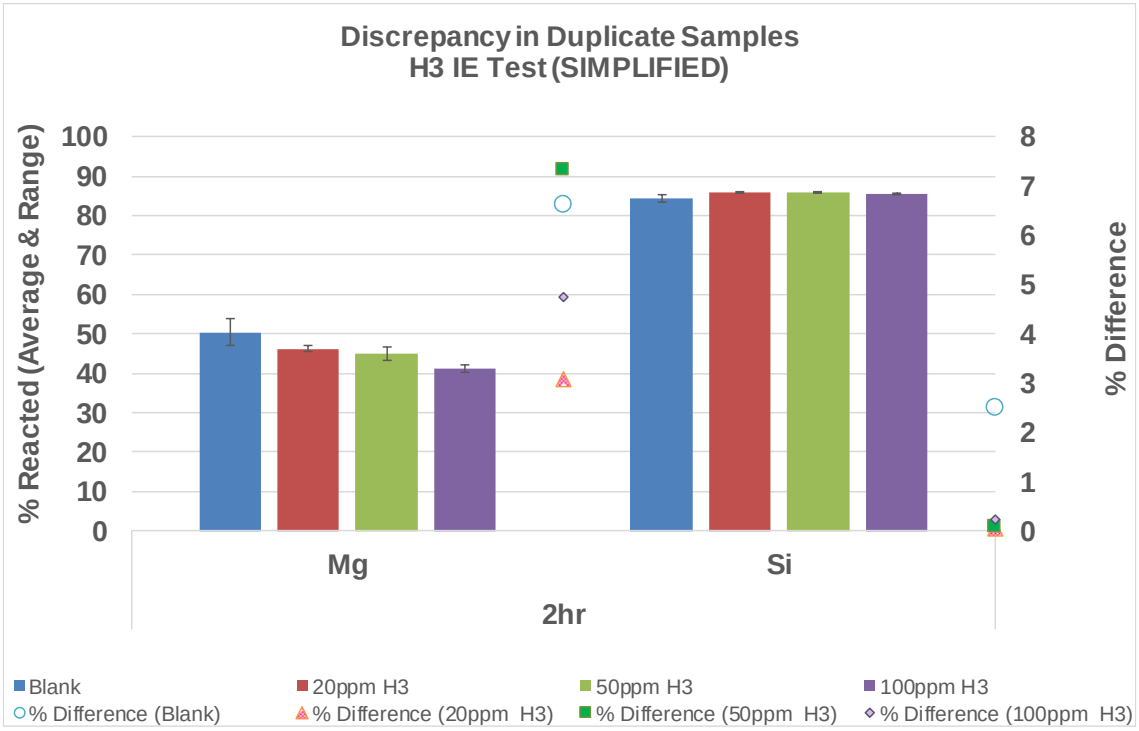

Figure 5-33 Discrepancy in duplicate samples of blank 60Mg:940Si (No H3) and various amount of H3-containing brine in H3 IE Test (Simplified)

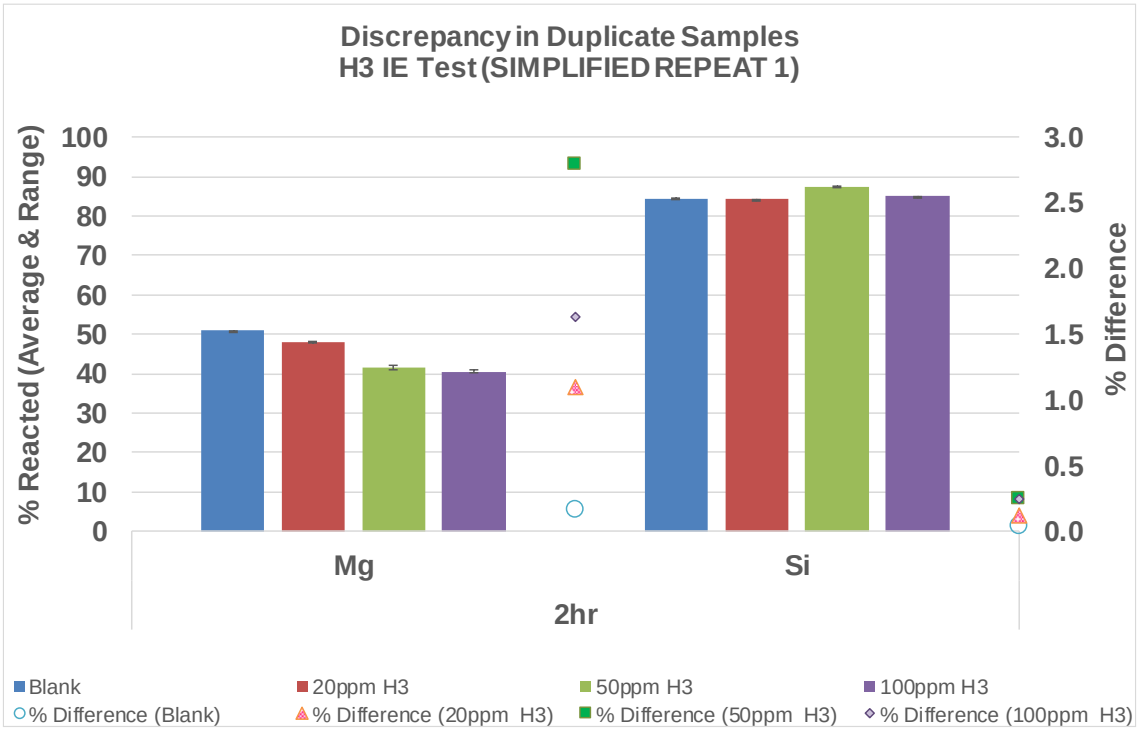

Figure 5-34 Discrepancy in duplicate samples of blank 60Mg:940Si (No H3) and various amount of H3-containing brine in H3 IE Test (Simplified Repeat 1)

5.3. SILICATE STATIC BOTTLE TESTS IN VARIOUS SILICATE SYSTEM AT 60ºC, pH8.5

It is worth noting that the blank (uninhibited) sample tests for the various silicate systems were conducted in multiple tests from the highest level of silicon ion to the lowest silicon ion for a fixed magnesium level of 60ppm and 30ppm. The purpose of the test was to study if sufficient scale is produced in the blank solution and if the silicate scale solution could be inhibited by the tested inhibitors at lower inhibitor concentrations.

The tests were conducted initially in "*worst"* base case of 60Mg:940Si followed by 60Mg:752Si, 60Mg:564Si, "*intermediate"* base case of 60Mg:470Si and 60Mg:300Si accordingly. However, even after the addition of 300ppm of A5 in the silicate system of 60Mg:300Si, the silicate scale cannot be prevented as will be explained in Section 5.7. Therefore, the magnesium and silicon level were reduced further where various silicate systems were studied i.e. 30Mg:150Si, 30Mg:75Si and 30Mg:50Si. The silicate system with 30Mg:75Si was chosen as the *"manageable"* base case and further tested using the inhibitors A5, VS-Co and H3, as discussed in Section 5.8.

5.3.1 Static Bottle Test for Various Silicate Systems with Magnesium Level = 60ppm at 60ºC, pH8.5

The percentage amounts of ion reacted for various silicate systems i.e. the blank (non-inhibited) solutions at 60ºC, pH 8.5 is plotted in Figure 5-35. As can be seen in this figure, it is clear that the amounts of magnesium and silicon ion reacted is increasing with the increasing amount of Si ion. About 47% - 58.5% of magnesium ion and 55% - 86% of silicon ion reacted after 2 hours when 300ppm – 940ppm silicon was mixed with 60ppm magnesium ion. These reacted percentages increased to 50% - 67.8% of magnesium ion and 60% - 89% of silicon ion after 22 hours.

It can be seen from Figure 5-36 that the silicate system of 60Mg:940Si stays clear after being mixed and pH adjusted at room temperature. However, the mixed brine became cloudy after 2 hours and a gel-like precipitate was observed after 22 hours followed by the settling of the precipitate to the bottom leaving a clear layer of solution after 5 days. The silicate system of 60Mg:752Si became slightly cloudy after being mixed and pH-adjusted at room temperature. This system became cloudier after 2 hours and a gel-like

precipitate also formed after 22 hours. After 5 days, the precipitate settled to the bottom just like the 60Mg:940Si case, although the amount of the precipitate was less.

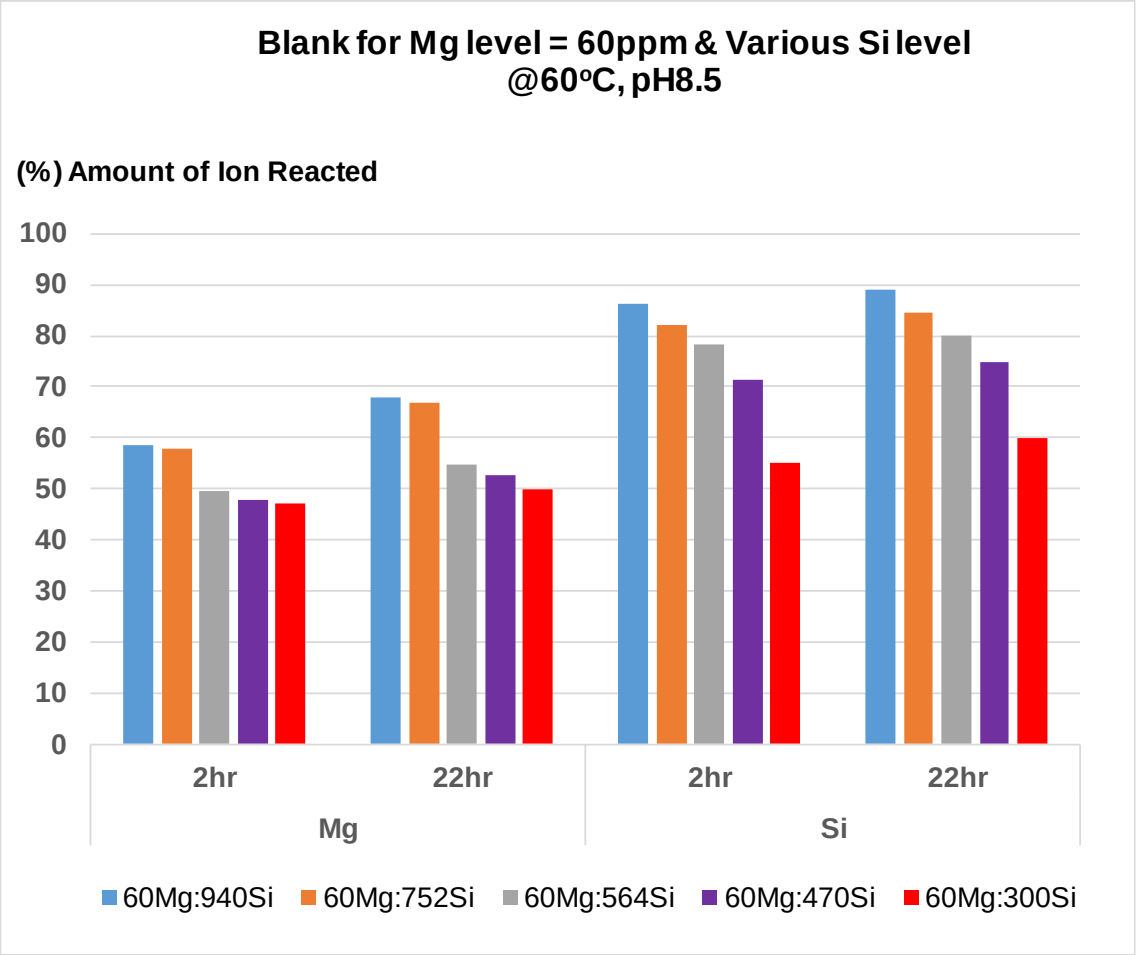

Figure 5-35 Percentage amount of ion reacted in various silicate system at 60°C, pH8.5 (Mg level = 60ppm)

For the silicate system of 60Mg:564Si and 60Mg:470Si, the mixed brine became cloudy immediately after being mixed and pH-adjusted at room temperature and they became hazier after 2 hours. Subsequently, a gel-like precipitate formed and the precipitate settled to the bottom leaving a clear layer of solution after 22 hours of reaction; the clear layer expanded after 5 days.

It is shown in the same figure that the amount of precipitate formed in the silicate system of 60Mg:300Si is the least compared to other silicate systems and this observation was consistent with the ICP-EOS data plotted in Figure 5-35.

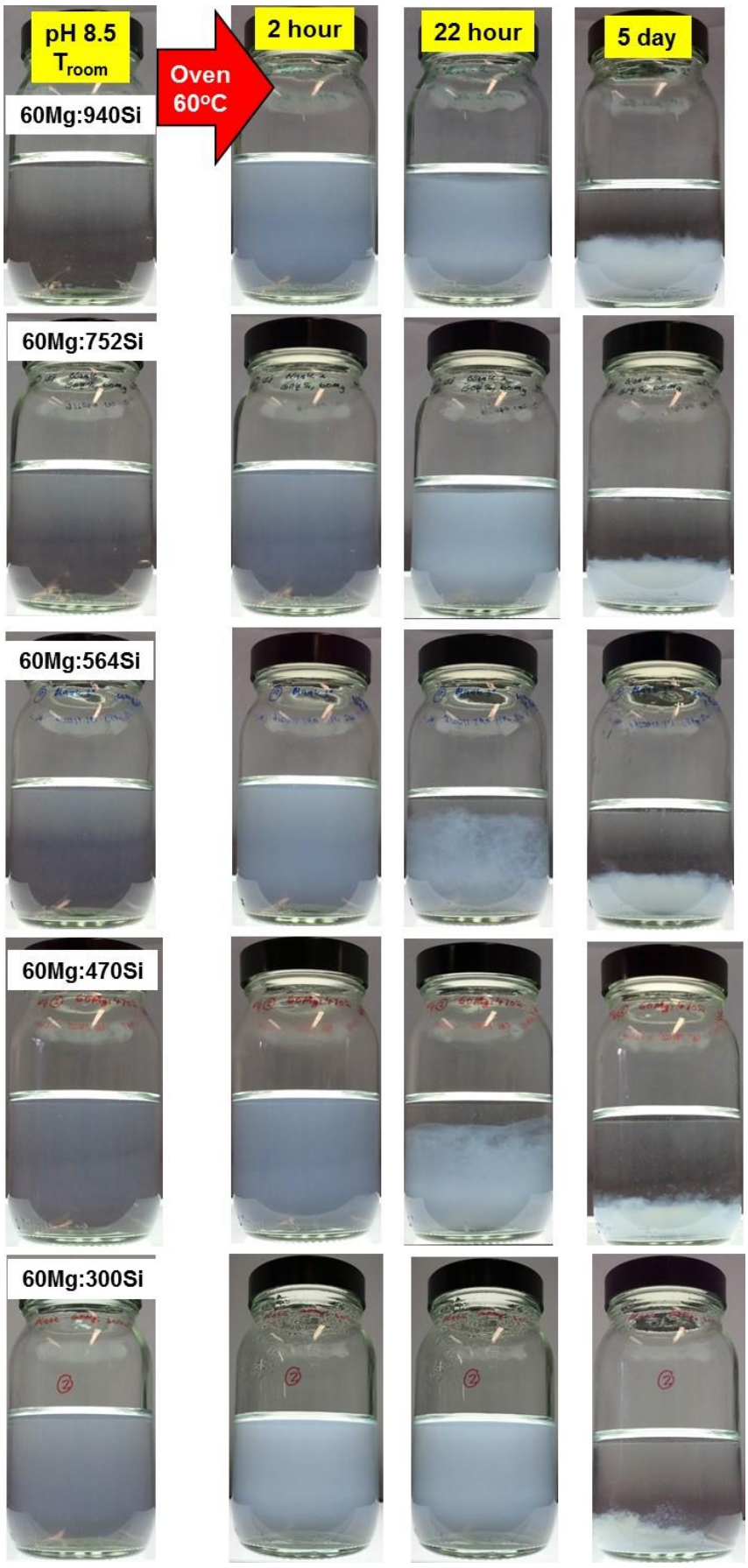

Figure 5-36 Observation of various silicate system at 60°C, pH8.5 (Mg level = 60ppm and Si level was varied from 300 to 940ppm)

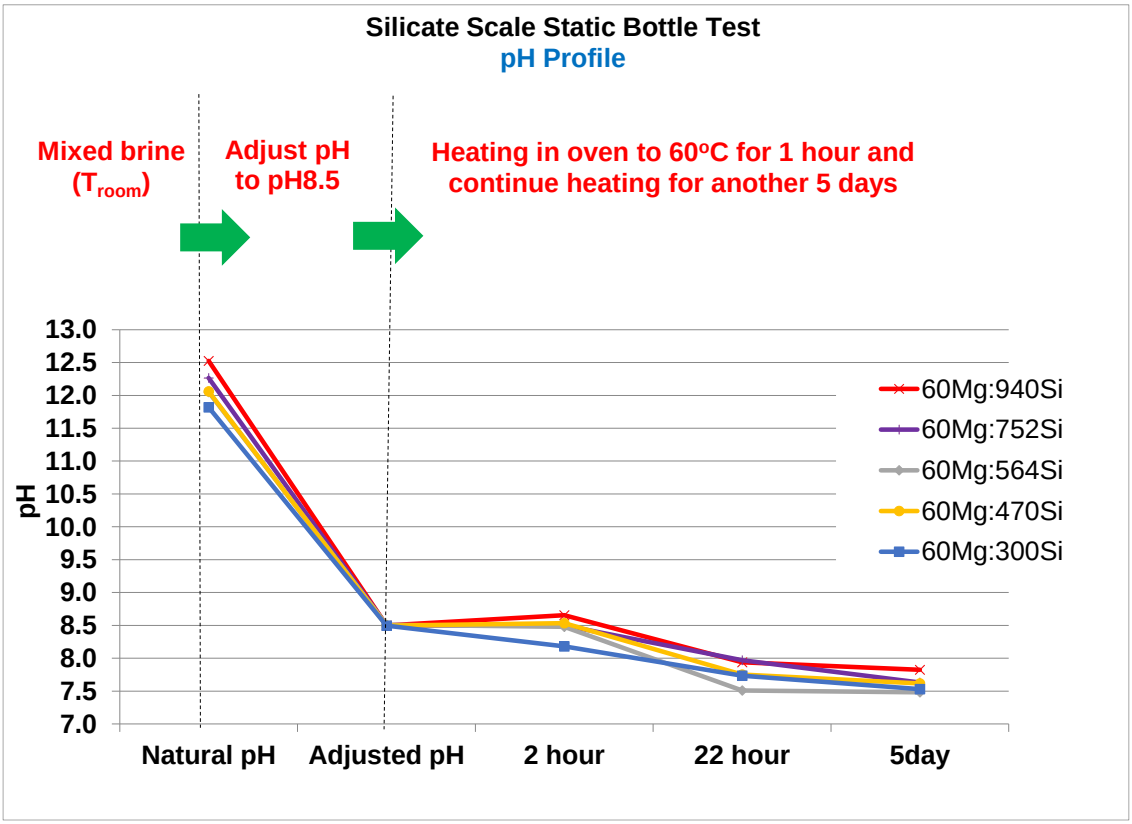

Figure 5-37 pH profiles for various silicate system of at 60°C, pH8.5 (Mg level = 60ppm and Si level was varied from 300 to 940ppm)

Figure 5-37 shows the pH changes in various silicate systems tested at 60°C, pH8.5. Generally, the natural pH of the mixed brine increased with the increasing amount of silicon ion with fixed magnesium ion level at 60ppm. The natural pH of 60Mg:940Si is approximately pH 12.5 while the pH is only about pH 11.8 for the 60Mg:300Si silicate system.

The plot of 60Mg:940Si showed that the pH increased after 2 hours of reaction before reducing back afterwards. For other silicate systems of 752ppm ≤ Si ≤ 470ppm, the pH is essentially the same as the initial adjusted pH i.e. pH8.5 up 2 hours before this pH value then reduced with time. The silicate system of 60Mg:300Si however, showed a reduction in pH value with time.

5.3.2 Static Bottle Tests for Various Silicate System with Magnesium Level = 30ppm At 60ºC, pH8.5

Figure 5-38 shows that about 13.6% - 24.6% of magnesium ion and 7.7% - 14.8% of silicon ion reacted after 2 hours when 50ppm – 150ppm silicon ion reacted with 30ppm magnesium ion. These percentages increased to ~14.1% - 29.3% of magnesium ion and 7% - 17.9% of silicon ions after 22 hours. The percentage amount of silicon ion reacted is considered very low (<10%) especially for the silicate system of 30Mg:50Si. However, this system does scale as can be seen clearly by direct observation, as shown in Figure 5-39.

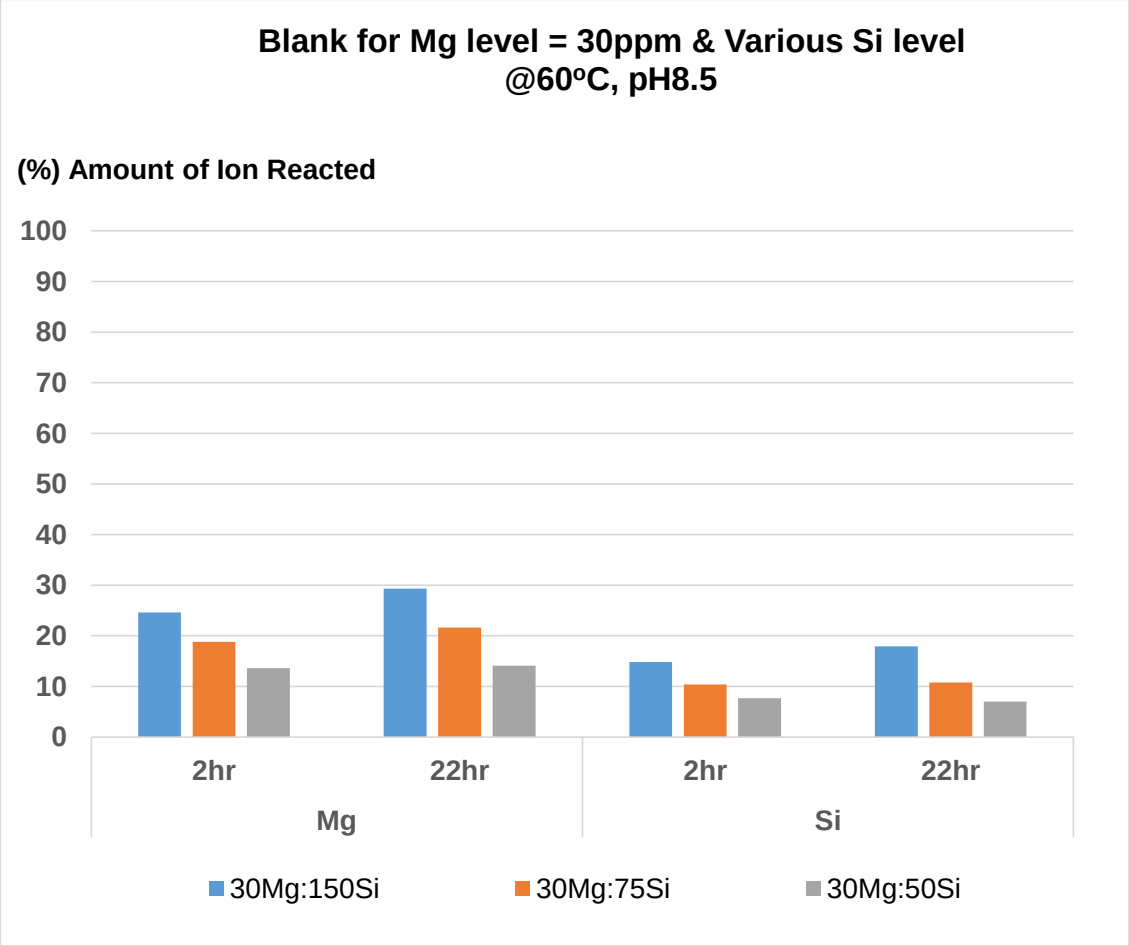

Figure 5-38 Percentage amount of ion reacted in various silicate system at 60ºC, pH8.5 (Mg level = 30ppm and Si level was varied from 50 to 150ppm)

For the silicate system, 30Mg:150Si, the mixed brine became slightly cloudy after being mixed and pH-adjusted at room temperature (see Figure 5-39). However, apparently the precipitate observed was formed 1 hour after heating in the oven (reaction time = 0). The amount of precipitate increased with residence time and settled to the bottom, leaving a clear supernatant solution after 22 hours.

The mixed brine of the silicate systems with 30Mg:75Si and 30Mg:50Si stayed clear throughout the 7 days of residence time with precipitate was detected as early as 1 hour after heating in the oven (reaction time=0).

Figure 5-40 shows that the pH values of all silicate systems reduced with time.

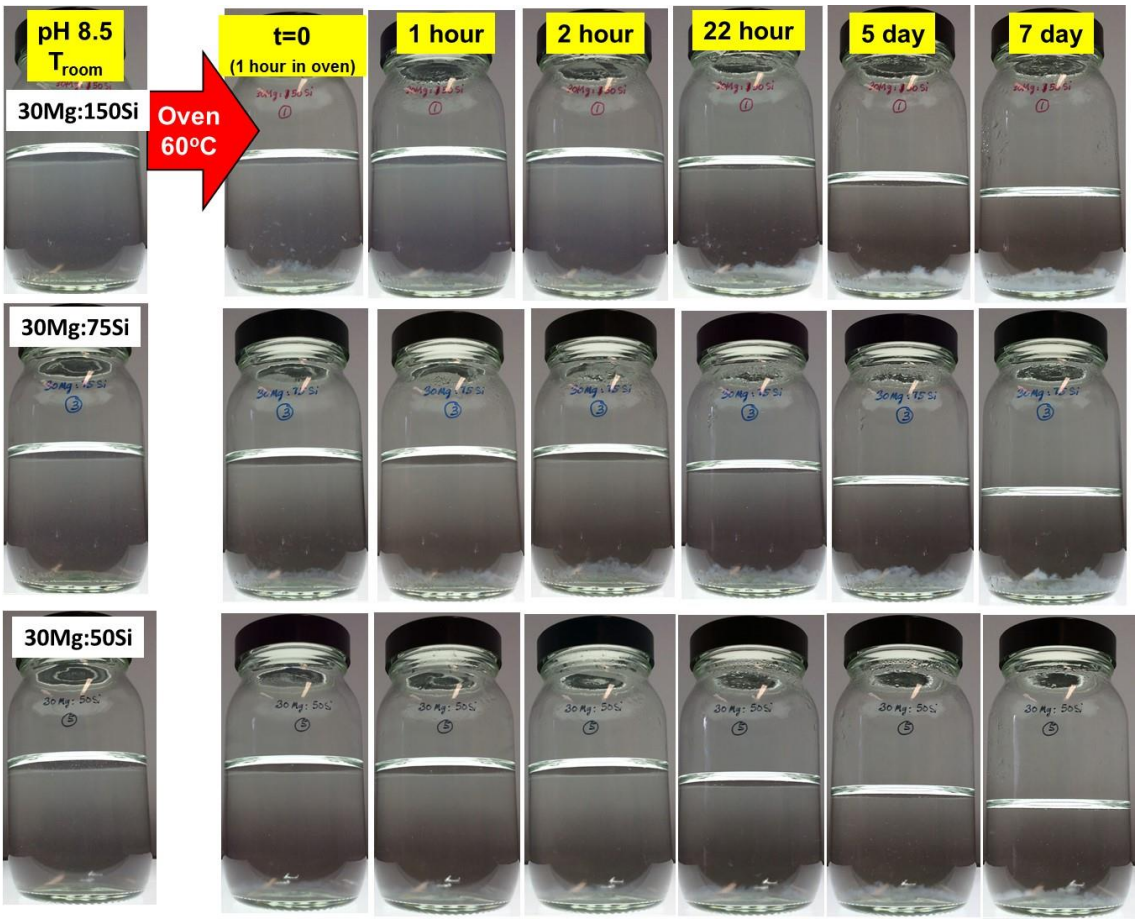

Figure 5-39 Observation of various silicate system at 60°C, pH8.5 (Mg level = 30ppm and Si level was varied from 50 to 150ppm)

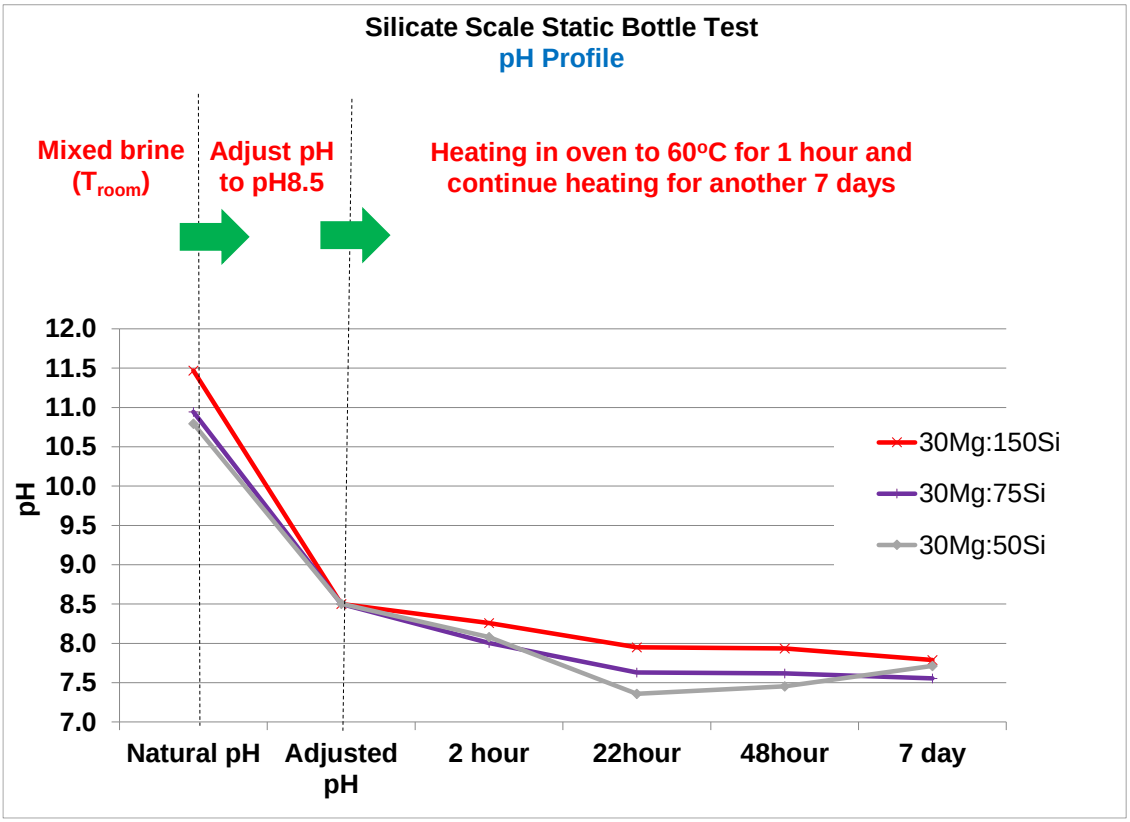

Figure 5-40 pH profiles for various silicate system of at 60°C, pH8.5 (Mg level = 30ppm and Si level was varied from 50 to 150ppm)

5.4. INHIBITION EFFICIENCY STUDY IN SILICATE SYSTEM 60Mg:940Si AT 60°C, pH8.5

These experiments were carried out following methodology described in section 5.2.6 to evaluate the performance of three inhibitors i.e. A5, VS-Co and H3 in the "*worst"* base conditions again; 60Mg:940Si at 60°C, pH8.5 at a range of inhibitor concentrations which are 20, 50 and 100ppm (and 500ppm for A5 and VS-Co). A central objective of current research within the FAST group, and in the oil industry in general, is to find a chemical that can inhibit the silicate scale at economical concentration.

5.4.1 Observations

The blank (uninhibited) sample in the silicate system of 60Mg:940Si at 60°C, pH8.5 produced a gel-like precipitate at 2 hours after heating in the oven. This precipitate settled to the bottom leaving a clear layer on top of the solution after 5 days; this can be observed in Figure 5-41. The addition of 100ppm A5 also produced a cloudy solution and gel-like precipitate at 2 and 22 hours, respectively, and the precipitate settled to the bottom leaving a cloudy layer on top of the solution after 5 days.

The mixed brine stays clear even after 5 days while being heated in the oven when 500ppm A5 polymer was added. All of these observations are consistent with the ICP-EOS data analysis.

However, it is worth stating that for the lower A5 concentrations (i.e. 20, 50, and 100ppm), the tests were conducted in HDPE bottles, and so no pictures are available. Also, it is worth noting that the mixed brine is probably in between the conditions seen in the blank and the 100ppm A5 in appearance.

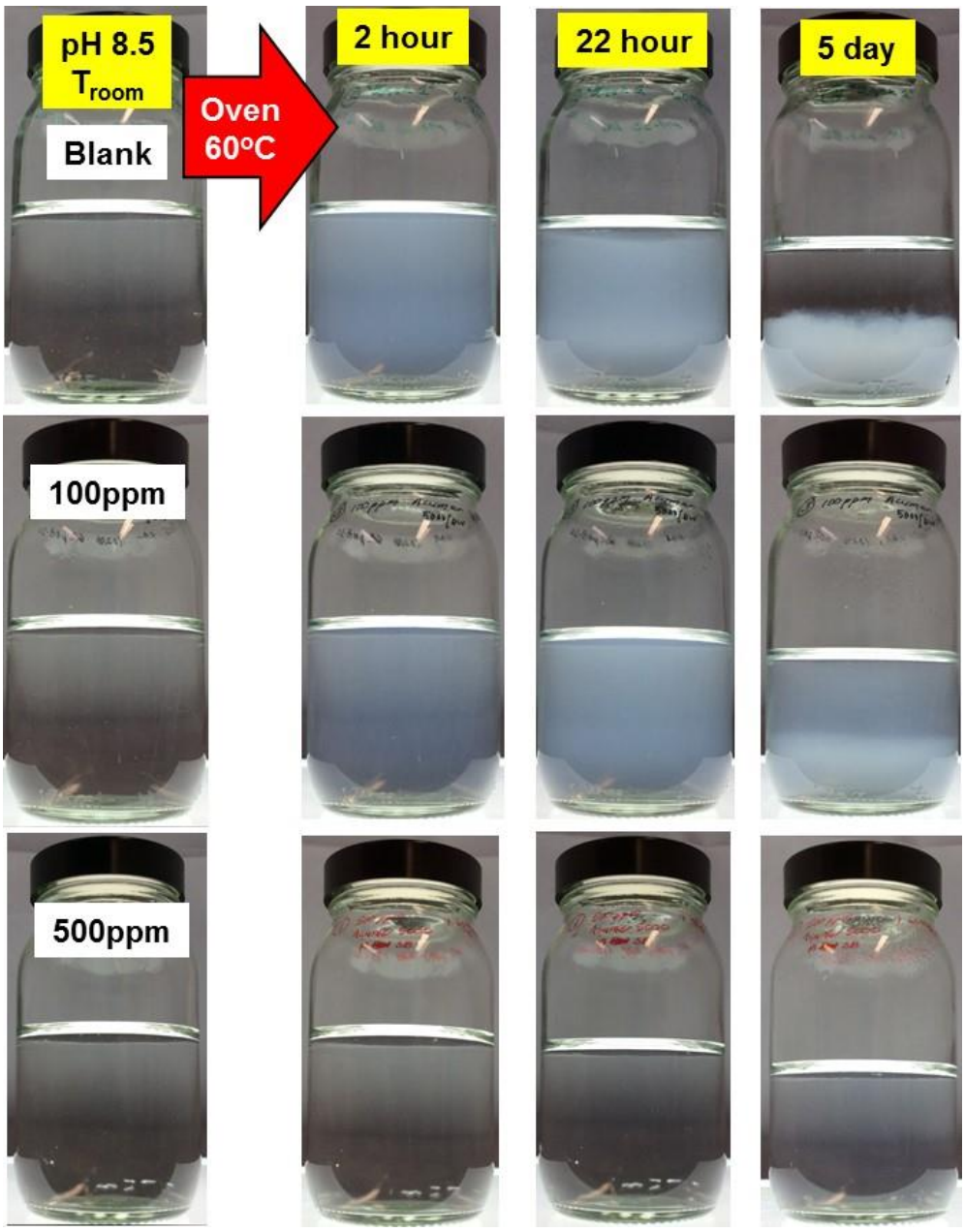

Figure 5-41 A5 IE Test observation in silicate system of 60Mg:940Si at 60°C, pH8.5 (0 to 500ppm A5)

The same observation can be made for the *blank* in the VS-Co IE Test (see Figure 5-42) which means that the blank is repeatable and reproducible. Gel-like precipitates were observed in the mixed brine with the addition of 20, 50 and 100 ppm VS-Co, 2 hours after heating in the oven and the precipitate settled to the bottom leaving a clear layer solution after 5 days. At 500ppm of VS-Co, the mixed brine became slightly cloudy after 2 hours heating. However, no pictures of this system are available for H3 IE Test as the test was conducted in HDPE bottles.

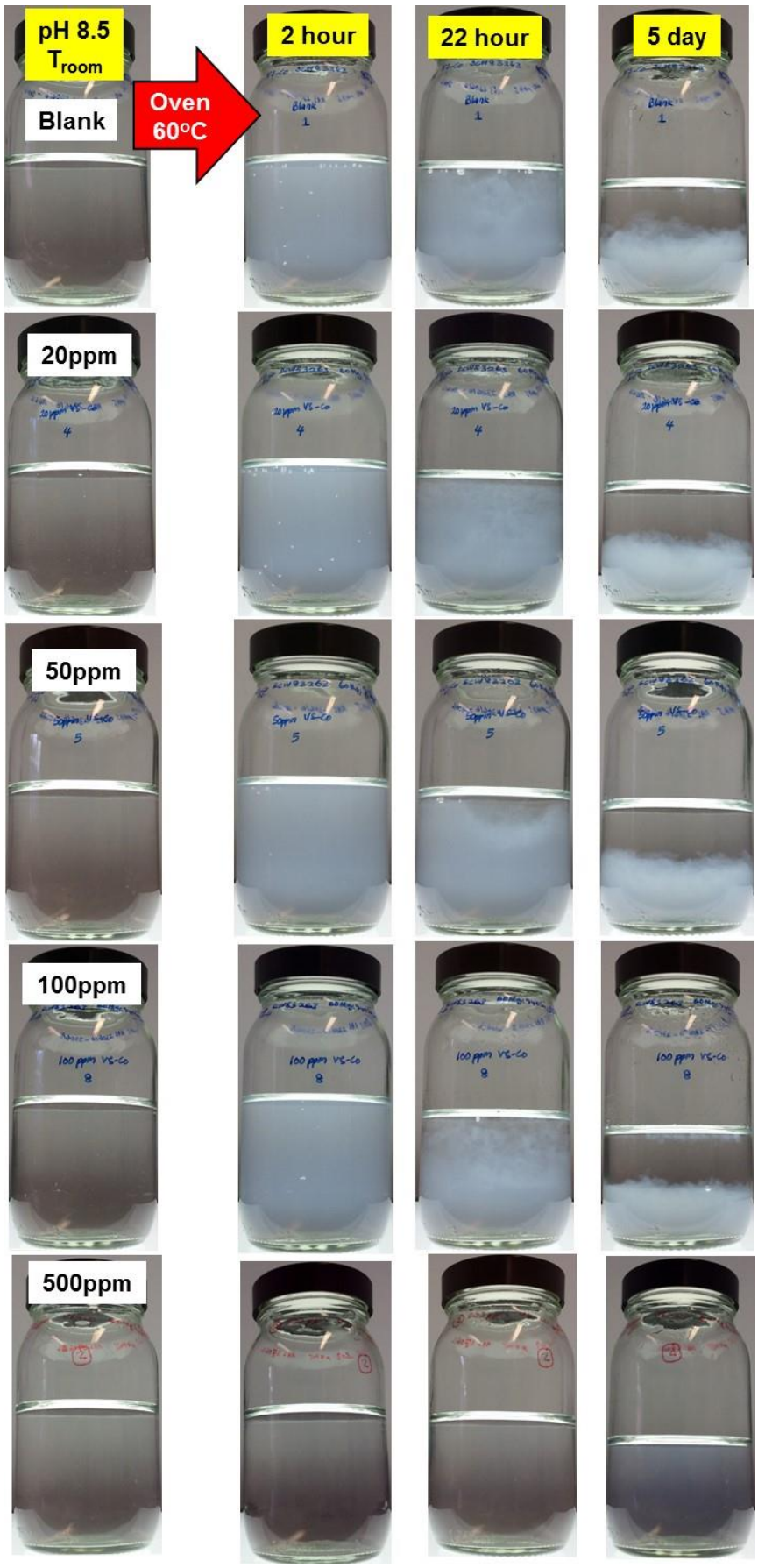

Figure 5-42 VS-Co IE Test observation in silicate system of 60Mg:940Si at 60°C, pH8.5 (0 to 500ppm VS-Co)

5.4.2 ICP-EOS Analysis

ICP-EOS data analysis revealed that A5 and VS-Co have little inhibition (5 to 18%) towards amorphous magnesium silicate scale (see Figure 5-43) and none towards amorphous silica scale (see Figure 5-44) at concentrations up to 100ppm. As shown in the same figures, H3 achieves about 30-40% inhibition efficiency towards the amorphous magnesium silicate scale but none to amorphous silica at 100ppm.

Figure 5-43 and Figure 5-44 clearly indicate that at 500ppm, A5 can stop both silicate scales i.e. ≥90% at 2 and 22 hours while VS-Co shows good inhibition with 79-82% towards amorphous magnesium silicate scale and 75-78% towards amorphous silica.

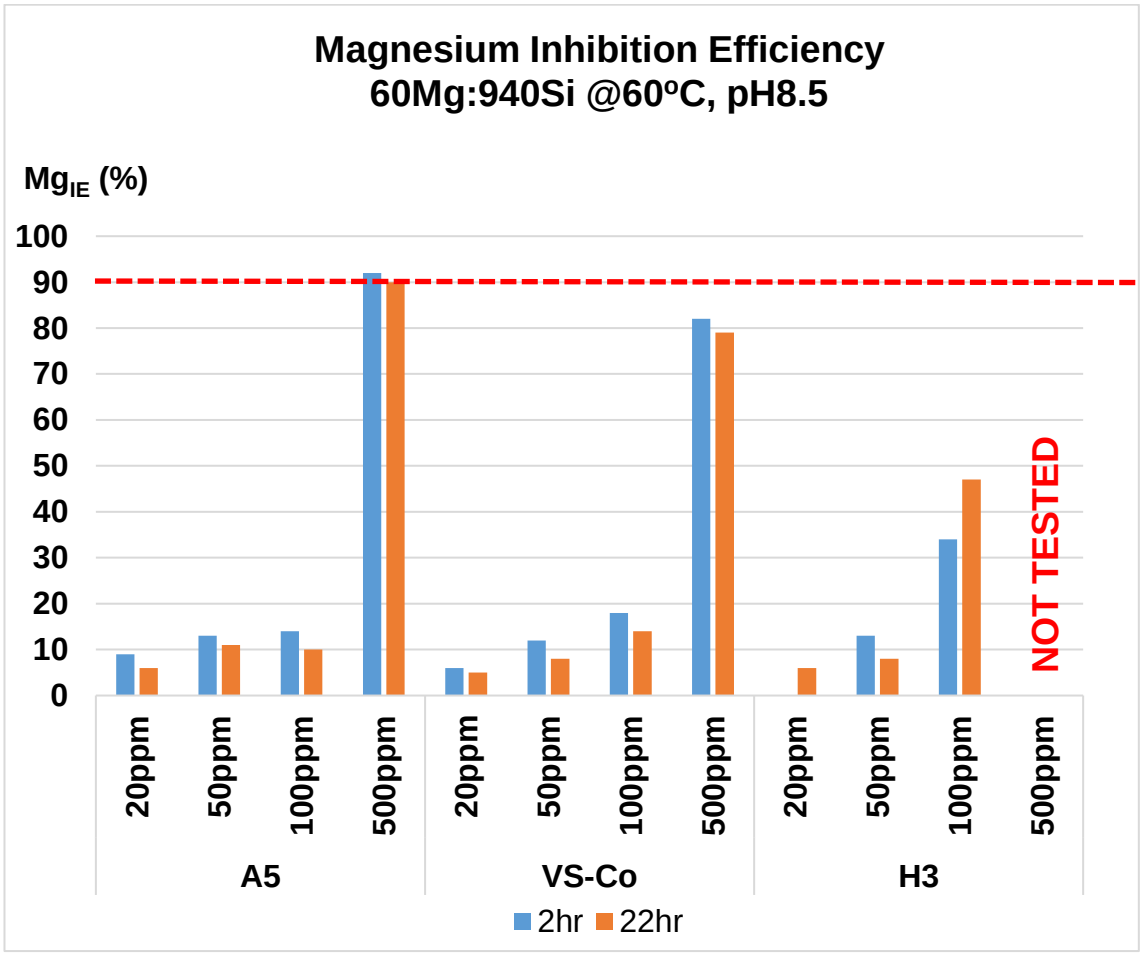

Figure 5-43 Inhibition efficiency percentage (Mg as precipitated ion in scaled solution) for silicate system of 60Mg:940Si at 60°C, pH8.5

Interestingly, A5 showed excellent inhibition efficiency to stop silicate scale (i.e. both amorphous magnesium silicate scale and amorphous silica) at 500ppm. However, this concentration is considered too high to be economically feasible and hence much lower A5 concentrations were subsequently tested (see below).

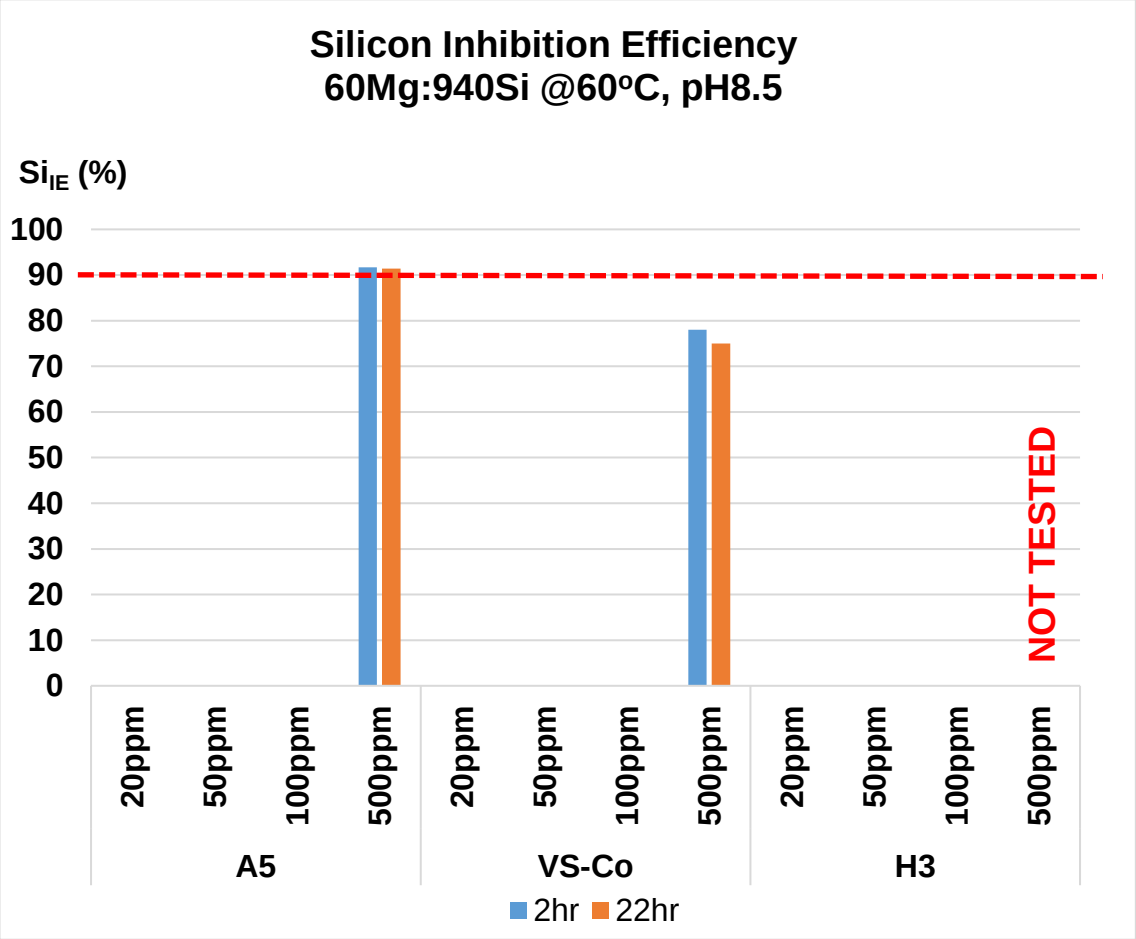

Figure 5-44 Inhibition efficiency percentage (Si as precipitated ion in scaled solution) for silicate system of 60Mg:940Si at 60ºC, pH8.5

5.4.3 pH Profiles

Figure 5-45, Figure 5-46 and Figure 5-47 show the pH profiles for the A5, VS-Co and H3 IE Tests correspondingly.

As can be seen in Figure 5-45, generally the pH value for the "blank" and "Mg/Si/A5 - for 20, 50 and 100ppm" increased slightly within 2 hours (pH>8.5) and then the pH reduced subsequently; i.e. between 7.8<pH<8.3 at 22 hours and between 7.6<pH<7.8 at 5 days.

When 500ppm of A5 was added to the mixed brine, the pH increased after 2 hours (pH 8.8) before reducing back to ~pH8.5 after 22 hours and then to ~pH8.3 after 5 days.

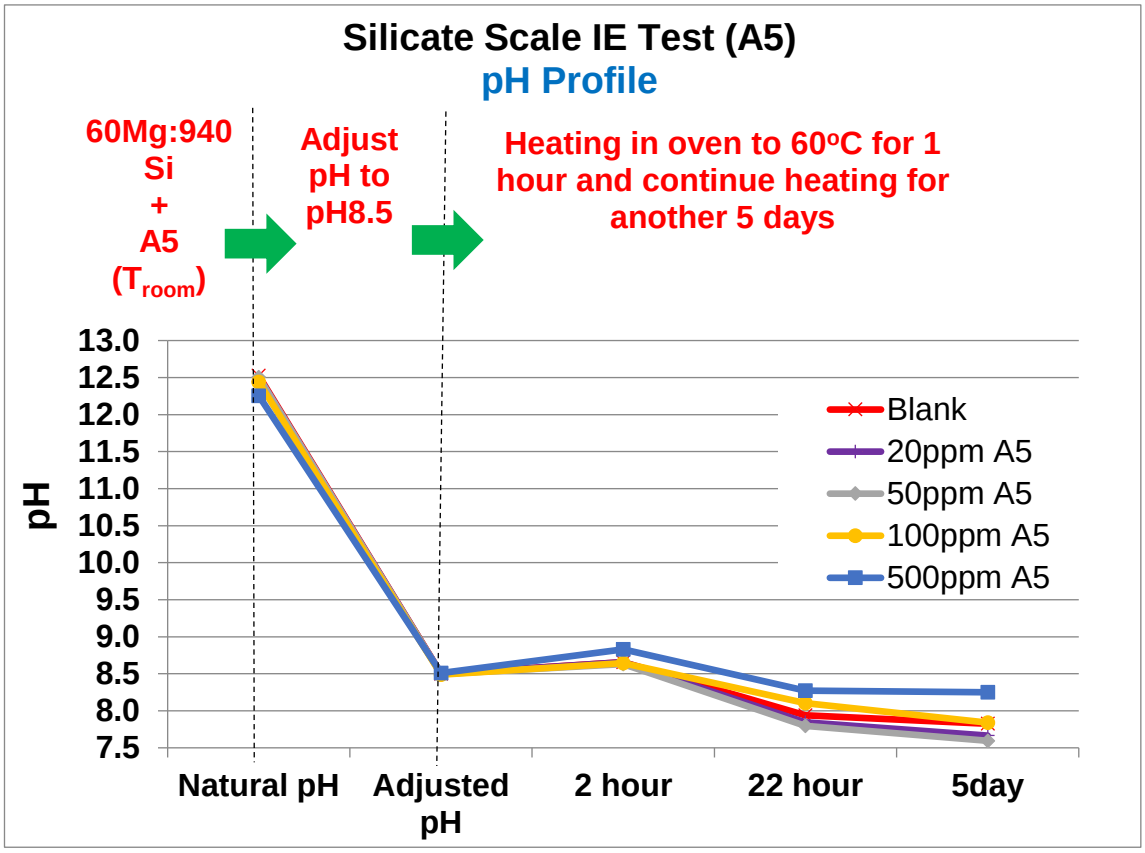

Figure 5-45 pH profiles for A5 IE Test in silicate system of 60Mg:940Si at 60°C, pH8.5

Results in Figure 5-46 demonstrate that, generally the pH value for the "blank" and "Mg/Si/VS-Co - for 20, 50 and 100ppm" increased slightly within 2 hours (8.5<pH<8.6) and then reduced back subsequently i.e. ~pH8 at 22 hours and 7.6<pH<7.8 at 5 days.

When 500ppm of VS-Co is added to the mixed brine, the pH increased after 2 hours (pH8.9); before reducing back to ~pH8.6 after 22 hours; then to ~pH8.5 after 5 days.

The pH profiles for the samples in the H3 test are plotted in Figure 5-47 showing that pH generally increased after 2 hours and then the pH subsequently reduced to a lower value. However, the pH profile within 2 and 22 hours was not studied in the context of this test.

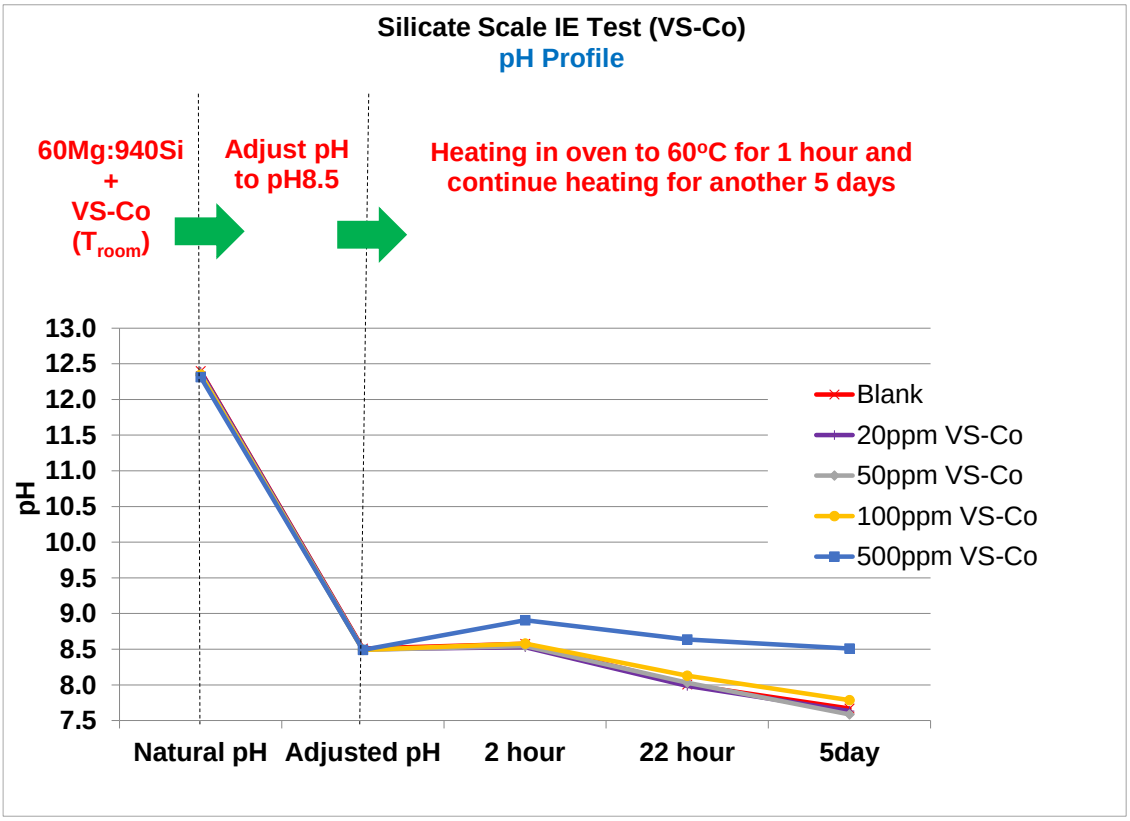

Figure 5-46 pH profiles for VS-Co IE Test in silicate system of 60Mg:940Si at 60°C, pH8.5

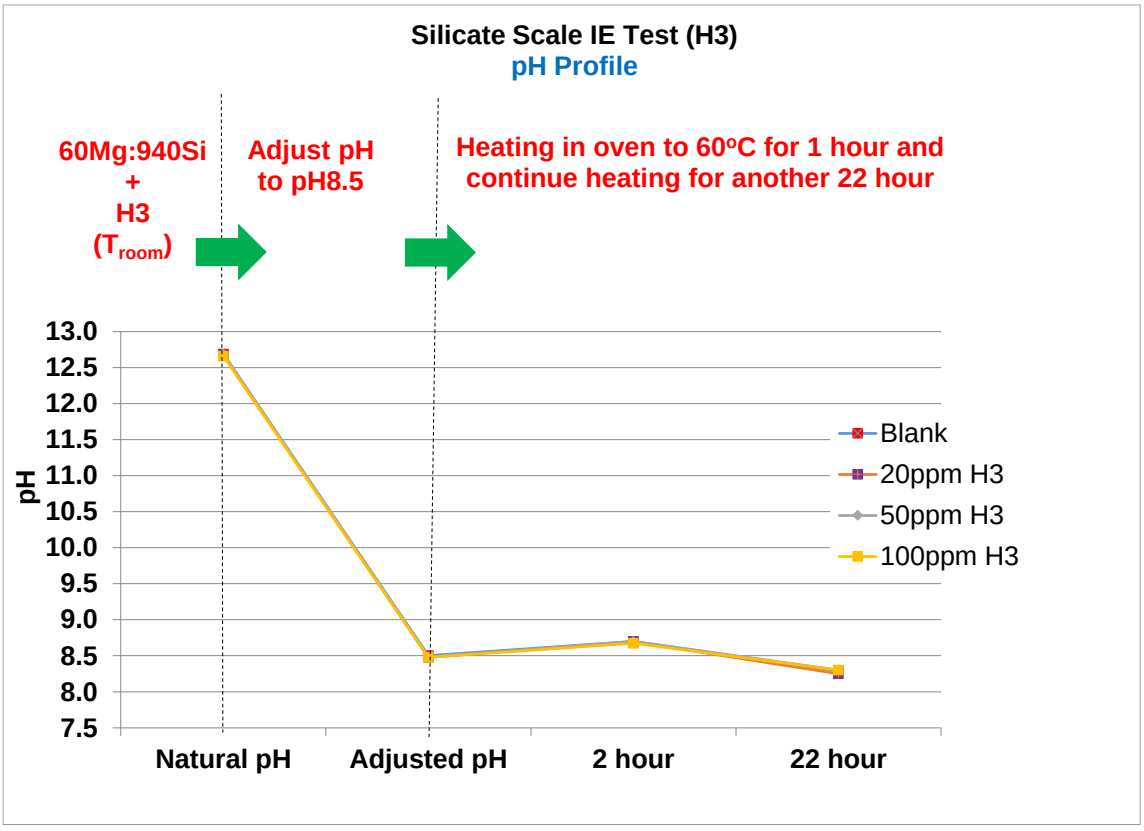

Figure 5-47 pH profiles for H3 IE Test in silicate system of 60Mg:940Si at 60°C, pH8.5

5.4.4 A5 Minimum Inhibitor Concentration (MIC_{static})

The Minimum Inhibitor Concentration under static conditions (MIC_{static}) for A5 was further investigated and determined as shown in Figure 5-48. It can be seen evidently that 500ppm of A5 successfully stops the formation of silicate scales (i.e. IE $_{Mg}$ % and IE $_{Si}$ % >90%) for this silicate scaling system (60Mg:940Si). This low molecular weight, water soluble polymer (Terpolymer of acrylic acid, 2-acrylamido-2-methylpropane sulfonic acid, non-ionic monomer) was found to be very effective at inhibiting the silicate scale at high concentration.

This will continue with further investigation of spectra produced from "*worst"* base case 60Mg:940Si when we tried inhibit this system using 100ppm of A5, VS-Co and H3 respectively. It is clearly shown Figure 5-49 that all spectra produced are the same for all inhibitors tested i.e. 100ppm A5, VS-Co and H3 respectively. A further analysis of the spectra indicated to us that no band appeared at bandwidth ~1278 to 1558cm^{-1} which means no magnesium hydroxide was produced in this silicate system.

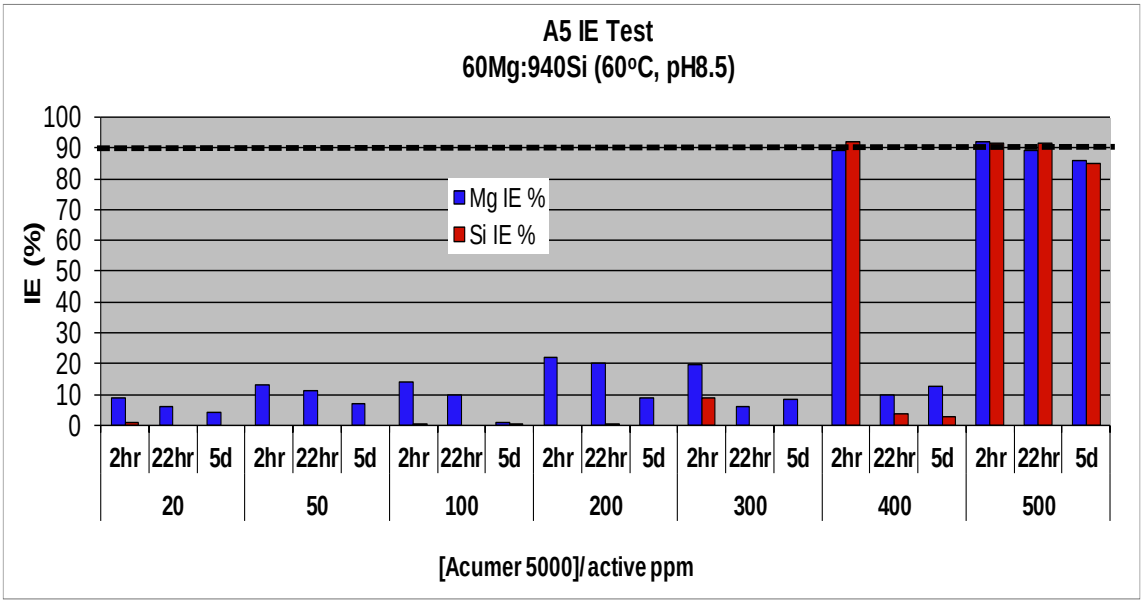

Figure 5-48 A5 inhibition efficiency percentage for silicate system of 60Mg:940Si at 60°C, pH8.5

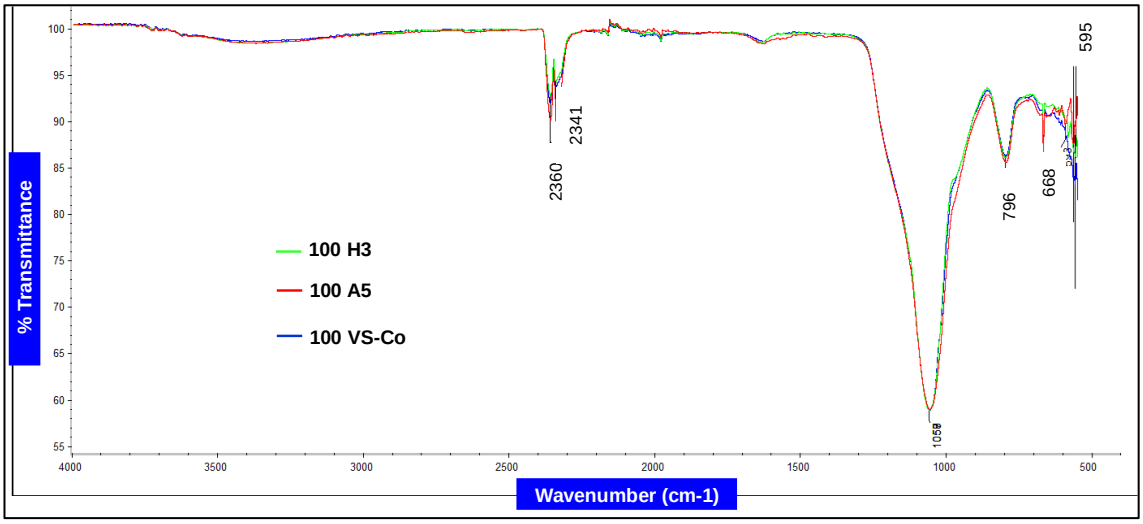

Figure 5-49 FTIR spectra of "*worst*" base case 60Mg:940Si in IE Test at test condition of 60ºC, pH8.5; [SI] = 100ppm

5.5. INHIBITION EFFICIENCY STUDY IN SILICATE SYSTEM 60Mg:752Si AT 60ºC, pH8.5

We continued to study the most promising scale inhibitor (i.e. A5) but for these tests the silicon level was reduced to 752ppm (10% lower than the *"worst"* base case). This study was carried out to investigate further if this inhibitor could work better at a much lower concentration than 500ppm A5.

5.5.1 Observations

Results in Figure 5-50 show that the blank in the silicate system of 60Mg:752Si became slightly cloudy after being mixed and pH-adjusted at room temperature. The system became cloudy after 2 hours and gel-like precipitate formed after 22 hours. After 5 days, the precipitate settled to the bottom leaving a clear layer of solution. When 100ppm of A5 was added to the same silicate system, the mixed brine stays clear even after being pH-adjusted at room temperature. The mixed brine only became slightly cloudy after 2 hours and only became slightly hazier, even after 5 days.

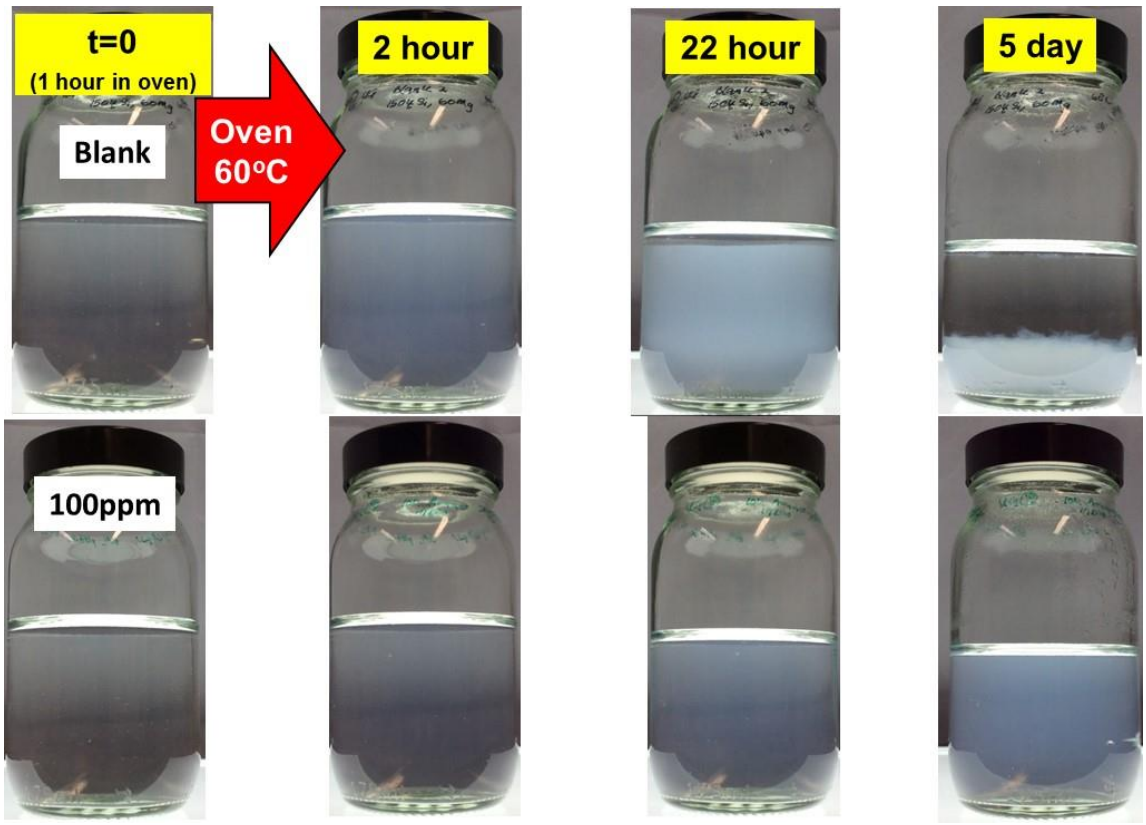

Figure 5-50 A5 IE Test observation in silicate system of 60Mg:752Si at 60°C, pH8.5 (0 to 100ppm A5)

5.5.2 ICP-EOS Analysis

As can be seen from the A5 IE results in Figure 5-51, the inhibition efficiency towards amorphous magnesium silicate scale is slightly improved ~30% at 2 and 22 hour while there is only a little inhibition towards amorphous silica, IE $_{Si}$ % ~15-17%.

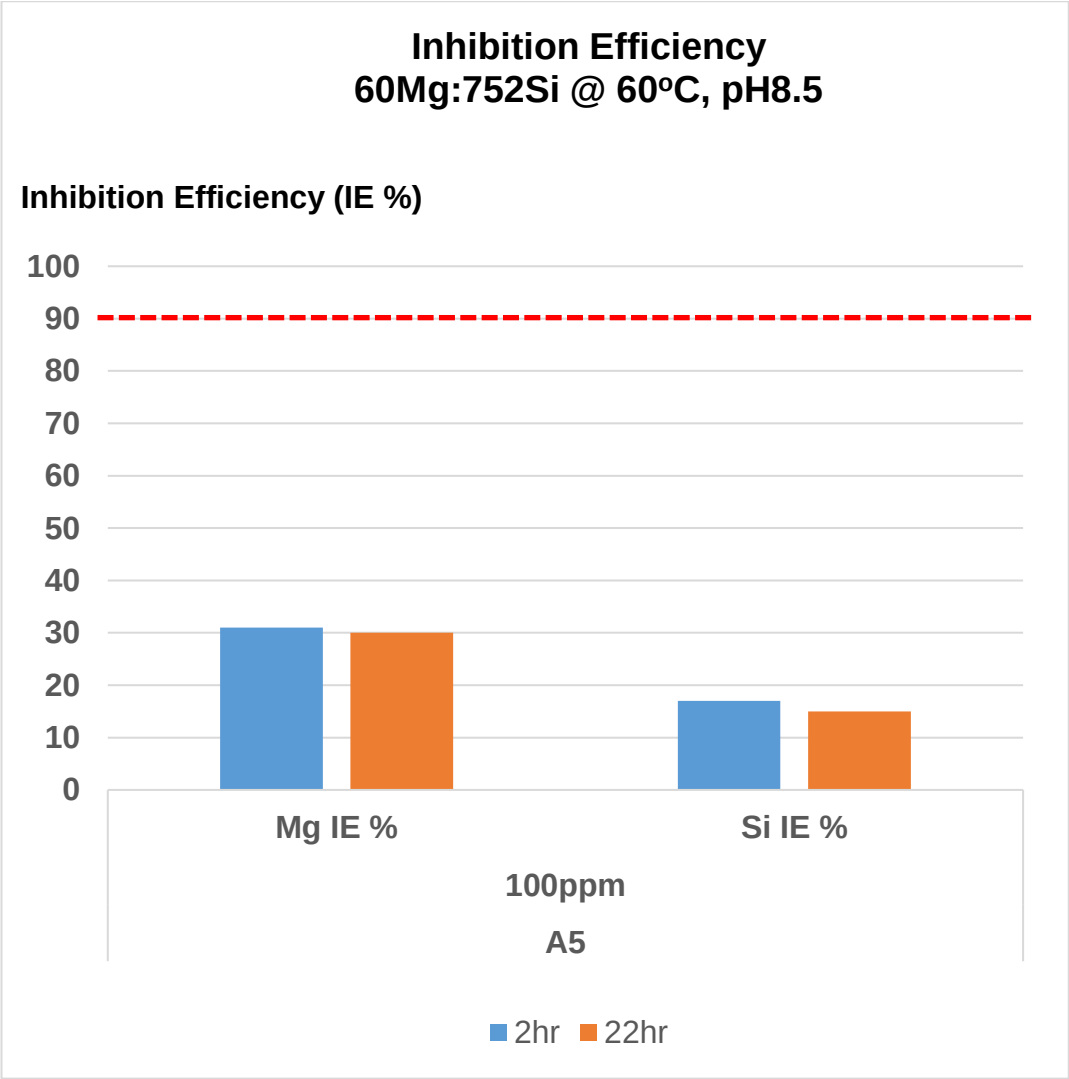

Figure 5-51 IE $_{Mg}$ % (Mg as precipitated ion in scaled solution) and IE $_{Si}$ % (Si as precipitated ion in scaled solution) for silicate system of 60Mg:752Si at 60ºC, pH8.5

5.5.3 pH Profiles

The results in Figure 5-52 show that the pH for this silicate system reduced with time, i.e. ~pH8.5 at 2 hours, ~pH8.0 at 22 hours and between 7.5<pH<8.0 after 5 days.

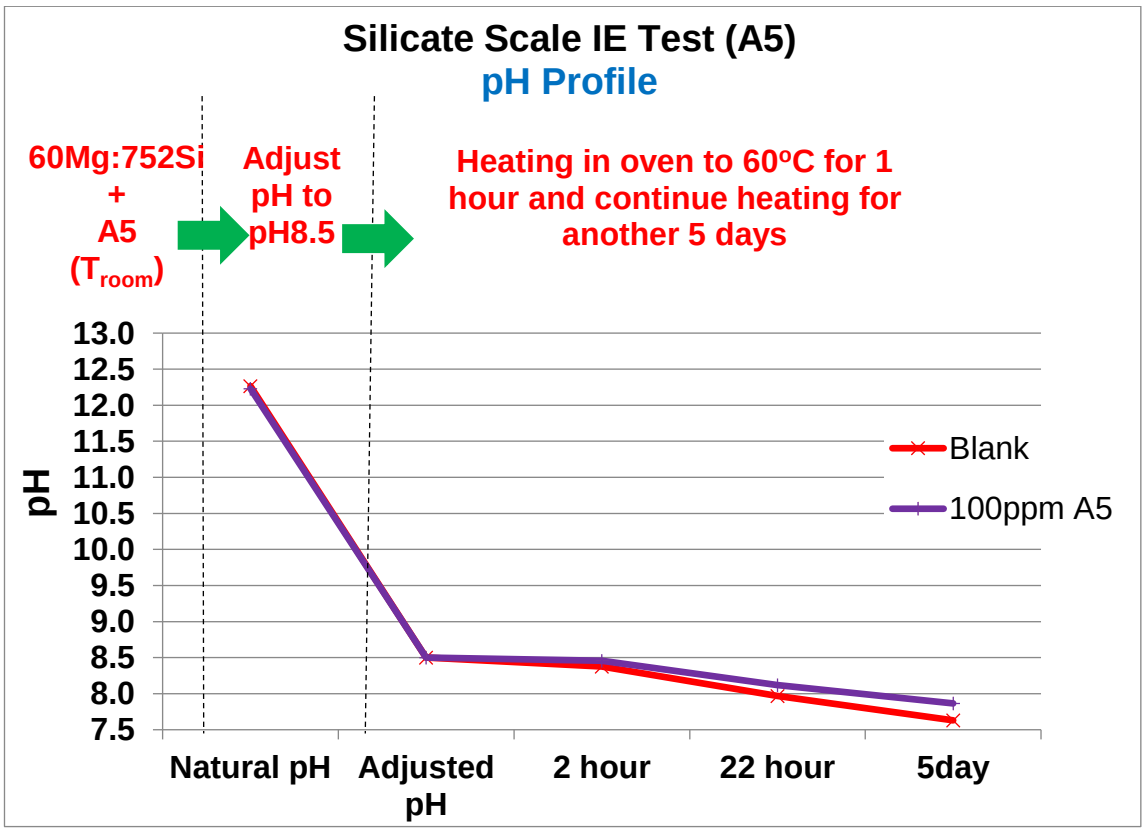

Figure 5-52 pH profiles for A5 IE Tests in silicate system of 60Mg:752Si at 60°C, pH8.5

5.6. INHIBITION EFFICIENCY STUDY IN SILICATE SYSTEM 60Mg:564Si AT 60°C, pH8.5

As discussed in Section 5.5, it was shown that the addition of 100ppm A5 to the 60Mg:752Si system was unsuccessful in stopping the formation of silicate scale. Therefore, the IE test was reduced to a silicon level of 564ppm (20% lower than the base case). This experiment was performed to further investigate if this inhibitor (A5) would work better at much lower concentrations. Four concentrations of A5 i.e. 20, 50, 100 and 200ppm were tested in a silicate system with 60Mg:564Si.

5.6.1 Observations

The pictures for the silicate system with the addition of 20 and 50ppm are not available as the test were conducted separately in HDPE bottles. It is quite clear that the physical appearance of the mixed brine of this silicate system was not very different from the

previous system (i.e. 60Mg:752Si) when the same 100ppm of A5 was added. As can be seen in Figure 5-53, the mixed brine (with 100ppm A5) stays clear when pH is adjusted at room temperature and this mixed brine became only slightly cloudy and the cloudiness increased with residence time.

The mixed brine with 200ppm of A5 was almost clear, even after 2 hours. It can be seen that the mixed brine was less hazy compared to when 100ppm A5 was added to the same silicate system.

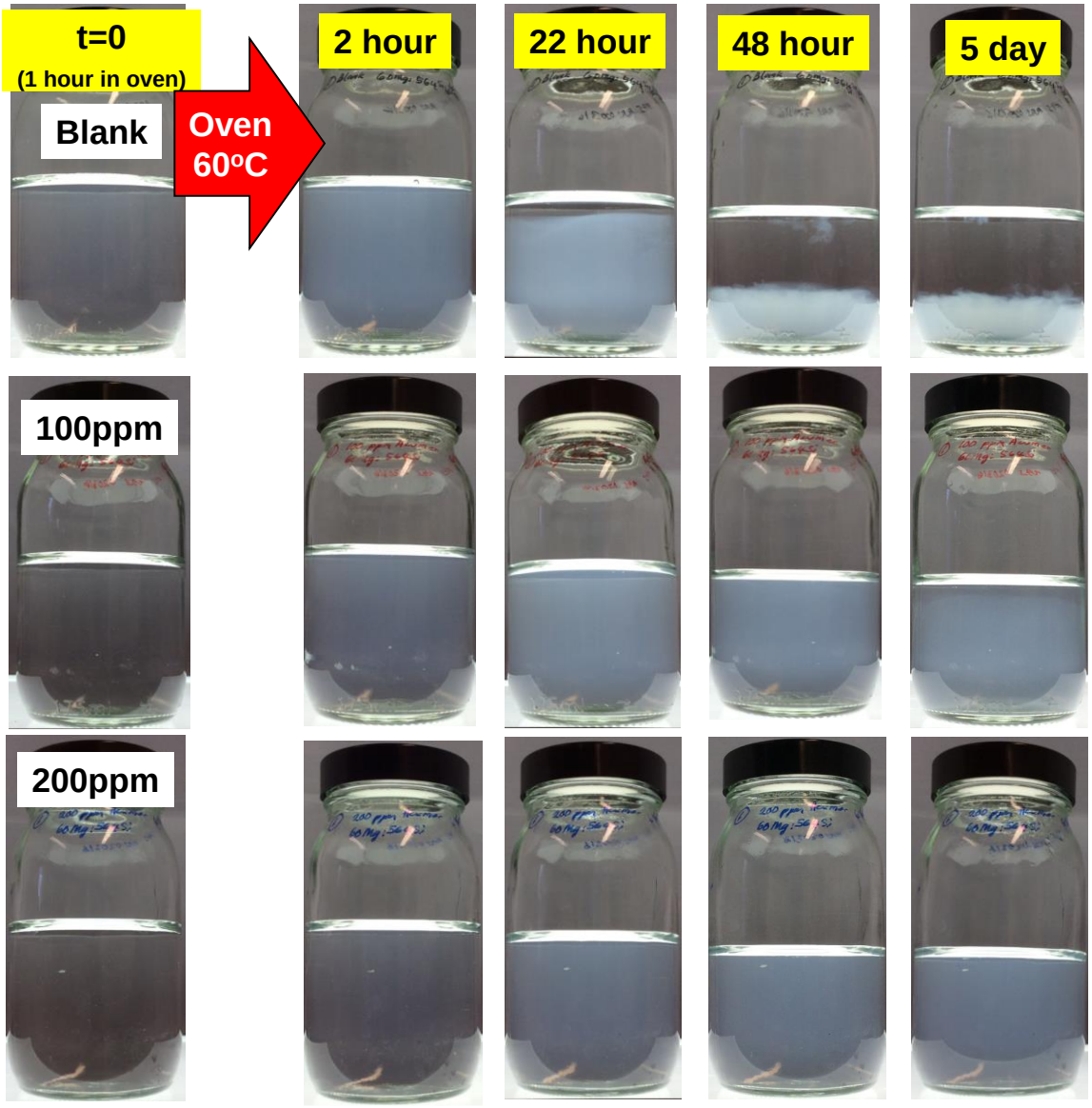

Figure 5-53 A5 IE Test observations in silicate system of 60Mg:564Si at 60°C, pH8.5 (0 to 200ppm A5)

5.6.2 ICP-EOS Analysis

Figure 5-54 shows that the A5 failed to inhibit the amorphous magnesium silicate even at the highest concentration of 200ppm. The IE $_{Mg}$ % at 200ppm is only ~29% and also, the addition of 200ppm of A5 had no effect in inhibiting amorphous silica scale.

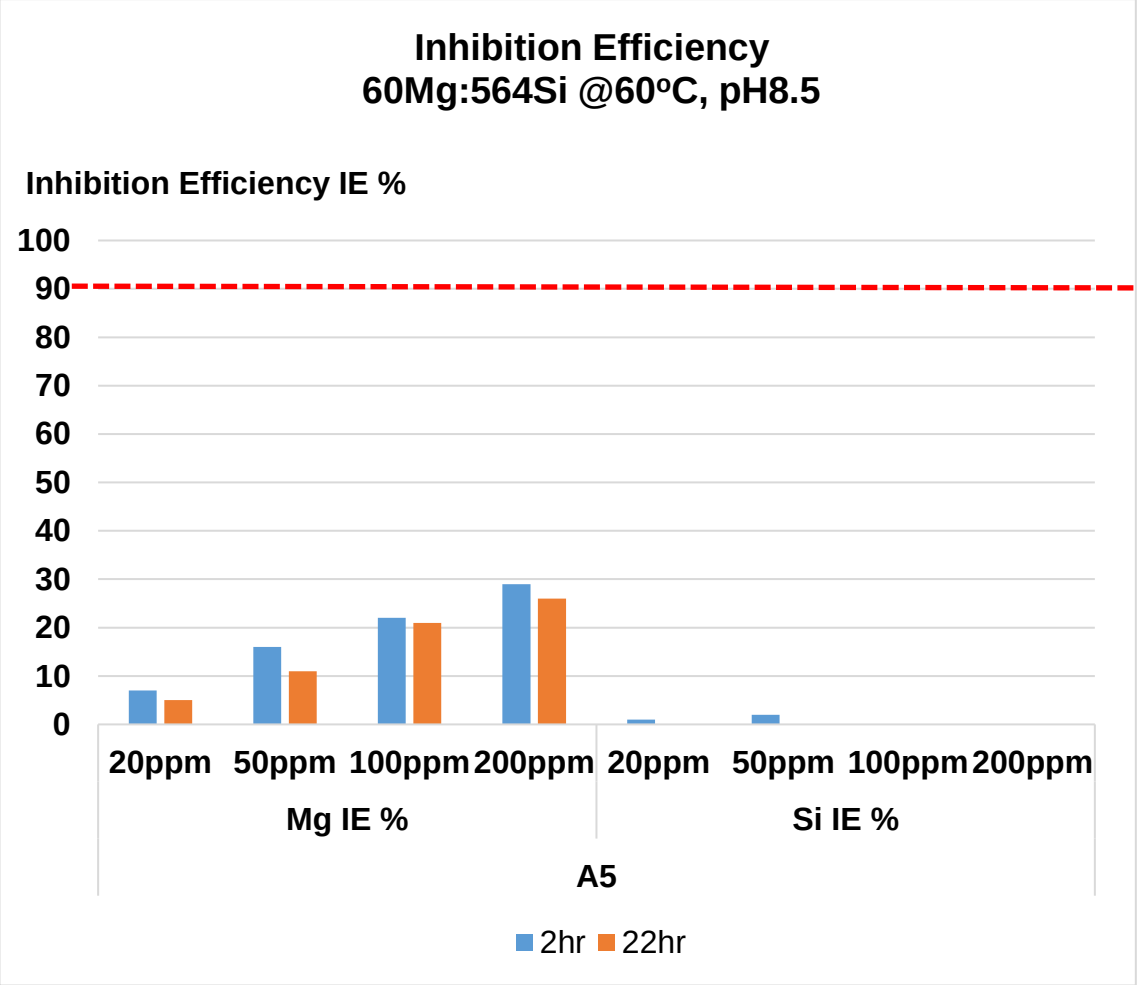

Figure 5-54 IE $_{Mg}$ % (Mg as precipitated ion in scaled solution) and IE $_{Si}$ % (Si as precipitated ion in scaled solution) for silicate system of 60Mg:564Si at 60ºC, pH8.5

5.6.3 pH Profiles

Figure 5-55 shows the pH profiles for the silicate system of 60Mg:564Si when 20 to 200ppm A5 was added. Generally, the pH value for all blank and inhibitor-containing brine at all concentrations was essentially not changed up to 2 hours (~pH8.5) before reducing to pH ~ 7.5 at 5 days.

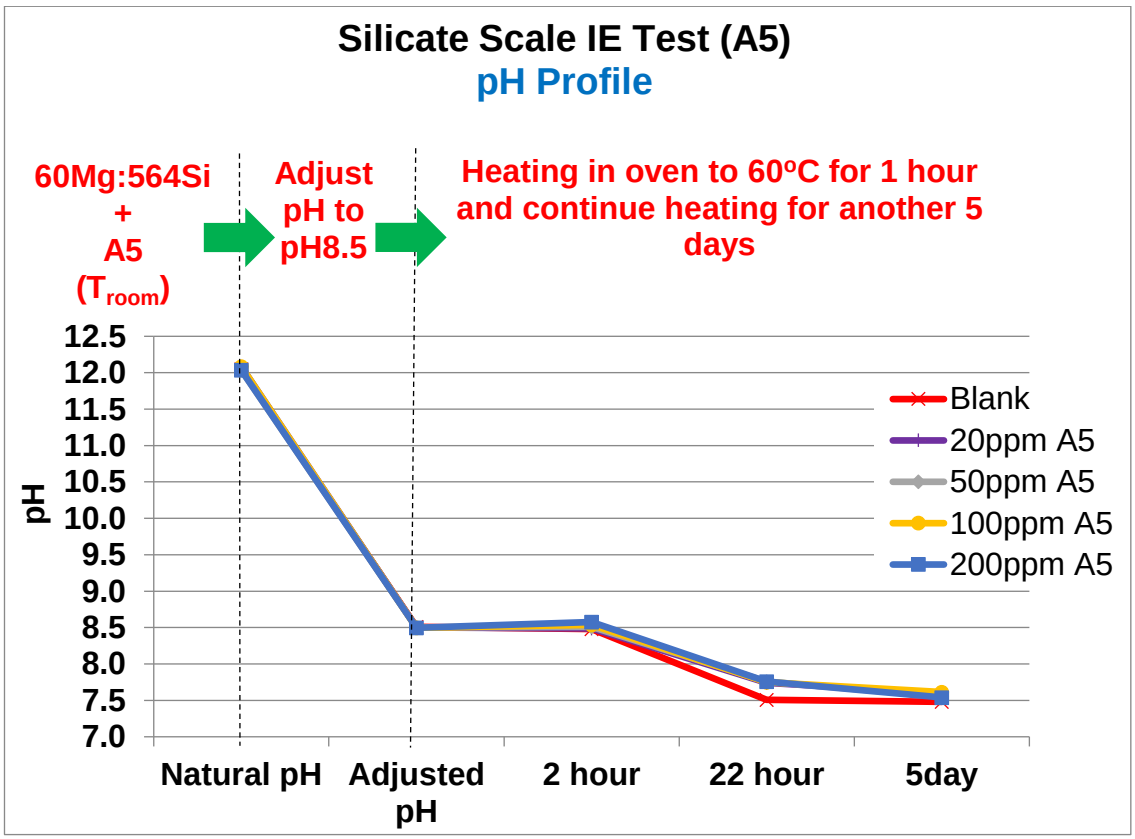

Figure 5-55 pH profiles for A5 IE Tests in silicate system of 60Mg:564Si at 60°C, pH8.5

5.7. INHIBITION EFFICIENCY STUDY IN SILICATE SYSTEM 60Mg:300Si AT 60°C, pH8.5

These experiments were carried out after it was observed in section 5.6 that the addition of 200ppm of A5 in the silicate system of 60Mg:564Si at 60°C, pH at 8.5, could only stop 30% of the amorphous magnesium silicate scale from forming and it had no effect on the amorphous silica scale. Hence, a further investigation was conducted at a much lower silicon level of [Si] = 300ppm i.e. the system containing only about one third of the *"worst"* base case silicon concentration.

5.7.1 Observations

Figure 5-56 shows the physical appearance of the silicate system 60Mg:300Si at 60°C, pH8.5 with the addition of 100ppm and 300pppm A5. It can be seen that A5 can inhibit the silicate scale formation when 100ppm of A5 was added, as the mixed brine became only slightly cloudy after 22 hours as compared to the blank solution. In fact, the mixed

brine with 100ppm A5 remains slightly cloudy even after 7 days. The silicate scales appear to be completely inhibited when 300ppm of A5 was added since the mixed brine stayed clear up to 48 hours after mixing (but later ICP-EOS analysis revealed that IE < 90% i.e. IE $_{Mg}$ % = 78-84% & IE $_{Si}$ % = 69-79%) and only became slightly hazy after 7 days (it was less hazy compared to 100ppm A5 at the same residence time). These observations are very consistent with the ICP-EOS analysis discussed in Section 5.7.2.

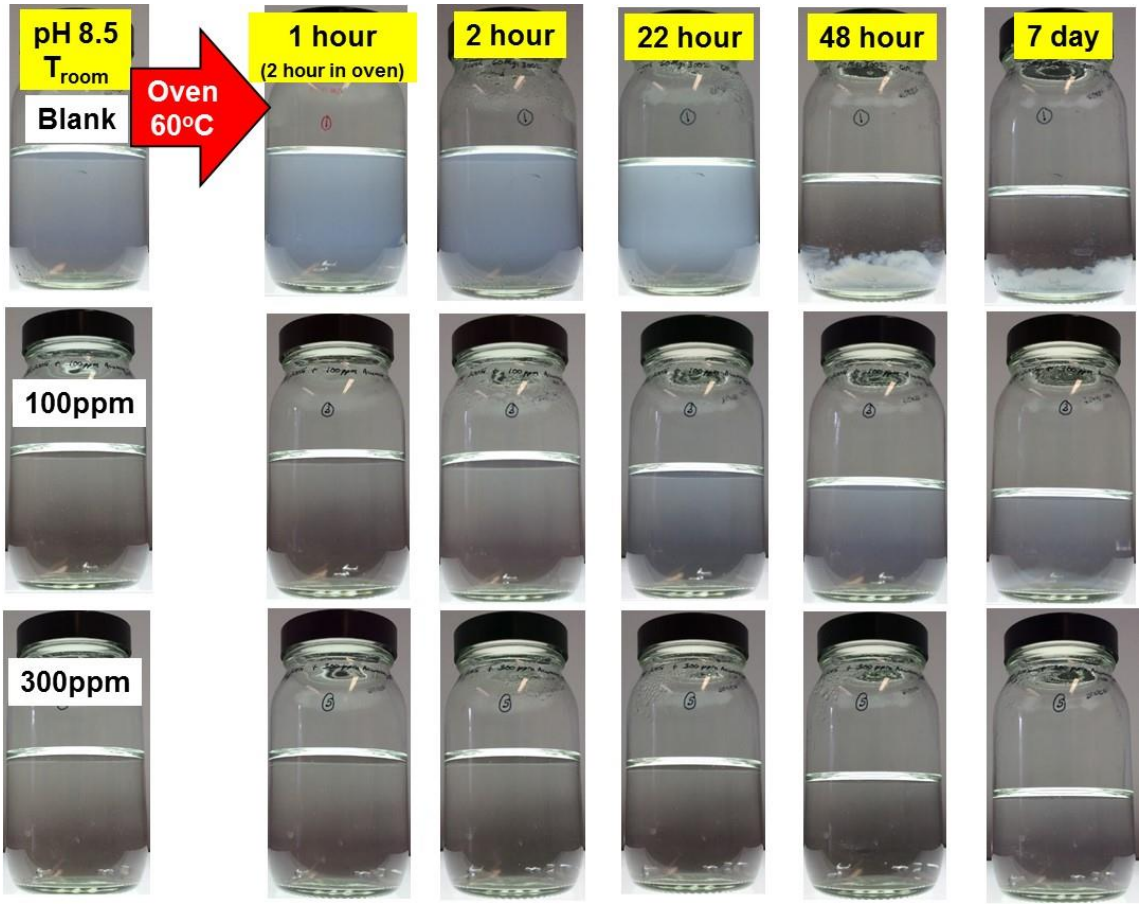

Figure 5-56 A5 IE Test observations in silicate system of 60Mg:300Si at 60°C, pH8.5 (0 to 300ppm A5)

Figure 5-57 showed that the addition of 100ppm VS-Co to the same silicate system shows that the mixed brine started to appear slightly cloudy only after 1 hour. This mixed brine became cloudier and the precipitate settled to the bottom leaving a clear solution on top, just like in the blank after 5 days. This did not occur for the brine with 100ppm A5 where the mixed brine became only slightly cloudy even after 7 days. It is evident that A5 is more efficient in combating silicate scale than is the VS-Co.

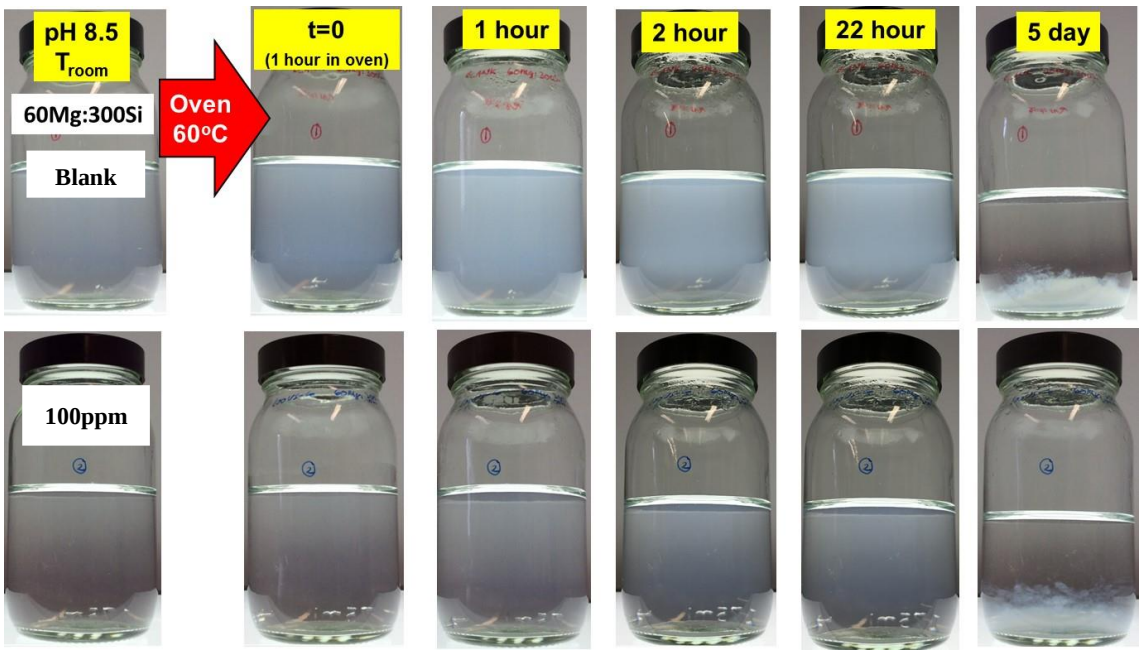

Figure 5-57 VS-Co IE Test observations in silicate system of 60Mg:300Si + 100VS-Co at 60°C, pH8.5

5.7.2 ICP-EOS Analysis

Results in Figure 5-58 show that the addition of 100ppm of A5 in this silicate system was much better at controlling the formation of amorphous magnesium silicate; an IE $_{Mg}$ % ~37 - 52% is observed for the magnesium silicate although little inhibition of the amorphous silica scale is seen (IE $_{Si}$ % ~8%). VS-Co also demonstrates approximately the same inhibition efficiency towards the formation of amorphous magnesium silicate scale; i.e. IE $_{Mg}$ % ~48 – 53% but almost no inhibition towards amorphous silica scale (IE $_{Si}$ % ~0%).

With the addition of 300ppm A5, not only is there an increase in the inhibition of the amorphous magnesium silicate scale (IE $_{Mg}$ % ~78 - 84%) but there is also a significant improvement in the inhibition of amorphous silica scale (IE $_{Si}$ % ~69 - 79%). Nonetheless the scale is not completely stopped (IE % is still less than 90%) in this silicate system and 300ppm of inhibitor is still considered as being too high to be economically feasible.

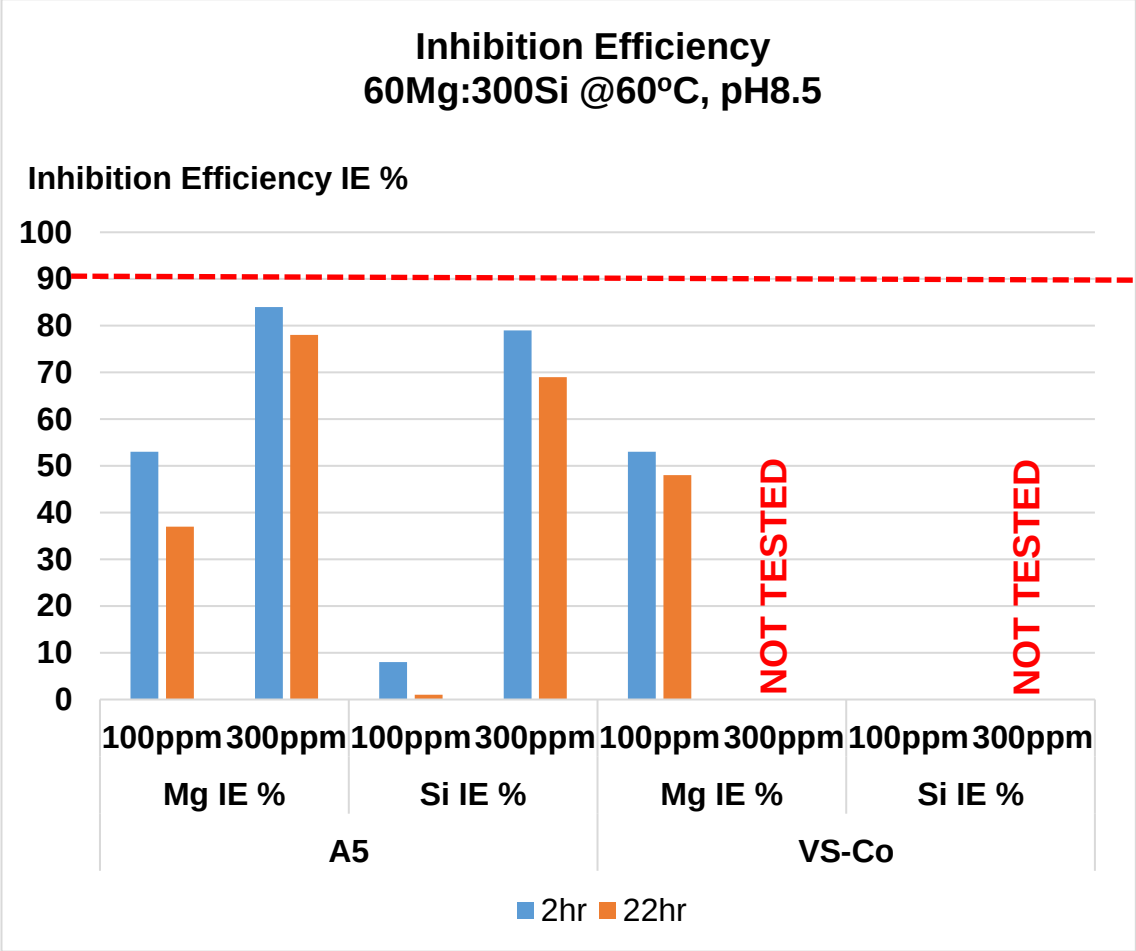

Figure 5-58 IE $_{Mg}$ % (Mg as precipitated ion in scaled solution) and IE $_{Si}$ % (Si as precipitated ion in scaled solution) for silicate system of 60Mg:300Si at 60ºC, pH8.5

5.7.3 pH Profiles

Figure 5-59 and Figure 5-60 show the pH profiles for the inhibition efficiency test for the 60Mg:300Si system at 60ºC, pH8.5 using A5 and VS-Co polymer, respectively. Generally, the pH values of the mixed brines for both inhibitors at all concentrations decreased gradually with reaction time.

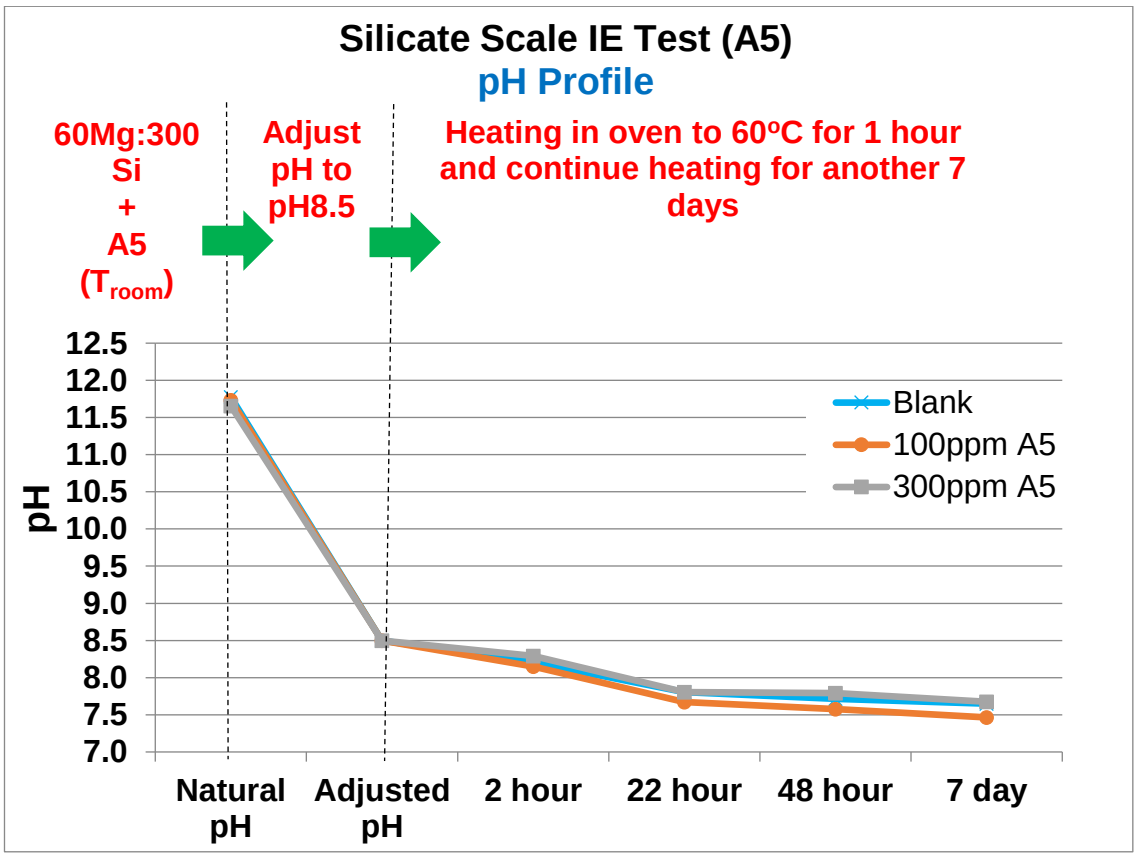

Figure 5-59 pH profiles for A5 IE Tests in silicate system of 60Mg:300Si at 60°C, pH8.5

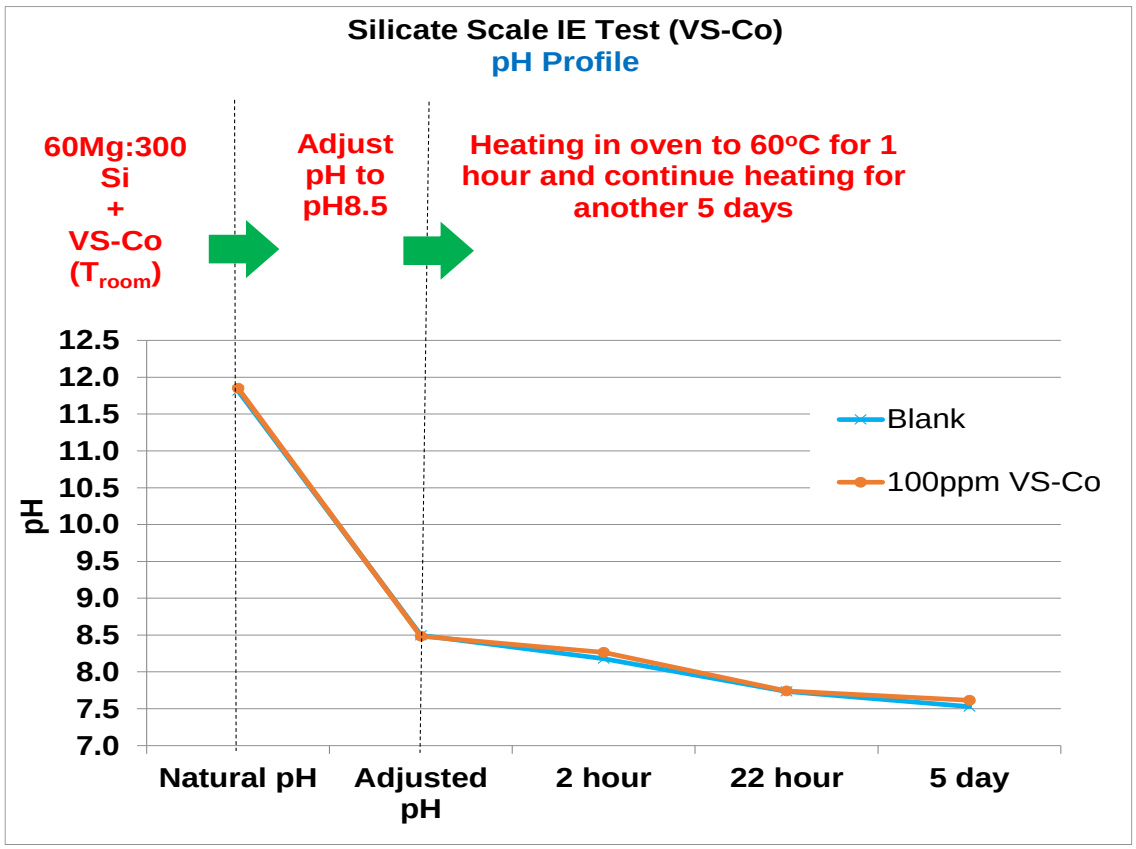

Figure 5-60 pH profiles for VS-Co IE Tests in silicate system of 60Mg:300Si at 60°C, pH8.5

5.8. INHIBITION EFFICIENCY STUDY IN SILICATE SYSTEM 30Mg:75Si AT 60°C, pH8.5

As discussed in the previous section, the addition of 300ppm A5 to the silicate system of 60Mg:300Si at 60°C, pH8.5 gave very promising IE results for the inhibition of both the amorphous magnesium silicate scale (IE_{Mg} % = 78 - 84%) and the amorphous silica scale (IE_{Si} % = 69 - 79%). However, these silicate scales cannot be completely stopped even at this relatively high inhibitor concentration.

Therefore, both magnesium and silicon ions were reduced further to 30Mg:75Si. These levels were quite similar to those in the water samples from the Forth Plant Daqing Field as reported by Jing et al. (2013). However, these chosen concentrations in our work are somewhat higher than those reported in the Daqing Field study; i.e. 75% and 25% higher for magnesium and silicon ions respectively, so that a more severe silicate scaling case is being considered in this study.

5.8.1 Observations

The observations of the mixed brine in the 30Mg:75Si silicate system with the addition of 20 to 300ppm A5 are shown in Figure 5-61 and Figure 5-62. The precipitate started to form in the blank solution as early as 1 hour after being heated in the oven (reaction time = 0). However, the other mixed brine (SI-containing brine) stays completely clear (to the naked eye) up to 7 days even at the lowest concentration of 20ppm A5. This can be explained by the IE_{Mg}% and IE_{Si}% that was ~70% at 20ppm and these values increased when the A5 concentrations were increased.

Precipitate appeared in the mixed brine (30Mg:75Si) with 20ppm VS-Co after 1 hour of heating in the oven (reaction time = 0) as can be seen in Figure 5-63. When 50ppm VS-Co was added to this silicate system, small particles were detected 2 hours after heating in the oven (reaction time = 1hr). This could only be seen in strong light and it is not quite visible in the pictures. Precipitate appeared after 4 days and this can be seen clearly in the pictures. In 100ppm VS-Co containing brine, small particles were observed 23 hours after being heated in the oven (reaction time = 22hour) and more particles were seen after 4 days. Again, these observations are not visible in the pictures but they could be seen directly under sufficiently strong light.

Figure 5-61 A5 IE Test observations in silicate system of 30Mg:75Si at 60°C, pH8.5 (0 to 50ppm A5)

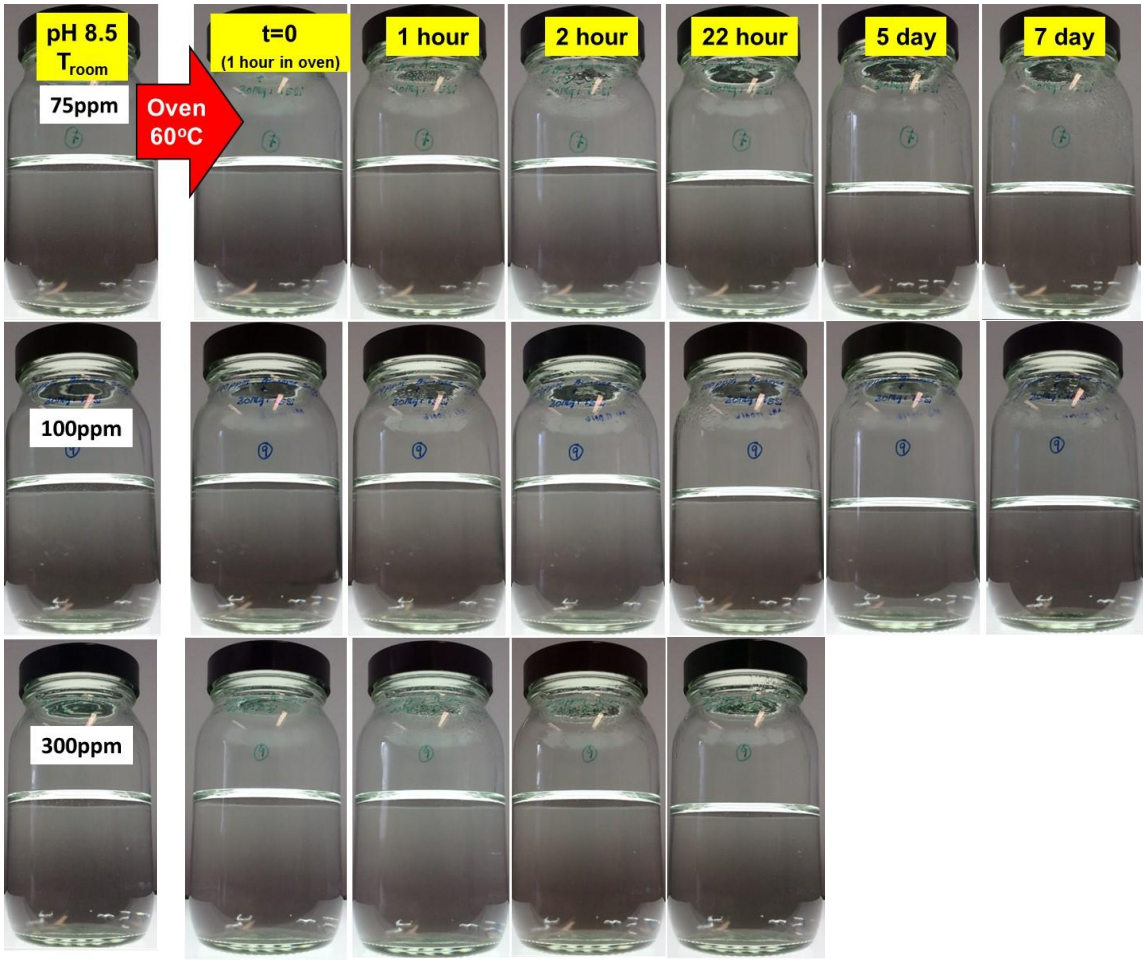

Figure 5-62 A5 IE Test observations in silicate system of 30Mg:75Si at 60ºC, pH8.5 (75 to 300ppm A5)

Figure 5-63 VS-Co IE Test observations in silicate system of 30Mg:75Si at 60°C, pH8.5 (0 to 100ppm VS-Co)

Figure 5-64 shows the observations recorded for the H3 inhibition efficiency test for the same silicate system (30Mg:75Si). For all H3 concentrations; small particles started to be detected after 1 hour of heating in the oven (reaction time = 0) although these particulates are not visible in the pictures.

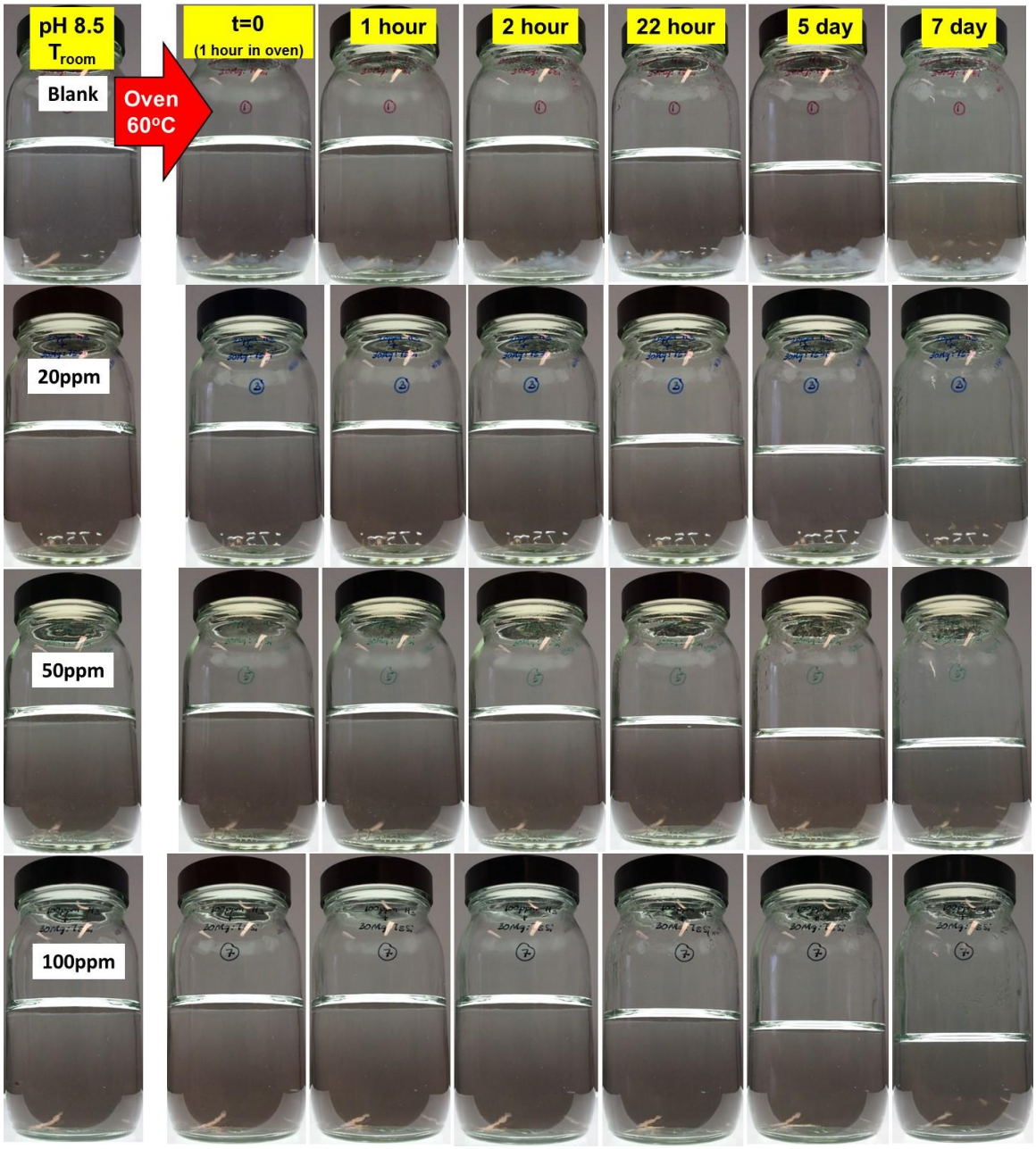

Figure 5-64 H3 IE Test observations in silicate system of 30Mg:75Si at 60°C, pH8.5 (0 to 100ppm H3)

5.8.2 ICP-EOS Analysis

The results in Figure 5-65 demonstrate that A5 and VS-Co successfully inhibit the amorphous magnesium silicate scale formation at 50ppm (i.e. IE $_{Mg}$ % >90%). However, as shown in Figure 5-66, the addition of 50ppm A5 stopped the formation of amorphous silica scale completely, whereas the VS-Co could only stop it to a level of IE $_{Si}$ % ~43 - 65% at the same inhibitor concentration. Also, the IE $_{Si}$ % was only about 58 - 62% when 100ppm VS-Co was added to the silicate system. These findings mean that the VS-Co cannot fully stop the formation of silicate scales even at the highest concentration tested i.e. 100ppm.

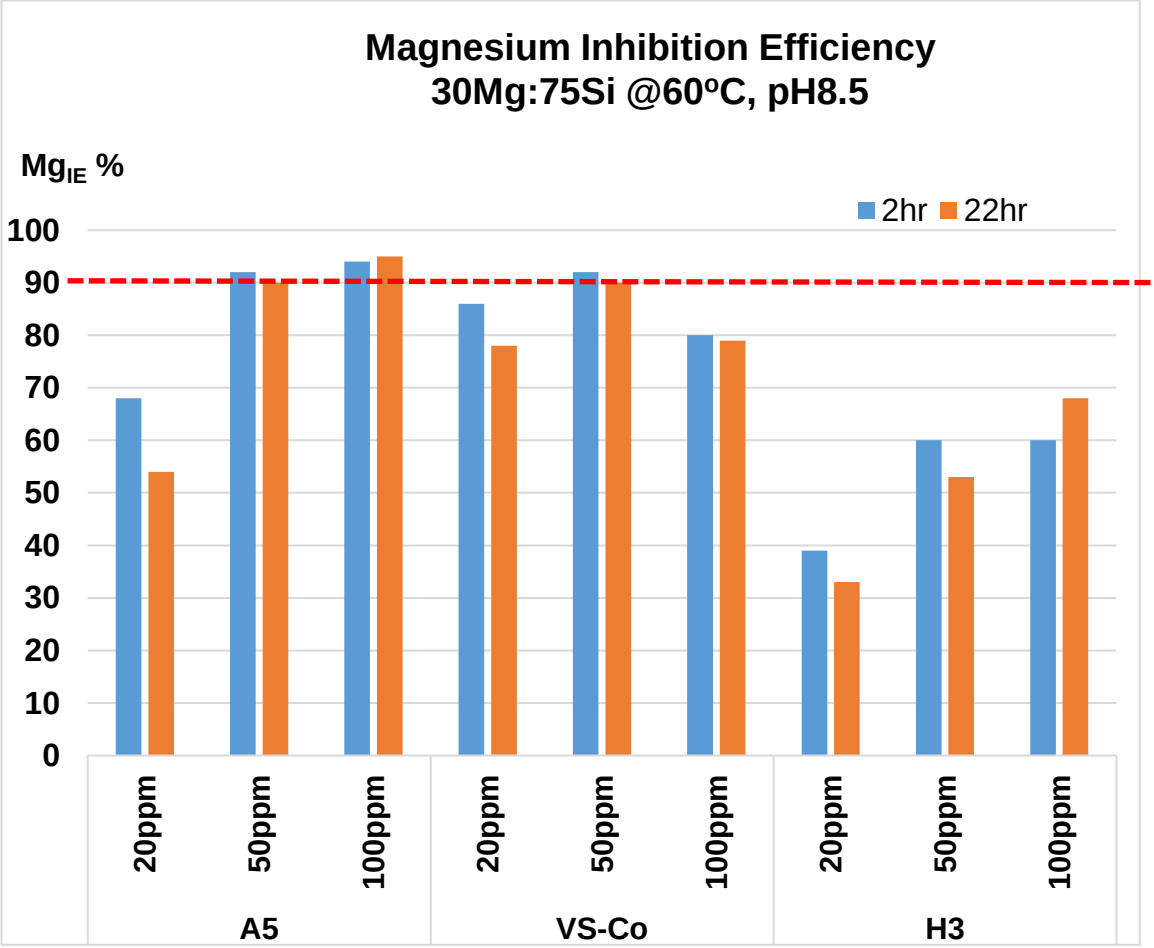

Figure 5-65 Inhibition efficiency percentage (Mg as precipitated ion in scaled solution) for silicate system of 30Mg:75Si at 60ºC, pH8.5

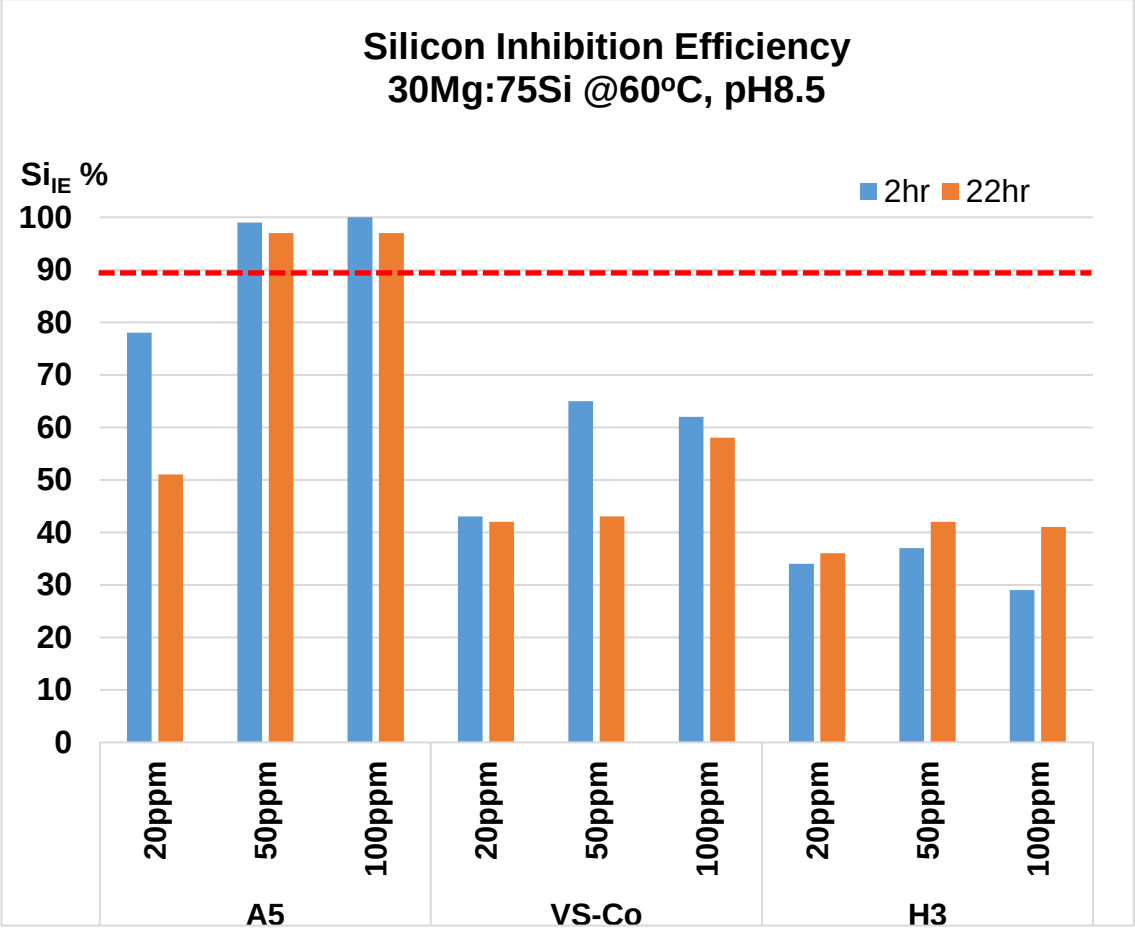

Figure 5-66 Inhibition efficiency percentage (Si as precipitated ion in scaled solution) for silicate system of 30Mg:75Si at 60ºC, pH8.5

The polymeric inhibitor, H3, was found to be the least efficient in preventing the silicate scale formation since the IE $_{Mg}$ % is only ~60 - 68% (see Figure 5-65) while the IE $_{Si}$ % is only 29 - 41% (see Figure 5-66) even when 100ppm H3 was added to the silicate system.

5.8.3 pH Profiles

The pH values for all A5 concentrations show the same reducing trend for residence times up to 22 hours, before in some cases showing a slight increase after 5 days (plotted in Figure 5-67). The pH values seem to be approximately constant between 5 to 7 days.

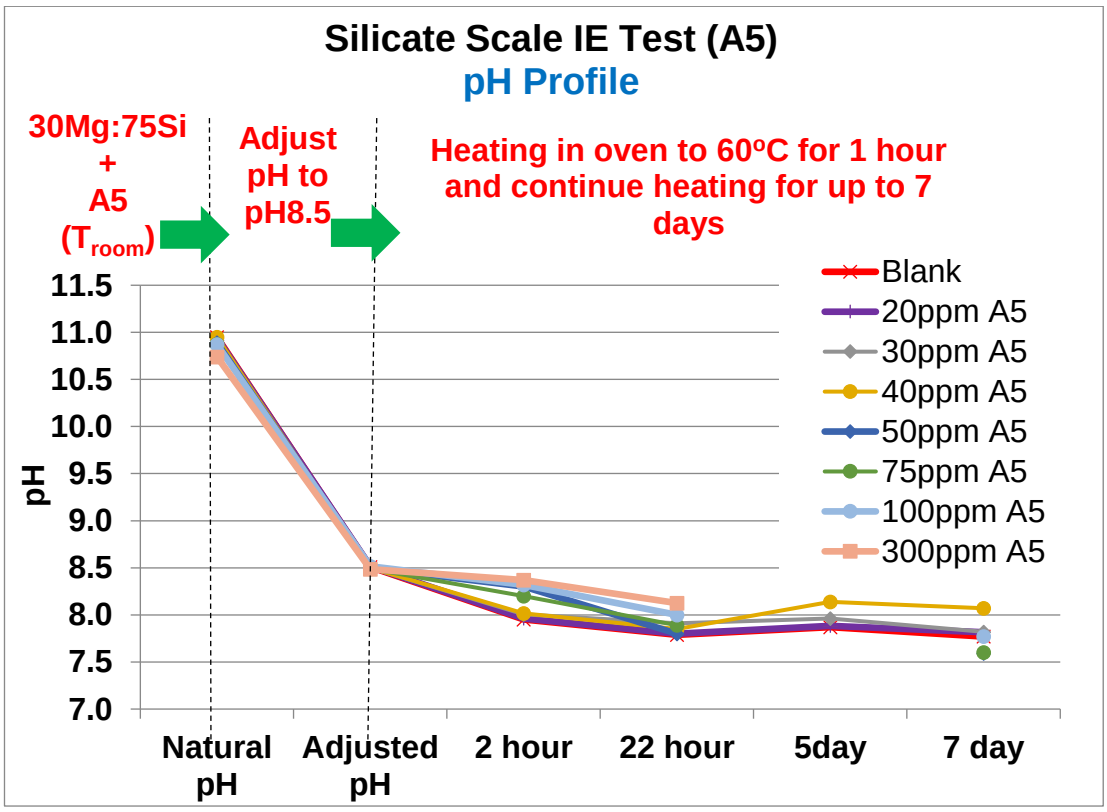

Figure 5-67 pH profiles for A5 IE Tests in silicate system of 30Mg:75Si at 60°C, pH8.5

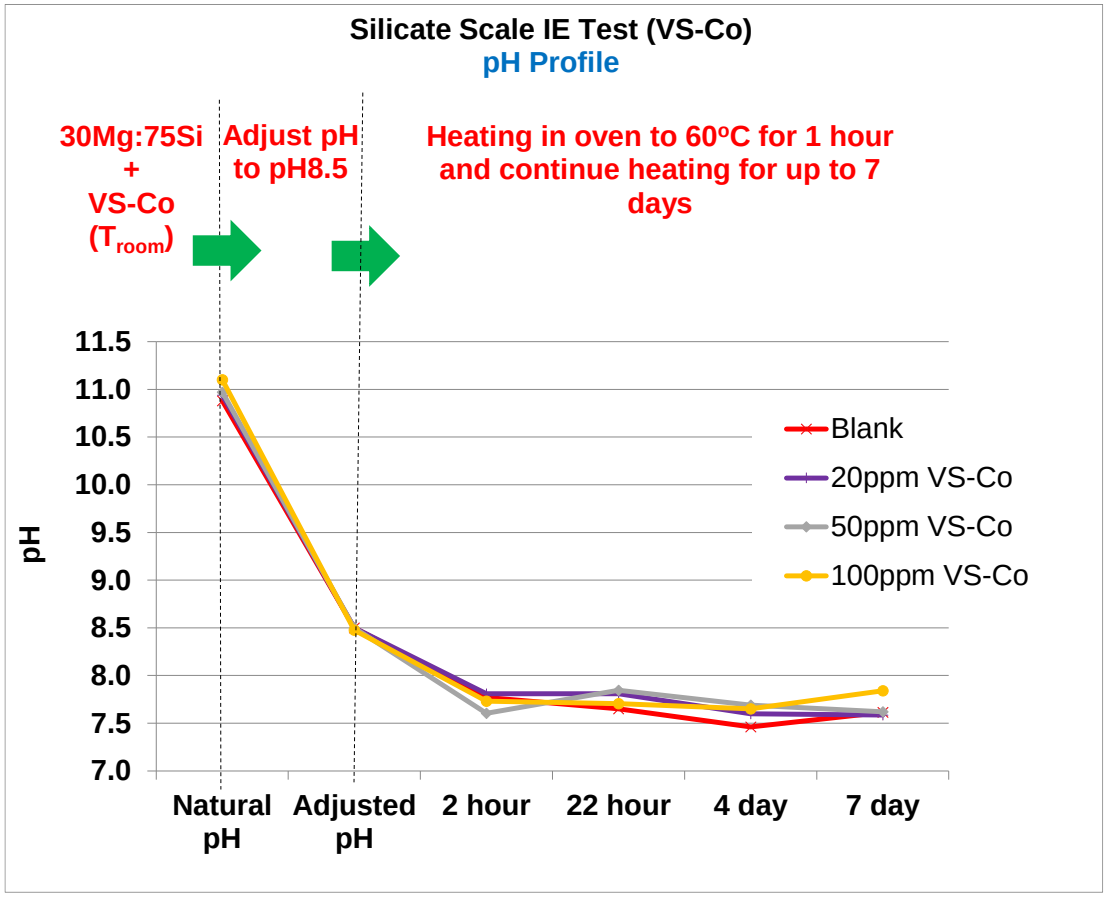

Figure 5-68 pH profiles for VS-Co IE Tests in silicate system of 30Mg:75Si at 60°C, pH8.5

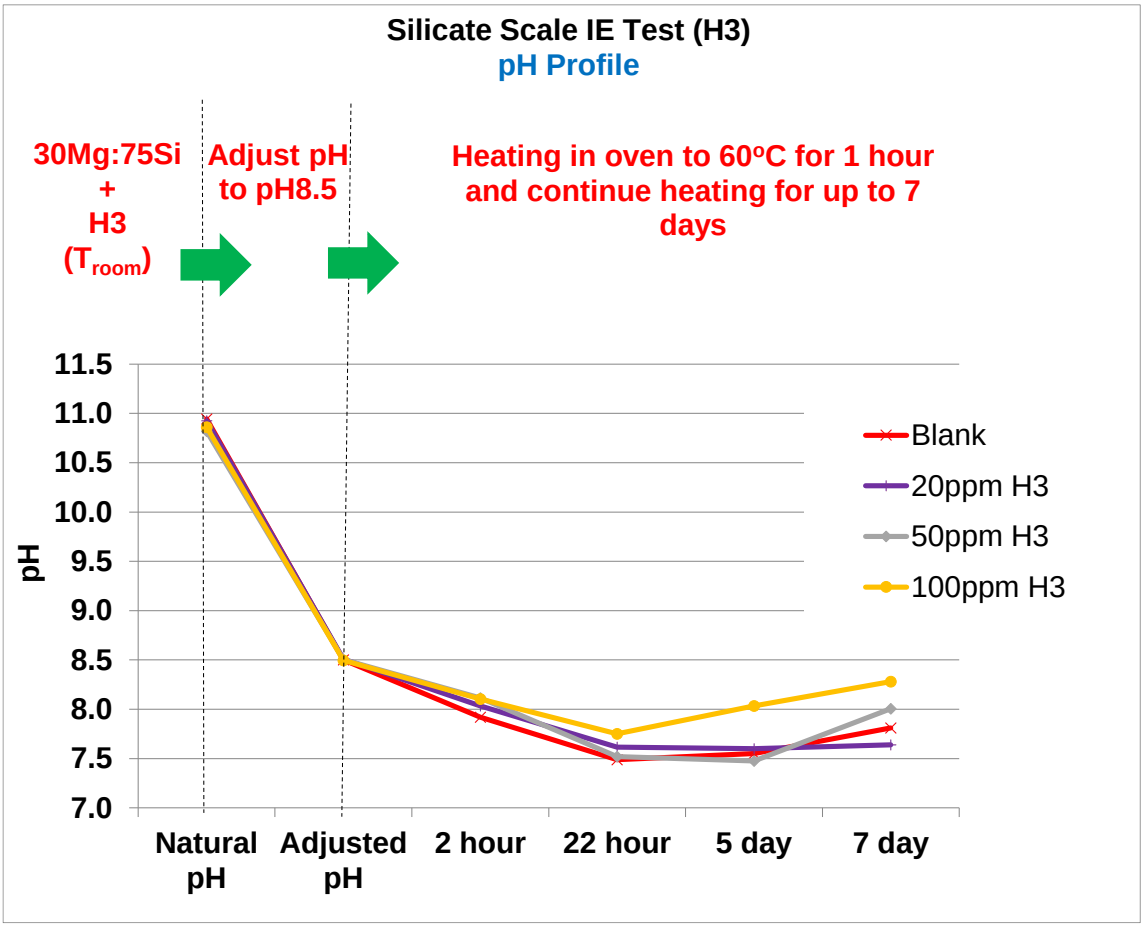

Figure 5-69 pH profiles for H3 IE Tests in silicate system of 30Mg:75Si at 60°C, pH8.5

Figure 5-68 shows the pH profiles for the VS-Co IE Tests for the same silicate system. In general, the pH values are decreasing with residence time.

The pH values of all H3 concentrations are also decreasing with residence time up to 22 hours but increases slightly afterwards as shown in Figure 5-69.

5.8.4 A5 Minimum Inhibitor Concentration (MIC_{static})

The Minimum Inhibitor Concentration under static conditions (MIC_{static}) for A5 was further investigated and determined as shown in Figure 5-70 and Figure 5-71. It is seen that 50ppm of A5 successfully stops the formation of silicate scales (i.e. IE $_{Mg}$ % and IE $_{Si}$ % >90%) for this silicate scaling system (30Mg:75Si), and so for this system we take the MIC ~ 50ppm of A5.

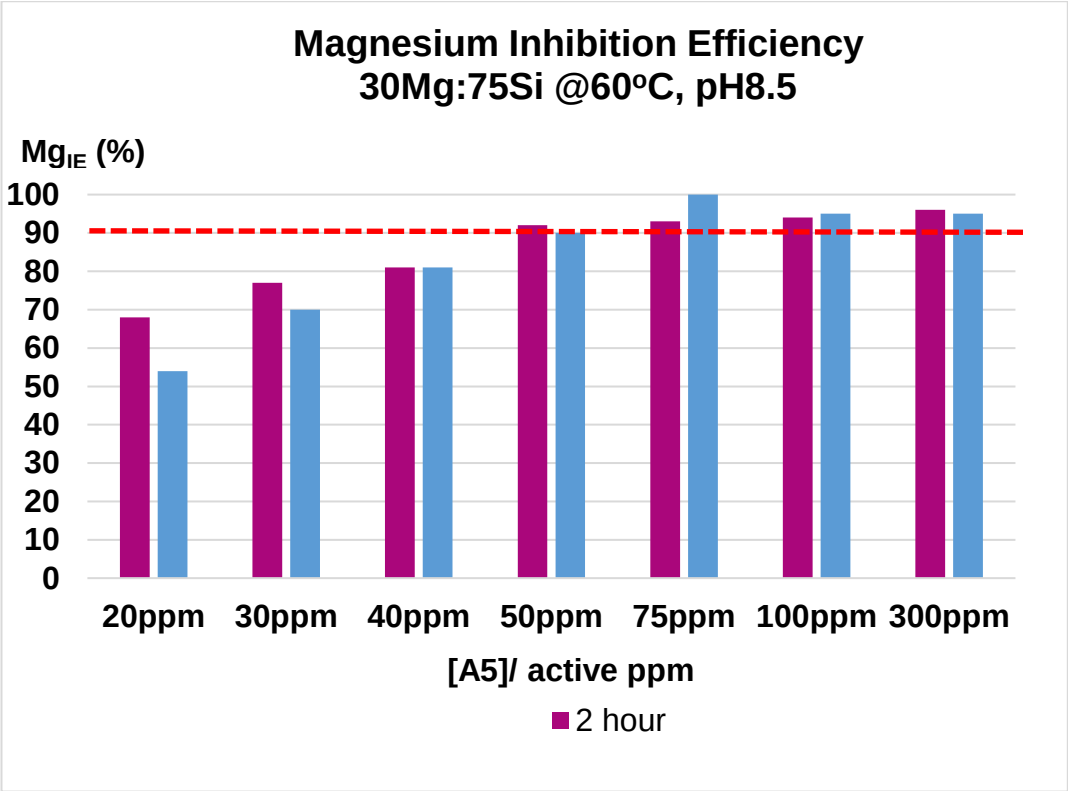

Figure 5-70 A5 inhibition efficiency percentage (Mg as precipitated ion in scaled solution) for silicate system of 30Mg:75Si at 60ºC, pH8.5

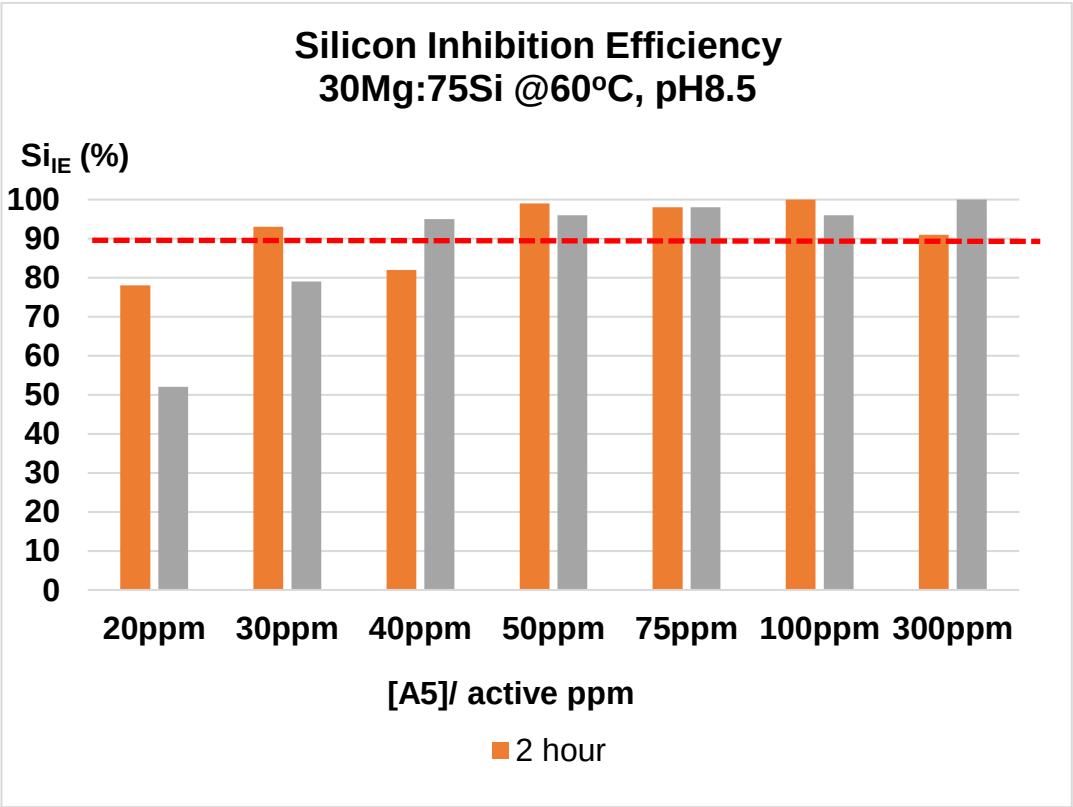

Figure 5-71 A5 inhibition efficiency percentage (Si as precipitated ion in scaled solution) for silicate system of 30Mg:75Si at 60ºC, pH8.5

5.8.5 Conjectures and New Findings

The ability of several inhibitors namely A5, VS-Co and H3 to inhibit the silicate scale in 30Mg:75Si was discussed in section 5.8. According to the results obtained and analysed, the ability of the tested inhibitors to stop the silicate scales in the silicate system of 30Mg:75Si at 60°C, pH8.5 can be grouped into 4 categories, shown in Table 5-8. Based on the 4 inhibition capabilities defined in Table 5-8, results in Figure 5-65 and Figure 5-66 can be further summarized into Table 5-9 and Table 5-10.

Table 5-8 Inhibitors category

IE_{Mg} % or IE_{Si} %	>90%	70 – 89%	50 –69%	<50%
Inhibition Capability	Excellent (E)	Good (G)	Average (A)	Poor (P)

Table 5-9 IE Tests summary of silicate system of 30Mg:75Si at 60°C, pH8.5

	20ppm			50ppm			100ppm		
	A5	VS-Co	H3	A5	VS-Co	H3	A5	VS-Co	H3
Amorphous Magnesium Silicate Inhibition	A	G	P	E	E	A	E	G	A
Amorphous Silica Scale Inhibition	A to G	P	P	E	P to A	P	E	A	P

Note: E – Excellent G – Good A – Average P – Poor

Table 5-10 MIC of inhibitors in IE static tests of silicate system of 30Mg:75Si at 60°C, pH8.5

Inhibitor (ppm)	A5		VS-Co		H3	
	Amorphous Magnesium Silicate Inhibition	Amorphous Silica Inhibition	Amorphous Magnesium Silicate Inhibition	Amorphous Silica Inhibition	Amorphous Magnesium Silicate Inhibition	Amorphous Silica Inhibition
20	X	X	X	X	X	X
50	√	√	√	X	X	X
100	√	√	X	X	X	X

Note: √ - totally inhibit (excellent inhibition) X – cannot totally inhibit (poor to good)

Excellent inhibition is achieved when the scale could be completely inhibited i.e. IE $_{Mg}$ % **AND** IE $_{Si}$ % >90% and no scale observed in the mixed brine.

The above tabulated results show that **A5 successfully** inhibited both scales (IE $_{Mg}$ % - 90-92% **AND** IE $_{Si}$ % - 97-99%) at **50ppm** (MIC_{static}).

VS-Co only achieves ***good*** inhibition towards amorphous magnesium silicate scale (79-80%) and ***average*** inhibition towards amorphous silica scale (58-62%) scale at the highest concentration tested, 100ppm.

H3 was found to be the least efficient inhibitor in this silicate system where it can only achieve ***average*** inhibition towards amorphous magnesium silicate scale (60-68%) and ***poor*** inhibition towards amorphous silica scale (29-41%) at the highest concentration tested, 100ppm.

Base on the limited information that we have (the inhibitors tested are proprietary), we can characterize all the inhibitors to the extent shown in Table 5-11.

Table 5-11 Summary of functional groups present in the inhibitors tested in silicate system of 30Mg:75Si at 60ºC, pH8.5

Inhibitors tested		**A5**	**VS-Co**	**H3**
Molecular weight (g/mol)		5000	<4000	Higher Molecular weight
Low molecular weight?		√	√	
Functional Groups present	Acrylamide (A)	√		√
	Sulfonate (B)	√	√	√
	Carboxylate (C)	√	√	
	Maleic Acid (D)	√		
	Non-ionic polymer (E)	√		

Based on the results discussed (and summarized in

Table 5-11), it is proposed that inhibitors with the ability to inhibit the silicate scale may possess the following properties:

1. Low molecular weight (<5000g/mol)

2. Sulfonate and carboxylate groups are probably able to stop the formation of amorphous magnesium silicate scale

3. Acrylamide, maleic acid and non-ionic polymer are probably able to stop the formation of amorphous silica scale

5.9. SUMMARY AND CONCLUSIONS

Following a systematic investigation on the repeatability and reproducibility of IE tests results, an experimental methodology to determine performance of any chemicals to inhibit silicate scale has established. This chapter presents the experimental results from a series of silicates scales with various Mg/Si levels and the results prove that the silicate scale is possible to inhibit.

A new *"manageable"* base case 30Mg:75Si is defined whereby this Mg/Si level can be inhibited. This case is more severe than a reported case from an ASP oilfield application. The new base case silicate system allowed different SI (with different functional groups) to be analysed/ compared. These results show clearly that silicate scales can be totally inhibited at reasonable SI concentrations and treatments would be economically feasible. Although others have shown that amorphous silica scale is hard to inhibit, we find that, it can be inhibited with 50ppm A5, which is an important new finding in silicate scale inhibition.

Evidence clearly shows that VS-Co and H3 failed to totally inhibit silicate scale even although 100ppm was added in the *"manageable"* base case. MIC_{static} of the most promising scale inhibitor, A5, in *"worst"* base case and *"manageable"* base case are 500ppm and 50ppm, respectively.

It is hoped that our conjectures on how functional groups affect IE % is useful and will help in the development of novel inhibitors or in search of a more suitable commercial inhibitor that can work for more severe silicate scaling systems.

CHAPTER 6. EFFECT OF FERROUS ION ON SILICATE FORMATION AND INHIBITION

6.1. INTRODUCTION

In this chapter, we consider the effect of ferrous iron (Fe^{2+}) on both the formation and inhibition of silicate scales. Oil reservoirs exist as anaerobic and strongly reducing environments and any oxygen which is injected into them tends to be rapidly consumed. Iron occurs in nature either in a trivalent state (Fe^{3+} - ferric) under oxidising conditions or in a divalent state (Fe^{2+}- ferrous) under reducing conditions.

The amounts and kinds of dissolved ions or molecules containing iron in the ferrous and ferric states are related to the pH and Eh of the water in which they occur. Iron must be mostly in the ferrous state and this ferrous iron is oxidized to ferric when the waters are exposed to air though this reaction is slow in strong acid (U.S. Geological Survey, 1962). Gallup (1989) studied iron silicate scale formation and inhibition at the Salton Sea Geothermal Field where it was claimed that Fe^{2+} had been oxidised to Fe^{3+}; in this case, the brine contained only 2-10ppm Fe^{3+} compared to 30ppm found in the scale.

Several studies have been carried out by researchers on the effect of Fe^{3+} in surface (atmospheric) water treatment system. The effects studied have included the antagonistic effect on the scale inhibitor; and how ferric hydroxide $Fe_2(OH)_3$ was seeding the silica polymerization on the membrane system. Indeed, even when the ferric hydroxide was removed, silica scaling continued to grow. Also, it was reported in the presence of as low as 0.05ppm Fe^{3+}, the silica tends to precipitate even below its saturation level. According to Zuhl and Amjad (2013), the Fe^{3+} ion present in the water as a result of raw water or carry over from the clarifier, is able to form soluble and insoluble complexes with hydroxide or/ and inhibitors. Therefore, less inhibitor is available to inhibit the scale formation. It was reported that Fe^{3+} negatively affects the calcium phosphate inhibitor and iron oxide dispersant due to the formation of insoluble hydroxide, $Fe(OH)_3$.

Wang and Wei (2016) studied the Fe-silicate formation and control in steam generator in ASP flooding through the scale modelling, lab testing, scale characterization and field observation. They found that the modelling results was appeared consistent with the

quantitative XRD results. The formation of this Fe-silicate scale caused the equipment failure due to tube plugging and overheating.

Rodríguez (2006) detected not only ferric ion but also ferrous ion in the iron silicate scales in the surface pipelines of the Miravelle Geothermal Field, Costa Rica. He suggested that Fe^{2+} is more soluble so that reducing agent sodium formate (NaHCOO) was used to effectively convert 99% of the ferric iron into ferrous ion which is more soluble at high temperature (250^{o}C). This also acts as corrosion mitigation as ferric iron is a well-known corrosive agent towards metallic corrosion materials.

This chapter presents our first results from anaerobic static bottle tests on silicate scale formation and inhibition for systems with a range of concentrations of ferrous ion (Fe^{2+}). This work has been carried out in one of our previously established "base case" silicate scaling systems. Here we present results for the *"manageable"* base case 30Mg:75Si at 60^{o}C, pH8.5; i.e. for the brine mix which initially has 30ppm of Mg^{2+} and 75 ppm of Si and initial pH 8.5.

6.2. FIRST RESULTS OF GLOVE BOX EXPERIMENT – 30Mg:75Si + 50Fe AT 60^{o}C, pH8.5

This section gives a detailed description of the first experimental work carried out and a discussion of the results obtained. The first task was to develop an appropriate experimental methodology to investigate the effect of ferrous ion to the silicate system and inhibitor performance in the absence of oxygen.

6.2.1 Experimental Setup

The objective of this experiments is to study the effect of ferrous ion on the silicate scaling system. In this experiment, we introduced 50ppm of ferrous ion into the "*manageable"* base case silicate system of 30Mg:75Si at 60^{o}C, pH8.5. The primary objective in this initial test was to establish whether or not the Fe^{2+} had an impact on the extent of reaction. This experiment was designed such that only ferrous ion was present, in the test samples, hence a reducing environment had to be maintained. These purely anaerobic tests were performed in the nitrogen glove box shown in Figure 6-1. The flowchart diagram shown in Figure 6-2 summarizes the experimental approach used in this test.

Figure 6-1 Nitrogen glove box

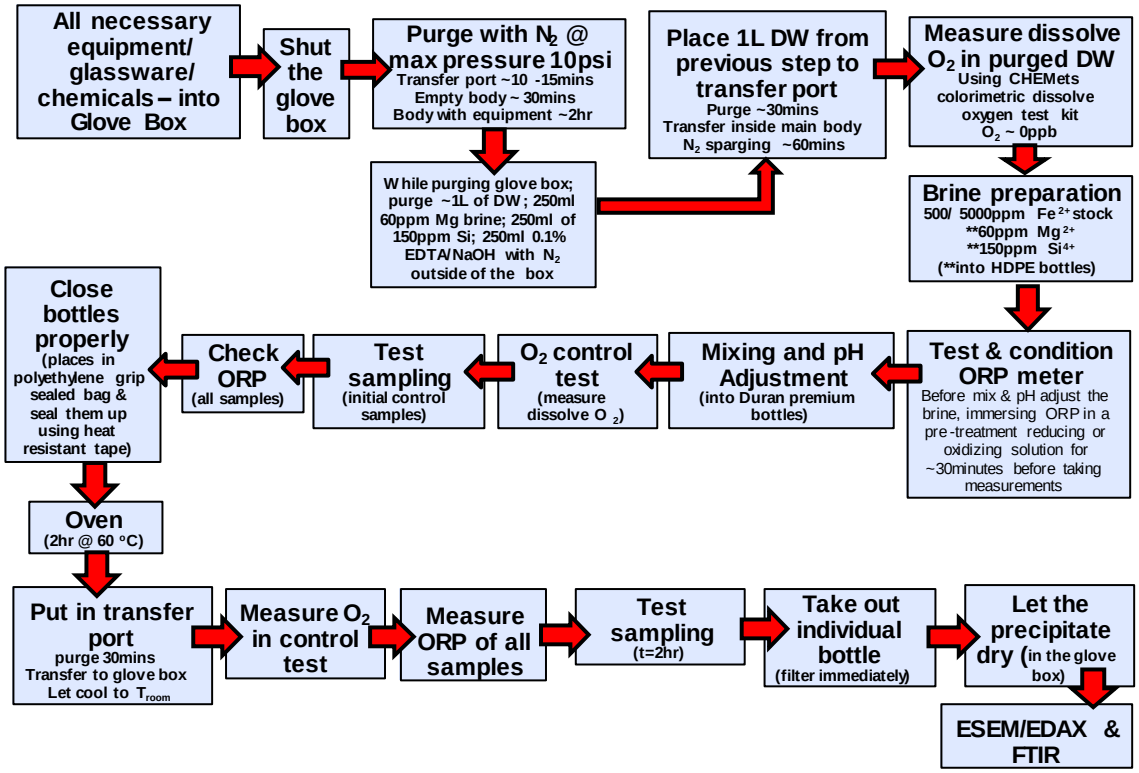

Figure 6-2 Summary of experimental methodology: Effect of ferrous ion (Fe^{2+}) on silicate system 30Mg:75Si at 60°C, pH8.5, anaerobic condition

In this set of experiments, two sets of brines, a 150ppm silicon brine and a 60ppm magnesium brine, were prepared by dissolving appropriate quantities of salts ($MgCl_2.6H_2O$ and $Na_2SiO_3.5H_2O$) in distilled water with the compositions given in Table 6-1. These magnesium and silicon brines were pre-prepared at ambient conditions and they were filtered using a 0.45µm filter as in the normal test procedure. These brines were then purged with nitrogen for about two hours and then put into the glove box and the oxygen content was checked to ensure that a <5ppb oxygen level was achieved.

Table 6-1 Brines and Fe^{2+} stock solution preparation

Manageable Case Scenario 30Mg:75Si	**Ion**	**Mg^{2+} Concentration {ppm (mg / L)}**	**Amount of $MgCl_2.6H_2O$ Required**				
			g / L	**g / 5L**	**g / 10L**	**g / 15L**	**g / 20L**
	Mg^{2+}	60	0.5018	2.5088	5.0175	7.5263	10.035
	Ion	**Si^{4+} Concentration {ppm (mg / L)}**	**Amount of $Na_2SiO_3.5H_2O$ Required**				
			g / L	**g / 5L**	**g / 10L**	**g / 15L**	**g / 20L**
	Si^{4+}	150	1.1330	5.6649	11.3300	16.9947	22.6596
	Ion	**Stock Fe^{2+} Concentration {ppm (mg / L)}**	**Amount $(NH_4)_2Fe(SO_4)_2 \cdot 6H_2O$ Required (g/100ml)**				
	Fe^{2+}	500	0.3511				
	Fe^{2+}	5000	3.5110				

500ppm and 5000ppm Fe(II) stock solutions were also prepared by dissolving an appropriate amount of an Fe stable salt, commonly known as Mohr's salt; ammonium iron (II) sulphate hexahydrate - $(NH_4)_2Fe(SO_4)_2 \cdot 6H_2O$) in distilled water (Refer Table 6-1). Ferrous stock solution was prepared in the glove box using the deoxygenized distilled water ensuring the presence of Fe^{2+} only. A small amount of this Fe(II) stock solution were then filtered using a syringe filter GD/X 25 0.2µm NYL.

In these experiments, we formed the silicate scale by mixing a 50ml sample of the silicon brine (Si Brine) with 50ml of the magnesium brine (Mg Brine). Then, 1ml of filtered 5000ppm ferrous stock solution was added to the mixed Mg/Si brine solution to give final concentrations of 30Mg:75Si:50Fe. Three sets of experiments were prepared i.e. 2 and 22-hour tests; and another 2-hour *repeat* test was carried out to ensure the repeatability and reproducibility of the approach.

All tests were performed in duplicate where bottles were numbered, and every even number was the duplicate of the preceding odd number, i.e. 1 and 2 were duplicates, 3 and 4 were duplicates etc. A pair of duplicates containing no inhibitor, the blank tests, was included in every batch. Essentially, it involved the mixing process of appropriate volume of Mg/ Si/ Fe^{2+} before this mixed brine was pH-adjusted to pH8.5 using 10% HCl solution. The mixing and pH adjustment steps were critical as they may have affected the repeatability and reproducibility of the test results. These steps should be handled with extra care and these procedures are illustrated in Figure 6-3.

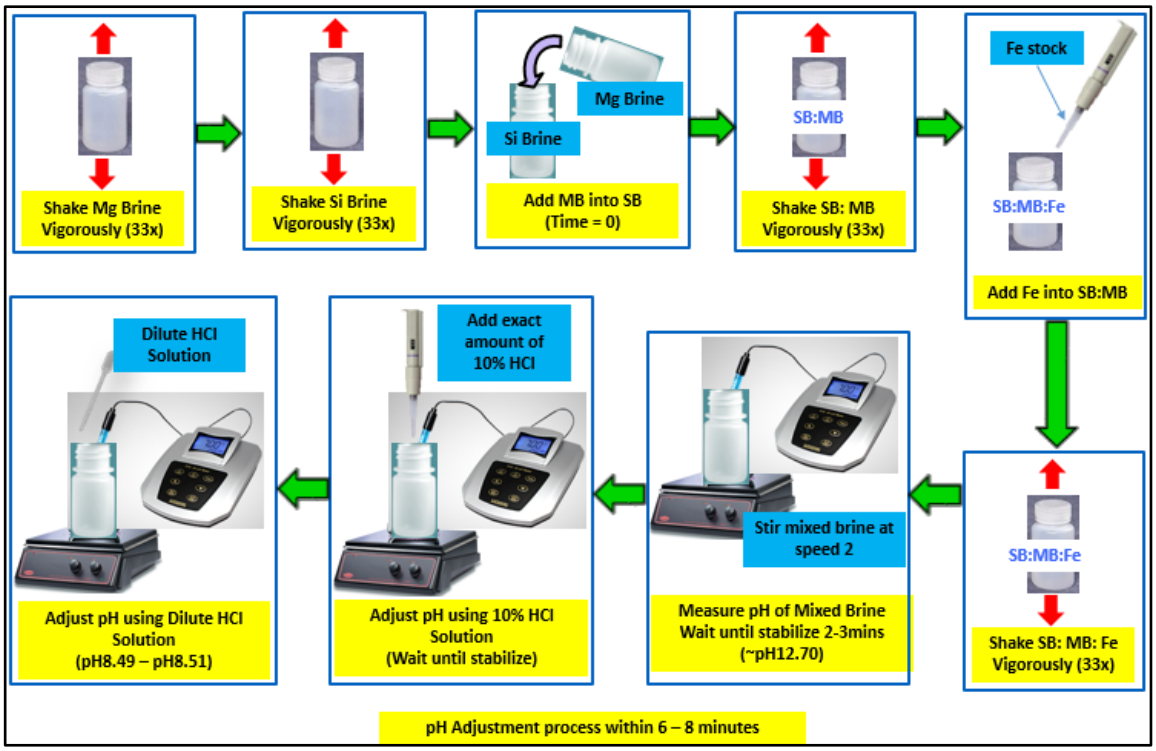

Figure 6-3 Brine mixing and pH adjustment procedure (Inside glove box)

The brines in sealed plastic bottles were then heated in the oven to the test temperature, T = 60°C from ambient conditions. It was important to ensure that the oxygen level was kept at <5ppb in the prepared mixed Mg/Si/Fe brine throughout the heating process. This was achieved by making sure that bottles lids were closed properly. An *O_2 control* was also included in this experiment for oxygen level monitoring and this was heated in the oven for the entire reaction time. The *O_2 control* was prepared by pouring 100ml of deoxygenized distilled water into an empty glass bottle. Since the *O_2 control* test bottle

contained only the deoxygenized distilled water, then the oxygen level could be measured using CHEMets Colorimetric Dissolved Oxygen Test Kit. Note that the presence of ferrous ion in the test samples did not allowed the oxygen level to be measured using the same test kit. All test bottles, including *O_2 control*, were placed in a polyethylene grip sealed bags, leaving as little gas inside as it is possible. The bags were closed properly, before sealed them up with heat resistant tape.

The test samples were then being ICP sampled at 2 hours. The ICP measurement allows us to determine the extent of reaction of magnesium and silicon ion as compared to the blank solution (i.e. the sample which contained no ferrous ion). By doing this, we could investigate how the ferrous ion affected the silicate system.

The oxygen level was kept at <5ppb level in the glove box and in all brines and distilled water at all time so that a reducing environment was achieved. A strict oxygen reduction regime was developed with the sole aim of keeping the amount of (O_2) as low as possible (all tests were successfully conducted at <5ppb O_2; ideally the oxygen level should be kept at <10ppb (it will be shown later in section 6.4.2 that oxygen level up to 10ppb is still acceptable). To support this argument, test samples tested in section 6.2.2(b) were observed to be contaminated i.e. the brine turned a dirty greenish colour at 0hour when 20ppb oxygen level was found to be present in the glove box).

~50ml deoxygenized distilled water was left in a beaker (*Glove Box O_2 control*) for oxygen level monitoring purposes so that we could monitor any oxygen contamination that may have occurred. All necessary solutions such as 0.1% EDTA/NaOH quenching solution, 150ppm silicon brine, 60ppm magnesium brine and distilled water were sparged using the N_2-sparging line outside the glove box for at least 2 hours (Other solutions with smaller quantities such as 10% HCl and dilute HCl needed for pH adjustment; all glassware/ equipment/ chemicals were purged with nitrogen gas using the N_2-sparging line appropriately; these were done one after another inside the glove box at the same time). All sparged solutions were then transferred into the glove box and sparged was continued using the N_2-sparging line. (The sparged solution were purged at least for another 1 hour and were checked to ensure they were oxygen-free). It is worth noting here that this 0.1% EDTA/NaOH solution is a lower concentration than normally used; in comparison to the aerobic silicate scale static test of 1% whereby the lower concentration of 0.1% was prepared to take into consideration the presence of the Fe ion which drops out in a 1% EDTA/NaOH solution.

Measuring Dissolved Oxygen using CHEMets Colorimetric Dissolved Oxygen Test Kit

The dissolved oxygen was measured in the nitrogen glove box using the CHEMets Colorimetric Dissolve Oxygen Test Kit (K-7599/R-7540) that has capability to measure the dissolve oxygen ranging from 0ppb to 100 ppb with MDL of 5ppb. The method detection limit (MDL) is defined as the minimum measured concentration of a substance that can be reported with 99% confidence that the measured concentration is distinguishable from method blank results.

The Oxygen (0 – 100 ppb) CHEMets test employs the Rhodazine D Method. Dissolved oxygen reacts with the pale yellow coloured leuco form of Rhodazine D to produce a deep rose colour. The resulting colour is proportional to the dissolved oxygen concentration in the sample. Results are expressed in ppm O_2. Refer Figure 6-4.

1. Place the CHEMets ampoule in the sample cup. Snap the tip by pressing against the side of the cup to fill the ampoule, leaving a small bubble at the top to allow for mixing.
2. Quickly mix the contents by inverting the ampoule, allowing the bubble to travel form end to end. Wipe away any liquid on the outside of the ampoule. The colour comparison must be made **within 30 seconds.**
3. Place the ampoule flat end down into the centre tube of the comparator. Direct the top of the comparator up towards a bright source of light while viewing from the bottom. Rotate the comparator until the colour standard below the ampoule shows the closest match. If the colour of the CHEMet ampoule is between two colour standards, a concentration estimate can be made.

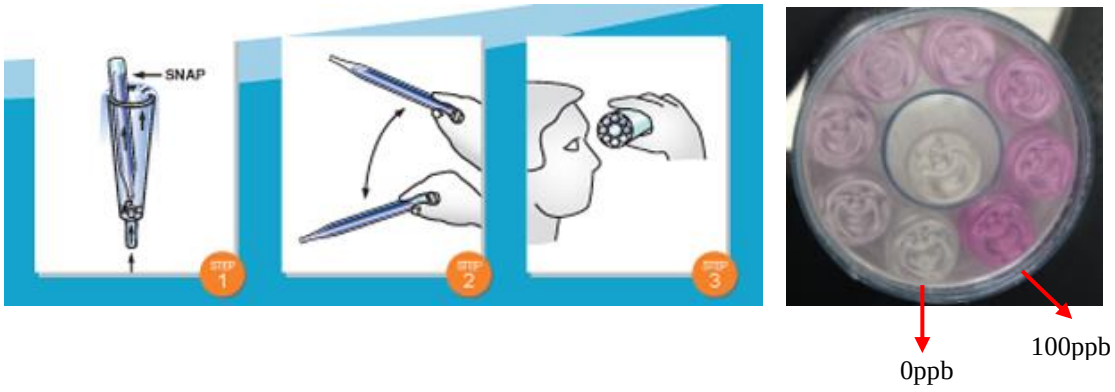

Figure 6-4 Measuring dissolved oxygen using CHEMets colorimetric dissolved oxygen test kit procedure and comparator

6.2.2 Experimental Results

(a) Original Test (Reaction time = 2 hour)

The first experiment which was carried out in this work involved the addition of a relatively high amount of ferrous ion, i.e. [Fe^{2+}] = 50ppm. The objectives of this first experiment were as following:

1. To investigate if the anaerobic environment is achievable in this glove box set up.
2. To establish if the ferrous ion affects the silicate system.

It is worth noting here that all bottles/ glassware equipment & others (e.g. test tubes, syringes, pipette tips etc.) were sparged with N_2 to ensure they were all O_2 free before any brine preparation. It was observed that <5ppb O_2 level was achievable in the glove box and in the nitrogen-sparged distilled water. This level was confirmed using CHEMets Colorimetric Dissolved Oxygen Test Kit. In addition, the Fe^{2+} stock prepared was also O_2 free as there were no colour changes in the test samples which indicated that no oxidation of Fe^{2+} had occurred.

Further visual inspection of the test samples at initial time, 2hr-ICP sampling time and after >24 hours in Figure 6-5 clearly showed that no perceptible changes in colour took place. It can be seen quite clearly that the test sample became cloudy after mixing and pH adjustment (at time 0 hour). The precipitate formed in the test sample 2 hours after reaction at T = 60°C and this precipitate settle to the bottom leaving a cloudy supernatant solution.

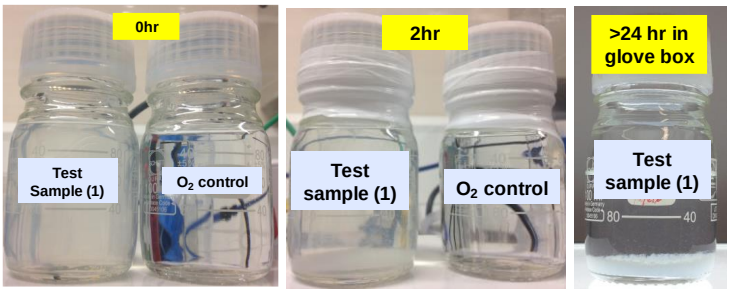

Figure 6-5 Visual observation of 30Mg:75Si + 50Fe in "Original Test"

In this initial set of experiments, the amount of magnesium, silicon and ferrous ion reacted were determined using the ICP analysis and the results are shown in Figure 6-6. These results clearly show that the amount of all ions reacted is higher in the brine containing 50 ppm of the Fe^{2+}- when compared with blank solution. This indicates that Fe^{2+} ion does affect the extent of the scaling reaction in the silicate system. When compared with scaling reaction in the base case silicate system of 30Mg:75Si at 60°C, pH8.5; we found that the amount of Mg^{2+} and Si^{4+} reacted increased by >1.5X and >4.5X respectively with almost all of the Fe^{2+} reacted.

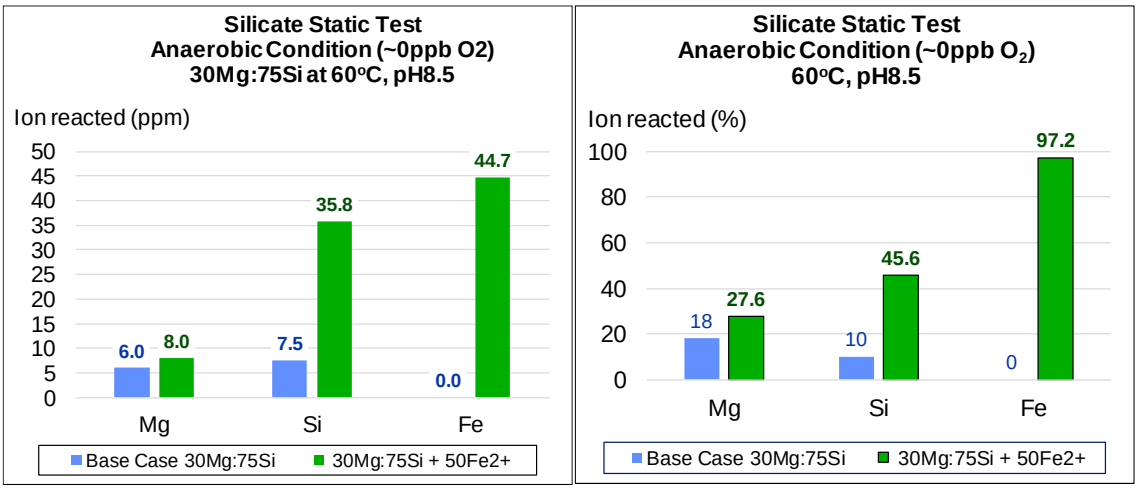

Figure 6-6 Amount of ion reacted when 50ppm of Fe(II) present in the "*manageable*" base case 30Mg:75Si. Ion reacted in ppm (Left) and Ion reacted in % (Right)

(b) Repeat Test 1 (Reaction time = 2 hour)

The experiment described above was repeated to check the reproducibility of the method. The oxygen measurement in the *Glove Box O_2 control* indicated that <5ppb O_2 level was again achievable in the glove box after sparging the glove box for more than 2 hours. The deoxygenated distilled water that was used to prepare the ferrous stock solution and as rinsing solution was also found to be oxygen free (0ppm O_2).

In this experiment, we again observed that the test samples of 30Mg:75Si:50Fe became cloudy after all brines had been mixed and pH-adjusted to pH8.5 similar to the one observed in *original test*. However, the colour changed to light green indicating that some oxidation of Fe^{2+} had probably taken place due to O_2 contamination; this can be seen in

Figure 6-7. These duplicate samples were prepared along with an *O_2 control*. The oxygen level measurement in the *O_2 control* showed that the oxygen level was between 20-30ppm even although the deoxygenized distilled water was confirmed (prior to test sample preparation) as being totally oxygen free. This may be due the fact that all bottles/ glassware equipment & others (e.g. test tubes, syringes, pipette tips etc.) were not sparged with N_2. Hence, there was possibility of oxygen contamination via these glassware equipment while preparing the test samples. This observation suggested that it is important to keep the O_2 level <10ppb in the *O_2 control* (as explained earlier in section 6.2.1) by purging all glassware/ equipment/ chemicals with nitrogen sparging line inside glove box.

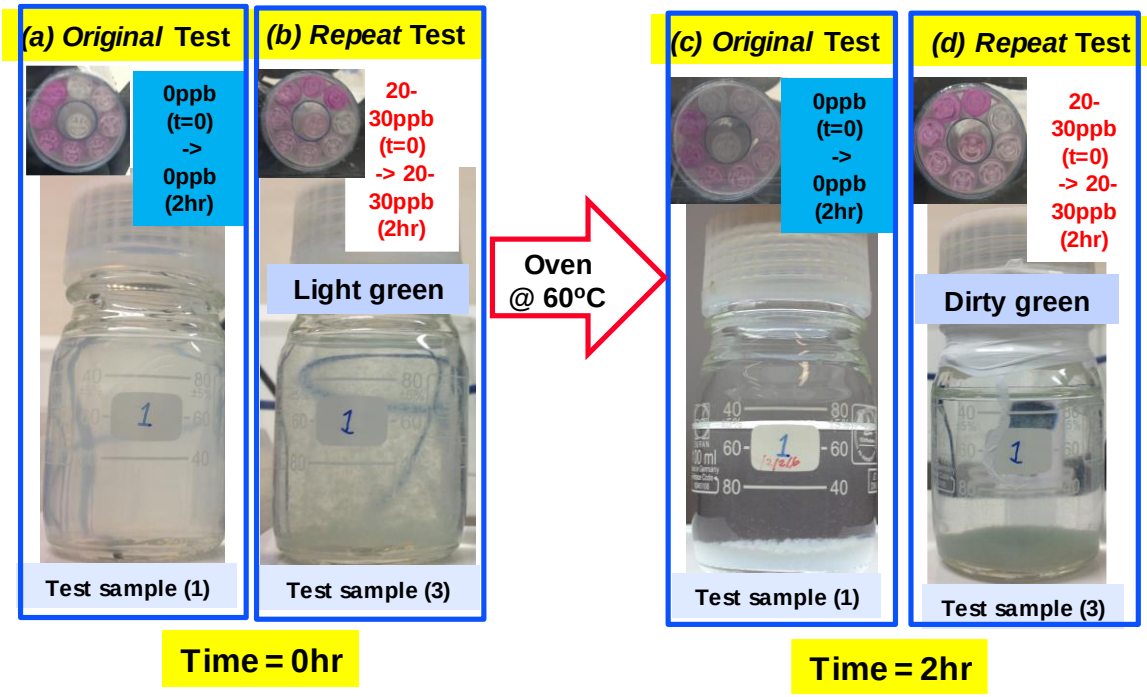

Figure 6-7 Observation of 30Mg:75Si + 50Fe at 60°C, pH8.5. After pH-adjusted in glove box (Left) and After heated in the oven for 2 hour (Right).

The oxygen level was maintained at 20-30ppb throughout the reaction in the oven at 60°C. However, the observation in Figure 6-7 suggested that even at this oxygen concentration, the oxidization of ferrous ion to ferric ion may have already occurred. The presence of Fe^{3+} increased the extent of scaling reaction in the silicate system after 2 hour (as compared to purely anaerobic condition) as shown in the results in Figure 6-8**.**

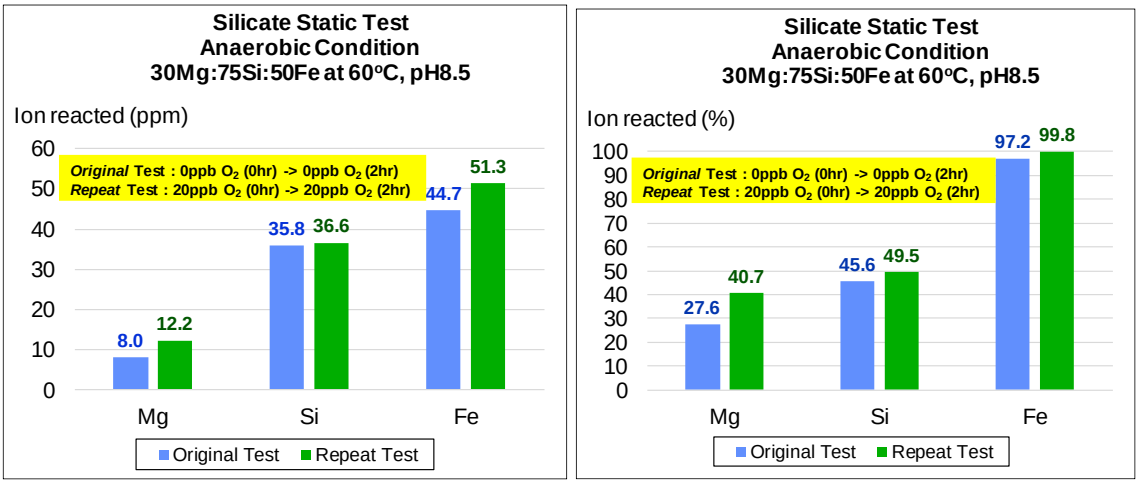

Figure 6-8 Effect of 50ppm Fe in the *"manageable"* base case 30Mg:75Si at 60°C, pH8.5 (Purely anaerobic condition vs. Oxygen contaminated condition). Ion reacted in ppm (Left) and Ion reacted in % (Right).

(c) Repeat Test 2 (Reaction time = 22 hour)

In the experiment described in this section, our aim objective was to investigate if the anaerobic condition were maintained over 22 hour of reaction time. This would establish whether or not our results can be trusted at 22 hours. Thus, another duplicated set of the 30Mg:75Si:50Fe^{2+} case was prepared and left to react for 22 hours in anaerobic conditions before being ICP-sampled at 2 and 22 hours.

The test samples were visually inspected and photographed from time to time. Performing such continuous monitoring of the physical condition of the tested brine allowed us to observe whether the anaerobic conditions were maintained and, if it did happen, then the time the oxygen started to leak into the test samples could be established. The test samples became slightly cloudy after being mixed and pH-adjusted to pH8.5 at room condition which was in good agreement with observation made in the previous *original* test that was performed in fully anaerobic condition. Also, from the observation recorded in Figure 6-9, it was quite clear that the anaerobic conditions were successfully maintained for up to 17 hours; however, the test samples became slightly greenish in colour at ~19 hours. This is explained by the fact that the oxygen level started to build up in the test sample and this oxidized some of the ferrous ion into ferric ion before these ferric ions further bridged the silicate ion which then resulted in the greenish colour observed.

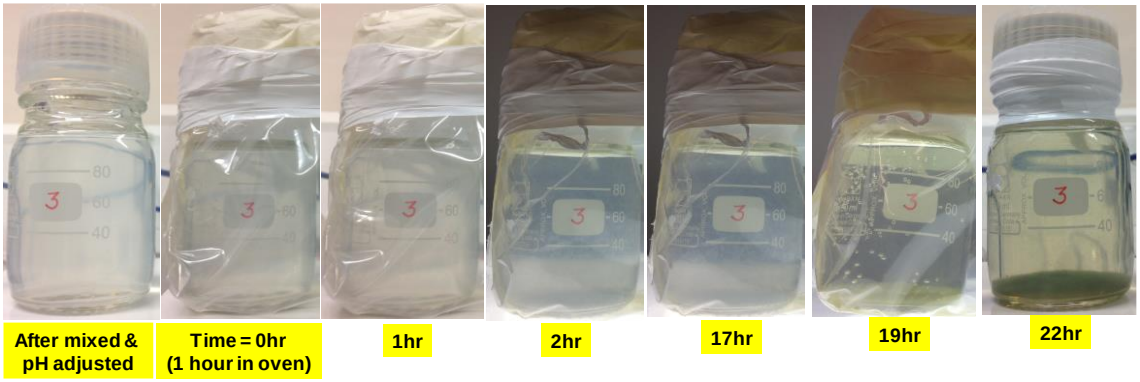

Figure 6-9 Observation of 30Mg:75Si + 50Fe at 60°C, pH8.5 up to 22 hours of reaction time

Figure 6-10 shows the physical observation for the test samples at 22 hour with the previous two repeating tests at 2 hours. It can be seen clearly that the precipitate formed in *22hr* test is darker than the one produced in the *Repeat 2hr* test. Also, the oxygen level was determined to be more than 100ppb in the *22hr* test samples as compared to only 20-30ppb found in the *Repeat 2hr* test samples. This indicates that the higher the oxygen level that is present, the more ferrous ions are oxidized to ferric ion before being readily incorporated into the silicate scale; hence the darker colour observed.

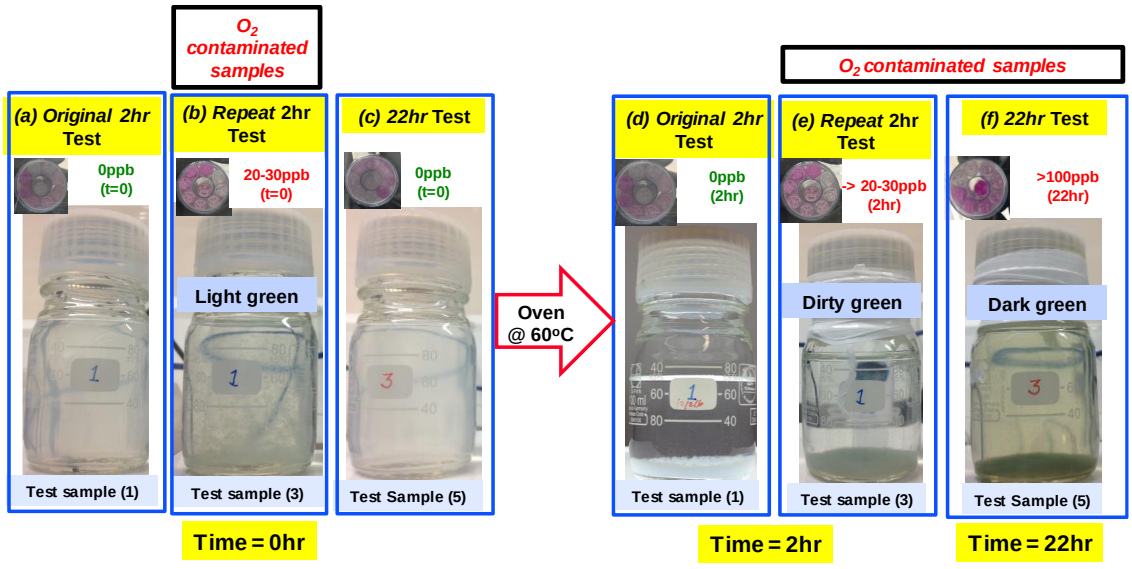

Figure 6-10 Observation of *2hr* and *22hr Test* in 30Mg:75Si + 50Fe

Figure 6-11 shows some interesting results that indicate that the amount of all ions (i.e. Mg, Si and Fe) in both tests is essentially the same regardless the reaction time. These findings may be explained by the presence of Fe^{3+} in both samples (both of the test samples were contaminated after 2 & 22 hr respectively) which resulted in approximately the same extent of reaction.

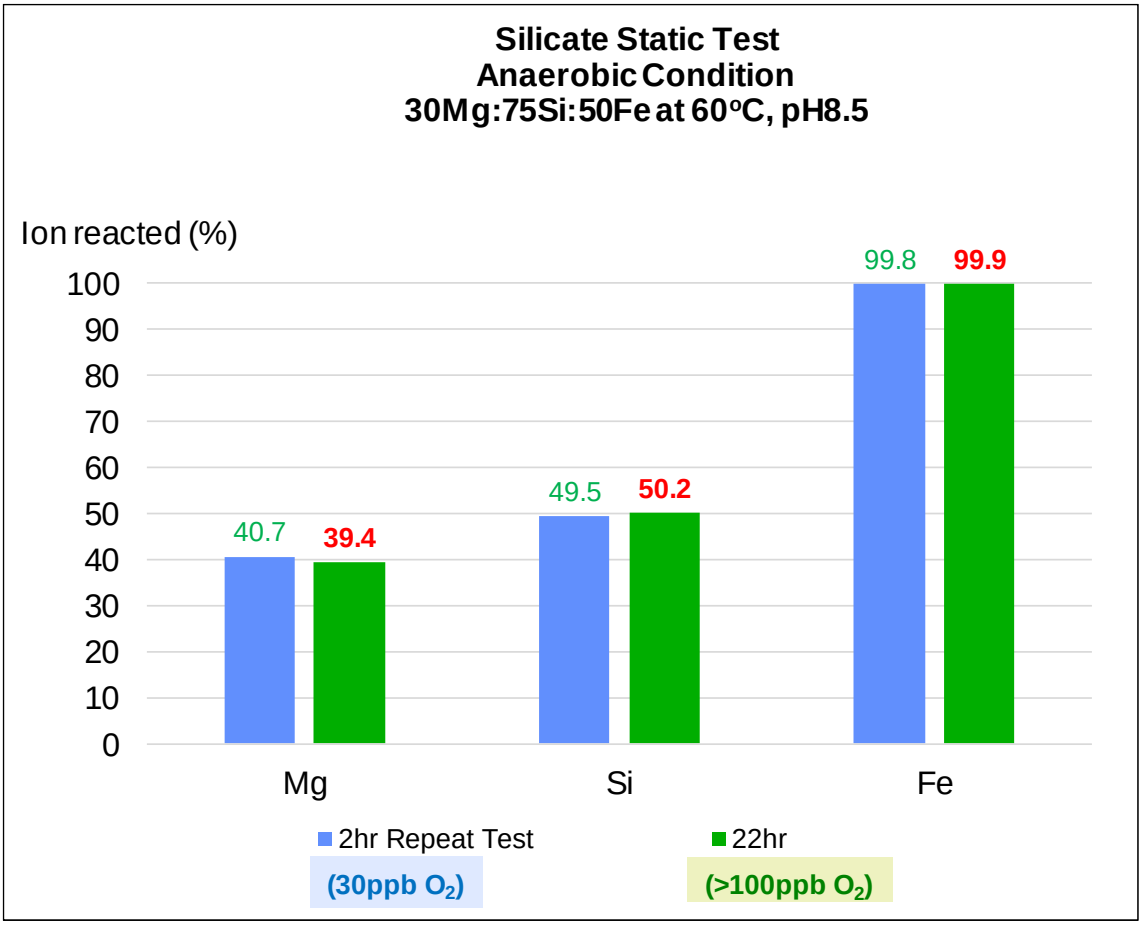

Figure 6-11 Comparison in amount of ion reacted between "*Repeat 2hr* Test" and "*22hr* Test" in silicate system of 30Mg:75Si + 50Fe at 60°C, pH8.5

All precipitates produced in these three first experiments were filtered and analysed using ESEM/EDAX. ESEM images are shown in Figure 6-12 and these results suggest that that all scale produces are amorphous in nature.

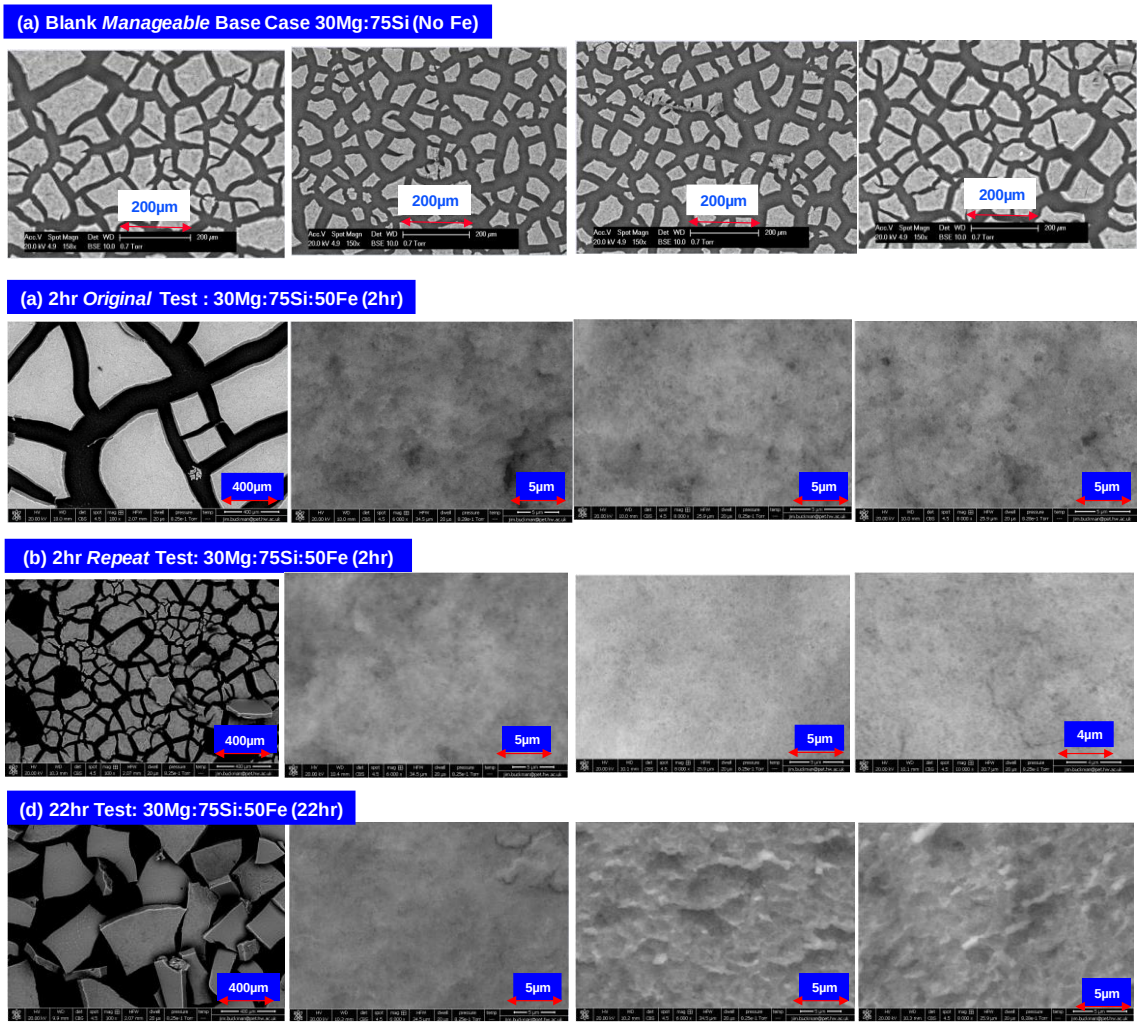

Figure 6-12 ESEM images of First Results in Silicate Scale Static Bottle Test of *blank* (No Fe) and 30Mg:75Si + 50Fe at 60ºC, pH8.5

Figure 6-13 shows the atomic % values obtained from the precipitates using EDAX analysis while Figure 6-14 shows plots of the amounts of ion reacted (i.e. that formed the precipitate) determined from ICP analysis. These data are useful in determining the stoichiometry (i.e. the Si:Mg molar ratios in the precipitates) which result from both techniques (EDAX and ICP) and these are shown in Figure 6-15. Note that there is very good agreement in the Si:Mg molar ratios for each technique in all tests.

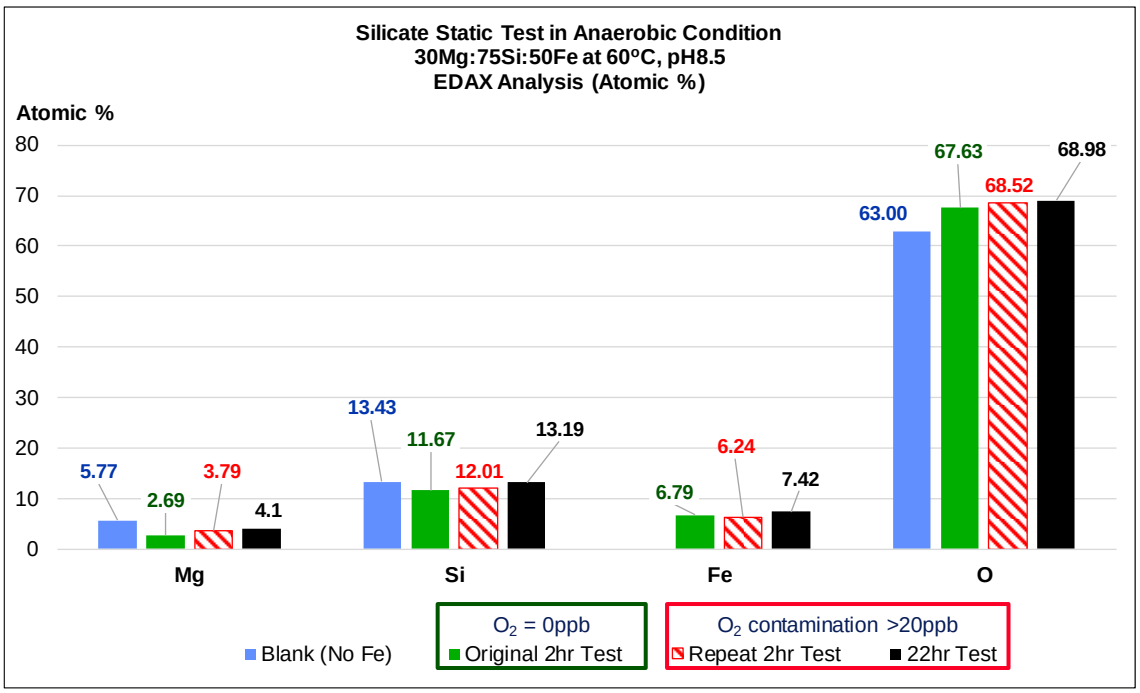

Figure 6-13 Atomic % in precipitate of *blank* (No Fe) and 30Mg:75Si + 50Fe at 60°C, pH8.5 – EDAX data

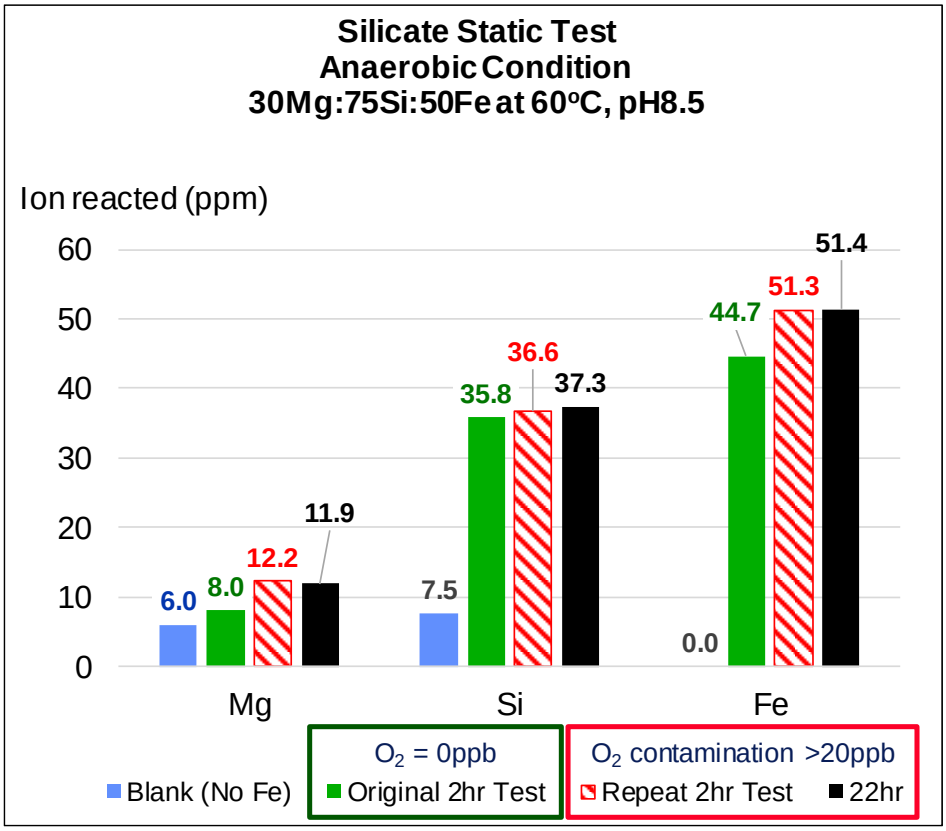

Figure 6-14 Amount of ion reacted in the precipitate of *blank* (No Fe) and 30Mg:75Si + 50Fe at 60°C, pH8.5 – ICP analysis

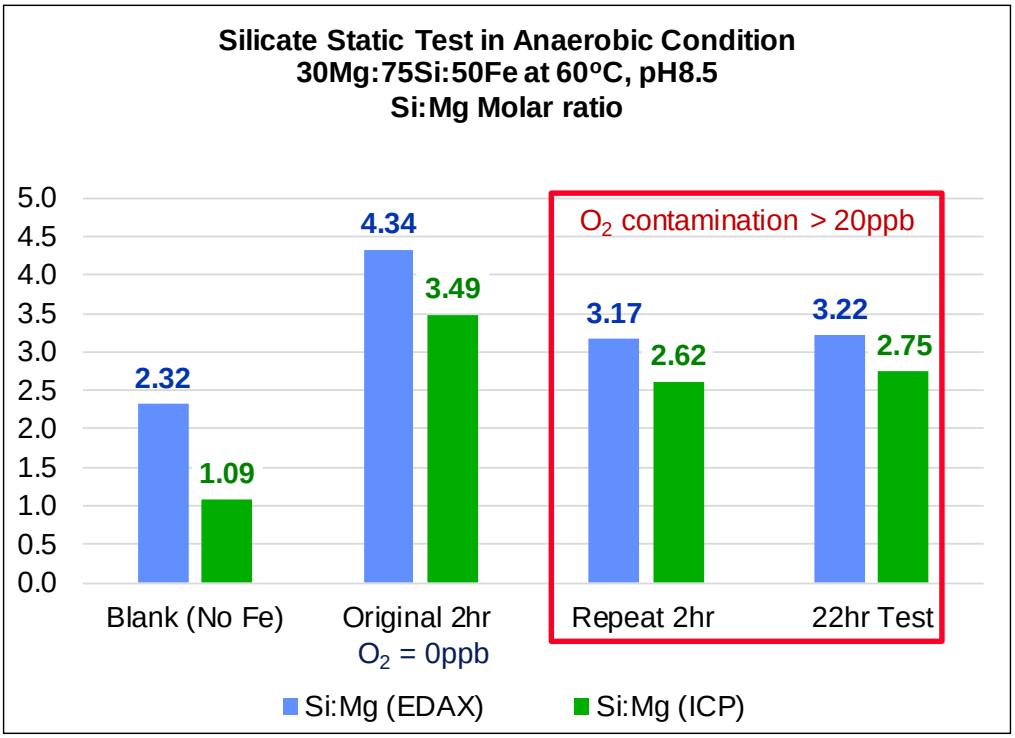

Figure 6-15 Si:Mg molar ratio of First Results in Silicate Scale Static Bottle Test of *blank* (No Fe) and 30Mg:75Si + 50Fe at 60°C, pH8.5

Further examination on the precipitate by using FTIR analysis revealed that all bands produced are almost the same for all three tests. It can be seen that the spectra for the O_2 contaminated test i.e. *Repeat* 2hr Test and 22hour Test are almost exactly the same (Refer Figure 6-16).

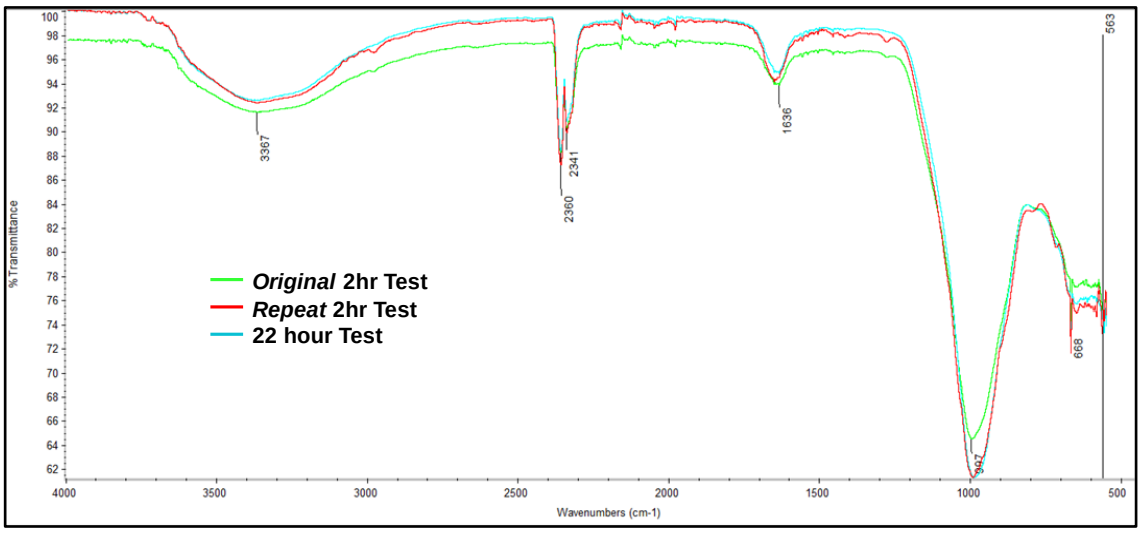

Figure 6-16 FTIR spectra of First Experiments (%Transmittance vs. Wavenumbers cm-1)

6.2.3 Summary and Conclusions

In conclusion, the experimental methodology to study the effect of ferrous ion on silicate scaling is now established with good results which are reproducible, as shown above. It was observed that a total reducing environment (O_2 content <5ppb) is achievable in the glove box equipment following the procedures described in section 6.2.1.

The purely anaerobic condition was also maintained and achievable throughout the 2 hours of reaction. Although, there was some oxygen contamination issues for the 22-hour test, the oxygen level was successfully kept essentially at <5ppb (concluded from physical observation only) up until ~17 hours. Hence, with some care and further improvements in the test procedure, the purely anaerobic environment may be achievable for the 22-hour tests. However, due to time constraint on this experimental work, we proceeded to study the effects of ferrous ion on the inhibited silicate system. Results on the performance of the silicate inhibitor A5 up to 2 hours only will be covered in the next section.

Following the results discussed above, we conclude that the silicate scale system of the "*manageable"* base case of 30Mg:75Si at 60^{o}C, pH8.5 ***was*** affected when ferrous ion was present in the solution. We found that the amounts of Mg and Si reacted to a higher extent in the presence of 50ppm Fe^{2+} as compared with the base case. These first results are useful in providing a case from which the effect of various ferrous ion concentration levels present in the silicate system can be studied.

The present of as low as 20ppb oxygen in the silicate system may results in oxidization of ferrous ion to ferric ion. The presence of ferric ion in the solution suggested a more severe scaling condition as compared to when only ferrous ion was present. We cannot conclude the precise amount of ferric ion that initiated the antagonistic effect to the silicate system since the ICP analysis only measured the total Fe rather than individual ferrous and ferric ions. Therefore, it is important to achieve the purely anaerobic condition in this test although it will be shown later in 6.4.2(a) that with the oxygen level must be kept to < 10ppb in order to prevent ferrous ion oxidization.

ESEM analysis on the precipitate produced confirmed that the silicate scale produced are not crystalline but rather amorphous in nature. The Si:Mg molar ratio determined from both ICP and EDAX analysis agreed with each other very well.

6.3. EFFECT OF FERROUS ION ON SILICATE SYSTEM

Following the results described above, we undertook a systematic investigation to study the effect of various concentrations of ferrous in the "*manageable"* silicate scaling base case and results are discussed in this section. The objective of this study is to determine the threshold ferrous ion concentration that may affect the extent of scaling reaction in the silicate system.

This set of experiments was conducted at 5 concentration of Fe(II) which are [Fe^{2+}] = 0ppm (blank), 5ppm, 10ppm, 25ppm and 50ppm. In these experiments, we formed the silicate scale by mixing the silicon brine (Si Brine) with the magnesium brine (Mg Brine) in a 50:50 ratio before an appropriate amount of filtered ferrous ion stock solution was added. The conditions for each test are tabulated in Table 6-2.

Table 6-2 The brine composition and preparation in "Effect of Ferrous Ion in Static Test"

Test	Fe^{2+} (ppm)	Fe^{2+} stock (ppm)	Fe^{2+} stock added (ml)	60ppm Mg^{2+} added (ml)	150ppm Si^{4+} added (ml)	Natural pH
1	0	-	0	50	50	10.95
2	5	500	1	50	50	10.71
3	10	500	2	50	50	10.69
4	25	500	5	50	50	10.72
5	50	5000	1	50	50	9.90

6.3.1 Experimental Results

(a) Physical Observations

A simple visual check was carried out in this test ensuring there was no oxygen contamination in the test samples. It was observed that all Fe-containing brine produced a white cloudy solution after being mixed and pH-adjusted at room temperature in the reducing environment. A slightly cloudy mixed brine was observed with the presence of 5ppm Fe and the turbidity increasing as the ferrous ion concentration increased. Likewise, all brines produced a white precipitate after 2 hours of reaction with the amount of precipitate increasing as the Fe concentration was increased as can be seen in Figure 6-17.

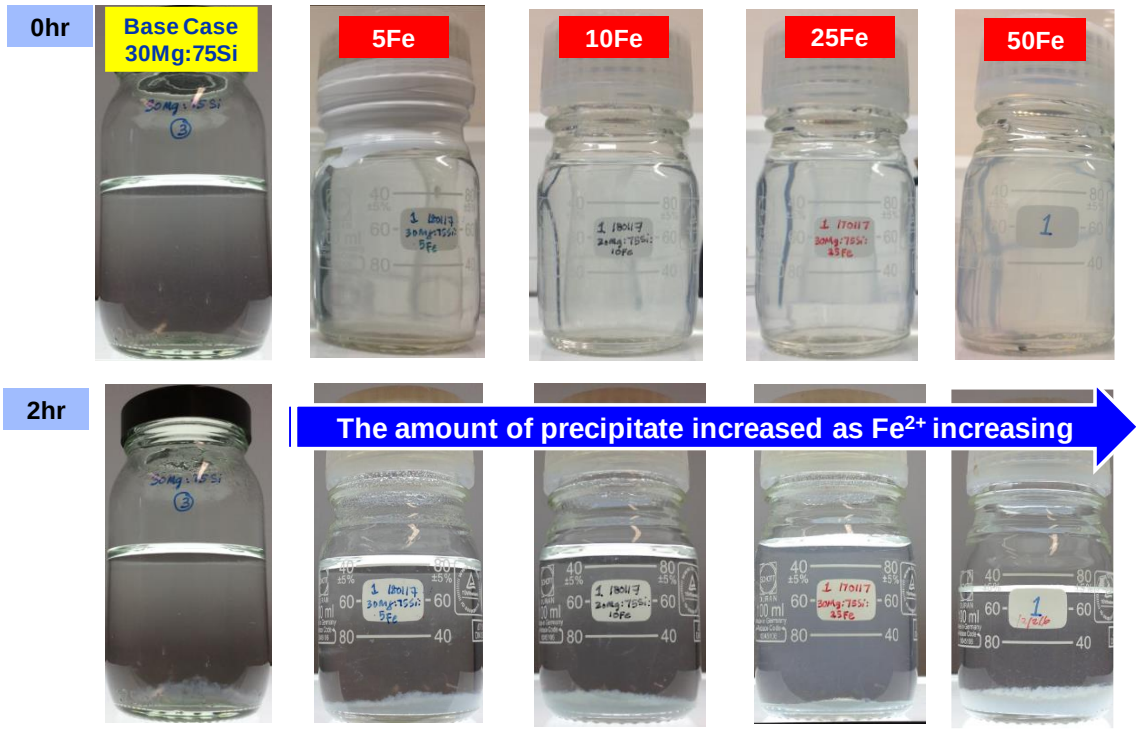

Figure 6-17 Physical observation of silicate system in Static Test with various Fe(II) ion concentrations at 0hr (Top) and 2hr (Bottom). *Please note that at 0hr, the picture of the base case was taken in different set of background.

(b) ICP Analysis

The ICP sampling at 2 hours was taken as per standard procedure, slightly below the surface. The ICP analysis plotted in Figure 6-18 and Figure 6-19 show the amount of ion reacted when various amount of ferrous ion were present in actual amounts of ion reacted (ppm) and in terms of percentage values, respectively. These figures show some interesting trends that demonstrate a clear increase in silicon ion reacted as the amount of ferrous ion added increased. It is shown that the addition of as low as 5ppm ferrous ion does affect the severity of silicate scaling produced whereby the amount of silicon and magnesium ion reacted doubled the amount reacted in the *blank* solution.

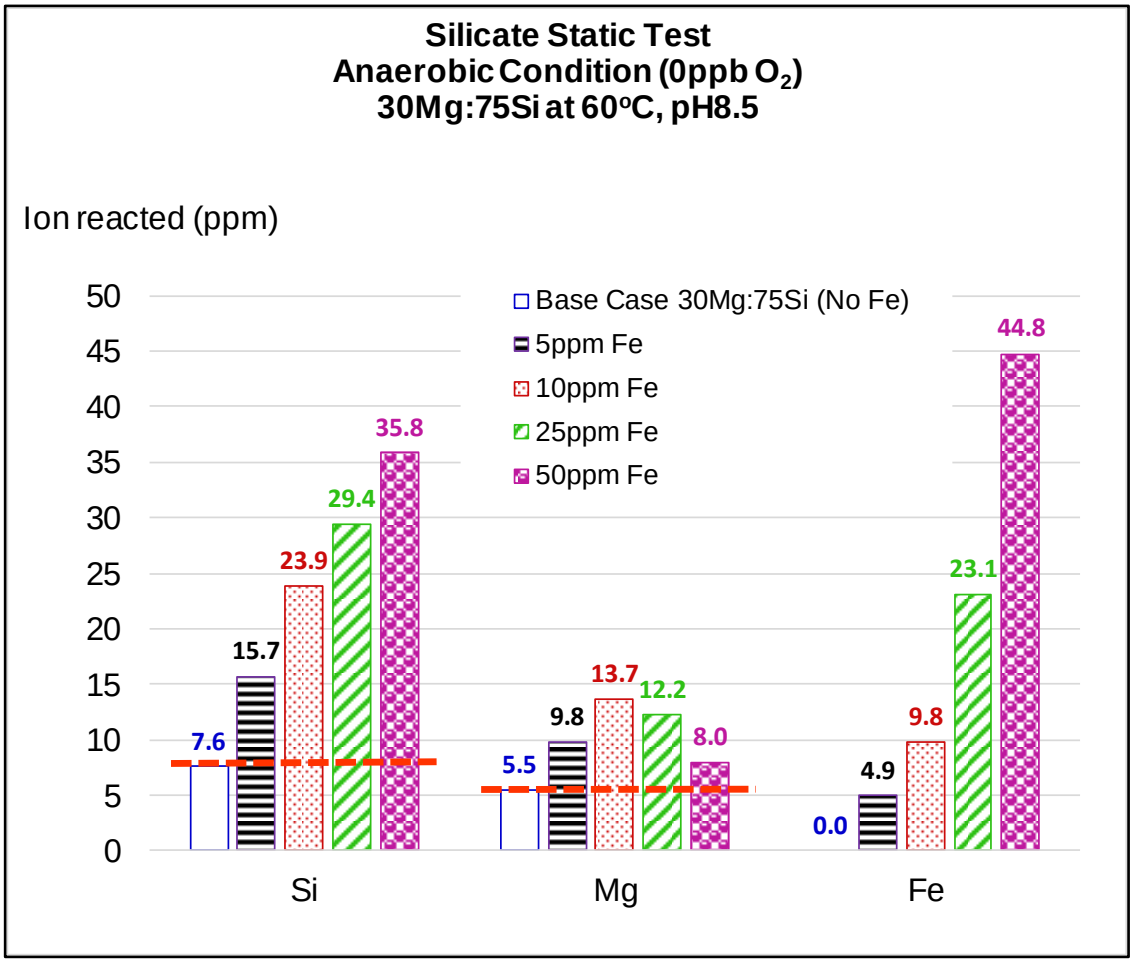

Figure 6-18 Amount of ion reacted (ppm) in silicate system of 30Mg:75Si when various amount of ferrous ion added

Results also showed that almost all ferrous ion reacted regardless of the total amount present initially; with more than 96% of any initial amount of ferrous ion reacting, i.e. being incorporated into the silicate scale.

The results for the Mg ion reacted in Figure 6-18 are a little more complex. It can also be seen from these results that the amount of magnesium ion reacted with 50ppm ferrous ion found to be less than observed in the lower ferrous ion concentrations. If this is a genuine result, it may be explained by the fact that the amount of ferrous ion reacted at this concentration are far higher than other cases. Hence, the magnesium ion may have to compete with the ferrous ion for incorporation into the silicate scale that resulted and hence slightly less magnesium ion was reacted. However, this result should be repeated and it deserves further study.

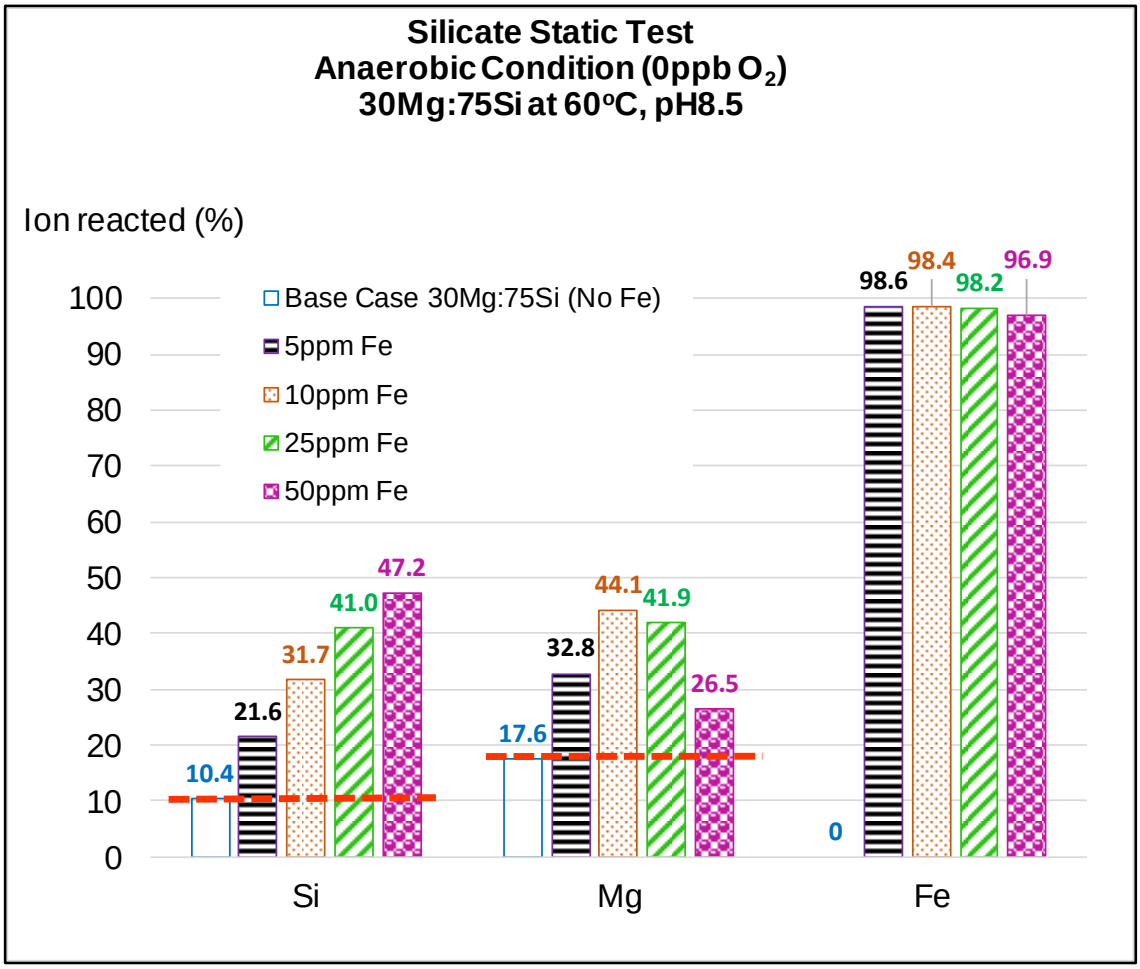

Figure 6-19 Amount of ion reacted (%) in silicate system of 30Mg:75Si when various amount of ferrous ion added

In these static bottle tests, the initial pH of the mixed brines was found to be in the range of 9.90 (when 50ppm Fe added) to 10.95 (blank) with the pH values reducing with the addition of ferrous ion. The pH values after 2 hours were found to be in the range from pH ~ 8 to ~8.20, as shown in Figure 6-20.

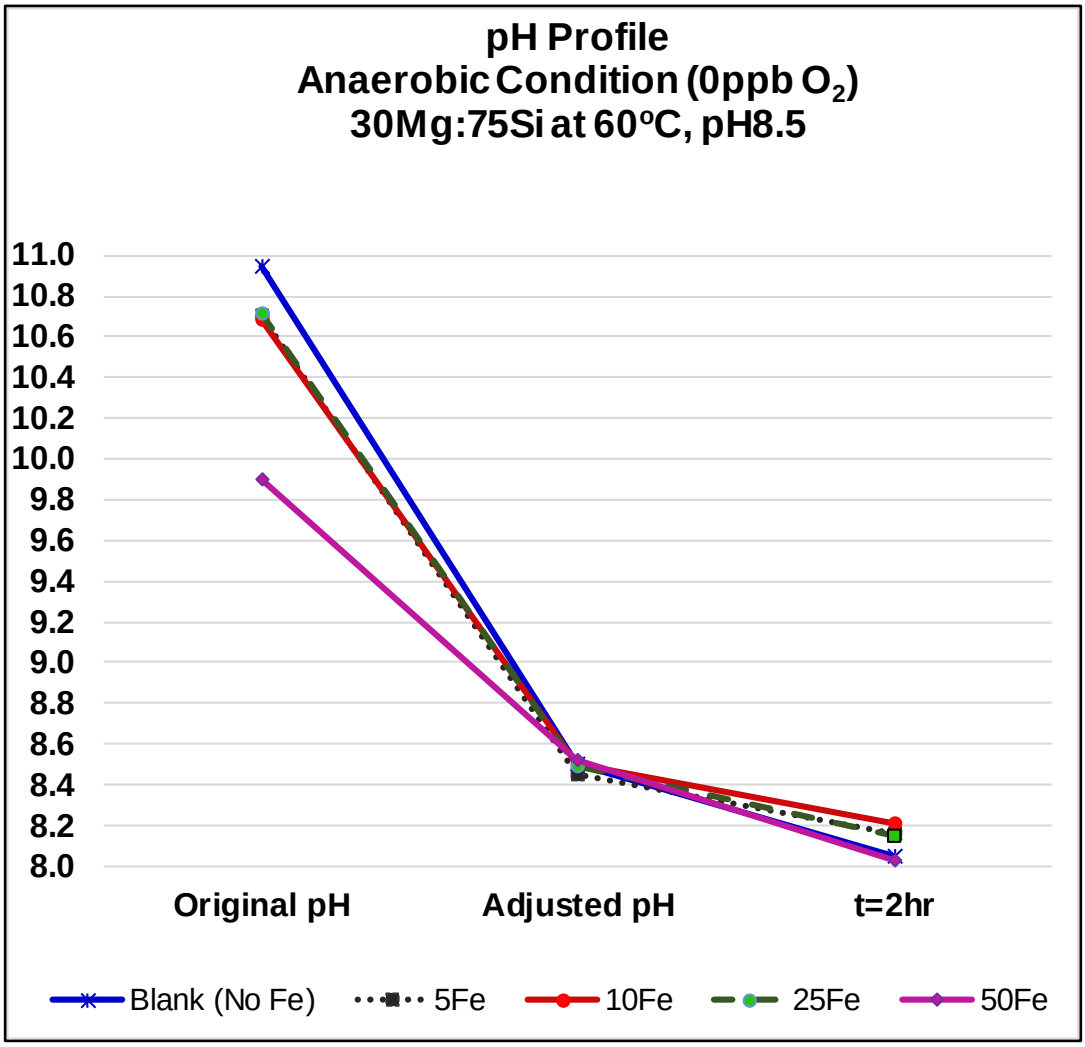

Figure 6-20 pH profile for "Effect of Ferrous Ion in Static Test" in silicate system of 30Mg:75Si

(c) ESEM/ EDAX Analysis

The precipitated silicate samples produced in these tests were filtered and examined by ESEM/EDAX analysis to study the composition and the nature of the scale. All of the mixed solutions were filtered by using 0.2 μm filters and rinsed using distilled water under aerated condition although this was carried out as quickly as possible. The filter cake samples, shown in Figure 6-21, were then left to dry at room temperature in the glove box in a reducing environment for at least 24 hours. It was observed that the higher the initial ferrous ion concentration present in the mixed solution, the thicker and the darker was the precipitated filter cake produced.

ESEM images of the precipitates produced in these tests are shown in Figure 6-22 where it can be seen that they are amorphous in nature.

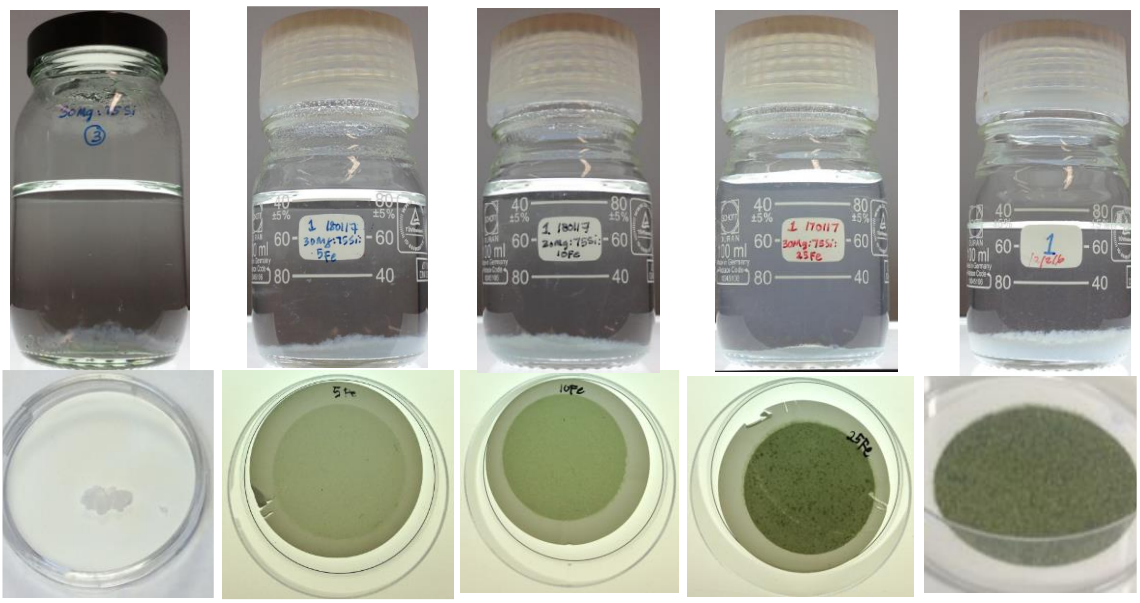

(i) Blank (ii) 5ppm Fe (iii) 10ppm Fe (iv) 25ppm Fe (v) 50ppm Fe

Figure 6-21 Precipitate formed for various amounts of Fe(II) present in Silicate Static Bottle Tests

The study presents an examination of the precipitate produced in the ferrous-containing silicate brines in a reducing environment. From the ICP data analysis plotted in Figure 6-18, we can calculate the effective stoichiometry of the silicate precipitates in terms of Si:Mg, and Fe:Mg and Fe:Si molar ratios, for each set of experimental conditions. The atomic % from EDAX analysis is plotted in Figure 6-23 where this information will be useful to check the effective stoichiometry on the actual precipitate. The stoichiometry ratio i.e. Si:Mg, and Fe:Mg and Fe:Si molar ratios determined from (i) the actual precipitate measured by ESEM/EDAX and (ii) the values determined from the ICP measurement, are shown in Figure 6-24, Figure 6-25 and Figure 6-26, respectively.

Generally, results indicate that the Si:Mg, Fe:Mg and Fe:Si molar ratios determined from the ICP measurement increased as the amount of ferrous ion initially in the mixed brine increased. All of these values are in good agreement with values determined from EDAX analysis on the actual precipitates. An interesting trend on the relationship between Si:Mg and Si:Fe molar ratios is observed in Figure 6-27. These results indicate that the Si:Mg molar ratios increases as the ferrous ion increased, which is the opposite of what is observed for the Si:Fe molar ratios.

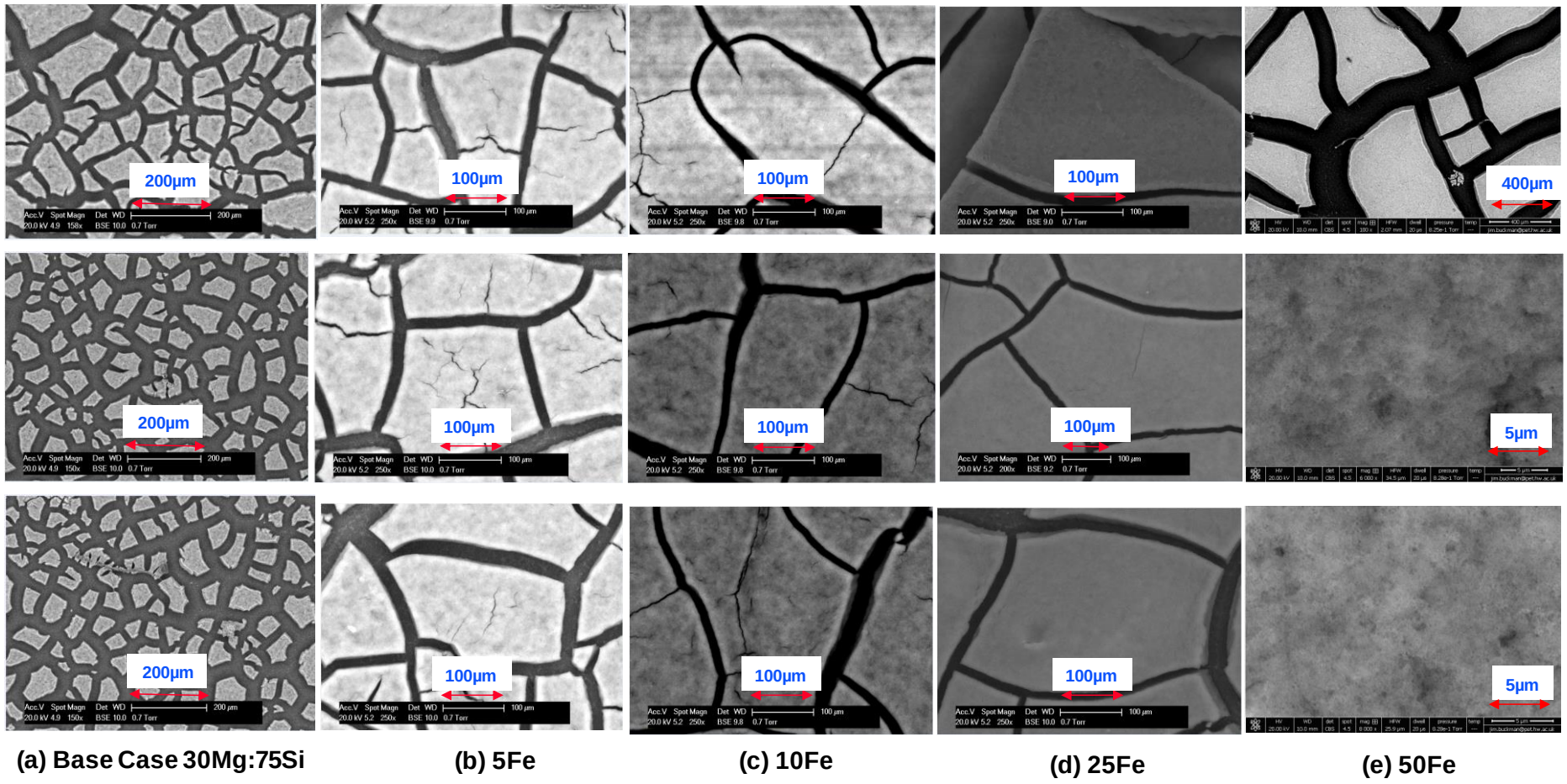

Figure 6-22 ESEM images of ferrous-containing silicate solution system of 30Mg:75Si at 60°C, pH8.5

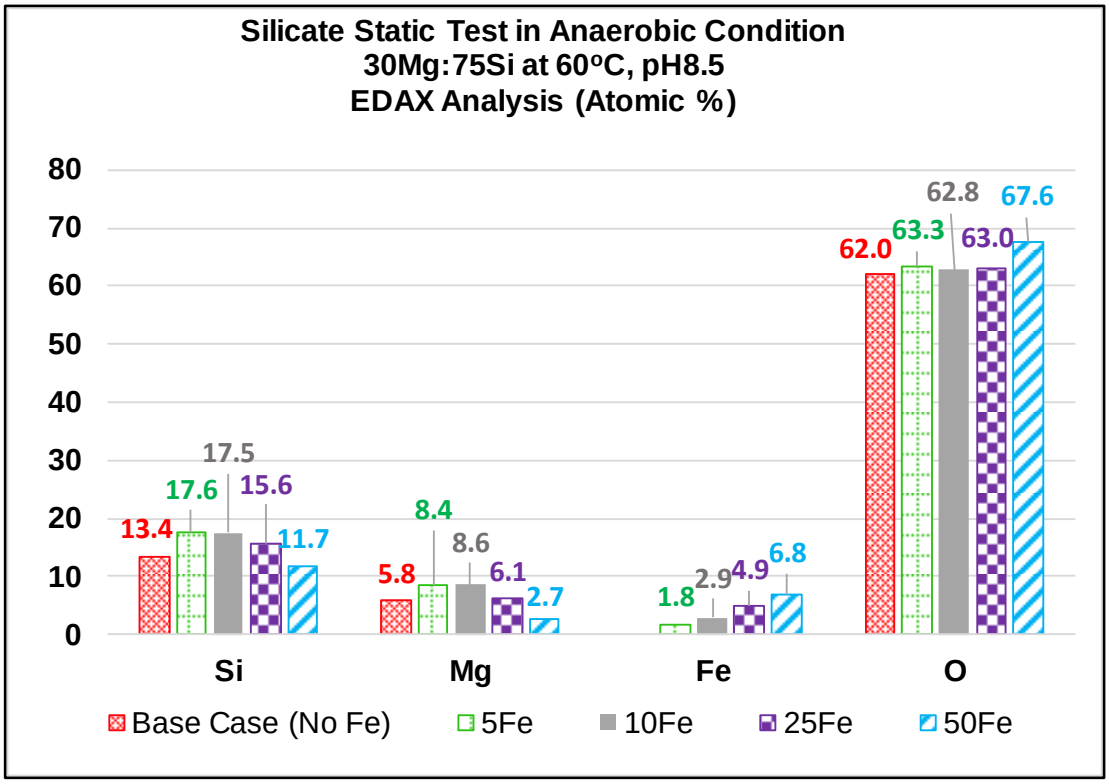

Figure 6-23 Atomic % in precipitate of *blank* (No Fe) and 30Mg:75Si + 50Fe at 60°C, pH8.5 – EDAX data

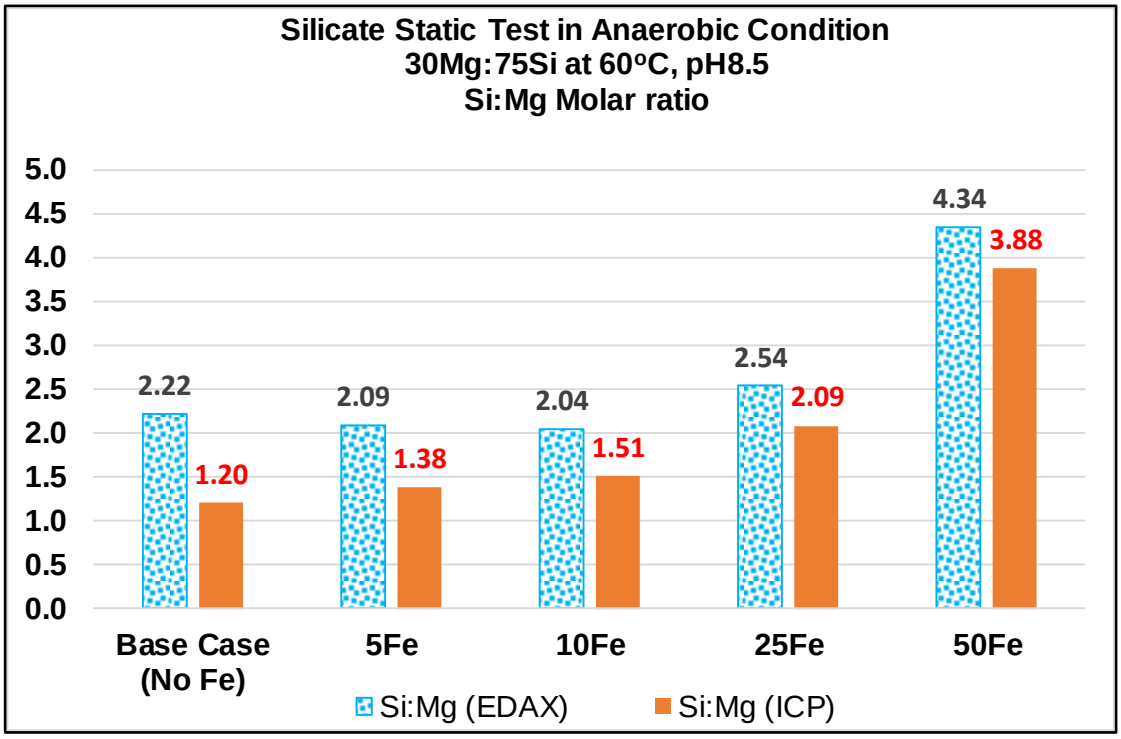

Figure 6-24 Si:Mg molar ratio of *blank* (No Fe) and 30Mg:75Si + Fe at 60°C, pH8.5 – EDAX analysis vs. ICP analysis

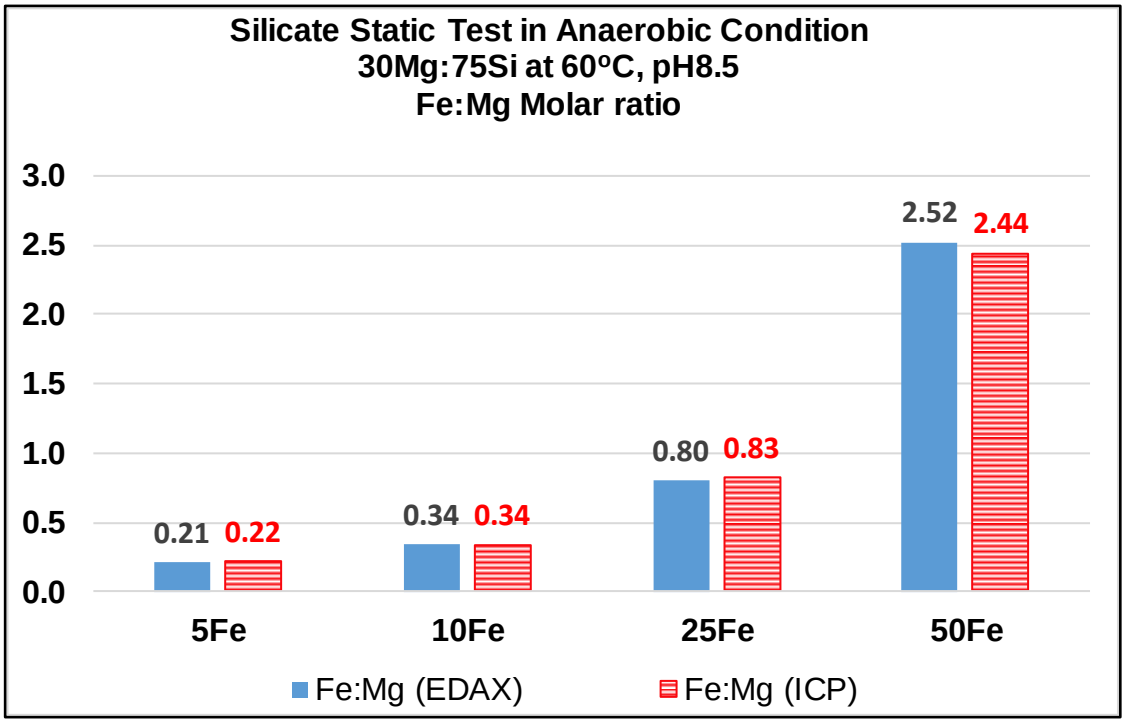

Figure 6-25 Fe:Mg molar ratio of *blank* (No Fe) and 30Mg:75Si + Fe at 60°C, pH8.5 – EDAX analysis vs. ICP analysis

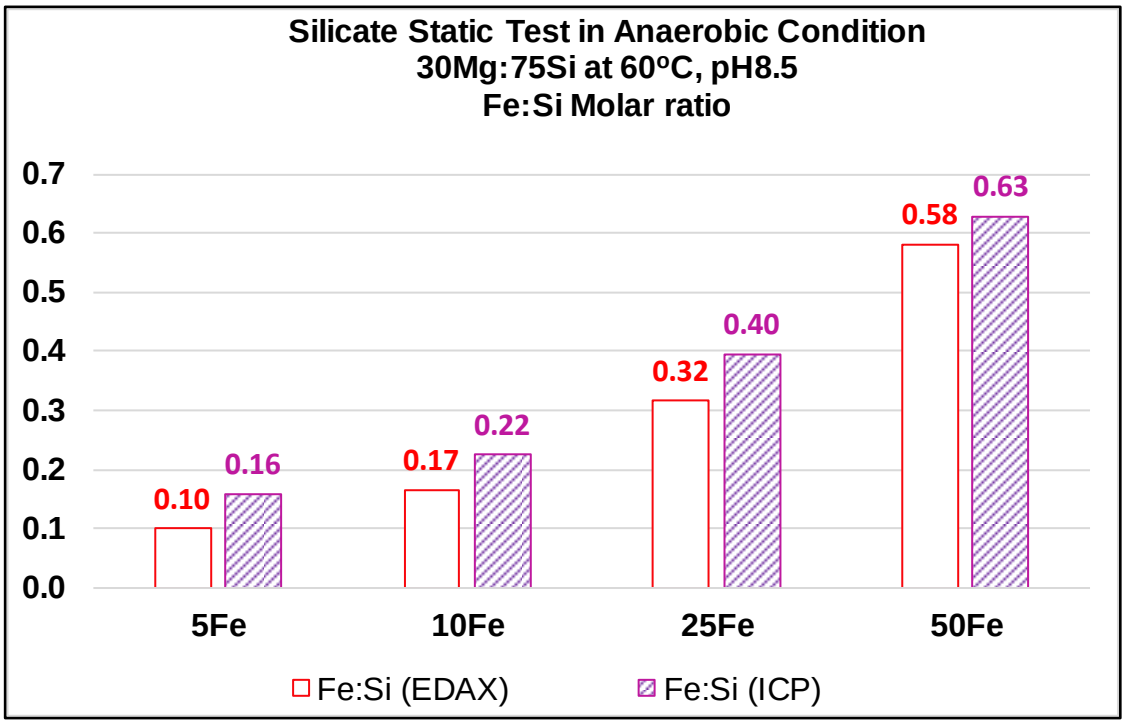

Figure 6-26 Fe:Si molar ratio of *blank* (No Fe) and 30Mg:75Si + Fe at 60°C, pH8.5 – EDAX analysis vs. ICP analysis

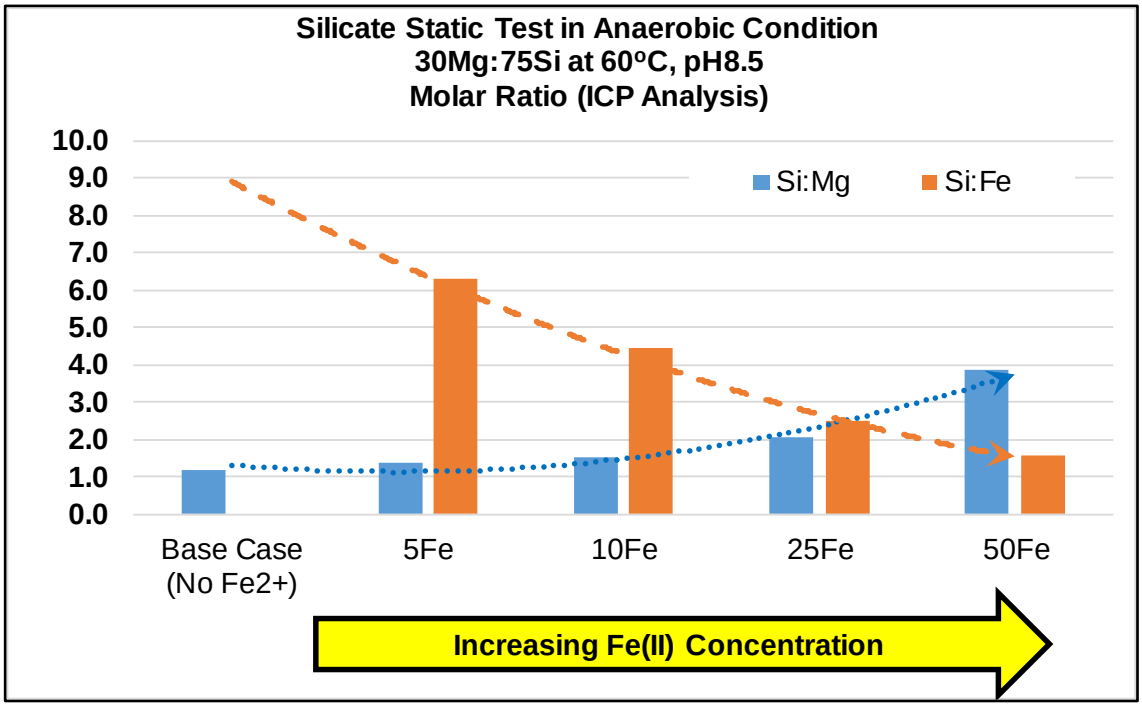

Figure 6-27 Relationship between Si:Mg and Si:Fe

(d) FTIR Analysis

The ICP analysis discussed above allowed us to determine the extent of reaction of magnesium, silicon and ferrous ion in the mixed silicate brine. Further analysis using the ESEM/EDAX enabled us to determine the elemental composition in the precipitates. Both techniques (ICP and ESEM/EDAX) suggested that all ions were reacted to some extent and this information helps us to anticipate the type of scale(s) that may form in this system. ESEM/EDAX analysis not only gives a useful microscopic pictures of the precipitate surface but also gives an approximate elemental composition of the precipitates.

Considering the fact that only a small amount of precipitate was produced in each test (< 1g), further characterization using MS and XRD may not be possible. FTIR-ATR is a versatile and non-destructive techniques which can be applied to a variety of materials. This technique also requires minimal preparation. Hence, we further analyse the precipitate using FTIR to identify the characteristic structural groups (functional groups) present in these molecules. The fingerprint region 600 – 1400cm^{-1} of the spectrum contains a complex set of absorptions, which are unique to each compound. Although

these are hard to interpret visually, by comparison with spectral lines from reference samples, they allow the identification of specific functional groups within compounds.

Considering all ions present initially that reacted at test condition of pH8.5 in the reducing environment, we can expect to see the scales in Table 6-3, while all possible scales are tabulated in Table 6-4 (some of which do not form):

Table 6-3 Precipitate that impossible to form (At test condition of pH8.5, <5ppb O_2)

	Salts	Solubility in water (ppm)	Description
1	$Mg(OH)_2$	6.4	Magnesium hydroxide only precipitate at pH>9.2 (Liu, S.T. and Nancollas, G.H., 1973) and (Chieng, C. and Nancollas, G.H., 1982)
2	$Fe(OH)_2$	7200	a. Solid bluish-green ferrous hydroxide at pH>8.5 (Lehigh University, 2000) b. May exist at pH>10 (U.S. Geological Survey, 1962) c. Iron (II) hydroxide is white if O_2 is excluded. In reality forms a "dirty green" and exposure to air, rapidly turning brown on oxidation to Fe (III) (Brown, 2000)
3	$Fe_2(OH)_3$	Insoluble at pH7	Orange solid ferric hydroxide. Not formed as O_2 is kept at <5ppb in this experiment
4	$Fe_2(SiO_3)_3$		Amorphous Fe (III) silicate not formed as O_2 is kept at <5ppb in this experiment

Table 6-4 Precipitate that may formed (At test condition of pH8.5, <5ppb O_2)

	Salts	Common Name	Description
1	$MgSiO_3$	Amorphous enstatite	Ilminite, antishovite
2	Mg_2SiO_4	Amorphous forsterite	Magnesium-rich end member of olivine – colorless, green, yellow, yellow green, white
3	$FeSiO_3$	Amorphous ferrous silicate	One of the scale formed in the superheaters and steam path of turbine

4	Fe_2SiO_4	Amorphous fayalite	Iron chrysolite Iron-rich end member of olivine –darker color than forsterite; brown, black
5	$(Mg, Fe)_2SiO_4$	Amorphous olivine	Color pale olive green to yellow green; occasionally brown, white Amorphous olivine with various compositions
6	$MgFeSiO_4$	Amorphous olivine	
7	$Mg_{0.8}Fe_{1.2}SiO_4$	Amorphous olivine	
8	$MgFeSi_2O_6$	Amorphous pyroxene	

FTIR spectra of the precipitate produced in ferrous-containing silicate brines in these static bottle tests in this reducing environment are shown in Figure 6-28. Some of the fingerprints are always seen in silicate type scale. Our aim is to identify the type of scale(s) that may have formed in the precipitate.

Rauch and Keppler (1998) and Bolfan-Casanova et al. (1998, 2000) found that clinoenstatite ($MgSiO_3$) consisted of three strong band and sharp bands at low frequency (~3600cm-1) and two weak and broad bands (~3000 and ~3400cm-1). These bands related to $MgSiO_3$ are not seen in our spectra. Karakassides et al. (1997, 1999) found that absorption due to the Si-O-Si and Si-O-M groups (M=Al, Mg, Fe) was seen at 950-1200cm-1 which matched bands observed in the test precipitates. These findings hence confirmed the presence of Si-O-Mg. The bands described earlier by Rauch and Keppler (1998) and Bolfan-Casanova et al. (2000, 2013) were probably hindered by many –OH stretching band ~3585cm-1 and bands due to water; an asymmetric broad band ranging from 2750 to 3800cm-1 with a shoulder around 3260cm-1 as proposed by Fukuda (2012).

Hernández-Ortiz et al. (2012) showed that absorption bands near 1100, 790, and 480cm-1 are common to all silicates with tetrahedrally coordinated silicon Si-O-Si and a band due to SiO_2 can be seen at about 1200cm-1. Ying (2007) also showed that a band due to Si-O-Si at 795-799cm-1 was not observed in his work on poly-silicic-ferric coagulant. In our samples, the band at ~795cm-1 is very weak when 5ppm ferrous ion is present in our brine and this band became less intense as the ferrous ion concentration increased. These observations may suggest that the scale may have transform from Si-O-Si to Si-O-Fe in higher ferrous concentration.

Day (1981) showed that bands due to Fe(II)-silicate scale i.e. $FeSiO_3$ and Fe_2SiO_4 appeared at 950cm-1 and 980cm-1 respectively. In our work, we observed that absorption band near 1100cm-1 have shifted to 993-1000cm-1. This may be explained by the fact that the Fe^{2+} may have already bridged the tetrahedrally coordinated silicon Si-O-Si to form Si-O-Fe.

Parveen et al. (2010) concluded in her work that $Fe(OH)_2$ has important characteristic peaks – a pair at 796 & 899 cm-1 which cannot be observed in our precipitates. This has supported our discussion earlier that ferrous hydroxide is probably not produced in our system as the pH profile was between 8-8.5 throughout the reaction. The small peak at 1456 cm^{-1} due to the bending vibration of OH bond as found in $Mg(OH)_2$ precipitate reported by Jiang et al. (2009) is not seen in our FTIR spectra. These findings again support our argument that magnesium hydroxide was not formed in our precipitate, as it may only precipitate in solutions with pH >9.2. Karakassides et al. (1999) confirmed that a band due to Si-O-Fe(III) is seen at 974cm-1 which again is not observed in our precipitate.

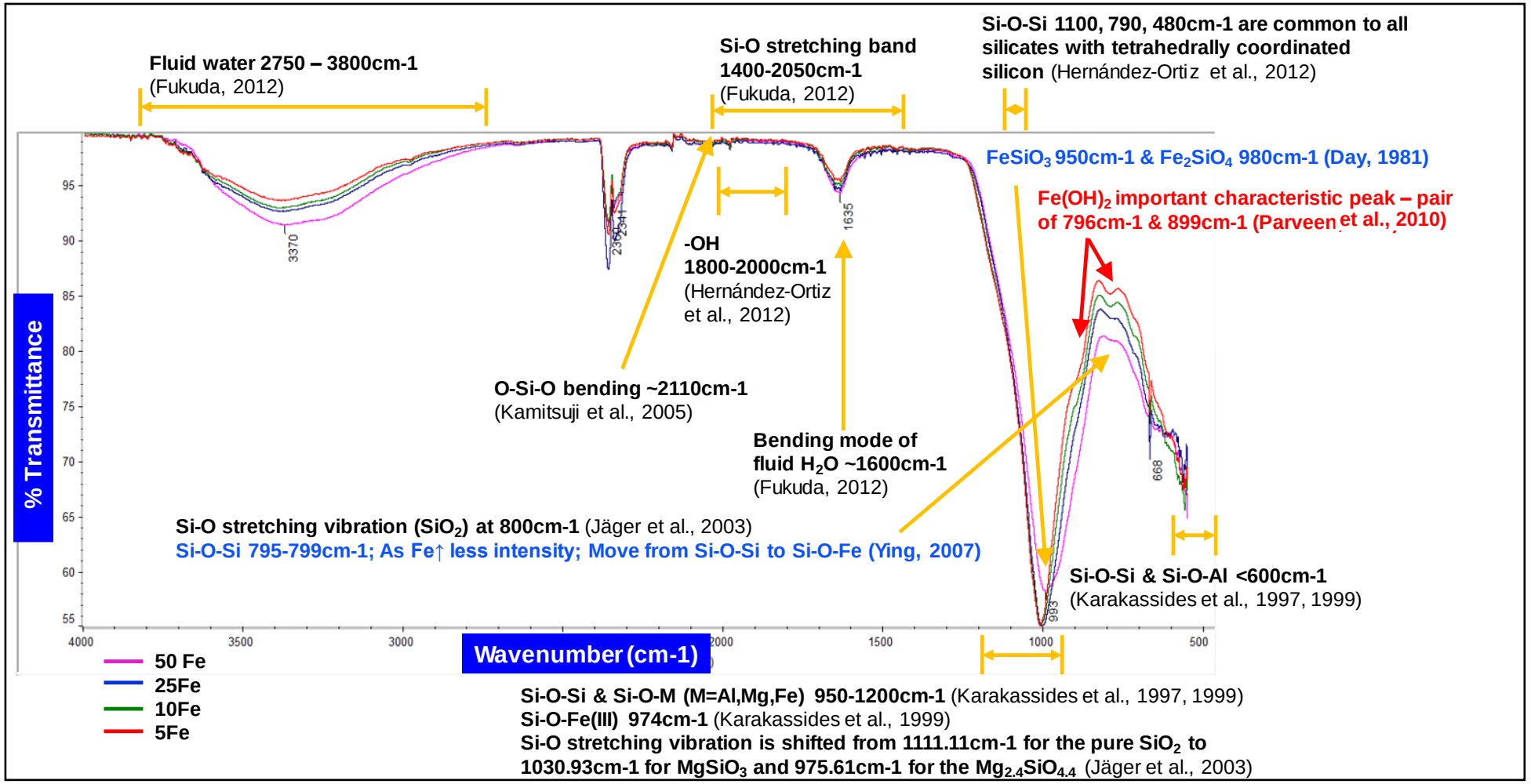

Figure 6-28 FTIR spectra analysis - Precipitate formed in the silicate system 30Mg:75Si at 60ºC, pH8.5, anaerobic condition with the presence of various ferrous ion concentrations

6.3.2 Summary and Conclusions

Our initial work on the effect of ferrous ion on the silicate system had been further extended to include various ferrous ion concentrations. Results obtained are repeatable and reproducible and a number of novel findings on how ferrous ion will affect the silicate system have been found as follows;

a) Fe^{2+} does affect the silicate scaling system and this was demonstrated for the 30Mg:75Si base case. It was demonstrated that the amount of Mg and Si ion reacted was considerably higher than in the *blank* (with no Fe^{2+});

b) Generally, the amount of ions reacted (i.e. Mg & Si) increased with increasing amount of Fe^{2+}; the amount of Mg/Si reaction was doubled when 5ppm of Fe^{2+} ion was present;

c) Almost all the initial ferrous ion reacted, regardless of the amount introduced initially into the system. This ferrous ion was completely incorporated into the silicate scale, suggesting that the ferrous ion more readily bridges the silicate scale as compared with the magnesium ion;

d) From the ESEM/EDAX analysis, we confirmed that the silicate scale produced in the presence of Fe^{2+} is amorphous in nature;

e) Generally, the molar ratio (Si:Mg , Si:Fe, Fe:Mg) in the precipitate formed calculated by both techniques i.e. ICP analysis & EDAX analysis agreed with each other which confirmed the repeatability and reproducibility of the experimental techniques deployed;

f) The FTIR spectra for the static test silicate (+Fe) precipitates confirmed the presence of following functional groups Si-O-Si, Si-O-Fe, Si-O-Mg, $MgSiO_3$, Fe(II)- within the silicate scale. These results do not conclusively identify the exact chemical nature of the precipitate. However, the scales produced are likely to be a mixture of amorphous silica, amorphous Mg-silicate, amorphous Fe-silicate and amorphous Mg-Fe-silicate;

g) The FTIR spectra for static silicate (+Fe) test confirmed the ***absence*** of following salts - $Fe(OH)_2$, $Mg(OH)_2$, $Fe(OH)_3$, Si-O-Fe(III).

6.4. EFFECT OF FERROUS ION ON THE INHIBITION EFFICIENCY OF A5

Following the results described above, we now know that ferrous ion will affect the silicate scaling system by producing much more silicate scale in the presence ferrous ion. It has also been established that both the magnesium ion and the ferrous ion are incorporated into the silicate scale. At that point, we then undertook a systematic investigation to study the effect of the same ferrous ion concentrations tested in section 6.3 on the performance of one of the best silicate inhibitors (or dispersants), denoted as A5, which we had tested in previous work for the silicate system (30Mg:75Si) in the absence of Fe. Due to time constraint with this study, work focused on the A5 performance only, as A5 performed the best and totally inhibit the silicate scale in the "*manageable"* base case (30Mg:75Si) as discussed in section 5.8.

6.4.1 Experimental Details

The experimental methodology deployed for this study was essentially the same as that described earlier, except the silicon brine was prepared with A5 as shown in Figure 6-29. Five ferrous concentration as used previously (0, 5, 10, 25, 50 ppm) were added into the brine mix finally containing 30Mg:75Si:50A5 (i.e. 50ppm of A5 was used) as shown in Table 6-5.

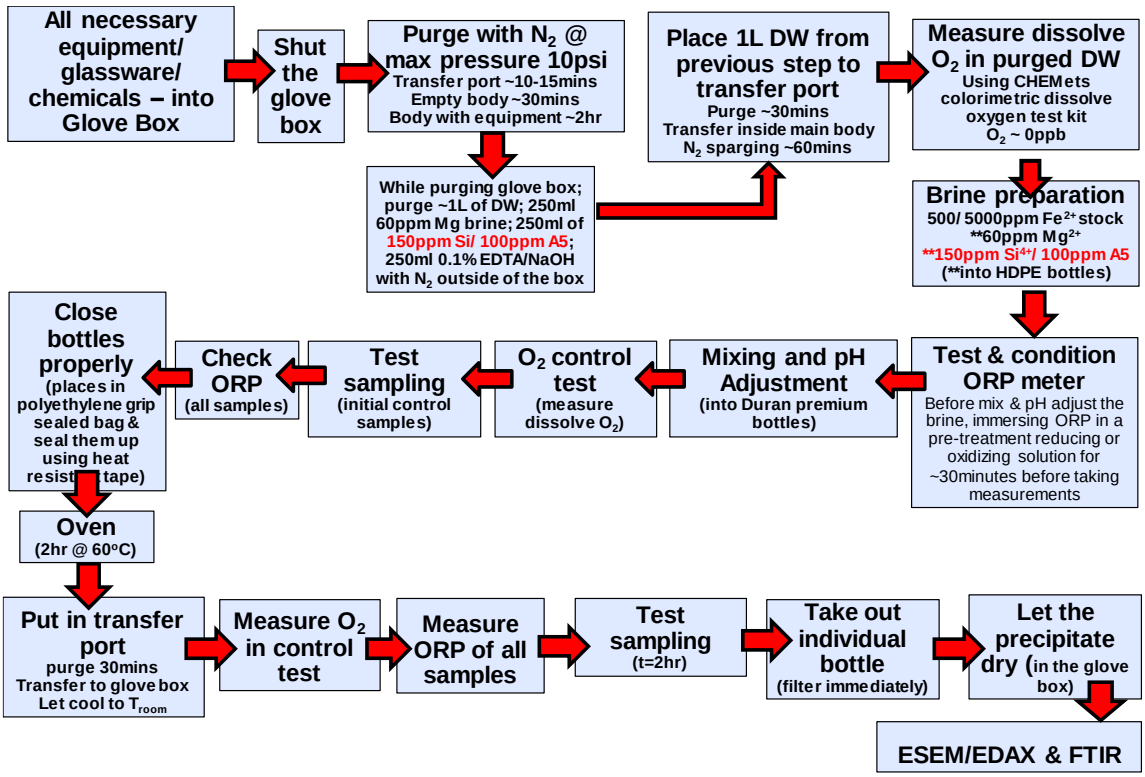

Figure 6-29 Summary of experimental methodology: Effect of ferrous ion on the A5 performance in silicate system 30Mg:75Si at 60°C, pH8.5, anaerobic condition

Table 6-5 The brine composition and preparation in "Effect of Ferrous Ion in Static IE Test"

Test	Fe^{2+} (ppm)	Fe^{2+} stock (ppm)	Fe^{2+} stock added (ml)	60ppm Mg^{2+} added (ml)	150ppm Si^{4+} / 100ppm A5 added (ml)	Natural pH
1	0 (*Blank*)	-	0	50	50	10.95
2	5	500	1	50	50	10.67
3	10	500	2	50	50	10.52
4	25	500	5	50	50	10.14
5	50	5000	1	50	50	9.72

6.4.2 Experimental Results

(a) Physical Observations

The oxygen content in all *inhibited blanks (mixed brine of 30Mg:75Si with 50A5 but no Fe^{2+})* and test samples was monitored throughout the test ensuring that a reducing environment was maintained. As explained in the test methodology section, the O_2 content was measured in the *O_2 control* samples only whereas all test samples were monitored throughout by physical observation only; i.e. by checking whether or not they may have experience colour changes that might indicate the oxidation of the ferrous ion.

As tabulated in Table 6-6, purely anaerobic conditions (i.e. <5ppb O_2) were achieved in all test condition except for the test with 50ppm Fe. Oxygen content in the 50ppm Fe case was measured to be within 0-10ppb, although no colour changes was observed in the test samples at 0hour. Also, it is worth noting that the oxygen level was successfully maintained at the same level 0-10ppb throughout the 2-hr reaction where the brine appears as a white cloudy solution. This information will be useful in determining the cut off value of the oxygen level that is allowed in this study. Observations in section 6.2.2(b) already indicated that the ferrous ion may have already oxidized to ferric ion when the oxygen level was as low as 20ppb. Yet, it is always good practice to ensure the <5ppb O_2 level is achieved in the glovebox and maintained throughout the reaction.

The photographs in Figure 6-30 clearly show that all Fe-containing brines with up to 25ppm ferrous ion stay clear after being mixed and pH-adjusted at room temperature. However, for the 50ppm Fe-containing brine, the solution became slightly cloudy immediately after being mixed and pH-adjusted, as can be seen in the same figure. All of the brines except the *inhibited blanks* became cloudy after being left for two hours in the

oven and the turbidity of the solutions increased with increasing ferrous ion concentration.

Table 6-6 O_2 content monitoring – O_2 measurement and physical observations

Test Condition	O_2 content monitoring			
	O_2 control samples (ppb)		Physical Observation in Test Samples	
Fe^{2+} (ppm)	t=0hr	t=2hr	t=0hr	t=2hr
0 (*Blank*)	<5	<5	Clear solution	Clear solution
5	<5	<5	Clear solution	Slightly cloudy
10	<5	<5	Clear solution	Slightly cloudy
25	<5	<5	Clear solution	Slightly cloudy
50	<10	<10	Slightly cloudy	Cloudy

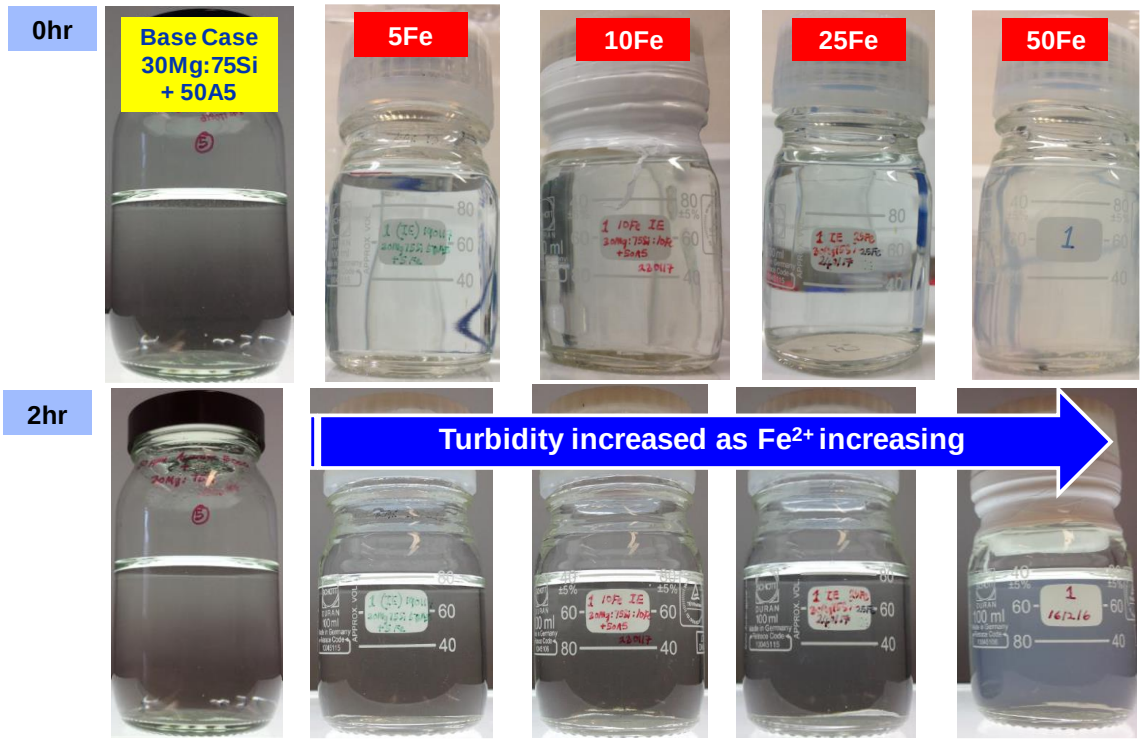

Figure 6-30 Physical observation of silicate system in A5 Static IE Test with various Fe(II) ion concentrations at 0hr (Top) and 2hr (Bottom). *Please note that at 0hr, the picture of the base case was taken in different set of background.

(b) ICP Analysis

The ICP measurement allows us to determine the severity of silicate scale production and to confirm and quantify the above observations. Figure 6-31 and Figure 6-32 shows the amount of ions reacted when 50ppm A5 was added to the Mg/Si/Fe mixed brine, plotted as actual concentration in ppm unit and as percentages, respectively.

Generally, we can conclude that observation made in Figure 6-30 are in good agreement with the ICP analysis. The graphs plotted in Figure 6-31 and Figure 6-32 clearly show that the amount of magnesium, silicon and ferrous ion reacted increased as the amount of ferrous ion added increases. This may explain the increasing in turbidity observable in Figure 6-30.

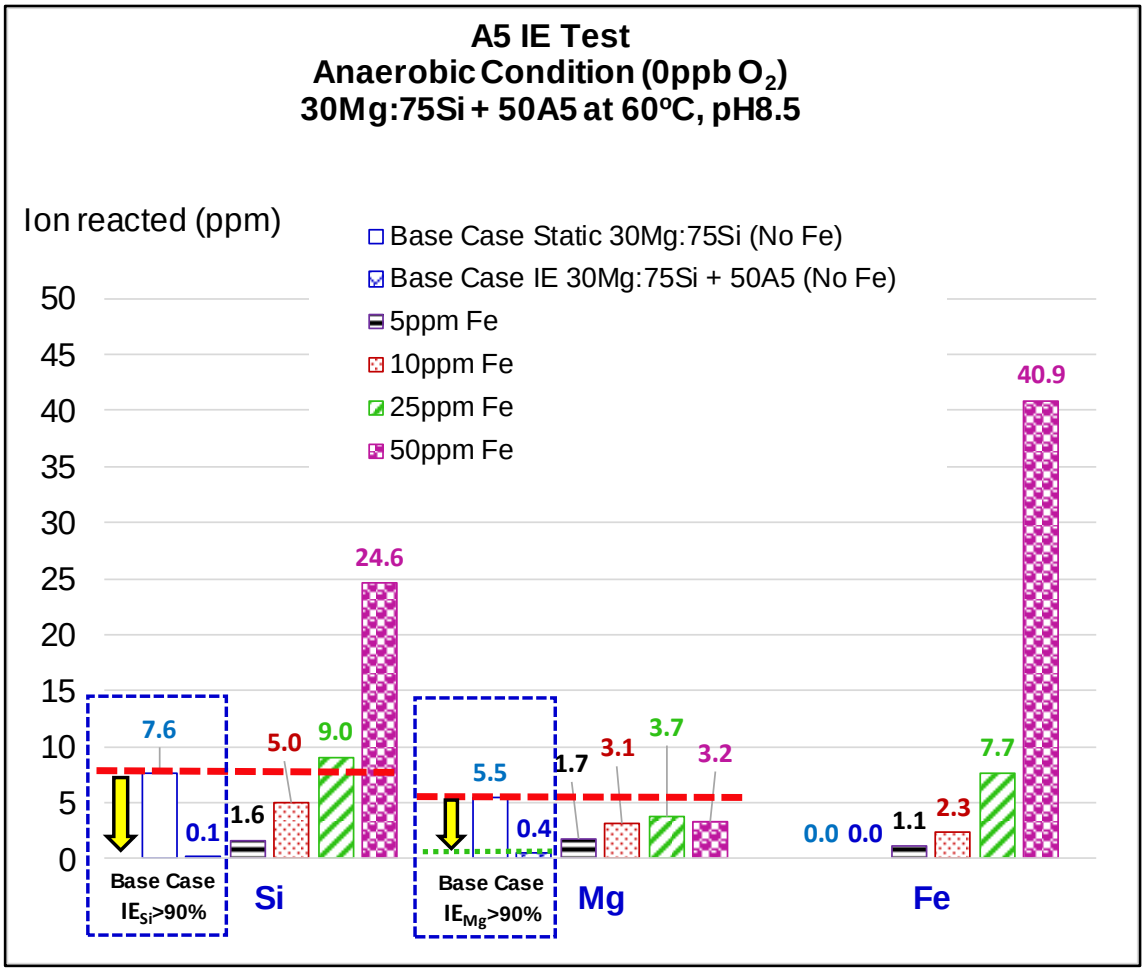

Figure 6-31 Amount of ion reacted (ppm) in Anaerobic Static IE Test of silicate system 30Mg, 75Si at 60°C, pH8.5

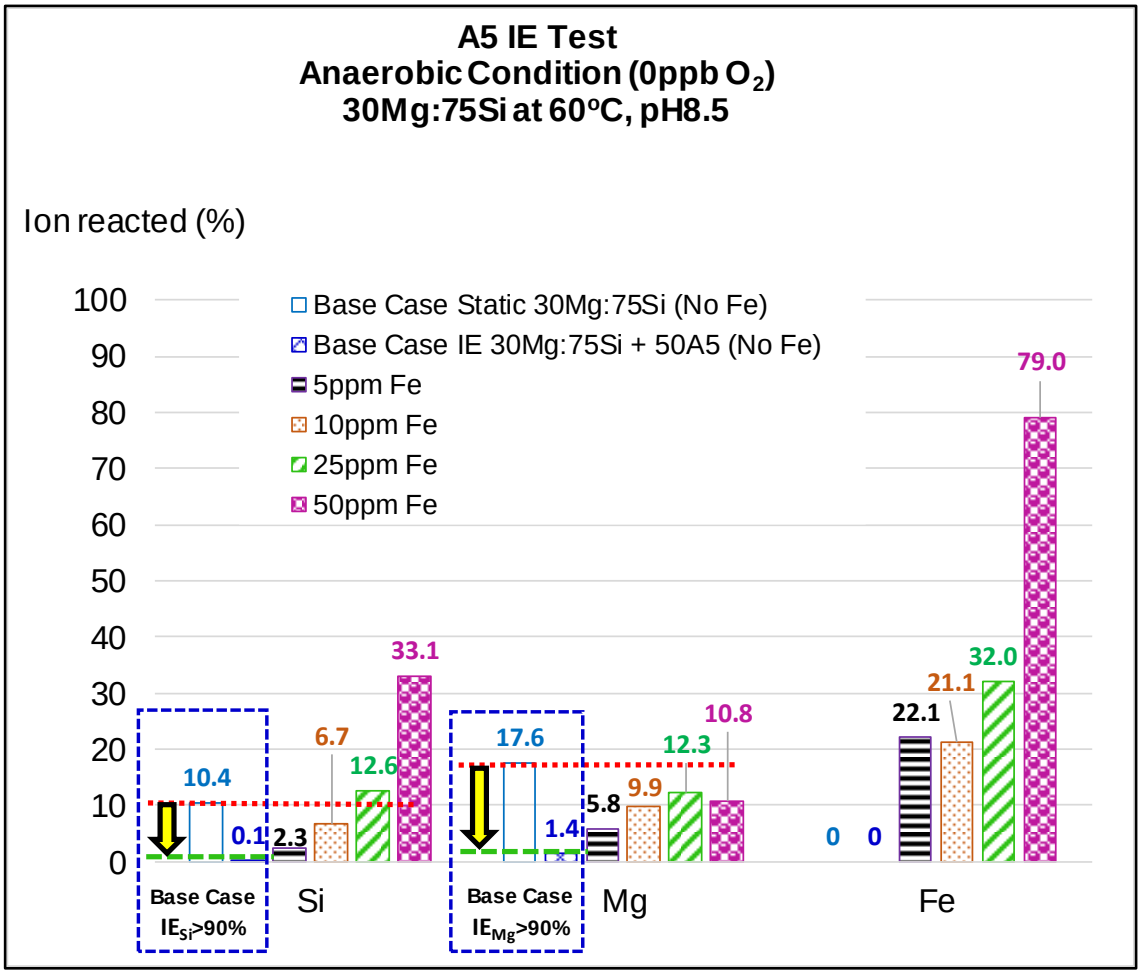

Figure 6-32 Amount of ion reacted (%) in Anaerobic Static IE Test of silicate system 30Mg:75Si + 50A5 at 60°C, pH8.5

Results obtained from ICP analysis indicated that Fe^{2+} ***does*** affect the performance of A5 where we observe that the addition of 5ppm Fe^{2+} resulted in 4 times higher and 20 times higher in Mg ion reacted and Si ion reacted respectively (i.e. when compared with scaling reaction in the *inhibited blank "manageable"* base case Silicate IE Test of 30Mg:75Si:50A5 at 60°C, pH8.5). These results suggested that Fe^{2+} does severely affect the capability of the A5 species to inhibit Si polymerization. The results also show that the A5 performance towards Mg-silicate is not much affected since the addition of ferrous ion as high as 50ppm showed that the amount of magnesium reacted was still less than the amount reacted in the *non-inhibited blank* (*(mixed brine of 30Mg:75Si with no A5 and no* Fe^{2+}*)* solution. Nevertheless, from the same figures, it is evident that the addition of 25 and 50ppm of ferrous ion has severely affected the performance of the A5 to inhibit the amorphous silica; it can be seen that the amount of silicon reacted in both cases is much higher than is observed in the *non-inhibited blank* solution. Results however shows

some interesting finding; for example, the A5 worked quite well to stop 70-80% of ferrous ion from reacting when there was 5-25ppm ferrous ion introduced into the solution. However, at the higher ferrous ion concentration, i.e. 50ppm, A5 was less able to prevent the formation of the ferrous-silicate scale; at 50ppm Fe, then only one fifth of the ferrous ion can be stopped from reacting.

The A5 performance results are plotted in Figure 6-33 in terms of IE_{Mg} % and IE_{Si} % respectively. However, the IE_{Mg} % and IE_{Si} % terms are now not exactly as explained in *Chapter 5* since the scales produced could be a mix of amorphous silica, amorphous Mg-silicate, amorphous Fe-silicate and amorphous Mg-Fe-silicate scale as discussed in section 6.3.2. IE_{Mg} % and IE_{Si} % are now defined as the inhibition efficiency percentage of A5 to stop magnesium ion and silicon ion from reacting. It is worth noting here that IE% calculated based on the individual blank (non-inhibited mixed brine of 30Mg:75Si + Fe^{2+}) of each Fe^{2+} concentration present initially in the inhibited brine of 30Mg:75Si + 50A5; which mean C_B is different depending on the ion concentration in the individual [Fe^{2+}] blank solution at the sampling time. For example, for IE% when 5ppm of Fe present in the inhibited mixed brine i.e. 30Mg:75Si:50A5 + 5Fe; C_B is the blank of non-inhibited mixed brine i.e. 30Mg:75Si + 5Fe.

As can be seen from Figure 6-33, the inhibition efficiency of A5 stopping the magnesium ion from participating in the reaction is reduced to about ~12% when as low as 5ppm of ferrous ion is present in the brine. Likewise, the addition of more ferrous ion in solution further reduces the performance of A5 to stop the reaction of magnesium ion to only ~18% at 2 hours. Generally, the IE% of Mg & Si were declining as the amount of ferrous ion present initially in the inhibited brine increased. The performance of A5 to stop the silicon ion reacting is severely affected when 25ppm and 50ppm of ferrous ion is present in the samples, as can be observed in the same graph. When 25ppm of Fe^{2+} is present in the inhibited brine, A5 is only ~69% and ~72% efficient against Si and Mg ions from reacting further. Likewise, the performance of 50ppm A5 to inhibit this *"manageable"* silicate system was severely affected with the presence of 50ppm of ferrous ion where it is ~28% and ~59% efficient against Si and Mg ions from reacting further. It is also shown that A5 can only stop ~19% of ferrous ion (of total 50ppm Fe^{2+} present initially) being incorporated into the silicate chain. These findings suggest that the addition of >25ppm of ferrous ion severely affects the A5 ability to inhibit the silicate scale.

As a conclusion, Fe^{2+} (as low as 5ppm) has a detrimental effect on the A5 IE %. This means that more A5 will be required to prevent silicate scale when ferrous ion is present. The pH profile throughout the reaction is plotted in Figure 6-34. The results in this figure show that the pH values reduced with time to pH ~8 to ~8.20.

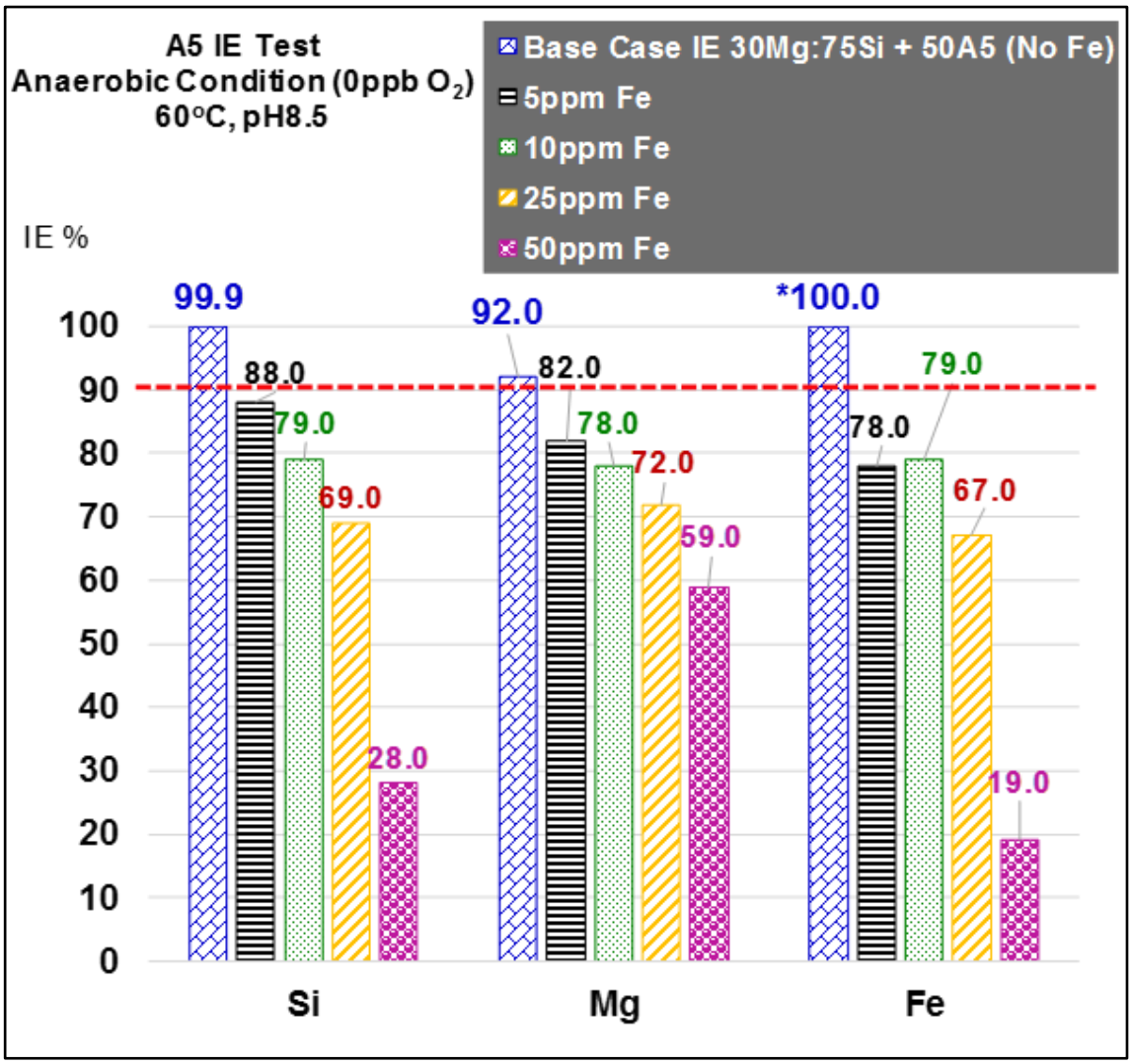

Figure 6-33 A5 performance in terms of IE_{Si} % and IE_{Mg} % in Anaerobic Static IE Test of silicate system 30Mg:75Si + 50A5 at 60°C, pH8.5 when various amount of ferrous present

***No Fe in the base case**

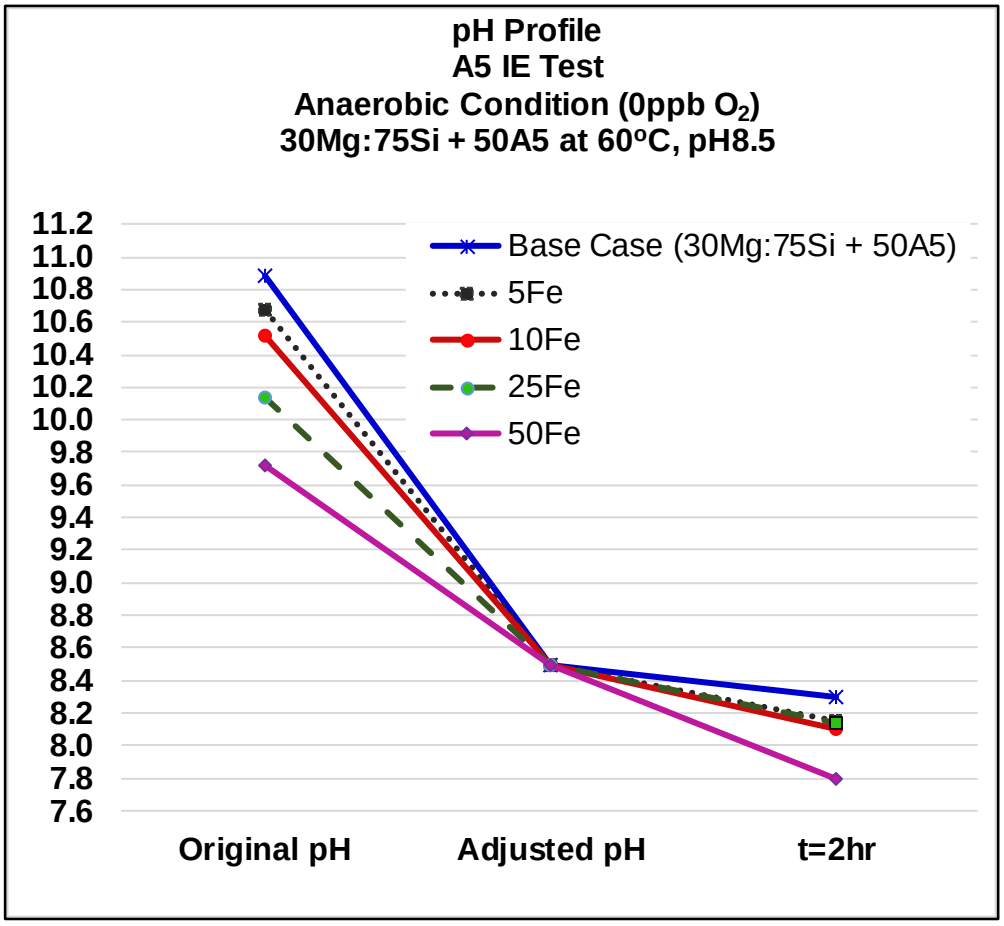

Figure 6-34 pH profile (%) in Anaerobic Static IE Test of silicate system 30Mg:75Si + 50A5 at 60°C, pH8.5

The ICP results are now used to determine the stoichiometric ratios in the silicate scales which were produced. The Si:Mg, Fe:Si and Fe:Mg molar ratio are plotted in Figure 6-35, Figure 6-36, and Figure 6-37 respectively.

Results in Figure 6-35 show that the Si:Mg molar ratios increased as the ferrous ion concentration is increasing. This is expected as the addition of more ferrous ion caused the A5 to lose its ability to stop silicon ion from reacting which resulted in more silicon ion reacting, especially when Fe(II) > 25ppm.

Likewise, the Fe:Si molar ratios increased at higher ferrous ion concentrations in the mixed brine. Yet, the value is lower for 10ppm Fe(II) and it is worth noting that amounts of both Si and Fe ions increased with increasing Fe ion concentrations. The same trend was observed for the Fe:Mg molar ratio which indicate that ferrous ion is much easier to bridge into the tetrahedrally coordinated silicon Si-O-Si. Hence, much more ferrous ion reacted than magnesium ion.

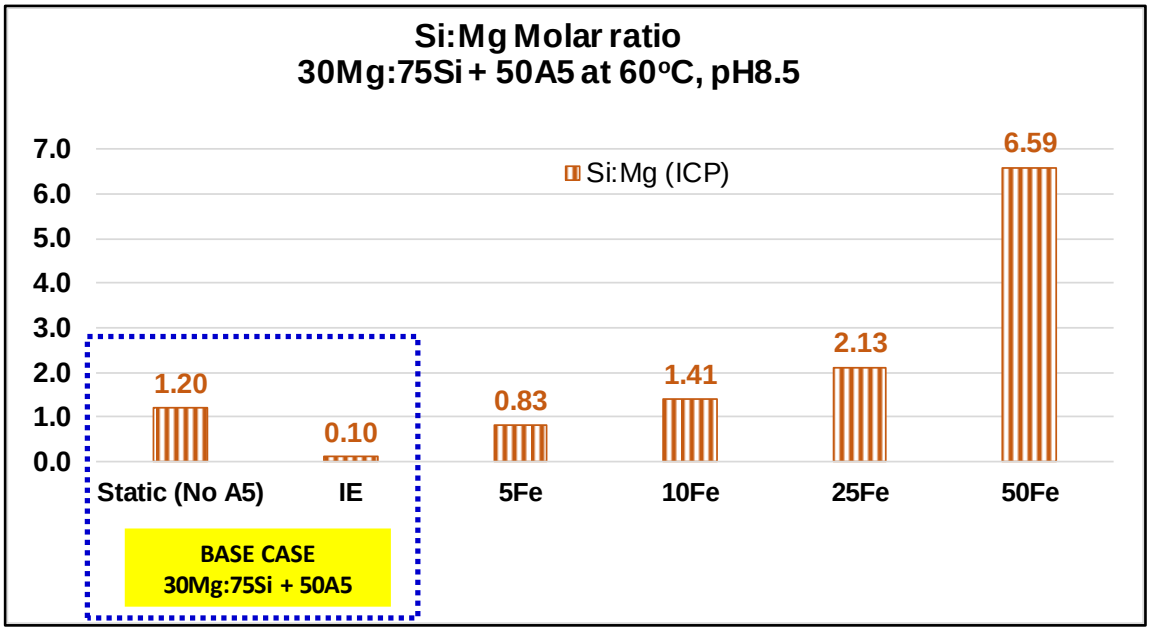

Figure 6-35 Si:Mg molar ratio in Anaerobic Static IE Test of silicate system 30Mg:75Si + 50A5 at 60°C, pH8.5

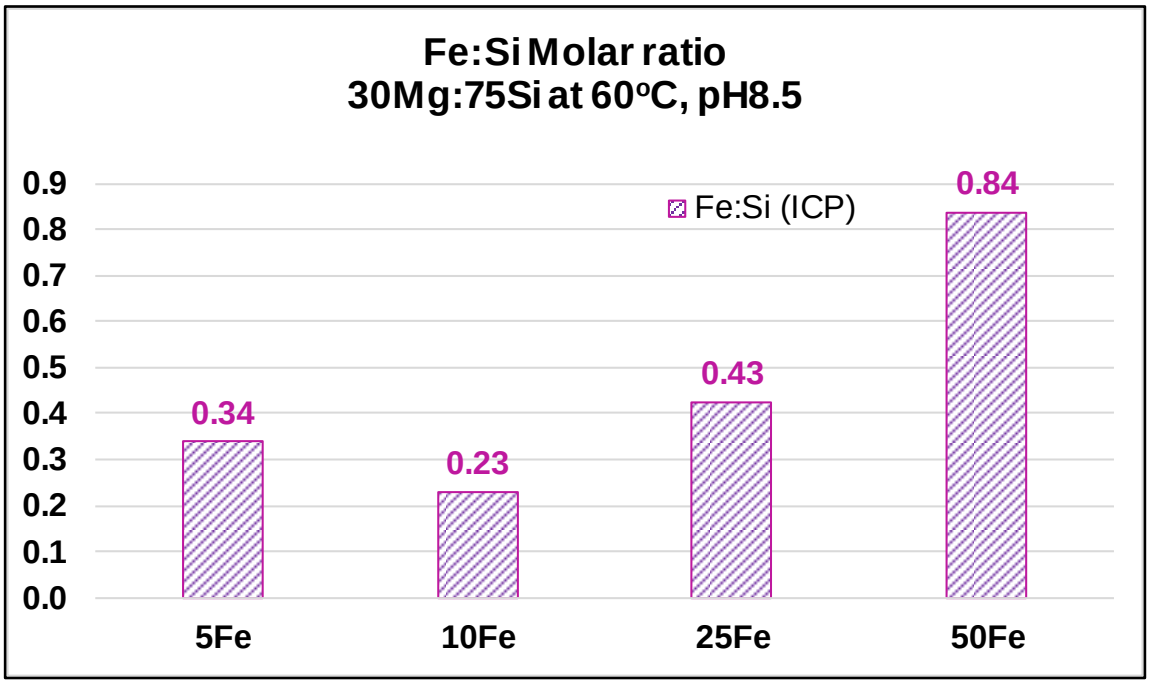

Figure 6-36 Fe:Si molar ratio in Anaerobic Static IE Test of silicate system 30Mg:75Si + 50A5 at 60°C, pH8.5

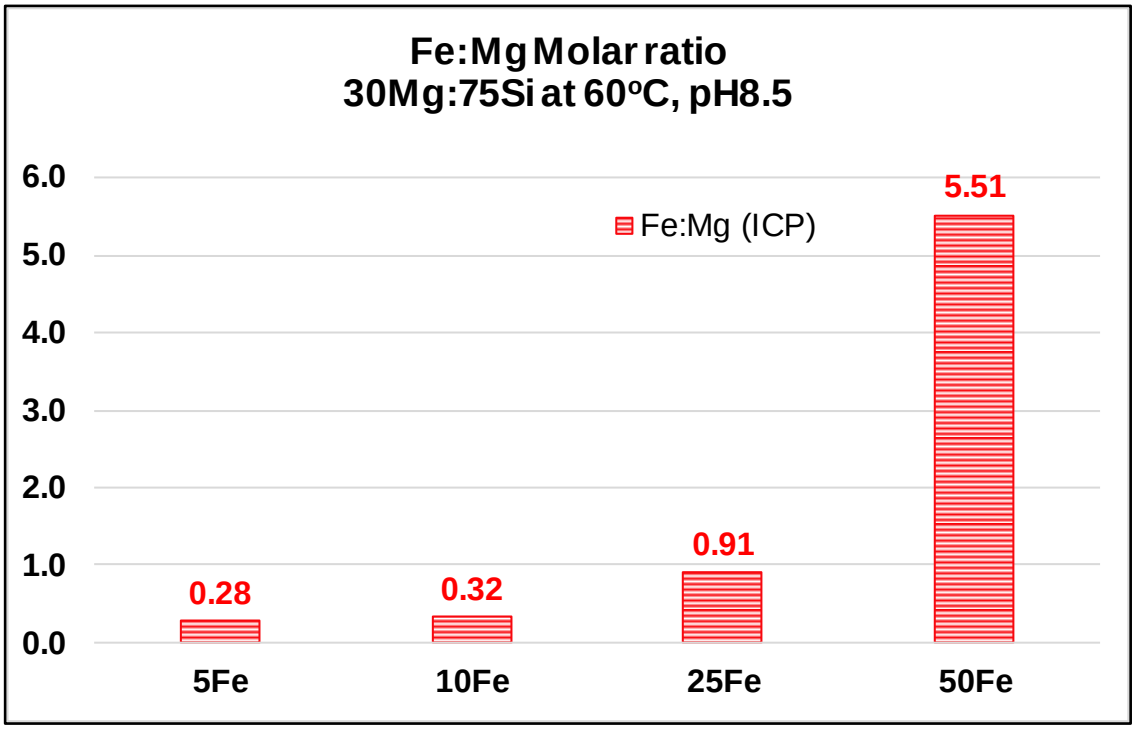

Figure 6-37 Fe:Mg molar ratio in Anaerobic Static IE Test of silicate system 30Mg:75Si + 50A5 at 60°C, pH8.5

(c) ESEM/ EDAX Analysis

ICP analysis shown in Figure 6-31 shows that the amount of ion reacted is < 10ppm Si, < 4ppm Mg and < 8ppm Fe reacted when up to 25ppm of ferrous ion was present in the A5-containing brine at initial conditions. Also, the mixed brine containing up to 25ppm only became slightly cloudy as shown in Figure 6-30. This may explain why almost nothing can be seen or can be caught by filtration. Yet, all these 'precipitates' have been analysed by ESEM/EDAX in order to confirm these results. Figure 6-38 obviously shows that only mixed brine containing 50ppm ferrous ion at initial condition produced a thin layer cake and their ESEM Images indicated that this precipitate is amorphous in nature.

The above observations were made using ICP analysis, visual observation on the mixed brine at 2-hours and by observing the 'precipitate' caught by filtration. These results are in agreement with the ESEM images and EDAX analysis shown in Figure 6-39 and Figure 6-40.

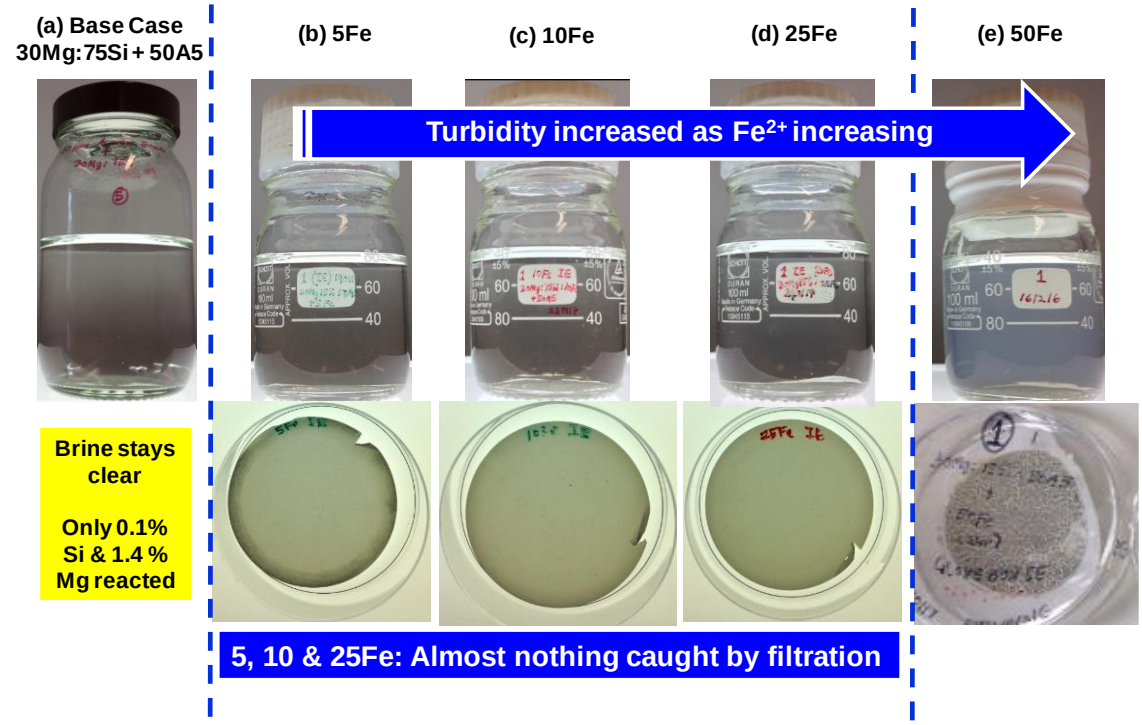

Figure 6-38 Precipitate filtered in Anaerobic Static IE Test of silicate system 30Mg:75Si + 50A5 at 60ºC, pH8.5

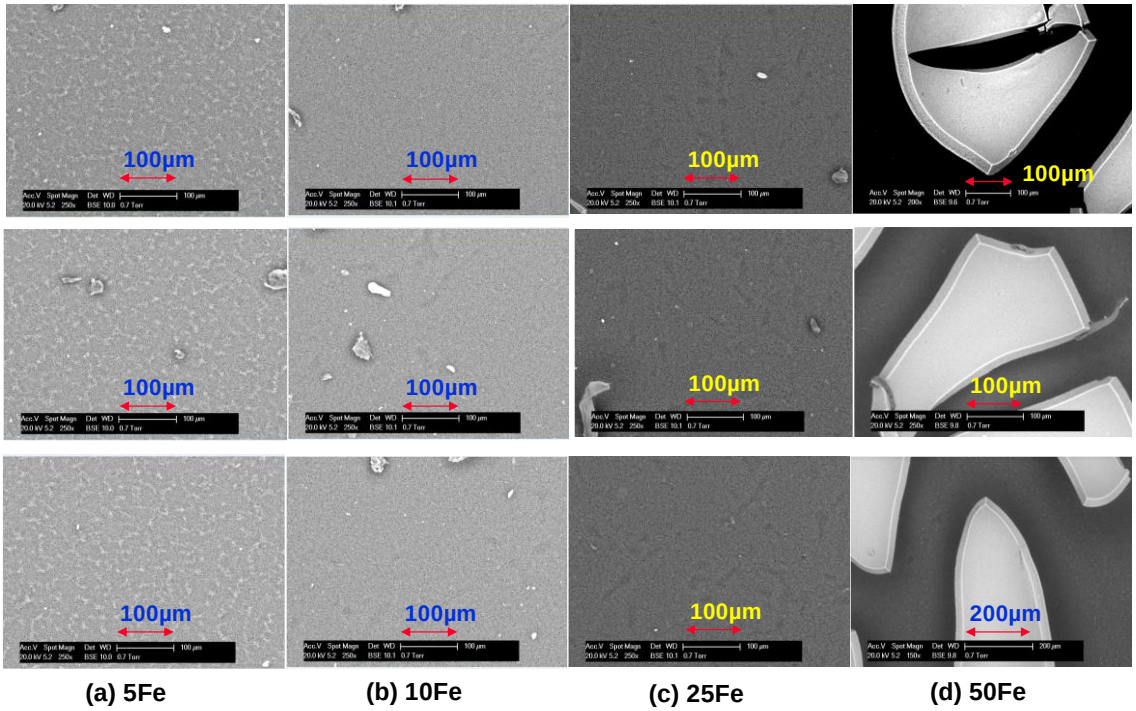

Figure 6-39 ESEM images of precipitate formed in Anaerobic Static IE Test of silicate system 30Mg:75Si + 50A5 at 60ºC, pH8.5

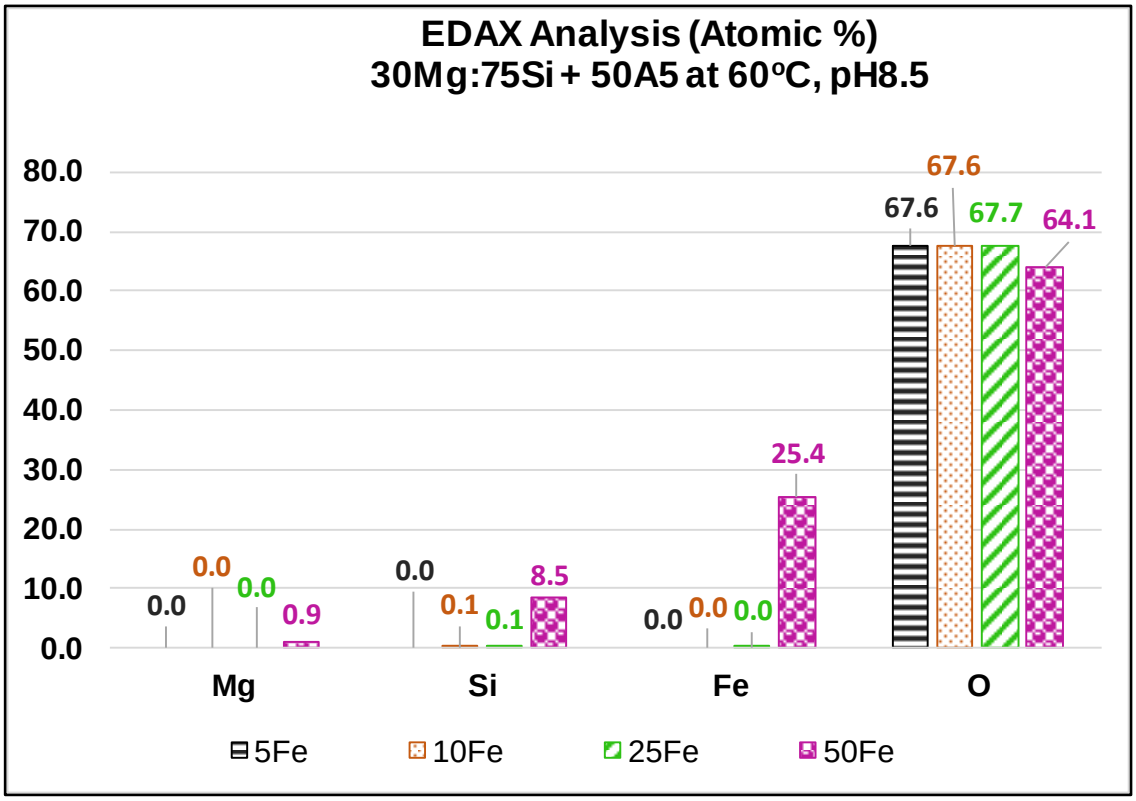

Figure 6-40 EDAX analysis of precipitate formed in Anaerobic Static IE Test of silicate system 30Mg:75Si + 50A5 at 60°C, pH8.5

Figure 6-40 shows that for the 'precipitate' of up to 25ppm Fe(II); no magnesium and ferrous ion was detected by EDAX analysis, while only small amounts of Si were detected. We can see ~0.9%, 8.5% and 25.4% of magnesium, silicon and ferrous ion detected, respectively, when 50ppm Fe-containing brine was analysed.

(d) FTIR analysis

We further investigate the behaviour of the silicate deposits when inhibitor A5 and ferrous ions were present using FTIR analysis. Performing such analysis may allow us to understand the reason behind the A5 failure to inhibit the silicate scale. This information will be useful to check the nature of the antagonistic effects due to Fe(II), for example:

a) Fe(II) is simply incorporated into the silicate scale altering the scale solubility in such a way as to make it more difficult to inhibit; or

b) Fe(II) interferes with A5 and thus prevents it from functioning properly as scale inhibitor i.e. Fe(II) chelated by A5 produce complex which may have already reduce A5 site available to chelate Mg and Si ions from reacting.

Figure 6-41 shows the comparison between the FTIR spectra when 50ppm Fe^{2+} is introduced into the silicate system of 30Mg:75Si and IE Test 30Mg:75Si:50A5. Spectra of the later test suggested that the present of ferrous ion may have altered the spectra at bandwidth ~1278 to 1558cm-1. We cannot compare these altered spectra with the *Base Case IE* (No Fe) i.e. 30Mg:75Si +50A5 because that scale was totally inhibited by the addition of 50ppm A5. The spectra observed suggest that scale produced in static and IE test are essentially the same as discussed in section 6.3.1(d). The band alteration may be explained by the complex of Fe(II)-A5 formed. However, this conjecture may be refuted by further experimental research.

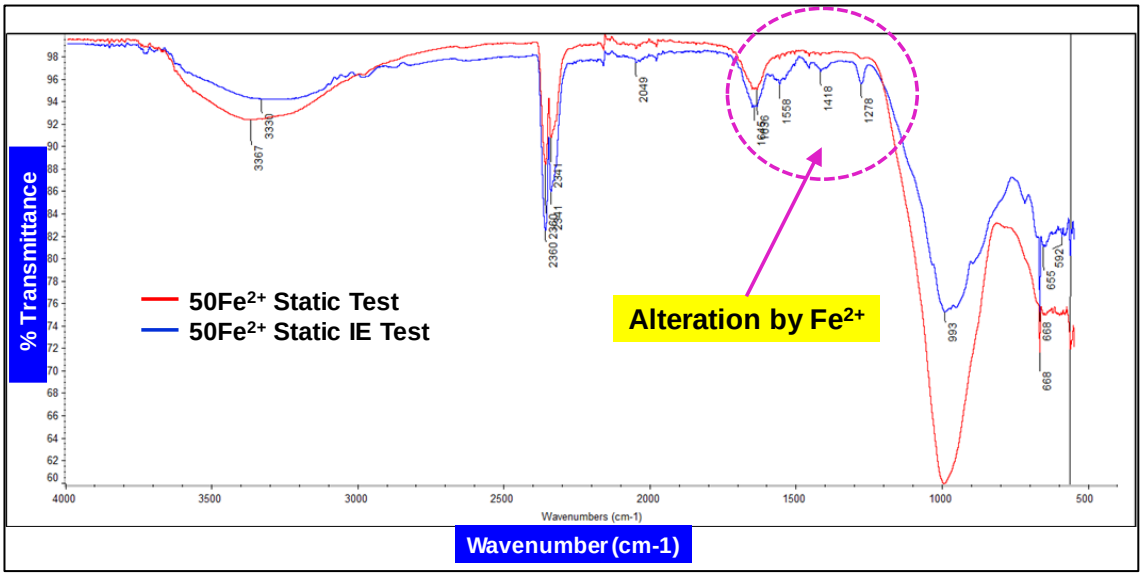

Figure 6-41 FTIR spectra of Static Test 30Mg:75Si:50Fe and IE Test 30Mg:75Si:50Fe + 50A5 at test condition of 60°C, pH8.5

6.4.3 Summary and Conclusions

The effect of ferrous ion on the performance of the A5 silicate inhibitor has been carried out successfully and some novel findings have emerged, as follows:

a) Fe^{2+} does significantly affect the performance of A5 and this has been demonstrated in the 30Mg:75Si silicate scaling case in the presence of various concentrations of ferrous ion. The presence of Fe causes a reduction in the

inhibition efficiency (IE) of both Mg and Si i.e. IE Mg % & IE Si % are both lower in the presence of Fe^{2+};

b) Generally, the IE% (i.e. IE Mg % & IE Si %) decreased with increasing amount of Fe^{2+};

c) The FTIR spectra revealed the alteration of ferrous ion at bandwidth ~1278 to ~1558cm-1.

6.5. ADDITIONAL FINDINGS – EFFECT OF FE ON THE SILICATE SYSTEM AND A5 PERFORMANCE IN AEROBIC CONDITION

In the experiment described here, the normal procedure of silicate static test methodology in normal aerated condition will be deployed but with the addition of Fe ion hence we know that all ferrous ion is now oxidized to ferric ion.

This experiment was designed so that ferric-silicate scale can be reproduce in the silicate static test and the effect of ferric ion on the A5 performance could be evaluated.

6.5.1 Effect of Fe(III) on Silicate System

Figure 6-42 shows that 30Mg:75Si:50Fe immediately changed to an orange colour upon mixing due to the fact that the ferrous ion is now oxidized to the ferric ion. When compared with the *blank* solution after 7 days of reaction, it produced relatively smaller amount of precipitate (by visual inspection).

However, ICP analysis plotted in Figure 6-43 tells us, on the contrary, that the amount of magnesium and silicon ion reacted in the ferric-containing brine is a factor of x2 higher than was found in the *blank* solution. The pH values in this brine were lower than the blank solution with a final pH of ~7.3 as compared to the blank pH ~ 7.8.

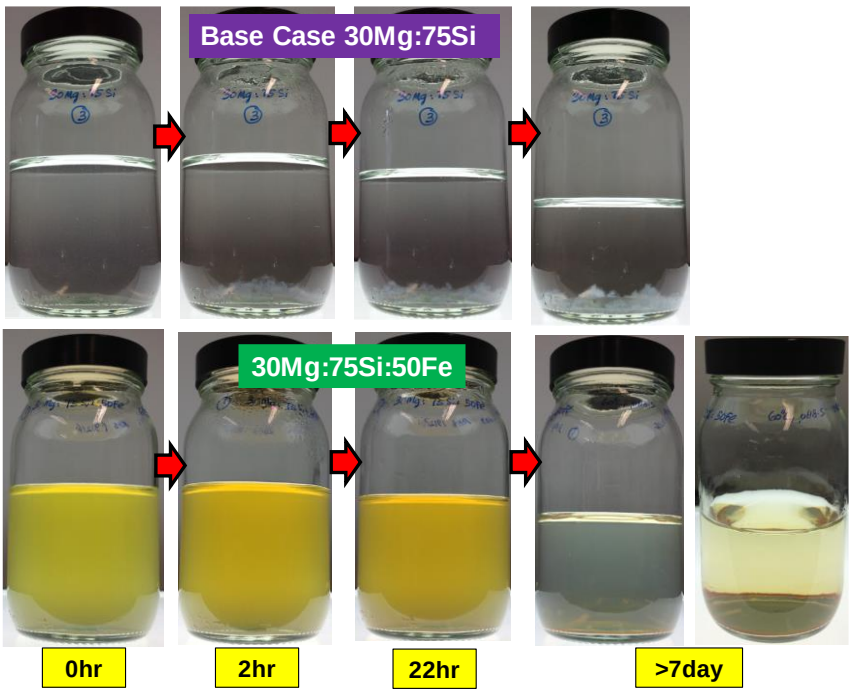

Figure 6-42 Observation of "*manageable*" base case blank (Top) vs. 30Mg:75Si:Fe50(III) (Bottom) in Static Test aerated condition at 60ºC, pH8.5

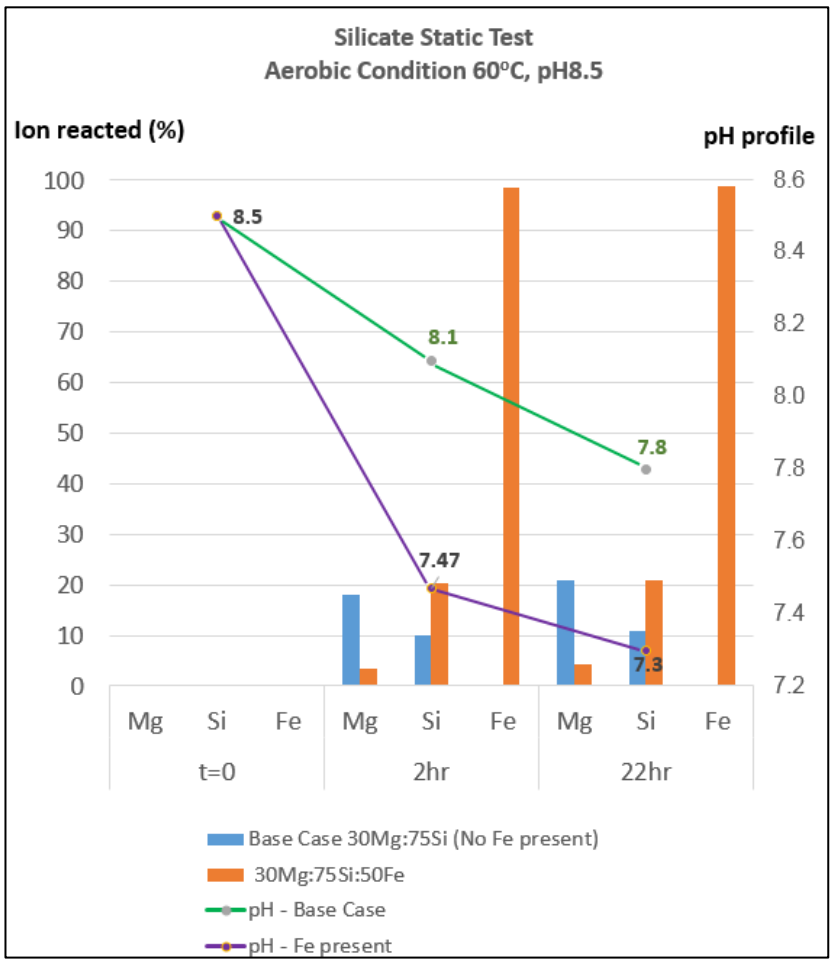

Figure 6-43 % amount of ion reacted of "*manageable*" base case (Blank) vs. 30Mg:75Si:50Fe(III) in Silicate Static Test at aerated condition, 60ºC, pH8.5

6.5.2 Effect of Fe(III) on A5 Performance

All test samples were visually inspected and photographed as shown in Figure 6-44. The addition of 50ppm A5 into the "*manageable"* base case resulted in clear solutions throughout 7 days of reaction while Fe(III)-containing brine produced orange coloured scale.

ICP analysis in Figure 6-45 revealed that the A5 performance in stopping magnesium and silicon from further reaction was severely affected by the presence of 50ppm Fe(III) where it obviously shown that the amount of magnesium reacted with A5 are much higher than found in the *blank* solution.

Results also showed that almost all ferric ion was reacted in static tests and the addition of 50ppm A5 can only makes <10% of the ferric ion stay in solution.

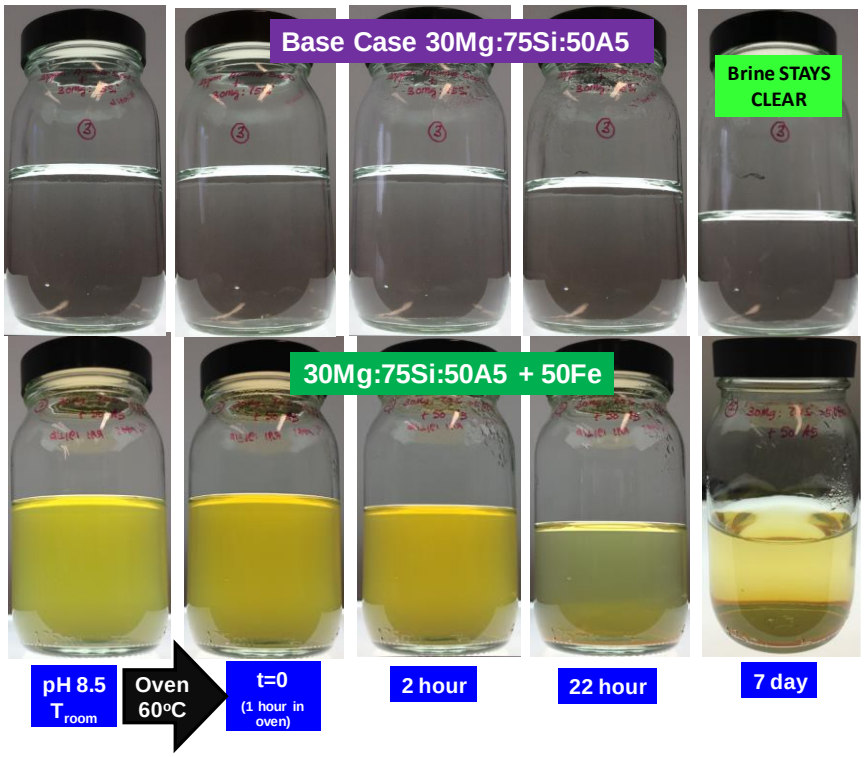

Figure 6-44 Observation of inhibited blank "*manageable*" base case of 30Mg:75Si:50A5 (Top) vs. Inhibited mixed brine of 30Mg:75Si:50A5 + 50Fe(III) (Bottom) in Static IE Test at aerated condition, 60°C, pH8.5

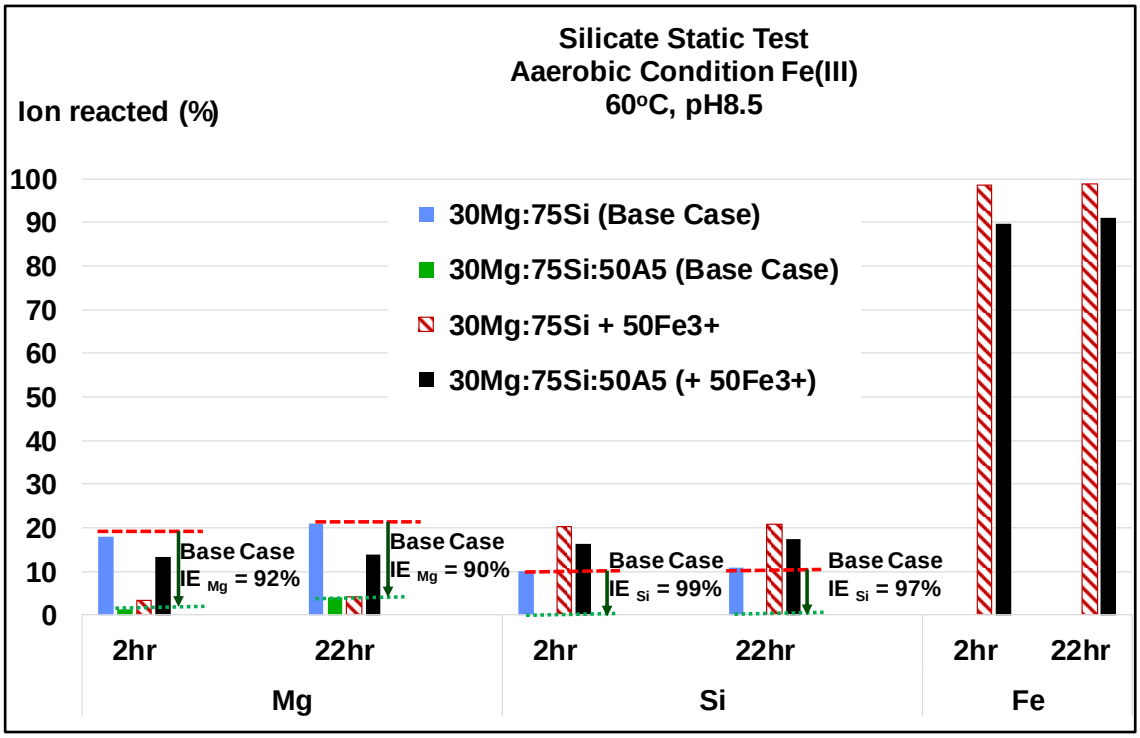

Figure 6-45 % amount of ion reacted of non-inhibited & inhibited blank *"manageable"* base case of 30Mg:75Si vs. Non-inhibited & inhibited mixed brine of 30Mg:75Si:50Fe(III) in Static & IE Test at aerated condition at 60°C, pH8.5

6.5.3 ESEM Analysis

ESEM Images for the precipitate formed in both static and IE tests are shown in **Figure 6-46** which clearly show that the precipitate is amorphous.

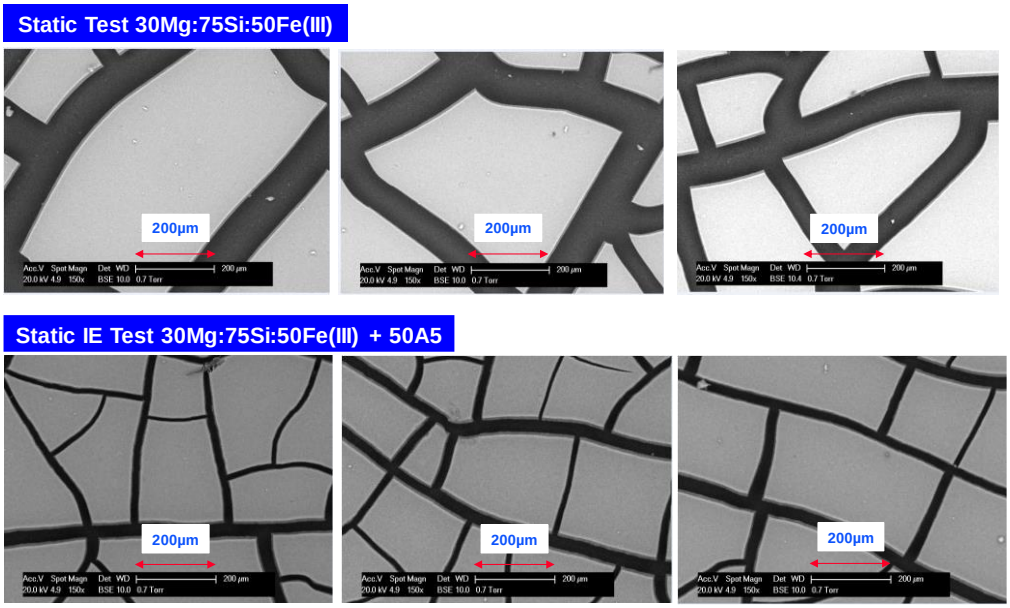

Figure 6-46 ESEM images of Fe(III)-containing brine in Static Test and Static IE Test

6.5.4 FTIR Analysis

We further examine the precipitate produced in both static and IE tests so that a conclusive determination can be made. Figure 6-47 revealed that the spectra of the IE test also been altered by the presence of ferric ion at essentially ~1279 to ~1558cm-1.

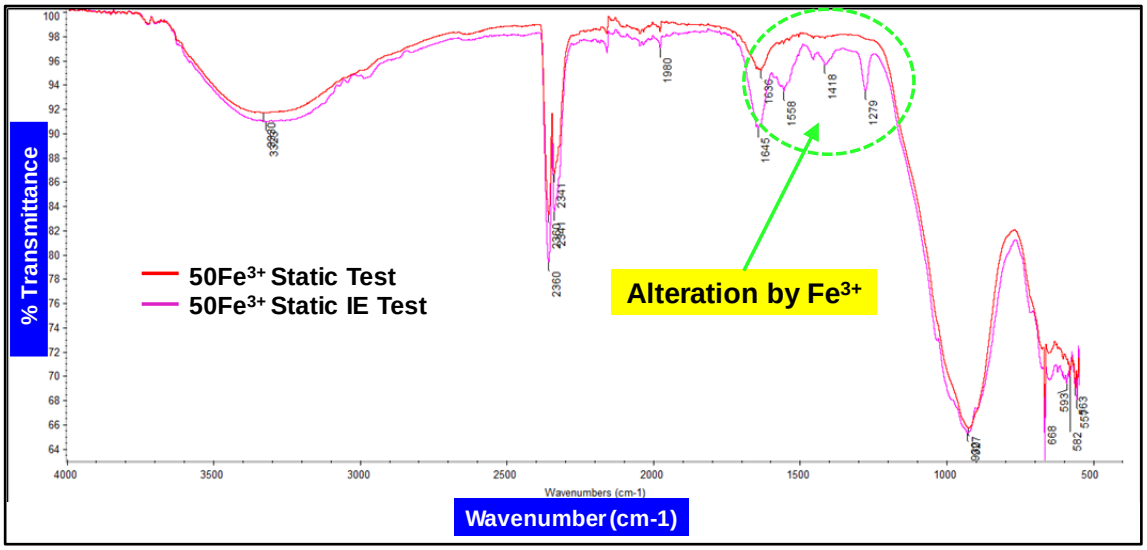

Figure 6-47 FTIR spectra of Static Test 30Mg:75Si:50Fe(III) and IE Test 30Mg:75Si:50Fe(III) + 50A5 at test condition of 60°C, pH8.5

Figure 6-48 shows the comparison between spectra produced by the precipitate in the static test with 50ppm ferrous ion conducted in anaerobic condition, and the precipitate produced in the experiment performed in aerated condition. All bands match exactly except those near ~1100cm-1 band whereby we could observe that this band can be seen at ~997cm-1 in Fe(II)-containing brine. This band was further moved to shorter wavelength i.e. ~930cm-1 when Fe(III) was present in the mixed brine. These findings agreed with Russel (1979) in his work on the infrared spectroscopy of ferri-hydrite.

Likewise, the same observation can be made for the spectra of the IE test when Fe(II) and Fe(III) were present in the mixed inhibited brine, respectively. Both Fe(II) and Fe(III) alter the spectra at the same bandwidths of ~1279 to ~1558cm-1 (Refer Figure 6-49).

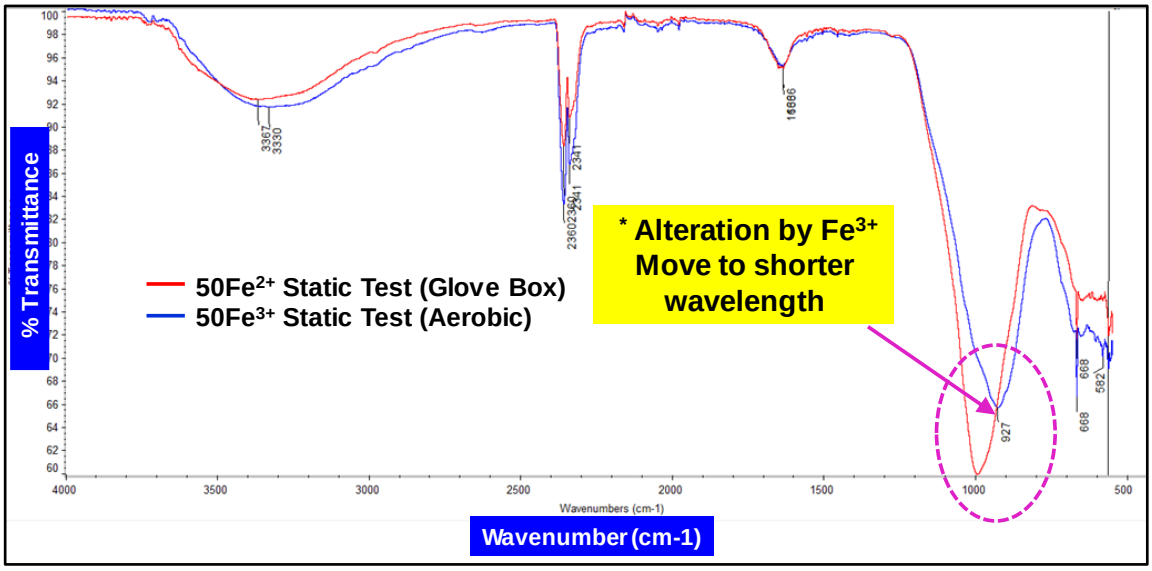

Figure 6-48 FTIR spectra of Static Test 30Mg:75Si:50Fe(II) and Static Test 30Mg:75Si:50Fe(III) at test condition of 60ºC, pH8.5

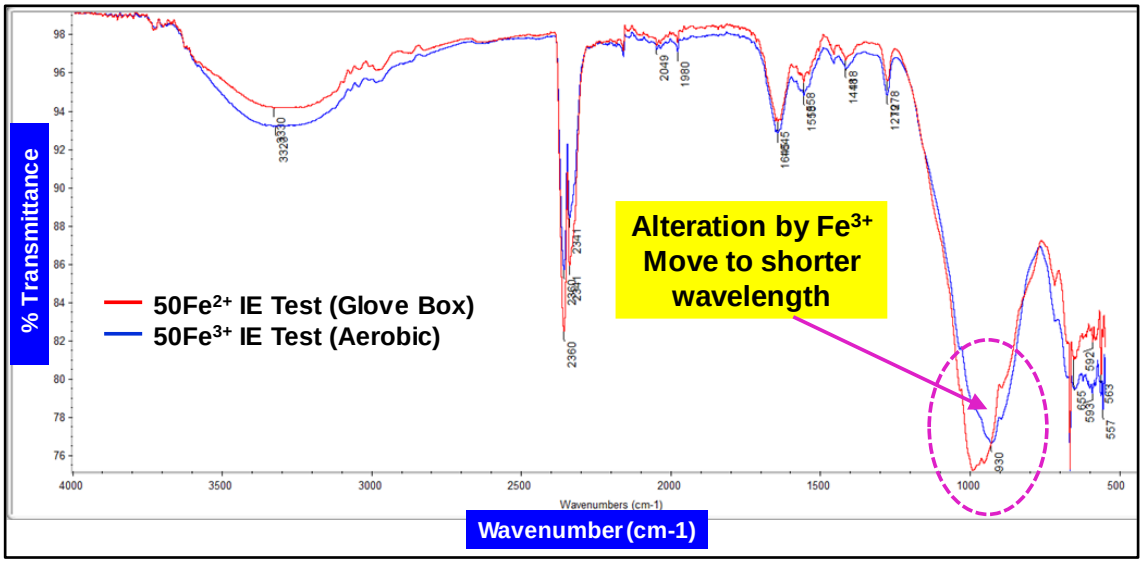

Figure 6-49 FTIR spectra of Static A5 IE Test 30Mg:75Si:50Fe(II) and Static A5 IE Test 30Mg:75Si:50Fe(III) at test condition of 60ºC, pH8.5

Spectra shown in Figure 6-50 confirmed the results discussed earlier in this chapter. The fingerprint band near ~1100cm-1 is ~1050cm-1 for the *blank*; this was then move to ~997cm-1 for Fe(II)-containing brine; and further moved to ~930cm-1 for the Fe(III)-containing brine.

The band due to Si-O-Si that generally can be seen at 795-799cm-1 will be reduce in intensity as the ferrous or ferric ion concentration increased in the mixed brine. Ferrous ion and ferric ion may alter the spectra that show multiple alteration at bandwidth ~1279 to ~1558cm-1.

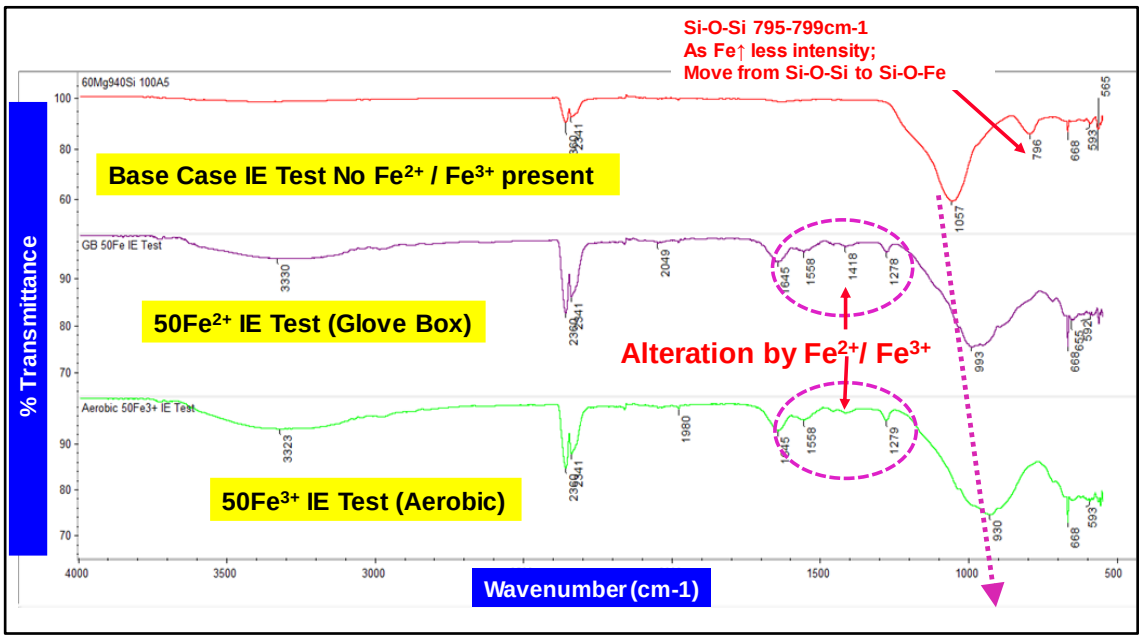

Figure 6-50 Band ~1100cm-1 and useful fingerprint for *blank* IE Test, Fe(II) IE Test and Fe(III) IE Test at 60ºC, pH8.5

6.6. SUMMARY AND CONCLUSIONS

The sections above have presented the specific conclusions in each area of this study. Here, we summarise the general findings from this study of silicate scaling in the presence of ferrous ions, as follows:

1. An experimental methodology to study the effect of ferrous ions on the silicate scaling system has been established. The central feature of this has been to maintain a reducing environment using an anaerobic glove box.
2. This experimental methodology has been applied to study the formation of Mg/silicate scale in the presence of various levels of Fe^{2+} from $[Fe^{2+}] = 0 – 50$ppm. It is shown that the ferrous iron does enhance the silicate formation and the Fe itself is fully incorporated into the silicate scale which is formed.
3. In addition to the presence of Fe affecting the severity of the silicate scale formation, it also shows an antagonistic effect to the silicate inhibitor tested in this work (the polymeric silicate inhibitor A5).
4. The silicate scales formed in the absence and presence of Fe are amorphous in nature and their stoichiometry (i.e. Mg:Si, Fe:Si ratios) can be worked out using ICP of the bulk liquid phase or by analysis of the resulting silicate precipitates using ESEM/EDAX techniques. The results obtained by each of these methods are in very good agreement.
5. Some additional characterisation of the nature of the functional groups present in the silicate scales is provided using FTIR spectroscopy. This has been used in cases where Fe is present and absent and new peaks are identified in the presence of Fe which is incorporated into the silicate scale which forms.

CHAPTER 7. CONCLUSIONS AND RECOMMENDATIONS

7.1. MAJOR CONCLUSIONS

In this work, we describe an integrated experimental study of silicate scale formation and inhibition conducted in an environment which is intended to mimic reservoir conditions under ASP flooding or other reservoir processes where silicates occur. The experimental approach uses mainly static bulk methods involving extensive silicate solution monitoring and solid silicate scale characterization using various spectroscopic techniques viz. ESEM/EDAX, XRD and FTIR.

The main conclusions from this work on the silicate scaling system and its inhibition are presented in this chapter. The conclusions presented here are a reaffirmation of those objectives outlined in *Chapter 1*; the five main objectives and the findings and a brief description of our findings against each objective, are as follows:

Objective 1: To develop an experimental bulk silicate scaling and inhibition methodology

Our initial experiments followed the previous work by Arensdorf et al. (2010) and we have shown that silicate scaling can be reproduced in the laboratory. However, we have greatly extended the earlier methodology to include a quantitative assay for [Mg] and [Si] and also to study of the silicate precipitated by ESEM/EDAX, FTIR and XRD techniques. This development has added a much more ***quantitative*** dimension to the characterisation of silicate scaling systems.

A robust and reliable methodology for studying silicate scale formation and inhibition has now been established involving *both* qualitative and quantitative techniques. To quantify silicate scale formation, we apply ICP analysis and this has elucidated several issues which have arisen while dealing with the colloidal nature of the mixed solution produced in the silicate reaction process. Among the issues that have been solved in this study include establishing the correct quenching solution, the location of ICP sampling, the effect of sample centrifuging and stirring and filtering while ICP sampling, and the use of glass or HDPE bottles for the tests.

The experimental methodology developed proved to be repeatable and reproducible, although the system is very sensitive to initial pH and much care must be taken in order to obtain reproducible results. The validity of our test methodology is supported by the close experimental agreement of the *Si:Mg molar ratio* acquired by both of the independent techniques, i.e. ICP analysis of the Mg-Silicate solution compared with ESEM/EDAX analysis of the solid silicate deposits.

The sensitivity/reproducibility issue was observed from the high dependency of silicate system to initial pH and this was successfully dealt with. The pH adjustment of the mixed brine must be very carefully controlled to test pH and the experimentalist must be very consistent in the precise details of the methods used, as described in the thesis (See *Chapter 5* - Section 5.2 discussed the sensitivity of silicate system to initial pH).

Objective 2: To understand the mechanisms of silicate scale formation and investigate several influencing factors affecting scaling conditions in ASP flooding

The initial development work on silicate scaling identified a "*worst"* base case and this was studied to understand the mechanism of silicate scaling reaction, as described in section 3.4.2. It was observed that the scaling reaction rate of the "*worst"* base case proceeded slowly and continuously rather than suddenly or instantaneously, reaffirming the observation made by other researchers. This may due to the fact that dissolved silica undergoes a polymerization reaction forming dimers, trimers, tetramers, and n-mers etc., until the structure resembles nano fragments of amorphous solid rather than large molecules; e.g. with n of order n ~ 10 - 30. This reaction proceeds with the growth of particles in a random process until they reach critical nucleus size beyond which they grow rapidly, coagulate and flocculate. The particles linked together into branched chains, then networks, finally extending throughout the liquid medium, thickening it to a gel, before settling on solid surfaces (Weres et al., (1979) and Iler (1979)).

Evidence is presented showing that the formation of silica-silicate scales in aqueous systems depends on several important factors, viz. *pH, temperature, silica brine ageing,* and the *initial amount of Mg ion in solution.* All of these factors were studied and evaluated by establishing the types and morphology of the silicate precipitates produced using spectroscopic analysis viz. ESEM/EDAX, FTIR and XRD; and by measuring the *Si:Mg molar ratio* by ICP analysis of the silicate solution and EDAX analysis on the

actual precipitates. This work which is discussed in *Chapter 4* has helped us gain a much better understanding of the mechanism of silicate scaling during ASP flooding and in other more conventional reservoir processes.

From the analysis of ICP results, it emerges that pH is the dominant factor that strongly influences the silicate scaling reaction compared to the effect of temperature. Precipitate formed in the silicate system mimics the pH condition of the well under ASP flooding and subsequent connate water mixing; i.e. at pH8.5 mostly amorphous silica SiO_2 and some amount of magnesium silicate $MgO.SiO_2$ is formed. Scale characterization using various spectroscopic analysis methods has confirmed no magnesium hydroxide $Mg(OH)_2$ formed under these conditions and the results from using ESEM/EDAX, FTIR and XRD to characterize the scale formed complemented each other. At higher pH values (pH ~ 10 – 11), it was shown that $Mg(OH)_2$ scale co-precipitated with other silicate scales. More magnesium silicate is precipitate at this high pH as compared with the lower pH8.5. These observations are consistent with work reported previously by Hauksson et al. (1995) and Amjad and Zuhl (2010) and Amjad (2016).

Following the previous obtained results in section 4.4.3, we found that the initial Si:Mg molar ratio clearly affected the final Si:Mg molar ratio in the precipitate. Two main conclusions are drawn based on different test conditions; conditions mimic-ing ASP flooding at 60^{o}C, pH8.5 and at elevated pH i.e. 25^{o}C, ~pH10.

a) For silicate system reacted at room temperature and natural pH (pH ~10); the Si:Mg in the precipitate does not changing much, having a value between ~1 to ~1.3, when $(Si:Mg)_o$ varied from ~0.76 to ~3.11 respectively. Also, in high pH reactions (>pH9.5) then co-produced of Mg-silicate and $Mg(OH)_2$ occurs, as discussed in section 4.4.1.

a) For silicate systems reacted at 60^{o}C and pH~8.5; the Si:Mg in the precipitate will vary between ~0.6 to ~21 as the initial $(Si:Mg)_o$ is varied from ~1.41 to ~13.56 respectively whereby only amorphous silica and amorphous Mg-silicate scale are produced.

Aged Silicon Brine (SB) showed extensive reaction of Si for both pH values studied (pH 8.5 and 7.6) at 22 hours but this was polymerized into amorphous silica and remain suspended in the solution. If this is maintained in solution, then the formation of hard scale vitreous silica on the surface will be avoided. The suspended polymerized scale

formed in both aged solution a weakly cemented floc-like material. Hence, the supersaturation condition due to monomeric silica is reduced due to the formation of this relatively nonadhesive polymeric form. Also, it is observed that the aged mixed brine we are able to successfully inhibit ~80% of the magnesium ion from reacting, as compared to fresh mixed brine. This means that much less magnesium silicate was produced under these ageing conditions. This may mean that in reservoir systems, there is a lower risk of the deposition of amorphous magnesium silicate scale.

Objective 3: To understand the mechanisms and the performance of various polymer in silicate scale inhibition.

The established experimental methodology to determine performance of any chemicals to inhibit silicate scale was adopted to determine the performance of several polymers; VS-Co, H3 and A5. A new "*manageable"* base case 30Mg:75Si is defined, whereby this Mg/Si level can be inhibited. Despite the fact that is our mildest case, it is higher than that reported by Jing et al., (2013) in and ASP oilfield application. This new "*manageable*" base silicate system allowed different scale inhibitors (SIs; having different functional groups) to be analysed/ compared. These results show clearly that silicate scales can be totally inhibited at reasonable SI concentrations; i.e. at concentrations which are economically feasible in the field. Despite work by others showing that amorphous silica can be very difficult to inhibit, we show that our *"manageable"* base case can be inhibited with ~50ppm of polymeric silicate inhibitor/dispersant A5. This is an important new finding in silicate scale inhibition. It is evident that inhibitors with the ability to inhibit the silicate scale should possess some or all of the following properties => (i) low molecular weight (<5000g/mol); (ii) contain sulfonate and carboxylate groups that may able to stop the formation of amorphous magnesium silicate scale; and (iii) comprise acrylamide, maleic acid and non-ionic polymer which are probably able to stop the formation of amorphous silica scale. Our conjectures on how these functional groups affect IE % will hopefully be useful in the development of novel silicate inhibitors or in the search for more commercial inhibitors that will work for more severe silicate scaling systems.

Objective 4: To develop the experimental methodology of studying the effect of ferrous ion on the silicate scaling system and inhibition in a reducing environment

It is shown that a reducing (anaerobic) environment using the glove box was successfully achieved in our study the effect of ferrous ion on the silicate scaling system. The experimental methodology is now established with results that are reproducible and it was observed that a totally reducing environment (O_2 content <5ppb) was achieved in the glove box equipment following the procedures described in section 6.2.1.

The purely anaerobic condition was also maintained and achievable throughout the first 2 hours of reaction. However, there was some oxygen contamination in our 22-hour tests although the oxygen level was successfully kept at <5ppb up until 17 hours (NB this was concluded from physical observation only). Hence, with further improvement in the test procedure, a purely anaerobic environment may be achievable for the full 22-hour test duration. Also, it is important to keep the oxygen level to be less than 10ppb in order to prevent ferrous ion oxidization (ideally, the purely anaerobic condition should be maintained throughout the experiment).

Objective 5: To study the effect of ferrous ion on (i) the silicate scaling system; (ii) the performance of A5 in silicate inhibition

Our work on the effect of ferrous ion on the silicate system and inhibition had been successfully investigated using the experimental methodology established in section 6.2.1. At least for the 2 hour tests, we can be sure that ferric ion (Fe^{3+}) contamination was avoided which would have interfered with the test results.

The most important finding is that the presence of ferrous ions ***does*** affect the severity of silicate scaling reaction. The application of FTIR spectra in characterizing the produced silicate scale in this static test confirmed the presence of following functional groups Si-O-Si, Si-O-Fe, Si-O-Mg, $MgSiO_3$, Fe(II)-silicate. The spectroscopic analysis is indicative but does not prove the exact composition of the Fe-silicate scale. However, the results are at least consistent with the conjecture that the scales produced are probably a mixture of amorphous silica, amorphous Mg-silicate, amorphous Fe-silicate and amorphous Mg-Fe-silicate scale. The FTIR spectra for static test also confirmed the absence of following salts that are $Fe(OH)_2$, $Mg(OH)_2$, $Fe(OH)_3$, Si-O-Fe(III).

Several new findings on how ferrous ion affected the A5 silicate inhibitor performance are observed. Indeed, Fe^{2+} ***does*** affect the performance of A5 in the 30Mg:75Si *"manageable"* scaling system. It is evident that ferrous ion has an antagonistic effect on the A5 capability to inhibit the silicate scale; it was found that IE Mg % and IE Si % are lower with the presence of Fe^{2+}. Generally, the IE% (i.e. IE Mg % & IE Si %) decreased with increasing amount of Fe^{2+}. The FTIR spectra revealed the alteration of ferrous ion at bandwidth ~1279 to ~1558cm-1 which did not appear in the blank inhibited system.

7.2. RECOMMENDATIONS FOR FUTURE WORK

This thesis has studied several aspects of silicate scale formation and inhibition where new insights into the mechanisms of silicate scale formation and inhibition are revealed. There are several areas that we have identified which would merit further study and these are discussed, as follows;

Modelling the silicate system using PHREEQC

It would be useful to model the silicate system using the PHREEQC program to determine if the existing silicate models can validate the experimental results presented in this thesis. Owing to issues of complexity and the time scales involved, it is often not possible to conduct sufficiently realistic laboratory experiments to observe the long-term behaviour and factors governing the silicate reaction. Hence, this is a goal that is largely unattainable owing to the complexity of silicate systems, the inadequacy of field data, and uncertainty relating to how the system will change over time.

A model is, more or less by definition, a simplification of reality and should always be treated as a powerful heuristic tool (i.e. not a source of absolute truth). Although by no means a substitute for experiment, modelling and computer simulation is a valuable predictive tool that can be used to bridge the gap between laboratory experiments, field observations, and the long-term behaviour of silicate systems.

The established and reported experimental data on silicate scale formation and inhibition in this thesis is beneficial in modelling the reactions involved by applying the existing PHREEQC geochemical models. Among them are ***inverse modelling*** which attempt to

establish reaction mechanisms that explain measured chemical changes that occur as water composition evolves along an ASP slug propagation from the injection well to the production well. In addition to that, ***reaction path (mass transfer)*** modelling is dynamic in the sense that it allows the simulation of how changes in water and mineral phase composition occur over time as defined primary minerals are dissolved in an incremental fashion. At each step in the calculation, the aqueous speciation is calculated, and secondary minerals are dissolved or precipitated in order to maintain equilibrium. In ***mixing processes*** modelling, the mixing of injected ASP fluids and formation (connate) fluids can be simulated to assess the silicate scaling potential of the mixed fluid. PHREEQC can be used as a speciation program to calculate saturation indices, the distribution of aqueous species, and the density and specific conductance of a specified solution composition (Parkhurst and Appelo, 2013).

Some of relevant work conducted in effort of modelling the silicate scaling system using geochemical modelling are work done in Miravalles Geothermal Field, Costa Rica. Mixing or titration modelling (***reaction path modelling)*** is the most suitable for understanding the processes that occur during the mixing between fluids from wells PGM-17 (neutral fluids) and PGM-19 (acidic fluids) added to the fact that acidic fluids are richer in iron than neutral fluids, sets the scenario for the amorphous iron silicate to precipitate. On the basis of a series of mixing scenarios, acidification of neutral fluids to a pH value of 6.0 is suggested in order to prevent the formation of these amorphous iron silicate scales (Rodríguez, 2006).

Another modelling work was done by Leech (2016) in Olkaria, Kenya geothermal system to model the possible geochemical effect of geothermal reinjection in this well. The scaling potential of hot reinjection into Olkaria wells were assessed prior to production and during reinjection. A comparison of the two would enable evaluation of how mixing of fluids can modify saturation states and eventually affect the scaling potential in reinjection wells and in the receiving aquifer. This study used the analytical results from the separated water and gas samples from relevant wells (i.e. OW-703, OW-708 and OW-911) to calculate the aquifer deep fluid composition using the WATCH speciation program version 2.4 that enable the calculation of the mineral saturation indices of anhydrite, calcite, and silica (*they were considered as the baseline data prior to reinjection). The second step involved mixing of reinjected fluid with the aquifer fluid

using ***mixing processes*** PHREEQC version 3.7. It was concluded that the mixing ratio, changes in pH and temperature affects the saturation state of the mixed fluid.

The silicate prediction model may also be extended to higher pressure condition that are not yet possible to test in laboratory work without using expensive and time-consuming equipment. It would be very beneficial for the oil and gas industry to have a model capable of predicting the occurrence and rate of deposition of silicate scales and this would be a useful tool in a silicate scale treatment program.

Further studies on the ageing brine system and modifying the inhibition studies

It has been demonstrated that amorphous magnesium silicate can be inhibited in the aged-mixed brine. Following observation made in the ageing brine test at room temperature, then further investigation would be very important. In particular, it would be very interesting to establish the time needed for such and aged system to achieve critical nucleus size, so that the amorphous colloid silica can be totally inhibit through the introduction of scale inhibitor. It is also recommended to repeat the ageing test at an elevated temperature condition to mimic the reservoir ASP flooding conditions at a temperature of say T =60^{o}C to see how this will affect the kinetic of silicate scaling. Going on from these experiments, a further test on how A5 will perform in those modified silicate system should be conducted.

Testing more scale inhibitor to validate conjectures

It is proposed that the silicate inhibition studies should be extent to a wider range of potential silicate scale inhibitors/dispersants in order to develop a better understanding of the behaviour of all polymeric scale inhibitors and to test conjectures presented in *Chapter 5*. This will be useful in identifying the actual functional groups that responsible for the inhibition of the silicate scale.

To study the inhibition efficiency testing by the dynamic tube blocking (TBR) test

It is established that the MIC of A5 in the "*manageable"* base case of 30Mg:75Si was [MIC] ~ 50ppm. It is proposed to further study the A5 (and other potential inhibitors) inhibition studies to include ***dynamic*** testing in tube blocking rig (TBR) tests. The TBR test evaluates short-term IE performance, which can of often give rise to different selection and ranking of scale inhibitor products than that obtained through conventional static IE tests. Working from TBR test MICs, it is possible to calculate the performance quotient as following equation:

$$PQ = \frac{\boldsymbol{MIC_{ST}}}{\boldsymbol{MIC_{TB}}}$$

To study the effect of co-precipitation with the calcite ($CaCO_3$)

Amorphous silica formation via silica polymerization, colloidal silica suspension, precipitation of metal silicates and coprecipitation of silica with mineral salts (e.g. calcium carbonate, calcium sulfate) are different processes responsible for the deposition of silica-based deposits. Preventing the formation of silica-silicate based deposits requires control of all these processes simultaneously (Gill, 1993). According to Amjad and Zuhl (2010), the ideal candidate(s) must have two distinct properties: (a) disperse both silica and magnesium silicate and (b) disperse scalant particles (e.g., calcium carbonate, calcium sulfate) that can act as nuclei for silica-silicate deposits. Therefore, it is worth extending this work to study the effect of calcium carbonate on the silicate scale formation and inhibition.

APPENDIX A GENERAL EQUIPMENT AND APPARATUS

I. Solution Preparations and Experimental Procedures

II. Inductively Coupled Plasma - Optical Emission Spectroscopy (ICP-OES)

III. Environmental Scanning Electron Microscopy - Energy Dispersive X-Ray (ESEM-EDX)

IV. Fourier Transform Infrared (FTIR) - iD5 ATR Thermo Scientific

V. D8 Advance High Res PXRD Bruker D8 Advance GX000208

I. Solution Preparations and Experimental Procedures

1. Brine Preparation

Magnesium brine (MB) was mixed with silicon brine (SB) in 50:50 ratio at test temperature and test pH in various base cases studied to give final concentration as shown in Table A-1.

Table A-1 The brine composition and preparation for difference base cases studied

Base Case Categories	Final Concentration of [Mg] and [Si] in 50:50 of MB:SB mixed brine			Mixed brine preparation 50ml MB + 50ml SB	
	Mixed brines	**Mg^{2+} Concentration (ppm)**	**Si^{2+} Concentration (ppm)**	MB (ppm)	SB (ppm)
"Worst" base case Scenario	1200Mg:1020Si	1200	1020	2400	2040
	900Mg:1020Si	900	1020	1800	2040
	60Mg:1020Si	600	1020	1200	2040
	450Mg:1020Si	450	1020	900	2040
	120Mg:1020Si	120	1020	240	2040
	90Mg:1020Si	90	1020	180	2040
	60Mg:1020Si	60	1020	120	2040
	45Mg:1020Si	45	1020	90	2040
	900Mg:940Si	900	940	1800	1880
	450Mg:940Si	450	940	900	1880
	300Mg:940Si	300	940	600	1880
	120Mg:940Si	120	940	240	1880
	90Mg:940Si	90	940	180	1880
	60Mg:940Si	60	940	120	1880
"Intermediate" base case scenario	60Mg:752Si	60	752	120	1504
	60Mg:564Si	60	564	120	1268
	60Mg:470Si	60	470	120	940
	60Mg:300Si	60	300	120	600
"Worst" base case scenario	30Mg:150Si	30	150	60	300
	30Mg:75Si	30	75	60	150
	30Mg:50Si	30	50	60	100

MB was prepared by weighing out and dissolving the magnesium chloride hexahydrate salt ($MgCl_2.6H_2O$) salt in an appropriate volume of distilled water as shown in Table A-2. The salt is ensured to completely dissolve by stirring for at least 2 hours and the brine is left overnight before using.

Table A-2 Preparation of magnesium brine (MB)

MB ppm (mg/L)	Amount of $MgCl_2.6H_2O$ Required				
	g / L	g / 5L	g / 10L	g / 15L	g / 20L
60	0.5018	2.5088	5.0175	7.5263	10.0350
90	0.7527	3.7635	7.5270	11.2905	15.0540
120	1.003	5.017	10.035	15.052	20.069
180	1.505	7.526	15.052	22.578	30.104
240	2.007	10.035	20.069	30.104	40.138
600	5.017	25.087	50.173	75.260	100.347
900	7.530	37.630	75.260	112.890	150.600
1200	10.03	50.17	100.35	150.52	200.69
1800	15.05	75.26	150.52	225.78	301.04
2400	20.07	100.35	200.69	301.04	401.38

Notes:

a) All prepared brines are filtered using 0.45μm Whatman filter paper. This is to remove any dirt or other impurities during filtration.
b) No degassing is required.
c) Brine is prepared couple of days before the experiment starts

SB was prepared by weighing out and dissolving the sodium metasilicate pentahydrate salt ($Na_2SiO_3.5H_2O$) salt in an appropriate volume of distilled water as shown in Table A-3. The salt is ensured to completely dissolve by stirring for at least 2 hours and the brine is left overnight before using.

Detailed procedure to prepare 5L of synthetic SB or MB:

1. All brines are prepared using distilled water.
2. All salts used are AnalaR reagent grade.
3. Remember labelling: contents, experimentalists name and date of preparation
4. Weigh out the appropriate salt ($MgCl_2.6H_2O$ or $Na_2SiO_3.5H_2O$) on a weighing boat.
5. Add the salt to the 1 litre beaker, whilst rinsing out container with distilled water, to ensure that all the individual salts are added into the beaker.
6. Make sure all salt is completely dissolve.
7. Pour this solution into a 5L volumetric flask whilst rinsing out container with distilled water, to ensure that all the individual salts are added into the volumetric flask
8. Make up to 5 litres of distilled water to the volumetric flask. Use the washings from the beaker and distilled water to bring it up to 5 litres,
9. Use a magnetic stirrer to stir the solution for at least 2 hours.

10. Once all of the solids are dissolved the solution can be transferred into 5L HDPE bottle.
11. Filter the solution through a 0.45µm membrane filter under reduced pressure prior to use.

Table A-3 Preparation of silicon brine (SB)

SB ppm (mg/L)	Amount of $Na_2SiO_3.5H_2O$ Required				
	g / L	g / 5L	g / 10L	g / 15L	g / 20L
100	0.755	3.777	7.553	11.330	15.107
150	1.133	5.665	11.330	16.995	22.660
300	2.266	11.330	22.660	33.990	45.320
600	4.530	22.660	45.320	67.980	90.640
940	7.100	35.500	71.000	106.500	142.000
1128	8.520	42.600	85.200	127.800	170.400
1504	11.360	56.800	113.600	170.400	227.200
1880	14.200	71.000	142.000	213.000	284.000
2040	15.409	77.043	154.085	231.128	308.170

Notes:

a) All prepared brines are filtered using 0.45µm Whatman filter paper. This is to remove any dirt or other impurities during filtration.
b) No degassing is required.
c) Brine is prepared couple of days before the experiment starts
d) Brine is transferred into HDPE bottle immediately after being prepared i.e. after the salt is completely dissolved

2. Preparation for ICP Standards

The diluent must match the samples.

The diluent / matrix used in static test and inhibition efficiency test under aerobic condition is 100% of 1% EDTA/NaOH (aq); however the diluent/ matrix used in Glove Box Experiment under anaerobic condition is 0.1% EDTA/NaOH (aq).

Prepare 100ml of each concentration of the ICP standards by diluting appropriate volume of standards in appropriate diluent as shown in Table A-4.

Table A-4 Preparation of ICP Standards

$[Si^{4+}]$ / ppm	Volume of Si^{4+} Standard 1,000ppm Solution Required
0	**0ml**
5	{(5/1,000)*100}ml = **0.5ml**
10	{(10/1,000)*100}ml = **1.0ml**
25	{(25/1,000)*100}ml = **2.5ml**
50	{(50/1,000)*100}ml = **5ml**
100	{(100/1,000)*100}ml = **10ml**
$[Mg^{2+}]$ / ppm	Volume of Mg^{2+} Standard 1,000ppm Solution Required
0	**0 ml**
5	{(5/1,000)*100}ml = **0.5ml**
10	{(10/1,000)*100}ml = **1.0ml**
20	{(20/1,000)*100}ml = **2.0ml**
$[Fe^{2+}]$ / ppm	Volume of Fe^{2+} Standard 1,000ppm Solution Required
0	**0 ml**
1	{(1/1,000)*100}ml = **0.1ml**
2.5	{(2.5/1,000)*100}ml = **0.25ml**
5	{(5/1,000)*100}ml = **0.5ml**
10	{(10/1,000)*100}ml = **1.0ml**

3. Preparation for 1% EDTA/NaOH

This diluent is used for all the silicate static test and IE tests under aerobic condition. Diluent Solution is used to dilute samples taken for ICP analysis. For all the analysis in these experiments, the samples were diluted 10 times so that they would match the calibrated standards. At any sampling times, filter 10 ml of the brine using 0.2µm Nylon filter then dilute 1ml. Take 1ml of filtered sample into 9ml of 1% EDTA/NaOH quenching solution.

This solution was prepared by dissolving 50g of sodium hydroxide and 50g of Na_2-EDTA in 5L of distilled water. Use a 5L Volumetric Flask. Monitor its natural pH (in between pH13 to 13.5).

Note: This 1% solution is a lower concentration than normally used, in comparison to the flow cell surface dissolver tests of 5% and scale dissolver dissolution tests of 15%

4. Preparation for 0.1% EDTA/NaOH

This diluent is used for all the silicate static test and IE tests in the anaerobic condition conducted in glove box apparatus. For all the analysis in these experiments, the samples were diluted 10 times so that they would match the calibrated standards. At any sampling times, filter 10 ml of the brine using 0.2µm Nylon filter then dilute 1ml. Take 1ml of filtered sample into 9ml of 0.1% EDTA/NaOH quenching solution.

This solution was prepared by dissolving 0.5g of sodium hydroxide and 1g of Na_2-EDTA in 1L of distilled water. Use a 1L Volumetric Flask. Monitor its natural pH (in between pH11.8 to 11.9), nitrogen purged.

Note: This 0.1% solution is a lower concentration than normally used, in comparison to the flow cell surface dissolver tests of 5% and scale dissolver dissolution tests of 15% and aerobic silicate scale static test of 1%

The lower concentration of 0.1% was prepared to take into consideration the presence of the Fe ion which drops out in a 1% EDTA/NaOH solution.

5. Preparation for Glassware and Apparatus:

a) Apparatus: Fan assisted oven, balance, magnetic stirrer, Glove Box Apparatus, and 5000ml, 1000ml, 250ml and 150ml plastic bottles.
b) For pH measurement: pH meter, pH10, pH 7and pH 4 buffer solutions for calibration.
c) For Scale Inhibitor Dilutions: 5L volumetric flask, 5L plastic container, 1L beaker and funnel.
d) For filtration: filtering equipment's like vacuum pump, conical flasks and tubing and filter papers (0.45µm) and (0.20)
e) For ICP preparation: 250ml volumetric flasks, 10ml and 2.5ml variable and 1ml variable pipettes, 0.2µm Nylon filter

6. List of Inventories:

Table A-5 Chemicals used

CHEMICAL	SUPPLIER
Ammonium iron (II) sulphate hexahydrate	Sigma Aldrich
Magnesium chloride 6-hydrate	Merck
Sodium metasilicate pentahydrate	Sigma-Aldrich
Ethylenediaminetetraacetic acid disodium salt dihydrate EDTA	VWR Chemicals
Sodium hydroxide	VWR Chemicals
pH 4 buffer solution (phthalate)	Fisher Chemicals
pH 7 buffer solution (phosphate)	Fisher Chemicals
pH 10 buffer solution (borate)	Fisher Chemicals
Mineral Oil	-
Nitrogen	BOC
35% HCl Solution	VWR
Mg 1000ppm ICP std	Romil Pure chemistry
Si 1000ppm ICP std	CPI International
Iron 1,000ppm ICP std	Romil
ORP Test Solution for Electrodes 240mV at 25^{o}C	Hanna Instruments
Oxidizing Pretreatment Solution	Hanna Instruments
Reducing Pretreatment Solution	Hanna Instruments
CHEMets Dissolved Oxygen Test Kit	Chemetrics
Argon, refrigerated, liquid	BOC
Nitrogen, refrigerated, liquid	BOC
Triton X100	Sigma Aldrich
VS-Co	A
H3	B
A5	C

7. Experimental Procedures for Static Test (Aerobic condition):

In these tests each individual test condition is conducted in duplicate to allow anomalous results to be immediately recognised. Tests would be repeated if the difference in the recorded duplicate results was > 5 – 10%. Below are procedures for static test of mixed brine 60Mg:940Si at 60^{o}C, Natural pH & pH8.5. The procedures may be changed accordingly for different mixed brine concentration and test conditions.

1. Prepare the two sets of brines: MB (i.e. 120ppm Mg), and SB (i.e. 1880ppm Si) by weighing out and dissolving the appropriate salt in an appropriate volume of distilled water. The salt is ensured to completely dissolve by stirring for at least 2 hours and the brine is left overnight before using.
2. Vacuum filter brines separately through 0.45μm membrane filter paper.
3. **Pre-test for pH adjustment**:
    a. Check the initial pH of all filtered brines (i.e. 120ppm MB, 1880ppm SB) separately

       Note: pH of the 1880ppm SB ~pH12.9; pH of the 120ppm MB ~pH5.5
    b. Check the initial pH of the mixed solution
        - "*50ml 120ppm MB with 50ml 1880ppm SB"*

       Note: the pH of above mixed solution is ~pH12.70

    c. Then, adjust the pH of mixed solution in step 3b. to test pH by deliberately adding 10% HCl solution (Record the number of drops of 10% HCl solution used – as guidance on amount needed to adjust the pH in actual experiment below).

       Note: As guidance only. Adding **1.82ml** of 10% HCl solution into the mixed 100ml of SB/MB solution will adjust the pH of the mixed solution from ~**pH12.7** to ~**pH8.5**

Test Condition 1 (Natural pH~12.70 - Initial mixed concentration of 60Mg:940Si): HDPE 100ml Bottles 1 & 2

4. Prepare two (2) HDPE bottles of mixed solution (HDPE bottles to be labelled as 1 & 2) to get final concentration of 60ppm Mg and 940ppm Si with its natural pH ~12.7.

5. This can be done by measuring out appropriate volumes of MB and SB into different 100ml HDPE bottle.
6. Measure out appropriate volumes of SB (50ml) into the labelled 1 & 2 bottles. Measure out appropriate volumes of MB (50ml) into additional 100ml HDPE bottles.
7. For a 50:50% mix to a total of 100ml, pour the MB bottle contents into the SB bottles and immediately shake the solution vigorously. Check the initial pH of the mixed solution.
8. Place the bottles containing the SB/MB mixed brines into an oven, set to the required temperature (60^{o}C). Leave for ~60 minutes to reach test temperature. After 60 minutes, start a stopclock (t = 0).
9. After 2 hours of mixing time, the two HDPE bottles (labelled as 1 & 2) are then centrifuged until a clear top solution is observed (for this experiment samples are centrifuged at the highest speed ~3600rpm for 30 minutes). The centrifuged tests are then sampled as described below (remove sample from generated clear top solution or alternatively, the samples can be ICP sampled using a GD/X 25 0.2µm Nylon filter if cloudy top layer is produced).

   Note: This centrifuging step was replaced with filtering step in the established methodology that guarantee the repeatability and reproducibility of the test results as detailed was discussed in section 4.3.4 to 4.3.6 and summarized in section 4.3.7.
10. Check the final pH of the mixed solutions (HDPE bottles labelled 1 & 2) after it has cooled down to room temperature i.e. after being ICP sampled (of only the top clear solution – do not disturb the precipitate).
11. The two bottles are then filtered using 0.2µm filter paper and will be analysed by SEM/EDX, FTIR (and XRD, if possible – if sufficient amount of scale produced).

Test Condition 2 (pH8.5 of 60Mg:940Si): HDPE 100ml Bottles 3 & 4

12. Prepare another two (2) HDPE bottles of mixed solution (HDPE bottles to be labelled as 3 & 4) to get final concentration of 60ppm Mg and 940ppm Si with the mixed initial pH adjusted to pH8.5.
13. This can be done by measuring out appropriate volumes of MB and SB into different 100ml HDPE bottle.

14. Measure out appropriate volumes of SB (50ml) into the labelled 3 & 4 bottles. Measure out appropriate volumes of MB (50ml) into additional 100ml HDPE bottles.
15. For a 50:50% mix to a total of 100ml, pour the MB bottle contents into the SB bottles and immediately shake the solution vigorously.
16. Adjust the pH of all the mixed brines by deliberately adding 10% HCl solution to pH8.5 (pH must be adjusted immediately after the brine been mixed i.e. brine should be mixed followed by pH adjustment before the next bottle in step 15 can be prepared).

Note: pH adjustment is to be done by constantly stirring the solution at speed 2. 10% HCl solution is added only after the natural pH is recorded and stabilized. The adjusting time (time started from the brines being mixed until the pH being adjusted) should be kept between 6 – 8 minutes.

17. Place the bottles containing the SB-SI/MB mixed brines into an oven, set to the required temperature (60^{o}C). Leave for ~60 minutes to reach test temperature. After 60 minutes, start a stopclock (t = 0).
18. After 2 hours of mixing time, the two HDPE bottles (labelled as 3 & 4) are then centrifuged until a clear top solution is observed (for this experiment, samples are centrifuged at the highest speed ~3600rpm for 30 minutes). The centrifuged tests are then sampled as described below (remove sample from generated clear top solution or alternatively, the samples can be ICP sampled using a GD/X 25 0.2µm Nylon filter if cloudy top layer is produced).

    Note: This centrifuging step was replaced with filtering step in the established methodology that guarantee the repeatability and reproducibility of the test results as detailed was discussed in section 4.3.4 to 4.3.6 and summarized in section 4.3.7).
19. Check the final pH of the mixed solutions (HDPE bottles labelled 3 & 4) after it has cooled down to room temperature i.e. after being ICP sampled (of only the top clear solution – do not disturb the precipitate).
20. The two bottles are then filtered using 0.2µm filter paper and will be analysed by SEM/EDX, FTIR (and XRD, if possible – if sufficient amount of scale produced).
21. Prepare the required ICP calibration standards in the appropriate background matrix (see below).
22. ICP analysis of samples for [Si^{4+}] and [Mg^{2+}].

Sampling and Analysis

The sampling procedure is carried out as follows:

After the required time interval, filter 10ml of the brine using a 0.2µm Nylon filter into a separate HDPE bottle; then dilute 1ml. 1ml of the particular test supernatant water (filtered sample) is removed using an Eppendorf 1ml automatic pipette and immediately added to the 9ml of 1% EDTA/NaOH quenching solution. The samples are then analysed by ICP for the particular ions of interest, e.g. silicon, and magnesium ions. The remaining filtered sample is allowed to cool to room temperature for pH measurement. ICP calibration standards and control solution are prepared as shown in Table A-6 and Table A-7.

Table A-6 ICP calibration Standards for Static Test (Aerobic condition)– Preparation Details

Si^{4+} in 0.1% EDTA / NaOH (aq) Mg^{2+} in 0.1% EDTA / NaOH (aq) The diluent must match the samples. In this case, the diluent will be 100% of 0.1% EDTA/NaOH (aq) Concentration of ICP calibration standards: 0ppm, 25ppm, 50ppm and 100ppm Si^{4+} and 0ppm, 5ppm, and 10ppm Mg^{2+} Prepare 100ml of each concentration	
$[Si^{4+}]$ / ppm	Volume of Si^{4+} Standard 1,000ppm Solution Required
0	**0ml**
25	{(25/1,000)*100}ml = **2.5ml**
50	{(50/1,000)*100}ml = **5ml**
100	{(100/1,000)*100}ml = **10ml**
$[Mg^{2+}]$ / ppm	Volume of Mg^{2+} Standard 1,000ppm Solution Required
0	**0 ml**
5	{(5/1,000)*100}ml = **0.5ml**
10	{(10/1,000)*100}ml = **1.0ml**

Use as repeating standard only/not in calibration = 25ppm Si^{4+}
Use as repeating standard only/not in calibration = 5ppm Mg^{2+}

Table A-7 Control Samples for Static Bottles Test (Aerobic condition) – Preparation Details

Control	Volume of 120ppm MB (ml)	Volume of 1880ppm SB (ml)	Volume of 1% EDTA/NaOH (aq) (ml)
Control 1 (x20) 120ppm Mg	5		**95**
Control 2 (x20) 1880ppm Si		5	**95**
Control 3 (x10) 120ppm Mg & 1880ppm Si	5	5	**90**

Control $[Si^{4+}]$ = $\frac{(1880)}{20}$ = **94ppm**
Control $[Mg^{2+}]$ = $\frac{(120)}{20}$ = **6ppm**
Control $[Si^{4+}]$ = $\frac{(1880*0.5)}{10}$ = **94ppm**
Control $[Mg^{2+}]$ = $\frac{(120*0.5)}{10}$ = **6ppm**

8. Experimental Procedures for Static IE Test (Aerobic condition):

In these tests each individual test condition is conducted in duplicate to allow anomalous results to be immediately recognised. Tests would be repeated if the difference in the recorded duplicate results was > 5 – 10%. Below are procedures for static IE test of mixed brine 30Mg:75Si + [A5] at 60^{o}C, pH8.5. The procedures may be changed accordingly for different mixed brine concentration, types of SI, [SI] and test conditions.

1. Prepare the two sets of brines: MB (i.e. 60ppm Mg), and SB (i.e. 150ppm Si) by weighing out and dissolving the appropriate salt in an appropriate volume of distilled water. The salt is ensured to completely dissolve by stirring for at least 2 hours and the brine is left overnight before using.
2. Vacuum filter brines separately through 0.45μm membrane filter paper.
3. Dissolve the inhibitors in "150ppm Silicon brine" to create stock solutions of 1,000ppm active SI (0.1% stock SI).
4. The inhibitor solutions prepared in Step 3 are then further diluted in silicon brine (SI/SB solutions) to give the required concentration for the particular test. Each inhibitor concentration is tested in duplicate.

   Note 1: the concentration of inhibitor in SB (SI/SB) must be higher than that required for the test by a factor which accounts for the dilution when mixed with the magnesium brine.

   Note 2: the SI was chosen to be diluted into silicon brine solution in this experiment (instead of magnesium brine solution) due to possible silicon polymerization. However, it might be worth to dilute the SI in the magnesium brine to check for any differences.

5. **Pre-test for pH adjustment**:
   a. Check the initial pH of all filtered brines (i.e. 60ppm MB, 150ppm SB) and SI stock solution (i.e. 1,000ppm A5) separately

   Note: pH of the 150ppm SB ~pH11; pH of the 60ppm MB ~pH5.5; pH of the SI stock solution ~pH11

   b. Check the initial pH of all the mixed solution

   "*50ml 60ppm MB with 50ml 150ppm SB"* **30Mg:75Si**

   "*50ml 60ppm MB with 50ml 150ppm SB/ 40ppm SI*" **30Mg:75Si + 20ppm A5**

   "*50ml 60ppm MB with 50ml 150ppm SB/ 60ppm SI*" **30Mg:75Si + 30ppm A5**

"*50ml 60ppm MB with 50ml 150ppm SB/ 80ppm SI*" **30Mg:75Si + 40ppm A5**

"*50ml 60ppm MB with 50ml 150ppm SB/ 100ppm SI*" **30Mg:75Si + 50ppm A5**

"*50ml 60ppm MB with 50ml 150ppm SB/ 150ppm SI*" **30Mg:75Si + 75ppm A5**

"*50ml 60ppm MB with 50ml 150ppm SB/ 200ppm SI*" **30Mg:75Si+100ppm A5**

"*50ml 60ppm MB with 50ml 150ppm SB/ 300ppm SI*" **30Mg:75Si+300ppm A5**

Note: the pH of all above mixed solution is ~pH10.7 (with 300ppm A5) to ~pH10.95 (non-inhibited blank)

c. Then, adjust the pH of mixed solutions to pH8.5 by deliberately adding 10% HCl solution (Record the number of drops of 10% HCl solution used – as guidance on amount needed to adjust the pH in actual experiment below).

Note: As guidance only. Adding ~0.085ml of 10% HCl (into 300ppm SI/SB/MB) to ~0.11ml of 10% HCl (Non-inhibited blank) solution into the mixed 100ml of SB/MB/SI solution will adjust the pH of the mixed solution from ~pH11 to ~pH8.5. Then, further adjust the pH using the diluted HCl solution. Refer Table A-8.

Table A-8 Guidance on pH adjustment – Amount of 10% HCl needed in silicate system of 30Mg:75Si

SI concentration (ppm)	Original pH	Amount 10% HCl added (ml)
0 (Non-inhibited BLANK)	10.9 – 11.0	0.110
20	10.9 – 11.0	0.105
30	10.9 – 11.0	0.105
40	10.9 – 11.0	0.105
50	10.87 – 10.92	0.100
75	10.87 – 10.88	0.100
100	10.85 – 10.88	0.100
300	10.73 – 10.75	0.085

Table A-9 Scale Inhibitor Activity

Scale Inhibitor name	Activity %
Acumer 5000	42

Calculation

1g in 1L = 1,000ppm as supplied

xg = 1g x (100/activity %)

i.e. xg = 1 x (100/42) = 2.381g/L for **Acumer 5000** at 42% active

1.1905g in 500mL = 1,000ppm = 0.1% therefore 0.1% act stock

Table A-10 Scale Inhibitor Stock Solution (0.1% act stock)

Scale Inhibitor name	Weight	Actual weight for 500ml
Acumer 5000	1 x (100/42) = 2.381g/L	**1.1905g**/500ml

Now preparing SI solutions to be used in tests. Remember there is a 50:50% SB:MB dilution upon mixing brines, therefore initial [SI] = mix [SI]*100/50.

Table A-11 Scale Inhibitor Dilution

Scale Inhibitor name	SI Activity (%)	Concs. required v/v before mix / ppm active	Concs. v/v after mix / ppm active	Volume of 1,000ppm active SI stock solution diluted (in 250ml "150ppm Silicone brine")
Acumer 5000	42	40	20	40/1,000*250 = **10ml** of stock SI soln
		60	30	60/1,000*250 = **15ml** of stock SI soln
		80	40	80/1,000*250 = **20ml** of stock SI soln
		100	50	100/1,000*250 = **25ml** of stock SI soln
		150	75	150/1,000*250 = **37.5ml** of stock SI soln
		200	100	200/1,000*250 = **50ml** of stock SI soln
		600	300	600/1,000*250 = 1**50ml** of stock SI soln

Note 1: in the above table, 250ml of each SI at each concentration has been prepared. This enables the same solution to be used in 2 bottles (2 x 50ml) i.e. a test and duplicate bottle at each sampling times i.e. 2 hr, 22 hr, 5 day & 7 day, for each test condition. Discard the remaining leftover solutions.

Note 2: The IE Test was conducted in 3 separate tests with repeated blank and 1 concentration to ensure enough time for sample preparation (i.e. allow accurate sample preparation and 2 hour sampling conducted in the same day).

Example of series of tests;

IE Test 1: **Blank**, 20/ 30/ **40ppm** Acumer 5000

IE Test 2: **Blank**, **40**/ 50/ **75ppm** Acumer 5000

IE Test 3: **Blank**, **75**/ 100/ 300ppm Acumer 5000

Test Condition 1 (Blank - Initial mixed concentration of 30Mg:75Si): Glass 175ml Bottles 1 & 2

6. Prepare two (2) glass bottles of mixed solution (Glass bottles to be labelled as 1 & 2) to get final concentration of 30ppm Mg and 75ppm Si.
7. This can be done by measuring out appropriate volumes of MB and SB into different 100ml HDPE bottle.
8. Measure out appropriate volumes of SB (50ml) into the labelled 1 & 2 bottles. Measure out appropriate volumes of MB (50ml) into additional 100ml HDPE bottles.
9. Shake MB and SB bottles vigorously. For a 50:50% mix to a total of 100ml, pour the MB bottle contents into the SB bottles and immediately shake the solution vigorously.
10. Adjust the pH of all the mixed brines by deliberately adding 10% HCl solution to pH8.5 (pH must be adjusted immediately after the brine been mixed i.e. brine should be mixed followed by pH adjustment before the next bottle in step 9 can be prepared).

    Note: pH adjustment is to be done by constantly stirring the solution at speed 2. 10% HCl solution is added only after the natural pH is recorded and stabilized. The adjusting time (time started from the brines being mixed until the pH being adjusted) should be kept between 6 – 8 minutes.

11. The mixing and pH adjustment procedure explained in section 5.2.6 and is illustrated in Figure 5-32.
12. Immediately, transfer the pH-adjusted mixed brine into the appropriately labelled glass bottle.
13. Place the glass bottles containing the SB/MB/SI mixed brines into an oven, set to the required temperature (60^{o}C). Leave for ~60 minutes to reach test temperature. After 60 minutes, start a stopclock (t = 0).
14. After 2 hours of mixing time, take the two glass bottles out of the oven and visually inspect them. Take picture as a record. Then, filter 10ml of the samples using 0.2µm Nylon filter as per $BaSO_4$ IE sampling into an appropriately labelled HDPE bottle (also labelled as 1 & 2). Then dilute 1 ml of the filtered tests as described below.
15. Place these two glass bottles back in the oven.

16. Check the pH of the remaining filtered samples (in HDPE bottles labelled 1 & 2) after it has cooled down to room temperature i.e. after being ICP sampled using filter techniques.
17. Repeat steps 14-15 at every sampling time i.e. 22hour, 5 day and 7 day (or any sampling times).
18. The two glass bottles are then filtered using 0.2µm filter paper and will be analysed by SEM/EDX, FTIR (and XRD, if possible – if sufficient amount of scale produced).

Test Condition 2 (20ppm A5 in initial mixed concentration of 30Mg:75Si): 175ml Glass Bottles 3 & 4

19. Prepare another two (2) glass bottles of mixed solution (Glass bottles to be labelled as 3 & 4) to get final concentration of 30ppm Mg and 75ppm Si with 20ppm A5.
20. This can be done by measuring out appropriate volumes of MB and SB/SI (prepared in step 4 by diluting 10ml of 0.1% act stock solution into 250ml SB) into different 100ml HDPE bottle. Refer to Table A-9 to Table A-11 for the SI dilution.
21. Measure out appropriate volumes of SB/SI (50ml) into the labelled 3 & 4 bottles. Measure out appropriate volumes of MB (50ml) into additional 100ml HDPE bottles.
22. Repeat steps 9 – 18 for these HDPE/ Glass bottles labelled 3 & 4.
23. Repeat steps 1 – 22 for other [SI] as listed in Table A-8.

24. Prepare the required ICP calibration standards in the appropriate background matrix.
25. ICP analysis of samples for [Si^{4+}] and [Mg^{2+}].

Sampling and Analysis

The sampling procedure is carried out as follows:

After the required time interval, filter 10 ml of the brine using 0.2µm Nylon filter into a separate HDPE bottle; then dilute 1ml. 1ml of the particular test supernatant water (filtered sample) is removed using an Eppendorf 1ml automatic pipette and immediately added to the 9ml of 1% EDTA/NaOH quenching solution. The samples are then analysed by ICP

for the particular ions of interest, e.g. silicon and magnesium ion. The remaining filtered sample is allowed to cool to room temperature for pH measurement. ICP calibration standards and control samples are prepared as shown in Table A-12 and Table A-13.

Table A-12 ICP calibration Standards for Static IE Test (Aerobic condition) Bottle Test – Preparation Details

Si^{4+} in 0.1% EDTA / NaOH (aq) Mg^{2+} in 0.1% EDTA / NaOH (aq) The diluent must match the samples. In this case, the diluent will be 100% of 0.1% EDTA/NaOH (aq) Concentration of ICP calibration standards: 0ppm, 5ppm, and 10ppm Si^{4+} and 0ppm, 5ppm, and 10ppm Mg^{2+} Prepare 100ml of each concentration	
$[Si^{4+}]$ / ppm	Volume of Si^{4+} Standard 1,000ppm Solution Required
0	**0ml**
5	{(5/1,000)*100}ml = **0.5ml**
10	{(10/1,000)*100}ml = **1.0ml**
$[Mg^{2+}]$ / ppm	Volume of Mg^{2+} Standard 1,000ppm Solution Required
0	**0 ml**
5	{(5/1,000)*100}ml = **0.5ml**
10	{(10/1,000)*100}ml = **1.0ml**

The required efficiencies for silicate scale inhibition are then calculated using the following equation:

$$\%Efficiency(t) = \frac{(M_B - M_I)x100}{M_B} = \frac{(C_O - C_B) - (C_O - C_I)x100}{(C_O - C_B)} = \frac{(C_I - C_B)x100}{(C_O - C_B)}$$

Equation A-1

Where;

- M_B = Mass of silicon (or other cations) precipitated in supersaturated blank solution.
- M_I = Mass of silicon (or other cations) precipitated in test solution.
- C_O = Concentration of silicon (or other cations) originally in solution (i.e. t=0).
- C_I = Concentration of silicon (or other cations) at sampling.
- C_B = Concentration of silicon (or other cations) in the blank solution (no inhibitor) at the same conditions and sampling time as C_I above.
- (t) = Sampling time.

Note: C_O is determined by adding the test SB and MB to the 1% EDTA/NaOH quenching solution in the appropriate ratio, as used for the quenched test solutions. Therefore, for these tests, **5ml** SB and **5ml** of MB made up to **100ml** with 1% EDTA/NaOH (refer Table A-13). C_O samples are added to the ICP analysis of test samples at regular intervals to allow for instrumental errors to be accounted for.

Table A-13 Control Samples for Static IE (Aerobic condition) Bottles Test – Preparation Details (prepare 100ml)

Control	Volume of 60ppm MB (ml)	Volume of 150ppm SB (ml)	Volume of 1% EDTA/NaOH (aq) (ml)
Control 1 (x20) 60ppm Mg	**5**		**95**
Control 2 (x20) 150ppm Si		**5**	**95**
Control 3 (x10) 60ppm Mg & 150ppm Si	**5**	**5**	**90**
Control $[Si^{4+}]$ = (150)/20 = **7.5ppm** Control $[Mg^{2+}]$ = (60)/20 = **3ppm** Control $[Si^{4+}]$ = (150*0.5)/10 = **7.5ppm** Control $[Mg^{2+}]$ = (60*0.5)/10 = **3ppm**			

9. Experimental Procedures for Static Test (Anaerobic condition):

In these tests each individual test condition is conducted in duplicate to allow anomalous results to be immediately recognised. Tests would be repeated if the difference in the recorded duplicate results was > 5 – 10%. Below are procedures for static test of mixed brine 30Mg:75Si at 60^{o}C, pH8.5. The procedures may be changed accordingly for different mixed brine concentration and test conditions.

150ppm SB & 60ppm MB will be pre-prepared in ambient condition & will be filtered using 0.45µm as for the normal test procedure control and will be purged with nitrogen before putting into the glove box. Below procedure is to study the effect of 50ppm Fe^{2+} on the silicate system of 30Mg:75Si at 60^{o}C, pH8.5. The procedures may be changed accordingly for different $[Fe^{2+}]$.

5000ppm Fe stock solution will be prepared in glove box and will be filtered using 0.2µm Nylon syringe filter as only small volume (1ml) of this stock will be required for the test.

1. Weigh Mohr's salt $(NH_4)_2Fe(SO_4)_2 \cdot 6H_2O$ in an appropriately marked plastic cup to prepare the Fe stock solution and put it into the glove box. **Note:** do **not** dissolve this prior to placing into the glove box.
2. Purge 100ml 0.1% EDTA/NaOH solution with nitrogen for ~10 min outside of the glove box.
3. Purge 100ml 150ppm SB with nitrogen for ~10 min outside of the glove box.
4. Purge 100ml 60ppm MB with nitrogen for ~10 min outside of the glove box.
5. Purge ~25ml 10% HCl solution and ~25ml dilute HCl with nitrogen for ~10 min outside of the glove box.
6. Place all necessary equipment/glassware/chemicals into the glove box:
    - Redox meter with test solution
    - CHEMets Colorimetric Dissolved Oxygen Test Kit
    - 10ml Eppendorf pipettes
    - 1ml Eppendorf pipettes
    - 10ml pipette tips (1)
    - 1ml pipette tips (5)
    - Pasteur pipettes (3)
    - box of tissues
    - 1*100ml volumetric flask (for Fe^{2+} stock solutions)
    - Duran premium bottles with lids – 100ml (2) – before placing them into the box, write down test conditions (SI conc.) on the bottles
    - 150ml HDPE bottles for brine preparation before mixing – Mg & Si (2)
    - 25ml Duran premium bottles with lids for filtered samples prior to ICP sampling at 2 hour (1)
    - 250ml HDPE bottle for waste disposal (1)
    - 100ml measuring cylinder (2)
    - DW safety-labelled wash bottle for rinsing electrodes (1)
    - 4 test tubes with lids
    - Test tube stand
    - Empty plastic cup for deoxygenized water for proper brine preparation (1)
    - Empty plastic beaker for rinsing electrodes (1)
    - Magnetic stirrer plate
    - Magnetic bar (2)
    - Magnetic retriever (1)

- Polyethylene grip sealed bag (1)
- Heat resistant tape **- FLUOLION (PTFE) Thread Tape 25.4mm width 85°C**
- GD/X 0.2microns Nylon Filter (1)
- 10ml syringe for ICP sampling at 2 hour (1)
- ~25ml of HCl 10%, ~25ml dilute HCl for pH adjustment – **purged with nitrogen inside the glove box**
- ~100ml 0.1% EDTA/NaOH quenching solution – **purged with nitrogen in transfer port**
- ~1L DW for brine preparation and electrode rinsing – **purged with nitrogen in transfer port**
- ~100ml of 60ppm Mg brine – **purged with nitrogen in transfer port**
- ~100ml of 150ppm Si brine – **purged with nitrogen in transfer port**
- Pre-measured samples of $(NH_4)_2Fe(SO_4)_2 \cdot 6H_2O$
- Buffer solution pH4 - ~25ml in 25ml Duran premium bottles with lids – **purged with nitrogen inside the glove box**
- Buffer solution pH7 - ~25ml in 25ml Duran premium bottles with lids – **purged with nitrogen inside the glove box**
- Buffer solution pH10 - ~25ml in 25ml Duran premium bottles with lids – **purged with nitrogen inside the glove box**

Note: Once transferred into the main body, sparge all of these items with nitrogen for about 1-2 minutes inside the glove box (using the nitrogen sparging line)

7. Shut the glove box and purge it with nitrogen, at max pressure 10psi. The transfer port is suitably purged after ~ 10-15 minutes. The empty main body requires ~ 30 minutes, with equipment placed inside ~2 hours.
8. While purging the glove box, purge ~1L of DW with nitrogen outside of the box using 1L Duran bottle with purging lid for 1 hour before placing it into the glove box. This will be used for the Fe^{2+} stock solutions and for rinsing the pH/ORP electrodes while using them inside the glove box.

Note: All further steps must be carried out in a glove box purged continually with nitrogen (2-5psi) in order to reach and maintain anaerobic conditions.

9. Place 1L bottle of DW from Step 8 into the transfer port, purge it for 30mins and transfer it inside the main body. Purge the DW again in the glove box for 1 hour.
10. Measure the [dissolved oxygen] in the purged DW (Step 8) using the CHEMets Colorimetric Dissolved Oxygen Test Kit. The testing procedure can be found below. If the amount of dissolved oxygen exceeds 0.5 ppb, repeat purging as long as it is necessary to reach an oxygen level in the DW of less than 0.5 ppb.

Note: Use CHEMets Colorimetric Dissolved Oxygen Test only for the solution which does not contain any Fe in it. Fe itself affects the CHEMets test, reacting with the components and leading to incorrect test results.

11. Dissolve the $(NH_4)_2Fe(SO_4)_2 \cdot 6H_2O$ (weighed in Step 1) in the 100ml volumetric flasks, using the DW from Step 7. Note: Prepare 1 bottle of 50ml SB, 1 bottles of 50ml MB
12. Prepare two (2) DURAN bottles of mixed solution (DURAN bottles to be labelled as 1) to get final concentration of 30ppm Mg and 75ppm Si with 50ppm Fe^{2+}.
13. Shake one MB and one SB bottles (prepared in step 10) vigorously. For a 50:50% mix to a total of 100ml, pour the MB/ Fe^{2+} bottle contents into the SB bottles and immediately shake the solution vigorously. Then add 1ml of 5000ppm Fe^{2+} stock solution. Shake vigorously
14. Adjust the pH of the mixed brines by deliberately adding 10% HCl solution to pH8.5 (pH must be adjusted immediately after the brine has been mixed).

Note: pH adjustment is to be done by constantly stirring the solution at speed 2. 10% HCl solution is added only after the natural pH is recorded and stabilized. The adjusting time (time started from the brines being mixed until the pH being adjusted) should be kept between 6 – 8 minutes.

15. The mixing and pH adjustment procedure explained in steps 13 - 14 is explained in section 5.2.6 and illustrated in Figure 5-32.
16. Immediately, transfer the pH-adjusted mixed brine into the appropriately labelled DURAN bottle. Take 1ml of sample from each test bottle, and add to the test tubes with 9 ml DW – this will give initial control samples.
17. Pour ~100 ml DW into a separate bottle. Measure the O_2 concentration in it. This will be an O_2 control test bottle for monitoring changes of O_2 concentration during the test.

18. Check the redox-potential of all prepared solutions, including the O_2 control test bottle. Test and condition ORP meter using test, oxidising and reducing solutions prior to the measurement. To do this, check the meter by immersing it in the 240mV at 25°C test solution. The reading should be within the range, 235-245 mV at 25°C. For more accurate readings, condition the meter by immersing it in a pre-treatment reducing or oxidizing solution for ~30 minutes before taking measurements.

    Note: If ORP is smaller than -600 mV at pH8.5/25°C, then Fe is predominantly stable as $Fe(OH)_2$ (s); -600 to -300 mV at pH8.5/25°C, then Fe is predominantly stable as Fe_3O_4(s); larger than -300mV at pH8.5/25°C, then Fe is predominantly stable as Fe_2O_3(s) (refer to Pourbaix diagram - see Figure A-1).

19. Make sure that bottles are closed properly. Place the bottles, including O_2 control test bottle, in a polythene grip sealed bags, leaving as little gas inside as it is possible. Close the bags properly, and seal them up with heat resistant tape. Take the bags with the bottles in them, out of the glove box and place them into an oven, set to 60°C. Leave for ~60 minutes to reach test temperature. After 60 minutes, start a stopclock (t = 0). Monitor solutions colour change every 30 min and take pictures when necessary.
20. After 2 hours, put them back into the transfer port, leave there for nitrogen purging for 30mins, and after, transfer into the glove box. Allow the test bottles to cool to room temperature.

    Note 1: after placing the bags to the oven at 60°C, the volume of gas inside the bag will increase due to a temperature increase which may cause damage to the bag. This leads to the bottles being exposed to increasing O_2 concentration => oxidising.

    Note 2: Before transferring anything inside the glove box, ***always*** purge the items with nitrogen in transfer port for at least 15mins (depending on size/number)!

21. Measure the O_2 concentration in the O_2 control test bottle. Check, if the low oxygen level has been maintained after the bottles were taken out, heated and replaced in the glove box.
22. Check ORP (see Step 18).
23. Then, filter 10ml of the sample using the 0.2µm Nylon filter as per $BaSO_4$ IE sampling into an appropriately labelled 25ml Duran premium bottles. Then dilute 1ml of the filtered test sample as described below.

Outside of Glove Box

24. Immediately (to avoid re-speciation of Fe^{2+} to Fe^{3+} in the precipitate before filtration), filter all liquid + solid through 0.22µm filter paper and collect the precipitate. Wash the precipitate with *a little* DW. These precipitates will be analysed by SEM/EDX, FTIR (and XRD, if possible – if sufficient amount of scale produced).
25. Prepare the required ICP calibration standards in the appropriate background matrix (see below).
26. ICP analysis of samples for [Si^{4+}], [Mg^{2+}] and [Fe^{2+}].
27. **Note:** Keep samples in glove box until the ICP's are ready to analyse them

Sampling and Analysis

The sampling procedure is carried out as follows:

After the required time interval, filter 10ml of the brine using a 0.2µm Nylon filter into a separate HDPE bottle; then dilute 1ml. 1ml of the particular test supernatant water (filtered sample) is removed using an Eppendorf 1ml automatic pipette and immediately added to the 9ml of 0.1% EDTA/NaOH quenching solution. The samples are then analysed by ICP for the particular ions of interest, e.g. silicon, magnesium and iron ions. The remaining filtered sample is allowed to cool to room temperature for pH measurement. ICP calibration standards and control samples are prepared as shown in Table A-14 and Table A-15.

Table A-14 ICP calibration Standards for Static Anaerobic Test– Preparation Details

Si^{4+} in 0.1% EDTA / NaOH (aq) Mg^{2+} in 0.1% EDTA / NaOH (aq) The diluent must match the samples. In this case, the diluent will be 100% of 0.1% EDTA/NaOH (aq) Concentration of ICP calibration standards: 0ppm, 25ppm, 50ppm, and 100ppm Si^{4+} and 0ppm, 5ppm, and 10ppm Mg^{2+} 0ppm, 50ppm, and 100ppm Fe^{2+} Prepare 100ml of each concentration	
$[Si^{4+}]$ / ppm	Volume of Si^{4+} Standard 1,000ppm Solution Required
0	**0ml**
5	{(5/1,000)*100}ml = **0.5ml**
10	{(10/1,000)*100}ml = **1.0ml**
$[Mg^{2+}]$ / ppm	Volume of Mg^{2+} Standard 1,000ppm Solution Required
0	**0 ml**
5	{(5/1,000)*100}ml = **0.5ml**
10	{(10/1,000)*100}ml = **1.0ml**
$[Fe^{2+}]$ / ppm	Volume of Fe^{2+} Standard 1,000ppm Solution Required
0	**0 ml**
5	{(5/1,000)*100}ml = **0.5ml**
10	{(10/1,000)*100}ml = **1.0ml**

Table A-15 Control Samples for Static Anaerobic Bottles Test – Preparation Details

Control	Volume of 60ppm MB (ml)	Volume of 150ppm SB (ml)	Volume of 1% EDTA/NaOH (aq) (ml)
Control 1 (x20) 60ppm Mg	**5**		**95**
Control 2 (x20) 150ppm Si		**5**	**95**
Control 3 (x10) 60ppm Mg & 150ppm Si	**5**	**5**	**90**

Control $[Si^{4+}] = \frac{(150)}{20} =$ **7.5ppm**

Control $[Mg^{2+}] = \frac{(60)}{20} =$ **3ppm**

Control $[Si^{4+}] = \frac{(150*0.5)}{10} =$ **7.5ppm**

Control $[Mg^{2+}] = \frac{(60*0.5)}{10} =$ **3ppm**

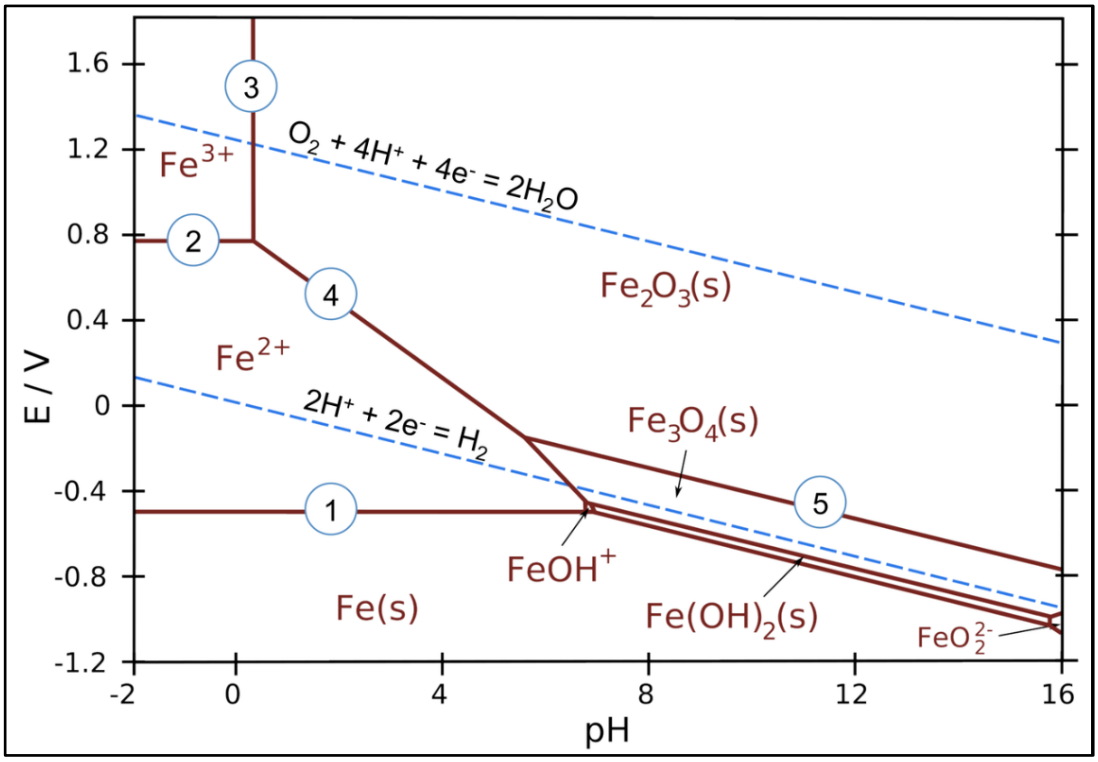

Figure A-1 Pourbaix diagram for 1mM Iron Solution

II. Inductively Coupled Plasma - Optical Emission Spectroscopy (ICP-OES)

In this study, ICP results relating to scale inhibitor analysis were are presented, where the detection limit is within the scope of the experiments. These experiments require analysis for magnesium, silicon and on occasion iron. The ICP-OES (Figure A-2) is less time consuming than the wet chemical assays the calibration range/methods used have been adapted over time.

The procedures followed for each of the elements is similar. However different concentrations of calibration standards are employed for the different elements. The measurement time for each element method is 2 seconds, mode 5 is used for single point analysis and primary/secondary slits of 18/81 respectively are used. The exception to this is the PPCA analysis, which uses the Gaussian mode of 2 and primary/secondary slits of 18/15 respectively. In between samples there is a rinse time of 60sec before it returns to analyze the samples. The sampling times allow for sample introduction; 3 minutes to analyze 1 element and 5-6 minutes to analyze 4 elements.

Figure A-2 ICP-OES Ultima 2 Machine

Experimental Procedure:

1. Clean and start up the ICP. Allow to heat up for 0.5-1 hour with distilled water flowing through the machine. The rinse solution between analyses is 5% Nitric acid and flows for 60sec before moving back to the next sample.

2. Prepare the element calibration standards within the same matrix (normally synthetic SW, FW or 1% NaCl solution) that the samples have been diluted in. In these experiments, the diluent used are 1% EDTA/NaOH and 0.1% EDTA/NaOH.

3. After the heat up period, select the method to be used to analyze the samples ensuring that the same method shows in the box at the top of the analysis sheet. This ensures that the correct elements are analyzed.

4. Set up an analysis run to auto-search, auto-attenuate and auto-search again on the highest calibration standard. The next highest standard can now be auto-searched. This process is continued until all of the element containing calibration standards (not standard LOW, which is matrix solution) have been auto-searched. Once the run begins check that the peaks observed are in the middle of the wavelength window and the top standard is the full height of the screen.

5. The machine is now ready to calibrate. Set–up a run to calibrate for the elements in the selected method/matrix.

6. After calibration has been achieved, i.e. a straight line through zero, with an R square number of approximately 1, the ICP is now ready to analyze samples.

7. The samples are placed in the auto-sampler racks. Calibration standards are placed in a rack at the end of the samples. When setting up the analysis run, begin with selecting each of the standards to be analyzed as a sample, and then analyze 10-12 samples before returning to the standards. Repeat these formations until all samples are analyzed, ending with a set of standards.

8. At the bottom of the sample run, add in a description of the run to help with later identification under the specific method. The analysis file is then saved onto the computer.

9. The calculated concentrations, with respect to the previous calibration, are then stored on the computer and printed out.

10. If the results for the calibration standards throughout the run have drifted from their intended concentrations, then the samples can be drift corrected.

Table A-16 ICP-OES wavelengths and calibration standards used for different elements

Element	Wavelength (nm)	Calibration (Standard)
Barium	233.527	0,10, 25, 50
Strontium	338.071	0,10, 25, 50
Calcium	317.933	0, 50, 200
Magnesium	279.806	0,25,100
Iron	259.940	0, 10, 40
Lithium	670.784	0,5,20
Aluminium	308.215	0, 5, 50, 250
Silicon	212.412 or 250.690	0, 5, 50, 250
Sodium	330.237 <100ppm 589.592 >100ppm	0, 10, 100, 1000
Cobalt	237.86	0, 2, 5
Chromium	205.55	0, 2, 5
Copper	324.754 or 224.700	0, 10, 100
Nickel	221.64	0, 2, 5
Zinc	213.856 or 334.502	0, 10, 100
Molybdenum	202.03	0, 2, 5
Germanium	265.118 or 209.426	0, 10, 100
Boron	249.67	0, 10, 100
Potassium	766.490	0, 20, 100, 1000
Phosphorus - phosphonate	177.440 (->50ppm) 214.914 (0, 50, 500, 2500)	0, 5, 50, 500, 2500
Phosphorus - PPCA	177.440 (->50ppm) 177.441 (0, 50, 500, 2500)	0, 5, 50, 500, 2500
Lead	220.353	0, 5, 10
Tin	189.989 0r 235.484	0, 10, 100
Tungsten	209.47	0, 2, 5
Sulphur	180.676	0, 5, 10 or 0, 10, 50, 250

Examples of Diluents: NaCl, DW, SW, FW, KCl/PVS, EDTA/KOH, DTPA/KOH, 5% Nitric acid and Acetic acid. In these experiments the diluents are 1% EDTA/NaOH and 0.1% EDTA/ NaOH

III. Environmental Scanning Electron Microscopy - Energy Dispersive X-Ray (ESEM-EDX)

For this study, a Philips XL30 Environmental Scanning Electron Microscope (ESEM), with an Oxford Instruments cryo-stage, and an EDAX energy dispersive x-ray detector (EDX) was used for the analysis. These can be used to image and/or analyze virtually any substance, including wet, oily and out gassing samples that cannot be examined by more conventional SEM's (http://www.pet.hw.ac.uk/cesem/intro.htm). This is presented in Figure A-3.

Figure A-3 ESEM - Philips XL30 at Heriot-Watt University (Source: FAST: GLP/RA)

An ESEM is specifically designed to be able to examine micro-structural and ultrastructural details of samples, within a SEM chamber, in their uncoated natural state. An ESEM is able to examine wet, oily and out-gassing samples, without any form of preparation, and is able to maintain specimens within their natural state for prolonged periods within the ESEM viewing chamber. The ESEM works at low vacuum (typically 2 - 6 Torr), and utilizes a chamber gas for imaging, charge suppression and sample humidity.

ESEM is specifically suited to dynamic experimentation of the micron scale and below. ESEM technology allows for dynamic experiments involving fluids, and the possibility of imaging samples undergoing compression and tension. ESEM can therefore be regarded as a micro dynamic experimentation chamber where materials can be examined at a range of pressures, temperatures, under a variety of gases/fluids.

In simpler terms, scanning electron microscopy occurs when an electron beam is scanned across the surface of a sample. As the electrons strike the sample, a variety of signals are generated and it is the detection of these signals that produces an image or the elemental composition of a sample. There are a number of detectors that can be used under a number of different conditions, such as low or high vacuum, cryo-SEM and wet ESEM work. These detectors themselves can be split into categories depending on how they detect the sample signals. For instance, there are secondary electron detectors, solid state backscattered detectors, the environmental secondary electron detector and gaseous secondary electron detectors.

In the XL30 ESEM, the two detectors for high vacuum mode are an Everhardt-Thornley secondary electron detector and a solid state backscattered detector. Both these detectors are permanently within the chamber whereas the various environmental detectors available, all clip into the detector socket at the back of the chamber and are inserted as and when required. A summary of detectors and their suitable detection conditions are presented in Table 22 (Philips XL30 ESEM Instruction manual).

The signals that provide the greatest amount of sample information in SEM are the secondary electrons, backscattered electrons and X-rays. The processes behind these techniques can be detailed as;

(a) Secondary electrons are emitted from the atoms occupying the top surface and are therefore able to produce a readily interpretable image of the surface,

(b) Backscattered electrons are primary beam electrons that are ‘reflected’ from atoms in the solid,

(c) X Spectrometry or EDX is the interaction of the primary beam with atoms in the sample that causes shell transitions, resulting in the emission of x-rays. The emitted Xrays have an energy, characteristic of the parent element. Detection and measurement of the energy permits elemental analysis (Energy Dispersive X-ray Spectroscopy or EDX).

EDX can provide rapid qualitative, or with adequate standards, quantitative analysis of elemental composition with a sampling depth of 1-2 microns. X-rays may also be used to form maps or line profiles, showing the elemental distribution in a sample surface.

Before using ESEM or EDX, always refer to the manufacturers instruction manual (Philips XL30 ESEM Instruction manual) and receive training before commencing work. However, a very general summary of the procedure is as follows;

a. Select the required detector.

b. Load samples into chamber.

c. Select mode – high, low, environmental and the corresponding conditions.

d. Ensure chamber is ready for use.

e. Focus the detector.

f. The SEM is now ready to image/analyse the samples.

g. When the process is finished, release the samples from the chamber.

Table A-17 ESEM- Summary of detectors and their detection conditions

Detector	Working Mode	Position
Everhardt-Thornley secondary electron	High vacuum	Permanently inside chamber
Backscattered detector	High vacuum	Permanently inside chamber, parked at back
Solid state backscattered detector	High or low vacuum (0.1 – 100Torr)	Stored at back of chamber in a sleeve. To use, remove sleeve and mount under the pole piece.
Environmental secondary electron detector	Environment 500micron detectors – P ≤ 10 Torr 300micron detectors for higher P	Primarily SE but incorporates a substantial BSE signal. Detector is cap shaped and fits over the wet mode insert/ bullet. Used in conjunction with a hook adaptor which plugs into the GSED (Gaseous SED)
Gaseous secdary electron detector	Environmental, P ≥ 6 Torr	Fits over end of wet mode bullet/ insert and clips into

	500microns wet specimens remain hydrated at P ≤ 10 Torr 1000micron – wider field of view but P ≤ 5 Torr	GSED connector at back of chamber
Large field gaseous secondary electron detector (LF-GSED)	Low vacuum (0.1-1.00 Torr) Can be used in a water vapour atmosphere or another gas such as Nitrogen	Contains a component of BSE. Used in conjunction with low vac/ high vac bullet/ insert and is plugged into the GSED connector socket at the back of ESEM chamber
Gaseous backscattered secondary electron detector (GBSED)	Full environmental, P ≤ 10 Torr for 500micron aperture.	3 modes – SE, SE&BSE and BSE. Changes made by using pull-down 'detectors' menu. The detector must be worked at a distance of 10mm due to its size.
Bullet	High or ≤ 1 Torr low vacuum	Screwed into pole piece. It changes pumping regime of lower part of column and forms an attachment point for the various environmental and BSE detectors.
ESEM bullet	Full wet ESEM work	Screwed into pole piece. It changes pump regime of lower part of column and forms an attachment point for the various environmental and BSE detectors.

IV. Fourier Transform Infrared (FTIR) iD5 ATR Thermo Scientific

FTIR stands for Fourier Transform InfraRed, the preferred method of infrared spectroscopy. In infrared spectroscopy, IR radiation is passed through a sample. Some of the infrared radiation is absorbed by the sample and some of it is passed through (transmitted). The resulting spectrum represents the molecular absorption and transmission, creating a molecular fingerprint of the sample. Like a fingerprint no two unique molecular structures produce the same infrared spectrum. This makes infrared spectroscopy useful for several types of analysis.

An infrared spectrum represents a fingerprint of a sample with absorption peaks which correspond to the frequencies of vibrations between the bonds of the atoms making up the material. Because each different material is a unique combination of atoms, no two compounds produce the exact same infrared spectrum. Therefore, infrared spectroscopy can result in a positive **identification** (qualitative analysis) of every different kind of material. In addition, the size of the peaks in the spectrum is a direct indication of the **amount** of material present. With modern software algorithms, infrared is an excellent tool for quantitative analysis.

The precipitate from the silicate scaling static bottle test was tested using ESEM/EDX. SEM provides detailed high-resolution images of the sample by rastering a focused electron beam across the surface and detecting secondary or backscattered electron signal. An Energy Dispersive X-Ray Analyser (EDX or EDS) is also used to provide elemental identification and quantitative compositional information. This means the SEM/EDX instrument is a powerful and flexible tool for solving a wide range of product and processing problems for a diverse range of metals and materials. However, EDX could only provide the relative amount of elements presents in the precipitate and does not provide the structural information these elemental are in. While FTIR can provide the information of the functional groups present in the compound analysed which could be a useful indicator of compound present when used together with the EDX analysis.

It is a non-destructive technique and requires very minimal of sample preparation. It also requires a very small amount of sample to be able to be perform the FTIR technique.

Procedures:

To run a background (it must be done once a day by the first user):

1. Double-click the OMNIC icon. In "Smart Accecory Change" window: Choose Organic Teaching Lab (iD5_ATR_Diamond.exp). Click "OK". See Figure A-4.

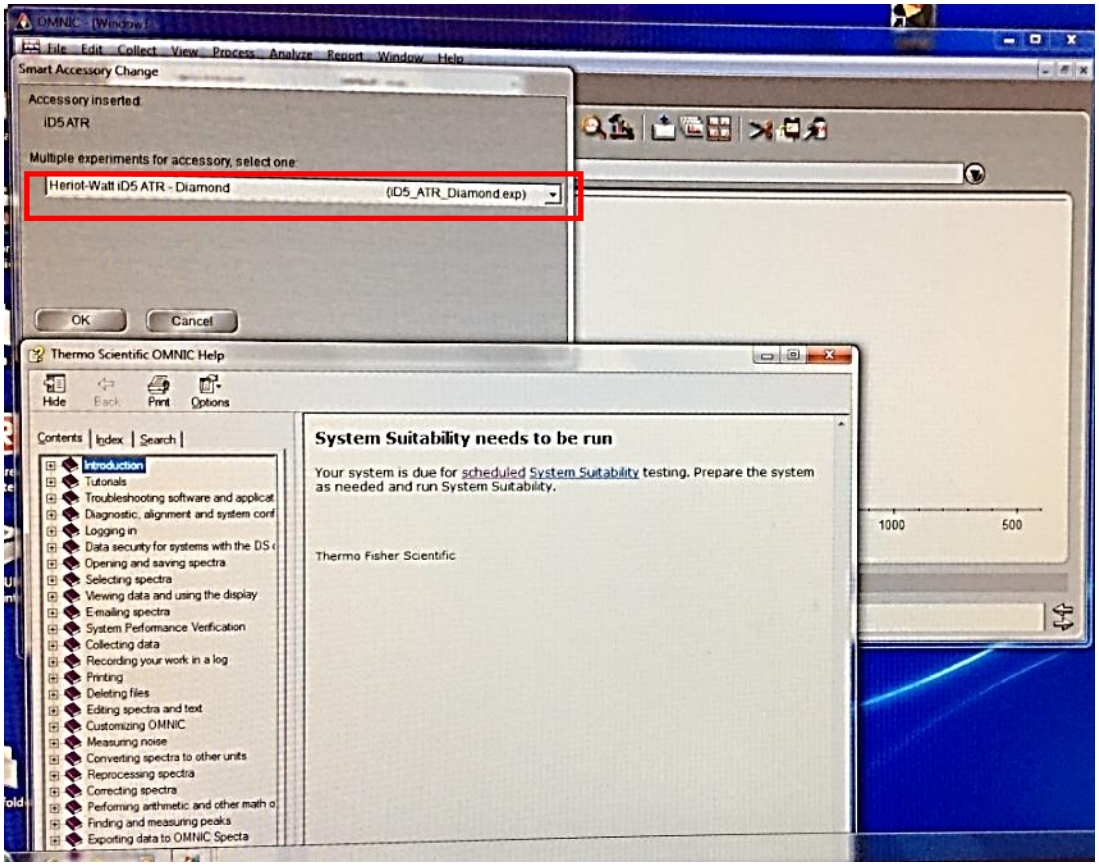

Figure A-4

2. In the "Collect" taskbar, select "Collect Background" icon. See Figure A-5.
   Make sure the diamond crystal is clear and unclamped. The crystal can be cleaned using the ethanol solution by spraying a piece of tissue before wiping the crystal. See Figure A-6.

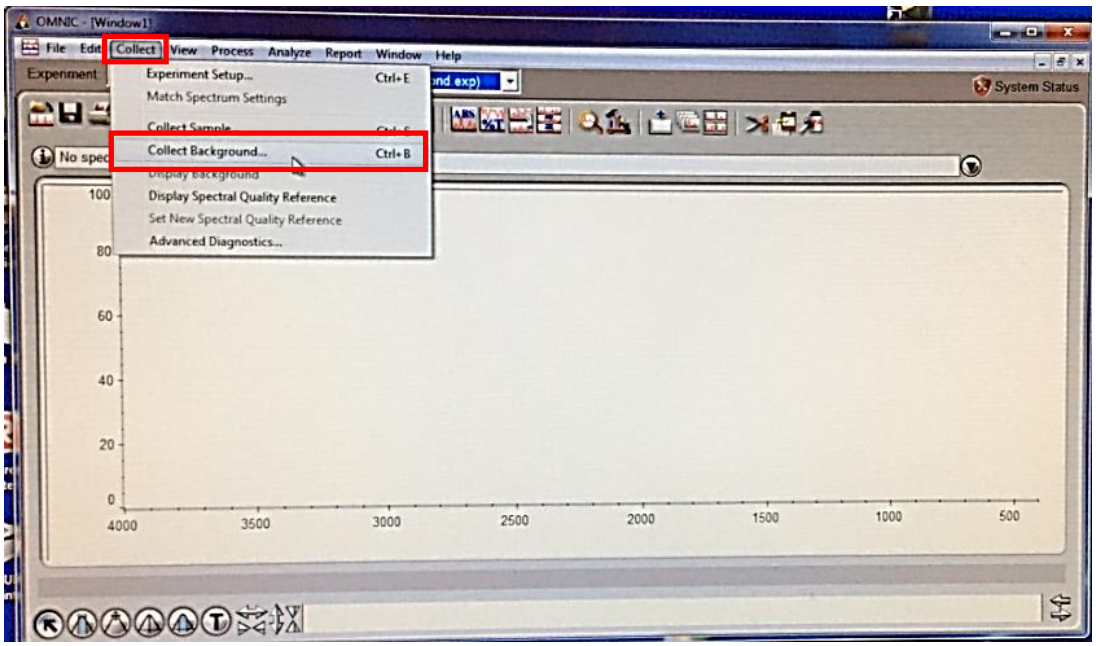

Figure A-5

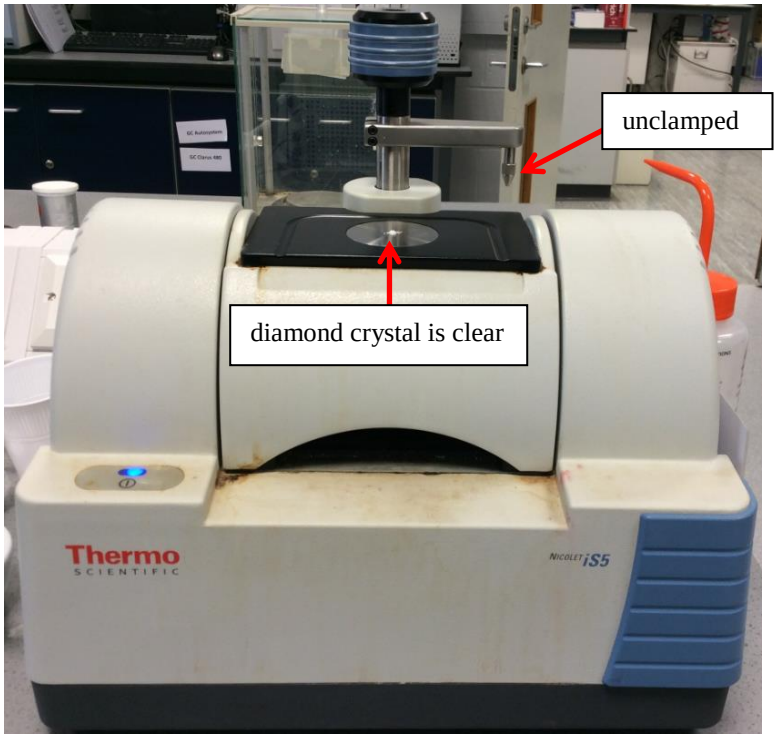

Figure A-6

3. Click “OK” confirmation window (progress of 16 scans is shown in bottom left corner). See Figure A-7 and Figure A-8.

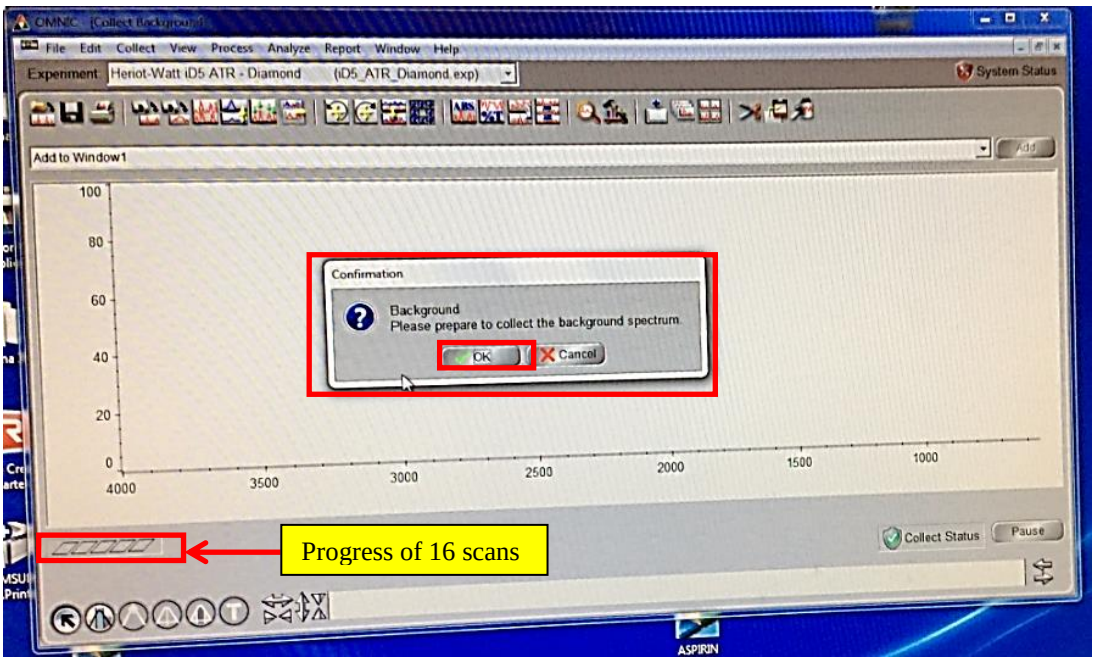

Figure A-7

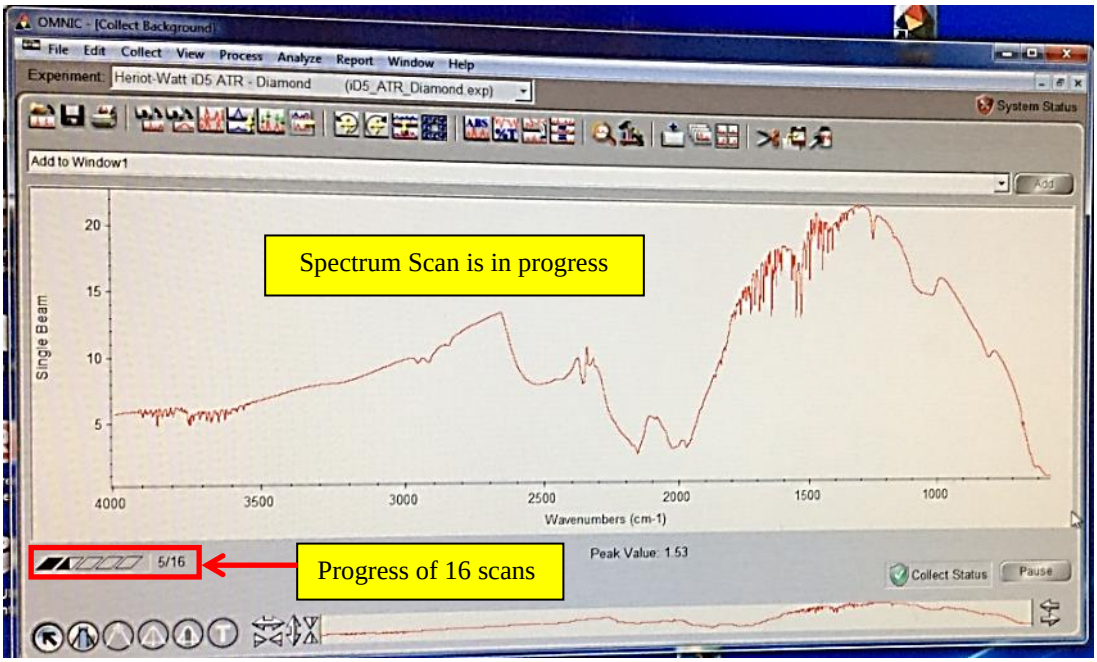

Figure A-8

4. Click “Yes” to “Add to Window…” in Confirmation window. See Figure A-9.

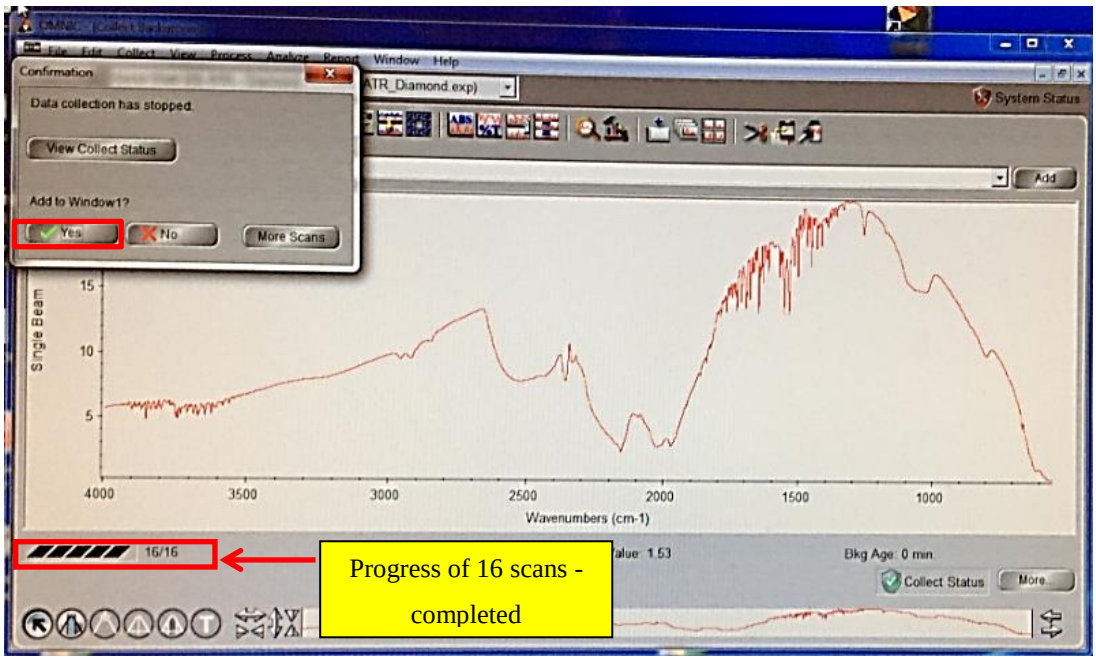

Figure A-9

5. In the "Edit" taskbar, select "Clear" icon in taskbar to remove background spectrum (Note: The background adjustment will stay active though invisible). See Figure A-10 and Figure A-11.

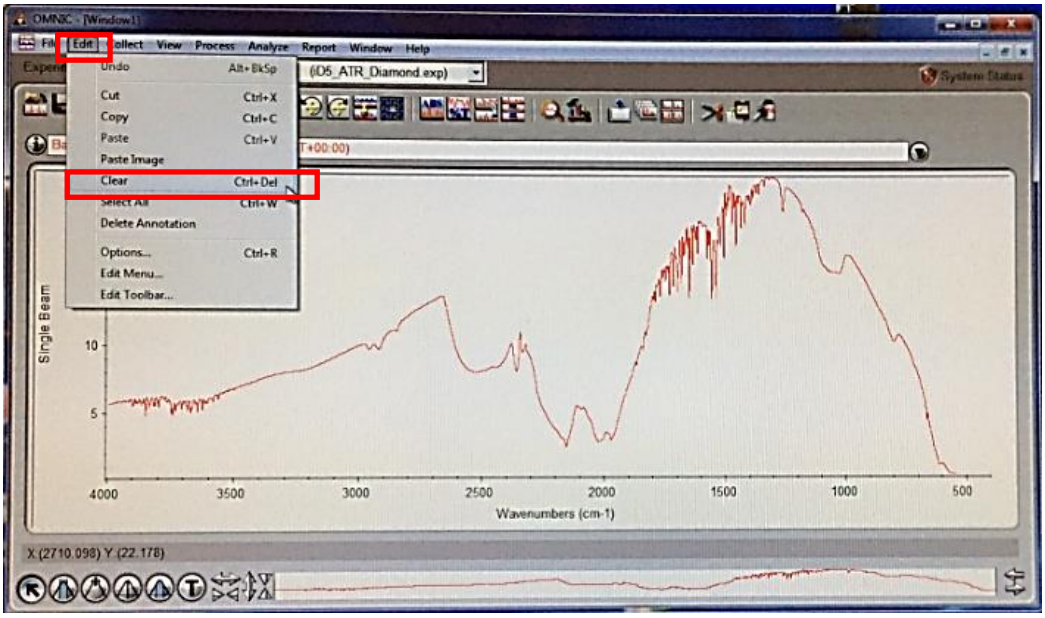

Figure A-10

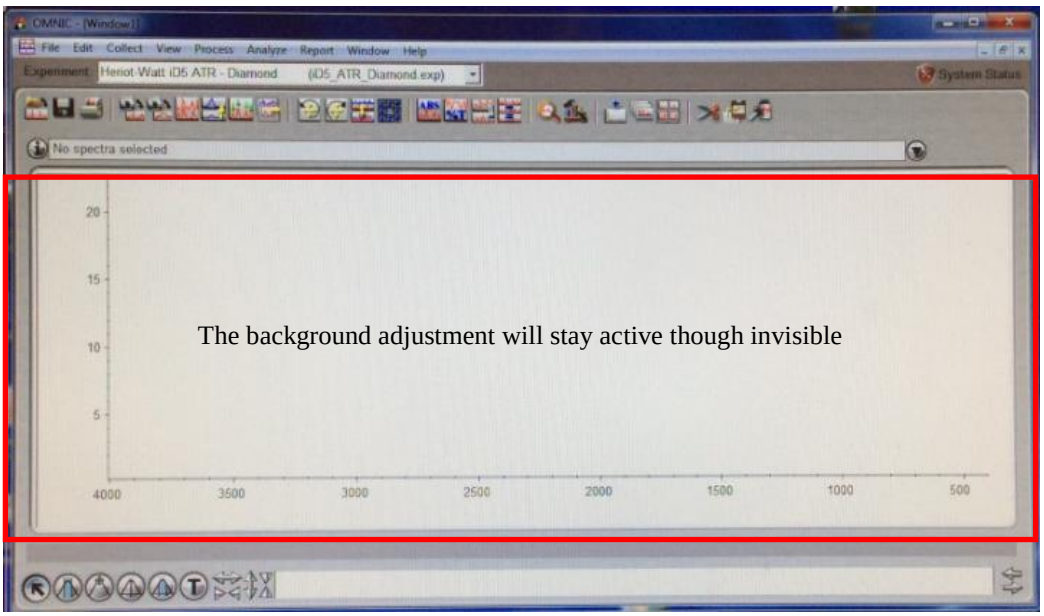

Figure A-11

To run sample:

6. In the “Collect” taskbar, select “Collect Sample” icon. See Figure A-12.

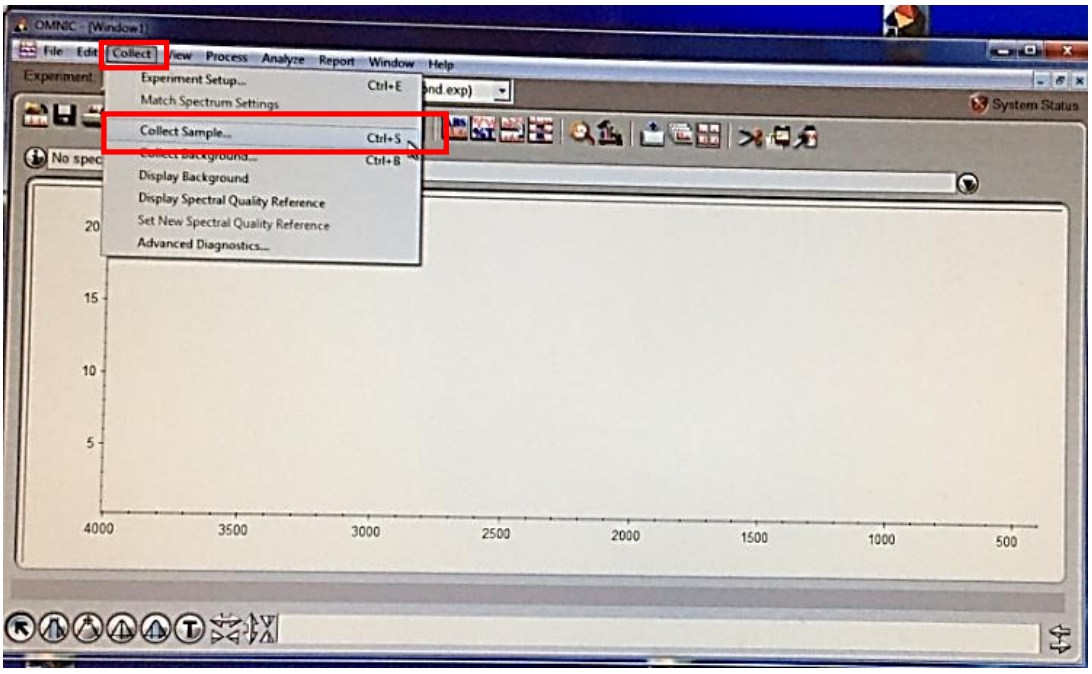

Figure A-12

7. In “Collect Sample” window, enter spectrum title or leave as it is. Click “OK”. See Figure A-13.

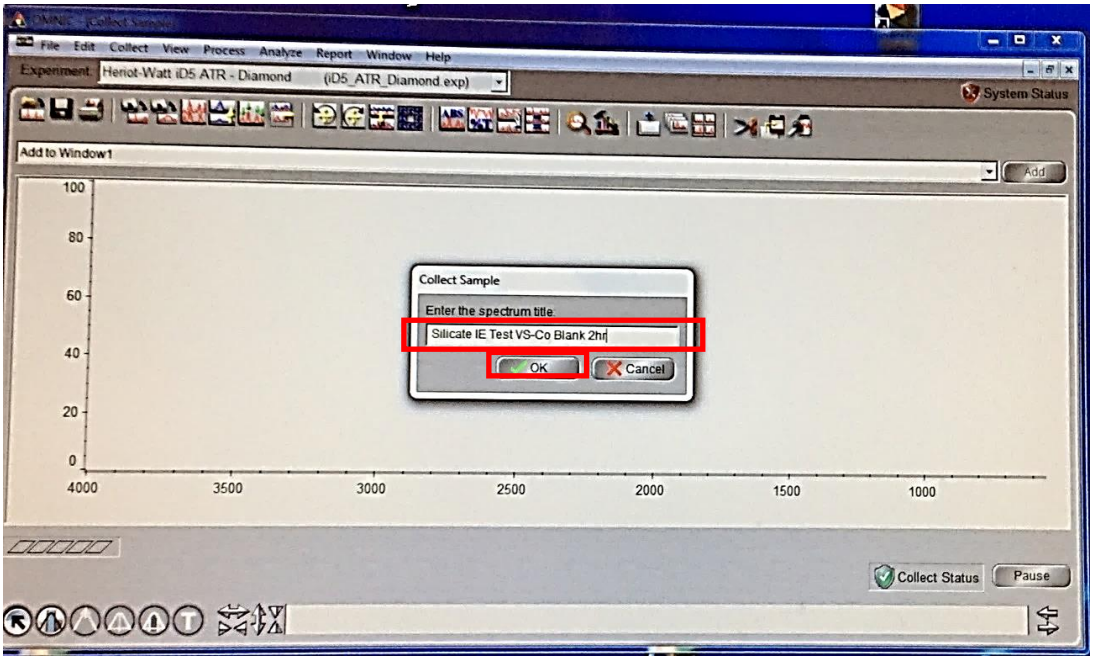

Figure A-13

<u>Prepare sample on crystal:</u>

8. If “solid” samples, make sure it is in small and tiny powder form. The big chunks of solid can be crushed using a mortar and pestel. See Figure A-14.
   Cover the crystal with a small amount of sample by using a spatula. Clamp until you hear a click sound. See Figure A-15.

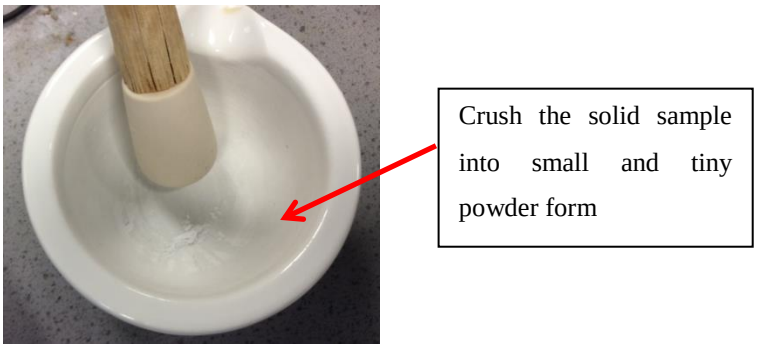

Figure A-14

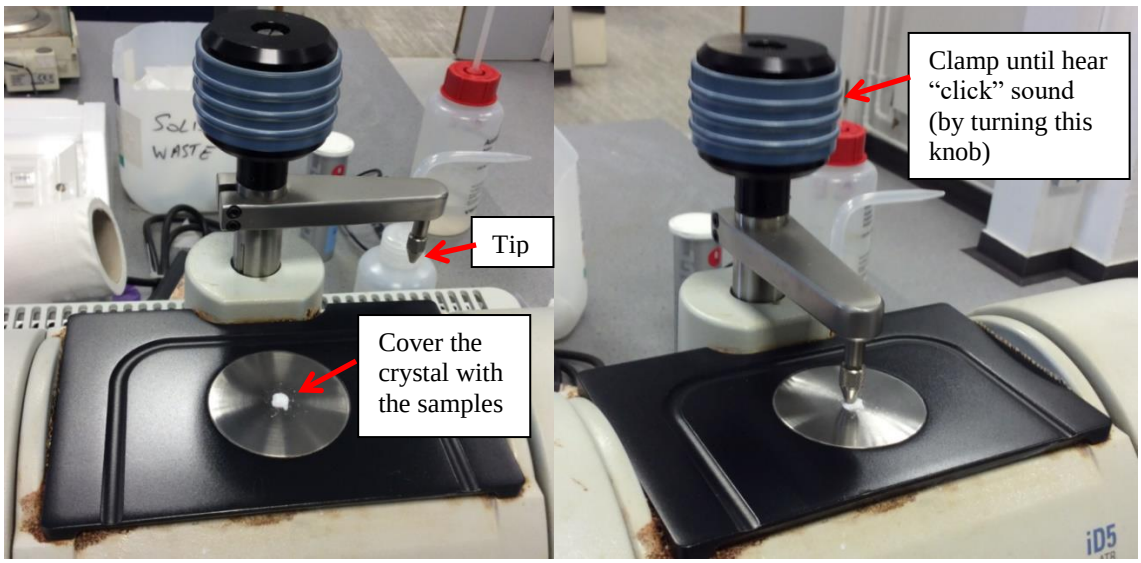

Figure A-15

9. If "liquid" sample, cover the crystal with the liquid by using pipette. But do not clamp. Note: If the liquid is very volatile, make sure it covers the crystal throughout the 16 scans.
10. Click "OK" confirmation window (progress of 16 scans is shown in bottom left corner). See Figure A-16 and Figure A-17.

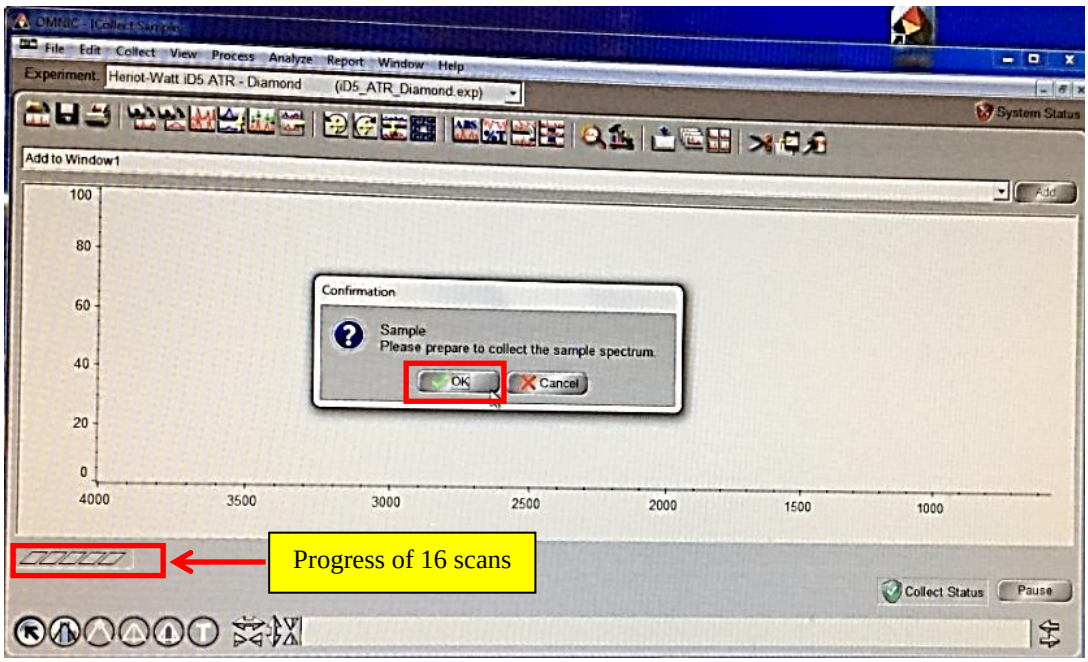

Figure A-16

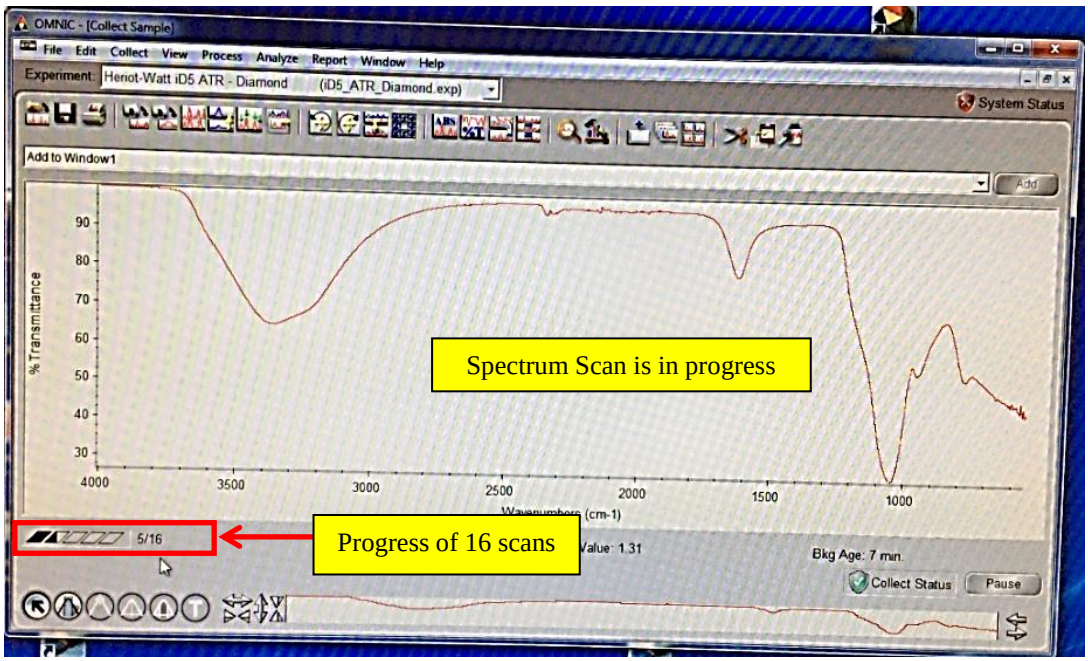

Figure A-17

11. Click “Yes” to “Add to Window…” in Confirmation window. See Figure A-18.

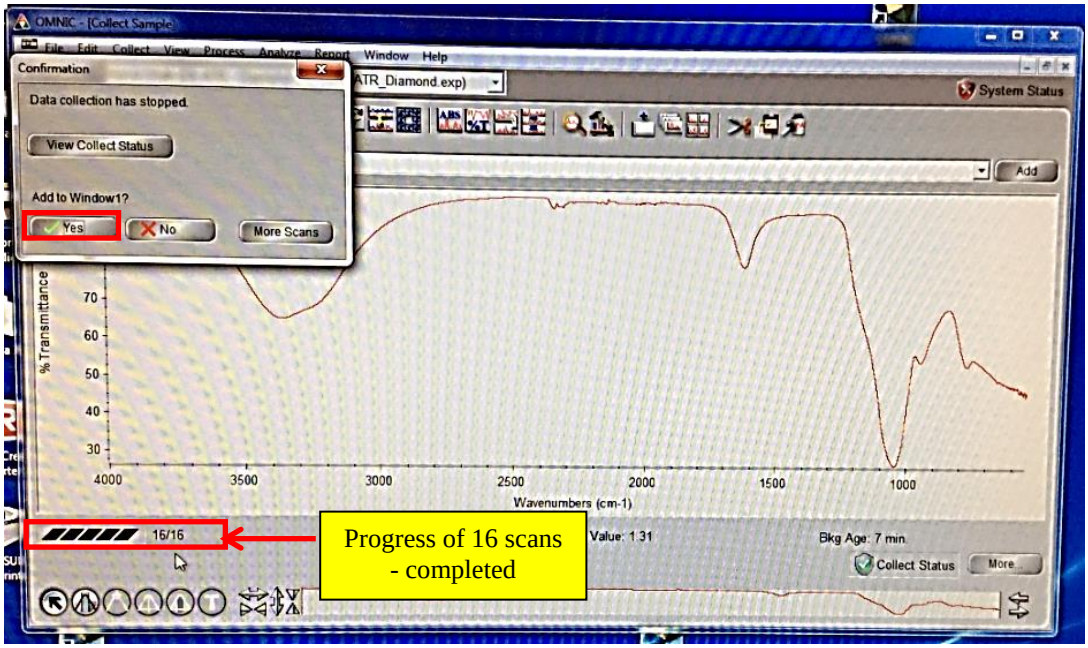

Figure A-18

12. In the “Analyze” taskbar, click “Find Peaks” icon for peak annotation; click anywhere above the vertical cursor to move up the annotation threshold. See Figure A-19, Figure A-20 and Figure A-21.

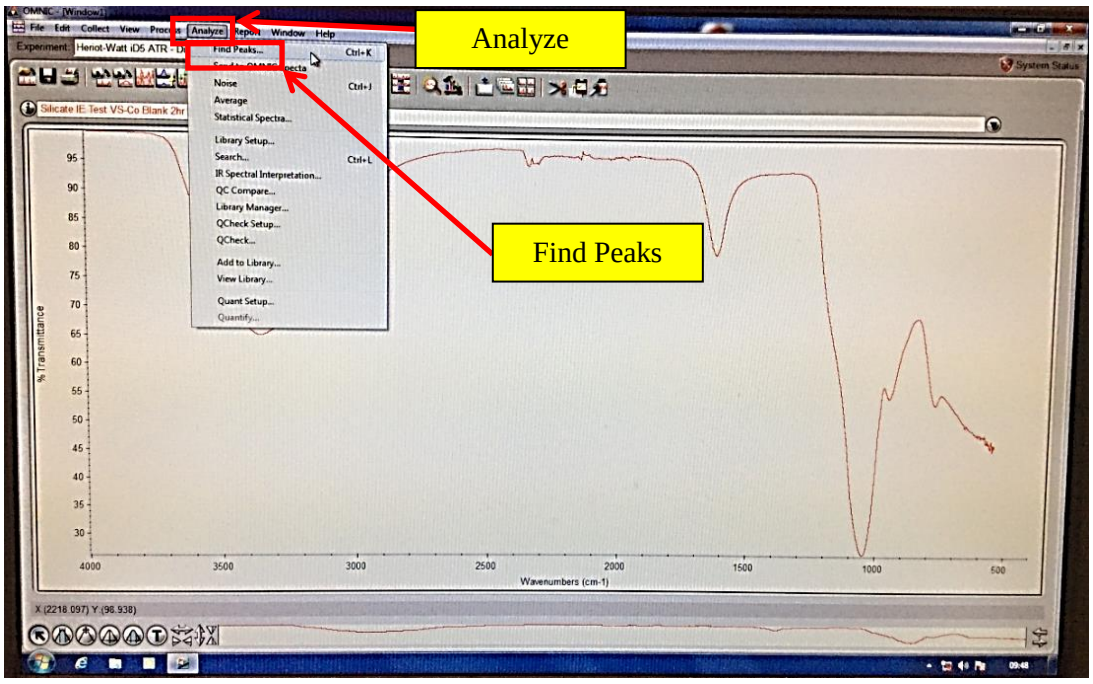

Figure A-19

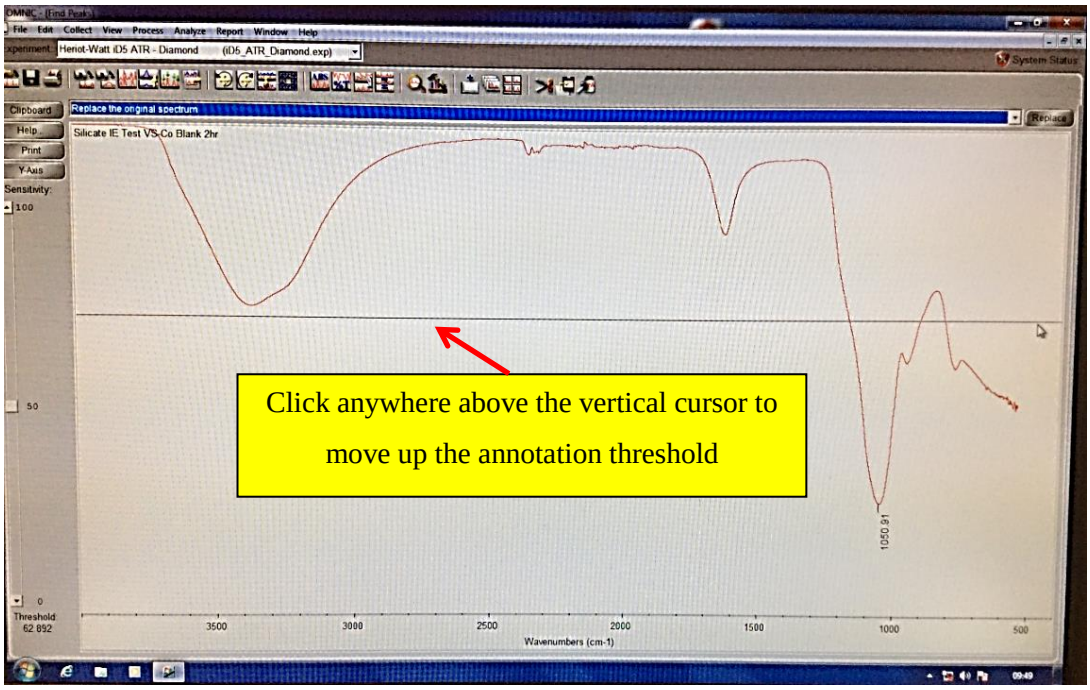

Figure A-20

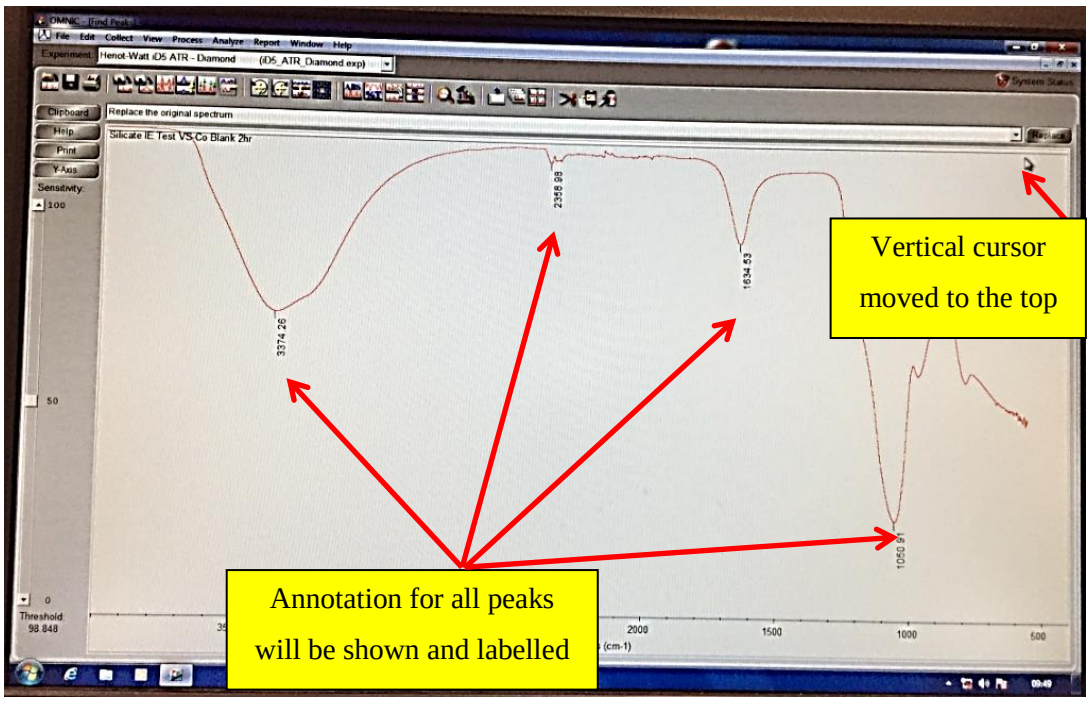

Figure A-21

13. Click “Replace” or “Add” button in top right corner of the screen. See Figure A-22.

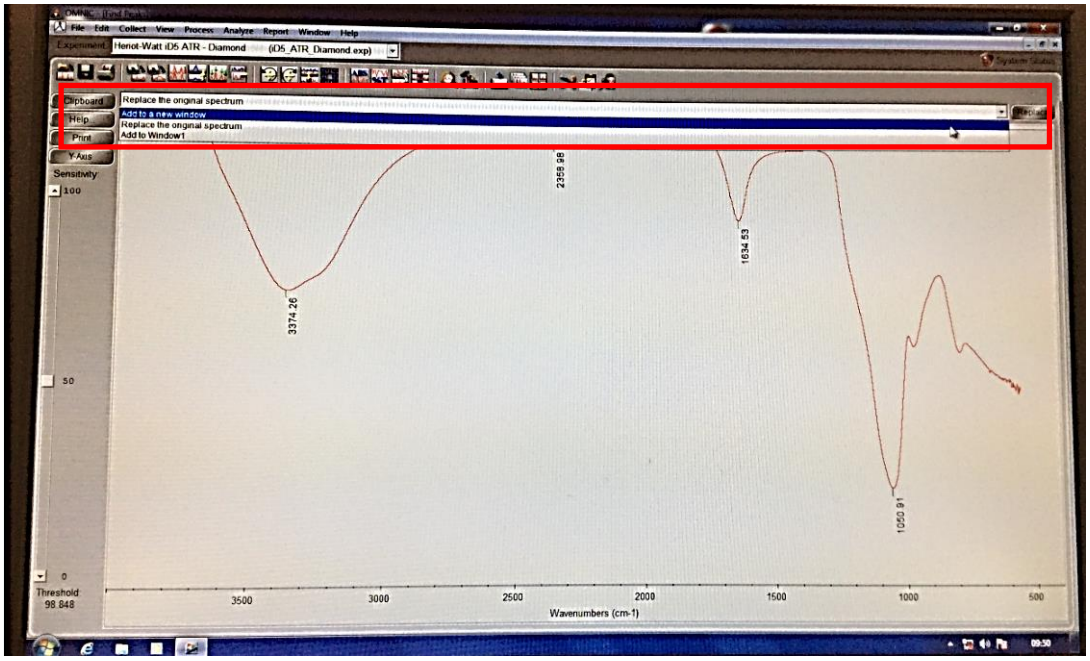

Figure A-22

14. Click “Full Scale” icon (under the “View” tab) to move image up, placing all annotation on screen, then PRINTS.
15. Once finished, clean the crystal and the tip using ethanol solution. It can be done by spraying a small amount of ethanol on a clean tissue before cleaning the crystal and the tip.
16. Close the OMNIC application but leave the computer on for the next user.

V. D8 ADVANCE HIGH RES PXRD BRUKER D8 ADVANCE GX000208

Bruker D8 Advance

The instrument is a Bruker D8 Advance powder diffractometer, operating with Ge-monochromated Cu Kα1 radiation (wavelength = 1.5406 Å) and a LynxEye linear detector in reflectance mode. Data were collected over the angular range 5-85 degrees in two-theta over one hour per sample.

The Bruker D8 Advance has a theta:theta geometry (often called Bragg-Brentano or focusing geometry) with a copper sealed tube x-ray source producing Cu kα radiation (technically kα1 and kα2 with kβ being removed by the primary optic) at a wavelength of 1.5406 Å from a generator operating at 40 keV and 40 mA. A parallel beam of monochromatic x-ray radiation is produced by the use of a Göbel mirror optic (primary optic). The diffracted x-rays are recorded on a scintillation counter detector located behind a set of long Soller slits/parallel foils. The sample remains flat throughout the measurement but can be rotated to allow for better sampling and removal of preferred orientation effects.

Lynxeye Detector

The LynxEye is a linear position sensitive detector (PSD). It can be used in two different modes:

- The 0° mount mode is used for fast reciprocal space mapping. When positioned in the 0° mount mode, the length of the LynxEye runs along the diffraction circle.
- The detector can observe 2.1° 2Theta simultaneously. This mode allows the LynxEye to collect a 2Theta (detector) scan without moving. This allows the LynxEye to quickly collect reciprocal space maps, since it is measuring a large portion of reciprocal space simultaneously. However, in this mode the LynxEye has limited resolution and limited dynamic range.

Figure A-23 D8 Advance high res PXRD Bruker D8 Advance (Bruker, 2016)

Sample submission

1. The samples need to be supplied as a finely ground powder with similar particle sizes, ideally sieved. This means you get better quality data
2. The amount should be a large spatula size to fill the sample holder of 25mm across and about 3mm deep.
3. The samples should be in screw topped vials or in sealed plastic bags and labelled clearly with the user name and sample name which will not rub off
4. The samples and sample forms should be submitted together and placed in the plastic pocket attached to the door of WPG05. This is the ground floor of the Perkin Building, Heriot-Watt University, Edinburgh, UK.
5. Dr Georgina Rosair supply background subtracted plots and visually match patterns to the data, for this she need to know elemental composition and likely components of the sample

Data collection

The sample is compacted into a sample holder, so it is flat and level with the top of the sample holder to minimise errors in peak positions. Data is collected using the Bruker XRD Commander program. Patterns are background subtracted an smoothed using the Bruker EVA software and qualitative pattern matching using the Powder Diffraction file PDF2 from 2007 was used to identify phases.

Further information

Additionally, this machine has robot for sample mounting and dismounting, so our samples are added and removed from the racks

Goniometer Accuracy

You commonly find instrument quality reduced to some goniometer accuracy, underpinned by direct beam measurements or some reproducibility measurements in a limited angular range. Albeit a prerequisite, this is not sufficient to ensure that the instrument is working properly over the entire angular range. That is why Bruker AXS additionally guarantee an unparalleled instrument alignment equal or better than ±0.01° 2Theta over the entire angular range, verified against the most recent NIST standard reference material SRM1976 (Bruker, 2016).

Accurate, precise and verifiable instrument alignment is a prerequisite for accurate and reliable data and results. Only verification against an internationally accepted standard reference material ensures that the entire system is working properly.

LIST OF REFERENCES

Ahmed A. F., and Elraies K. A. (2014) 'The effect of water salinity and reservoir temperature on silica dissolution during ASP flood: Static Model', *Proceedings of the International Conference on Integrated Petroleum Engineering and Geo sciences (ICIPEG),* Kuala Lumpur, Malaysia, 3-5 June. doi: 10.1007/978-981-287-368-2_9.

Alexander, G.B., Heston, W.M., and ller, R.K. (1954) 'The solubility and amorphous silica in water', *The Journal of Physical Chemistry,* 58(6), pp. 453-455. doi: 10.1021/j150516a002.

Alforjani, S. (2005) 'Effect of ferrous ions on the performance of calcium sulfate inhibitors', *Proceedings of the Ninth International Water Technology Conference,* Sharm El-Sheikh, Egypt, 17-20 March. Available at: http://iwtc.info/2005_pdf/12-7.pdf (Accessed: 11 November 2015).

Amjad, Z. (2014) 'Impact of iron oxide (rust) on the performance of calcium phosphate scale inhibitors for industrial water systems', *International Journal of Corrosion and Scale Inhibition,* 3(3**)**, pp. 177–189. doi: 10.17675/2305-6894-2014-3-3-177-189.

Amjad, Z. (2016) 'Silica scale control by non-ionic polymers: The influence of water system impurities', *International Journal of Corrosion and Scale Inhibition*, 5(2), pp. 100–111. doi: 10.17675/2305-6894-2016-5-2-1.

Amjad, Z. and Yorke, M.A. (1985) *Carboxylic functional polyampholytes as silica polymerization retardants and dispersants.* U.S. Patent No. US4510059A. Available at: https://www.google.ch/patents/US4510059?dq=U.+S.+Patent+No.+4,510,059+(1985), &hl=de&sa=X&ved=0ahUKEwir2KXWga7TAhXLJFAKHa05A8IQ6AEIJDAA (Accessed: 24 August 2014).

Amjad, Z., and Zuhl, R. W. (2008b) 'An evaluation of silica scale control additives for industrial water systems', *Proceedings of the NACE International CORROSION 2008,* New Orleans, Louisiana, 16-20 March. Available at: https://www.onepetro.org/download/conference-paper/NACE-08368?id=conference-paper%2FNACE-08368 (Accessed: 20 March 2015).

Amjad Z., Zibrida, J. F., and Zuhl R. W. (1997) 'A new antifoulant for controlling silica fouling in reverse osmosis systems', *Proceedings of the International Desalination Association World Congress on Desalination and Water Reuse,* Madrid, Spain, 6-9 October. Available at: https://webcache.googleusercontent.com/search?q=cache:-eor0q3EfnwJ:https://www.lubrizol.com/-/media/Lubrizol/Water-Treatment/Documents/TEC-RO/IDA-97-Silica-Antifoulant.pdf%3Fla%3Den+&cd=1&hl=en&ct=clnk&gl=uk (Accessed: 20 March 2015).

Amjad, Z. and Zuhl, R.W. (2008a) 'Laboratory evaluation of process variables impacting the performance of silica control agents in industrial water treatment programs', *Proceeding of the Association of Water Technologies Annual Convention,* Texas, USA, 5-8 November. AWT-08 (Nov-08). Available at: https://webcache.googleusercontent.com/search?q=cache:-9NJ6Hfu_ckJ:https://www.lubrizol.com/-/media/Lubrizol/Water-Treatment/Documents/Carbosperse/LaboratoryEvaluationofProcessVariablesImpactingthePerformanceofSilicaControlAgentsinIndustrialWaterT.pdf+&cd=1&hl=en&ct=clnk&gl=uk (Accessed: 24 August 2014).

Amjad Z., and Zuhl R.W. (2009) 'Silica control in industrial water systems with a new polymeric dispersant', *Association of Water Technologies, Inc.: Annual Convention and Exposition*. The Westin Diplomat, Hollywood, 26-29 August. Ohio: Lubrizol Advanced Materials, Inc., pp. 1-25.

Amjad, Z. and Zuhl, R.W. (2010) 'The role of water chemistry on preventing silica fouling in industrial water systems', *Proceeding of the NACE International Corrosion 2010 Conference & Expo,* San Antonio, Texas, USA, 14-18 March. Available at: https://www.academia.edu/27593509/THE_ROLE_OF_WATER_CHEMISTRY_ON_PREVENTING_SILICA_FOULING_IN_INDUSTRIAL_WATER_SYSTEMS

Amjad Z., and Zuhl R.W. (2011) 'Factors impacting silica-silicate control agent performance in industrial water systems', *Proceedings of the International Water Conference,* Orlando, Flourida, 13-17 November. Available at: https://webcache.googleusercontent.com/search?q=cache:XOwXCZAZaugJ:https://www.lubrizol.com/-/media/Lubrizol/Water-Treatment/Documents/Carbosperse/IWC-1161Final16Oct24.pdf+&cd=1&hl=en&ct=clnk&gl=uk (Accessed: 07 April 2015).

Andhika, M., Castañeda, M. H., and Regenspurg, S. (2015) 'Characterization of Silica Precipitation at Geothermal Conditions' *Proceedings of the World Geothermal Congress 2015,* Melbourne, Australia, 19-25 April. Available at: https://pangea.stanford.edu/ERE/db/WGC/papers/WGC/2015/27026.pdf

Andhika, M. and Regenspurg, S. (2013) 'Characterization of Silica Precipitation Kinetics under High Temperature Geothermal Field Conditions Using Ultrasonic Techniques', *Proceedings of the NACE International CORROSION 2013,* Orlando, Florida, USA, 17-21 March. Available at: https://www.onepetro.org/download/conference-paper/NACE-2013-2627?id=conference-paper%2FNACE-2013-2627 (Accessed: 20 March 2015).

Arensdorf, J. J., Hoster, D., McDougall, D. B., and Yuan, M. (2010) 'Static and dynamic testing of silicate scale inhibitors', *Proceedings of the CPS/SPE international oil & gas conference and exhibition,* Beijing, China, 8-10 June. doi:10.2118/132212-MS.

Arensdorf, J.J., Kerr, S., Miner, K. and Ellis-Toddington, T.T. (2011) 'Mitigating silicate scale in production wells in an oilfield in Alberta', *Proceeding of the SPE International symposium on oilfield chemistry,* The Woodlands, Texas, USA, 11-13 April. doi: http://dx.doi.org/10.2118/141422-MS.

Arnórsson, S. (2004). Environmental impact of geothermal energy utilization. In: Energy, Waste and the Environment (eds. R. Giore and P Stille). Publication of the Geological Society of London (In print).

Basbar, A.E.A, Elraies, K.A., and Osgouei, R.E. (2013) 'Formation of silicate scale inhibition during alkaline flooding: static model', *Proceedings of the North Africa Technical Conference and Exhibition,* Cairo, Egypt, 15-17 April. doi: https://doi.org/10.2118/164669-MS.

Baumann, H. (1959) 'Polymerization und depolymerization der kieselsäure unter verschiedenen bedingungen', *Kolloid Zeischrift,* 162, pp. 28-35.

Bishop, A. D., and Baer, J. L. (1972) 'The thermodynamics and kinetics of the polymerisation of silicic acids in dilute aqueous solution', *Thermochima Acta,* 3(5), pp. 399-409.

Björke, J. K., Mountain, B.W., and Seward, T. M. (2012) 'The solubility of amorphous aluminous silica: implications for scaling in geothermal power stations', *Proceedings of the New Zealand Geothermal Workshop 2012.* Auckland, New Zealand, 19 - 21 November. Available at: https://www.geothermal-energy.org/pdf/IGAstandard/NZGW/2012/46654final00087.pdf (Accessed: 20 March 2015).

Bolfan – Casanova, N., Keppler, H., and Rubie, D.C. (1998) *Distribution of water between nominally anhydrous minerals in the system $MgSiO_3$ - H_2O.* Available at: http://www.bgi.uni-bayreuth.de/index.php?page=5&lng=en&view=1&year=1998&content=56 (Accessed: 3 January 2017).

Bolfan – Casanova, N., Keppler, H., and Rubie, D.C. (2000) 'Water partitioning between nominally anhydrous minerals in the MgO-SiO_2-H2O system up to 24 GPa: implications for the distribution of water in the Earth's mantle', *Earth and Planetary Science Letters*, 182, pp. 209-221.

Boo, B.H. (2011) 'Infrared and Raman spectroscopic studies of Tris(trimethylsilyl)silane derivatives of $(CH_3)_3Si)_3Si$-X [X = H, Cl, OH, CH_3, OCH_3, $Si(CH_3)_3$]: vibrational assignments by Hartree-Fock and density-functional theory calculations', *Journal of the Korean Physical Society*, 59(5), pp. 3192-3200.

Brown K. Mineral scaling in geothermal power production. United Nations University, Reykjavic, Iceland; 2013. Geothermal Training Programme Reports 2013 no. 39.

Brown, K. (2011) 'Thermodynamics and kinetics of silica scaling', *Proceedings of the International Workshop on Mineral Scaling 2011*, Manila, Philippines, 25-27 May. Available at: https://www.geothermal-energy.org/pdf/IGAstandard/WPRB/2011/01_Brown.pdf (Accessed: 20 March 2015).

Cenovus Energy Inc. (2009) *IETP project 03-053 Suffield conventional heavy oil chemical flood annual report*. Available at: http://www.energy.alberta.ca/xdata/IETP/IETP%202009/03-053%20Suffield%20Conventional%20Heavy%20Oil%20Chemical%20Flood/03-053_Annual%20Report%202009.pdf (Accessed: 9 February 2016).

Brown, P. (2000) *Doc Brown's Chemistry.* Available at: http://www.docbrown.info/page07/transition06Fe.htm (Accessed: 01 March 2017).

Chan S.H. (1989) 'A review on solubility and polymerization of silica', *Geothermics*, 18(1/2), pp. 49-56.

Chan, S.H., Neusen, K.F. and Chang, C.T. (1987b), 'The solubility and polymerization on amorphous silica in geothermal energy applications', *Proceedings of the ASME-JSME Thermal Engineering Joint Conference*, Honolulu, Hawaii, March 22-27, pp. 103-108.

Chan, S.H., Zhou, D.Z. and Neusen, K.F. (1987a), 'A semi-analytical model of silica fouling. Heat Transfer in Geophysical and Geothermal Systems', *Proceedings of the 24th National Heat Transfer Conference*, Pittsburgh, Pennsylvania, USA, pp. 45-51.

Charest, M. Alkaline-Surfactant-Polymer (ASP) flooding in Alberta: Small amounts of the right chemicals can make a big difference. Canadian Discovery Ltd. Canada; 2013. Canadian Discovery Digest no. 1.

Chen, C-T.A. and Marshall, W.L. (1982) 'Amorphous silica solubilities IV. Behavior in pure water and aqueous sodium chloride, sodium sulfate, magnesium chloride, and magnesium sulfate solutions up to 350°C', *Geochimica et Cosmochimica Acta*, 46, pp. 279-287.

Cheng, J., Zhou, W., Wang, Q., Cao, G., Bai, W., Zhou, C., and Luo, M. (2014) 'Technical Breakthrough in Production Engineering Ensures Economic Development of ASP Flooding in Daqing Oilfield', *Proceedings of the SPE Asia Pacific Oil & Gas Conference and Exhibition,* Adelaide, Australia, 14-16 October. doi: 10.2118/171506-MS.

Chernev, I.I., Okrugin, V.M., Okhapkin, N.S., Andreeva, E.D., Shadrin, A.A. and Yablokova, D.A. 'Technogenic precipitation in the structures of Mutnovsky Geothermal Power Complex (South Kamchatka)', *Proceedings of the* World Geothermal Congress 2015, Melbourne, Australia, 19-25 April. Available at: https://pangea.stanford.edu/ERE/db/WGC/papers/WGC/2015/27043.pdf (Accessed: 20 March 2015).

Chieng, C., and Nancollas, G.H. (1982) 'The crystallization of magnesium hydroxide, constant composition study', *Desalination,* 42(2), pp. 209-219.

Darton, E.G. (1999) ‘RO plant experiences with high silica waters in the Canary Islands’, *Desalination,* 124(1-3), pp. 33-41. doi: https://doi.org/10.1016/S0011-9164(99)00086-7.

Day, K.L. (1981) ‘Infrared extinction of amorphous iron silica’, *The astrophysical journal,* 246, pp. 110-112 1981.

Demadis K. D. (2003) ‘Water Treatment’s ‘Gordian Knot’’, *Chemical Processing,* 66(5), pp. 29-34. Available at: https://www.researchgate.net/publication/288317715_Water_treatment%27s_%27Gordian_Knot%27 (Accessed: 20 March 2016).

Demadis K.D. (2010) ‘Recent Development in Controlling Silica and Magnesium Silicate Foulants in Industrial Water Systems’, in Amjad, Z. (ed.) *The Science and Technology of Industrial Water Treatment.* USA: Taylor and Francis Group, LLC, pp. 179-203.

Demadis, K.D., Mavredaki, E., Stathoulopoulou, E., Neofotistou, E., and Mantzaridis, C. (2007) ‘Industrial water systems: problems, challenges and solutions for the process industries’, *Desalination,* 213(1-3), pp. 38–46.

Demadis, K.D., Neofotistou, E. (2004) ‘Inhibition and Growth Control of Colloidal Silica: Designed Chemical Approaches’, *Materials performance,* 43(4), pp. 38-42.

Dhaouadi, H., Chaabane, H., and Touati, F. (2011) ‘Mg(OH)2 nanorods synthesized by a facile hydrothermal method in the presence of CTAB’, *Nano-Micro Letters,* 3(3), pp. 153-159.

Dowas, W.F., Rimstidt, J.D., and Barnes, H.L. (1976) ‘Kinetics of silica scaling’, *Conference on Scale Management in Geothermal Energy Development.* San Diego, CA, 2-4 August. United States: Pennsylvania State University, University Park, PA, pp. 9-17.

Dublin, L. (1986) *Silica inhibition: prevention of silica deposition by boric acid/orthorborate ion.* U.S. Patent No. US4584104A. Available at: http://www.google.com/patents/US4584104 (Accessed: 24 August 2014).

Eisenberg, D. & Kauzman, W. (1969). The Structure and Properties of Water, Oxford University Press, Oxford

Ellis A.J. and Mahon W.A.J. (1977) *Chemistry and Geothermal Systems*. New York: Academic Press.

Euvrard M., Hadi L., and Foissy A. (2007) ‘Influence of PPCA (phosphinopolycarboxylic acid) and DETPMP (diethylenetriaminepentamethylenephosphonic acid) on silica fouling’, *Desalination*, 205 (1-3), pp. 114–123.

Fan, C., Shi, W., Zhang, P., Lu, H., Zhang, N., Work, S., Al-Saiari, H. A., Kan, A. T. and Tomson, M. B. (2011) ‘Ultra-HTHP Scale Control for Deepwater Oil and Gas Production’, *Proceeding of the SPE International Symposium on Oilfield Chemistry*, The Woodlands, Texas, USA, 11-13 April. doi: 10.2118/141349-MS.

Flaaten, A., Nguyen, Q.P., Zhang, J., Mohammadi, H., and Pope, G.A. (2008) ‘ASP chemical flooding without the need for soft water’, *SPE Annual Technical Conference and Exhibition*. Denver, Colorado, 21-24 September. Texas: Society of Petroleum Engineers, pp. 1-20. doi: https://doi.org/10.2118/116754-MS.

Fleming B. A., and Crerar D. A. (1982) ‘Silicic Acid Ionization and Calculation of Silica Solubility at Elevated Temperature and pH Application to Geothermal Fluid Processing and Reinjection’, *Geothermics*, 11(l), pp. 15-29.

Fortin, D**.,** Ferris, F.G., and Scott, S.D. (1998) ‘Formation of Fe-silicates and Fe-oxides on bacterial surfaces in samples collected near hydrothermal vents on the Southern Explorer Ridge in the northeast Pacific Ocean’, *American Mineralogist*, 83(11-12), pp. 1399–1408.

Fournier, R.O., and Rowe, J.J. (1977) ‘The solubility of amorphous silica in water at high temperatures and pressures’, *American Mineralogist*, 62(9-10), pp.1052-1056.

Fukuda, J. (2012) ‘Water in rocks and minerals – species, distributions, and temperature dependences’, in Theophanides, T. (ed.) *Infrared Spectroscopy - Materials Science, Engineering and Technology*. Croatia (European Union): Intech, pp. 77-96. Available at: https://cdn.intechopen.com/pdfs-wm/36169.pdf (Accessed: 25 January 2017).

Gaffney, S.H., Jackson, G.E. and Lyons, A.J.S. (1988) ‘The Effect of Iron(II) on the Barium Sulphate Scale Inhibition Performance of Diethylenetriaminepentamethylenephosphonic Acid (DETPMPA)’, *Proceedings of the Chemistry in the Oil Industry 3rd International Symposium*, University of Manchester, Manchester, UK, 19-20 April, pp.135-139.

Gallup, D.L. (1989) ‘Iron silicate scale formation and inhibition at the Salton Sea Geothermal Field’, *Geothermic,* 18(1-2), pp. 97-103.

Gallup, D. L. and Reiff, W. M. (1991) ‘Characterization of geothermal scale deposits by Fe-57 Mossbauer spectroscopy and complementary x-ray diffraction and infra-red studies’, *Geothermics,* 20(4), pp. 207-224.

Gill, J. S. (1993) ‘Inhibition of Silica-Silica Deposit in Industrial Waters,’ *Colloids and Surfaces,* 74(1), pp. 101-106.

Gill, J.S. (1998) ‘Silica scale control’, *Proceedings of the NACE International CORROSION 1998,* San Diego, California, USA, 22-27 March. Available at: https://www.onepetro.org/download/conference-paper/NACE-98226?id=conference-paper%2FNACE-98226 (Accessed: 20 March 2015).

Graham, G.M., Stalker, R. and McIntosh, R. (2003) ‘The impact of dissolved iron on the performance of scale inhibitors under carbonate scaling conditions’, *Proceedings of the International Symposium on Oilfield Chemistry,* Houston, Texas, 5-7 February. doi: https://doi.org/10.2118/80254-MS.

Guerra, C.E. and Jacobo, P.E. pH modifications for silica control in geothermal fluids. United Nations University Geothermal Training Programme UNU-GTP and LaGeo, Santa Tecla, El Salvador; 2012. Short Course on Geothermal Development and Geothermal Wells.

Gunnarsson, A., and Arnórsson, S. (2003) ‘Silica scaling: The main obstacle in efficient use of high-temperature geothermal fluids’, *Proceedings of the International Geothermal Conference,* Reykjavík, Iceland, 14-17 September. Available at: https://rafhladan.is/bitstream/handle/10802/9400/S13Paper118.pdf?sequence=1 (Accessed: 20 March 2015).

Gunnarsson, A., and Arnórsson S. (2005) ‘Impact of silica scaling on the efficiency of heat extraction from high-temperature geothermal fluids’, *Geothermics,* 34(3), pp. 320-329. doi: http://doi.org/10.1016/j.geothermics.2005.02.002.

Harrar, J.E., Lorensen, L.E. and Locke, F.E. (1982*) Method for inhibiting silica precipitation and scaling in geothermal flow systems.* U.S. Patent No. US4328106A. Available at: https://www.google.ch/patents/US4328106 (Accessed: 24 August 2014).

Hauksson, T., Pórhallsson, S., Gunnlaugsson, E., and Albertsson, A. (1995) ‘Control of magnesium silicate scaling in district heating systems’, *World Geothermal Congress.* Florence, Italy, 18-31 May. Italy: International Geothermal Association, pp. 2487-2490.

Henley, R.W. (1983) ‘pH and silica scaling control in geothermal field development’, *Geothermics,* 12(4), pp. 307-321.

Hernández-Ortiz, M. Acosta-Torres, L.S., Hernández-Padrón, G., Mendieta, A.I., Bernal, R., Cruz-Vázquez, C., and Castaño, V.M. (2012) ‘Biocompatibility of crystalline opal nanoparticles’, *BioMedical Engineering OnLine,* 11(78), pp. 1-10. doi**:** 10.1186/1475-925X-11-78.

Hirasaki, G.J., Miller, C.A., and Puerto, M. (2011) ‘Recent Advances in Surfactant EOR’, *SPE Journal,* 16(4), pp. 889-906. doi: https://doi.org/10.2118/115386-PA.

Holmes-Farley, S. R. (2005) *What is that Precipitate in My Reef Aquarium?.* Available at: http://reefkeeping.com/issues/2005-07/rhf/index.htm#20 (Accessed: 14 June 2014).

Hou, J.R., Liu, Z.C., Zhang, S.F., Yue, X.A., Yang, J.Z. (2005) ‘The role of viscoelasticity of alkali/surfactant/polymer solutions in enhanced oil recovery’, *Journal of Petroleum Science and Engineering*, 47(3-4), pp. 219– 235.

Hunt, D. (2012) *General Chapter <1660> Evaluation of the Inner Surface Durability of Glass Containers.* Available at: http://www.usp.org/sites/default/files/usp_pdf/EN/USPNF/revisions/c1660.pdf (Accessed: 3 March 2015).

Husky Oil Operation Limited (2010) *Innovative Energy Technologies Program Application 01-023 Taber S Mannville B Alkaline-Surfactant-Polymer Flood Warner ASP Flood 2009 Annual Report*. Available at: http://www.energy.alberta.ca/xdata/IETP/IETP%202009/01-023%20Taber%20S%20Alkaline-Surfactant-Polymer%20Flood/2009%20Annual%20Report%20Application%2001-023%20Print.pdf (Accessed: 9 February 2016).

Icopini, G.A., Brantley, S.L., and Heaney, P.J. (2005) ‘Kinetics of silica oligomerization and nanocolloid formation as a function of pH and ionic strength at 25°C’, *Geochimica et Cosmochimica Acta,* 69(2), pp. 293–303.

Iler, R.K. (1979) *The chemistry of silica,* New York: John Wiley.

ISO 3534-2 (2006) Statistics – vocabulary and symbols – part 2: applied statistics. International Organization for Standardization, Geneva.

Jäger, C., Dorschner, J., Mutschke, H., Posch, Th. and Henning, Th. (2003) 'Steps toward interstellar silicate mineralogy VII. Spectral properties and crystallization behaviour of magnesium silicates produced by the sol-gel method', *Astronomy & Astrophysics,* 408(1), pp 193–204, doi: 10.1051/0004-6361:20030916

Jephcott, C. M. and Johnston, J. H. (1950) 'Solubility of silica and alumina', *Arch. Indust. Hyg. & Occupational Med.,* 1(3), pp.323-340.

Jiang, W., Hua, X., Han, Q., Yang, X., Lu, L., and Wang, X. (2009) 'Preparation of Lamellar Magnesium Hydroxide Nanoparticles via Precipitation Method', *Powder Technology,* 191(3), pp 227-230. doi: 10.1016/j.powtec.2008.10.023.

Jing, G. Tang, S., Li, X., Yu, T. and Gai, Y. (2013) 'The scaling conditions for ASP flooding oilfield in the fourth Plant of Daqing oilfield', *Journal of Petroleum Exploration and Production Technology,* 3(3), pp. 175-178. doi:10.1007/s13202-013-0061-2.

Joint Committee for Guides in Metrology (JCGM) (2008) International vocabulary of metrology – basic and general concepts and associated terms (VIM). International Organization for Standardization, Geneva.

Jørgensen, S.S. (1968) 'Solubility and dissolution kinetics of precipitated silica in I M NaCl at 25 ° C', *Acta Chemica Scandinavica,* 22, pp. 335-341.

Kamitsuji, K., Suzuki, H., Kimura, Y., Sato, T., Saito, Y., and Kaito, C. (2005) 'Crystalline Mg_2SiO_4 and amorphous Mg-bearing silicate grain formation by coalescence and growth', *Astronomy & Astrophysics,* 429(1), pp. 205-208.

Karakassides, M. A., Gournis D., and Petridis, D. (1997) 'Infrared reflectance study of thermally treated Li- and Cs-montmorillonites', *Clays and Clay Minerals,* 45(5), pp. 649-658.

Karakassides, M.A., Gournis, D., and Petridis, D. (1999) 'An infrared reflectance study of Si-O vibrations in thermally treated alkali saturated montmorrilonites clay minerals', *Clay Minerals,* 34(3), pp. 429-438.

Karpov, I.K., Chudnenko, K.V., and Kulik, D.A. (1997) ‘Modeling chemical mass transfer in geochemical processes: thermodynamic relations, conditions of equlibria, and numerical algorithms’, *American Journal of Science*, 297(8), pp.767-806.

Kashpura V.N., and Potapov V.V. (2000) ‘Study of the amorphous silica scales formation at the Mutnovskoe Hydrothermal Field (Russia)’, *Proceedings of the Twenty-Fifth Workshop on Geothermal Reservoir Engineering.* Stanford University, Stanford, California, 24-26 January. Available at: https://www.geothermal-energy.org/pdf/IGAstandard/SGW/2000/Potapov.pdf (Accessed: 07 April 2014).

Kelland, M.A. (2011) ‘Effect of Various Cations on the Formation of Calcium Carbonate and Barium Sulfate Scale with and without Scale Inhibitors’, *Industrial & Engineering Chemistry Research,* 50(9), pp. 5852–5861. doi: 10.1021/ie2003494.

Khan, M. Y., Samanta, A., Ojha, K., and Mandal, A. (2009) ‘Design of Alkaline/Surfactant/Polymer (ASP) Slug and its use in Enhanced Oil Recovery’, *Petroleum Science and Technology*, 27(17), pp. 1926-1942. doi: 10.1080/10916460802662765.

Kitahara, S. (1960) ‘The polymerization of silicic acid obtained by the hydrothermal treatment of quartz and the solubility of amorphous silica’, *The Review of Physical Chemistry of Japan,* 30(2), pp. 131-137.

Kristmannsdóttir, H., Ó1afsson, M., and Thórhallsson, S., (1989) ‘Magnesium silicate scaling in district heating systems in Iceland’, *Geothermics,* 18(1-2), pp. 191–198.

Kronenberg, A.K. & Wolf, G.H. (1990) ‘Fourier transform infrared spectroscopy determinations of intragranular water content in quartz-bearing rocks: implications for hydrolytic weakening in the laboratory and within the earth’, *Techtonophysics*, 172 (3-4), pp 255-271. doi:10.1016/0040-1951(90)90034-6.

Krumrine, P.H., Mayer, E.H., Brock, G.F. (1985) ‘Scale Formation during Alkaline Flooding’, *Journal of Petroleum Technology*, 37(08), pp. 1466-1474. doi: https://doi.org/10.2118/12671-PA.

Kwon, H., and Park, D.G. (2009) ‘Infra-Red study of surface carbonation on polycrystalline magnesium hydroxide’, *Bulletin of the Korean Chemical Society*, 30(11), pp. 2567-2573.

Leech, C.N. Modelling the Geochemical Effects of Geothermal Fluid Injection in the Olkaria Geothermal Field, Kenya. United Nations University, Orkustofnun, Iceland; 2016. UNU Geothermal Training Programme Reports 2016 no.24.

Lehigh University (2000) *The LEO EnviroSci Inquiry.* Available at: http://www.ei.Lehigh.edu/envirosci/enviroissue/amd/links/chem1.html (Accessed: 04 January 2017).

Li, J., Li, T., Yan, J., Zuo, X., Zheng, Y. and Yang, F. (2009) 'Silicon containing scale forming characteristics and how scaling impacts sucker rod pump in ASP Flooding', *SPE Asia Pacific Oil and Gas Conference and Exhibition.* Jakarta, Indonesia, 4-6 August. Texas: Society of Petroleum Engineers, pp. 1-3. doi: SPE-122966-MS.

Lindsay, W.L. (1972) *Chemical Equilibria in Soil*. New York: John Wiley & Sons.

Liu, S.T., and Nancollas, G.H. (1973) 'The crystallization of magnesium hydroxide', *Desalination*, 12(1), pp. 75-84.

Malki, M. (2014) 'Case study: The impact of ferrous ion oxidation on silica scaling in RO systems, *Proceeding of the AWWA/AMTA Membrane Technology Conference & Exposition*, Las Vegas, Nevada, USA, 10-14 March. Available at: https://www.membranechemicals.com/wp-content/uploads/2017/02/The-impact-of-ferrous-ion-oxidation-on-silica-scaling-in-RO-systems-AWWA-AMTA-2014-1.pdf (Accessed: 3 July 2015).

Manceau, A., Ildefonse, P.H., Hazemann, J.-L., Flank, A-M., and Gallup (1995) 'Crystal chemistry of hydrous iron silicate scale deposits at the Salton Sea geothermal field', *Clays and Clay Minerals*, 43(3), pp. 304-317.

Marshall, W. L. (1980) 'Amorphous silica solubilities—I. Behavior in aqueous sodium nitrate solutions; 25–300°C, 0–6 molal', *Geochimica et Cosmochimica Acta,* 44(7), pp.907-913.

Marshall, W. L. and Chen, C.T.A. (1982) 'Amorphous Silica Solubilities V. Predictions of Solubility Behavior in Aqueous Mixed Electrolyte Solutions to 300°C', *Geochimica et Cosmochimica Acta*, 46(2), pp. 289-291.

Marshall, W.L. and Warakomski, J.M. (1980) 'Amorphous silica solubilities II. Effect of aqueous salt solutions at 25°C', *Geochimica et Cosmochimica Acta,* 44, pp. 915-924.

Mayer, E.H., Berg, R.L., Charmichael, J.D., Weinbrandt, R.M. (1983) 'Alkaline Injection for Enhanced Oil Recovery - A Status Report', *Journal of Petroleum Technology*, 35(01), pp. 209-221. doi: https://doi.org/10.2118/8848-PA.

McDonald, R.S. (1958) 'Surface Functionality of Amorphous Silica by Infrared Spectroscopy', *J. Phys. Chem., 62* (10), pp 1168–1178. doi**:** 10.1021/j150568a004.

McLin, K.S., Moore, J.N., Hulen, J., Bowman, J.R. and Berard, B. (2006) 'Mineral characterization of scale deposits in injection wells; Coso and Salton Sea geothermal fields, CA', *Proceedings of the Thirty-First Workshop on Geothermal Reservoir Engineering*, Stanford University, Stanford, California, 30 January – 1 February. Available at: https://pangea.stanford.edu/ERE/pdf/IGAstandard/SGW/2006/mclin.pdf: (Accessed: 20 March 2015).

Meyers, P. (1999) 'Behavior of silica in ion exchange and other systems', *The International Water Conference: 60th Annual Meeting.* Western William Penn Hotel, Pittsburgh, Pennsylvania, 18-20 October. Pennsylvania: Engineer's Society of Western Pennsylvania, pp. 492-501.

Meyers, P. (2004) Behavior of Silica: *Technologies Available and How They Rate.* Arizona, US: Water Conditioning & Purification Magazine.

Mroczek, E.K., and McDowell, G. (1990) 'Silica scaling field experiments', *Geothermal Resources Council (Transactions)*, 14(11), pp. 1619-1625.

Musić, S., Filipović-Vinceković, N. and Sekovanić, L. (2011) 'Precipitation of Amorphous SiO_2 Particles and Their Properties', *Brazilian Journal of Chemical Engineering*, 28(01), pp 89 – 94. doi: 10.1590/S0104-66322011000100011.

Neofotistou, E., and Demadis, K.D. (2004) 'Use of antiscalants for mitigation of silica (SiO_2) fouling and deposition: fundamentals and applications in desalination systems', *Desalination*, 167, pp. 257-272.

Ning, R.Y. (2002) 'Discussion of silica speciation, fouling, control and maximum reduction', *Desalination*, 151(1), pp. 67-73.

Olsen, D.K., Hicks, M.D., Hurd, B.G., Sinnokrot, A.A. and Sweigart, C.N. (1990) 'Design of a novel flooding system for an oilwet Central Texas carbonate reservoir', *SPE/DOE Seventh Symposium on Enhanced Oil Recovery*. Tulsa, Oklahoma, 22–25 April. Texas: Society of Petroleum Engineers, pp. 507-516.

Park, J., Norman, D., McLin, K., and Moore, J. (2006) 'Modeling amorphous silica precipitation: a strategy to reduce silica precipitation near Coso injection wells', *Proceedings of the Thirty-First Workshop on Geothermal Reservoir Engineering*, Stanford University, Stanford, California, 30 January – 1 February. Available at: https://pangea.stanford.edu/ERE/pdf/IGAstandard/SGW/2006/park.pdf: (Accessed: 20 March 2015).

Parkhurst, D.L., and Appelo, C.A.J., 2013, Description of input and examples for PHREEQC version 3—A computer program for speciation, batch-reaction, one-dimensional transport, and inverse geochemical calculations: U.S. Geological Survey Techniques and Methods, book 6, chap. A43, 497 p., available only at https://pubs.usgs.gov/tm/06/a43/

Parveen, M. F., Umapathy, S., Dhanalakshmi, V., and Anbarasan, R. (2010) 'Synthesis and characterization of nanosized Iron (II) hydroxide and Iron (II) hydroxide/ poly(vinylalcohol) nanocomposite', *Journal of Applied Polymer Science*, 118(3), pp. 1728-1737.

Perez, L. A., Brown, J. M., and Nguyen, K. T. (1993) *Method for controlling silica and water-soluble silicate deposition.* US Patent No. 5256302. Available at: https://docs.google.com/viewer?url=patentimages.storage.googleapis.com/pdfs/US5256302.pdf (Accessed: 21 July 2017).

Rashid, I., Daraghmeh, N., Al-Remawi, M., Leharne, S. A., Chowdhry, B. Z., and Badwan, A. (2009) 'Characterization of Chitin–Metal silicates as binding superdisintegrants', *Journal of Pharmaceutical Sciences*, 98(12), pp. 4887-4901. doi: 10.1002/jps.21781.

Rauch, M., and Keppler, H. (1998) *Comparison of the water solubility in synthetic pure $MgSiO_3$ enstatite and in a natural, aluminous enstatite from Tanzania.* Available at: http://www.bgi.uni-bayreuth.de/index.php?page=5&lng=en&view=1&year=1998&content=58 (Accessed: 3 January 2017).

Rodríguez, A. Amorphous iron silicate scales in surface pipelines: characterization and geochemical constraints on formation conditions in the Miravalles geothermal field, Costa Rica. United Nations University, Orkustofnun, Iceland; 2006. UNU Geothermal Training Programme Reports 2006 no.19.

Rothbaum. H.P. and Rohde, A.G. (1979) 'Kinetics of silica polymerisation and deposition from dilute solutions between 5 and 180ºC', *Journal of Colloid and Interface Science*,71(3), pp. 533-559.

Rothbaum, H. P., and Wilson, R. D. (1977) 'Effect of temperature and concentration on the rate of polymerization of silica in geothermal waters' *Geochemistry*. New Zealand Department of Science and Industrial Resources Bulletin, pp. 37-43.

Said, S.A. (1997) *Genesis of silica-enriched agricultural pans in soils managed under wheat-fallow cropping systems*. Master thesis. Oregon State University. Available at: https://ir.library.oregonstate.edu/xmlui/handle/1957/33736 (Accessed: 14 August 2015).

Samanta, A., Bera, A., Ojha, K., and Mandal, A. (2012) 'Comparative studies on enhanced oil recovery by alkali–surfactant and polymer flooding', *Journal of Petroleum Exploration and Production Technology*, 2(2), pp. 67-74. doi: 10.1007/s13202-012-0021-2.

Sazali, R.A., Sorbie, K.S., and Boak, L.S. (2014) *Silicate Scaling.* Internal FAST 5 Report 2 May 2014. Unpublished.

Sazali, R.A., Sorbie, K.S., and Boak, L.S. (2014) *Silicate Scaling.* Internal FAST 5 Report 3 November 2014. Unpublished.

Sazali, R.A., Sorbie, K.S., and Boak, L.S. (2015) *Silicate Scaling.* Internal FAST 5 Report 4 May 2015. Unpublished.

Sazali, R.A., Sorbie, K.S., and Boak, L.S. (2015) *Silicate Scaling.* Internal FAST 5 Report 5 October 2015. Unpublished.

Sazali, R.A., Sorbie, K.S., and Boak, L.S. (2016) *Silicate Scaling.* Internal FAST 5 Report 6 May 2016. Unpublished.

Sazali, R.A., Sorbie, K.S., and Boak, L.S. (2016) *Silicate Scaling.* Internal FAST 6 Report 1 November 2016. Unpublished.

Sazali, R.A., Sorbie, K.S., and Boak, L.S. (2016) *Silicate Scaling.* Internal FAST 6 Report 2 May 2017. Unpublished.

Shaw, S.S. (2012) *Investigation into the mechanisms of formation and prevention of barium sulphate oilfield scale.* PhD thesis. Heriot-Watt University. Available at: http://www.ros.hw.ac.uk/handle/10399/2550 (Accessed: 14 August 2015).

Sheng, J. J. (2013) 'A comprehensive review of Alkaline-Surfactant-Polymer (ASP) Flooding', *SPE Western Regional & AAPG Pacific Section Meeting 2013 Joint Technical Conference.* Monterey, California, 19-25 April. Texas: Society of Petroleum Engineers, pp. 1-20.

Sheng, J.J. (2014) 'A comprehensive review of alkaline–surfactant–polymer (ASP) flooding', *Asia-Pacific Journal of Chemical Engineering*, 9(4), pp. 471-489. doi: 10.1002/apj.1824.

Shupe, R.D. (1981) 'Chemical Stability of Polyacrylamide Polymers', *Journal of Petroleum Technology*, 33(8), pp. 1513-1529.

Sinclair L. A. (2012) *Development of Silica Scaling Test Rig.* Master thesis. University of Canterbury. Available at: https://ir.canterbury.ac.nz/handle/10092/7002 (Accessed: 14 August 2015).

Singhal, A. (2011) *Preliminary review of IETP projects using polymers.* Calgary, Alberta, Canada: Premier Reservoir Engineering Services Ltd. Available at: http://www.energy.alberta.ca/Oil/pdfs/IETPPolymerStudy.pdf (Accessed: 21 May 2014).

Sonne, J., Miner, K., and Kerr S. (2012a) 'Potential for inhibitor squeeze application for silicate scale control in ASP flood', *Proceedings of the SPE EOR Conference at Oil and Gas West Asia*, Muscat, Oman, 16-18 April.

Sonne, J., Kerr, S., and Miner, K. (2012b) ‘Application of silicate scale inhibitors for ASP flooded oilfields: A novel approach to testing and delivery’, *Proceedings of the SPE International Conference and Exhibition on Oilfield Scale,* Aberdeen, UK, 30-31 May. doi:10.2118/154332-MS.

Sorbie, K.S., and Laing, N. (2004) ‘How scale inhibitors work: Mechanisms of selected barium sulphate scale inhibitors across a wide temperature range’, *Proceeding of the SPE International Symposium on Oilfield Scale,* Aberdeen, United Kingdom 26-27 May.

Stathoulopoulou, A., and Demadis, K.D. (2008) ‘Enhancement of silicate solubility by use of “green” additives: linking green chemistry and chemical water treatment’, *Desalination,* 224 (1-3), pp. 223–230.

Stefánsson, A., Arnórsson, S., Gunnarsson, I., Kaasalainen, H., and Gunnlaugsson, E. (2011) ‘The geochemistry and sequestration of H_2S into the geothermal system at Hellisheidi, Iceland’, *Journal of Volcanology and Geothermal Research,* 202(3), pp. 179–188.

Stoll, W.M., Al-Shureqi, H., Finol, J., Al-Harthy, S.A.A, Oyemade, S.N., de Kruijf, A., Van Wunnik, J.M.N., Arkesteijn, F., Bouwmeester, R., and Faber, M.J. (2010) ‘Alkaline-Surfactant-Polymer flood: from the laboratory to the field’, *SPE EOR Conference at Oil & Gas West Asia*. Muscat, Oman, 11-13 April. Texas: Society of Petroleum Engineers, pp. 1-15. doi: https://doi.org/10.2118/129164-MS.

Stoppelenburg, L.S., and Yuan, M. (2000) ‘The performance of barium sulfate inhibitors in iron containing waters in both aerated and anaerobic systems’, *Proceedings of the CORROSION 2000,* Orlando, Florida, 26-31 March. Available at: https://www.onepetro.org/download/conference-paper/NACE-00114?id=conference-paper%2FNACE-00114 (Accessed: 11 November 2015).

Sui, X., Liu, Y., Wang, B., Wu, H., and Dong, J. (2014) ‘Study on morphology of silicic acid polymerization process in different systems’, *Journal of Chemical and Pharmaceutical Research,* 6(1), pp. 681-685.

Tobbler, D.J. (2008) *Molecular pathways of silica nanoparticle formation and biosilicification.* PhD thesis. The University of Leeds. Available at: http://etheses.whiterose.ac.uk/359/ (Accessed: 14 August 2015).

U.S. Geological Survey (1962) *Chemistry of iron in natural water*. Washington, U.S.: United States Government Printing Office. Available at: https://pubs.usgs.gov/wsp/1459a/report.pdf/ (Accessed: 01 April 2017).

Umar, A.A., and Saaid, I.M. (2013) 'Silicate Scales formation during ASP Flooding: A Review', *Research Journal of Applied Sciences, Engineering and Technology*, 6(9), pp. 1543-1555.

Umar A.A. and Saaid I.M., (2014) 'Effect of Temperature on Silicate Scale Inhibition During ASP Flooding, *Journal of Applied Sciences,* 14(15), pp. 1769-1774.

Unomah, O.U. (2013) *Chemical enhanced oil recovery utilizing alternative alkalis*. PhD thesis. The University of Texas at Austin. Available at: https://repositories.lib.utexas.edu/handle/2152/22386 (Accessed: 14 August 2015).

Wang, W. and Wei, W. (2016) 'Silica and silicate scale formation and control: Scale Modelling, Lab Testing, Scale Characterization, and Field Observation', *Proceeding of the SPE International Oilfield Scale Conference and Exhibition,* Aberdeen, UK, 11-12 May. doi: http://dx.doi.org/10.2118/179897-MS.

Weres, O., and Apps, J.A. (1982) 'Prediction of chemical problems in the reinjection of geothermal brines', *Geological Society of America, Special Paper 189*, pp. 407-426.

Weres, O., Yee, A. and Tsao, L. Kinetics of silica polymerization. Lawrence Berkeley National Laboratory. University of California, California, USA; 1980. LBNL Paper LBL-7033.

Weres, O., Yee, A., and Tsao, L. (1979) 'Kinetic equations and type curves for predicting the precipitation of amorphous silica from geothermal brines', *SPE Oilfield and Geothermal Chemistry Symposium*. Houston, Texas, 22-24 January. Texas: Society of Petroleum Engineers, pp. 249-255.

Weres, O., Yee, A. and Tsao, L. (1981) 'Kinetics of silica polymerization' *Journal of Colloid and Interface Science,* 84(2), pp. 379-402.

Willey, J. D. (1974) 'The effect of pressure on the solubility of amorphous silica in seawater at 0^{o}C', *Marine Chemistry,* 2(4), pp.239-250.

Ying, F. (2007) ‘Reaction mode between Si & Fe & evaluation of optimal species in poly-silicic-ferric coagulant’, *Journal of Environment Sciences,* 19(6), pp. 678-688.

Zhang, Z., Liu, Y., Dai, Z., Bhandari, N., Zhang, F., Yan, F., Ruan, G., Alsaiari, H., Lu, Y-T., Deng, G., Kan, A. and Tomson, M. (2016) ‘Impact of FeIII/FeII on scale inhibition’, *Proceeding of the SPE International Oilfield Scale Conference and Exhibition*, Aberdeen, Scotland, 11-12 May. doi: SPE-179905-MS.

Zhang, Z., Zhang, F., Wang, Q.L., Bhandari, N., Yan, F., Liu, Y., Dai, Z., Wang, L., Bolanos, V., Kan, A.T. and Tomson, M.B. (2015) ‘Ferrous iron impact on phosphonate and polymeric scale inhibitors at temperature ranging from 25 to 70°C’, *Proceeding of the SPE International Symposium on Oilfield Chemistry*, The Woodlands, Texas, USA, 13-15 April. doi: https://doi.org/10.2118/173770-MS.

Zuhl, R.W. and Amjad, Z. (2013) ‘Solution Chemistry Impact on Silica Polymerization by Inhibitors’, in Amjad, Z. (ed.) *Mineral Scales in Biological and Industrial Systems*. New York, USA: CRC Pressbook, Taylor and Francis Group, pp. 173-200.